

IAEA-TECDOC-1665

***Impact of
Soil Conservation Measures on
Erosion Control and Soil Quality***



IAEA

International Atomic Energy Agency

Impact of Soil Conservation Measures on Erosion Control and Soil Quality

The following States are Members of the International Atomic Energy Agency:

AFGHANISTAN	GHANA	NORWAY
ALBANIA	GREECE	OMAN
ALGERIA	GUATEMALA	PAKISTAN
ANGOLA	HAITI	PALAU
ARGENTINA	HOLY SEE	PANAMA
ARMENIA	HONDURAS	PARAGUAY
AUSTRALIA	HUNGARY	PERU
AUSTRIA	ICELAND	PHILIPPINES
AZERBAIJAN	INDIA	POLAND
BAHRAIN	INDONESIA	PORTUGAL
BANGLADESH	IRAN, ISLAMIC REPUBLIC OF	QATAR
BELARUS	IRAQ	REPUBLIC OF MOLDOVA
BELGIUM	IRELAND	ROMANIA
BELIZE	ISRAEL	RUSSIAN FEDERATION
BENIN	ITALY	SAUDI ARABIA
BOLIVIA	JAMAICA	SENEGAL
BOSNIA AND HERZEGOVINA	JAPAN	SERBIA
BOTSWANA	JORDAN	SEYCHELLES
BRAZIL	KAZAKHSTAN	SIERRA LEONE
BULGARIA	KENYA	SINGAPORE
BURKINA FASO	KOREA, REPUBLIC OF	SLOVAKIA
BURUNDI	KUWAIT	SLOVENIA
CAMBODIA	KYRGYZSTAN	SOUTH AFRICA
CAMEROON	LATVIA	SPAIN
CANADA	LEBANON	SRI LANKA
CENTRAL AFRICAN REPUBLIC	LESOTHO	SUDAN
CHAD	LIBERIA	SWEDEN
CHILE	LIBYAN ARAB JAMAHIRIYA	SWITZERLAND
CHINA	LIECHTENSTEIN	SYRIAN ARAB REPUBLIC
COLOMBIA	LITHUANIA	TAJKISTAN
CONGO	LUXEMBOURG	THAILAND
COSTA RICA	MADAGASCAR	THE FORMER YUGOSLAV REPUBLIC OF MACEDONIA
CÔTE D'IVOIRE	MALAWI	TUNISIA
CROATIA	MALAYSIA	TURKEY
CUBA	MALI	UGANDA
CYPRUS	MALTA	UKRAINE
CZECH REPUBLIC	MARSHALL ISLANDS	UNITED ARAB EMIRATES
DEMOCRATIC REPUBLIC OF THE CONGO	MAURITANIA	UNITED KINGDOM OF GREAT BRITAIN AND NORTHERN IRELAND
DENMARK	MAURITIUS	UNITED REPUBLIC OF TANZANIA
DOMINICAN REPUBLIC	MEXICO	UNITED STATES OF AMERICA
ECUADOR	MONACO	URUGUAY
EGYPT	MONGOLIA	UZBEKISTAN
EL SALVADOR	MONTENEGRO	VENEZUELA
ERITREA	MOROCCO	VIETNAM
ESTONIA	MOZAMBIQUE	YEMEN
ETHIOPIA	MYANMAR	ZAMBIA
FINLAND	NAMIBIA	ZIMBABWE
FRANCE	NEPAL	
GABON	NETHERLANDS	
GEORGIA	NEW ZEALAND	
GERMANY	NICARAGUA	
	NIGER	
	NIGERIA	

The Agency's Statute was approved on 23 October 1956 by the Conference on the Statute of the IAEA held at United Nations Headquarters, New York; it entered into force on 29 July 1957. The Headquarters of the Agency are situated in Vienna. Its principal objective is "to accelerate and enlarge the contribution of atomic energy to peace, health and prosperity throughout the world".

IAEA-TECDOC-1665

**IMPACT OF SOIL CONSERVATION
MEASURES ON EROSION
CONTROL AND SOIL QUALITY**

INTERNATIONAL ATOMIC ENERGY AGENCY
VIENNA, 2011

COPYRIGHT NOTICE

All IAEA scientific and technical publications are protected by the terms of the Universal Copyright Convention as adopted in 1952 (Berne) and as revised in 1972 (Paris). The copyright has since been extended by the World Intellectual Property Organization (Geneva) to include electronic and virtual intellectual property. Permission to use whole or parts of texts contained in IAEA publications in printed or electronic form must be obtained and is usually subject to royalty agreements. Proposals for non-commercial reproductions and translations are welcomed and considered on a case-by-case basis. Enquiries should be addressed to the IAEA Publishing Section at:

Sales and Promotion, Publishing Section
International Atomic Energy Agency
Vienna International Centre
PO Box 100
1400 Vienna, Austria
fax: +43 1 2600 29302
tel.: +43 1 2600 22417
email: sales.publications@iaea.org
<http://www.iaea.org/books>

For further information on this publication, please contact:

Soil and Water Management and Crop Nutrition Section
International Atomic Energy Agency
Vienna International Centre
PO Box 100
1400 Vienna, Austria
email: Official.Mail@iaea.org

**IMPACT OF SOIL CONSERVATION MEASURES
ON EROSION CONTROL AND SOIL QUALITY**

IAEA, VIENNA, 2011
IAEA-TECDOC-1665
ISBN 978-92-0-113410-3
ISSN 1011-4289
© IAEA, 2011
Printed by the IAEA in Austria
October 2011

FOREWORD

The present world population of 6 billion is expected to reach 9.3 billion by the year 2050. Most of the population increases will occur in developing countries, where the largest fraction depends upon agriculture for their livelihoods. Against the background of projections on increased population growth and pressure on the availability of land and water resources worldwide, several developing countries will face major challenges to achieve food security in a sustainable manner, considering their available per capita land area, severe scarcity of freshwater resources and particular infrastructure and socio-economic conditions. This is further compounded by severe global soil degradation, in particular Sub-Saharan Africa and South Asia, and increased risks of soil erosion. Worldwide, soil degradation is currently estimated at 1.9 billion hectares and is increasing at a rate of 5 to 7 million hectares each year. As climate change and variability worsen, they will undoubtedly increase the incidences of extreme weather events such as storms, droughts and floods and, at the same time, will increase even more the risks of land degradation and in particular soil erosion.

Global cost estimates of the soil loss by soil erosion are of the order of US \$400 billion per year (US \$ 1992). Therefore it is imperative that we conserve the top soil on which plants and livestock depend. This challenge can only be tackled by integrated agricultural systems, such as conservation agriculture, combining reduced tillage, retention of crop residues and contrasting crop rotations. In view of the above there is an urgent need to obtain reliable quantitative data on the extent and rates of soil erosion to provide a more comprehensive analysis of the problems and to underpin soil conservation strategies, including the assessment of their economic and environmental impacts. The quest for alternative techniques for assessing soil erosion to complement classical methods has directed attention to the use of radionuclides, particularly ^{137}Cs , as tracers to obtain quantitative estimates of the effectiveness of soil conservation measures in controlling erosion and improving soil quality.

This Coordinated Research Project (CRP) entitled 'Assessing the effectiveness of soil conservation measures for sustainable watershed management and crop production using fallout radionuclides' (D1.50.08), was approved and implemented between 2002 and 2008 and was conceived as a follow-up of the CRP on 'Assessment of soil erosion through the use of ^{137}Cs and related techniques as a basis for soil conservation, sustainable production and environmental protection' coordinated by the Joint FAO/IAEA Division of Nuclear Techniques in Food and Agriculture. The implementation of this IAEA CRP, during the period of 1996-2001, has made a major contribution to coordinating efforts to refine and standardize the ^{137}Cs technique. These methodological developments are documented in a Handbook for the Assessment of Soil Erosion and Sedimentation using Environmental Radionuclides published by Kluwer in 2002. The efficacy and value of the approach has been demonstrated by investigations in a range of environments. These findings are reported in two special issues of the journals *Acta Geologica Hispanica* (2000) and *Soil and Tillage Research* (2003). They have paved the way to both extending the approach to other environmental radionuclides (^{210}Pb and ^7Be) and expanding applications exploiting the essentially unique advantages provided by the technique.

The overall objective of this CRP D1.50.08 was to develop improved land use and management strategies for sustainable watershed management through effective soil erosion control practices. A range of soil conservation measures were tested in sixteen countries to provide information about their effectiveness in controlling soil erosion and improving soil quality by using fallout radionuclides, which were found to be effective and efficient tools for short and medium term assessment of soil erosion. This publication contains the manuscripts prepared by the participants and was edited by G. Dercon and F. Zapata of the Joint

FAO/IAEA Division of Nuclear Techniques in Food and Agriculture, and G. Hancock from CSIRO Land and Water (Australia). The IAEA officer responsible for this publication was G. Dercon of the Joint FAO/IAEA Division of Nuclear Techniques in Food and Agriculture.

EDITORIAL NOTE

The papers in these proceedings are reproduced as submitted by the authors and have not undergone rigorous editorial review by the IAEA.

The views expressed do not necessarily reflect those of the IAEA, the governments of the nominating Member States or the nominating organizations.

The use of particular designations of countries or territories does not imply any judgement by the publisher, the IAEA, as to the legal status of such countries or territories, of their authorities and institutions or of the delimitation of their boundaries.

The mention of names of specific companies or products (whether or not indicated as registered) does not imply any intention to infringe proprietary rights, nor should it be construed as an endorsement or recommendation on the part of the IAEA.

The authors are responsible for having obtained the necessary permission for the IAEA to reproduce, translate or use material from sources already protected by copyrights.

CONTENTS

SUMMARY.....	1
COUNTRY REPORTS	
Models for deriving estimates of erosion and deposition rates from fallout radionuclide (caesium-137, excess lead-210, and beryllium-7) measurements and the development of user-friendly software for model implementation	11
<i>D.E. Walling, Y. Zhang, Q. He</i>	
Sediment budgets and source determinations using fallout caesium-137 in a semiarid rangeland watershed, Arizona, USA.....	35
<i>J.C. Ritchie, M.A. Nearing, F.E. Rhoton</i>	
Using tracers to assess the impacts of sediment and nutrient delivery in the lake burragorang catchment following severe wildfire	49
<i>S. Wilkinson, P. Wallbrink, W. Blake, R. Shakesby, S. Doerr</i>	
Assessment of the contribution from surface erosion of forest floors to suspended sediment in mountainous forested catchments in the tsuzura watershed, southern Japan.....	61
<i>Y. Onda, S. Mizugaki, H. Kato</i>	
Assessment of soil losses from managed and unmanaged sites in a subcatchment of Rawal dam, Pakistan using fallout radionuclides.....	73
<i>M. Rafiq, M. Ahmad, N. Iqbal, J.A. Tariq, W. Akram, M. Shafiq</i>	
Assessment of soil erosion severities and conservation effects on reduction of soil loss and sediment yield by using the caesium-137 and excess lead-210 tracing techniques in the upper Yangtze River basin, China.....	87
<i>X. Zhang, Y. Long, X. He, A. Wen, M. Feng, Y. Qi, J. Zheng, J. Fu, L. He, Y. Zhang, Y. He, H. Li, D. Yan, Y. Zhang, L. Bai, D.E. Walling</i>	
The use of excess lead-210, beryllium-7 and caesium-137 in investigations of sediment delivery dynamics in the homerka and dunajec catchments in the Polish Flysh Carpathians	115
<i>W. Froehlich, D.E. Walling</i>	
Application of the radionuclide technique and other methods for assessing the effectiveness of soil conservation measures at the Novosil study site, Orel region, Central Russia.....	131
<i>V.N. Golosov, V.R. Belyaev, M.V. Markelov, N.N. Ivanova, Y.S. Kuznetsova</i>	
Estimates of long and short term soil erosion rates on farmland in semi-arid West Morocco using caesium-137, excess lead-210 and beryllium-7 measurements.....	159
<i>M. Benmansour, A. Nouria, A. Benkdad, M. Ibn Majah, H. Bouksirat, M. El Oumri, R. Mossadek, M. Duchemin</i>	
The use of caesium-137 measurements for assessing soil erosion and sedimentation in the Riva basin (Istanbul, NW Turkey)	175
<i>S. Hacıyakupoglu, M.S. Kiziltas, H. Saygin, F. Gokbulak, A. Hizal, D.E. Walling, T.A. Ertek, A.E. Erginal</i>	
Erosion/disposition data derived from fallout radionuclides (FRNS) using geostatistics.....	185
<i>L. Mabit</i>	

Application of caesium-137 and beryllium-7 to assess the effectiveness of soil conservation technologies in the Central Highlands of Vietnam	195
<i>P.S. Hai, T.D. Khoa, N. Dao, N.T. Mui, T.V. Hoa, P.D. Hien, T.C. Tu</i>	
Assessment of effectiveness of soil conservation measures in reducing soil erosion and improving soil quality in China using fallout radionuclide techniques	207
<i>Y. Li, H.Q. Yu, X.C. Geng, M.L. Nguyen, R. Funk</i>	
Assessing the impacts of riparian zones on sediment retention in Brazilian sugarcane fields by the caesium-137 technique and WEPP modeling	225
<i>O.O.S. Bacchi, G. Sparovek, M. Cooper, S.B.L. Ranieri, V. Correchel</i>	
Use of fallout caesium-137 and beryllium-7 to assess the effectiveness of changes in tillage systems in promoting soil conservation and environmental protection on agricultural land in Chile	241
<i>P. Schuller, A. Castillo, D.E. Walling, A. Iroumé</i>	
Using caesium-137 techniques to estimate soil erosion and deposition rates on agricultural fields with specific conservation measures in the Tutova rolling hills, Romania	259
<i>N. Popa, E. Filiche, G. Petrovici, R.M. Margineanu</i>	
Combined use of caesium-137 methodology and conventional erosion measurements in the Mistelbach watershed (Austria)	279
<i>L. Mabit, A. Toloza, A. Klik, A. Geisler, U.C. Gestmann</i>	
Using the concept of a soil quality index (SQI) TO evaluate agricultural soils with and without soil protection measures in Lower Austria	297
<i>A. Klik, J. Hofmann</i>	
Analytical performance of 14 laboratories taking part in proficiency test for the determination of caesium-137 and total lead-210 in spiked soil samples	311
<i>A. Shakhashiro, L. Mabit</i>	
RECENT IAEA PUBLICATIONS ON SOIL AND WATER MANAGEMENT AND CROP NUTRITION	325
LIST OF PARTICIPANTS	327

SUMMARY

The Coordinated Research Project (CRP) entitled 'Assessing the effectiveness of soil conservation measures for sustainable watershed management and crop production using fallout radionuclides' established a research network and supported the efforts of teams of scientists in sixteen Member States (Australia, Austria, Brazil, Canada, Chile, China, Japan, Morocco, Pakistan, Poland, Romania, Russian Federation, Turkey, United Kingdom, United States of America, Vietnam). The aim of this CRP was the development of improved land use and management strategies for sustainable watershed management through effective soil erosion control practices. The specific objectives of the project were: i) To further develop fallout radionuclide methodologies, with particular emphasis on the combined use of ^{137}Cs , ^{210}Pb and ^7Be for measuring soil erosion over several spatial and time scales, ii) To establish standardized protocols for the combined application of the above techniques, and iii) To utilize these techniques to assess the impact of short term changes in land use practices and the effectiveness of specific soil conservation measures.

The achievements of this CRP, as reflected in this publication, demonstrated that fallout radionuclide based techniques are powerful tools to assess soil erosion at several spatial and temporal scales in a wide range of environments and to determine the effectiveness of soil conservation measures in controlling soil erosion. The CRP network confirmed that the ^{137}Cs technique is now recognized worldwide to be the primary and most widely isotopic tracer for long term soil erosion/sedimentation investigations, while the ^7Be technique has been further developed for application in short term soil redistribution studies.

The main specific research results and recommendations arising from this CRP are summarized below.

1. Development and refinement of fallout radionuclide methodologies

The key focus of this CRP was to develop novel applications of environmental or fallout radionuclides (FRNs) for assessing the impact of soil conservation measures on soil erosion and sedimentation. ^{137}Cs and excess ^{210}Pb ($^{210}\text{Pb}_{\text{ex}}$) and ^7Be were identified as the primary radionuclides for inclusion. New protocols were developed and tested for the combined application of ^{137}Cs , ^{210}Pb and ^7Be to obtain information on soil redistribution rates over short and long term time scales and spatial patterns (Benmasour et al., Froehlich et al., Golosov et al., Li et al., Onda et al., Hai et al., Schuller et al., Wilkinson et al., Zhang et al.).

The following potential approaches involving these radionuclides were identified and tested.

a) ^{137}Cs

Schuller et al. from Chile exemplified in her report the potential of the use of detailed measurements of ^{137}Cs depth distributions and inventories to establish changes in soil redistribution rates over the period covered by bomb fallout in response to a major change in land management. The Chilean research team developed a simplified method for using ^{137}Cs depth distribution datasets to estimate soil loss or accumulation at a sampling point under conventional tillage and after the shift to a no-till system. The approach should be applicable in Chile or elsewhere, where a change from conventional tillage to no-till has occurred. However, due to the long half-life of ^{137}Cs the approach is constrained by the requirement for relatively long periods (10 to 15 years) under the contrasting tillage systems.

In Russian Federation the use of ^{137}Cs was tested by Golosov et al. to investigate changes in soil redistribution rates associated with the post-Chernobyl period (after 1986). The utilization

of this approach is limited to those areas of Europe where bomb (from the 1950-1960s) and Chernobyl fallout inventories were of similar magnitude. However, Golosov et al. found that the technique seemed to overestimate the actual erosion rates, due to the influence of extreme erosion during the period immediately after the Chernobyl accident and prior to incorporation of the fresh Chernobyl fallout into the plough layers by tillage.

b) ^7Be

This CRP also demonstrated the potential for using ^7Be to provide information on short term rates of soil redistribution. The successful use of ^7Be measurements to quantify erosion rates during individual events or short periods of heavy rainfall has been reported by the teams from Morocco, Vietnam, Chile, Austria and China (Benmansour et al. Hai et al. Schuller et al. Wilkinson et al. Li et al.). The approach clearly involves a number of complexities, as it requires careful selection of the study period and detailed soil sampling and the need to monitor fallout inputs. To determine the effectiveness of soil conservation measures, it is necessary to have control areas for comparison purposes. The information on event-related erosion generated by the ^7Be measurements can provide a useful complement to the use of ^{137}Cs measurements to document (for example) the mean annual erosion rates associated with specific land use systems, and the effects of different soil conservation practices.

c) ^{210}Pb

The potential for using ^{210}Pb measurements to estimate soil redistribution rates was also explored. Only 31% of the participants were able to provide acceptable results for total ^{210}Pb analyses (Shakhashiro and Mabit). Once this analytical capacity is improved it seems that the use of ^{210}Pb measurements as a complement to ^{137}Cs has an important role to play (Benmansour et al.; Froehlich et al.; Golosov et al.; Li et al.; Onda et al.; Wilkinson et al.; Zhang et al.). However, in Russian Federation Golosov et al. found that $^{210}\text{Pb}_{\text{ex}}$ fallout was characterised by substantially higher local variability than that of ^{137}Cs , posing an important potential limitation in the use of $^{210}\text{Pb}_{\text{ex}}$ for estimating soil redistribution. Nevertheless it was found that the variation of $^{210}\text{Pb}_{\text{ex}}$ along their studied transects followed a similar pattern as that of ^{137}Cs . The results from the CRP generally support the conclusion that $^{210}\text{Pb}_{\text{ex}}$ can potentially be employed for quantification of soil redistribution. However, more research is needed to evaluate the various factors influencing the spatial variability of fallout inputs and its initial fallout variability. Because of this variability there is an need to consider carefully both the number of reference sites to be sampled when using $^{210}\text{Pb}_{\text{ex}}$ and the number of sampling points at individual reference sites.

d) Combined use of ^{137}Cs , $^{210}\text{Pb}_{\text{ex}}$ and ^7Be

The CRP focussed strongly on the combined use of ^{137}Cs , $^{210}\text{Pb}_{\text{ex}}$ and ^7Be . The studies reported by Benmansour et al., Froehlich and Walling, Golosov et al., Li et al., Onda et al., Hai et al., Schuller et al., Wilkinson et al. and Zhang et al. demonstrated the potential for using two or three of these radionuclides in combination to derive information on changes in soil redistribution rates through time, sediment source identification and on the efficiency of soil conservation measures. Examples of this combined use are provided below in section 3.

Additionally, Froehlich and Walling, Onda et al., Ritchie et al., Wilkinson et al. and Zhang et al. demonstrated the potential for using fallout radionuclides as tracers for discriminating and identifying the sources of suspended sediment. Coupled with an appropriate experimental design this approach can afford a powerful tool for assessing changes in sediment sources resulting from the introduction of soil conservation measures. In a study of the lake Burragorang catchment in Australia following a severe wildfire, Wilkinson et al. compared

the ^{137}Cs and $^{210}\text{Pb}_{\text{ex}}$ concentrations associated with eroded surface soil and river sediments and showed that a high proportion of the post-fire river sediment comprised soil surface material. Similarly, Ritchie et al. used ^{137}Cs measurements to establish which sub-areas within a semi-arid rangeland watershed in Arizona, USA, were contributing to the suspended sediment load in a stream. Based on these results it was suggested that management of these semi-arid rangelands must consider techniques that will protect grass dominated areas from shrub invasion. Froehlich and Walling also proved for the Polish Flysh Carpatians Mountains how changes in the $^{210}\text{Pb}_{\text{ex}}$, ^7Be and ^{137}Cs content of suspended sediment transported by a river during flood events reflected changes in the relative contribution of different sediment sources. Unpaved roads were identified as the main source of the suspended sediment load. Onda et al. could also identify the forest floor as the most important source of fluvial sediment in the studied mountainous forested catchments in southern Japan by comparing the radionuclide content of suspended sediment with that of potential source materials and suspended sediment.

Fallout radionuclides can also be used to provide an improved understanding of organic carbon losses from fields and watersheds. Li et al. and Mabit et al.) showed how estimates of soil redistribution rates, based on ^{137}Cs and $^{210}\text{Pb}_{\text{ex}}$ measurements, could be used to better understand how soil organic carbon content is influenced by soil erosion, and how the related soil health (Klik et al.) can be improved by specific soil conservation measures.

2. Establishment of standardized protocols for the combined application of the above techniques

Although basic procedures, in particular for ^{137}Cs based techniques, are now well established, the different case studies described in this publication identified a number of technical challenges in applying and developing the approaches outlined above. These challenges, which are described below, make clear that there is not a single method that can be used when applying fallout radionuclide based techniques in estimating soil redistribution or assessing the efficiency of soil conservation measures. Methods are specific to the fallout radionuclides being used, the research questions being asked, the environmental conditions under which the study is being carried out and the local land management conditions. However, the CRP teams addressed most of the main challenges involved in the use of fallout radionuclides to develop improved land use and management strategies for sustainable watershed management through effective soil erosion control practices.

a) Environmental conditions

The environmental conditions, under which fallout radionuclides have been applied in this CRP, vary considerably. One of the most impacting consequences was the wide range of inventory levels and associated fallout radionuclide deposition histories. In some circumstances low fallout radionuclide levels (e.g. ^{137}Cs inventories in the southern hemisphere, $^{210}\text{Pb}_{\text{ex}}$ in coastal zones with prevailing onshore winds or high levels of supported ^{210}Pb relative to excess ^{210}Pb) can be dealt with by counting samples for a longer duration (requiring more detectors, longer studies, or alternate sampling strategies – bulking) or by using more efficient detectors (requiring further capital investment). However, practical limits may exist.

The importance of using geostatistical tools in studies using fallout radionuclides (^{137}Cs , ^{210}Pb and ^7Be) to estimate soil redistribution rates and isotope and sediment budgets has been demonstrated by Mabit et al. The use of such spatial analysis techniques and tools helps

develop an understanding of the impact of land and water management practices on soil redistribution, so that the best and most-effective conservation practices can be identified to maximize the efficiency of soil and water conservation.

b) Reference sites

Reliable reference sites can be difficult to establish due to the high degree of variability in local precipitation (e.g. Golosov et al.) and the difficulty of identifying undisturbed stable sites (e.g. Hacıyakupoglu et al.). In particular finding suitable reference sites in mountainous regions and areas under intensive cultivation can be a challenge (e.g. Mabit et al.). In addition when the study areas are large, it is important to select several reference sites. In this respect, it is essential that care should be taken when establishing the reference inventory of fallout radionuclides in a study area. Mabit et al. described in detail how soil sampling was carried out on their reference site in Mistelbach, Austria.

c) Experimental design

Measurements themselves cannot provide the information or answers required. They must be used as a tool within an appropriate and sound experimental design. This CRP showed both through the approaches used as well as through different experimental designs how fallout radionuclides are a perfect tool to answer a manifold of questions related with the impact of land use practices in inducing or controlling soil erosion (Benmansour et al., Hacıyakupoglu et al., Onda et al., Ritchie et al.), land use change (Froehlich et al., Popa et al., Wilkinson et al.), and the effectiveness of soil conservation measures (Bacchi et al., Golosov et al., Li et al., Hai et al., Mabit et al., Popa et al., Rafiq et al., Schuller et al., Zhang et al.)

d) Quality assurance /quality control

The measurement of the radionuclides by HPGe gamma spectrometry forms an essential component of the application of fallout radionuclides techniques in soil erosion and sedimentation studies. From the performance evaluation of the proficiency test carried out during this CRP by Shakhashiro et al. it was found that 66% of the laboratories reported 'acceptable' results for the ^{137}Cs measurements, whereas only 31% of the participants were able to provide acceptable results for total $^{210}\text{Pb}_{\text{ex}}$ analyses. Difficulties were also apparent in the measurement of low activity levels of ^{137}Cs activity ($2.6 \pm 0.2 \text{ Bq kg}^{-1}$) with more than 40% of results scored as unacceptable. In general, the analytical uncertainties associated with the results were appropriate for the analytes and matrices considered in the current proficiency test. The results from the proficiency test underline the necessity for the IAEA to regularly organize intercomparison exercises of fallout radionuclide analyses for laboratories participating in Coordinated Research projects and Technical Cooperation (TC) projects and working in soil erosion/sedimentation studies.

e) Conversion models

In this CRP, a generally applicable set of conversion models was developed by researchers at the University of Exeter for use with ^{137}Cs , $^{210}\text{Pb}_{\text{ex}}$ and ^7Be measurements to estimate soil redistribution rates (Walling et al.). The models include six models for use with ^{137}Cs measurements, three models for use with $^{210}\text{Pb}_{\text{ex}}$ measurements and a single model for use with ^7Be measurements. The ^{137}Cs and $^{210}\text{Pb}_{\text{ex}}$ models include models applicable to either cultivated or uncultivated land. The model developed for ^7Be is applicable to both cultivated and uncultivated land. Furthermore, in order to facilitate the application of the models in a standardised manner, and to promote their use by the wider scientific community, a user-

friendly software package, based on an Excel Add-in has been produced and made available to interested persons. The model software also contains several routines for estimating key parameters. In addition a refined ^7Be conversion model which extended the timescale over which ^7Be measurements can be used from a few weeks to several months was also developed.

The models are available on the following website: <http://www-naweb.iaea.org/nafa/swmn/swmcn-databases.html>. It is hoped that the use of a standardised set of conversion models by researchers will facilitate exchange and comparison of results and that the wider testing of the conversion models will generate an improved understanding of their advantages and limitations and thus assist the further development and improvement of such models.

3. Use of fallout radionuclide techniques to assess the impact of short- and medium term changes in land use practices and the effectiveness of specific soil conservation measures

Fallout radionuclide techniques have been used to assess the impact of land use and agricultural management practices in inducing or controlling soil erosion. These studies have investigated the impacts of different land management practices (Benmansour et al., Hacıyakupoglu et al., Onda et al., Ritchie et al.), land use change (Froehlich et al., Popa et al., Wilkinson et al.), the effectiveness of soil conservation measures such as riparian strips, zero-tillage, conservation agriculture, grass barriers, contour cropping, and others (Bacchi et al., Golosov et al., Li et al., Hai et al., Mabit et al., Popa et al., Rafiq et al., Schuller et al., Zhang et al.). Some examples are provided below.

In Southern Chile Schuller et al. tested the effectiveness of conservation agriculture (with zero tillage and the retention of crop residues) in controlling soil erosion and reported that implementing conservation agriculture, about 16 years ago, reduced the mean annual net erosion rates in a cereal field, as documented using ^{137}Cs measurements, by about 87% (from $11 \text{ t ha}^{-1} \text{ year}^{-1}$ to $1.4 \text{ t ha}^{-1} \text{ year}^{-1}$) with the proportion of the study area subject to erosion reducing from 100% to 57%. However the beneficial effects of such management change can be readily lost if the mulch layer of old crop residues is removed by burning. The same research team used the short-lived radionuclide ^7Be to document the erosion resulting from a short period of intense rainfall occurring after the dramatic burning of the crop residues. The results provided evidence of substantial net erosion of 12 t ha^{-1} over this 27 day exceptionally wet period (400 mm rainfall). This represented a dramatic increase over the average annual soil loss under conservation agriculture from 1.4 t ha^{-1} on a year basis. Li et al. similarly used ^7Be measurements in their studies in NE China to show that zero-tillage in combination with the retention of crop residues could reduce soil erosion by 33% as compared with conventional tillage practices in NE China. Similar results were reported by Benmansour et al. from Morocco.

The importance of post-fire erosion was demonstrated in Australia (Wilkinson et al.), as significant amounts of sediment and attached nutrients were eroded from burnt hillslopes in the months following a fire event (Wilkinson et al.). Comparison of the concentrations of ^{137}Cs and $^{210}\text{Pb}_{\text{ex}}$ associated with eroded surface soil and river sediment showed that the latter was derived primarily from surface erosion of the hillslopes after the fire, in contrast to the pre-fire situation, where the sediment was dominated by sub-surface material mobilised from river channels and gullies.

Using the ^{137}Cs technique Bacchi et al. were able to show that the minimum established width of 30 m for riparian zones, prescribed by Brazilian Environmental Law, is not always enough

to ensure the sediment trapping function of the riparian vegetation. Bacchi et al. also used the ^{137}Cs measurements to calibrate the process based WEPP erosion model to better predict soil loss and sediment deposition in complex landscapes, such as riparian systems.

Zhang et al. showed, based on ^{137}Cs and $^{210}\text{Pb}_{\text{ex}}$ measurements on the sloping cultivated land in the Sichuan basin in China, that the traditional and centuries-old soil conservation measures can reduce soil losses by up to 35% compared to losses on steep arable land without conservation measures.

In Romania, the extent of the area under soil conservation practices has declined by more than 60% since 1991, as a result of a change in government policy. The related law stipulated that the land had to be reassigned to the original landowners resulting in the division of the agricultural land in long and narrow plots, which are often oriented downslope. The major impact of the law was the restoration of the old traditional agricultural system leading to increased soil erosion. Popa et al. showed that erosion on the long and narrow plots without conservation was three times higher than in locations where soil conservation measures still existed.

The CRP has created an effective network of research scientists and national research institutes involved in the use of fallout radionuclides to document soil redistribution rates and to assess the relative impacts of different soil conservation measures on soil erosion and land productivity. The success of the CRP has stimulated an interest in many Member States in the use of these methodologies to identify factors and practices that can enhance sustainable agriculture and minimize land degradation. At present there are 37 Member States where fallout radionuclides are being used to address issues relating to sustainable land management through Technical Co-operation (TC) projects at both national and regional levels. For example, a major regional project on ‘Sustainable Land Use and Management Strategies for Controlling Soil Erosion and Improving Soil and Water Quality’ (RCA Project RAS/5/043) has recently been concluded. This project involved participants from the following 14 Member States in the East Asia and Pacific region: Australia, Bangladesh, China, India, Indonesia, Republic of Korea, Malaysia, Mongolia, Myanmar, Pakistan, Philippines, Sri Lanka, Thailand and Vietnam. The fallout radionuclide methodology has been successfully used by the participating countries to assess soil erosion, to evaluate soil conservation measures (e.g. forestation, terracing, contour cropping, contour hedgerow systems), and to understand better the link between soil redistribution and soil quality (e.g. Soil Organic Matter) in the landscape.

The success outlined above has stimulated additional commitment from the Agency in responding to requests from Member States in Latin America. In 2009, a new regional Technical Co-operation project RLA5051 on ‘Using Environmental Radionuclides as Indicators of Land Degradation in Latin American, Caribbean and Antarctic Ecosystems’ was initiated. This has been approved to run for 5 years, from 2009 until 2013. The following 14 Member States are participating: Argentina, Bolivia, Brazil, Chile, Cuba, Dominican Republic, El Salvador, Jamaica, Haiti, Mexico, Nicaragua, Peru, Uruguay and Venezuela. The project aims to enhance soil conservation and environmental protection in Latin American, Caribbean and Antarctic environments in order to ensure sustainable agricultural production and reduce the on and off-site impacts of land degradation.

The CRP network also acknowledged the potential for further development of fallout radionuclide applications linked with fingerprinting technologies, in particular in the area-wide assessment of the impact of agricultural systems and land use practices on the extent of land degradation and the identification of hot-spots of critical land degradation. The network

recommended that the IAEA should support these investigations through the Co-ordinated Research Programme. In this context, action was taken by organizing a Consultants Meeting on Integrated approaches for the assessment of land use impacts on soil loss and related environmental problems in Vienna, from 5-7 November, 2007. A new CRP proposal (D1.20.11: 'Integrated Isotopic Approaches for an Area-wide Precision Conservation to Control the Impacts of Agricultural Practices on Land Degradation and Soil Erosion') emphasising the identification of critical areas of soil loss was formulated and approved and the project started in June 2009. This CRP focuses on the catchment scale integration of Compound Specific ^{13}C Isotope Analysis with the use of fallout radionuclides. Carbon (C) is an essential part of soil organic matter. Its isotopic signature (^{13}C) depends on the type of land use, e.g. arable land or dairy farming, and hence it can be used to distinguish the sources of eroded soils, and place soil conservation measures where most needed.

COUNTRY REPORTS

MODELS FOR DERIVING ESTIMATES OF EROSION AND DEPOSITION RATES FROM FALLOUT RADIONUCLIDE (CAESIUM-137, EXCESS LEAD-210, AND BERYLLIUM-7) MEASUREMENTS AND THE DEVELOPMENT OF USER-FRIENDLY SOFTWARE FOR MODEL IMPLEMENTATION

D.E.WALLING, Y. ZHANG, Q. HE
University of Exeter, School of Geography,
Exeter, Devon, United Kingdom

Abstract

Within the framework of an IAEA CRP, an attempt has been made to develop a generally applicable set of conversion models for use with ^{137}Cs , $^{210}\text{Pb}_{\text{ex}}$ and ^7Be measurements to estimate soil redistribution rates. The models include six models for use with ^{137}Cs measurements, three models for use with $^{210}\text{Pb}_{\text{ex}}$ measurements and a single model for use with ^7Be measurements. In the case of ^{137}Cs , four of the models are applicable to cultivated land, namely the proportional model, a simple mass balance model, a more comprehensive mass balance model and a mass balance model incorporating the effects of tillage. The other two ^{137}Cs models are applicable to uncultivated sites and include the profile distribution model and the diffusion and migration model. For $^{210}\text{Pb}_{\text{ex}}$, the models include two that are applicable to cultivated land, namely a comprehensive mass balance model and a mass balance model incorporating tillage, and a diffusion and migration model that is applicable to uncultivated land. The profile distribution model developed for ^7Be is applicable to both cultivated and uncultivated sites. In order to facilitate the use of the models, a user-friendly software package based on an Excel Add-in has been developed. Guidelines for model selection and for establishing parameter values are provided and the model software contains several routines for estimating key parameters.

1. INTRODUCTION

The fallout radionuclides caesium-137 (^{137}Cs), excess lead-210 ($^{210}\text{Pb}_{\text{ex}}$), and beryllium-7 (^7Be), are being increasingly used to estimate soil redistribution rates in soil erosion and sediment budget investigations [1–5]. Work undertaken in a wide range of environments in different areas of the world has demonstrated that their use, both independently or in combination, affords a valuable means of estimating rates of soil loss and sediment deposition, which possesses many advantages over conventional monitoring techniques [6]. These main advantages include the potential for deriving retrospective estimates of erosion and deposition rates based on a single site visit and for assembling distributed information for individual points in the landscape, which can be used to study spatial patterns of soil redistribution and to validate distributed soil erosion models [7].

Use of fallout radionuclide measurements to estimate rates of erosion and deposition is commonly founded on comparison of the inventories at individual sampling points with a reference inventory representing the local fallout input and thus the inventory to be expected at a site experiencing neither erosion nor deposition. A measured inventory for an individual sampling point, which is less than the reference value is indicative of erosion, whereas an inventory greater than the reference value is indicative of deposition. Although such comparisons of measured inventories with the local reference value provide useful *qualitative* information on the spatial distribution of erosion and deposition in the landscape on the relative magnitude of the values involved, in most instances *quantitative* estimates of erosion and deposition rates are required. The derivation of *quantitative* estimates is much dependent upon the existence of a reliable means of converting the relationship between the measured inventory at a specific sampling point and the local reference inventory to an estimate of the rate of erosion or deposition at that point.

To date, most work aimed at developing procedures, or so-called conversion models, for deriving estimates of erosion and deposition rates from a comparison of measured fallout radionuclide inventories within a study site with the local reference inventory has focussed on ^{137}Cs . Many different approaches have been used to convert ^{137}Cs measurements to quantitative estimates of erosion and deposition rates [8,9,10]. These methods include both empirical relationships, and theoretical models and accounting procedures. In an effort to standardise the methods and procedures employed within a past IAEA CRP that investigated the use of fallout radionuclides in erosion and sedimentation investigations, Walling and He, in 2001, developed PC-compatible software that implemented a number of models (procedures), which appeared to provide meaningful results. The models varied in complexity from the simple proportional model to more complex mass balance models and models which attempt to describe the key processes controlling the distribution of ^{137}Cs in the soil profile. Models applicable to both cultivated and uncultivated (e.g. rangeland and permanent pasture) soils were included. This readily available standardised software has played an important role in promoting the use of ^{137}Cs in soil erosion and sedimentation-related studies across the world. However, a number of deficiencies in the software, which potentially limit its application, have become apparent. These deficiencies range from the difficulties in specifying several of the model parameters, through rigid requirements for data structures within a file, to lack of error trapping and handling capacities.

Since the release of the software, further progress has also been made in the application of other fallout radionuclides, in addition to ^{137}Cs , in soil erosion investigations, and more particularly excess ^{210}Pb ($^{210}\text{Pb}_{\text{ex}}$) and ^7Be [e.g.11-13]. The use of these other radionuclides involves most of the basic assumptions associated with the ^{137}Cs technique, e.g.

- (1) Wet deposition from rainfall is the dominant source.
- (2) Strong affinity of the radionuclide with soil and sediment particles, particularly the finer particles.
- (3) Exponential decrease of mass concentration and inventory with depth within an undisturbed soil profile and a homogenised distribution within the plough layer at cultivated sites.
- (4) Near-uniform spatial distribution of fallout inventories across a study site.
- (5) Post-fallout redistribution of the radionuclide occurs in association with soil and sediment redistribution.

It has therefore proved possible to adapt some of the conversion models formerly applied to ^{137}Cs measurements for use with $^{210}\text{Pb}_{\text{ex}}$ and ^7Be , providing the key contrasts with ^{137}Cs are taken into account. Together these three radionuclides are able to provide information on soil redistribution over temporal scales ranging from a few days, through decades to around 100 years. Furthermore, use of the individual radionuclides in combination offers potential to identify temporal trends in soil erosion and sedimentation rates.

Against this background, the original PC based software has been updated to overcome the known problems, to incorporate new procedures or conversion models for fallout radionuclides other than ^{137}Cs , and to provide an integrated computational framework that can convert radionuclide inventories on a platform accessible to most researchers. This paper provides an overview of the conversion models for use with ^{137}Cs , $^{210}\text{Pb}_{\text{ex}}$ and ^7Be and the development of user-friendly software for model implementation.

2. DESCRIPTION OF THE CONVERSION MODELS

This section presents a brief description of the theoretical basis of the models incorporated into the software and provides some guidelines regarding the advantages and limitations of the individual models. Since the conversion models developed for $^{210}\text{Pb}_{\text{ex}}$ and ^7Be were adapted from those used for ^{137}Cs , emphasis will be placed on the latter. The discussion of the models provided for $^{210}\text{Pb}_{\text{ex}}$ and ^7Be will focus on their differences from the conversion models employed for ^{137}Cs .

2.1. Models for use with caesium-137 measurements

The first four models described below are for application to cultivated soils and the last two for use with uncultivated soils (rangelands or permanent pasture).

2.1.1. The proportional model

The proportional model is probably the simplest of the conversion models used for ^{137}Cs measurements. It is based on the premise that ^{137}Cs fallout inputs are completely mixed within the plough or cultivation layer and the simple assumption that the depth of soil removed by erosion is directly proportional to the fraction of the original ^{137}Cs inventory removed from the soil profile by erosion since the beginning of ^{137}Cs fallout or the onset of cultivation, whichever is later. Thus, if half of the ^{137}Cs input has been removed, the total soil loss over the period is assumed to be 50% of the plough depth. Division of this depth by the number of years elapsed since the beginning of significant ^{137}Cs fallout provides an estimate of the annual rate of surface lowering. Inclusion of a value for the bulk density of the soil makes it possible to calculate an erosion rate in units of mass per unit time (i.e. $\text{t ha}^{-1} \text{ year}^{-1}$). A particle size correction factor is often incorporated into the model to make allowance for the size selectivity of sediment mobilisation and the preferential association of ^{137}Cs with the finer fractions of the soil. The model can be represented as follows:

$$Y = 10 \frac{B d X}{100 T P} \quad (1)$$

where:

Y is the mean annual soil loss ($\text{t ha}^{-1} \text{ a}^{-1}$);

d is the depth of plough or cultivation layer (m);

B is the bulk density of soil (kg m^{-3});

X is the percentage reduction in total ^{137}Cs inventory (defined as $(A_{\text{ref}} - A)/A_{\text{ref}} \times 100$);

A_{ref} is the local ^{137}Cs reference inventory (Bq m^{-2});

A is the measured total ^{137}Cs inventory at the sampling point (Bq m^{-2});

T is the time elapsed since the initiation of ^{137}Cs accumulation or the commencement of cultivation whichever is later (a);

P is the particle size correction factor for erosion.

An inference from the assumptions of the proportional model is that the ^{137}Cs concentration of the eroded sediment remains constant through time. The ^{137}Cs concentration of deposited sediment at a depositional point may therefore be assumed to be constant. In cases where the ^{137}Cs inventory A for a sampling point is greater than the local reference inventory A_{ref} , deposition of sediment may be assumed and the annual deposition rate Y' ($\text{t ha}^{-1} \text{ a}^{-1}$) may be estimated using the following equation:

$$Y' = 10 \frac{B d X'}{100 T P'} \quad (2)$$

where:

X' is the percentage increase in total ^{137}Cs inventory (defined as $(A - A_{ref})/A_{ref} \times 100$);
 P' is the particle size correction factor for deposition.

Advantages and limitations: The proportional model requires very little information to provide an estimate of the erosion or deposition rate at the sampling point. In addition to the values of ^{137}Cs inventory for the sampling points and the local reference inventory, only an estimate of the plough depth and a value for the bulk density of the soil are required. It is therefore easy to apply. However, the assumptions of this model are a considerable oversimplification of reality in terms of the accumulation of ^{137}Cs in the soil. The accumulation of ^{137}Cs takes place over several years and some of the fallout input will remain at the soil surface prior to incorporation into the soil profile by cultivation. If some of the ^{137}Cs accumulated on the surface is removed by erosion prior to incorporation into the profile the estimates of soil loss provided by the model will overestimate actual rates of soil loss. Perhaps more importantly, however, this model does not take into account the fact that the depth of the plough layer is maintained by incorporating soil from below the original plough depth as the surface is lowered by erosion, this in turn causes a progressive dilution of ^{137}Cs concentrations in the soil within the plough layer. As a result, the model is likely to underestimate the actual rates of soil loss. Similarly, if the model is used to estimate deposition rates, the values obtained will underestimate the actual deposition rates, since no account is taken of the progressive reduction in the ^{137}Cs content of the deposited soil as erosion proceeds upslope. In view of these important limitations, use of the proportional model is not generally recommended.

2.1.2. Simplified mass balance model (mass balance model 1)

Mass balance models attempt to overcome some of the limitations of the simple proportional model by taking account of both inputs and losses of ^{137}Cs from the profile over the period since the onset of ^{137}Cs fallout and the progressive lowering of the base of the plough layer in response to removal of soil from the soil surface by erosion. Zhang *et al.* [14] proposed a simplified mass balance model, which assumes that the total ^{137}Cs fallout occurred in 1963, instead of over the longer period extending from the mid 1950s to the mid 1970s. In its original form this simplified mass balance model did not take account of particle size effects but a correction factor P has been included in the model incorporated into the software.

For an eroding site ($A(t) < A_{ref}$), assuming a constant rate of surface lowering R (m a^{-1}), the total ^{137}Cs inventory (A , Bq m^{-2}) at year t (a) can be expressed as:

$$A(t) = A_{ref} \left(1 - P \frac{R}{d}\right)^{t-1963} \quad (3)$$

By re-arranging the above equation, the erosion rate Y ($\text{t ha}^{-1} \text{a}^{-1}$) can be calculated as:

$$Y = \frac{10 d B}{P} \left[1 - \left(1 - \frac{X}{100}\right)^{1/(t-1963)} \right] \quad (4)$$

where:

A_{ref} is the local reference inventory (Bq m^{-2});
 Y is the mean annual erosion rate ($\text{t ha}^{-1} \text{a}^{-1}$);

d is the depth of plough or cultivation layer (m);
 B is the bulk density of soil (kg m^{-3});
 X is the percentage reduction in total ^{137}Cs inventory (defined as $(A_{ref}-A)/A_{ref}\times 100$);
 P is the particle size correction factor.

For a depositional site ($A(t) > A_{ref}$), assuming a constant deposition rate R' ($\text{kg m}^{-2} \text{a}^{-1}$) at the site, the sediment deposition rate can be estimated from the ^{137}Cs concentration of the deposited sediment $C_d(t')$ (Bq kg^{-1}) according to:

$$R' = \frac{A_{ex}(t)}{\int_{1963}^t C_d(t') e^{-\lambda(t-t')} dt'} = \frac{A(t) - A_{ref}}{\int_{1963}^t C_d(t') e^{-\lambda(t-t')} dt'} \quad (5)$$

where:

$A_{ex}(t)$ is the excess ^{137}Cs inventory of the sampling point over the reference inventory at year t (defined as the measured inventory less the local reference inventory) (Bq m^{-2});
 $C_d(t')$ is the ^{137}Cs concentration of deposited sediment at year t' (Bq kg^{-1});
 λ is the decay constant for ^{137}Cs (a^{-1});
 P' is the particle size correction factor.

Generally, the ^{137}Cs concentration $C_d(t')$ of deposited sediment can be assumed to be represented by the weighted mean of the ^{137}Cs concentration of sediment mobilised from the upslope contributing area. $C_d(t')$ and can therefore be calculated as:

$$C_d(t') = \frac{1}{\int_S R dS} \int_S P' C_e(t') R dS \quad (6)$$

where: S (m^2) is the upslope contributing area and $C_e(t')$ (Bq kg^{-1}) is the ^{137}Cs concentration of sediment mobilised from an eroding point, which can be calculated from Equation 3 according to:

$$C_e(t') = P \frac{A(t')}{d} = \frac{P}{d} A_{ref}(t') \left(1 - P \frac{R}{d}\right)^{t'-1963} = \frac{P}{d} A_{ref}(t) e^{\lambda(t-t')} \left(1 - P \frac{R}{d}\right)^{t'-1963} \quad (7)$$

where: $A_{ref}(t)$ is A_{ref} .

Advantages and limitations: The simplified mass balance model takes into account the progressive reduction in the ^{137}Cs concentration of the soil within the plough layer due to the incorporation of soil containing negligible ^{137}Cs from below the original plough depth and thus represents an improvement over the proportional model. This model is also easy to use and requires only information on plough depth. However, this model does not take into account the possible removal of freshly deposited ^{137}Cs fallout before its incorporation into the plough layer by cultivation, which may occur during rainfall events which produce surface runoff and therefore erosion. The assumption that the total ^{137}Cs fallout input occurs in 1963 is also an oversimplification.

2.1.3. Mass balance model 2

A more comprehensive mass balance model requires consideration of the time-variant fallout ^{137}Cs input and the fate of the freshly deposited fallout before its incorporation into the plough layer by cultivation.

For an eroding point ($A(t) < A_{ref}$), the change in the total ^{137}Cs inventory $A(t)$ with time can be represented as:

$$\frac{dA(t)}{dt} = (1 - \Gamma) I(t) - \left(\lambda + P \frac{R}{d}\right) A(t) \quad (8)$$

where:

$A(t)$ is the cumulative ^{137}Cs activity per unit area (Bq m^{-2});

R is the erosion rate ($\text{kg m}^{-2} \text{a}^{-1}$);

d is the cumulative mass depth representing the average plough depth (kg m^{-2});

λ is the decay constant for ^{137}Cs (a^{-1});

$I(t)$ is the annual ^{137}Cs deposition flux ($\text{Bq m}^{-2} \text{a}^{-1}$);

Γ is the proportion of the freshly deposited ^{137}Cs fallout removed by erosion before being mixed into the plough layer;

P is the particle size correction factor.

If an exponential distribution for the initial distribution of ^{137}Cs fallout at the surface of the soil profile can be assumed, following He and Walling [15], Γ can be expressed as:

$$\Gamma = P \gamma (1 - e^{-R/H}) \quad (9)$$

where:

γ is the proportion of the annual ^{137}Cs input susceptible to removal by erosion;

H is the relaxation mass depth of the initial distribution of fallout ^{137}Cs in the soil profile (kg m^{-2}).

If t_0 (a) represents the year when cultivation started, from Equations 8 and 9, the total ^{137}Cs inventory $A(t)$ at year t can be expressed as:

$$A(t) = A(t_0) e^{-(PR/d+\lambda)(t-t_0)} + \int_{t_0}^t (1 - P \gamma (1 - e^{-R/H})) I(t') e^{-(PR/d+\lambda)(t-t')} dt' \quad (10)$$

where: $A(t_0)$ (Bq m^{-2}) is the ^{137}Cs inventory at t_0 (a):

$$A(t_0) = \int_{1954}^{t_0} I(t') e^{-\lambda(t'-t_0)} dt' \quad (11)$$

The erosion rate R can be estimated by solving Equation 10 numerically, when the ^{137}Cs deposition flux and values of the relevant parameters are known. The ^{137}Cs concentration of mobilised sediment $C_e(t')$ can be expressed as:

$$C_e(t') = \frac{I(t')}{R} P \gamma (1 - e^{-R/H}) + P \frac{A(t')}{d} \quad (12)$$

For a depositional point ($A(t) > A_{ref}$), assuming that the excess ^{137}Cs inventory A_{ex} (Bq m^{-2}) (defined as the measured total inventory $A(t)$ less the local direct fallout input A_{ref}) at an aggrading point is due to the accumulation of ^{137}Cs associated with deposited sediment, the excess ^{137}Cs inventory can be expressed as:

$$A_{ex} = \int_{t_0}^t R' C_d(t') e^{-\lambda(t-t')} dt' \quad (13)$$

where: R' ($\text{kg m}^{-2} \text{a}^{-1}$) is the deposition rate and $C_d(t')$ (Bq kg^{-1}) is the ^{137}Cs concentration of deposited sediment. $C_d(t')$ will reflect the mixing of sediment and its associated ^{137}Cs concentration mobilised from all the eroding points that converge on the aggrading point. $C_d(t')$ essentially comprises two components, the first of which is associated with the removal of the freshly deposited ^{137}Cs , and the second is associated with erosion of the accumulated ^{137}Cs stored in the soil. Again, $C_d(t')$ can be estimated from the ^{137}Cs concentrations of the mobilised sediment from the upslope eroding area S :

$$C_d(t') = \frac{1}{\int_S R dS} \int_S P' C_e(t') R dS \quad (14)$$

From Equations 13 and 14, the mean soil deposition rate R' can be calculated from the following equation:

$$R' = \frac{A_{ex}}{\int_{t_0}^t C_d(t') e^{-\lambda(t-t')} dt'} \quad (15)$$

Advantages and limitations: The mass balance model described here takes account of both the temporal variation of the ^{137}Cs fallout input and its initial distribution in the surface soil, prior to incorporation into the plough layer by tillage. Results obtained using this model are likely to be more realistic than those provided by the simplified mass balance model 1 presented in the previous section. However, in order to use this model, information on the plough depth h , relaxation mass depth H and the parameter γ is required. Although the first is relatively easy to estimate from the ^{137}Cs depth distribution at a non-eroding point, the latter two are more difficult to specify. The relaxation mass depth H is best estimated experimentally for the local soil type and the parameter γ can be estimated from available long term rainfall records and information on the timing of tillage operations at the study site. Since the model requires information on the ^{137}Cs concentration of soil eroded from upslope, the sampling points used with the model must be arranged along a downslope transect. Normally, a uniform spacing of sampling points is assumed.

2.1.4. A mass balance model incorporating soil movement by tillage (Mass balance model 3)

The mass balance models described previously do not take account of soil redistribution caused by tillage operations. As tillage results in the redistribution of soil in a field, the ^{137}Cs contained in the soil will also be redistributed, and such redistribution needs to be taken into account when using the ^{137}Cs measurements to derive estimates of rates of soil erosion by water. If the effects of tillage redistribution on ^{137}Cs inventories can be quantified and taken into account, the remaining component of redistribution will reflect the impact of water erosion.

The effect of tillage in redistributing soil can be represented by a downslope sediment flux. Following Govers et al. [16], the downslope sediment flux F_Q ($\text{kg m}^{-1} \text{a}^{-1}$) from a unit contour length may be expressed as:

$$F_Q = \phi \sin \beta \quad (16)$$

where: β ($^\circ$) is the slope angle and ϕ ($\text{kg m}^{-1} \text{a}^{-1}$) is a site-specific constant.

If a flow line down a slope is divided into several sections and each section can be approximated as a straight line, then for the i^{th} section (from the hilltop), the net soil redistribution induced by tillage R_t ($\text{kg m}^{-2} \text{a}^{-1}$) can be expressed as:

$$R_t = (F_{Q,out} - F_{Q,in}) / L_i = \phi (\sin \beta_i - \sin \beta_{i-1}) / L_i = R_{t,out} - R_{t,in} \quad (17)$$

where: L_i (m) is the slope length of the i^{th} segment, and $R_{t,out}$ ($\text{kg m}^{-2} \text{a}^{-1}$) and $R_{t,in}$ ($\text{kg m}^{-2} \text{a}^{-1}$) are defined as:

$$\begin{aligned} R_{t,out} &= \phi \sin \beta_i / L_i \\ R_{t,in} &= \phi \sin \beta_{i-1} / L_i \end{aligned} \quad (18)$$

For a point experiencing water erosion (rate R_w ($\text{kg m}^{-2} \text{a}^{-1}$)), variation of the total ^{137}Cs inventory $A(t)$ (Bq m^{-2}) with time t can be expressed as:

$$\frac{dA(t)}{dt} = (1 - \Gamma) I(t) + R_{t,in} C_{t,in}(t) - R_{t,out} C_{t,out}(t) - R_w C_{w,out}(t) - \lambda A(t) \quad (19)$$

where: $C_{t,in}$, $C_{t,out}$ and $C_{w,out}$ (Bq kg^{-1}) are the ^{137}Cs concentrations of the sediment associated with tillage input, tillage output and water output respectively. The net erosion rate R ($\text{kg m}^{-2} \text{a}^{-1}$) is:

$$R = R_{t,out} - R_{t,in} + R_w \quad (20)$$

For a point experiencing water-induced deposition (rate R'_w , ($\text{kg m}^{-2} \text{a}^{-1}$)), variation of the total ^{137}Cs inventory with time can be expressed as:

$$\frac{dA(t)}{dt} = I(t) + R_{t,in} C_{t,in}(t) - R_{t,out} C_{t,out}(t) + R'_w C_{w,in}(t) - \lambda A(t) \quad (21)$$

where: $C_{w,in}$ (Bq kg^{-1}) is the ^{137}Cs concentration of the sediment input from water-induced deposition.

The net erosion rate R is:

$$R = R_{t,out} - R_{t,in} - R'_w \quad (22)$$

The ^{137}Cs concentration of the soil within the plough layer $C_s(t')$ (Bq kg^{-1}) can be expressed as:

$$\begin{aligned} C_s(t') &= \frac{A(t')}{d} \quad \text{for a net erosion site} \\ C_s(t') &= \frac{1}{d} \left[A(t') - \frac{|R|}{d} \int_{t_0}^{t-1} A(t'') e^{-\lambda t''} dt'' \right] \quad \text{for a net deposition site} \end{aligned} \quad (23)$$

where: $|R|$ ($R < 0$) is the net deposition rate. The relationships between C_s and $C_{t,in}$ and $C_{t,out}$ are as follows:

$$\begin{aligned} C_{t,in}(t') &= C_{t,out}(t') = C_s(t') \\ C_{w,out}(t') &= P C_s(t') + \frac{I(t')}{R_w} P \gamma (1 - e^{-R_w/H}) \end{aligned} \quad (24)$$

while the ^{137}Cs concentration of water-derived deposited sediment $C_{w,in}(t')$ (Bq kg^{-1}) can be expressed as:

$$C_{w,in}(t') = \frac{1}{\int_s R dS} \int_s P' C_{w,out}(t') R dS \quad (25)$$

For a given point, the tillage-derived erosion or deposition rate ($R_{t,out}-R_{t,in}$) can be calculated from Equations 17 and the net soil erosion rate ($R>0$) or deposition rate ($R<0$) can be estimated by solving Equations 19, 20, 24 and 25 numerically.

Advantages and limitations: The mass balance model described here represents an important improvement over the two mass balance models presented previously in that it takes into account the effects of tillage-induced soil movement. The estimates of soil redistribution rates associated with water erosion provided by this model are likely to be closer to reality for cultivated soils than those provided by the other two mass balance models. However, this model requires more information than the previous two mass balance models. Furthermore, in its current form, the model can only be used for individual slope transects.

2.1.5. The profile distribution model (for uncultivated soils)

For uncultivated soils, the depth distribution of ^{137}Cs in the soil profile will be significantly different from that in cultivated soils where the ^{137}Cs is mixed within the plough or cultivation layer. In most situations, the depth distribution of ^{137}Cs in an undisturbed stable soil will exhibit a well-defined exponential decline with depth that may be described by the following function [see 14,8]:

$$A'(x) = A_{ref} (1 - e^{-x/h_0}) \quad (26)$$

where:

- $A'(x)$ is the amount of ^{137}Cs above the depth x (Bq m^{-2});
- A_{ref} is the ^{137}Cs reference inventory (Bq m^{-2});
- x is the depth from soil surface (kg m^{-2});
- h_0 is the coefficient describing profile shape (kg m^{-2})

If it is assumed that the total ^{137}Cs fallout occurred in 1963 and that the depth distribution of the ^{137}Cs in the soil profile is independent of time, the *erosion rate* Y for an eroding point (with total ^{137}Cs inventory A_u (Bq m^{-2}) less than the local reference inventory A_{ref} (Bq m^{-2})) can be estimated as:

$$Y = \frac{10}{(t-1963) P} \ln\left(1 - \frac{X}{100}\right) h_0 \quad (27)$$

where:

- Y is the annual soil loss ($\text{t ha}^{-1} \text{ a}^{-1}$);
- t is the year of sample collection (a);
- X is the percentage ^{137}Cs loss in total inventory in respect to the local ^{137}Cs reference value (defined as $(A_{ref}-A_u)/A_{ref} \times 100$);
- A_u is the measured total ^{137}Cs inventory at the sampling point (Bq m^{-2});
- P is the particle size correction factor.

For a depositional location, a tentative estimate of the deposition rate R' can be estimated from the excess ^{137}Cs inventory $A_{ex}(t)$ (Bq m^{-2}) (defined as $A_u - A_{ref}$) and the ^{137}Cs concentration of deposited sediment C_d :

$$R' = \frac{A_{ex}}{\int_{t_0}^t C_d(t') e^{-\lambda(t-t')} dt'} = \frac{A_u - A_{ref}}{\int_S \frac{P'}{R} dS \int_S A_{ref} (1 - e^{-R/h_0}) dS} \quad (28)$$

C_d can be calculated using the same approach as used in Equations 6 and 14.

Advantages and limitations: The profile shape model is simple and easy to use. However, this model involves a number of simplifying assumptions. Most importantly, it does not take account of the time-dependent behaviour of the ^{137}Cs fallout input and the progressive development (downward movement) of the depth distribution of the ^{137}Cs within the soil profile after deposition from the atmosphere. As such, it is likely to overestimate rates of soil loss, since the amount of ^{137}Cs removed with a given depth of soil is likely to be greater than suggested by the present day depth distribution of ^{137}Cs in the soil.

2.1.6. The diffusion and migration model (for uncultivated soils)

Although the depth distribution model described above can be used to obtain estimates of soil erosion or deposition rates for uncultivated soils, a more realistic approach needs to consider the time-dependent behaviour of the ^{137}Cs depth distribution, which reflects both the timing of the ^{137}Cs fallout input and the progressive redistribution and downward movement of ^{137}Cs in the soil profile after deposition from the atmosphere [e.g.17, 18, 15]. Under certain circumstances, the redistribution of ^{137}Cs in uncultivated soils can be represented using a one-dimensional diffusion and migration model characterised by an effective diffusion coefficient and migration rate (see 17, 19, 15]. For example, in some situations, the ^{137}Cs depth profile in uncultivated soils exhibits a broad concentration peak with the maximum concentration located below the soil surface. In this situation variation of the ^{137}Cs concentration $C_u(t)$ (Bq kg^{-1}) in surface soil with time t (a) may be approximated as:

$$C_u(t) \approx \frac{I(t)}{H} + \int_0^{t-1} \frac{I(t') e^{-R/H}}{\sqrt{D \pi (t-t')}} e^{-V^2 (t-t')/(4D) - \lambda(t-t')} dt' \quad (29)$$

where:

D is the diffusion coefficient ($\text{kg}^2 \text{m}^{-4} \text{a}^{-1}$);

V is the downward migration rate of ^{137}Cs in the soil profile ($\text{kg m}^{-2} \text{a}^{-1}$).

For an eroding point, if sheet erosion is assumed, then the erosion rate R may be estimated from the reduction in the ^{137}Cs inventory $A_{ls}(t)$ (Bq m^{-2}) (defined as the ^{137}Cs reference inventory A_{ref} less the measured total ^{137}Cs inventory A_u (Bq m^{-2})) and the ^{137}Cs concentration in the surface soil $C_u(t')$ given by Equation 29 according to:

$$\int_0^t P R C_u(t') e^{-\lambda(t-t')} dt' = A_{ls}(t) \quad (30)$$

For a depositional location, the deposition rate R' can be estimated from the ^{137}Cs concentration of deposited sediment $C_d(t')$ and the excess ^{137}Cs inventory $A_{ex}(t)$ (defined as the total measured ^{137}Cs inventory A_u less the local reference inventory A_{ref}) using the following relationship:

$$R' = \frac{A_{ex}}{\int_{t_0}^t C_d(t') e^{-\lambda(t-t')} dt'} = \frac{A_u - A_{ref}}{\int_{t_0}^t C_d(t') e^{-\lambda(t-t')} dt'} \quad (31)$$

where: $C_d(t')$ can be calculated from:

$$C_d(t') = \frac{1}{\int_s R dS} \int_s P' P C_u(t') R dS \quad (32)$$

Advantages and limitations: Since the diffusion and migration model described here takes into account the time-dependent behaviour of both the ^{137}Cs fallout input and its subsequent redistribution or downward movement in the soil profile, it therefore represents an improvement over the profile shape model presented in the previous section. However, to use this model, more information on the behaviour of ^{137}Cs in undisturbed soils is needed. More particularly, estimates of the diffusion coefficient D and the migration rate V are required. These can be derived from detailed measurements of the ^{137}Cs depth distribution.

2.2. Conversion models for use with excess lead-210 and beryllium-7 measurements

Excess ^{210}Pb has long been employed to determine sedimentation rates in depositional environments, such as reservoirs, lakes, floodplains, etc. [e.g. 20, 21]. The presence of ^7Be has also been used to assess the degree of short term surface mixing in a estuarine and coastal sediments [22]. The use of $^{210}\text{Pb}_{ex}$ and ^7Be measurements for estimating soil redistribution rates is, however, is still in its infancy and not as well established as that of ^{137}Cs . The physico-chemical behaviour of these two radionuclides in different soils worldwide still requires further investigation, before their full potential can be exploited with confidence. The development of the conversion models for $^{210}\text{Pb}_{ex}$ and ^7Be presented here should therefore be seen as an attempt to encourage the use of these two radionuclides in different environments and, in turn, to identify the shortcomings of the new models and to improve them accordingly. The similarities between the three fallout radionuclides have already been emphasized in the introduction section. They provide the theoretical basis for extending the ^{137}Cs technique, in terms of site selection, sampling procedures, sample treatment, etc., to the other two radionuclides. As background for a discussion of the adaptation of the ^{137}Cs conversion models to $^{210}\text{Pb}_{ex}$ and ^7Be , Table 1 provides a summary of the key characteristics of the three radionuclides. Several of the conversion models used for ^{137}Cs have been modified to accommodate these differences.

2.2.1. A conversion model for beryllium-7 measurements

As indicated in Table 1, ^7Be has a much shorter half-life than ^{137}Cs and, therefore, provides a valuable tracer for investigating short term soil redistribution processes. Because its short half-life limits its residence time in the soil, the opportunity for downward diffusion and migration are greatly reduced and its penetration depth is commonly limited to less than 2 cm. Tillage operations between the ^7Be deposition and the time of sampling will restrict its use, as the mixing effects of tillage operations will reduce the ^7Be concentration in the tillage layer to below the detection level. The depth distributions of ^7Be documented on cultivated land are very similar to those found in uncultivated soils, since, as indicated above, the action of mixing by tillage reduces the concentrations below the level of detection. Although the exponential form of the depth distribution has some similarities to that found for ^{137}Cs on

uncultivated soils, the depth of penetration is much smaller and the profile shape factor (see Equation 26) is much lower, reflecting the restricted penetration depth.

To use measurements of ^7Be inventories collected along a downslope transect to estimate erosion and deposition rates, the profile distribution model used for ^{137}Cs and described above has been modified as follows:

- (1) The modelling period is reduced from decades to a single event or a short period encompassing several events.
- (2) Annual natural decay is no longer important;
- (3) The value for the profile shape factor is much lower (e.g. $<20 \text{ kg m}^{-2}$)

In all other respects, the application of the profile distribution model is essentially the same as its use for ^{137}Cs . A detailed discussion of the conversion model and its application can be found in papers by Blake et al. and Walling et al. [11,13].

TABLE 1. A COMPARISON OF THE KEY CHARACTERISTICS OF THE FALLOUT RADIONUCLIDES CAESIUM-137, EXCESS LEAD-210, AND BERYLLIUM-7

Radionuclide	^{137}Cs	Excess ^{210}Pb	^7Be
Origin	Artificial, weapons-testing	Natural geogenic	Natural cosmogenic
Half-life	30.2 years	22.3 years	53.3 days
Time period of application	Since 1954	ca. 100 years	Days-months
Temporal pattern of fallout input	Main global input commenced in 1954 peaked in 1963 and ceased in 1980s ^a	Continuous input with limited inter-annual variation	Short term (e.g. daily) inputs must be considered
Global pattern of fallout input and reference inventories	High in northern hemisphere, low in southern hemisphere	Unknown	Unknown
Depth distribution at eroding sites under cultivation (a) and pasture (b)	(a) uniform distribution, (b)exponential decrease,	(a) uniform distribution, (b) exponential decrease	(a) & (b) exponential decrease
Tillage influence	Possible	Possible	Not applicable
Time basis of estimated rates	Annual average	Annual average	Event(s) based

^a An exception is the Chernobyl accident which caused ^{137}Cs deposition in adjacent regions in 1986. Significant Chernobyl fallout is primarily restricted to Europe.

2.2.2. Conversion models for use with excess lead-210 measurements

$^{210}\text{Pb}_{\text{ex}}$ has a comparable half-life (22.3 years) to ^{137}Cs . However, its natural origin and its essential continuous input provide potential for deriving estimates of soil distribution rates averaged over longer periods (e.g. 100 years). Two mass balance models (one with a tillage

component included and the other without) have been developed for use with the $^{210}\text{Pb}_{\text{ex}}$ inventories for samples collected from cultivated sites. They represent adaptations of mass balance model 2 and mass balance model 3, respectively. The migration and diffusion model for ^{137}Cs has also been modified for use with $^{210}\text{Pb}_{\text{ex}}$ measurements obtained for samples collected from uncultivated fields. The key modifications made to the ^{137}Cs conversion models are as follows:

- (1) The modelling period has been set to extend back 100 years from the sampling date. It is assumed that any $^{210}\text{Pb}_{\text{ex}}$ deposition prior to this point in time will have become essentially insignificant due to decay. In theory, only around 4% of the original deposition will remain after 100 years. The time of sampling is not used in the calculation. It is only relevant for interpreting the results obtained from the model.
- (2) It is assumed that the annual $^{210}\text{Pb}_{\text{ex}}$ fallout remains effectively constant through time and that because the reference inventory will represent a steady state balance between input and decay, the reference inventory will remain the same through time. The deposition flux ($I_{(t)}$) can be determined from the local reference inventory (A_{ref}) as:

$$I_{(t)} = A_{\text{ref}} \ln(2) / 22.3 \quad (32)$$

- (3) Due to its shorter half-life, the decay constant for $^{210}\text{Pb}_{\text{ex}}$ differs from that for ^{137}Cs .

Most of the parameters used in the conversion models for $^{210}\text{Pb}_{\text{ex}}$ inventories are very similar to those used for the ^{137}Cs models. However, a degree of caution is needed in their specification, since the behaviour of $^{210}\text{Pb}_{\text{ex}}$ in soils could be different from that of ^{137}Cs . Further information related to the application of $^{210}\text{Pb}_{\text{ex}}$ in soil erosion studies on cultivated land can be found in papers by Walling and He [12] and Walling et al. [23].

3. SELECTING A MODEL FOR USE WITH CAESIUM-137 AND EXCESS LEAD-210 MEASUREMENTS

A single model is provided for use with ^7Be measurements, but for ^{137}Cs and $^{210}\text{Pb}_{\text{ex}}$, there is a choice of several conversion models. The discussion of the advantages and limitations of these different models provided in the previous sections will provide some help to users in making an appropriate choice. Factors that should be considered include:

- (1) The intended use of the resulting estimated erosion and deposition rates,
- (2) The land use history of the study sites,
- (3) The availability of the relevant parameters and other data and the feasibility of obtaining these if they are not available.

While it is impossible to generalise as to which model is likely to be most appropriate for any specific project, some general guidelines are provided by the flow charts presented in Fig. 1. In addition to data availability, an understanding of site-specific radionuclide redistribution processes is an important prerequisite, when selecting a model. Collection of sectioned cores from some critical points /sites will not only help to refine the sampling strategy, but also yield valuable information about the ongoing redistribution processes in the soil profile. For example, the depth of the maximum concentration down the profile for a reference site provides an indication of the migration rate for ^{137}Cs . The magnitude of the reduction in the inventory at the very top of a slope can provide an indication of the intensity of tillage translocation.

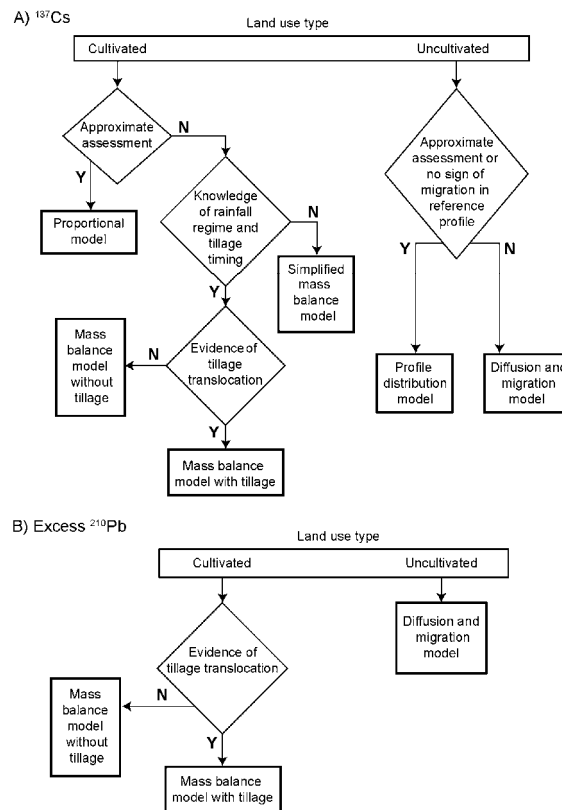


FIG. 1. General guidelines for choosing a conversion model for ^{137}Cs (A) and $^{210}\text{Pb}_{\text{ex}}$ (B).

4. DEVELOPMENT OF AN EXCEL ADD-IN FOR IMPLEMENTING THE CAESIUM-137, EXCESS LEAD-210 AND BERYLLIUM-7 CONVERSION MODELS

As indicated above, conversion of radionuclide inventories to estimates of erosion and depositional rates attempts to numerically infer the rate of removal or accretion of the radionuclide over a specific time period and thereby produce an estimate of the rate of soil redistribution. The complexities and uncertainties associated with the various soil redistribution processes means that the conversion models should initially be applied with caution and where possible the results obtained validated against independent information or evidence of the erosion and deposition rates involved. To facilitate the use of the conversion models described in the previous section, software has been developed for converting ^{137}Cs , $^{210}\text{Pb}_{\text{ex}}$, and ^7Be inventories to soil erosion and deposition rates using VBA (Visual Basic Application). The software has been designed to deal with point data collected along a single downslope transect that follows the flow line (direction of maximum slope), and assumes that there is no sediment contribution from upslope areas or significant across slope soil redistribution.

Implemented as a standard Add-in within Microsoft Excel, the updated software has the following advantages and characteristics:

- (1) It can take full advantages of the data management and data analysis functions available in Excel. The conversion results can be readily related to other environmental variables or factors for further analysis.
- (2) To ensure meaningful model parameterisation, limitations have been placed on the acceptable ranges for individual parameters and default values have been provided. Procedures have also been included to derive or estimate some parameters.

- (3) Conversion models for ^{137}Cs , $^{210}\text{Pb}_{\text{ex}}$ and ^7Be can be accessed with a uniform, consistent, interactive interface in a user-friendly manner. The design of the interfaces follows the logical flow of data analysis involving input data at the top, parameter specification in the middle, and storage of the results at the bottom.
- (4) Help information has been integrated into the programme. Relevant information and guidance is provided at the appropriate time.
- (5) There are no restrictions on folder names /paths, data file locations and, thus, the user is given more flexibility in programme installation and data management.

The conversion models available within the Add-in are listed in Table 2.

TABLE 2. CONVERSION MODELS AVAILABLE WITHIN THE ADD-IN

	Cultivated	Uncultivated (Pasture)
^{137}Cs	<ul style="list-style-type: none"> • Proportional model • Simplified mass balance model (Mass balance model 1) • Mass balance model 2 • Mass balance model with tillage (Mass balance model 3) 	<ul style="list-style-type: none"> • Profile shape model • Diffusion and migration model
^{210}Pb	<ul style="list-style-type: none"> • Mass balance model 2 • Mass balance model with tillage (Mass balance model 3) 	<ul style="list-style-type: none"> • Diffusion and migration model
^7Be	<ul style="list-style-type: none"> • Profile shape model 	

For each model, the sample inventories, the reference inventory and the particle size correction factor (if it is available) are required. Other parameters and data requirements are detailed in Table 3.

It is clear that each model has its own specific set of parameters, although some parameters are common between models. More importantly, the models differ in their underlying assumptions, the process description and the representation of temporal variability. A sound understanding of the models and the meaning and derivation of their parameters is an essential precursor to their successful application. In order to assist in applying the appropriate model and to avoid their possible misuse, these issues will be addressed in the following sections.

TABLE 3. PARAMETERS AND DATA REQUIREMENTS FOR THE INDIVIDUAL MODELS

Model type	Parameter and data requirements
Proportional model and Simplified mass balance model	Tillage depth, bulk density, year of tillage commencement
Mass balance model 2	Tillage depth, year of tillage commencement, proportion factor, relaxation depth, record of annual fallout flux ^a
Mass balance model with tillage (Mass balance model 3)	Tillage depth, tillage constant, proportion factor, relaxation depth, slope length and slope gradient for each section of the transect, record of annual fallout flux*
Diffusion and migration model	Diffusion coefficient, relaxation depth, migration coefficient, record of annual fallout flux*
Profile shape model	Profile shape factor

^a Only required for ^{137}Cs models.

5. PARAMETER SPECIFICATION AND DERIVATION

As with any model, the reliability of the conversion models outlined in the previous section depends heavily on the specification and derivation of the model parameters. Some of these are more difficult to derive than others. Procedures for the derivation of the individual parameters are described in this section.

5.1. The reference inventory

The reference inventory is a critical parameter for any study using ^{137}Cs , $^{210}\text{Pb}_{\text{ex}}$, and ^7Be measurements to estimate soil redistribution rates. The value provided will govern whether a sampling point is designated as having undergone erosion or deposition, and the magnitude of the redistribution rates involved. For ^{137}Cs , an algorithm has been developed and included in the software to estimate a region-specific value for any area of the world, based on known relationships between the reference inventory, geographic location (longitude and latitude) and annual rainfall [24]. It must be emphasised that the predicted value is seen only as providing an estimate of the likely magnitude of the reference inventory at a study site and the value should not be used in the conversion models. It is necessary to obtain a reliable estimate of the local reference inventory, based on field measurements, prior to applying a conversion model. There are currently no procedures available to predict the likely magnitude of reference inventories for ^{210}Pb , and ^7Be . It is recommended that the sampling of reference sites should include some depth incremental sampling, as well as the collection of bulk cores, in order to confirm that the site has not been disturbed (e.g. cultivated). The associated depth or profile distributions may also be needed to derive other parameters, such as the profile shape factor, and the migration and diffusion rate etc.

5.2. Particle size correction factors for eroding and depositional sites

The particle size correction factors are incorporated into the conversion models, in order to take account of the grain size selectivity of erosion and sedimentation processes and the likely preferential association of the fallout radionuclides with the finer fractions of the soil or sediment. Thus, for example, if erosion is associated with the preferential removal of fine particles, which are characterized by high concentrations of the radionuclide, the erosion rate is likely to be overestimated if this is not taken into account. Equally, if deposition involves the preferential deposition of coarser particles with low radionuclide activity, the deposition rate may be under-estimated if this is not considered. However, although the need to incorporate particle size correction into conversion models is clear, there have been few attempts to derive the necessary correction factors. These are likely to vary according to both the soil type and the radionuclide being considered, as well as the degree of selectivity associated with the sediment mobilisation erosion and deposition processes.

For an eroding site, the correction factor will reflect the ratio of the radionuclide concentration of the mobilised sediment to that of the original soil [see 25]. Because the grain size composition of mobilised sediment is usually enriched in fine soil particles compared with the original soil, the ratio is generally greater than 1.0, due to the strong affinity of ^{137}Cs for fine particles. Its value is therefore a function of the grain size composition of both mobilised sediment and the original soil. For a deposition site, the correction factor will be a function of the ratio of the ^{137}Cs concentration of deposited sediment to that of the mobilised sediment. Because the grain size composition of deposited sediment is frequently depleted in fine fractions compared with the mobilised sediment, its value is generally less than 1.0

In order to estimate values for the particle size correction factor for eroding sites (P) and depositional sites (P'), information on the grain size distribution of the soils and the mobilised sediment is needed. Values of P and P' can be estimated using the procedures described by He and Walling [21]. If the specific surface area of mobilised sediment is S_{ms} ($\text{m}^2 \text{g}^{-1}$), and that of the original soil is S_{sl} ($\text{m}^2 \text{g}^{-1}$), P can be calculated as:

$$P = \left(\frac{S_{ms}}{S_{sl}} \right)^{\nu} \quad (33)$$

where: ν is a constant with a value of ca. 0.65. If the specific surface area of deposited sediment is S_{ds} ($\text{m}^2 \text{g}^{-1}$), P' can be calculated as:

$$P' = \left(\frac{S_{ds}}{S_{ms}} \right)^{\nu} \quad (34)$$

The value of ν in Equation 34 is the same as that in Equation 33. The following relationship therefore exists:

$$PP' = \left(\frac{S_{ms}}{S_{sl}} \right)^{\nu} \left(\frac{S_{ds}}{S_{ms}} \right)^{\nu} = \left(\frac{S_{ds}}{S_{sl}} \right)^{\nu} \quad (35)$$

5.3. The proportion factor

The proportion factor represents the proportion of the annual radionuclide fallout that is susceptible to mobilisation by heavy rainfall, prior to its incorporation into the soil by tillage. This will depend on the temporal distribution of the local rainfall in relation to the timing of cultivation. In locations where the annual wet season and associated high intensity rainfall, which can generate surface runoff and thus mobilise sediment, occur shortly before the period of cultivation, the fallout input already accumulated at the soil surface as well as additional input directly associated with the high intensity rainfall events will be susceptible to removal by erosion. In these circumstances, the value for the proportional factor can be assumed to be ca. 1.0, if there is only one cultivation operation. In cases where the main period of high intensity rainfall events occurs immediately after cultivation has been completed and the remainder of the rainfall occurring during the year is unlikely to generate surface runoff, the fallout input accumulated at the soil surface before the occurrence of these events will have been incorporated into the plough layer by tillage, and only that directly associated with the intense rainfall occurring immediately after tillage will be susceptible to removal by erosion. Under these circumstances, the value of proportion factor may be approximated by the ratio of the depth of rainfall associated with the main period of heavy rainfall, which produces surface runoff, to the total annual rainfall. If there is more than one cultivation operation each year, the temporal pattern of precipitation in relation to each cultivation operation needs to be considered.

5.4. The tillage constant

The potential significance of tillage translocation on within-field redistribution of fallout radionuclides has been emphasized by a number of recent studies [16,26]. The contribution of tillage translocation to the redistribution of ^{137}Cs and $^{210}\text{Pb}_{\text{ex}}$ has been incorporated, albeit in a simple manner, in mass balance model 3 by use of a tillage constant that represents a slope-independent specific soil flux. It is a lumped value for the time period under investigations

(about 40 years for ^{137}Cs and 100 years for $^{210}\text{Pb}_{\text{ex}}$). No temporal and spatial variation is considered. While there are some data available on the value for the tillage constant associated with specific implements, the direct application of such values in the conversion models is frequently complicated by the need to account of the use of different implements over a period of several decades. An alternative approach to estimating the tillage constant is provided by considering the inventories of eroding sites located at the top of a slope where the contribution of water erosion and deposition can be treated as negligible, due to the lack of a significant upslope to contribute runoff.

Assuming that there is no significant water erosion, the tillage erosion rate R_t ($\text{kg m}^{-2} \text{a}^{-1}$) can be estimated from the measured total ^{137}Cs inventory $A_I(t)$ (Bq m^{-2}) of a eroding point using the following Equation (derived from equation 10):

$$A_I(t) = A_I(t_0) e^{-(R_t/d+\lambda)(t-t_0)} + \int_{t_0}^t I(t') e^{-(R_t/d+\lambda)(t-t')} dt' \quad (36)$$

The tillage constant can be estimated from the erosion rate:

$$\phi = \frac{R_{t,\text{out},1} L_1}{\sin \beta_1} = \frac{R_t L_1}{\sin \beta_1} \quad (37)$$

A separate Add-in has been developed to solve the above equations numerically for the tillage constant, using the measured inventories of ^{137}Cs or $^{210}\text{Pb}_{\text{ex}}$ and site-specific values for the reference inventory, tillage depth, slope gradient and soil bulk density. For ^{137}Cs , the year of tillage commencement and the sampling year can also be specified. It is provided as an optional component of the software.

5.5. The profile shape factor, the migration rate and the diffusion coefficient

The profile shape factor (h_0) describes the rate of exponential decrease in inventory or radioactivity with depth for a soil profile from an uncultivated site. The larger the value of the profile shape factor, the deeper the ^{137}Cs or ^7Be penetration into the soil profile. If depth incremental samples are available for a reference site, h_0 can be estimated in Excel via curve-fitting. To estimate the value of h_0 , an exponential function in the form of $f(z) = f(0)e^{-z/h_0}$ can be fitted to the relationship between sampling depth and mass concentration or inventory, where $f(0)$ is the fallout concentration (inventory) at the surface soil and z is the sampling depth in cumulative mass above.

The diffusion coefficient (D) and the migration rate (V) represent the evolution of the shape of the ^{137}Cs or $^{210}\text{Pb}_{\text{ex}}$ profile with time. High values of D and V will imply a deeper penetration of ^{137}Cs into the soil profile. Although more precise values of D and V can be obtained through solving the one-dimensional transport equation (see 15], in the case of ^{137}Cs they may be approximated using the following equations:

$$V \approx \frac{W_p}{t - 1963} \quad (38)$$

$$D \approx \frac{(N_p - W_p)^2}{2 \times (t - 1963)} \quad (39)$$

where:

- t is the year when the soil core was collected (a);
- W_p is the mass depth of the maximum ^{137}Cs concentration (kg m^{-2});
- N_p is the distance between the depth of the maximum ^{137}Cs concentration and the point where the ^{137}Cs concentration reduces to $1/e$ of the maximum concentration (kg m^{-2}).

For ^{137}Cs , D ($\text{kg}^2 \text{m}^{-4} \text{a}^{-1}$) and V ($\text{kg m}^{-2} \text{a}^{-1}$) are normally in the range of 30-50 $\text{kg}^2 \text{m}^{-4} \text{a}^{-1}$ and 0.2-1.0 $\text{kg m}^{-2} \text{a}^{-1}$, respectively. With $^{210}\text{Pb}_{\text{ex}}$, D is related to V as follows [15]:

$$\frac{1}{h_0} = 0.5 \times \left(\sqrt{\frac{V^2}{D^2} + \frac{4\lambda}{D}} - \frac{V}{D} \right) \quad (40)$$

Assuming $V = 0$, since the maximum $^{210}\text{Pb}_{\text{ex}}$ activity will commonly be found at the surface, rather than, as in the case of ^{137}Cs , just below the surface, D can be calculated using the above equation. Routines have been developed for estimating h_0 , D , and V for reference sites where values of depth incremental sample mass and corresponding values of mass concentration are available. These are activated when a migration and diffusion model is selected. It is important to note that the estimated values will be influenced by the thickness of the depth increment used in sectioning the core. Since soil erosion is a surface processes, it is vital to have detailed information near the top of the profile.

5.6. The annual deposition flux

Except for the simplified mass balance model, all other mass balance models use the annual deposition flux in their calculations. For $^{210}\text{Pb}_{\text{ex}}$, the annual deposition flux is assumed to effectively constant through time and it is calculated by the software, using the given reference inventory and assuming a steady-state between the annual input and the loss of the radionuclide by decay. For ^{137}Cs , the annual fallout deposition flux since 1954 must be provided. Few, if any, studies will have these data available for specific sites. The software therefore uses the given reference inventory value and generalised information on the temporal distribution of annual fallout to synthesise the annual series for a study site. Assuming that the study site has the same relative annual variation as that of the reference station used to characterize the temporal pattern of annual fallout, although different in absolute magnitude, the record of the local ^{137}Cs deposition flux $I(t)$ can be synthesised using the following equation:

$$I(t) = \alpha I_n(t) \quad (41)$$

where:

- $I_n(t)$ is the ^{137}Cs deposition flux for the reference station ($\text{Bq m}^{-2} \text{a}^{-1}$);
- α is a scaling factor which can be calculated as follows:

$$\alpha = \frac{A_{\text{ref}}}{\int_{1954}^t I_n(t') e^{-\lambda(t-t')} dt} = \frac{A_{\text{ref}}}{A_n} \quad (42)$$

where: A_n (Bq m^{-2}) is the present total atmospheric fallout inventory for the ^{137}Cs deposition at the reference station. The reference station file is a plain text file that contains a single column of numbers listing the annual flux in Bq m^{-2} from 1954. The default value for years after 1983 is zero. Representative station files for both the northern and south hemisphere, without Chernobyl-related ^{137}Cs inputs, are included in the help documentation. They can be

copied, saved and modified. A customised annual deposition flux file can also be generated for those areas where the Chernobyl- related ^{137}Cs input is known to be significant, if the additional deposition flux that occurred in 1986 is known or can be estimated.

6. MANAGEMENT OF THE ADD-IN SOFTWARE AND ITS APPLICATION

6.1. System requirements and installation

The software distributed is a standard Microsoft (Ms) Excel Add-in. It consists of one Add-in file (named radiocalc.xla), one compiled html help file (named radiocalc.chm) and one rainfall data file if the approximate local reference inventory has to be estimated. The minimum software environment is a copy of Excel 97 operating on Windows 98 and Internet Explorer 5.0. It was developed on a PC running Windows 98 and Excel 2000. User's feedbacks on its performance on other system combinations would be most welcome.

6.1.1. Add-in installation

To install the programme, one only has to move the files to a user-preferred folder. It is highly recommended that all three files should be saved in one folder. The ideal location is the 'Add-in' folder created by the Windows setup programme.

One way to find the location of this folder on your PC is to try saving a workbook as an Add-in and note down the full path to the prompted default folder provided by Excel.

When you use the Add-in for the first time, the following steps must be followed to prepare it for use:

- (1) Start Excel
- (2) Navigate the menu system as follow: **Tools** | **Add-in**. If the files have been saved in the recommended folder, the Add-in named 'radiocalc.xla' should be in the list of Add-in available. Otherwise, click the **Browse** button, find the file 'radiocalc.xla' and open it. It should, then, appear on the list. Make sure the leading box in front of the 'radiocalc.xla' is checked by clicking it if necessary.
- (3) Close the Add-in window and a new menu item named 'radionuclide inventories conversion' should be added to the **Tools** menu. Then, you can use the Add-in by simply clicking this newly added menu item.
- (4) If you have to save help files separately from the Add-in file itself, you need to specify the correct path via the 'options' button on the main menu before the online help for the Add-in can function properly.
- (5) Apart from 'Add-ing' one entry to the windows registry, no other files or modifications to the user's system files and configuration are required.

6.1.2. Removing the Add-in

Removal of the Add-in from your computer involves two steps:

- (1) Remove the added menu item from the menu system: navigate the Add-in list via: **Tools** | **Add-in**. Then, remove the Add-in by clicking on the leading box. The programme will also delete its entry to the windows's registry.
- (2) Remove the files themselves: go to the folder and delete the files as usual.

When you go to the Add-in list next time, you will be prompted by the Excel to delete the Add-in from the list.

Caution: deleting the files before removing the added menu item is not good practice and should be avoided.

6.2. Using the Add-in

6.2.1. Input data management

The data for the sampling points should be entered into an Excel worksheet and listed in columns which run from the top to the bottom of the slope. The same numbers of entries will be expected for the values relating to sample inventory, particle size correction factor, etc. With the current version of the programme, an active worksheet is required for it to run. All input data are expected to be in this worksheet and the output results will also be saved in it.

6.2.2. Interaction with the interface

The interface of the Add-in should be familiar to any Microsoft Windows user. Designed as a tool for research purpose, it is assumed that the user knows how to deal with command buttons, option buttons, input boxes, etc., in a Windows operating system.

With this Add-in, users also have to select a particular set of values or range (multiple cells in a single column) for data input and output. This can be done by selecting the first cell in the range, holding down the mouse, dragging it over the cells, and releasing the mouse when you reach the last cell. If a mistake is made, one can simply click the first cell and start all over again. Where a range is expected, the text input box is locked (no keyboard entry will be allowed) to avoid error in its specification. Instead, an arrow-labelled button is provided to its right. The user simply clicks the button to select a range interactively from the active worksheet.

6.3. Provision of help

The Add-in has online help included. It is a compiled html help file that can be viewed while the programme is running or independently as an ordinary file as long as you have Microsoft Internet Explorer (version 5 and above) installed.

7. CONCLUSIONS

Conversion models are a key requirement in the use of fallout radionuclides to obtain information on soil redistribution rates, since they are able to convert measurements of the reduction or increase in the radionuclide inventory of a sampling point, relative to the local reference inventory, into a quantitative estimate of the erosion or deposition rate involved.

A wide range of conversion models are available for use with ^{137}Cs measurements and a limited number of models are now being developed for use with $^{210}\text{Pb}_{\text{ex}}$ and ^7Be .

In order to obtain a degree of consistency and standardisation in the use of such conversion models across a group of researchers involved in an ongoing IAEA Coordinated Research Project, a group of nine models covering applications involving both cultivated and uncultivated areas and the three fallout radionuclides, has been developed and documented.

Furthermore in order to facilitate the application of the models in a standardised manner and to promote their use by the wider scientific community, a user-friendly software package, based on an Excel Add-in has been produced and made available to interested persons. It is hoped that the use of a standardised set of conversion models by the CRP participants and other researchers will facilitate exchange and comparison of results and that the wider testing of the conversion models will generate an improved understanding of their advantages and limitations and thus assist the further development and improvement of such models.

ACKNOWLEDGEMENTS

The work on assembling, developing and documenting the set of nine conversion models described in this contribution and the production of the user-friendly software to assist in applying the models were undertaken to support implementation of the IAEA Coordinated Research Project on 'Assessing the effectiveness of soil conservation techniques for sustainable watershed management using fallout radionuclides' (D1-50-08), through technical contract UK-12094.

REFERENCES

- [1] RITCHIE, J.C., RITCHIE, C.A., "¹³⁷Cs use in erosion and sediment deposition studies: promises and problems", IAEA-TECDOC-828, Vienna (1995) 11-201.
- [2] WALLING, D.E., QUINE, T.A., "The use of fallout radionuclides in soil erosion investigations", IAEA Publ. ST1/PUB/947, Vienna (1995) 597-619.
- [3] WALLING, D.E., "Opportunities for using environmental radionuclides in the study of watershed sediment budgets", Proceedings of the International Symposium on Comprehensive Watershed Management, Beijing, September 1998, Beijing (1998) 1-16.
- [4] WALLING, D.E., "Tracing versus monitoring: New challenges and opportunities in erosion and sediment delivery research", Soil Erosion and Sediment Redistribution in River Catchments, (OWENS, P.N., COLLINS, A.J. Eds.), CABI, Wallingford (2006) 13-27.
- [5] ZAPATA, F. (Ed.), Handbook for the Assessment of Soil Erosion and Sedimentation Using Environmental Radionuclides, Kluwer, The Netherlands (2002).
- [6] LOUGHRAN, R.J., The measurement of soil erosion, Progress in Physical Geography **13** (1989) 216-233.
- [7] HE, Q., WALLING, D.E., Testing distributed soil erosion and sediment delivery models using ¹³⁷Cs measurements, Hydrological Processes **17** (2003) 901-916.
- [8] WALLING, D.E., QUINE, T.A., "Use of Caesium-137 as a Tracer of Erosion and Sedimentation", Handbook for the Application of the Caesium-137 Technique. University of Exeter, UK (1993).
- [9] WALLING, D.E., HE, Q., Improved models for estimating soil erosion rates from ¹³⁷Cs measurements, Journal of Environmental Quality **28** (1999) 611-622.
- [10] WALLING, D.E., et al., "Conversion models for use in soil- erosion, soil-redistribution and sedimentation investigations", Handbook for the Assessment of Soil Erosion and Sedimentation Using Environmental Radionuclides, (ZAPATA, F. (Ed.) Kluwer, The Netherlands (2002) 111-162.
- [11] BLAKE, W.H. et al., Fallout beryllium-7 as a tracer in soil erosion investigations, Applied Radiation and Isotopes **51** (1999) 599-605.

- [12] WALLING, D.E., HE, Q., Using fallout lead-210 measurements to estimate soil erosion on cultivated land, *Soil Science Society America J.* **63** (1999) 1404-1412.
- [13] WALLING, D.E., et al., Use of ^7Be and ^{137}Cs measurements to document short- and medium term rates of water-induced soil erosion on agricultural land, *Water Resources Research* **35** (1999) 3865-3874.
- [14] ZHANG, X.B. et al., A preliminary assessment of the potential for using caesium-137 to estimate rates of soil erosion in the Loess Plateau of China, *Hydrological Sciences J.* **35** (1990) 267-276.
- [15] HE, Q., WALLING, D.E., The distribution of fallout ^{137}Cs and ^{210}Pb in undisturbed and cultivated soils, *Applied Radiation Isotopes* **48** (1997) 677-690.
- [16] GOVERS, G. et al., The relative contribution of soil tillage and overland flow erosion to soil redistribution on agricultural land, *Earth Surface Processes and Landforms* **21** (1996) 929-946.
- [17] PEGOYEV, A.N., FRIDMAN, S.D., Vertical profiles of cesium-137 in soils, *Pochvovedeniye* **8** (1978) 77-81.
- [18] WALLING, D.E., HE, Q., "Towards improved interpretation of ^{137}Cs profiles in lake sediments", *Geomorphology and Sedimentology of Lakes and Reservoirs* (MCMANUS, J. DUCK, R.W., Eds.) Wiley, Chichester, UK, (1993) 31-53.
- [19] REYNOLDS, W.D., et al., Evaluation of distribution coefficients for the prediction of strontium and cesium migration in a uniform sand, *Canadian Geotechnical J.* **19** (1982) 92-103.
- [20] APPLEBY, P.G., OLDFIELD, F. "Application of ^{210}Pb to sedimentation studies", *Uranium Series Disequilibrium*. (IVANOVICH, M., HARMON, R.S. Eds.) Oxford University Press (1992) 731-778.
- [21] HE, Q., WALLING, D.E., Use of fallout Pb-210 measurements to investigate longer-term rates and patterns of overbank sediment deposition on the floodplains of lowland rivers, *Earth Surface Processes and Landforms* **21** (1986) 141-154.
- [22] BOPP, R.F., et al., Sediment-derived chronologies of persistent contaminants in Jamaica Bay, *Estuaries* **16** (1993) 606-616.
- [23] WALLING, D.E., et al., Using unsupported lead-210 measurements to investigate soil erosion and sediment delivery in a small Zambian catchment, *Geomorphology* **52** (2003) 193-213.
- [24] WALLING, D.E., HE, Q., "The global distribution of bomb-derived ^{137}Cs reference inventories", *Final Report on IAEA Technical Contract 10361/RO-R1*, (2000).
- [25] HE, Q., WALLING, D.E., Interpreting the particle size effect in the adsorption of ^{137}Cs and unsupported ^{210}Pb by mineral soils and sediments, *J. Environmental Radioactivity* **30** (1996) 117-137.
- [26] GOVERS, G., et al., Tillage erosion and translocation: emergence of a new paradigm in soil erosion research, *Soil and Tillage Research* **51** (1999) 167-174.

SEDIMENT BUDGETS AND SOURCE DETERMINATIONS USING FALLOUT CAESIUM-137 IN A SEMIARID RANGELAND WATERSHED, ARIZONA, USA

J.C. RITCHIE

US Department of Agriculture - Agricultural Research Service –
Hydrology and Remote Sensing Laboratory,
Beltsville

M.A. NEARING

US Department of Agriculture- Agricultural Research Service –
Southwest Watershed Research Center,
Tucson

F.E. RHOTON

US Department of Agriculture- Agricultural Research Service - National
Sedimentation Laboratory,
Oxford

USA

Abstract

Analysis of soil redistribution patterns and sediment sources in semiarid and arid watersheds provides information for understanding watershed sediment budgets and for implementing management practices to improve rangeland conditions and reduce sediment loads in streams. The purpose of this research was to develop sediment budgets and to identify potential sediment sources using ¹³⁷Caesium (¹³⁷Cs) and other soil properties in a series of small semiarid subwatersheds on the USDA ARS Walnut Gulch Experimental Watershed near Tombstone, Arizona, USA. Soils were sampled in a grid pattern on two small subwatersheds and along transects associated with soils and geomorphology on six larger subwatersheds. Soil samples were analyzed for ¹³⁷Cs and selected physical and chemical properties (i.e. bulk density, rocks, particle size, soil organic carbon). Suspended sediment samples collected at flume sites on the Walnut Gulch Experimental Watershed were also analyzed for the same properties. Sediment budgets measured using ¹³⁷Cs inventories for a small shrub and a small grass subwatersheds found eroding areas in these watersheds were losing 5.6 and 3.2 t ha⁻¹ a⁻¹, respectively; however, a sediment budget for each of the small subwatersheds, including depositional areas, found net soil loss to be 4.3 t ha⁻¹ a⁻¹ from the shrub watershed and near zero t ha⁻¹ a⁻¹ from the grass subwatershed. The suspended sediments collected at the flumes of the larger subwatersheds were enriched in silt, clay, and ⁴⁰K, but not for ¹³⁷Cs. Using multivariate mixing models to determine sediment source indicated that the shrub dominated subwatersheds were contributing most of the suspended sediments measured at the outlet flume of the Walnut Gulch Experimental Watershed. Both methodologies (sediment budgets and sediment source analyses) indicate that shrub dominated systems provide more suspended sediments to the stream systems. These studies also suggest that sediment yields measured at the outlet of a watershed may be a poor indicator of actual soil redistribution within a watershed. Using ¹³⁷Cs provided useful information on soil redistribution within watersheds and sediment source areas for developing management strategies. Management of these semiarid rangelands must consider techniques that will protect grass dominated areas from shrub invasion.

1. INTRODUCTION

Degradation of semiarid and arid rangelands is a major concern and is usually described in terms of soil movement/erosion and changing plant communities [1, 2, 3]. A U.S. National Research Council Report [4] cited a need to develop a methodology to monitor and assess this degradation and its impact on rangelands and rangeland conditions. Understanding the patterns of soil erosion, soil redistribution, and sediment yield are key factors for monitoring and assessing soil quality, rangeland condition, water quality, and managing semiarid

rangelands [5]. Maintaining or improving soil quality or rangeland conditions requires managing soil erosion and soil organic carbon movement and losses at the field and watershed levels [5, 6, 7]. Recent studies indicate that soil erosion and subsequent redeposition of this eroded material within the same field play a significant role in understanding soil organic matter patterns and therefore soil quality at field and landscape levels [7, 8]. The stability of semiarid rangeland ecosystems has been defined as the capability of a site to limit redistribution and loss of soil resources (including nutrients and organic matter) by wind and water [9, 10].

Determination of sediment budgets, sediment sources, and soil redistribution in watersheds is important for management of natural and agricultural systems and accessing environmental problems. Soil losses are a major concern around the world with degradation of both onsite and off-site resources. Pimentel et al. [11] estimated the annual cost for soil redistribution at \$37 billion in the United States in the mid 1990's. With the growing recognition of the enormity of this problem, methods need to be developed for determining soil redistribution patterns in watersheds, for relating suspended sediments to source areas in the watershed, and for determining the effectiveness of management practices on the runoff and soil redistribution. With the growing concern about degradation of semiarid and arid rangelands [4], a better understanding of soil redistribution patterns of these ecosystems is necessary to develop management plans to maintain or improve rangeland conditions.

Two general approaches (monitoring and fingerprinting) have been used to identify sediment sources in watersheds. In both approaches, suspended sediments are compared with potential sources areas using geomorphological, physical, chemical, and mineralogical properties. Monitoring of source areas employs erosion pins, runoff plots, and suspended sediment samples [12, 13]. Fingerprinting uses mixing models to compare potential sediment source and suspended sediment properties to determine potential sediment sources from the watershed [12, 14, 15, 16]. Physical, chemical, and fallout radionuclide (^{137}Cs) are among the many properties that have been used for fingerprinting suspended sediments [14, 16, 17, 18, 19]. These physical and chemical properties are evaluated for the source areas and the suspended sediments using simple or multivariate mixing models [12, 14, 16].

The objective of this research was to use radioactive fallout ^{137}Cs distribution patterns to determine soil redistribution patterns for determining sediment budgets and with other physical and chemical properties to identify source of sediments by fingerprinting in a semiarid subwatershed of the Walnut Gulch Experimental Watershed near Tombstone, Arizona, USA.

2. MATERIALS AND METHODS

2.1. Study area

The study area (Fig. 1) is located in the Southeastern Arizona Basin and Range province on the United States Department of Agriculture (USDA), Agriculture Research Service (ARS) Walnut Gulch Experimental Watershed near Tombstone, Arizona USA (31° 43' N. Latitude, 110° 41' W. Longitude). The watershed is approximately 150 km² in a high foothill alluvial fan of the San Pedro River Watershed at elevations ranging from 1220 to 1950 m. Mean annual temperature is 17°C ranging from 1°C in January to 35°C in June. Mean annual precipitation in the Watershed is approximately 356 mm ranging from 250 to 500 mm a⁻¹, with approximately two thirds of the rainfall occurring in the monsoon season (July-August). Most of the surface runoff occurs during the monsoon period [20].

Walnut Gulch Experimental Watershed, Arizona

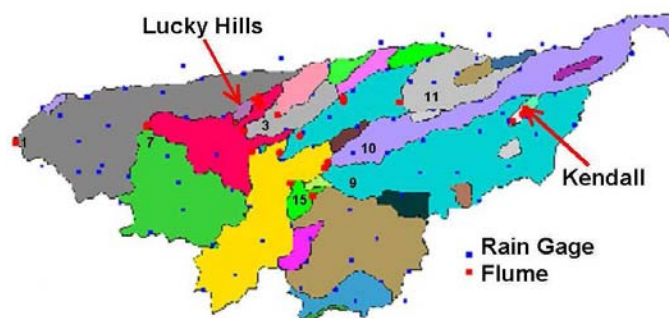


FIG.1. Map of Walnut Gulch Experimental Watershed, Tombstone, Arizona, USA showing the subwatersheds used in this study.

Soils in the Walnut Gulch Experimental Watershed are closely related to their parent material [21,22,23]. The watershed soils have developed on Precambrian to Tertiary-age sandstone, conglomerates, limestone, volcanic, granodiorite, and quartz monzonite materials [22]. Quaternary alluvium from limestone makes up approximately 80% of the watershed surface [24]. The soils formed on this parent material are well-drained, calcareous gravelly loams [25]. Watershed soils formed in alluvium and colluvium from andesite and basalt, and residuum from granodiorite were generally finer textured, shallow, and well-drained. Rock contents at the soil surface range from 0 to 70% [26].

At lower elevations in the watershed (Fig. 2), shrub species of creosote bush [*Larrea tridentata* (DC.) Coville; *Larrea divaricata* Cav.]¹, whitethorn [*Acacia constricta* Benth.], tarbush [*Flourensia cernua* DC.], snakeweed [*Gutierrezia sarothrae* (Perch) Britton & Rusby], and burroweed [*Isocoma tenuisecta* Greene] dominate the landscape. At higher elevations, grass species of black grama [*Bouteloua eriopoda* (Torr.) Torr.], blue grama [*Bouteloua gracilis* (Kunth) Lag. ex Griffith], sideoats grama [*Bouteloua curtipendula* (Michx.) Torr.], curly mesquite [*Hilaria belangeri* (Steud.) Nash] and bush muhly [*Muhlenbergia porteri* Scribn. Ex Beal] dominate the vegetation [27,28]. The Walnut Gulch Experimental Watershed serves as grazing land for cattle and horses. Grazing has occurred in the area since the establishment of Spanish ranches in the early 1800s with intensive grazing in the area beginning in the 1880s.

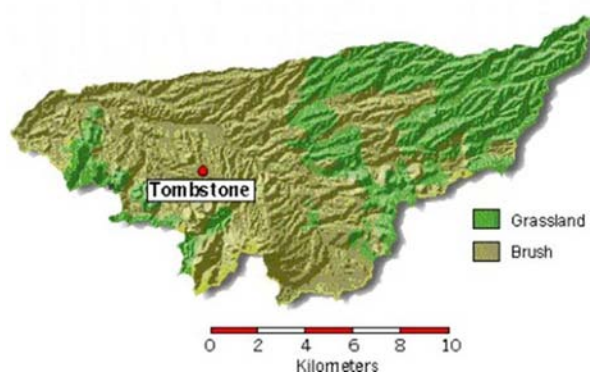


FIG. 2. Map of Walnut Gulch Experimental Watershed, Tombstone, Arizona, USA showing vegetation patterns.

¹ Scientific nomenclature of plant names according to the USDA, ARS, National Genetic Resources Program, Germplasm Resources Information Network - (GRIN) [Online Database], National Germplasm Resources Laboratory, Beltsville, Maryland. URL: <http://www.ars-grin.gov/cgi-bin/npgs/html/index.pl?language=en> (28 August 2007).

2.1.1. Study sites for assessing sediment budgets

Sediment budgets were determined for the Lucky Hills and Kendall subwatersheds (Fig. 1) of the Walnut Gulch Experimental Watershed. The Lucky Hills watershed has an area of 3.7 hectares and the Kendall watershed has an area of 1.9 hectares. Mean hillslope gradients of the Lucky Hills and Kendall watersheds are 7.7% and 12.3%, respectively. The Lucky Hills watershed is a shrub dominated semiarid rangeland with approximately 25% canopy cover and a gravelly sandy loam soils with a primary particle size distribution of 52% sand, 26% silt, and 22% clay. The Kendall watershed is a grass dominated semiarid rangeland with approximately 35% canopy cover with a few shrubs and forbs having a gravelly fine sandy loam soils with a primary particle size distribution of 55% sand, 20% silt, and 25% clay. The organic carbon contents of the soils from the Lucky Hills and Kendall Watersheds are approximately 0.8% and 1.1%, respectively. Both watersheds were historically used as grazing land; however, the Lucky Hills watershed was fenced in 1963 limiting the grazing by domestic livestock. The Kendall watershed continues to be grazed [29]. These watersheds are instrumented with flumes for runoff and suspended sediment measurements [30].

2.1.2. Study sites for identifying sediment sources

The sediment source research was conducted on subwatersheds 3, 7, 9, 10, 11, and 15 of the Walnut Gulch Experimental Watershed (Fig. 1). Dominant vegetation in subwatersheds 3, 7, and 15 is shrubs while the vegetation in subwatersheds 9, 10, and 11 is grass [27]. These subwatersheds, as well as the outlet of the Walnut Gulch Experimental Watershed, are instrumented with supercritical flumes for runoff measurements and sample collection [30].

2.2. Field Methods

2.2.1. Soil Sampling – Sediment Budget Studies

For the sediment budget studies in Lucky Hill and Kendall subwatersheds, soil samples were collected on a 25-m grid pattern. A differential GPS (Global Positioning System) was used to determine the latitude, longitude, and elevation of each sample site. Cover (i.e. vegetation, bare) was noted for the sample sites. Bulk soil samples at each site were collected for the 0-25 cm soil layer at three points and composited for analyses.

2.2.2. Soil Sampling - Sediment Source Studies

For the sediment source studies soil samples were collected from the six subwatersheds based on area occupied by different soil mapping units. A 1000 m transect was chosen for each 200 ha of a soil mapping unit. Transects were delineated so a range of surface geomorphology factors [31] were represented. At each selected location, samples were collected from the surface 5 cm at three points, approximately 10 m apart and perpendicular to the slope, and composited for analyses. This sampling depth generally represents the A horizon thickness [32] which is most affected by soil erosion processes. Site data were recorded for latitude, longitude, elevation, slope position, slope steepness, and slope aspect.

2.2.3. Suspended Sediment Sampling – Sediment Source Studies

Suspended sediments were collected with vertical samplers mounted on the face of the flumes on each of the six subwatersheds and at the outlet (Flume 1) of the Walnut Gulch Experimental Watershed. These samples were collected in 30.5 cm increments above the floor of the flume to a flow depth to 122 cm in 500 mL plastic sample bottles mounted inside the

sealed sampler at each depth. Additionally, 2 liter sample bottles were attached to the bottom of the samplers to ensure sufficient volumes of suspended sediments were obtained at the 30.5 cm flow depth during low flow events [21]. Suspended sediment samples collected between 1999 and 2003 were composited to provide a sample for each flume for this study.

2.3. Laboratory Analyses

Soil samples and suspended sediment samples were oven-dried at 60°C. All samples were sieved to pass a <2 mm screen. Weights of soil (<2 mm) and rock fragment (>2 mm) fractions were determined. Particle size analyses were determined by standard pipette analysis [33]. Total carbon and nitrogen were determined using a Leco CN-2000 carbon-nitrogen analyzer (Leco Corp., St. Joseph, MI²).

The soil fraction (<2 mm) was placed into counting beakers and sealed for analyses of ¹³⁷Caesium, ⁴⁰Potassium and ²²⁶Radium by gamma-ray spectrometry using a Canberra Genie-2000 Spectroscopy System that receives input from three Canberra high purity coaxial germanium crystals (HpC >30% efficiency) into three 8192-channel analyzers. The system is calibrated and efficiency determined using an Analytic mixed radionuclide standard (10 nuclides) whose calibration can be traced to U.S. National Institute of Standards and Technology. Measurement precision for ¹³⁷Cs is ± 4 to 6% [34].

2.4. Estimation of Soil Redistribution Rates – Sediment Budget Studies

Radioactive ¹³⁷Cs was globally distributed by the deposition of radioactive fallout material from atmospheric nuclear weapon tests from the mid 1950s to the mid 1970s mostly by rainfall [35,36,37]. While rainfall may be patchy in semiarid and arid landscapes, the assumption is that over the 20-year period of radioactive fallout, all areas would have approximately uniform rain and fallout ¹³⁷Cs deposition [9]. Since ¹³⁷Cs is quickly adsorbed by clays, any subsequent movement of ¹³⁷Cs across the landscape is due to physical processes (i.e., water erosion, wind erosion). Thus patterns of ¹³⁷Cs distribution across the landscape can be used to estimate soil redistribution rates and patterns based on the measurement of ¹³⁷Cs concentrations in the eroding or depositing sites and comparing it to measurements of ¹³⁷Cs concentration in reference soil sites where soil erosion has not occurred [15,38,39,40].

The Diffusion and Migration Model for Erosion and Deposition on Undisturbed Soils [38,39], which accounts the time-dependent behavior of both the ¹³⁷Cs fallout input and its subsequent redistribution in the soil profile, was used to convert from ¹³⁷Cs concentrations to net soil redistribution rates for the Kendall [41] and Lucky Hills [42] subwatersheds. The net soil redistribution rates were calculated by comparing the ¹³⁷Cs concentrations of the soil samples collected over the watersheds and the mean ¹³⁷Cs inventory of the soil samples taken at the reference sites on or near the Walnut Gulch Experimental Watershed.

Sediment budgets were calculated using interpolations and spatial analyses. Contour maps, maps of net soil redistribution and percent rock fragments were produced by using a Kriging interpolation method for the Lucky Hills and Kendall watersheds.

² Trade names are included for the benefit of the reader and do not imply an endorsement of or a preference for the product listed by the U. S. Department of Agriculture.

2.5. Sediment Sources Analyses

The relative contribution of each of the subwatersheds to the suspended sediment loads measured at the outlet (Flume 1) of the Walnut Gulch Experimental Watershed was estimated using the multivariate mixing model methods described by Walling and Woodward [16] and Walling et al. [43] to compare the physical and chemical parameters measured for the soil and suspended sediment samples. Each property was normalized by its standard deviation. This mixing model allowed the measured parameters of suspended sediments at flume 1 to be expressed in terms of possible contributions from flumes 3, 7, 9, 10, 11, and 15 and the subwatershed soil samples.

3. RESULTS AND DISCUSSION

3.1. Development of Sediment Budgets

Sixteen soil samples collected at sites with little evidence of physical or biological disturbance of the surface were for use as reference soil sites for determining soil redistribution patterns for the sediment budgets studies. The mean ^{137}Cs concentration in these samples was $1839 \pm 792 \text{ Bq m}^{-2}$. This variability in reference samples is similar to variability measured in other studies [44,45]. We assumed that this ^{137}Cs concentration ($1839 \pm 792 \text{ Bq m}^{-2}$) represented the ^{137}Cs input to the watershed area and used it as the reference value in the Diffusion and Migration Model [38,39] to calculate soil redistribution rates and patterns for the sediment budget studies in the Lucky Hills and Kendall watersheds. Samples collected at 1 cm intervals were used to estimate the diffusion coefficients.

The spatial patterns of soil redistribution in the two watersheds are shown in Figs. 3 and 4. Erosion rates were greater in the Lucky Hills watershed than in the Kendall watershed with eroding sites in Lucky Hills watershed averaging $5.6 \text{ t ha}^{-1} \text{ a}^{-1}$ erosion while the Kendall watershed averaged $3.2 \text{ t ha}^{-1} \text{ a}^{-1}$. Results indicated that 85% of the sampling sites in the Lucky Hills watershed were eroding compared to 53% of the sites for the Kendall watershed. There were more deposition sites (47% of the sample sites) in the Kendall watershed than in the Lucky Hills watershed (15% of the sites). The Kendall watershed had higher deposition rates ($3.9 \text{ t ha}^{-1} \text{ a}^{-1}$) than the Lucky Hills watershed ($3.4 \text{ t ha}^{-1} \text{ a}^{-1}$) at the deposition sites.

When the total soil redistribution budget was calculated, there was more soil loss from the Lucky Hills watershed than from the Kendall watershed. The calculated soil loss from the Lucky Hills watershed was $-4.3 \text{ t ha}^{-1} \text{ a}^{-1}$, while the calculated soil loss from the Kendall watershed was $+0.1 \text{ t ha}^{-1} \text{ a}^{-1}$ (which was not statistically significantly different from zero). These rates are similar to soil losses calculated from the suspended sediment loads measured at the flumes on these watersheds [41].

Differences in erosion rates between the two watersheds appear to be related largely to vegetation, while within watersheds variation in hillslope erosion rates appeared to be controlled by surface rocks. There was a significant positive linear relationship between soil erosion and percent rock fragments in both Kendall and Lucky Hills (Fig. 5). Less erosion in the areas with more rock fragments may be explained by the reduction of sediment transport capacity of flow with increasing hydraulic resistance on rocky surfaces [46,47]. Vegetation differences appear to be related to the patchiness of the vegetation. The vegetation (grass) cover is greater, more uniform, and less patchy in the Kendall watershed than that of the Lucky Hills watershed, where shrubs were essentially single plants separated by relatively wide inter-plant bare soil spaces. Slope at sampling points and slope curvature did not appear to have a significant influence on the hillslope erosion rates.

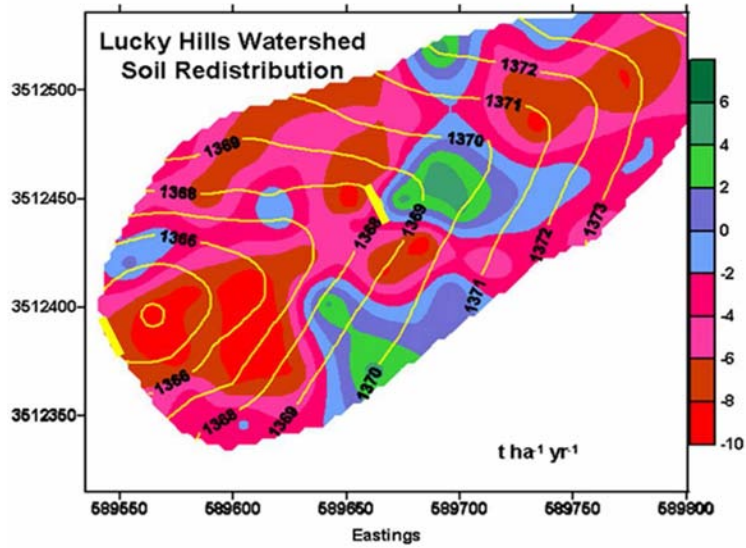


FIG.3. Soil redistribution patterns in the Lucky Hills subwatershed of the Walnut Gulch Experimental Watershed, Tombstone, Arizona, USA.

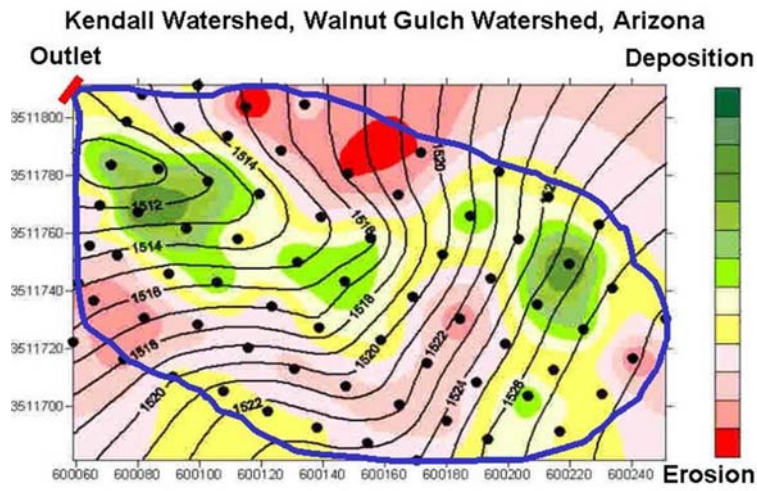


FIG.4. Soil redistribution patterns in the Kendall subwatershed of the Walnut Gulch Experimental Watershed, Tombstone, Arizona, USA.

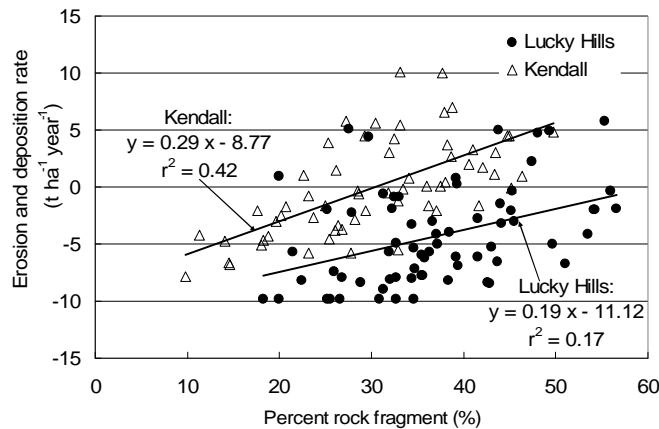


FIG. 5. Relationships between percent rock fragments in the upper 25 cm of the soil profile and calculated erosion and deposition rates in the Lucky Hills and Kendall watersheds [41].

The delivery of eroded soil to the outlet of each watershed appears to be due to differences in deposition between the two watersheds which were related to differences in the watersheds and drainage network morphology. The Lucky Hills watershed has a strongly incised channel network which facilitated transport of eroded sediments from the watershed. Conversely, the Kendall watershed had a swale area which slowed runoff, allowing much of the sediments in the runoff from the hillslopes to be deposited in the swale area before reaching the watershed outlet.

An important implication of this study is that sediment yield from a watershed may have little to do with actual rates of soil erosion rates (soil redistribution) and patterns within the watershed. The results from this study for the Kendall watershed are illustrative of that point. Even though the net soil loss from the watershed from the sediment budgets was negligible, and even though past actual measurements show sediment yield rates to be quite small, there was net soil erosion on 50% or more of the Kendall watershed area at rates as high as $7.9 \text{ t ha}^{-1} \text{ a}^{-1}$. Hillslopes at Kendall have been eroding over the past 40 years, even though very little sediment is being exported from the watershed at the site of the measuring flume.

3.2. Identification of Sediment Sources

Selected physical and chemical properties of the soils and suspended sediments (Tables 1 and 2) indicate that the particle size distributions of suspended sediments were finer than the watershed soils. For suspended sediments versus watershed soil properties, enrichment of clay content of the suspended sediments over the watershed soils ranged from 1.7 in subwatershed 3 to 1.0 in subwatershed 9 with an average 1.4 for all watersheds. This indicates that subwatershed 3 had the most erodible soils, and subwatershed 9 had the least erodible soils. Further, suspended sediments were enriched in silt-size material, relative to the clay fractions, in most subwatersheds by a factor of 2 to 3 times. These differences of particle size were probably due to the selectivity of soil erosion and sediment transport process to detach and move the finer particle sizes.

TABLE 1. SELECTED PHYSICAL AND CHEMICAL PROPERTIES IN SOILS AND SUSPENDED SEDIMENTS BY SUBWATERSHED. SUBWATERSHED/FLUME 1 IS THE OUTLET FLUME OF THE WALNUT GULCH EXPERIMENT WATERSHED. ALL SUBWATERSHEDS FLOW THROUGH FLUME 1. (ADAPTED FROM RHOTON et al. [21])

Subwatershed/Flume – Cover-	Clay (%)		Silt (%)		Organic Carbon (%)	
	Soils	Suspended Sediment	Soils	Suspended Sediment	Soils	Suspended Sediment
1	----	20.7	----	41.3	----	2.31
3 – Shrub	13.3	21.6	14.8	40.9	1.02	3.21
7 – Shrub	11.8	17.6	16.2	32.6	0.85	2.49
15 - Shrub	14.1	18.2	25.1	39.5	1.42	2.60
9 – Grass	16.3	15.7	18.4	33.7	1.21	1.99
10 – Grass	16.0	17.1	14.2	41.0	1.15	1.93
11 – Grass	13.3	16.8	13.6	32.0	1.18	2.16

TABLE 2. RADIONUCLIDE CONCENTRATIONS IN SOILS AND SUSPENDED SEDIMENTS BY SUBWATERSHED. SUBWATERSHED/FLUME 1 IS THE OUTLET FLUME OF THE WALNUT GULCH EXPERIMENT WATERSHED. ALL SUBWATERSHEDS FLOW THROUGH FLUME 1. (ADAPTED FROM RHOTON et al. [21])

Subwatershed/Flume Cover- Bq kg ⁻¹	¹³⁷ Caesium		⁴⁰ Potassium		²²⁶ Radium	
	Soils	Suspended Sediment	Soils	Suspended Sediment	Soils	Suspended Sediment
1	----	13.6	----	1098	----	85.1
3 – Shrub	11.2	9.1	620	1444	38.9	87.7
7 – Shrub	12.8	14.2	592	1239	25.7	75.8
15 - Shrub	12.8	18.5	515	1171	25.4	71.8
9 – Grass	14.2	10.5	581	1306	27.7	27.3
10 – Grass	16.5	7.0	737	1532	39.7	101.7
11 – Grass	11.1	12.7	498	1234	34.8	76.6

Organic carbon contents of the suspended sediments averaged 2.1 times higher than the watershed soils. Soil organic carbon varied significantly between subwatersheds with subwatershed 15 containing almost double the concentration of organic carbon as subwatershed 7 soils. Organic carbon contents of the suspended sediments averaged 2.4% compared to 1.1% for the watershed soils. Total soil nitrogen contents were closely related to organic carbon contents. The C/N ratios exhibited more mean separation between subwatersheds than the organic carbon and nitrogen components taken individually. C/N ratios were slightly higher in the suspended sediments than in the watershed soils.

The distribution of radionuclides in the watershed soils (Table 2) indicate that the ¹³⁷Cs concentrations ranged from 11.1 Bq kg⁻¹ (subwatershed 11) to 16.5 Bq kg⁻¹ (subwatershed 10) and averaged 13.1 Bq kg⁻¹ for all samples. The highest ¹³⁷Cs concentrations were found in subwatersheds with the highest clay contents. This is as expected since ¹³⁷Cs is rapidly and strongly adsorbed by the clay and organic matter fractions in soils and decreases exponentially with depth [40,48]. The ¹³⁷Cs concentrations in the suspended sediments were lower than the ¹³⁷Cs concentrations in the subwatersheds surface soils. This suggests that primary sediment sources are areas where rills, gullies, and streambanks erosion dominate rather than from sheet erosion of the surface soil.

The ⁴⁰K activities ranged from 515 Bq kg⁻¹ (subwatershed 15) to 737 Bq kg⁻¹ (subwatershed 10), and averaged 591 Bq kg⁻¹. These differences are probably due to parent material differences between watersheds. Wilson [49] showed that ⁴⁰K contents of igneous rocks are greater than sedimentary, and that granitic rocks were greater than basalt. Ibrahim et al. [50] reported ⁴⁰K concentrations in finer textured soils to be greater than sandy soils. Concentrations of ⁴⁰K averaged 1321 Bq kg⁻¹ in suspended sediments collected from the six subwatersheds indicating that the suspended sediments were enriched by a factor of 2.2 relative to the watershed soils.

3.3. Sediment Source Estimations

Physical and chemical properties of the suspended sediments were used with a mixing model to determine the relative contribution of each subwatershed to the suspended sediments

measured at flume 1. The shrub-dominated subwatersheds 3, 7, and 15 contributed 46%, 22%, and 18%, respectively while the grass dominated subwatersheds 9, 10, and 11 contributed only 4%, 6%; and 4%, respectively of the suspended sediments measured at Flume 1 at the outlet of Walnut Gulch Experimental Watershed (Fig. 1). Thus 86% of the suspended sediments leaving the Walnut Gulch Experimental Watershed originated from the shrub dominated subwatersheds 3, 7 and 15 with the other 14% coming from the grass dominated subwatersheds 9, 10, and 11. These shrub dominated subwatersheds had lower ground cover, lower clay content indicating more erodible soils, and are closest to flume 1, thus the suspended sediments contributed by these subwatersheds to the main channel does not undergo as much sorting prior to its delivery at flume 1. Also, the soils near flume 1 are similar to those in subwatershed 3. This could lead to an overestimation of the contribution from subwatershed 3. Some factors supporting the lower estimates of sediment source contributions from the grass dominated subwatersheds 9, 10, and 11 are greater ground cover, higher clay content indicating less erodible soils, and their greater distance from flume 1.

Stable carbon isotope (^{13}C) data (Data not shown) [21] indicate that 63.8% of the stable carbon isotopes in the suspended sediments at flume 1 are from C3 plant (shrubs) origin. At the flumes on the shrub dominated subwatersheds 3, 7, and 15, 68.1, 65.7, and 55.3% respectively of the stable carbon isotopes is from C3 plants. These data support the mixing model results which indicate subwatersheds 3, 7, and 15 are contributing most of the suspended sediments leaving Walnut Gulch Experimental Watershed at flume 1 and also suggest a strong relationship between stable carbon isotope composition, land cover, and soil erosion.

4. CONCLUSIONS

Both sediment budgets and sediment source analyses indicate that shrub dominated ecosystem are providing more suspended sediments at the Walnut Gulch Experimental Watershed than the grass dominated ecosystems. Sediment budgets and sediment source analyses using fallout ^{137}Cs provided useful data for understanding soil redistribution patterns and sediment sources areas to estimate which portions of the semiarid rangeland watershed are producing the suspended sediment loads in a stream. The sediment budget studies indicate that significant soil redistribution is occurring within the watershed before soil particles reach the watershed outlet, thus sediment yields measured at the outlet of a watershed may be a poor indicator of the magnitude of actual soil redistribution within a watershed.

Sediment source studies indicated that most of the suspended sediments measured at the outlet of the watershed were from shrub dominated subwatersheds. Expanding our sampling areas to include more eroding surfaces (i.e., streambanks, gully faces, etc.) as well as sheet erosion sites would allow inferences to be made about the relative contribution of streambank versus gully versus sheet erosion contributions from the subwatersheds. The ability to identify primary sediment sources in watersheds will contribute to a more efficient implementation of management practices to reduce pollutant loads, both suspended sediments and chemicals, from watersheds. Our studies suggest that management of these semiarid rangelands must consider techniques that will protect grass dominated areas from shrub invasion.

REFERENCES

- [1] TONGWAY, D.J., et al., Degradation and recovery processes in arid grazing lands in central Australia. Part 1: Soil and land resources, *J. Arid Environ.* **55** (2003) 301-326.
- [2] de SOYZA, A.M., et al., Indicators of Great Basin rangeland health, *J. Arid Environ.* **45** (2000) 289-304.
- [3] HERRICK, J.E., WHITFORD, W.G., Assessing the quality of rangeland soils: Challenges and opportunities, *J. Soil Water Conserv.* **50** (1995) 237-242.
- [4] NATIONAL RESEARCH COUNCIL, Rangeland Health: New methods to classify, inventory, and monitor rangeland, National Academy Press, Washington, DC, USA (1994).
- [5] WHITFORD, W.G., et al., Vegetation, soil, and animal indicators of rangeland health, *Environ. Monitor. Assess.* **51** (1998) 179-200.
- [6] LAL, R., et al., The potential of US cropland to sequester carbon and mitigate the greenhouse effect, Ann Arbor Press, Chelsea, Michigan, USA (1998).
- [7] RITCHIE, J.C., McCARTY, G.W., ¹³⁷Cesium and soil carbon in a small agricultural watershed, *Soil Tillage Res.* **69** (2003) 45-51.
- [8] McCARTY, G.W., RITCHIE, J.C., Impact of soil movement on carbon sequestration in agricultural ecosystems, *Environ. Pollut.* **116** (2002) 423-430.
- [9] RITCHIE, J.C., et al., Variability in soil redistribution in the northern Chihuahuan desert based on ¹³⁷Caesium measurements, *J. Arid Environ.* **55** (2003) 737-746.
- [10] SCHLESINGER, W.H., et al., Biological feedbacks in global desertification, *Sci.* **247** (1990) 1043-1048.
- [11] PIMENTEL, D.P., et al., Environmental and economic costs of soil erosion and conservation benefits, *Sci.* **267** (1995) 1117-1123.
- [12] SLATTERY, M.C., et al., The application of mineral magnetic measurements to quantify within-storm variations in suspended sediment sources, IAHS-AISH Publication **229** (1995) 143-151.
- [13] SUTHERLAND, R.A., BRYAN R.B., Variability of particle size characteristic of sheetwash sediments and fluvial suspended sediment in a small semiarid catchment, Kenya, *Catena* **16** (1989) 189-204.
- [14] WALLING, D.E., Tracing suspended sediment sources in catchments and river systems, *Sci. Total Environ.* **334** (2005) 159-184.
- [15] WALLING, D.E., Using environmental radionuclides as tracers in sediment budget investigations, IAHS-AISH Publication **283** (2003) 57-78.
- [16] WALLING, D.E., WOODWARD, J.C., 1992. Use of radiometric fingerprints to derive information on suspended sediment source, Erosion and sediment monitoring programmes in river basins, **210** (1992) 153-164.
- [17] SMITH, H.G., DRAGOVICH, D., Improving precision in sediment source and erosion process distinction in an upland catchment, south-eastern Australia. *Catena* **72** (2008) 191-203.
- [18] BONNIWELL, E.G., et al., Determining the times and distances of particle transit in a mountain stream using fallout radionuclides, *Geomorphol.* **27** (1999) 75-92.
- [19] WALLBRINK, P.J., et al., Relating suspended sediment to its original soil depth using fallout radionuclides, *Soil Sci. Soc. Am. J.* **63** (1999) 369-378.
- [20] NICHOLS, M.H., et al., Precipitation changes from 1956 to 1996 on the Walnut Gulch Experimental Watershed, *J. Am. Water Resour. Assoc.* **38** (2002) 161-172.
- [21] RHOTON, F.E., et al., Identification of suspended sediment sources using soil characteristics in a semiarid watershed, *Soil Sci. Soc. Am. J.* **72** (2008) 1102-1112.

- [22] OSTERKAMP, W.R., et al., Soils relative to geology and landforms in Walnut Gulch Experimental Watershed, Arizona, USA, *Water Resour. Res. Special Issue* (In press).
- [23] RHOTON, F.E., et al., Soil geomorphological characteristics of a semiarid watershed: Influence of carbon distribution and transport, *Soil Sci. Soc. Am. J.* **70** (2006) 1532-1540.
- [24] ALONSO, M.A. "Controls on erosion, sub-basins of Walnut Gulch, Arizona", *Proceedings of Conference on Management of Landscapes Disturbed by Channel Erosion*, (WANG, S., et al., Ed.), Center for Computational Hydroscience and Engineering University of Mississippi, Oxford, MS, USA (1997), 861-866.
- [25] GELDERMAN, F.W., *Soil Survey: Walnut Gulch Experimental Watershed, Arizona*, USDA-SCS Special Report. U.S. Government Printing Office, Washington, DC, USA (1970).
- [26] SIMANTON, J.R., TOY, T.J., The relation between surface rock-fragment cover and semiarid hillslope profile morphology, *Catena* **23** (1994) 213-225.
- [27] SIMANTON, J.R., et al., Spatial distribution of surface rock fragments along catenas in semiarid Arizona and Nevada, USA, *Catena* **23** (1994) 29-42.
- [28] WELTZ, M.A., RITCHIE, J.C., FOX, H.D., Comparison of laser and field measurements of vegetation heights and canopy cover, *Water Resour. Res.* **30** (1994) 1311-1320.
- [29] OSBORN, H.B., SIMANTON, J.R., Runoff estimates for thunderstorm rainfall on small rangeland watersheds, *Hydrol. Water Resour. Arizona and the Southwest* **13** (1983) 9-15.
- [30] RENARD, K.G., et al., Agricultural impacts in an arid environment: Walnut Gulch studies, *Hydrol. Sci. Technol.* **9** (1993) 145-190.
- [31] SCHOENEBERGER, P.J., et al., *Field book for describing and sampling soils*. Version 2.0, Natural Resources Conservation Service, National Soil Survey Center, Lincoln, Nebraska, USA (2002).
- [32] BRECKENFELD, D.J., SVETLIK, W.A., MCGUIRE, C.E., *Soil survey of Walnut Gulch Experimental Watershed*. U.S. Department of Agriculture, Soil Conservation Service, Washington, DC, USA (1995).
- [33] USDA-NATURAL RESOURCES CONSERVATION SERVICE, *Soil Survey Laboratory Methods Manual*, Soil Survey Investigations Report No.42. U. S. Government Printing Office, Washington, DC, USA (1996).
- [34] RITCHIE, J.C. Combining ¹³⁷Caesium and topographic surveys for measuring soil erosion/deposition patterns in a rapidly accreting area, *Acta Geologica Hispanica* **35** (2000) 207-212.
- [35] PLAYFORD, K., et al., *Radioactive fallout in air and rain: results to the end of 1991*, AEA-EE-0498, United Kingdom Atomic Energy Authority, Harwell, United Kingdom (1993).
- [36] CAMBRAY, R.S., et al., *Radioactive fallout in air and rain: Results to the end of 1988*, AERE-R-13575, U.K. Atomic Energy Authority Report, Harwell, United Kingdom (1989).
- [37] CARTER, M.W., MOGHISSI, A.A., Three decades of nuclear testing, *Health Phys.* **33** (1977) 55-71.
- [38] WALLING, D.E., HE, Q., Model for converting ¹³⁷Cs measurements to estimates of soil redistribution on cultivated and uncultivated soils, and estimating bomb-derived ¹³⁷Cs reference inventory (Including Software for Model Implementation). A contribution to the International Atomic Energy Agency Coordinated Research Programmes on Soil Erosion (D1.50.05) and Sedimentation (F3.10.01), Department of Geography, Exeter, United Kingdom (2001).

- [39] WALLING, D.E., HE, Q., Improved models for estimating soil erosion rates from Caesium-137 measurements, *J. Environ. Qual.* **28** (1999) 611-622.
- [40] RITCHIE, J.C., MCHENRY, J.R., Application of radioactive fallout Caesium-137 for measuring soil erosion and sediment accumulation rates and patterns: a review, *J. Environ. Qual.* **19** (1990) 215-233.
- [41] NEARING, M.A., et al., Spatial patterns of soil erosion and deposition in two small, semi-arid watersheds, *J. Geophys. Res. F: Earth Surface* **110** (2005) Article Number F04020.
- [42] RITCHIE, J.C., et al., Patterns of soil erosion and redeposition on Lucky Hills Watershed, Walnut Gulch Experimental Watershed, Arizona, *Catena* **61** (2005) 122-130.
- [43] WALLING, D.E., et al., A multi-parameter approach to fingerprinting suspended sediment sources, *Tracers in hydrology. Proc international symposium, Yokohama*, **215** (1993) 329-338.
- [44] WALLBRINK, P.J., et al., Measuring soil movement using ¹³⁷Cs: Implications of reference site variability, *Internat. Assoc. Hydrol. Sci. Publ.* **224** (1994) 95-102.
- [45] SUTHERLAND, R.A., Caesium-137 soil sampling and inventory variability in reference samples: Literature survey, *Hydrol. Process.* **10** (1996) 43-53.
- [46] NEARING, M.A., et al., Soil erosion by surface water flow on a stony, semiarid hillslope. *Earth Surf. Process. Landforms* **24** (1999) 677-686.
- [47] POESEN, J., et al., Concentrated flow erosion rates as affected by rock fragment cover and initial soil moisture content. *Catena* **36** (1999) 315-329.
- [48] CREMERS, A., et al., Quantitative analysis of radiocaesium retention in soils, *Nature* **335** (1998) 247-249.
- [49] WILSON, J.W., et al., Atmospheric ionizing radiation and human exposure, NASA Center for Aerospace Information (CASI), Hanover, Maryland, USA, (2005).
- [50] IBRAHIM, N.M., et al., Measurement of radioactivity levels in soil in the Nile delta and Middle Egypt, *Health Phys.* **64** (1993) 620-627.

USING TRACERS TO ASSESS THE IMPACTS OF SEDIMENT AND NUTRIENT DELIVERY IN THE LAKE BURRAGORANG CATCHMENT FOLLOWING SEVERE WILDFIRE

S. WILKINSON, P. WALLBRINK

Division of Land and Water,

Commonwealth Scientific and Industrial Research Organisation (CSIRO),

Canberra, Australia

W. BLAKE

University of Plymouth,

Plymouth, United Kingdom

R. SHAKESBY, S. DOERR

University of Wales,

Swansea, United Kingdom

Abstract

The paper summarises the findings of a four year project utilising fallout radionuclide's and geomorphologic methods to investigate the impacts on water quality of sediments and nutrients released following the 2001 bushfires to the Lake Burragorang catchment. This is the principal water supply for the city of Sydney which is the capital of the state of New South Wales, Australia. Three tracer budgets (^{137}Cs , $^{210}\text{Pb}_{\text{ex}}$ and ^7Be) were constructed and showed that significant amounts of mineral and organic sediment and attached nutrients were eroded from burnt hillslopes in the months following the fires. Some storage on flatter footslope areas indicates the capacity for these areas to act as hillslope sediment buffers. The fire had a large impact on the characteristics of sediment delivered to the river network and the reservoir. A comparison of ^{137}Cs and $^{210}\text{Pb}_{\text{ex}}$ concentrations on eroded surface soil and river sediments showed that a high proportion of the post-fire river sediment was derived from surface erosion of hillslopes, in contrast to the pre-fire sediment sources which were dominated by erosion of sub-surface material from rivers and gullies. The characteristics of post-fire river sediment returned towards pre-fire conditions over four years as the pulse of sediment was stored and evacuated from the river network. The below-average rainfall and runoff in the post-fire period of vegetation recovery however, limited the total post-fire sediment yield to Lake Burragorang well below the potential yield that could have occurred in wetter conditions. The sediment and nutrient yields to Lake Burragorang in post-fire runoff events were one to two orders of magnitude larger than in pre-fire conditions due to the increased availability of sediment and nutrients. Monitoring the potential for phosphorus-fuelled algal blooms following post-fire runoff events may be an important post-fire water quality management strategy.

1. INTRODUCTION

Fire has an impact on soil erosion as well sediment and nutrient redistribution by removing vegetation and surface litter cover, and to a lesser extent by affecting soil wettability; thereby increasing runoff. The literature (c.f. references in reviews by [2, 3] shows considerable variation in the impacts on hillslope sediment yield following Australian forest fires; with both large and negligible increases on pre-fire sediment delivery rates being recorded depending on fire severity. The impact of fire on sediment yield was also found to be determined by the extent to which post-fire rainfall events exceeded the erosion resistance of catchments during the post-fire recovery of litter and ground vegetation cover, soil structure and soil wettability. Elevated nitrogen, phosphorus, calcium, magnesium and potassium concentrations have been observed after wildfire, because of their release in combustion, and their affinity for fine sediment particles.

Lake Burragorang drains the Warragamba catchment and is the principal water supply storage for Sydney, NSW, Australia. It was subject to extreme wildfire in January 2002 which covered 225,000 ha and was the largest in the catchment in over 30 years. The aim of this project was to use measurements of fallout radio nuclides (^{137}Cs , $^{210}\text{Pb}_{\text{ex}}$ and ^7Be) as well as contemporary geomorphic approaches to investigate the transfer of sediments and nutrients between different components of the Nattai River sub catchment slopes to Lake Burragorang reservoir continuum following the major wildfire. An investigation of the combustion of vegetation at the field site, coupled with analysis of remote sensing data, indicated that the fire was of high to extreme severity over much of the burnt area [4,5]. There were several significant rainfall events in the weeks following the fire that delivered a pulse of black post-fire sediment to the river network draining the burnt area [4]. Consequently the three major tasks of this project were to:

- Use tracer budgets to investigate and quantify the redistribution of soil/sediment and attached nutrients that occurs within, and from, severely burnt hillslopes in the Sydney catchment.
- Determine the downstream impacts of post-fire erosion and sediment movement on water quality (suspended sediment and nutrients) in the immediate post-fire period.
- Compare the longer term impacts of post-fire sediment/nutrient losses over the lifespan of Lake Burragorang to that during periods of non-fire catchment erosion.

2. MATERIALS AND METHODS

2.1. Study area

The Lake Burragorang catchment lies within the Nattai National Park and is located approximately 100 km south-west of Sydney (Fig. 1). The region comprises steep, densely forested gorge country, typical of the Blue Mountains. The geology of the area is dominated by the Hawkesbury Sandstone of the Permo-Triassic Sydney Basin. The Nattai River, Little River and Blue Gum Creek – a tributary of Little River – are the main drainages of the Nattai catchment. The confluence of the Nattai and Little rivers lies downstream of the southernmost fetch of the Nattai Arm of Lake Burragorang. This southeastern arm of Lake Burragorang is some 30 km south of Warragamba Dam, which is on the Wollondilly River near its confluence with the Nepean River. Lake Burragorang catchment (Fig. 1) has a series of gorges with watershed ridges and gently sloping to flat plateaux of resistant sandstone beds. The climate is humid temperate with moist summers and cool winters and no marked dry season. The long-term mean annual rainfall is 900-1000 mm, although extremes of 400 and 1600 mm have been recorded.

The Blue Gum Creek catchment was subjected to a range of bushfire intensities that were representative of those that applied to the broader region. It drains an area of 44.6 km² and has headwaters at Thirlmere Lakes to the east (Fig. 2). Topographic relief in Blue Gum Creek catchment is of the order of 200 m; ridge crests are close to 500 m above Australian Height Datum (AHD) and valley floors below 300 m (AHD). Geomorphic units in the valley sides comprise: gentle ridge top slopes/plateaux, steep bedrock exposures and cliffs, talus-strewn mid to lower slopes, and footslopes which merge with the distinct valley floors. Soils in the area range from loamy sands to sandy loams on the slopes, with sandy clay loams occurring in sheltered locations. Dark loamy organic material is common at the surface, varying in thickness from 1 to 2 cm on ridges, increasing in depth on lower mid-slopes, foot-slopes and the valley floor. These soils have been mapped as Rudosols and Tenosols [6].

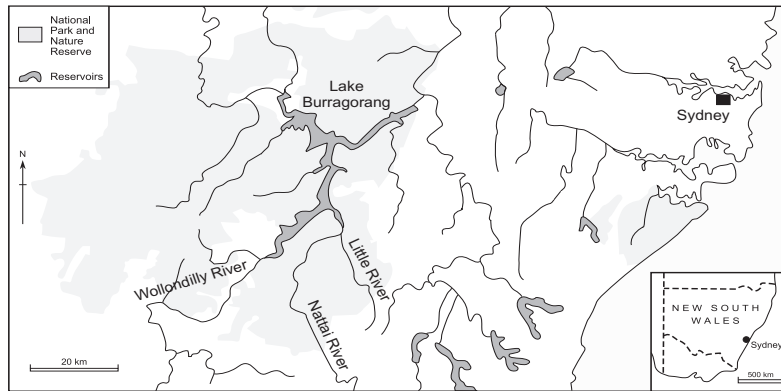


FIG. 1. Location of the study area, showing Little River and Nattai River to the south of Lake Burragorang.

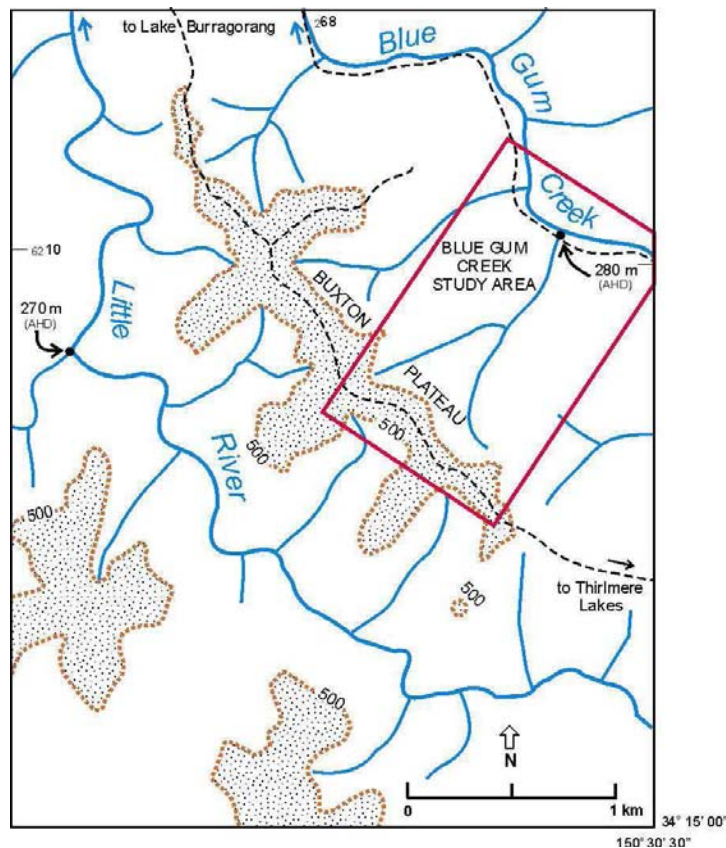


FIG. 2. Map of Lake Burragorang catchment showing the location of the Blue Gum Creek study area in which the hillslope process and sediment redistribution studies were undertaken.

The river network study encompassed the Little River and Nattai River and adjacent tributaries, and the impact on reservoir sedimentation focussed on the Nattai and adjacent Wollondilly arms of the reservoir [7].

Approximately 70% of the area has soil cover although this varies greatly between land units; the remaining 30% being exposed rock. Vegetation in the area is described as open dry Eucalypt woodland. The severely burnt south-western side of Blue Gum Creek was selected for the present study, the key features in this catchment are described in detail by [4]. In

addition to the research focus on the valley slope, ancillary sites not burnt in the fires were selected in surrounding ridgetop positions. These have similar soil and vegetation characteristics to corresponding slope positions in the catchment and were used as reference sites.

2.2. Quantification of post-fire material fluxes

The three phases of this project involved quantifying post-fire material (sediment and nutrient) fluxes at three scales in the lake Burragorang catchment; i.e. (1) the hillslope to river continuum, (2) the hillslope to downstream river network and (3) the hillslope to downstream receiving water body (i.e. the Nattai River delta). The research methods used at these three spatial scales are detailed below:

2.2.1. Hillslope tracer budgets

At the hillslope scale, measurements of fallout radionuclides ^{137}Cs , $^{210}\text{Pb}_{\text{ex}}$ and ^7Be were used to construct budgets quantifying the losses and redistribution of material within and between a series of geomorphic units of hillslope topography in the large rainfall events that occurred in the months following the fires [7,8,9]. These were i) the depositional fan, ii) the lower slope riparian zone, iii) a Pleistocene era depositional fan, iv) the sideslopes with slope angle >110 , and v) the ridgetop and plateau areas. Independent measurements of hillslope erosion and redistribution processes using erosion bridges and geomorphic investigations were also conducted to develop knowledge of post-fire processes [4,10].

2.2.2. Downstream sediment impacts

Radionuclide sediment tracers were used to quantify the spatial and temporal trends in sediment and nutrient fluxes over a four-year period following the fires within the river network downstream of the burnt area. A mixing model was used to determine the mixture of surface and sub-surface sources based on ^{137}Cs and $^{210}\text{Pb}_{\text{ex}}$ activities (Bq kg^{-1}) and how the contribution from these sources has changed over time [10]. Sediment particle magnetic characteristics were used as an additional tracer of surface sediment from burnt areas [11]. Sediment geochemistry was used to investigate the fire impact on phosphorus movement. Water quality monitoring data was also used to understand the event scale temporal dynamics of post-fire erosion on sediment and nutrient transport within the river network [12]. The sampling locations of deposited and river channel sediment are given in Fig. 3.

2.2.3. Hillslope to downstream water body

The long term contribution to reservoir sedimentation of fire relative to non-fire processes was investigated by reconstructing the chronology and source characteristics of sediment from cores and deposited sediment samples collected from the Nattai and Wollondilly arms of Lake Burragorang. The signature of the deposited sediments was compared against the signatures of burnt and non-burnt source material. A combination of ^{137}Cs , $^{210}\text{Pb}_{\text{ex}}$ and ratios of fallout plutonium isotopes was used in this analysis, as well as sediment geochemistry and physical characterisation of core strata [12].

The project experimental design required five multi day field expeditions and analyses were conducted on over 700 sediment samples.

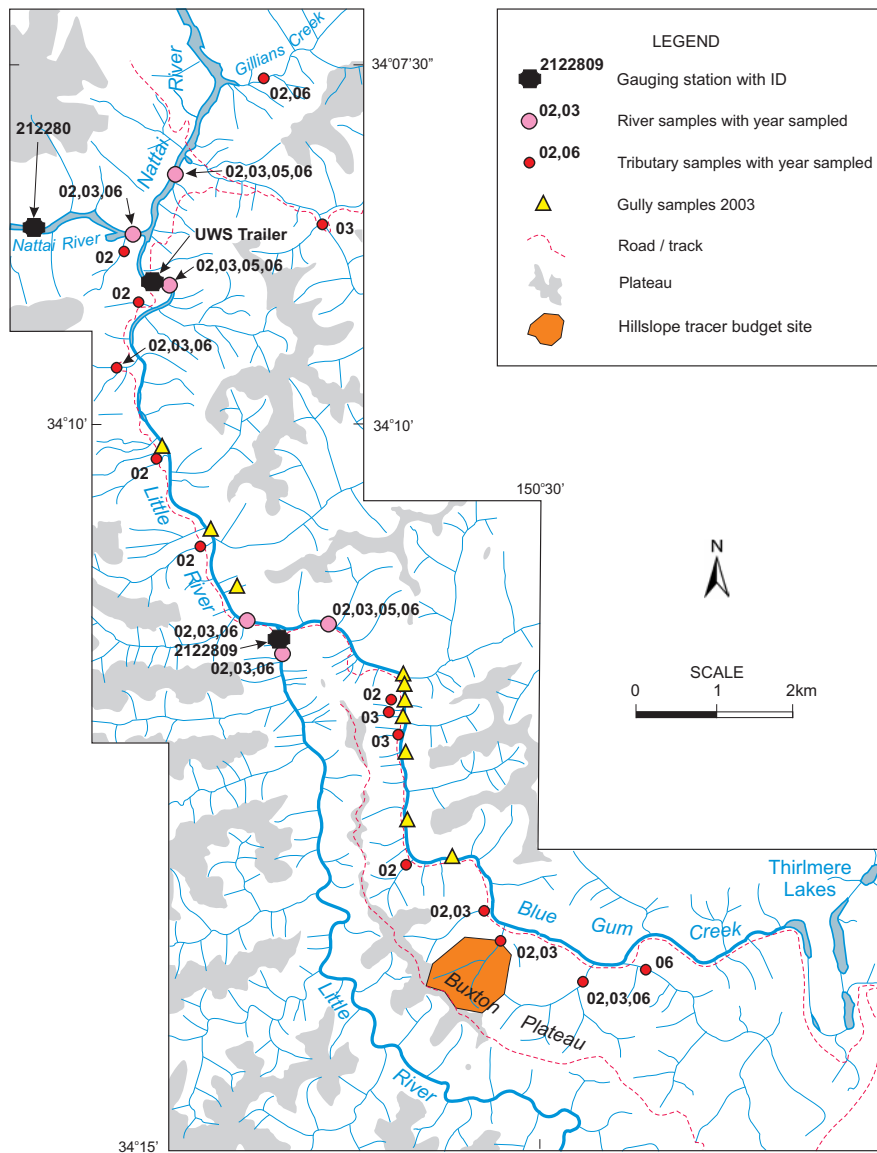


FIG. 3. Location of deposited river sediment samples and river gauges in the Nattai catchment.

3. RESULTS AND DISCUSSION

3.1. Fire extent and severity

The 2001 Sydney fires burnt 225 000 ha of eucalypt forest surrounding Lake Burragorang. Modelling of fire intensity based on fuel load biomass indicates extreme heat energy levels exceeding 70 000 kWm⁻¹. This extreme fire intensity was calculated from a combination of satellite imagery and field assessment, and corresponded to soil temperatures exceeding 350°C at depths averaging 1.5-2 cm and extensive consumption of woody vegetation [4].

By May 2002, large quantities of topsoil had been eroded from the burnt hillslopes and transported to the stream [4, 9]. Evidence of sediment movement was more prevalent in areas where the fire was of high severity than where the fire was of low severity. Some of the burnt topsoil and sub-surface material eroded from hillslopes was also deposited on lower gradient

footslopes. The spatial heterogeneity of soil wettability³ and widespread bioturbation on footslopes enhanced infiltration and so prevented larger amounts of hillslope transport from occurring.

3.2. Hillslope erosion and sediment redistribution

The Hillslope radionuclide budgets were constructed as per [7, 8], and show significant short term surface soil/sediment/ash redistribution on slopes in the Blue Gum Creek catchment. Erosion rates were highest on steep side slopes, and some deposition occurred on lower gradient foot-slopes adjacent to Blue Gum Creek [7, 8]. The estimated losses of the surface layers of litter and topsoil were several times those of the deeper sandy sub-soil layers [8, 13]. Independent soil erosion measurements support these findings, with erosion of sandy sub-soil 6.8-14.9 mm deep in some locations but deposition of similar magnitude elsewhere indicating generally local redistribution of sand-sized material. Litter dams and ant faunal activity were important factors in limiting sediment transport on hillslopes [4, 9]. In some places the fire also caused physico-chemical changes to sediment by fusing fine particles into sand-sized aggregates [14, 15]. These other factors and also spatial variability in soil wettability limited the erosion impact of fire-induced changes to soil wettability which have been found to be important elsewhere [16]. Comparisons between downstream sediment yields and hillslope erosion rates [17] also found that sediment storage on foot-slopes was an important buffer that constrained sediment delivery from the hillslope erosion to the river network. Importantly for the transport of nutrients, fine sediment and burnt organic material/ash were transported together [7].

3.3. Sediment and nutrient delivery to the river network

All the ¹³⁷Cs and ²¹⁰Pb_{ex} activities (Bq kg⁻¹) for sediment sources and river deposits (<10 µm fraction) are given in Fig. 4. The data show that the fire had a large impact on the characteristics of sediment delivered to the river network. The contribution of surface-derived material to river sediment in 2002 increased with the proportion of upstream catchment that was burnt, as illustrated in Fig. 5. In the Little River, with a completely burnt catchment, 84% of post-fire sediment was derived from surface erosion; in contrast Gillans Creek, with a very small proportion of catchment burnt, had less than 10% of sediment derived from surface erosion [10].

The sediment delivery to the river network in 2002 was approximately six times the pre-fire mean-annual rate in the fully burnt Little River catchment and 3 times the pre-fire amount in the partially burnt lower Nattai River [10, 18]. This result was supported by mineral magnetic analysis [19, 11]. Field observations indicate that the predominant sources of subsurface material in the catchment are gully and riverbank erosion. The gullies in this environment can be considered as part of the fluvial incision of the landscape rather than as a response to historical landuse change as they are on the tablelands. The erosion rates of the forested sandstone area are relatively high by Australian standards, which can be attributed to long term fluvial incision of the eastern Australian continental margin over the last 100 million years [20]. Declines in the radionuclide activities of river sediment towards pre-fire levels over the 4 years to March 2006 indicate that the majority of the post-fire sediment was delivered to the reservoir during this time, as shown in Fig. 6 [10].

¹Soil wettability is a dynamic soil property, which results from complex interactions between many other physical and chemical properties. As opposed to water repellency, soil wettability defines the ability of the soil to intake water.

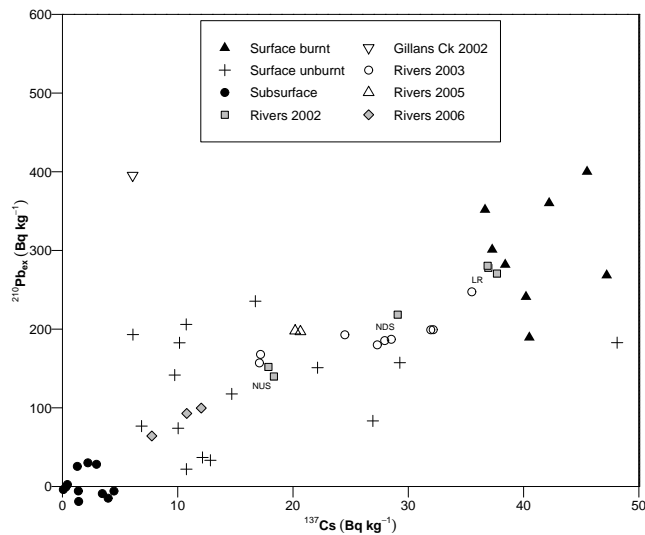


FIG. 4. ^{137}Cs and $^{210}\text{Pb}_{\text{ex}}$ activities for sediment sources and river deposits ($<10\ \mu\text{m}$ fraction). The data are corrected for radioactive decay from May 2002. The groups of 2002 river sediment are labelled LR=Little River, NUS=Nattai River upstream of Little River and NDS=Nattai River downstream of Little River.

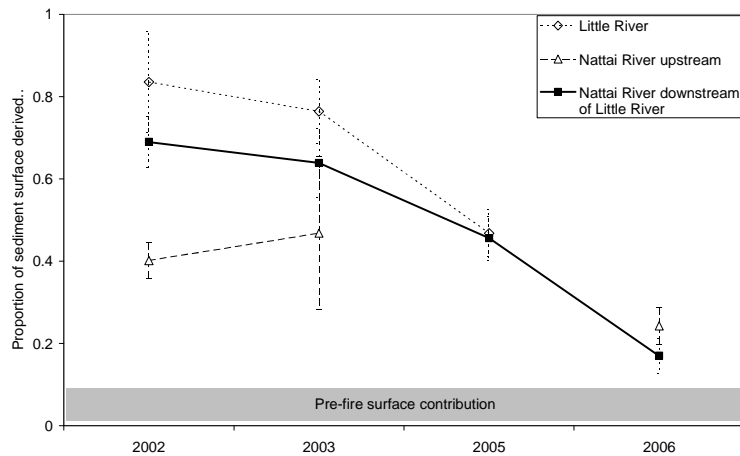


FIG. 5. Decline in the proportion of fine river sediment derived from surface erosion over the sampling period, for the Little River and for the Nattai River upstream and downstream of Little River. The error bars show 95% confidence intervals.

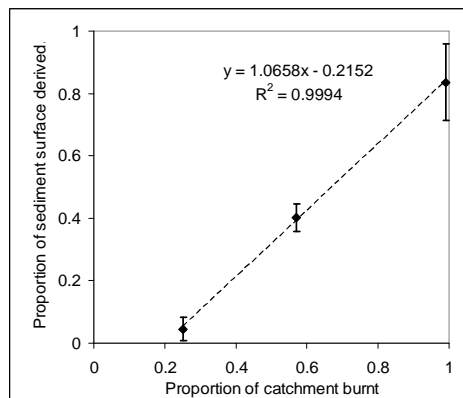


FIG. 6. Estimated proportions of river sediment that were derived from surface erosion in 2002. From left to right, the points correspond to Gillians Creek, Nattai River upstream of Little River, and Little River. The error bars show standard errors.

The post-fire concentrations of suspended sediment, phosphorus and nitrogen in Little River were much more sensitive to increasing runoff than before the fire, as a consequence of surface erosion being the dominant post-fire sediment source. The phosphorus concentration of river sediment in 2002 was six times that of pre-fire sources (Fig. 7).

Phosphorus was particularly associated with the organic fraction of sediment. This was attributed to the forest litter being consumed to ash and fused with forest soils during the fire and this fine surface material then having increased availability for transport in subsequent rainfall post-fire. Consequently, the post-fire transport of suspended sediment, phosphorus and nitrogen was much more rainfall event-driven. The yields from individual post-fire runoff events were 1–2 orders of magnitude higher than the yields for similar sized events before the fire (data not shown).

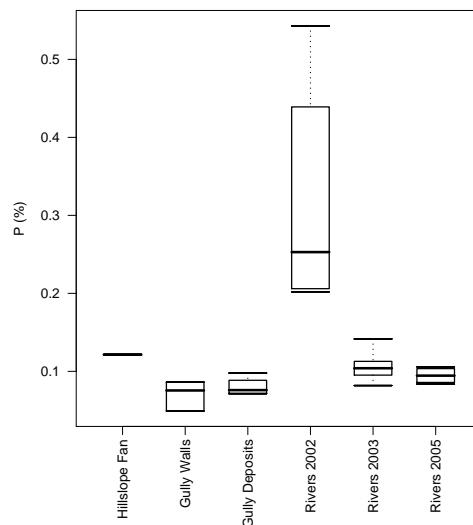


FIG. 7. Variation in P content of the <10 um fraction of sediment over time. The phosphorus concentration of river sediment in 2002 was six times that of pre-fire sources.

3.4. Sediment yields to the reservoir

Although the 2001 fire was of high to extreme severity, the post-fire period remained much drier than average, which limited post-fire erosion and sediment delivery from hillslopes [10], and also reduced the rate at which it was delivered to the reservoir. Independent of fire, the variability in runoff caused three orders of magnitude variation in annual sediment yield at the Nattai River gauge 212280; between one order of magnitude above and two orders of magnitude below the mean annual yield [4, 12, 21]. Consequently, although sediment delivery to the river network from the burnt area was several times the mean annual delivery, deposition of post-fire sediment in the Nattai and Wollondilly arms of the reservoir in 2002 was minor relative to pre-fire deposition [22]. The 2002 deposition was somewhat lower than the long term mean-annual rate of deposition since dam completion in 1960, and comprised less than 1–1.6% of total reservoir deposition [12].

Thus the erosion pulse associated with the fire event increased annual sediment yields from very low drought levels back towards the long term average. A worst case combination of severe fire and above-average runoff in the post-fire period could, however, have resulted in annual sediment yields two to three orders of magnitude above the mean yield.

Independent of the amount of sediment delivered from fires over the long term, the radically different characteristics of sediment released by post-fire erosion pose a risk to reservoir water quality. In particular the phosphorus concentration of post-fire sediment and the dissolved phosphorus concentration of post-fire runoff are both several times that of non-fire sources. Event yields of phosphorus can be 1–2 orders of magnitude larger after fire [10]. Therefore the risk of algal bloom in the reservoir is elevated after post-fire runoff events. Modelling the risk of algal bloom after post-fire runoff events, and also regular algae monitoring by direct measurement or remote sensing, may be useful methods for managing the risk of algal bloom to water quality.

4. CONCLUSIONS

From this study we concluded that the 2001 fires and subsequent rainfall triggered widespread erosion of hillslopes. The combustion of ground vegetation and forest litter also increased the hydrologic connectivity of hillslopes to streams. Steep side slopes and also plateaux were the major areas contributing post-fire sediment in the Blue Mountains sandstone terrain. It also appeared that lower gradient foot-slopes and riparian areas were the only hillslope units where net sediment deposition occurred. Therefore, preferential protection of riparian and foot slope areas from fire may be a useful strategy for buffering post-fire hillslope erosion from the river network.

The data suggested that post-fire sediment yields from the burnt area to the river network were approximately six times pre-fire levels, and that post-fire sediment was sourced predominantly from surface erosion rather than the erosion of sub-surface material from gullies and riverbanks characteristic of unburnt catchments. The post-fire river sediment contained several times more phosphorus than pre-fire sources. Sediment yields to the river network declined towards pre-fire levels over a four year period. The post-fire pulse in delivery of phosphorus was somewhat shorter than four years. Furthermore drier than average conditions in the post-fire period of vegetation recovery limited annual sediment yields to the reservoir to less than the long term average sediment yield in 2002, but greater than the yield that would have been experienced if the fire had not occurred.

We also conclude that after fire, individual runoff events can transport one to two orders of magnitude more sediment and nutrients than during pre-fire events. Therefore the risk of algal blooms may be elevated following post-fire runoff events. Modelling the risk of algal blooms after post-fire runoff events, and regular algal monitoring by direct measurement or remote sensing, may help identify the risks of algal blooms.

ACKNOWLEDGEMENTS

This research was part-funded by the Sydney Catchment Authority (SCA) and the UK Natural Environment Research Council (Grant Code: NER/A/S/2002/0043). Danny Hunt, Chris Leslie, Colin McLachlan and Paul Rustomji (CSIRO) provided technical assistance to the project. Gary Hancock and Vicky Farwig (University of Wales) contributed to the analysis of reservoir cores. Pauline English (CSIRO) contributed to data analysis and prepared Fig. 1. Chris Chafer, Bala Vigneswaran and Rob Mann (SCA) provided data and advice to the project.

REFERENCES

- [1] WALLBRINK, P., et al., Impacts on water quality by sediments and nutrients released during extreme bushfires: Report 1: A review of the literature pertaining to the effect of fire on erosion and erosion rates, with emphasis on the Nattai catchment, NSW, following the 2001 bushfires. Client Report, CSIRO Land and Water, Canberra, (2004),
http://www.clw.csiro.au/publications/consultancy/2004/nattai_catchment_fire_erosion.pdf
- [2] SHAKESBY, R.A., DOERR, S.H., Wildfire as a hydrological and geomorphological agent, *Earth-Science Reviews* 74 (2006) 269.
- [3] SHAKESBY, R.A., et al., Fire Severity, Water Repellency Characteristics and Hydrogeomorphological Changes Following the Christmas 2001 Sydney Forest Fires, *Australian Geographer* 34 (2003) 147-175.
- [4] CHAFER, C.J., et al., The post-fire measurement of fire severity and intensity in the Christmas 2001 Sydney wildfires, *International Journal of Wildland Fire* 13 (2004) 227-240.
- [5] ISBELL, (1996), *The Australian Soil Classification*, CSIRO, Melbourne, Australia (1996).
- [6] ENGLISH, P., et al., Impacts on water quality by sediments and nutrients released during extreme bushfires: Report 2: Tracer assessment of post-fire sediment and nutrient redistribution on hillslopes: Nattai National Park, NSW. Client Report, CSIRO Land and Water, Canberra, (2005),
<http://www.clw.csiro.au/publications/consultancy/2005/SCA-Report2.pdf>.
- [7] WALLBRINK, P.J., et al., "Using tracer based sediment budgets to assess redistribution of soil and organic material after severe bush fires", *IAHS Publ.* 292, IAHS Press, (2005), 223-230.
- [8] SHAKESBY, R.A., et al., "Hillslope soil erosion and bioturbation after the Christmas 2001 forest fires near Sydney, Australia.", *Soil erosion and sediment redistribution in river catchments*. P. N. Owens and A. J. Collins, CAB International, Wallingford, UK, (2006), 51-61.
- [9] WILKINSON, S., et al., Impacts on water quality by sediments and nutrients released during extreme bushfires: Report 3: Post-fire sediment and nutrient redistribution to downstream waterbodies, Nattai National Park, NSW. CSIRO Land and Water Science Report 64/06, Canberra, (2006a), 31 pp, www.clw.csiro.au/publications/science/2006/sr64-06.pdf.
- [10] BLAKE, W.H., et al., Magnetic enhancement in wildfire-affected soil and its potential for sediment-source ascription, *Earth Surface Processes And Landforms*, 31 (2006) 249-264.
- [11] WILKINSON, S., et al., Impacts on water quality by sediments and nutrients released during extreme bushfires: Report 4: Impacts on Lake Burragorang. CSIRO Land and Water Science Report 6/07, Canberra, (2007), 22 pp, <http://www.clw.csiro.au/publications/science/2007/sr6-07.pdf>.
- [12] SHAKESBY, R.A., et al., Distinctiveness of wildfire effects on soil erosion in south-east Australian eucalypt forests assessed in a global context, *Forest Ecology and Management* 238 (2007) 347-364.
- [13] BLAKE, W.H., et al., Impacts of wildfire on effective sediment particle size: implications for post-fire sediment budgets, *Sediment Budgets 1*, Seventh IAHS Scientific Assembly, Foz do Iguacu, Brazil, April 2005, *IAHS Publ.* 291, (2005), 143-150.

- [14] BLAKE, W.H., et al., Structural characteristics and behaviour of fire-modified soil aggregates, *Journal of Geophysical Research F: Earth surface*, 112 (2007) Article Number F02020
- [15] DOERR, S.H., et al., Effects of differing wildfire severities on soil wettability and implications for hydrological response, *Journal of Hydrology* 319 (2006), 295-311.
- [16] TOMKINS, K.M., et al., Contemporary versus long-term denudation along a passive plate margin, Australia: the role of extreme events, *Earth Surface Processes and Landforms*, 32 (2007) 1013-1031
- [17] WILKINSON, S., et al., A preliminary assessment of fire impacts on downstream water quality. Presentation to the Third RCM of Assessing the effectiveness of soil conservation techniques for sustainable watershed management using fallout radionuclides CRP D1.50.08, Vienna, Austria, 27-31 March, 2006.
- [18] BLAKE, W.H., et al., "Sediment redistribution following wildfire in the Sydney region, Australia: a mineral magnetic tracing approach", IAHS Publication 288, *Sediment Transfer through the Fluvial system*, IAHS Press, (2004) 52-59.
- [19] VAN DER BEEK, P., et al., Cenozoic landscape development in the Blue Mountains (SE Australia): lithological and tectonic controls on rifted margin topography, *Journal of Geology* 109 (2001) 35-56.
- [20] RUSTOMJI, P., WILKINSON, S., Estimated suspended sediment yields in the Lake Burrator catchment, *Journal of Geophysical Research*, (in review).
- [21] BLAKE, W.H., et al., "Using geochemical stratigraphy to indicate post-fire sediment and nutrient fluxes into a water supply reservoir, Sydney, Australia." IAHS Publication 306, *Sediment dynamics and the hydromorphology of fluvial systems*, Proceedings of an international conference at Dundee, Scotland, IAHS Press, (2006b), 363-370.

ASSESSMENT OF THE CONTRIBUTION FROM SURFACE EROSION OF FOREST FLOORS TO SUSPENDED SEDIMENT IN MOUNTAINOUS FORESTED CATCHMENTS IN THE TSUZURA WATERSHED, SOUTHERN JAPAN

Y. ONDA, S. MIZUGAKI, H. KATO
Laboratory of Integrative Environmental Sciences,
School of Life and Environmental Sciences,
University of Tsukuba,
Tsukuba, Japan

Abstract

In mountain areas of Japan overland flow and associated soil erosion from unmanaged forest plantations of Hinoki trees (*Chamaecyparis obtusa* (Siebold et Zucc.) Endl., Hinoki in Japan) seriously challenge the sustainability of watershed management. To identify the critical hot-spots for erosion and sources for suspended sediment the concentrations of fallout radionuclides such as ^{137}Cs and $^{210}\text{Pb}_{\text{ex}}$ were analyzed in a representative forested watershed (33 ha) in the Shimanto river basin located 700 km southwest of Tokyo. Soil sampling was conducted on hillslopes in various locations such as landslide scars, unmanaged plantations of Hinoki trees and unpaved forest roads and tracks. Additionally, detailed sampling in the stream bed and bank was carried out in several tributaries. The activities of ^{137}Cs and $^{210}\text{Pb}_{\text{ex}}$ of soils and fluvial sediments were determined by gamma-ray spectrometry. The radionuclides associated with potential source materials and mobilized sediment from the forest floor showed different properties according to the source type. The concentrations of ^{137}Cs and $^{210}\text{Pb}_{\text{ex}}$ of suspended sediment were found to lie between values given by the forest floor and river bed sediment. In the studied area of the unmanaged Hinoki plantation watershed the estimated contribution from the forest floor ranged from 31 to 55%. This suggests that forest floor should be recognized as the most important source of fluvial sediment in this watershed.

1. INTRODUCTION

In most forested hillslopes, precipitation infiltrates into the soil and Hortonian overland flow rarely generates due to the high infiltration rate of the top soil, resulting in the ground water flow and subsequent runoff to the stream. However, overland flow and resulting soil erosion in forest floors in unmanaged plantations of Japanese cypress (*Chamaecyparis obtusa* (Siebold et Zucc.) Endl., called 'Hinoki' in Japan) are a serious problem for sustainable watershed management in Japan. This is attributed to the dense coverage of the Hinoki tree canopies, limiting light penetration and the forest floor becoming too dark for normal growth of understory vegetation. In addition the litter from the Hinoki tree is easy to dissipate and susceptible to moving downward. Forest floors in unmanaged Hinoki plantations can be similar to bare land without any understory vegetation, and can therefore be subject to severe overland flow and associated surface soil erosion.

Surface soil erosion in unmanaged Hinoki plantations has been reported in the literature [1, 2, 3]. Miura et al. [2] investigated the sediment transport on the forest floor using sediment traps, suggesting that significant amounts of sediment were transported by raindrop impact. Nanko et al. [3] observed the amount of detached sediment by raindrops using splash cups and indicated that large kinetic energy associated with throughfall raindrops can enhance the splash erosion. These studies, however, have been conducted at plot or hillslope scale, and the contribution of sediment yield on the forest floor in unmanaged Hinoki plantations has never been evaluated at the watershed scale.

The fingerprinting approach using fallout radionuclides has been increasingly used to establish sediment sources in watershed scales in contrasting environments [e.g., 4, 5, 6, 7]. Fingerprinting of the suspended fine sediment is required to identify the relative contributions of the sources for developing sustainable watershed management in Japan. The purpose of this study is to estimate the contribution of the forest floor to the proportion of the suspended sediment yield in an unmanaged Hinoki watershed. The ^{137}Cs and $^{210}\text{Pb}_{\text{ex}}$ activities and other parameters such as organic matter content and particle size distribution in potential sources of surface soil and in suspended sediments were analyzed to ascertain the fluvial sediment sources in a forested watershed in southern Japan.

2. SAMPLING METHODS AND STUDY AREA

2.1. Study area

The study area is the headwater catchment (named as Hinoki 156) in the Tsuzura River watershed ($33^{\circ} 10' \text{ N}$, $132^{\circ} 57' \text{ E}$), a midstream tributary of Shimanto River basin, located 700 km southwest of Tokyo (Fig. 1). The average annual precipitation in the town of Taisho is 2735 mm and the mean annual temperature recorded at the Kubokawa weather station (17.5 km east of the site) was 14.6°C between 1979 and 2000. The catchment area is 33 ha ranging in elevation from 175 to 560 m above sea level. The bedrock of this area consists of sedimentary rocks of the Shimanto belt. The study area is dominated by Hinoki planted from 1965 to 1969. An unpaved truck road/trail with a length of c.a. 2.3 km and a width of 2 m to 4 m had been constructed around the area from 2001 to 2003. The density of the truck trails is 6 km km^{-2} .

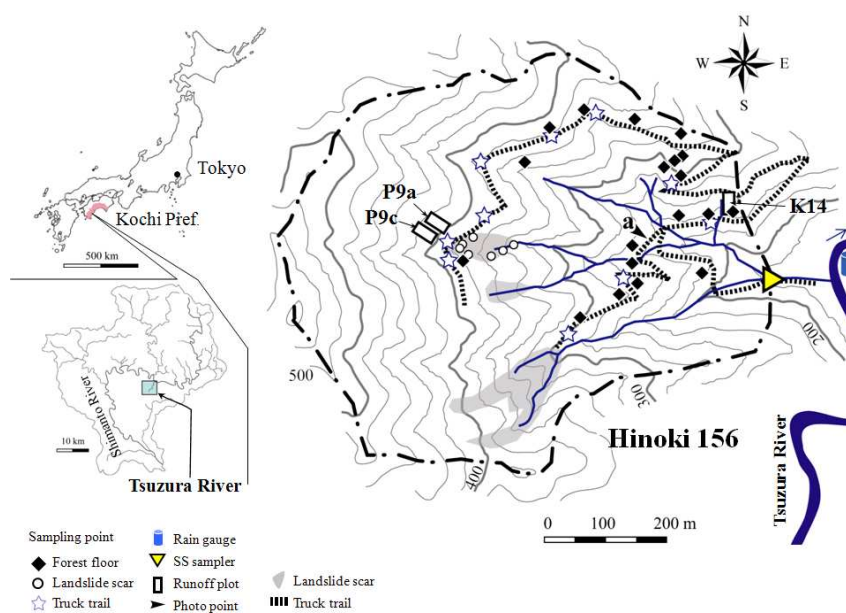


FIG. 1. Sampling points for potential sources. Suspended sediment sampler was placed at the outlet of the watershed.

2.2. Integrated suspended sediment sampler

There are many studies on fingerprinting of fluvial suspended sediment using ^{137}Cs , $^{210}\text{Pb}_{\text{ex}}$ and mineral composition [e.g., 7, 8, 9]. For fingerprinting studies using environmental radionuclides, however, it is important to obtain enough suspended sediment for analyzing its

radionuclide activities. In order to obtain the sample, a large amount of suspended sediment should be collected during the rainfall event, and filtered or centrifuged. Phillips et al. [10] developed a simple, inexpensive time-integrated suspended sediment sampler that employs the principles of sedimentation. Koga et al. [11] and Osanai et al. [12] conducted the sampling efficiency test of the sampler in a flume experiment, and found that the amount of suspended sediment obtained by the sampler linearly increases with flow velocity and sediment concentration. This suspended sediment sampler was adopted to collect the suspended sediment during the flood events (Fig. 2) at the outlet of watershed, and collected samples from June to November in 2004.



FIG.2. Suspended sediment sampler set in the stream at the outlet of the watershed.

2.3. Sampling methods

The possible sources of fine sediment to the river system were river banks, landslide scars, truck trails and the forest floor (Fig. 3). The soil sampling was conducted on hillslopes at various locations, such as landslide scars and the soil surface in unmanaged Hinoki plantations, and in the stream with detailed sampling in the river bed and banks of several tributaries. The source material samples were collected using a stainless core sampler (100 mL) with a diameter of 5 cm. To obtain an adequate number of samples for the analysis, core sampling was conducted several times at each sampling point and the surface materials (top 1 cm) were combined.

In order to observe overland flow on the floor in unmanaged Hinoki plantation forest, additionally three runoff plots (Fig. 4) were placed along the slope in Hinoki 156 (named as K14, P9a and P9c, with a size of 50 cm by 200 cm (170 cm for K14)). Overland flow was collected and the sediment transported by overland flow was trapped at the end of the plot. The sediment transported by the overland flow was trapped by a plankton net (pore size: 0.075 mm) at the outlet of the plot and collected from August 2004 to August 2006. Rainfall intensity was also measured with a 0.2-mm tipping bucket rain gauge (RC-10; Davis Instruments Corp., California, USA); tip time was recorded with 0.5-s accuracy by a data logger (HOBO Event; Onset Computer Corp., MA, USA) close to the Tsuzura River near the outlet of Hinoki 156 watershed (Fig. 1). Furthermore, mobilized sediment by surface erosion and fluvial sediment on the forest floor was also collected during extreme rainfall events (typhoon) to investigate sediment routing from forest floor to the stream channel.

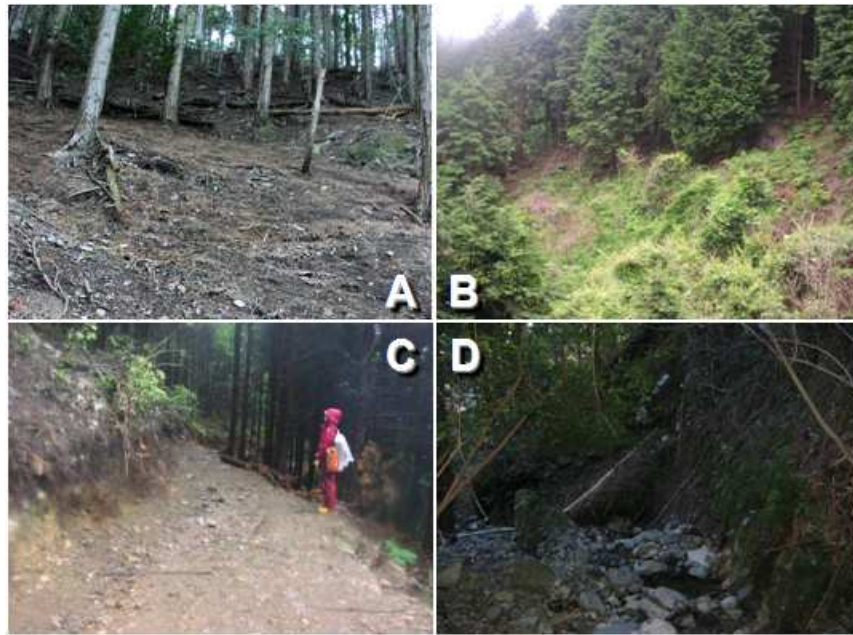


FIG. 3. Potential sources of suspended sediment. (A) Forest floor, (B) landslide scar, (C) truck trail, and (D) stream bank.



FIG. 4. Runoff plot system (A) established on the hillslope. The characters P, T, and R indicate the runoff plot, the tipping bucket for discharge measurement and the reservoir tank, respectively. (B) A detailed view on the runoff plot.

2.4. Radionuclide and other analyses

To measure the ^{137}Cs and $^{210}\text{Pb}_{\text{ex}}$ content, low-energy HPGe gamma spectrometers (Eurysis EGC-200-R; Eurysis EGC25-195-R) coupled with multi-channel analyzer gamma ray spectrometry were used at the laboratory in the University of Tsukuba. In gamma ray spectrometry, $^{210}\text{Pb}_{\text{ex}}$ activities are determined from the difference between total and supported ^{210}Pb activities [13]. Assuming equilibrium between ^{226}Ra and ^{222}Rn in the soil samples, the supported Pb-210 activity can be calculated from the activity of its short-lived daughter ^{214}Pb (half-life 27 minutes), which derives from ^{222}Rn in the ^{238}U decay series [13,14].

$$^{210}\text{Pb}_{\text{ex}} = (^{210}\text{Pb}_{\text{total}}) - (^{214}\text{Pb}) \quad (1)$$

The collected sediment samples were dried for 48 hours at 105 °C, sieved using a 2 mm open sieve, packed in a 100 cm³ plastic bin and sealed. These samples were sealed for more than five times the half-life period of ²²²Rn, or 21 days before analysis, to allow equilibrium to occur between ²²⁶Ra and ²²²Rn [13, 14]. For ¹³⁷Cs and excess ²¹⁰Pb analyses, the gamma activity of each sediment sample was measured for 43,200 to 86,400 seconds. Using a low-energy germanium detector, gamma activity was determined at the 661.6 keV photopeak for ¹³⁷Cs, 46.5 keV for total ²¹⁰Pb, and 352.0 keV photopeak for ²¹⁴Pb. All radionuclides detected were quantified as concentration (Bq kg⁻¹) from reference samples including ²¹⁰Pb and ¹³⁷Cs, and ¹⁵²Eu. The self-adsorption of gamma rays by the sample, and background effects during the measurement of gamma rays were calibrated by comparison with the reference samples. For the measurements of radionuclide activities of a small amount of suspended sediment samples, a well-type Ge detector (GCW 2521S of Canberra, Meriden, U.S.A.) from the National Institute for Agro-Environmental Sciences (Japan) was used. The energy and efficiency calibrations for this detector were carried out using a standard sample that included ²¹⁰Pb (46.5 keV), ⁵¹Cr (320.0 keV), ⁸⁵Sr (514.0 keV), ¹³⁷Cs (661.6 keV), and ⁵⁴Mn (834.8 keV).

To eliminate the effect of organic matter content on the ¹³⁷Cs or ²¹⁰Pb_{ex} associated with suspended sediment and potential source materials, the radionuclide activity associated with mineral fraction can be estimated as following:

$$C_{total} = C_m (1-OM) + C_{om} OM \quad (2)$$

where: C_{total} is total radionuclide activity associated with sediment or potential source material, C_m and C_{om} are radionuclide activity associated with mineral fraction and organic fraction, respectively, and OM is organic matter content of sediment or potential source material. C_{om} was measured using organic matter extracted from the surface soil of the forest floor in Hinoki 156, according to Wallbrink et al. [15].

In comparing the radionuclide content between suspended sediment samples and potential source materials for fingerprinting, it is important to take into account the difference due to the selective mobilization of fines. He and Walling [16] investigated the grain size effects in the adsorption of ¹³⁷Cs and unsupported ²¹⁰Pb by mineral soils, and they found a relationship between ¹³⁷Cs and unsupported ²¹⁰Pb and specific surface area. In order to remove this effect mentioned above, the particle-size correction factor P was proposed and can be calculated for each sample as following [16]:

$$P = (S_{ms} / S_{sl})^v \quad (3)$$

where: S_{ms} and S_{sl} are the specific surface area of mobilized sediment and original soil, respectively, and the exponent coefficient, v , is a constant with a value of 0.65 for ¹³⁷Cs and 0.76 for ²¹⁰Pb_{ex} for cultivated soil in the catchment of the Jackmoor Brook, Devon, UK, respectively.

In this study, the particle size distribution was measured by sieving for the sample larger than 425 μm and using the laser beam diffraction method for the samples smaller than 425 μm (Shimadzu SALD-3100, JAPAN) after hydrogen peroxide pretreatment. The Shimadzu SALD-3100 has a capacity of handling samples with grain size ranging from 0.05 to 3000 μm. The particles in the samples analyzed were classified into 51 size ranges. The specific surface areas of the samples were estimated using their grain size distribution and the spherical approximation of the particles in each class. The particle size composition of the

>425 μm fractions was obtained by sieving. It is stressed that the values of specific surface area calculated in this manner provide only approximate estimates.

Using the equation (3) and the ν value of 0.65 for ^{137}Cs and 0.76 for $^{210}\text{Pb}_{\text{ex}}$, respectively, the P values were calculated from the specific surface area of each sediment and source material. The specific surface area of the suspended sediment collected in the fourth period was adopted as S_{ms} . The corrected ^{137}Cs or $^{210}\text{Pb}_{\text{ex}}$ activity for each sample can be obtained by multiplying P by the mineral-associated ^{137}Cs or $^{210}\text{Pb}_{\text{ex}}$ activity (C_m) obtained in the equation (2). The organic matter content was also analyzed by measuring ignition loss after heating each sample at 450°C for 4 hours.

3. RESULTS

3.1. Radionuclides activities associated with potential source materials

The corrected ^{137}Cs and $^{210}\text{Pb}_{\text{ex}}$ activities, in which the effects of organic matter content and particle size were eliminated, showed different ranges for each potential source (Fig. 5). The forest floor exhibited high values of ^{137}Cs and $^{210}\text{Pb}_{\text{ex}}$ activities with a high variation, ranging from 19.6 Bq kg^{-1} to 114.4 Bq kg^{-1} for ^{137}Cs and from 84.9 Bq kg^{-1} to $1568.4 \text{ Bq kg}^{-1}$ for $^{210}\text{Pb}_{\text{ex}}$. The landslide scar exhibited corrected ^{137}Cs activities from 22.5 Bq kg^{-1} to 59.1 Bq kg^{-1} and corrected $^{210}\text{Pb}_{\text{ex}}$ activities from 180.1 Bq kg^{-1} to 401.1 Bq kg^{-1} , overlapping the low range of radionuclides activities of the forest floor. The truck trail exhibited lower corrected values of ^{137}Cs and $^{210}\text{Pb}_{\text{ex}}$ than those of the forest floor and the landslide scar: $<20.5 \text{ Bq kg}^{-1}$ for ^{137}Cs and $<188.5 \text{ Bq kg}^{-1}$ for $^{210}\text{Pb}_{\text{ex}}$. For the materials of the stream bank, the $^{210}\text{Pb}_{\text{ex}}$ activities were $<117.1 \text{ Bq kg}^{-1}$, as low as that for the truck trails; however, ^{137}Cs activities were not detected.

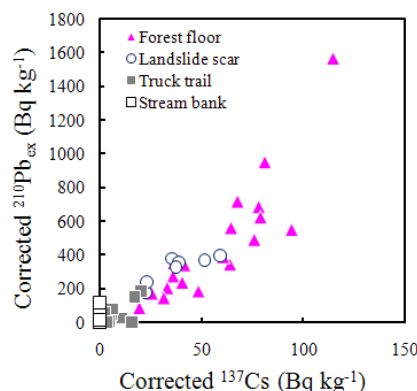


FIG. 5. Corrected ^{137}Cs and $^{210}\text{Pb}_{\text{ex}}$ activities of potential source materials.

3.2. Radionuclides activities associated with suspended sediments

The amount of suspended sediment and its organic matter content collected with the time-integrated suspended sediment sampler varied in each period. The amount of suspended sediment ranged from 0.7 g to 7.4 g. The organic matter content of suspended sediment ranged from 12.5% to 38.6%. Both the amount of suspended sediment and organic matter content showed no correlation with total rainfall.

The corrected values of both ^{137}Cs and $^{210}\text{Pb}_{\text{ex}}$ associated with the suspended sediment lay between those of the forest floor and the stream bank, and were considerably lower than that

of the runoff sediment (Fig. 6). The corrected values associated with the suspended sediment and the potential source materials lie along a linear gradient, except for that of the suspended sediment in the fifth period, suggesting that the suspended sediment can be predicted from a range of combinations of all the sources. The average concentration of the plot sediment is about the same as the average forest floor samples. These results confirm that the potential source material collected by the core sampling method represents the actual sediment isotopic signals from sediment sources.

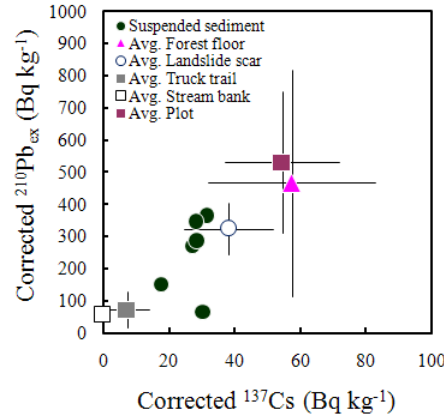


FIG. 6. Corrected ^{137}Cs and $^{210}\text{Pb}_{\text{ex}}$ activities of suspended sediment and potential sources. Error bars denote one sigma standard deviation.

4. DISCUSSION

Given the linearity in the relationship between ^{137}Cs and $^{210}\text{Pb}_{\text{ex}}$ activities associated with suspended sediment and potential source materials, a simple mixing model using a single parameter allowed fingerprinting of the suspended sediment. To estimate the contribution from the potential sources to suspended sediment using the simple mixing model, only two end-members should be chosen from among the potential sources: one with a higher radionuclide activity than suspended sediment, and the other with a lower activity. In this case, the higher radionuclide activities were found in the source material on the forest floor and lower in subsoil such as stream bank and truck trail (Fig. 6). If these forest floor and subsoil are adopted as the end-members, the contribution from forest floor (a) is calculated as follows:

$$a = \frac{C_{\text{ms}} - C_{\text{msub}}}{C_{\text{mf}} - C_{\text{msub}}} \quad (4)$$

where: C_{ms} is the corrected radionuclide activity associated with suspended sediment, and C_{msub} and C_{mf} are the average values of corrected radionuclide activity associated with the subsoil (stream bank and truck trail) and forest floor samples, respectively.

The contribution from forest floor calculated using ^{137}Cs and $^{210}\text{Pb}_{\text{ex}}$ as tracers in the equation (4) was plotted against the total rainfall during each observation period in Figure 7. Due to the higher variation in $^{210}\text{Pb}_{\text{ex}}$ activities associated with suspended sediment and potential sources than ^{137}Cs , the higher error can be introduced to the calculated contribution in the mixing model. The propagation error introduced from the equation (4) was significantly higher for $^{210}\text{Pb}_{\text{ex}}$ than for ^{137}Cs (Fig. 7). Therefore, in this case ^{137}Cs was the most useful tracer for estimating the contribution of forest floor to suspended sediment.

The contribution of the forest floor to the suspended sediment calculated by ^{137}Cs , ranged from 25% to 51%, and seemed to be almost constant and independent of rainfall events (Fig. 7). This result suggests that the forest floor can be considered as one of the most important sources of suspended sediment in the unmanaged Hinoki plantation watershed. It should be noted that although a low contribution (25%) of the forest floor was found in the fifth period, turbid water running through the truck trail and collapse of the stream bank were observed by field inspection. Therefore, the low value of forest floor contribution may be attributed to the erosion and collapse of the truck trail network (Fig. 8).

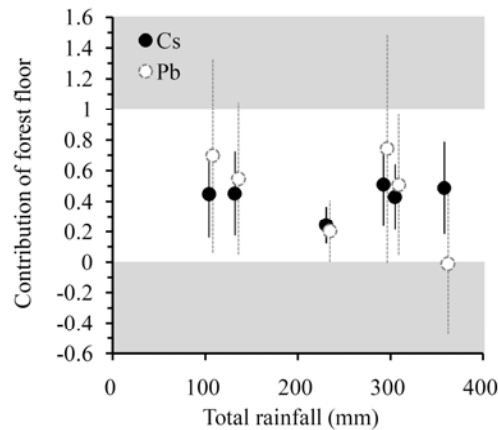


FIG. 7. Contribution of forest floor to suspended estimated by ^{137}Cs and $^{210}\text{Pb}_{ex}$. Error bars denote the propagation error in the calculation in Eq. (4). Gray zone denotes the area of the contribution of forest floor over than 1 and less than 0.



FIG. 8. Eroded truck trail after the typhoon event.

The average contribution over six periods was evaluated. For the calculation of average contribution, the value of radionuclide activity for each period should be weighted by the amount of suspended sediment sample, because the trapped sediment in the time-integrated suspended sediment sampler can increase with the suspended sediment concentration and/or flow velocity [11,12]. Then, the weighted average contribution is calculated based on the weighted average values of the radionuclide activity, organic matter content, and specific surface area of the suspended sediments derived from the following equation:

$$C_{\text{avg}} = \frac{\sum_{i=1}^6 C_{\text{si}} w_i}{\sum_{i=1}^6 w_i} \quad (5)$$

where: C_{avg} is the weighted average concentration of the radionuclide activity associated with the suspended sediments, C_{si} is the corrected radionuclide activity associated with the suspended sediments collected during period i , and w_i is the amount of suspended sediments collected during period i .

The weighted average values of the organic matter content and specific surface area are also calculated in the same way as that in Eq. (5). By using these weighted average values of the corrected radionuclide activities, organic matter content, and specific surface area, the relative contribution of the forest floor throughout the observation period can be calculated from the equations (2), (3), (4), and (5). The average contributions calculated from ^{137}Cs and $^{210}\text{Pb}_{\text{ex}}$ were 46% and 50%, respectively. The average contributions calculated by ^{137}Cs and $^{210}\text{Pb}_{\text{ex}}$ are almost identical, suggesting that $^{210}\text{Pb}_{\text{ex}}$ would be useful to fingerprint the suspended sediments when a sufficient amount of the suspended sediment sample can be collected.

Many researchers have indicated that forest road networks (including logging roads and truck trails) can be the dominant source of suspended sediment. Wemple et al. [17] investigated the erosion types and sediment budgets associated with forest road networks during an extreme storm event in two managed forested watersheds in Oregon. They indicated that fillslope cutting was the dominant process in the production of the sediment associated with the forest road. They also indicated that sediment interception and storage by roads was an important aspect in that study. Motha et al. [7] investigated the source composition of the suspended sediment for several rainfall events using tracers, including ^{137}Cs and $^{210}\text{Pb}_{\text{ex}}$, in a forested catchment in Australia. They indicated that the mean sediment contribution from undisturbed forest was 50% to 70%, but an unpaved road can be an important sediment source on a per unit area basis. Sidle et al. [18] assessed the effect of connectivity between truck trail networks and stream channels on the sediment budget in a tropical forested watershed after logging and indicated that truck trails can trap and store the sediment from upslope.

On the truck trail networks in the Hinoki 156 watershed it was often observed that the sediment from the upslope was transported and trapped by fluvial processes and gravity, and stored during the no-rainfall period (Fig. 3C). During rainfall, overland flow is easily generated on the truck trail networks, resulting in deep gully erosion and providing low ^{137}Cs and $^{210}\text{Pb}_{\text{ex}}$ sediments to the stream channel (Fig. 8). The overland flow on the truck trail networks can transport the material deposited on the road surface and the sediment from the upslope to the downslope and/or the stream channel [18]. Therefore, the truck trail networks can play a role as both pathway and source to the stream channel, resulting in low levels of radionuclides in the suspended sediment.

5. CONCLUSIONS

In this study, the fingerprinting of suspended sediment using radionuclides was conducted to estimate the contribution of the forest floor in unmanaged Hinoki (Japanese cypress) plantations to the production of sediments in suspension in the Tsuzura watershed in southern Japan. The ^{137}Cs and $^{210}\text{Pb}_{\text{ex}}$ activities associated with potential source materials and mobilized sediment from the forest floor showed different radionuclides properties according

to the source type. By comparing the radionuclides properties between potential source materials and suspended sediment, the suspended sediment was judged to originate from two source types: (1) surface material such as the forest floor, and (2) subsoil such as the stream bank or truck trail. A simple mixing model using fallout nuclide was found to be available to evaluate the contribution of forest floor to suspended sediment for each observation period. The contribution of forest floor to suspended sediment ranging from 25% to 51% with 46% in average indicated that the forest floor is an important sediment source. Furthermore, overland flow generated on the truck trail during the extreme typhoon event suggested the indirect input of sediment from the forest floor to the stream channel through truck trail networks. The results obtained in this study can contribute toward the understanding of water and sediment routing in the watershed and sediment or nutrient budget. This knowledge could be applied to the evaluation of the effect on the water quality and ecology downstream.

ACKNOWLEDGEMENTS

The manuscript is a contribution as IAEA research agreement JPN/12391 to the CRP on 'Assessing the effectiveness of soil conservation techniques for sustainable watershed management using fallout radionuclides (D1.50.08)'. This study was partially supported by a grant from Japan Science and Technology Agency to the CREST research project 'Field and modelling studies on the effect of forest devastation on flooding and environmental issues'. The authors are grateful for the field assistance provided by the students of the graduate school of Life and Environmental Sciences, University of Tsukuba.

REFERENCES

- [1] MIHARA, Y., Raindrop and soil erosion, *Bulletin of the National Institute of Agricultural Sciences* **A-1** (1951) 1–59 (in Japanese with English summary).
- [2] MIURA, S, et al., Transport rates of surface materials on steep forested slopes induced by raindrop splash erosion, *Journal of Forestry Research* **7** (2002) 201–211.
- [3] NANKO, K., et al., Estimation of soil splash detachment rates on the forest floor of an unmanaged Japanese cypress plantation based on field measurements of throughfall drop sizes and velocities, *Catena* **72** (2008) 348–361.
- [4] COLLINS, A.L., et al., Use of composite fingerprints to determine the provenance of the contemporary suspended sediment load transported by rivers, *Earth Surface Processes and Landforms* **23** (1998) 31–52.
- [5] COLLINS, A.L., et al., Using ^{137}Cs measurements to quantify soil erosion and redistribution rates for areas under different land use in the Upper Kaleya River basin, southern Zambia, *Geoderma* **104** (2001) 299–323.
- [6] WALLING, D.E., et al., Fingerprinting suspended sediment sources in the catchment of the River Ouse, Yorkshire, UK, *Hydrological Processes* **13** (1999) 955–975.
- [7] MOTHA, J.A., et al., Determining the source of suspended sediment in a forested catchment in southeastern Australia, *Water Resources Research* **39** (2003) 1056–1069.
- [8] ONDA, Y., et al., An experimental study identifying sediment sources using radio nuclides, *Journal of the Japan Society of Erosion Control Engineering* **50-4**: (1997) 19–24 (in Japanese, with English Abstract).
- [9] Wallbrink, P.J., et al., Determining sources and transit times of suspended sediment in the Murrumbidgee River, New South Wales, Australia, using fallout ^{137}Cs and ^{210}Pb , *Water Resources Research* **34** (1998) 879–887.

- [10] PHILLIPS, J.M., et al., Time integrated sampling of fluvial suspended sediment: a simple methodology for small catchments, *Hydrological Processes* **14** (2000) 2589–2602.
- [11] KOGA, S., et al. Experimental verification of the time-integrated suspended sediment sampler, *Bulletin of the Terrestrial Environment Research Center, the University of Tsukuba* **5** (2004): 109–114 (in Japanese).
- [12] OSANAI, N., et al., Experimental study on sampling efficiency of suspended load with time-integrated sampler, *TECHNICAL NOTE of National Institute for Land and Infrastructure Management* **266** (2005) 70 pp (in Japanese, with English Abstract).
- [13] JOSHI, S.R., Nondestructive determination of lead-210 and radium-226 in sediments by direct photon analysis, *Journal of Radioanalytical and Nuclear Chemistry* **116–1** (1987) 169–182.
- [14] MURRAY, A.S., et al., Analysis for naturally occurring radionuclides at environmental concentrations by gamma spectrometry. *Journal of Radioanalytical and Nuclear Chemistry* **115–2** (1987) 263–288.
- [15] WALLBRINK, P.J., et al., A tracer budget quantifying soil redistribution on hill slopes after forest harvesting, *Catena* **47** (2002) 179–205.
- [16] HE, Q., WALLING, D.E., Interpreting particle size effects in the adsorption of ¹³⁷Cs and unsupported ²¹⁰Pb by mineral soils and sediments, *Journal of Environmental Radioactivity* **30–2** (1996) 117–137.
- [17] WEMPLE, B.C., et al., Forest road and geomorphic process interactions, Cascade Range, Oregon, *Earth Surface Processes and Landforms* **26** (2001) 191–204.
- [18] SIDLE, R.C., et al., Sediment pathways in a tropical forest: Effects of logging roads and skid trails, *Hydrological Processes* **18** (2004) 703–720.

ASSESSMENT OF SOIL LOSSES FROM MANAGED AND UNMANAGED SITES IN A SUBCATCHMENT OF RAWAL DAM, PAKISTAN USING FALLOUT RADIONUCLIDES

M. RAFIQ, M. AHMAD, N. IQBAL, J.A. TARIQ, W. AKRAM
Pakistan Institute of Nuclear Science and Technology

M. SHAFIQ
National Agricultural Research Center

Islamabad, Pakistan

Abstract

Soil degradation by water erosion, which is further responsible for sedimentation in the irrigation water conveyance systems and reservoirs, is a matter of growing concern in Pakistan. The surface runoff and soil loss from a catchment depends upon rainfall and catchment characteristics. Conventional techniques for measuring erosion rates are time-consuming and need long data records. Caesium-137 (^{137}Cs), a fallout isotope produced from atmospheric nuclear weapon tests, has become a well-established radiotracer of soil movement. To assess and validate the technique as well as to compare the results with conventional methods of analysis the ^{137}Cs technique was applied in a sub-catchment of the Rawal Watershed of Islamabad, Pakistan. The reference inventory of ^{137}Cs , for an uneroded site, was $3280 \pm 138 \text{ Bq m}^{-2}$. Based on this reference value, the net soil loss from the studied sub-catchment was estimated at $10.2 \text{ t ha}^{-1} \text{ a}^{-1}$. The results obtained by National Agricultural Research Center (NARC) using conventional methods from a complete monitoring during the time period of 1990 - 1998 ranged from 0.3 to $28 \text{ t ha}^{-1} \text{ a}^{-1}$, with an average value of $11.3 \text{ t ha}^{-1} \text{ a}^{-1}$. The results obtained by using the ^{137}Cs and the conventional techniques were thus very comparative, indicating the effectiveness of fallout radionuclide technique over conventional/traditional methods. Using the ^{137}Cs technique, the calculated soil losses from two nearby deforested areas were $31.9 \text{ t ha}^{-1} \text{ a}^{-1}$ and $21.4 \text{ t ha}^{-1} \text{ a}^{-1}$ respectively. The net soil loss from an unmanaged hill slope in the same area was estimated as $37.7 \text{ t ha}^{-1} \text{ a}^{-1}$. The comparison of results from managed and unmanaged areas with different land use practices showed the impact of human activities on accelerating soil losses within the Rawal catchment. The ^{137}Cs technique proved to be less time consuming in the provision of information on soil loss and redistribution rates than direct measurement would have been and can be used to assess watershed management practices.

1. INTRODUCTION

Soil erosion and associated sedimentation are major agricultural and environmental problems worldwide. Soil erosion causes not only on-site degradation of a non-renewable natural resource but also off-site problems such as downstream sediment deposition in fields, floodplains and water bodies. Erosion and sediment deposition are natural processes forming the landscape but they can be accelerated by human intervention, through deforestation, overgrazing and poor farming practices. In view of their great impact on sustainable agricultural production and environmental conservation, there is an urgent need to assemble quantitative data on the extent, magnitude and actual rates of erosion/sedimentation as well on their economic and environmental consequences [1, 2] .

Pakistan comprises a wide range of terrestrial ecosystems varying from the ice clad rugged mountains in the Northern areas of the Potohar plateau, the Punjab plains, the deserts of Cholistan and Thar, the dry mountains of Baluchistan and a 1300 km long coastal belt. Pakistan is located in the transitional climatic zone characterized by the East Asia Monsoon and the Mediterranean climates. Annual rainfall varies widely from less than 100 mm to more than 2000 mm. Some areas in the north-eastern parts get enough rainfall, but mostly it occurs in the monsoon season (July-August). Due to high intensity rains, lack of vegetation cover and steep hill slopes, high sediment yields are generated.

For an agricultural country like Pakistan, land is the vital resource for production of food and agricultural commodities as well as for biodiversity conservation. About 55% of Pakistan's labour force is employed in agriculture, producing 30% of the nation's gross income. Although the country's soil resources are vast, good quality soils that sustain prime agriculture are limited. Out of 79.61 Mha of total area, 23 Mha is cultivated. Pakistan has the world's largest canal system in the famous Indus plains but still about 25% of the cultivated area is rain-fed because of water shortage. The present land use is not in accordance with its potential capability. There are many factors that affect the land capability potential directly, like soils, topography, climate, hydrology, type of vegetation cover, crop rotation, soil erosion, loss of nutrients etc. Erosion-affected land in Pakistan has been estimated to be around 8 Mha, about 10% of the country's total area or 33% of the cultivated area [3].

Conventional methods used for erosion assessment are long term monitoring of experimental plots, field survey of erosion features and erosion modeling. These methods of documenting rates of soil loss and sedimentation redistribution possess many limitations [4]. All these methods are limited in their capacity to provide complete and timely data. Numerous field studies reported in the literature have shown the potential of nuclear techniques for such studies. Bomb-derived caesium-137 (^{137}Cs with half life of 30.2 years) has been widely used for tracing the movement of soil and sediment particles within the landscape [1]. In particular ^{137}Cs measurements have been used to provide information on rates and patterns of soil erosion and deposition, mainly in agricultural regions [5, 6, 7], and on rates and patterns of sediment deposition on floodplains and in lakes [8, 9, 10].

Until recently no data on the fallout history of ^{137}Cs from atmospheric nuclear weapons tests or soil ^{137}Cs inventories for Pakistan were available. The first use of fallout ^{137}Cs in the country was started at Missa Kaswal in the Mangla Watershed in 2000. Since then, the role of FRNs has been studied at different locations of the Potwar area ranging from agricultural fields to hilly slopes. The present study has been carried out to estimate erosion rates and to assess erosion and sedimentation remediation practices. For this purpose a small sub-catchment of Rawal Lake was selected where the National Agricultural Research Center (NARC) has been already applying some management practices as well as monitoring soil losses from the area using conventional techniques. In this paper, the results of soil redistribution within a managed sub-catchment were compared with the soil distribution within an unmanaged sub-catchment by using the ^{137}Cs technique.

2. MATERIALS AND METHODS

2.1. Study Area

The Rawal Lake (33°42.42'N, 73°07.77'E) is located at an elevation of 535 m a.s.l. in the Park Area of Islamabad. The dam has been constructed in June 1962 on the Kurang River which occupies a catchment of 270 km² and drains about 1.1×10^8 m³ of water annually. The reservoir has a gross storage capacity of 5.856×10^7 m³. The pond is spread over an area of 7.68 km². Since the catchment area of the reservoir consists of hills with unmanaged steep slopes, the streams are flashy with high velocity of flowing water.

The drainage area of the reservoir comprises the Murree, Abbotabad, Rawalpindi and Hazara hills. Most of the catchment area is hilly with steep agricultural farmland, terraced in different pockets, forest and grassland. Most of the area is unmanaged and there is no organized control on deforestation, road cuts, leveling of agricultural land or general construction purposes, and no protection of stream and riverbanks. However, at very few locations, some government

departments are working to manage, monitor and protect the green areas and applying some management practices to reduce soil erosion within the catchment of Rawal Lake. Otherwise, there is no record on the extent of erosion in the area and therefore no data on spatial origin of soil material and sediment transported.

The main study site known as Satra Meel is located in a sub-catchment located approximately 15 km North of Islamabad at 33°45.92'N, 73°12.62'E (Fig. 1). The National Agriculture Research Center (NARC) has been monitoring this subcatchment for water and sediment yields since 1990. The basin is 12.64 ha in area and is underlain by shale and sandstone, on which is developed sandy loam and sandy clay loam soils (Orthents, Soil Taxonomy) with high stone content (up to 35% by volume, in the first 100 cm). The slopes are covered with low scrub forest (canopy of approximately 2-3 m) which is used for cattle grazing and wood cutting. NARC has also introduced some management practices, such as forestation, restricting the cutting of the bushes and cattle grazing in the area to reduce the sediment delivery from this sub-basin (this site is referred to as 'managed area' in the text). The average annual rainfall in the area is around 1200 mm (range of 959-1725 mm). Approximately 63-74% of total precipitation is received in the monsoon period (July to September). Number of rainy days per year varies from 54 to 91.

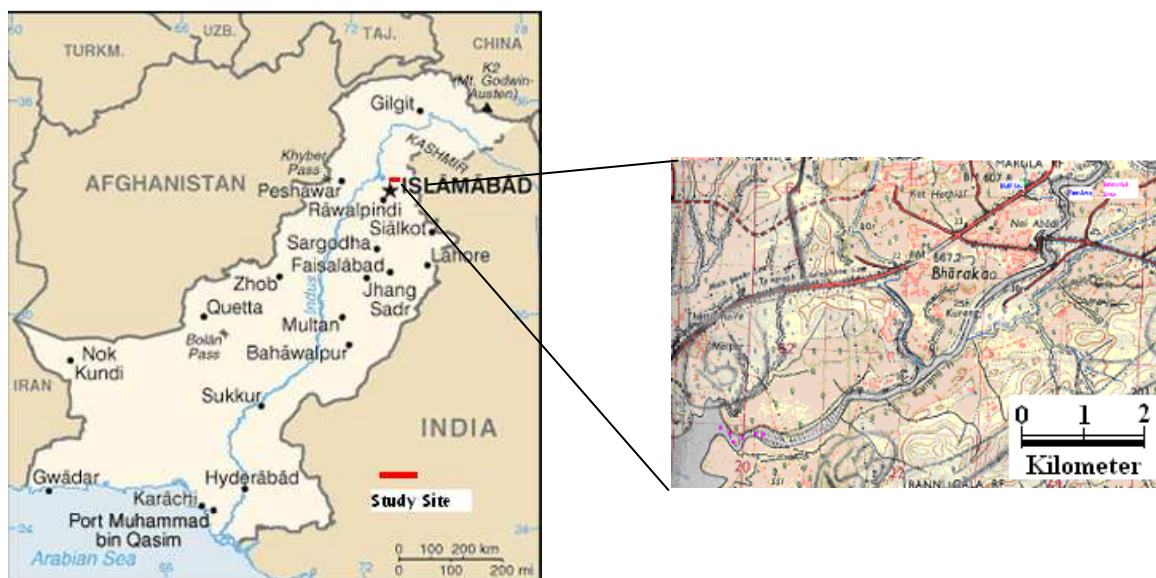


FIG. 1 Location map of study areas in the Rawal Dam catchment.

2.2. Reference sites

The history of land use and other vegetation cover of the area are not available because the NARC has only managed the site since 1990. Completely flat sites with no evidence of erosion or deposition were difficult to find in this area. However, one set of soil samples was taken from a reference site at the drainage divide that seemed to be stable. Because of high stone content, depth increments of 2 cm were taken to 10 cm only. The steel core (diameter of 9.1 cm) was used to take a bulk sample between 10 cm and 27.5 cm soil depth. In total eight bulk core samples were collected at hilltop sites for comparison with the ^{137}Cs depth profile.

Considering the very low ^{137}Cs inventory of the first site, a second reference site was selected on a flat area on a hill near the studied catchment. One scraper set of soil samples with depth increments of 2 cm was taken up to 24 cm and a bulk core was taken from 24 to 43 cm. Nine

bulk core samples were collected from the same site for comparison with the ^{137}Cs depth profile.

2.3. Sampling at watershed level

Soil sampling in the NARC managed sub-catchment was carried out at different locations across the hill slopes and in the valley. To compare the results with this managed site, samples were also collected from an unmanaged area outside the sub-catchment across different land use practices. In the managed area, the major potential sediment source seemed to be confined to the walking tracks (>1 meter in width). It was hypothesized that the ^{137}Cs inventory of soil samples collected from the tracks would be lower than in soils of the adjacent forest sites because the tracks showed an eroded appearance.

In this sub-catchment (Fig. 2) three transects were sampled (from all three hills) along with samples from the valley bottom. Transect 1 was sampled from hill 1 by coring (Diameter of 9.1 cm) for soil ^{137}Cs . Since the area is very bushy and different types of grasses are available, people in the vicinity have made many tracks to approach the green area for cattle grazing. Samples were collected from the walking track and the adjacent planted area. The second transect is sampled from the top of hill 2 along a less used track. The third transect was located on hill 3 and the samples were taken from top of the hill down to the main stream. Six samples were taken from the top of the hill 3 along different tracks and seven samples were taken along the main track from the top of hill to the stream. To find out the difference in erosion extent between the managed (NARC field station) and unmanaged sites (Fig. 1) outside the NARC field, soil samples were collected from a nearby deforested area and unmanaged patches along the main River Kurang.

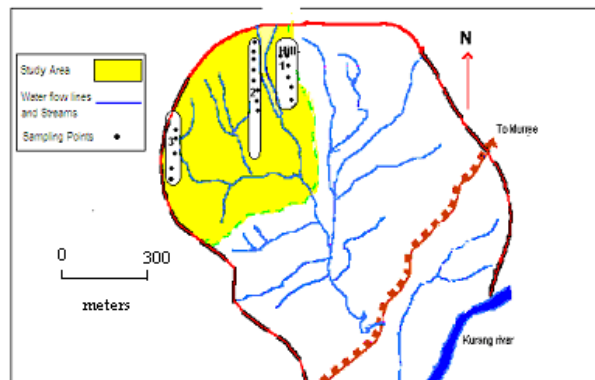


FIG. 2. Map of Satrameel Catchment within Sub-Catchment-2.

2.4. Analysis of soil samples for ^{137}Cs

Each soil sample was air-dried, weighed, and the aggregates were broken using a mortar and pestle. For some samples the larger concretions were removed by hand and the smaller ones were separated after passing the soil through a 2 mm mesh sieve. The concretions were weighed and the percentage of concretions in each sample was calculated on a weight basis. The bulk density of the concretions was used to correct the whole soil bulk density for the presence of concretions using the method described by Vincent et al. [11].

^{137}Cs was measured by gamma spectroscopy using Soil-6 (500 g), IAEA-375 (200 g) and IAEA-327 (200 g) as standards. Soil samples were put into 500 mL Marinelli beakers

(200 mL beakers for small samples) for equilibration and placed over a high purity coaxial germanium crystal enclosed in a lead castle connected to a EURISYS MEASURES Germanium Coaxial N Type detector connected to computer based MCA equipped with software 'Interwinner-4.1'. Energy resolution of the detector using standard ^{60}Co source is about 2.16 KeV and Peak to Compton ratio is ~ 72 at 1332 KeV. The relative efficiency of the detector determined at 1332 KeV is 52.73% at 25 ± 0.2 cm relative to $3'' \times 3''$ NaI detector. ^{137}Cs activity concentrations per unit mass (Bq kg^{-1}) were determined by counting the 661 keV gamma emissions for 10000 second counting intervals. Activity concentration (Bq kg^{-1}) of the samples was calculated by comparative method using count rate and activity of the standard. Total activity of the sample was converted to total aerial activity (Bq m^{-2}) using the corrected bulk density and the sampling depth.

2.5. Conversion Models

Estimation of rates of soil loss from ^{137}Cs measurement is generally based on a comparison of the inventory measured at a specific sampling point with the established reference inventory. For uncultivated soils, the calibration relationship required to convert the magnitude of the changes in the ^{137}Cs inventory to an estimate of the soil redistribution (erosion/deposition) rates commonly employs a theoretical profile distribution model (PDM) [12,13,14]. This model represents the vertical distribution of the ^{137}Cs inventory within the soil profile by a simple numerical function, which in turn can be used to estimate the depth of soil that would need to be removed to result in the measured ^{137}Cs inventory. In most cases an exponential function is used to represent the down-profile reduction in ^{137}Cs activity [13, 15].

$$A'(x) = A_{ref}(1 - e^{-x/h_0}) \quad (1)$$

where: x is the mass depth from soil surface (kg m^{-2}), $A(x)$ the ^{137}Cs inventory above depth x (Bq m^{-2}), A_{ref} the local reference inventory (Bq m^{-2}) and h_0 the relaxation depth describing the profile shape (kg m^{-2}). The greater the value of the shape factor h_0 , the deeper the ^{137}Cs penetrates into the soil profile.

Assuming, as a simplification, that the total ^{137}Cs fallout occurred in 1963, the year of maximum bomb fallout, and that the depth distribution of ^{137}Cs in the soil profile is independent of time, the erosion rate Y (for an eroding point, i.e. with a total inventory less than the reference inventory) can be estimated [16] as:

$$Y = \frac{10}{t - 1963} h_0 \ln\left(1 - \frac{X}{100}\right) \quad (2)$$

where: Y is the annual soil loss ($\text{t ha}^{-1} \text{ a}^{-1}$) (negative value), t the year of sample collection (a), X the percentage reduction in the ^{137}Cs inventory in relation to the local ^{137}Cs reference value (defined as $[(A_{ref} - A_u)/A_{ref}]100$ and A_u the measured total ^{137}Cs inventory at the sampling point (Bq m^{-2}).

Although this exponential PDM involves a number of simplifying assumptions, it is easy to apply and it has been widely used as a mean of estimating soil erosion rates from ^{137}Cs measurements in areas with undisturbed soils. Only a single parameter h_0 , needs to be estimated and this value can be derived from measurements of the vertical distribution of ^{137}Cs in the soil profile at the reference site, by fitting the following exponential function to those data, i.e.

$$A(x) = A(0)e^{-x/h_0} \quad (3)$$

where: x is the mass depth from soil surface (kg m^{-2}), $A(x)$ the concentration of ^{137}Cs at depth x (Bq kg^{-1}) and $A(0)$ the concentration of ^{137}Cs in the surface soil (Bq kg^{-1}).

Equation 3 has been fitted to the vertical distribution of ^{137}Cs activity (Bq kg^{-1}) for the reference site, using Lanarius least square regression. Values for the parameters $A(0)$ and h_0 were determined.

3. RESULTS AND DISCUSSION

3.1. Reference Site

The study area consists of stony hills without any past data on land use activities. Level sites without evidence of erosion or deposition were difficult to find. In total two reference inventories were established. The distribution of the ^{137}Cs inventory along the depth profile taken by the scraper plate at the reference site-1 is shown in Fig. 3. The total inventory was 1649 Bq m^{-2} . The ^{137}Cs inventory of the depth profile taken at the reference site-2 is shown in Fig. 4. The total inventory was 3280 Bq m^{-2} . Below the peak in activity concentration at 7-6 cm, the profile showed an exponential decline in ^{137}Cs activity with depth. At greater depth with increasing bulk density and declining infiltration rates, the remaining ^{137}Cs would be adsorbed. The concentration of ^{137}Cs would then decrease with depth. In comparison with ^{137}Cs inventories at the reference sites taken from Murree (around 50 km NE, 5796 Bq m^{-2}) and Missa Kaswal (around 70 km South, 4280 Bq m^{-2}), the inventory of the reference site-1 (1649 Bq m^{-2}) seems very low and that of reference site-2 (3280 Bq m^{-2}) seems reasonable. Most of the inventories on the basis of bulk cores taken from site-2 had higher values of ^{137}Cs with an average of 4256 Bq m^{-2} . Therefore the reference inventory used for calculations and data interpretation was 3280 Bq m^{-2} . This problem of unstable reference inventory is due to the high stoniness of the soil as the scraper plate does not allow depth penetration after a few centimetres [17]. However, no stone hindered the second reference inventory up to the depth of 24 cm.

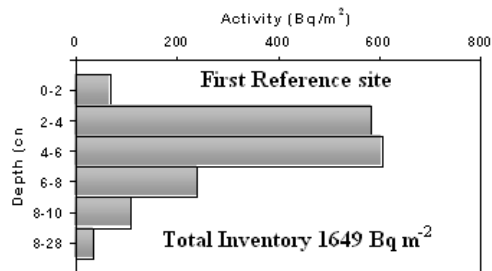


FIG. 3. Depth profile of ^{137}Cs inventory at Satrameel, first reference site.

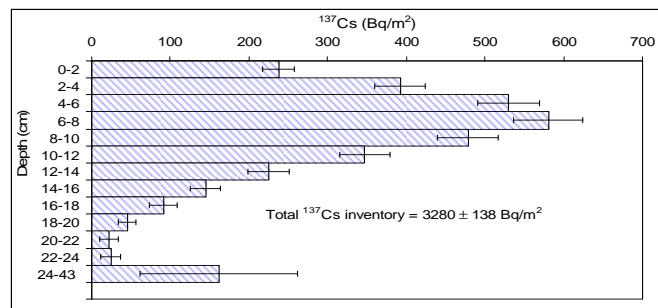


FIG. 4. Depth profile of ^{137}Cs inventory at Satrameel, second reference site.

3.2. Slope Transects

3.2.1. NARC managed sub-catchment

Data on soil cores collected from the different slope transects and valley floor are given in Tables 1-3.

The values of ^{137}Cs inventory obtained for 16 bulk cores ranged from 232 to 11391 Bq m^{-2} . Except for three locations (almost flat areas and thick bushes in between the slope), all the values were lower than the reference value of 3280 Bq m^{-2} . The significant reduction in inventory evident for most cores indicates that most of the sampling points have experienced appreciable net erosion over the period since the commencement of ^{137}Cs fallout in the mid 1950s.

Of the 24 bulk cores collected along the transect on hill 2, only 3 had ^{137}Cs inventories higher than the reference inventory indicating net soil accumulation, while 21 had lower ^{137}Cs inventories, indicating net soil loss. These three locations with deposition were on a reasonably flat area along the transect. The rest of the points indicated the presence of erosion. Very high erosion rates were observed at the lower portion of the transect because of low vegetation cover, steep slope gradient and accelerated run-off.

The results obtained at hill 3 indicated less erosion at the upper slope position because of good plant cover, the absence of walking tracks and a relatively lower slope gradient. The ^{137}Cs inventory obtained for 12 bulk cores ranged from 74 to 8691 Bq m^{-2} . However, the erosion accelerated downwards because of steeper slope gradients, accelerated run-off and less vegetation, especially at the lower part of the hill.

TABLE 1. CAESIUM-137 INVENTORIES AND SOIL REDISTRIBUTION AT THE TRANSECT ALONG HILL 1

Sample No	Inventory (Bq m^{-2})	Soil redistribution ($\text{t ha}^{-1} \text{a}^{-1}$) (Using Profile Distribution Model)
1	1652	-11.3
2	1439	-13.5
3	2728	-3.0
4	5303	10.2
5	3258	-0.1
6	515	-30.4
7	1958	-8.5
8	9433	31.3
9	11391	41.2
10	232	-43.5
11	1394	-14.0
12	637	-26.9
13	1122	-17.6
14	1760	-10.2
15	565	-28.9
16	1363	-14.4

TABLE 2. CAESIUM-137 INVENTORIES AND SOIL REDISTRIBUTION AT THE TRANSECT ALONG HILL 2

Sample N°	Inventory (Bq m ⁻²)	Soil redistribution (t ha ⁻¹ a ⁻¹) (Using Profile Distribution Model)
1	3910	3.2
2	376	-35.6
3	809	-23.0
4	2531	-4.3
5	7788	23.0
6	1617	-11.6
7	9405	31.3
8	1889	-9.1
9	9143	29.9
10	3121	-0.8
11	2898	-2.0
12	1203	-16.5
13	322	-38.1
14	1525	-12.6
15	1125	-17.6
16	1861	-9.3
17	1247	-15.9
18	2813	-2.5
19	317	-38.4
20	417	-33.9
21	218	-44.5
22	622	-27.3
23	711	-25.1
24	612	-27.6

TABLE 3. CAESIUM-137 INVENTORIES AND SOIL REDISTRIBUTION AT THE TRANSECT ALONG HILL 3

Sample N°	Inventory (Bq m ⁻²)	Soil redistribution (t ha ⁻¹ a ⁻¹) (Using Profile Distribution Model)
1	1673	-11.1
2	4126	4.3
3	8691	27.7
4	2658	-3.5
5	2828	-2.4
6	7962	23.9
7	3882	3.1
8	3555	1.4
9	472	-31.8
10	2377	-5.3
11	635	-27.0
12	74	-62.2

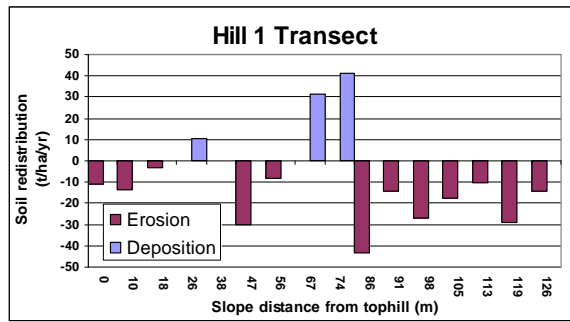


FIG. 5. Soil redistribution along the Hill 1 transect.

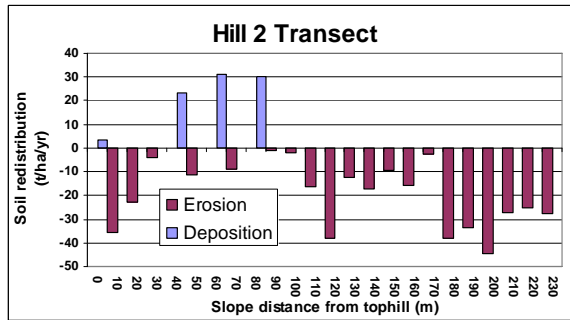


FIG. 6. Redistribution along the Hill 2 transect.

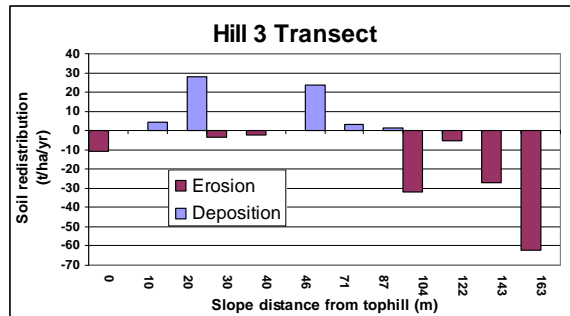


FIG. 7. Redistribution along the Hill 3 transect.

The average rate of soil loss from the NARC managed subcatchment 2 was $-10.2 \text{ t ha}^{-1} \text{ a}^{-1}$. However, the soil redeposition within the catchment is $\sim 30\%$ whereas the rest of the eroded soil is delivered to the channel.

3.2.2. Unmanaged area outside NARC sub-catchment

On the other hand, outside the NARC managed site different land use practices had different impacts on the redistribution of soil. For example, the cores taken from the top of the deforested hill down to the river Kurang bank had very low ^{137}Cs inventories showing very high erosion rates. The average redistribution rate along the transect using profile distribution model was $-31.9 \text{ t ha}^{-1} \text{ a}^{-1}$. The results are shown below in Table 4. Another profile taken from the adjacent deforested hill with relatively small slope gradient gave an average redistribution value of $21.4 \text{ t ha}^{-1} \text{ a}^{-1}$ (Table 5).

In a similar way the low ^{137}Cs inventories at the bottom of hill slope adjacent to a road under construction (where the natural land structure has been changed due to bulldozing, tree cutting etc.) show severe erosion and the results are shown in Table 6.

TABLE 4. CAESIUM-137 INVENTORIES AND SOIL REDISTRIBUTION AT THE TRANSECT IN FIRST DEFORESTED STUDY AREA

Sample N°	Inventory (Bq m ⁻²)	Soil redistribution (t ha ⁻¹ a ⁻¹) (Using Profile Distribution Model)
1	198.6	-41.1
2	338.9	-33.1
3	748.4	-21.3
4	589.3	-24.9
5	128.2	-47.6
6	2151.6 (relatively flat area)	-5.6
7	218.2	-39.7
8	72.6	-56.0
9	274.2	-36.3
10	1281.1 (Base flat area)	-13.3
	Average	-31.9

TABLE 5. CAESIUM-137 INVENTORIES AND SOIL REDISTRIBUTION AT THE TRANSECT SECOND DEFORESTED STUDY AREA

Sample N°	Inventory (Bq m ⁻²)	Soil redistribution (t ha ⁻¹ a ⁻¹) (Using Profile Distribution Model)
1	414	-29.2
2	1140	-14.5
3	466	-27.5
4	1236	-13.3
5	541	-25.3
6	799	-19.6
7	757	-20.4
8	843	-18.9
9	86	-52.1
10	923	-17.5
11	2050	-5.9
12	1012	-16.2
13	876	-18.3
	Average	-21.4

TABLE 6: CAESIUM-137 INVENTORIES AND SOIL REDISTRIBUTION AT TRANSECT AT THE LOWER SLOPE POSITION OF THE HILLSLOPE

Sample N°	Inventory (Bq m ⁻²)	Soil redistribution (t ha ⁻¹ a ⁻¹) (Using Profile Distribution Model)
1	465.2	-28.4
2	480	-27.9
3	124.2	-48.0
4	138	-46.5
	Average	-37.7

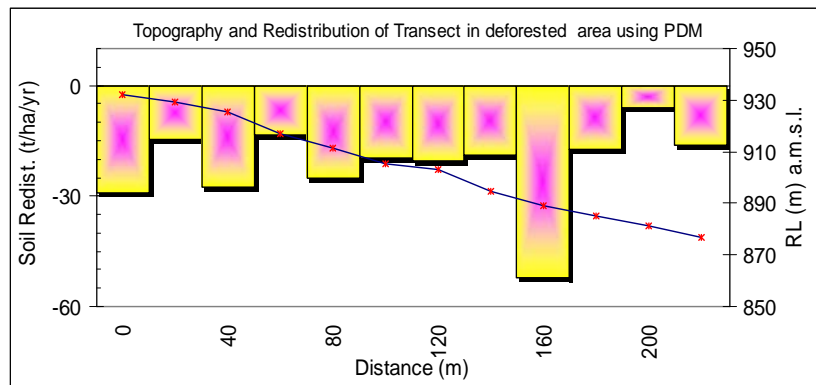


FIG. 8. Redistribution along the transect in deforested area.

The high net soil loss of 31.9, 21.4 and 37.7 t ha⁻¹ a⁻¹ can be attributed to land use and slope gradient in the areas outside the managed sub-catchment. The largest soil losses appear to be associated with the areas where bulldozing and land levelling have been carried out for the construction of civil structures and roads. The sediment flux values of between 40 and 90 t ha⁻¹ a⁻¹ have been reported in Sutherland in Bulldozing areas (18). The same trend is observed in the study area. The management practices in the NARC managed area seem very effective in controlling the erosion rates. However, soil loss rates of 10.2 t ha⁻¹ a⁻¹ suggest that much more efforts are needed to control the erosion from the slopes.

4. CONCLUSIONS

The use of ¹³⁷Cs in studies of soil erosion/redistribution provides useful information in the study area. Although, it does not discriminate different erosion processes, the Cs¹³⁷ inventories at the reference site, eroded slope (managed and unmanaged sites) and valley floor are still sufficient for use in soil erosion and sedimentation investigations in the sub-catchment of Rawal Lake. The erosion rates obtained by the ¹³⁷Cs technique (10.2 t ha⁻¹ a⁻¹) are in good agreement with the results obtained by conventional techniques (11.3 t ha⁻¹ a⁻¹). However, the results by conventional techniques took a long time to establish the soil loss (approximately 11 years), whereas by using ¹³⁷Cs technique, we were able to get the data within three years of study. The ¹³⁷Cs technique also provides information on the spatial soil redistribution within the catchment which is very difficult to be obtained by conventional methods.

The erosion rates from two deforested areas outside the NARC managed site are 31.9 and 21.4 t ha⁻¹ a⁻¹ respectively, whereas the value from area under civil work is around 37.7 t ha⁻¹ a⁻¹. The low values of redistribution (10.2 t ha⁻¹ a⁻¹) in the NARC managed sub-catchment indicate the potential of conservation/management practices in controlling the erosion. It also indicates that impacts of human activities are major contributors for soil erosion.

The ¹³⁷Cs technique provides an opportunity for quantifying the erosion/redistribution rates. Estimates of soil loss from the catchment derived by ¹³⁷Cs measurement provide a clear confirmation of the validity of the technique for estimating erosion and deposition processes within the sub-catchment. However, the determination of a reference inventory is very crucial. There is a need for more detailed studies of this type in order to understand the response of sediment redistribution and mobilization processes from sub-catchment to catchment scale.

ACKNOWLEDGEMENTS

The authors wish to thank the International Atomic Energy Agency for providing the financial and technical support under research contract N°. PAK-12392. Sincere thanks are due to Technical Officers and other IAEA Staff for their support in implementing the project. The authors are also thankful to the Pakistan Atomic Energy Commission Authorities, especially Director General, Pakistan Institute of Nuclear Science and Technology and Head, Isotope Application Division for facilitating the project. Cooperation of NARC (end-user department) is acknowledged with gratitude. The authors are also grateful Mr. Muhammad Zamir, Mr. Muhammad Gulistan and Mr. Amjad Ali for their help in collection and analysis of samples.

REFERENCES

- [1] RITCHIE, J.C., MCHENRY, J.R., Application of radiation fallout caesium-137 for measuring soil erosion and sediment accumulation rates and patterns: A review, *J. Environ. Qual.* **19** (1990) 215–233.
- [2] WALLING, D.E., QUINE, T.A., “The use of fallout radionuclide measurements in soil erosion investigations”, *Proc. Int. Symposium Nuclear Techniques in Soil-Plant Studies for Sustainable Agriculture and Environmental Preservation*, October 1994, Vienna, IAEA Proc. Series STI/PUB/947 (1995) 579–619.
- [3] MIAN, A., MIRZA, Y.A., *Pakistan’s Soil Resources, Environment and Urban Affairs Division*, Government of Pakistan and IUCN The World Conservation Union, ISBN 969-8141-03-0 (1993).
- [4] LOUGHRAN, R.J., The measurement of soil erosion, *Prog. Phys. Geog.* **13** (1989) 216–233.
- [5] MCHENRY, J.R., RITCHIE, J.C., Estimating field erosion and solid matter transport in inland waters, *IAHS Publication* **122** (1977) 26–33.
- [6] LOUGHRAN, R.J., et al., Estimation of soil erosion from ¹³⁷Cs measurements in a small, cultivated catchment in Australia, *Appl. Radiat. Isot.* **39** (1988) 1153–1157.
- [7] WALLING, D.E., QUINE, T.A., “The use of caesium-137 measurements in soil erosion surveys”, *Erosion and Sediment Transport Monitoring Programmes in River Basins* (BOGEN, J., et al., eds.), *IAHS Publication* **210** (1993) 143–152.
- [8] WALLING, D.E., HE, Q., “Use of Caesium-137 as a tracer in the study of rates and patterns of floodplain sedimentation”, *Tracers in Hydrology* (PETERS, N.E., et al., eds), *IAHS Publication* **215** (1993) 319–328.
- [9] WALLING D.E., et al., “Investigating contemporary rates of floodplain sedimentation”, *Lowland Floodplain Rivers: Geomorphological perspectives* (CARLING, P.A., PETTS, G.E., eds), Wiley, Chichester (1993) 166–184.
- [10] WALLING, D.E., et al., “Conversion models for use in soil-erosion, soil redistribution and sedimentation investigations”. *Handbook for the Assessment of Soil Erosion and sedimentation Using Environmental Radionuclides* (ZAPATA, F., ed), Kluwer Academic Publishers, Dordrecht (2002) 111–164.
- [11] VINCENT, K.R., CHADWICK, O.A., Synthesizing bulk density for soils with abundant rock fragments, *Soil Sci. Soc. Am. J.* **58** (1994) 455-464.
- [12] WALLING, D.E., QUINE, T.A., Calibration of caesium-137 measurements to provide quantitative erosion rate data, *Land Degrad. Rehabil.* **2** (1990) 161–175.
- [13] ZHANG, X., et al., A preliminary assessment of the potential for using caesium-137 to estimate rates of soil erosion in the Loess Plateau of China, *Hydrol. Sci. J.* **35** (1990) 267–276.\

- [14] WALLING, D.E., HE, Q., Models for converting ^{137}Cs measurements to estimates of soil redistribution rates on cultivated and uncultivated soils, estimating bomb-derived ^{137}Cs reference inventories (including software for model implementation), A Contribution to the IAEA Coordinated Research Programme on Soil Erosion (D1.50.05) and Sedimentation (F3.10.01) (2001).
- [15] ZHANG, X., et al., Soil erosion rates on sloping cultivated land on the Loess Plateau near Ansai, Shaanxi Province, China: An investigation using ^{137}Cs and rill measurements, *Hydrological Processes* **12** (1998) 171–189.
- [16] WALLING, D.E., HE, Q., Improved model for estimating soil erosion rates from cesium-137 measurements, *J. Environ. Qual.* **28** (1999) 611–622.
- [17] LOUGHRAN, R.J., et al., “Sampling methods”, Handbook for the assessment of soil erosion and sedimentation using environmental radionuclides (ZAPATA, F., ed), Kluwer Academic Publishers, Dordrecht (2002) 41–57.
- [18] SUTHERLAND, R.A., Caesium-137 estimates of erosion in agricultural areas, *Hydrological Processes* **6** (1992) 215–225.

ASSESSMENT OF SOIL EROSION SEVERITIES AND CONSERVATION EFFECTS ON REDUCTION OF SOIL LOSS AND SEDIMENT YIELD BY USING THE CAESIUM-137 AND EXCESS LEAD-210 TRACING TECHNIQUES IN THE UPPER YANGTZE RIVER BASIN, CHINA

X. ZHANG, Y. LONG, X. HE, A. WEN, M. FENG, Y. QI, J. ZHENG,
J. FU, L. HE, Y. ZHANG, Y. HE, H. LI, D. YAN
Chinese Academy of Sciences,
Institute of Mountain Hazards and Environment,
Chengdu, Sichuan China

Y. ZHANG, L. BAI
Sichuan University, Physics Department,
Sichuan, China

D.E. WALLING
University of Exeter, Department of Geography,
Exeter, Devon, United Kingdom

Abstract

In one of the most eroded regions of China, the Upper Yangtze River Basin, ^{137}Cs and $^{210}\text{Pb}_{\text{ex}}$ tracing techniques have been used to identify sediment sources and assess erosion rates and to evaluate soil conservation benefits and impacts of deforestation and reforestation on soil erosion. Dating of reservoir deposits by ^{137}Cs concentration variations in profiles provided reliable information on sediment yields and average soil losses in a catchment in the Hilly Sichuan Basin and the Three Gorge Region. The collected data indicated that specific sediment yields ranged between $566 \text{ t km}^{-2} \text{ a}^{-1}$ and $1869 \text{ t km}^{-2} \text{ a}^{-1}$. Further investigation of sediment sources by comparison of the ^{137}Cs and $^{210}\text{Pb}_{\text{ex}}$ concentrations in reservoir sediment and those in surface soils provided relative sediment contributions of 18%, 46% and 36% from steep forest slopes, gentle cultivated terraces and bare slopes, respectively, in a micro-catchment located in the Hilly Sichuan Basin. Additionally two forest and shrub fires, which occurred in 1960 and 1998, respectively, in the catchment, were identified from the variations of ^{137}Cs and $^{210}\text{Pb}_{\text{ex}}$ concentrations in a deposit profile in the Jiulongdian Reservoir (Yunnan Plateau). Dating of these reservoir deposits showed that sediment yields are highly responsive to vegetation changes in the catchment. Finally, assessment of soil losses from ^{137}Cs and $^{210}\text{Pb}_{\text{ex}}$ measurements on the sloping cultivated land in the Sichuan Hilly Basin showed that the traditional and centuries-old soil conservation measures (a drainage system combined with the 'Tiaoshamiantu' cultivation) have reduced soil losses up to 35% compared to losses on sloping land without conservation measures monitored by runoff plots.

1. INTRODUCTION

The Upper Yangtze River Basin is a mountainous and hilly region with a drainage area of $1.006 \times 10^6 \text{ km}^2$ and has an annual runoff of $4390 \times 10^8 \text{ m}^3$ and sediment yield of 5.23×10^8 tons, of which the bed load sediment yield only accounts for less than 5%. The Tibet Plateau and the Hengduanshan Mountain Range are located in the west of the basin, the Yunnan-Guizhou Plateau in the south, and Sichuan Hilly Basin and its surrounding mountain ranges in the east. Most of the basin is characterised by a subtropical climate except the high mountain regions that has a temperate climate. Annual precipitation mostly ranges between 800-1200 mm and more than half of it occurs during the wet season of June-September.

The basin has a population of 1.5×10^8 , most of which are living in the eastern part of the basin, where population density is mostly over $250 \text{ persons km}^{-2}$ and the highest reaches $600 \text{ persons km}^{-2}$ in the Hilly Sichuan Basin. The Upper Yangtze River Basin has a total arable

land area of 1.5×10^7 ha (0.1 ha per capital), 60% of which is sloping cultivated land. It is very common that some steep slopes over 30° are still under cultivation. Forest coverage ranges between 10-30% in the basin and most of the forests are secondary forests. The mean specific sediment yield is 520 t km^{-2} over the basin. However, sediment yield is very variable within the basin. It is less than $200 \text{ t km}^{-2} \text{ a}^{-1}$ in the Tibet Plateau region of the remote western basin and higher than $2000 \text{ t km}^{-2} \text{ a}^{-1}$ in some regions of the eastern basin such as the Lower Jinshajiang River Gorge Region, under steep terrain and fractured geology conditions, and the Upper Jialingjiang River Region underlain by loess deposit. Sediment delivery ratio ranges between 0.15-0.6 in the basin but its reliability is uncertain.

In 1988, the Upper Yangtze River Basin was identified by the Central Government as a key region for national soil and water conservation. Since then, a national project, titled 'Soil and Water Conservation Project', has been carried out to control the severe soil erosion in the Upper Yangtze River Basin. After 1998's big floods, additional national projects were launched, which deal with vegetation rehabilitation and natural forests protection. These projects have significant positive on-site and off-site impacts on the mountain environment and the Three Gorge Reservoir and the Middle and Lower Yangtze River Plains in general by reducing soil loss and sediment production. However, there is an urgent need for collecting information on soil erosion and sedimentation to evaluate the benefits of soil conservation measures, to predict future changes of soil erosion and to plan new environmental projects in the Basin. There is very limited information on erosion and sedimentation in the basin, because since 1950 most of research on soil erosion and sedimentation has been carried out in the Loess Plateau in China. Additionally, it is impossible to obtain such information in a few years by using classic methods, such as runoff plots and hydrological stations. Therefore, the ^{137}Cs and ^{210}Pb tracing techniques were used to investigate soil erosion severities and sediment sources and to evaluate soil conservation effects on reduction of soil loss and sediment yield.

Four case studies are reported in this paper:

- (1) Evaluation of soil loss reduction by traditional cultivation measures in the Sichuan Hilly Basin,
- (2) Sediment source identification by using ^{137}Cs and ^{210}Pb radionuclides in a small catchment of the Hilly Sichuan,
- (3) Investigation of erosion severities and sediment production by ^{137}Cs dating of reservoir and pond deposits in small catchments of the Hilly Sichuan Basin and the Three Gorges Region,
- (4) Evaluation of the impacts of vegetation destruction and recovery on sediment production since the end of 1950s in the Jiulongdian catchment from the variations of ^{137}Cs , $^{210}\text{Pb}_{\text{ex}}$ in reservoir deposit profiles.

2. EVALUATION OF SOIL LOSS REDUCTION BY TRADITIONAL CULTIVATION MEASURES IN THE SICHUAN HILLY BASIN

2.1. Study site

This study was carried out near the Jiajia Village, Jianyang County, in the Sichuan Hilly Basin to evaluate soil conservation benefits of the traditional and centuries-old soil conservation measure, such as a drainage system combined with the 'Tiaoshamiantu' cultivation, by using $^{210}\text{Pb}_{\text{ex}}$ in conjunction with ^{137}Cs . A sloping field of a small mound near

the Jiajia Village, Jianyang County, was selected as the focus of this investigation (Fig. 1). The field has a slope length of 17.5 m and consists of two subfields: the upper subfield has a length of 7 m with a gradient of 20°, while the lower subfield has a length of 10 m and a gradient of 10° (Fig. 1). The two subfields are separated by a small counter-ditch. To protect the cultivated soils from water erosion, the study site has an excellent traditional drainage system, which is widely adopted by steep-land farmers in the Sichuan Hilly Basin. Besides the middle counter-ditch between the two subfields, the field has as well an upper side counter-ditch and a lower side counter-ditch. The width and depth of those ditches are about 30 cm. The three counter-ditches are connected to a downslope drainage ditch. The upper side ditch prevents runoff water from the higher fields entering into the upper subfield, while the lower side ditch reduces the velocity of the runoff from the field and part of the sediments from the field silt up in the ditch. The middle ditch has the function of both upper and lower side ditches reducing the speed of the runoff water and capturing sediments. The deposited sediments in the ditches are returned to the field by the traditional cultivation measure of ‘Tiaoshamiantu’ each year.

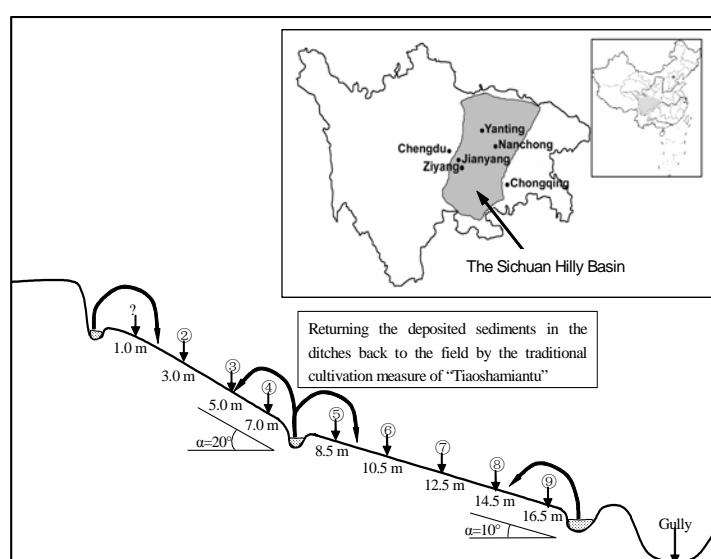


FIG. 1. A schematic representation of the traditional system of ‘Tiaoshamiantu’ and the location of the sampling points within the study field.

2.2. Methodology

To document soil redistribution by using the $^{210}\text{Pb}_{\text{ex}}$ and ^{137}Cs inventories, in total 18 soil cores, i.e. 16 bulk cores and 2 sectioned cores, were collected along two parallel downslope transects with a gap of 2 m between both transects. Along each transect, 4 and 5 soil cores were taken in the upper and lower subfield respectively, and the gap between the nearby cores along the transect was approximately 2 m (Fig. 1). To know the depth distributions of $^{210}\text{Pb}_{\text{ex}}$ and ^{137}Cs in the soils, two sectioned cores were located at the middle erosion site and the lower deposition site. To obtain the local ^{137}Cs and $^{210}\text{Pb}_{\text{ex}}$ reference inventories, one sectioned soil core was collected from the nearby waste grass land near a tomb and 8 bulk soil cores from the flat cultivated land on top of the mound. To ensure that the entire ^{137}Cs and $^{210}\text{Pb}_{\text{ex}}$ inventories of the soil profiles were measured, 30-60 cm deep soil cores were collected.

Sectioned soil core samples were collected using a combined core tube with a diameter of 9.7 cm. The tube comprised two segments, which could be separated to facilitate sectioning of the

core. The tube was propelled into the ground manually and the obtained soil cores were sectioned at 5 cm increments. Bulk soil core samples were collected using a 7.8 cm-diameter core tube. The tube was also put into the ground manually, but the obtained soil cores were not sectioned. Preparation of the soil samples was undertaken in the laboratory of Chengdu Institute of Mountain Hazards and Environment, Chinese Academy of Sciences. All samples were air-dried, ground and weighted. Measurements of $^{210}\text{Pb}_{\text{ex}}$ and ^{137}Cs activities were undertaken in the Sediment Research Facility of Department of Geography and Archaeology, Exeter University, Exeter, UK. The samples with a weight of ≥ 200 g were sealed for 20 days prior assay in order to achieve equilibrium between ^{226}Ra and its daughter ^{222}Rn . Measurements of $^{210}\text{Pb}_{\text{ex}}$ and ^{137}Cs activities in soil samples were undertaken by gamma spectrometry, using a high resolution, low background, low energy, hyper-pure n-type germanium coaxial γ -ray LOAX HPGe detector. The samples were placed in the detector and counted for ≥ 50000 s, providing a precision of approximately $\pm 10\%$ at the 90% level of confidence for the gamma ray measurements. The ^{137}Cs concentrations were obtained using 662 keV gamma ray. The total ^{210}Pb of the samples were obtained using the 46.5 keV gamma ray from ^{210}Pb , and the ^{226}Ra concentrations were obtained using the 351.9 keV gamma ray from ^{214}Pb , a short lived daughter of ^{226}Ra . Unsupported ^{210}Pb ($^{210}\text{Pb}_{\text{ex}}$) concentrations of the samples were calculated by subtracting the ^{226}Ra -supported ^{210}Pb concentrations from the total ^{210}Pb concentrations.

2.3. Depth distributions of $^{210}\text{Pb}_{\text{ex}}$ and ^{137}Cs in soils

Depth distributions of $^{210}\text{Pb}_{\text{ex}}$ and ^{137}Cs were very similar in both uncultivated and cultivated soils (Fig. 2). The profile for the uncultivated soil of the waste grass land shows that the maximum concentrations of the two radionuclides occurred in the surface horizon and decrease exponentially with depth. ^{137}Cs and $^{210}\text{Pb}_{\text{ex}}$ concentrations of the top 5 cm horizon were $27.57 \pm 0.80 \text{ Bq kg}^{-1}$ and $260.61 \pm 13.03 \text{ Bq kg}^{-1}$, respectively.

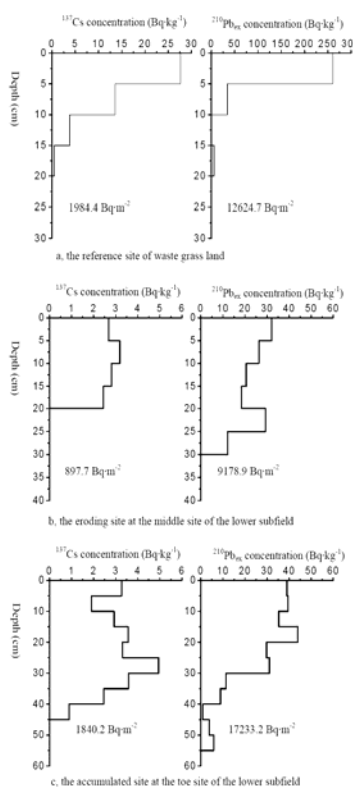


FIG. 2. Depth distributions of ^{137}Cs and $^{210}\text{Pb}_{\text{ex}}$ in cultivated and uncultivated soils.

With regards to the profile for the cultivated soil at the eroding middle site 7 of the lower subfield, the two radionuclides were quite evenly distributed within the plough layer of 20 cm, ^{137}Cs and $^{210}\text{Pb}_{\text{ex}}$ concentrations varied between $2.44 \pm 0.22 \text{ Bq kg}^{-1}$ and $3.19 \pm 0.29 \text{ Bq kg}^{-1}$ and between $18.44 \pm 1.45 \text{ Bq kg}^{-1}$ and $32.07 \pm 2.65 \text{ Bq kg}^{-1}$, respectively (Fig. 2). No ^{137}Cs was detected below the depth of 20 cm, but $^{210}\text{Pb}_{\text{ex}}$ existed in the layer at a depth of 20-30 cm. It may be caused by the deep ploughing campaign during the period of ‘the Great Leap Forward’ from 1958 to 1960. For the profile at the accumulated toe site 9 of the lower subfield, the ^{137}Cs concentration in the top 20 cm layer was close to those at the eroding middle site, and the maximum concentration of $4.95 \pm 0.34 \text{ Bq}\cdot\text{kg}^{-1}$ occurred in the depth layer of 25-30 cm, then it declined with depth and little ^{137}Cs was detected below the depth of 40 cm. By comparison of the ^{137}Cs depth distributions between the middle site and the toe site, it is estimated that 20 cm thick soils layer have been deposited at the toe site since 1963 resulting into an average accumulation rate of about 0.5 cm a^{-1} . The higher ^{137}Cs concentration in the layer at a depth of 25-30 cm as compared to the current plough layer of top 20 cm indicates that the ^{137}Cs concentration of plough soil has decreased since the middle of 1960s. However, for the accumulated profile at the toe site, $^{210}\text{Pb}_{\text{ex}}$ was quite evenly distributed in the top 30 cm layer with a concentration of $29.73 \pm 2.47 \text{ Bq}\cdot\text{kg}^{-1}$ and $43.91 \pm 3.16 \text{ Bq}\cdot\text{kg}^{-1}$, then the concentration significantly declined with depth. However, a little $^{210}\text{Pb}_{\text{ex}}$ was still detected in the deepest sampling layer at 55-60 cm. The decrease of $^{210}\text{Pb}_{\text{ex}}$ concentration with depth below the depth of 30 cm is suggested to be caused by the radio-decay of the radionuclide. According to the declining rate of the $^{210}\text{Pb}_{\text{ex}}$ concentration from the layer of 25-30 cm to the layer of 50-55 cm, the average accumulation rate is estimated to be 0.48 cm a^{-1} by the radio decay rate, which is close to the rate of 0.5 cm a^{-1} from the ^{137}Cs measurements.

2.4. Local ^{137}Cs and $^{210}\text{Pb}_{\text{ex}}$ reference inventories

The ^{137}Cs and $^{210}\text{Pb}_{\text{ex}}$ inventories of the sectioned soil core at the waste grass site were $1984.4 \pm 151.8 \text{ Bq m}^{-2}$ and $12624.7 \pm 836.7 \text{ Bq m}^{-2}$, respectively. The ^{137}Cs and $^{210}\text{Pb}_{\text{ex}}$ inventories of the 8 bulk soil cores on the flat cultivated land varied between $1267.5 \pm 131.4 \text{ Bq m}^{-2}$ and $2323.8 \pm 143.4 \text{ Bq m}^{-2}$ with a mean value of 1799.9 Bq m^{-2} for ^{137}Cs , and between $11052.5 \pm 660.7 \text{ Bq}\cdot\text{m}^{-2}$ and $14356.7 \pm 1023.3 \text{ Bq}\cdot\text{m}^{-2}$ with a mean value of $12889.3 \text{ Bq}\cdot\text{m}^{-2}$ for $^{210}\text{Pb}_{\text{ex}}$. The mean values of the ^{137}Cs and $^{210}\text{Pb}_{\text{ex}}$ inventories for the 9 soil cores were 1820.4 Bq m^{-2} and $12859.9 \text{ Bq m}^{-2}$, which were considered as local ^{137}Cs and $^{210}\text{Pb}_{\text{ex}}$ reference inventories. The reported ^{137}Cs references for the Sichuan Basin were 2600 Bq m^{-2} in 1991 in Yanting [1], and 2035.8 Bq m^{-2} in 1997 in Nanchong [2], and their corresponding values in 2002 were $2017 \text{ Bq}\cdot\text{m}^{-2}$ and 1812.8 Bq m^{-2} , respectively. The ^{137}Cs reference inventory at the study site was close to the Nanchong’s value. No $^{210}\text{Pb}_{\text{ex}}$ reference inventories or $^{210}\text{Pb}_{\text{ex}}$ fallout fluxes in the Sichuan Basin were reported. Despite the fact that such information is scanty for China, there are reports on $^{210}\text{Pb}_{\text{ex}}$ reference inventories in the Loess Plateau (5730 Bq m^{-2} , [3]) and in Taiwan province of China (34000 Bq m^{-2} , [4]). The $^{210}\text{Pb}_{\text{ex}}$ flux was reported to be $341.7 \text{ Bq m}^{-2} \text{ a}^{-1}$ in the estuary of the Yangtze River [5] and $149.7 \text{ Bq m}^{-2}\cdot\text{a}^{-1}$ [6] in the coast area of Xiamen, Fujian province of China, the corresponding $^{210}\text{Pb}_{\text{ex}}$ reference inventories of these sites were 11390 Bq m^{-2} and 4990 Bq m^{-2} , respectively. The limited information on deposition fluxes of fallout $^{210}\text{Pb}_{\text{ex}}$ in the world vary from 23 Bq m^{-2} to 367 Bq m^{-2} , the corresponding $^{210}\text{Pb}_{\text{ex}}$ reference inventories were 766.7 Bq m^{-2} and 12233 Bq m^{-2} , respectively [6]. Appleby and Oldfield [7] indicated that the values are reduced and generally increase from the west to east over the continents, due to the predominant west-east movement of air masses. Henderson and Maier-Reimer [8] used an atmosphere model of ^{222}Rn sources and transport to predict $^{210}\text{Pb}_{\text{ex}}$ deposition flux distribution over the oceans in the world and the $^{210}\text{Pb}_{\text{ex}}$

deposition flux prediction map shows that the East China Sea has the highest value of about 7700 Bq m⁻² in the world oceans. The ²¹⁰Pb_{ex} reference inventory of 12859.9 Bq m⁻² (385.8 Bq m⁻² a⁻¹) at the study area in the Sichuan Hilly Basin seems to be the highest value reported in the world, except the deposition flux of 34 000 Bq·m⁻² in the Yanminshan of Taiwan province with an annual precipitation of 4500 mm [4]. It is noticed that the local ⁷Be reference inventories were 117.4 Bq m⁻² and 169.9 Bq m⁻² before and after the wet season, respectively [9]. These data were obtained from the flat grass land of a meteorological observation yard of the Yanting Purple Soil Agricultural Ecology Station of CAS, Yanting County in the Sichuan Basin, 125 km northeast to the study site (Fig. 1). By comparison with the reported ⁷Be reference inventories or deposited fluxes in the similar latitude regions of the world, the inventories in Yanting of the basin are considerably low. It is suggested that the low ⁷Be and high ²¹⁰Pb_{ex} deposition fluxes in the Sichuan Basin are related to its topography and climate conditions. ²¹⁰Pb_{ex} is a geogenic radionuclide of ²²²Rn decay daughter (half-life 3.8 days), which is emitted from the continental crust, while ⁷Be is a cosmogenic radionuclide which is a spallation product of N or O atoms under the cosmic ray bombardment in the stratosphere and troposphere. The Sichuan Hilly Basin is surrounded by mountains and characterized with very cloudy and wet weather. The average annual relative humidity, cloud cover index and sunshine time are only about 75%, 8, and 1200 hrs, respectively, in the basin [10]. The thick clouds prevent cosmic rays piercing through to produce ⁷Be radionuclides in the lower troposphere as well as the local produced ²¹⁰Pb_{ex} radionuclides from the crust moving up into the upper troposphere. However, the ²¹⁰Pb_{ex} radionuclides are still transported into the atmosphere of the basin with air flows from other regions. Due to thick clouds, the basin has a low ⁷Be deposition flux or reference inventory but a high ²¹⁰Pb_{ex} fallout flux or reference inventory.

2.5. Downslope variations in both ¹³⁷Cs and ²¹⁰Pb_{ex} inventories

The ¹³⁷Cs and ²¹⁰Pb_{ex} inventories were characterised by similar downslope variation patterns for the study field (Table 1). For the steeper upper subfields with a slope gradient of 10°, the mean ¹³⁷Cs and ²¹⁰Pb_{ex} inventories¹ were 993 Bq m⁻² and 8028 Bq m⁻², which accounted for 55% and 62% of the reference values, while for the lower subfields of 20°, the inventories were 1298.6 Bq m⁻² and 11388.2 Bq m⁻², accounting for 71% and 89% of the reference value, respectively (Table 1). The depletion of ¹³⁷Cs and ²¹⁰Pb_{ex} inventories is related to the net soil losses and it is obvious that the net erosion rate in the upper subfield is greater than in the lower subfield. The differences of the ¹³⁷Cs and ²¹⁰Pb_{ex} inventories of cultivated soils from the reference values usually result from either water erosion or soil translocation by tillage [1, 11]. However, the differences may also partly result from the traditional cultivation measure of ‘Tiaoshamiantu’ on the study field, by which the deposited sediments in the counter ditches and in the micro sediment trapping tanks are being returned back to the field. Therefore, the downslope variations of the ¹³⁷Cs and ²¹⁰Pb_{ex} inventories in the study field are probably caused by the combination of water erosion, tillage and the ‘Tiaoshamiantu’ measure.

¹The data represent the mean values of the two parallel transects for each downslope distance.

TABLE 1. COMPARISON OF THE CAESIUM-137 AND EXCESS LEAD-210 INVENTORIES AND THE ESTIMATED ANNUAL SOIL LOSSES BASED ON CAESIUM-137 AND EXCESS LEAD-210 MEASUREMENTS

Sampling site	Distance (m)	¹³⁷ Cs inventory (Bq m ⁻²)	Annual soil losses estimated by ¹³⁷ Cs (cm a ⁻¹)	²¹⁰ Pb _{ex} inventory (Bq m ⁻²)	Annual soil losses estimated by ²¹⁰ Pb (cm a ⁻¹)	
Upper subfield	1	1.0	275	0.92	5210	0.88
	2	3.0	672	0.49	6975	0.51
	3	5.0	1916		11737	0.06
	4	7.0	1109	0.25	8189	0.34
Mean value		993		8028		
Lower subfield	5	8.5	1587	0.07	13204	
	6	10.5	1378	0.14	9779	0.19
	7	12.5	898	0.35	9178	0.24
	8	14.5	1115	0.24	10048	0.17
	9	16.5	1840		17233	
Mean value		1299		11388		

In the upper subfield, the ¹³⁷Cs and ²¹⁰Pb_{ex} inventories ranged from 275 Bq m⁻² and 5211 Bq m⁻² to 1916 Bq m⁻² and 11738 Bq m⁻², respectively, and ¹³⁷Cs and ²¹⁰Pb_{ex} inventories increased as slope length increased until the toe site 4. In the lower subfield, the ¹³⁷Cs and ²¹⁰Pb_{ex} inventories ranged from 898 Bq m⁻² and 9179 Bq m⁻² to 1840 Bq m⁻² and 17233 Bq m⁻², respectively, and the lowest inventories occurred at the middle site 7 while the two highest values were recorded at the toe site 9 and top site 5. Soil loss rates by water erosion usually increase and the rates by tillage usually decrease as slope length increases on a cultivated slope [11, 12]. The general tendency of decreasing ¹³⁷Cs and ²¹⁰Pb_{ex} inventories in the upper subfield should be mainly due to translocation of cultivated soils by tillage. Returning sediments from the upper side ditch back to the field by the process of ‘Tiaoshamiantu’ has no significant effect on the ¹³⁷Cs and ²¹⁰Pb_{ex} inventories at the top site 1 of the upper subfield, because the upslope cliff of only about 1 m high produces little sediments. The lower ¹³⁷Cs and ²¹⁰Pb_{ex} inventories at the toe site 4 than at the site 3 are partly due to the severe water erosion and the fact that that farmers liked to return the deposited sediments in the middle ditch back to the top of the lower subfield during ‘the Peoples Commune Period’ of 1950s-1970s. The spatial variability in ¹³⁷Cs and ²¹⁰Pb_{ex} inventories in the lower subfield, which is very short and only has a slope length of 9 m, was very different from either the water erosion pattern or the tillage pattern. Additionally, the lowest values occurred at the middle site 7 while the two highest values at the top site 5 and the toe site 9. It is suggested that the traditional cultivation measure of the ‘Tiaoshamiantu’ played an important role in redistribution of cultivated soils and the related ¹³⁷Cs and ²¹⁰Pb_{ex} inventories on the lower subfield.

2.6. Soil erosion rates

At an eroding site of the study field, the soil losses occurred by either water erosion or soil translocation by tillage, which led to a reduction in ¹³⁷Cs. Some of this soil loss was compensated by returning the deposited sediments in the ditches back to the fields, but generally this soil was replaced by ¹³⁷Cs free subsoil incorporated by the annual ploughing. Therefore, the mass balance model is still able to be used for estimating soil losses for the study fields and the annual soil loss depth at the site was calculated by following the simplified model [13, 14]:

$$A=A_0 (1-h/H)^{y-1963} \quad (1)$$

where:

- A is the ^{137}Cs inventory (Bq m^{-2});
- A_0 is the local ^{137}Cs reference inventory (Bq m^{-2});
- h is the annual soil loss depth (cm);
- H is the plough depth (20 cm);
- y is the sampling year.

The annual soil losses in the upper subfield were estimated to range between 0.25 cm and 0.92 cm (except for the site 3) and in the lower subfield between 0.14 cm and 0.35 cm (except for the site top and bottom sites) (Table 1).

Unlike ^{137}Cs , the $^{210}\text{Pb}_{\text{ex}}$ distribution is in a steady state for a continuous cultivated land over more than 100 years, such as the studied field. It means that the $^{210}\text{Pb}_{\text{ex}}$ inventory is constant at a non-deposition site, where the annual $^{210}\text{Pb}_{\text{ex}}$ loss due to the soil losses and radio decay is replaced by the annual $^{210}\text{Pb}_{\text{ex}}$ deposition flux. The annual soil loss depth at a non-deposition site can be therefore estimated by using the following model [15, 3]:

$$h=H (A_0-A) \lambda/A \quad (2)$$

where:

- A is the $^{210}\text{Pb}_{\text{ex}}$ inventory (Bq m^{-2});
- A_0 is the local $^{210}\text{Pb}_{\text{ex}}$ reference inventory (Bq m^{-2});
- λ is the radio decay coefficient (0.03).

The annual soil losses were estimated in the upper subfield to range between 0.34 cm and 0.88 cm, except for the site 3 and 9, in the lower subfield between 0.17 cm and 0.24 cm, except for the top site 5 and the bottom site (Table 1).

The estimated annual soil losses between the ^{137}Cs and $^{210}\text{Pb}_{\text{ex}}$ measurements were quite close and it strongly indicates that the continuous natural $^{210}\text{Pb}_{\text{ex}}$ can be used to assess soil rates for a medium to long timescale of about 50-100 years. It is suggested that very little erosion or accumulation has occurred at site 3 of the upper subfield, because the ^{137}Cs inventory was slightly higher than the reference inventory while the $^{210}\text{Pb}_{\text{ex}}$ inventory is slightly lower than the reference inventory. By combination of the erosion rates from the ^{137}Cs and $^{210}\text{Pb}_{\text{ex}}$ measurements, the weighted mean net soil erosion rate was estimated to be $4870 \text{ t km}^{-2} \text{ a}^{-1}$ for the upper subfield, taking $\gamma = 1.15 \text{ g cm}^{-3}$. At the top site of the lower subfield, ^{137}Cs inventory was 87.2% of the reference value and the $^{210}\text{Pb}_{\text{ex}}$ inventory 102.7% of the reference value. The annual soil loss depth of 0.07 cm from the ^{137}Cs measurement at the site was used for estimating the mean erosion rate soil loss of the lower subfield. As mentioned above, the accumulation rate at the bottom site of the lower subfield was estimated to be about 0.5 cm a^{-1} . By combination of the erosion and the accumulation rates from the ^{137}Cs and $^{210}\text{Pb}_{\text{ex}}$ measurements, the weighted mean net soil erosion rate was estimated to be $1691 \text{ t km}^{-2} \text{ a}^{-1}$ for the lower subfield.

The Ziyang agriculture experiment station of the Sichuan Academy of Agriculture, located in Ziyang County, has similar soil and landscape conditions to the study site, which is 45 km

northwest to the station (Fig. 1). The soil erosion rates from the runoff plot measurements of 1989-1995 at the station were $2590 \text{ t km}^{-2} \text{ a}^{-1}$ for the cultivated slope of 10° and $4221 \text{ t km}^{-2} \text{ a}^{-1}$ for the slope of 15° [16]. However, the net erosion rate of $1691 \text{ t km}^{-2} \text{ a}^{-1}$ for the lower studied subfield of 10° accounts for 65% of the measured erosion rate on the runoff plot of 10° from the runoff measurements, while the net erosion rate of $4870 \text{ t km}^{-2} \text{ a}^{-1}$ for the upper slope of 20° is close to the measured erosion rate of $4221 \text{ t km}^{-2} \text{ a}^{-1}$ on the runoff plot of 20° . The above comparison of the net erosion rates on the study field with the measured erosion rates on the runoff plots indicates that the traditional drainage system and 'Tiaoshamiantu' cultivation measure has significant positive effects on the conservation of the valuable steepland farmland in the Sichuan Hilly Basin.

3. SEDIMENT SOURCE IDENTIFICATION BY USING CAESIUM-137 AND EXCESS LEAD-210 RADIONUCLIDES IN A SMALL CATCHMENT OF THE HILLY SICHUAN

3.1. Study area

This study was carried out to identify sediment sources and assess sediment contributions from cultivated terraces, steep forest and grass slopes, bare slopes and river banks in a small catchment of the Wujia Gully located in the Hilly Sichuan Basin of Yanting County, Sichuan Province, by using radionuclide tracers such as ^{137}Cs and $^{210}\text{Pb}_{\text{ex}}$. The Wujia Gully, near the Yanting Ecology-Agriculture Station of Chengdu Institute of Mountain Hazards and Environment, CAS, in Yanting County of the Hilly Sichuan Basin, has a drainage area of 0.22 km^2 and the elevations range between 420 m and 560 m a.s.l. The catchment is underlain by horizontally bedded mudstones, siltstones and sandstones of the Jurassic Penglaizhen Group. The topography typically comprises steep sandstone cliffs with slopes of 25° - 30° separated by gentle terraces of $< 10^\circ$, underlain by mudstones and siltstones in the catchment. The gentle terraces and the steep slopes account for 1/3 and 2/3 of the catchment area, respectively. The gentle terraces have been cultivated for centuries, whereas the steep slopes were originally covered by waste grasses but have gradually been afforested with cypress trees since 1970s (Fig. 3). There are only a few bare slopes located on nearly vertical terrace banks. The purple soils on the cultivated terraces, forest and waste slopes in the catchment are derived from fast weathering of Jurassic rocks [5]. Average annual precipitation is 826 mm, 70% of which occurs in the wet season from June to September.

In 1956 a small reservoir for irrigation purposes was made at the outlet of the Wujia Gully catchment by constructing an earth dam with a height of 4.75 m. The reservoir has a current storage capacity of $25,000 \text{ m}^3$ with a maximum water depth of 3.0 m and a surface area of $9,200 \text{ m}^2$. This dam has a spillway and bottom culvert with several intakes on the left side. The maximum sediment deposition depth since 1956 was 1.3 m and 5000 m^3 of sediments had been deposited in the reservoir, which was estimated from the changes in water storage volume of the reservoir. Parts of the fringe areas in the reservoir were dredged in 1985. Based on the deposited sediment volume in the reservoir (since 1956), the specific sediment yield of the studied catchment is estimated to be $642 \text{ t km}^{-2} \text{ a}^{-1}$. The Wujia Gully catchment is very small and is characterised by steep terrain. The eroding purple soil is very fine, in which 99 per cent of the particles are less than 0.5 mm in diameter. Field investigation indicated that no significant deposition occurred in the gully bottom upstream of the reservoir. The average erosion rate over the catchment above the reservoir was suggested to be close to the specific sediment yield of $642 \text{ t km}^{-2} \text{ a}^{-1}$.

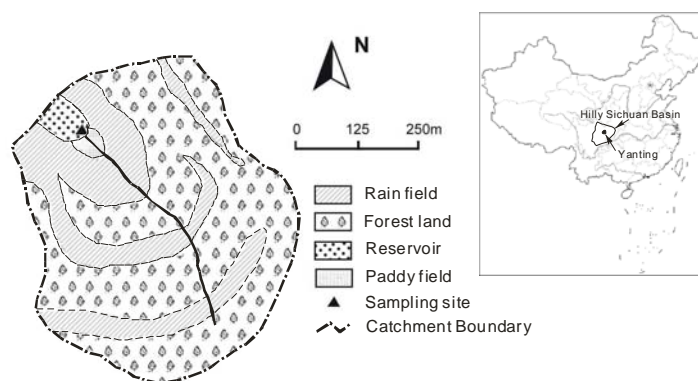


FIG. 3. A sketch map of the Wujia gully and the sampling location of sediment deposit profile in the reservoir.

3.2. Sampling and Measurements

In May 2002 a sediment deposit profile of 106 cm deep was made on the fringe of the reservoir by using a 95 mm diameter core tube comprising two segments, which could be separated to facilitate sectioning of the core. The profile was divided into 7 sections with intervals of 7-14 cm. Based on interviews with the local farmers, it was found out that a sediment layer of about 50 cm had been deposited at the sampling site since the reservoir was partly dredged in 1985. In total 14 surface soil samples of 0-5 cm in depth were collected using a soil scraper in the catchment; 6 samples for gentle cultivated terraces, 6 samples for steep forest slopes and 2 samples for bare slopes. ^{210}Pb , ^{226}Ra and ^{137}Cs activities of the soil and sediment samples were measured in the isotope laboratory of Department of Geography and Archaeology, Exeter University, Exeter, UK. The samples were air-dried, disaggregated and passed through a 2 mm sieve before they were sent to UK for the measurement by gamma spectroscopy, as described above.

3.3. Results and Discussion

3.3.1. ^{137}Cs , ^{210}Pb and $^{210}\text{Pb}_{\text{ex}}$ concentrations in source soils

The study carried out in 1994 in the Zhaojiawan Gully next to the Wujia Gully catchment showed that the local ^{137}Cs reference inventory was $2,600 \text{ Bq m}^{-2}$ and its corresponding value was $2,017 \text{ Bq m}^{-2}$ for 2002. The ^{137}Cs contents of ploughed soils on gentle cultivated terraces varied mostly between 4.0 and 8.0 Bq kg^{-1} with a mean value of 5.5 Bq kg^{-1} at that time [1].

Concentrations of ^{137}Cs , ^{210}Pb and $^{210}\text{Pb}_{\text{ex}}$ in the surface soils on forested slopes, cultivated terraces and bare slopes from this study are shown in Table 2. Surface soils on the steep forestland had the highest concentrations for all three radionuclides. ^{137}Cs concentrations ranged between 4.93 Bq kg^{-1} and 9.76 Bq kg^{-1} with a mean value of $7.15 \pm 0.40 \text{ Bq kg}^{-1}$ while ^{210}Pb concentrations between 135.7 and 206.3 Bq kg^{-1} with a mean value of $162.0 \pm 3.9 \text{ Bq kg}^{-1}$, and the $^{210}\text{Pb}_{\text{ex}}$ concentrations between 64.4 Bq kg^{-1} and $159.91 \text{ Bq kg}^{-1}$ with a mean value of $124.8 \pm 6.1 \text{ Bq kg}^{-1}$. Surface soils on the cultivated terraces had medium concentrations of those radionuclides, and ^{137}Cs concentrations ranged between 2.82 Bq kg^{-1} and 4.72 Bq kg^{-1} with a mean value of $4.01 \pm 0.31 \text{ Bq kg}^{-1}$ while ^{210}Pb concentrations between 59.35 Bq kg^{-1} and 84.05 Bq kg^{-1} with a mean value of $70.96 \pm 2.65 \text{ Bq kg}^{-1}$ and the $^{210}\text{Pb}_{\text{ex}}$ concentrations between 34.41 Bq kg^{-1} and 58.96 Bq kg^{-1} with a mean value of $45.52 \pm 3.11 \text{ Bq kg}^{-1}$. However, due to severe soil erosion, the surface soils on the bare slopes contained no ^{137}Cs and $^{210}\text{Pb}_{\text{ex}}$ and was characterised by the lowest values in ^{210}Pb , which ranged between 10.27 Bq kg^{-1} and 19.96 Bq kg^{-1} with a mean value of $15.12 \pm 1.22 \text{ Bq kg}^{-1}$.

TABLE 2. CAESIUM-137, LEAD-210 AND EXCESS LEAD-210 CONCENTRATIONS IN SURFACE SOILS

Land types	¹³⁷ Cs concentrations	²¹⁰ Pb concentrations	²¹⁰ Pb _{ex} concentrations
	(Bq kg ⁻¹)	(Bq kg ⁻¹)	(Bq kg ⁻¹)
	Range	Range	Range
	(Mean)	(Mean)	(Mean)
Cultivated terraces	2.82±0.27~4.72±0.38 (4.01±0.31)	59.35±2.60~84.05±3.00 (70.96±2.65)	34.41±2.68~58.96±4.04 (45.52±3.11)
Forest slopes	4.93±0.32~9.76±0.52 (7.15±0.40)	135.7±3.3~206.4±4.5 (162.0±3.9)	64.35±3.51~159.9±7.3 (124.8±6.1)
Bare slopes	0 (0)	10.27±1.02~19.96±1.42 (15.12±1.22)	0 (0)

3.3.2. ¹³⁷Cs, ²¹⁰Pb and ²¹⁰Pb_{ex} depth distributions in the profile of deposited sediment in the reservoir

¹³⁷Cs, ²¹⁰Pb, ²¹⁰Pb_{ex} and fine particle content (< 0.05 mm) of the deposited sediment in the reservoir are shown in Fig. 4. Soil deposits with high ¹³⁷Cs concentration were predominantly present in the upper part of the profile that was deposited after dredging in 1985. The maximum ¹³⁷Cs concentration of 4.20±0.31 Bq kg⁻¹ could be found in the middle of the profile at a depth of 39-50 cm but decreased gently towards the surface to 3.06±0.23 Bq kg⁻¹ in the top 12 cm layer, while the sediment below the 50 cm in depth contained no ¹³⁷Cs. There were significant differences in ²¹⁰Pb and ²¹⁰Pb_{ex} concentrations between the sediments in the profile from above and below a depth of 50 cm. ²¹⁰Pb concentrations in the upper 50 cm in the profile varied between 52.46±2.28 Bq kg⁻¹ and 82.46±1.89 Bq kg⁻¹ and ²¹⁰Pb_{ex} concentrations between 30.72±2.36 Bq kg⁻¹ and 62.63±2.91 Bq kg⁻¹. However, the sediments below 50 cm contained very little or no ²¹⁰Pb_{ex} and had low ²¹⁰Pb concentrations ranging between 16.91±1.33 Bq·kg⁻¹ and 34.07±1.85 Bq·kg⁻¹. It can be concluded that the upper 50 cm sediments in the profile were the deposits since 1985 and the lower part below 50 cm was the buried paddy soil, which may be deposited sediments from many years ago because the soil had a similar grain size composition as compared to the recently deposited sediments (Fig.4). The maximum ²¹⁰Pb_{ex} concentrations of 62.63±2.91 Bq kg⁻¹ and ²¹⁰Pb of 82.46±1.89 Bq kg⁻¹ were located in the sub-top layer at a depth of 12-26 cm and those concentrations decreased downwards to 30.72±2.36 Bq kg⁻¹ and 52.46±2.28 Bq kg⁻¹ in the sediment layer at a depth of 39-50 cm. ²¹⁰Pb_{ex} and ²¹⁰Pb concentrations were 50.87±2.17 Bq·kg⁻¹ and 72.66±1.61 Bq·kg⁻¹ in the top 12 cm layer, which was slightly less than the sub-top layer. Taking the top 50 cm sediments as the deposits since 1985, the mean deposit rate over the period of 1985-2002 was estimated to be 3.0 cm·a⁻¹.

The deposited sediments in the reservoir were a mixture of sediments originating from the following sources, i.e. forestland, cultivated terraces and bare steep land, and gully banks. For the rapidly silting reservoir in the study catchment, the delivered sediments were the main sources of the measured ¹³⁷Cs and ²¹⁰Pb_{ex} in the reservoir deposits. Besides radio decay, variation in ¹³⁷Cs, ²¹⁰Pb_{ex} and ²¹⁰Pb concentrations with depth in the profile were related not only to the changes of the fallout fluxes but also to the changes of the land use conditions in the catchment. The trend of decreasing ¹³⁷Cs concentration in the sediments from a depth at 50 cm towards the surface reflects the reduction of the radionuclide in the surface soils of steep forest slopes and gentle cultivated terraces due to surface soil erosion. If land use

conditions were constant since 1985, the maximum $^{210}\text{Pb}_{\text{ex}}$ concentration should have occurred in the top layer of the profile and it would have decreased downward due to radio decay of the nuclide. However, the maximum ^{210}Pb concentration did not occur in the top layer but in the sub-top layer and then it decreased downwards in the profile. It was suggested that the reduction in sediments originating from the soils containing high ^{210}Pb of the forested slopes was due to the optimal soil cover because of denser canopies of the growing cypress forests. There are no data on local $^{210}\text{Pb}_{\text{ex}}$ fluxes and such information is very limited in China. It was reported that the $^{210}\text{Pb}_{\text{ex}}$ flux was $341.7 \text{ Bq m}^{-2} \text{ a}^{-1}$ in the mouth area of the Yangtze River [17] and $149.7 \text{ Bq m}^{-2} \text{ a}^{-1}$ in the coast area of Xiamen, Fujian Province [3,2]. It was estimated to be $171.9 \text{ Bq m}^{-2} \text{ a}^{-1}$ from the $^{210}\text{Pb}_{\text{ex}}$ reference inventory of 5730 Bq m^{-2} at non-eroded grassland in Zichan, Shaanxi Province, the Loess Plateau. Taking $221.1 \text{ Bq m}^{-2} \text{ a}^{-1}$, the mean value of the above three fluxes, as the local $^{210}\text{Pb}_{\text{ex}}$ flux in the study area, the $^{210}\text{Pb}_{\text{ex}}$ precipitation on the water surface of the reservoir accounted for 10.4% of the $^{210}\text{Pb}_{\text{ex}}$ activities in the deposited sediments of the top 12 cm.

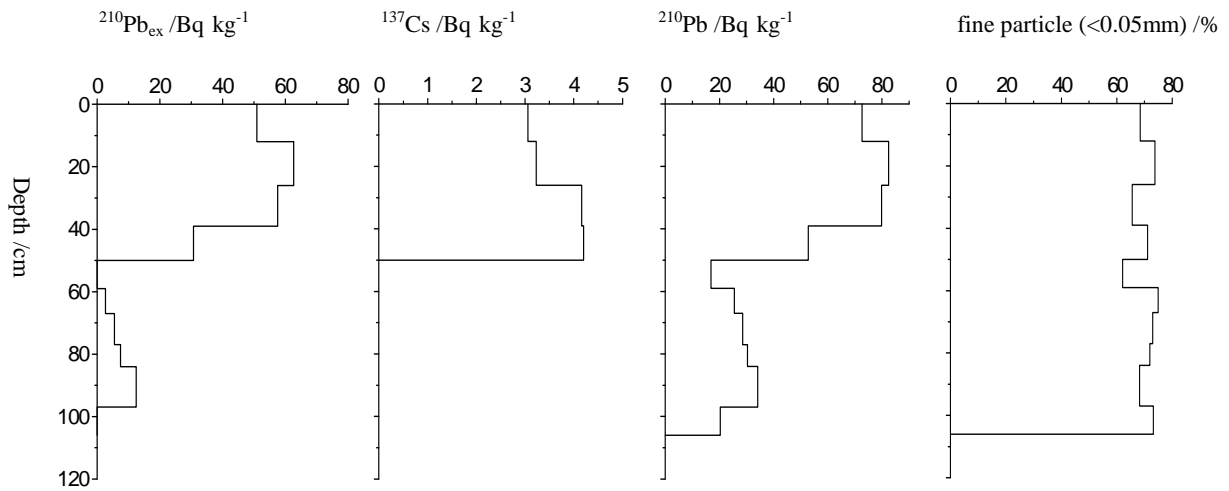


FIG. 4. Depth distributions of ^{137}Cs , ^{210}Pb , $^{210}\text{Pb}_{\text{ex}}$ and fine particle contents of the deposited sediments in the reservoir.

3.3.3. Relative sediment contributions

If particle selection is ignored, relative contributions of three types of soil sources to the delivering sediment in a catchment could be calculated from the concentrations of two tracers in the sediment and source soils by using the following mixing model:

$$C_d = C_1 \times f_1 + C_2 \times f_2 + C_3 \times f_3 \quad (3)$$

$$P_d = P_1 \times f_1 + P_2 \times f_2 + P_3 \times f_3 \quad (4)$$

$$f_1 + f_2 + f_3 = 1 \quad (5)$$

where:

C_d is the concentration of tracer C in sediment (Bq kg^{-1});

C_1, C_2, C_3 are the concentrations of tracer C in three types of soil sources, respectively, (Bq kg^{-1});

P_d is the concentration of tracer P in sediment (Bq kg^{-1});

P_1, P_2, P_3 are the concentrations of tracer P in three types of soil sources, respectively, (Bq kg^{-1});

f_1, f_2, f_3 are the relative sediment contributions of the three types of soil sources, respectively (%).

As mentioned above, the Wujia Gully is a very small and rather uniform catchment of 0.22 km^2 being characterised by steep slopes and fine eroding purple soil without significant deposition in the gully bottom upstream of the reservoir. Therefore the relative contributions of the forest slopes, cultivated terraces and bare slopes to the recent deposited sediment of the top 12 cm in the profile were estimated from two tracer groups, of which one consists of ^{137}Cs and ^{210}Pb and the other of ^{137}Cs and $^{210}\text{Pb}_{\text{ex}}$. The ^{210}Pb and $^{210}\text{Pb}_{\text{ex}}$ concentrations used for calculating the relative sediment contributions were determined by subtracting the direct fallout flux values on the water surface of the reservoir from the measured values of deposited sediment. The relative sediment contributions of the forest slopes, cultivated terraces, and bare slopes were estimated to be 18%, 46% and 36%, respectively, by using ^{137}Cs and ^{210}Pb as tracers, while those were 8%, 64% and 28%, respectively, by using ^{137}Cs and $^{210}\text{Pb}_{\text{ex}}$ as tracers. Taking the average erosion rate over the catchment as $642 \text{ t km}^{-2} \text{ a}^{-1}$ and that cultivated terraces and forest slopes account for 1/3 and 2/3 of the catchment area, the erosion rates were estimated to be $886 \text{ t km}^{-2} \text{ a}^{-1}$ for the cultivated terraces and $173 \text{ t km}^{-2} \text{ a}^{-1}$ for the forest slopes, respectively. The slightly lower $^{210}\text{Pb}_{\text{ex}}$ and ^{210}Pb concentrations in the top 12 cm deposits in the profile compared to those in the sub-top 12-26 cm deposits in the profile indicates that the proportion of sediment delivering from the forest slopes has decreased because the cypress forests were growing, improving the soil cover.

4. INVESTIGATION OF EROSION SEVERITIES AND SEDIMENT PRODUCTION BY CAESIUM-137 DATING OF RESERVOIR AND POND DEPOSITS IN SMALL CATCHMENTS OF THE HILLY SICHUAN BASIN AND THE THREE GORGES REGION

4.1. Study Areas

In 2003-2004, a study on erosion and sedimentation was carried out in four small catchments in Yanting County and Nanchong City of the Hilly Sichuan Basin and Kaixian County of the Three Gorges region based on analyses of deposits of small reservoirs and ponds by using the ^{137}Cs fingerprinting technique. Geomorphologically, Nanchong belongs to the medium hill region of the Hilly Sichuan Basin while Yanting is in the medium high hill region of the basin. Kaixian belongs to the parallel ridge-valley region with low mountains of the eastern Basin (Fig. 5). Geographical and land use conditions of the four catchments are showed in Table 3.

The Wujia Gully and Jiliu Gully catchments are both near the Yanting Ecology-Agriculture Station of Chengdu Institute of Mountain Hazards and Environment, CAS, in Yanting County, and have drainage areas of 0.22 km^2 and 0.09 km^2 , respectively. The two catchments have similar physical geography and land use conditions and elevations vary between 420 m and 560 m above sea level. The catchments are underlain by horizontally bedded mudstones, siltstones and sandstones of the Jurassic Penglaizhen Group. The landform typically comprises steep sandstone cliffs with slopes of 25° - 30° separated by gentle mudstone and siltstone terraces of $<10^\circ$. The gentle terraces and the steep slopes account for 1/3 and 2/3 of the catchment area, respectively. The gentle terraces have been cultivated for centuries,

whereas the steep slopes were originally covered by waste grasses but have gradually been afforested with cypress trees since 1970s.

The Tianmawan Gully catchment in Nanchong has a drainage area of 0.19 km² and elevations vary between 310 m and 420 m above sea level. The catchment is underlain by horizontally bedded mudstones and siltstones of the Jurassic Suining Group. The landform typically comprises dozens of small steep cliffs separated by short gentle terraces. The steep cliffs usually have heights of a few meters and are covered by waste grasses with widely dispersed young cypress trees, while the gentle terraces with slopes of <10° and with lengths of 10-30m are mostly rainfed lands. \

The Chunqiu Gully catchment in Kaixian County has a drainage area of 0.58 km² and elevations between 190 m and 400 m above sea level. The catchment is underlain by mudstones and sandstones of the Jurassic Shaximiao Group with an inclination of about 30°. The landforms are characterized with inclining bedded rocky low mountains which are typical in the parallel ridge-valley region of the Eastern Sichuan Basin. The catchment and bed rock have the same orientation direction. As the catchment face has same direction with the bedrock dip, bedding slopes occupy most of the catchment. Soils are thin on the bedding slopes and some of the slopes are bare. Part of the bedding slopes are rainfed lands and others are waste grass lands.

In all four study catchments the soils on the slopes are purple soils. These purple soils originated from different strata and have considerable differences in erosion resistance. Due to different proportions of sandstones, the purple soils of the Penglaizhen Group and the Suining Group have relatively high and low erosion resistances while the resistance of the Shaximiao Group is in between. As the size of the studied catchments is less than 1 km², the four small catchments have little valley areas and relatively high longitudinal channel gradients of 10-20%. Reclamation ratio in the Tianmawan Gully is 0.45, while the ratios are 0.25 in other three catchments. Annual precipitations are 1100 mm in Kaixian, 1010 mm in Nanchong and 826 mm in Yanting, respectively, 70% of which occur in the wet season from June to September.

A pond with an earth dam of 4-5m high was constructed at the outlet of each catchment during the period from 1949 to 1956 and had a storage volume of 1.5-5.1×10⁴ m³. The dams were made up of soils dug from the valley bottoms within the ponds. The four ponds have simple water delivery facilities of weirs or bottom culverts with intakes. The storage water in the ponds is used for irrigation in spring and summer. The two ponds in the Chunqiu Gully and in the Jiliu Gully have no flood spill ditches, while the pond in the Wujia Gully catchment has a ditch but it was seldom used. The delivered sediments from the upstream catchments have been predominantly deposited in the ponds in the three gullies. The pond of the Tianmawan Gully has a flood spill ditch, which has been used to prevent flood water with high sediment concentrations from entering into the pond of the Tianmawan Gully for preservation of the limited storage capacity, especially from 1981 onwards when the land use responsibility system was introduced in the rural area of China. However, before 1981 the spill ditch was seldom used and the delivered sediments from the upstream catchment predominantly deposited in the reservoir.

TABLE 3. THE BASIC INFORMATION ABOUT STUDY CATCHMENTS

Catchment	Drainage area (km ²)	Relative relief (difference between the lowest and highest altitude) (m a.s.l.)	Longitudinal channel gradient (%)	Strata bedding	Annual precipitation (mm)	Cropland precipitation ratio	Dam height (m)	Construction time	Storage capacity (m ³)
Penglaiizhen									
Wujia Gully, Yanting	0.22	140 (420-560)	11.8	Group (mudstones, siltstones and sandstones)	826	0.25	4.75	1956	25000
Penglaiizhen									
Jiliu Gully, Yanting	0.09	110 (420-530)	19.8	Group (mudstones, siltstones and sandstones)	826	0.25	5.0	1955	15000
Suning									
Tianmawan Nanchong	Gully, 0.19	110 (310-420)	12.7	Group (mudstones and siltstones)	1010	0.45	4.0	1949	21000
Shaximiao									
Chunqiu Kaixian	Gully, 0.58	210 (190-400)	9.7	Group (mudstones and sandstones)	1100	0.25	4.0	1955	51000

*Storage capacity of the Chunqiu Gully's pond is estimated from the counter map (1:10000) and the heights of dam, other reservoirs' capacities are according to interview to local technicians and farmers.



FIG. 5. A sketch map of the sampling locations.

4.2. Sampling and measurements

Incremental samples of sediment deposit profiles were collected in the four ponds in 2003-2004. The two ponds of the Wujia Gully and the Jiliu Gully catchments in Yanting were drained in the autumn of 2003 for construction of a new irrigation channel, so a pit was dug for sampling. Sediment samples of the complete deposit profiles of 120 cm and 190 cm deep were collected in the Wujia Gully and the Jiliu Gully, respectively. With regards to the Tianmawan Gully and the Chunqiu Gully catchments, sediment samples of the deposit profiles were collected by drilling a core with a diameter of 98 mm at the center of the ponds, and a PVC pipe with a diameter of 100 mm was used to protect the core during the drilling. Due to the homogeneous composition of the deposited sediments over the profiles, it was difficult to identify flood events in the profiles and the profiles of the four ponds were sectioned into about 5 cm lengths for sampling. It was noticed that a grey-green fine sand layer was visible at the depth of 50~55 cm in the deposit profile of the Jiliu Gully's pond. By interviewing local farmers, the layer could be linked with road construction in 1984 by which a grey-green sandstone layer of the bedrock was exposed to erosion. In the Tianmawan Gully catchment, additionally incremental samples of two paddy soil profiles were collected to investigate accumulation conditions in paddy fields in the valley upstream of the pond.

All samples were air-dried, disaggregated and passed through a 2 mm sieve prior to analysis of their ^{137}Cs activity by gamma spectrometry. Measurements of ^{137}Cs activities in samples were undertaken by gamma spectrometry, using a high resolution, low background, low energy, hyper-pure n-type germanium coaxial γ -ray LOAX HPGe detector. The samples with a weight of $\geq 380\text{g}$ were placed on the detector and counted for ≥ 50000 s, providing a precision of approximately $\pm 6\%$ at the 95% level of confidence for the gamma ray measurements. The ^{137}Cs concentrations were obtained using 662 keV gamma ray. Particle compositions of the sediment samples in the Jiliu Gully were analyzed using a pipette method.

4.3. Results and Discussion

The 1963's ^{137}Cs peak is clear and easy to be identified in the deposit profiles of the four ponds. The greatest and deepest ^{137}Cs peak occurred at a depth of 145 cm in the pond of the Jiliu Gully catchment whereas the shallowest peak was found at a depth of 25 cm in the pond of the Tianmawan Gully catchment. The variations in clay content ($<0.002\text{mm}$) with depth in the deposit profile of the Jiliu Gully's pond show that the deposited sediments are very fine with an average clay content of 27% and the content has no significant changes over the profile (Fig. 6).

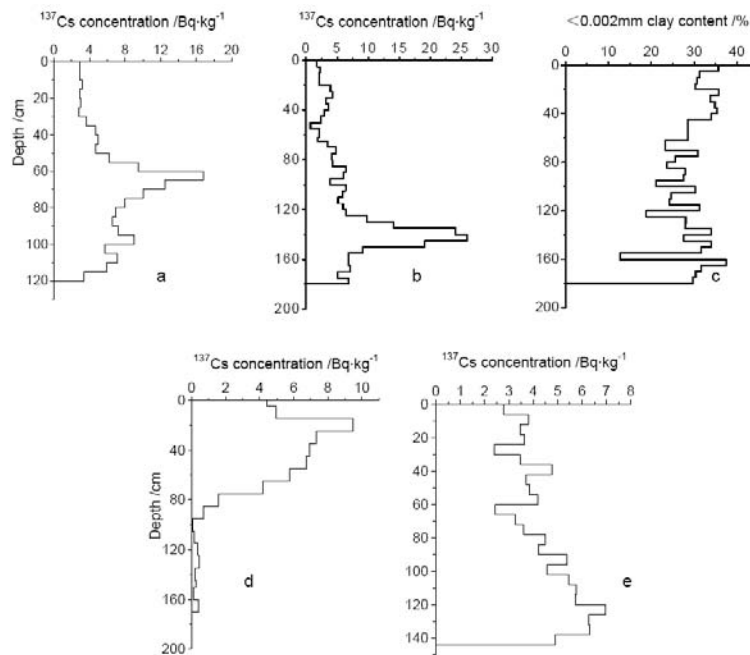


FIG. 6. Depth distributions of ^{137}Cs and clay content of the deposit profiles in the ponds (^{137}Cs concentration depth distributions of the Wujia Gully (a), the Jiliu Gully (b), the Tianmawan Gully (d) and the Chunqiu Gully (e); c. $<0.002\text{mm}$ fine particle content depth distribution of the Jiliu Gully, Yanting).

The deposition volumes of the four ponds since 1963 were estimated according to the 1963 ^{137}Cs peak depths and the deposition areas. As big floods were diverted out of the pond of the Tianmawan Gully since 1981, the estimated value for the pond is the deposition volume during the period from 1963 to 1981. However, the estimated values for the other three ponds are the deposition volumes during the period from 1963 to the sampling year. The specific sediment yields for deposition in the ponds were estimated from the deposition volumes and times, and the catchment areas. The estimated specific yield was $1869 \text{ t km}^{-2} \text{ a}^{-1}$ for the Chunqiu Gully in Kaixian, and $802 \text{ t km}^{-2} \text{ a}^{-1}$ and $713 \text{ t km}^{-2} \text{ a}^{-1}$ for the Wujia Gully and the Jiliu Gully in Yanting, respectively (Table 4). According to the depth of the 1984's grey-green fine sand layer in the profile, the estimated yield is $584 \text{ t km}^{-2} \text{ a}^{-1}$ since 1984, which is lower than the value since 1963. The reduction of the specific sediment yield was probably caused by forestation since the end of 1970s in Yanting.

As the original valley areas above the dam in the three catchments were predominantly occupied by the ponds, little sediment has been accumulated in the upstream valley of the ponds since the dam was built in the 1950s. In addition, the small gullies on the slopes above the valleys are steep and the bedrock beds of the gullies indicate no sediment accumulation occurring there. The sediment delivery ratio should be thus close to 1 for the slopes. It is reasonable to use the specific sediment yields for deposition in pond to represent the specific sediment yield of the three catchments, because there have been no valley areas for sediment accumulation since the dams were built and the sediment delivery ratio on the slopes is close to 1.

The new land created by silting at the upstream delta of the pond has been brought under cultivation as paddy fields in the Tianmawan Gully catchment. However, local farmers were unable to distinguish the new paddy fields from the old fields because the pond was built up long time ago. According to the current water surface area of the pond, the estimated

sediment deposit volume was 1384 m^3 between 1963 and 1981 and the related specific sediment yield for deposition in the pond was $566 \text{ t km}^{-2} \text{ a}^{-1}$, which should be lower than the real value. Investigation of sediment deposition in small reservoirs and ponds in the Liuxi River catchment, in which the Tianmawan Gully is located, showed that the average specific sediment yield for deposition in small reservoirs and ponds is $762 \text{ t km}^{-2} \text{ a}^{-1}$. Some researchers have thought that sediment accumulation is very severe in the paddy fields of the valleys in the Hilly Sichuan Basin, but, the conclusion has not been checked until now with measurements. The unchecked conclusion is important evidence for the low sediment delivery ratio in the basin. Most of valley areas above the pond in the Tianmawan Gully have not been submerged and have been cultivated as paddy fields for centuries. Two ^{137}Cs depth distribution profiles in the paddy fields of the valley above the pond show that ^{137}Cs distribution depths are 25 cm and 28 cm, respectively, and the fallout is quite evenly distributed within the soil layers of the depths (Fig. 7). Those ^{137}Cs distribution depths are closely linked with the plough depth of 25 cm in the paddy field. Therefore, it can be concluded that no severe sediment accumulation occurs in the valley areas of the Medium Hilly Regions, such as in Nanchong. It also implies that the sediment delivery ratio of 0.1 is too low for the region and that the ratio may be between 0.5 and 0.8 and the related average erosion rates are between $1000 \text{ t km}^{-2} \text{ a}^{-1}$ and $1500 \text{ t km}^{-2} \text{ a}^{-1}$.

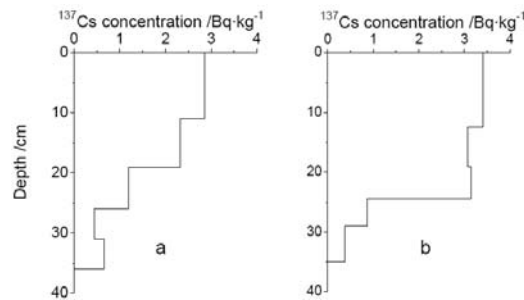


FIG. 7. Depth distributions of ^{137}Cs concentrations of the paddy fields of Tianmawan Gully in Nanchong (a. of No. 1 paddy field; b. of No. 2 paddy field).

The two ponds of the Jiliu and Wujia Gully catchments in Yanting were characterised by the highest ^{137}Cs peak concentrations in the deposit profiles, which were $26.0 \pm 1.4 \text{ Bq kg}^{-1}$ and $16.86 \pm 0.98 \text{ Bq kg}^{-1}$, respectively. The concentrations were $9.50 \pm 0.56 \text{ Bq kg}^{-1}$ and $6.95 \pm 0.43 \text{ Bq kg}^{-1}$ for the ponds of the Tianmawan Gully and Chunqiu Gully, respectively. The high ^{137}Cs peak concentrations in the deposit profiles of the two ponds in Yanting are probably due to the lithology of the Penglaizhen Group, in which sandstone is occupying a large proportion of the area upstream from the ponds. Bare sandstone cliffs are widely distributed in these two catchments. There was no soil to adsorb the precipitated ^{137}Cs fallout with rainfall on the bare rocky slopes during nuclear testing period and the fallout was prone to transport directly into the pond by runoff. The lower ^{137}Cs peak concentrations in the ponds of the two catchments probably resulted from the lower proportion of sandstone areas in the Suining Group of Nanchong and in the Shaximiao Group of Kaixian than in the Penglaizhen Group of Yanting. The Tianmawan Gully's pond had the highest ^{137}Cs concentrations of $4.44 \pm 0.29 \text{ Bq kg}^{-1}$ in the top layer of the deposit profile, while the Jiliu Gully's pond had the lowest value of $1.74 \pm 0.14 \text{ Bq kg}^{-1}$, and the concentrations for the Chunqiu gully and Wujia Gully's ponds were $2.78 \pm 0.20 \text{ Bq kg}^{-1}$ and $2.92 \pm 0.24 \text{ Bq kg}^{-1}$, respectively. The highest value occurred in the Tianmawan Gully's pond because the top layer is linked with deposits from 1981. The lowest value in the Jiliu Gully's pond is probably because of the filling earth on the sides of the road, which was built in 1984. This earth does not contain ^{137}Cs and the earth erosion makes considerable contributions to the pond sedimentation.

TABLE 4. CAESIUM-137 CONCENTRATIONS AT DIFFERENT DEPTHS IN DEPOSIT PROFILES AND SEDIMENT DEPOSITION VOLUMES

Catchments	Sampling time	Deposit area * (m ²)	Depth of the 1963's ¹³⁷ Cs peak (cm)	Concentration of the 1963's ¹³⁷ Cs peak (Bq kg ⁻¹)	¹³⁷ Cs concentration of the top layer (Bq kg ⁻¹)	Sediment volume after 1963 (m ³)	Specific sediment yield** (t km ⁻² a ⁻¹)
Wujia Gully, Yanting	2003.10	7349	60	16.86±0.98	2.92±0.24	4409	802
Jiliu Gully, Yanting	2003.5	1259	145	26.03±1.40	1.74±0.14	1826	713
Tianmawan Gully, Nanchong	2004.7	5534 (water surface area)	25	9.50±0.56	4.44±0.29	1384	566
Chunqiu Gully, Kaixian	2004.4	25400 (currently water surface area is 11400 m ²)	125	6.95±0.43	2.78±0.20	31750	1869

*The deposition areas in Table 4 comprises both of the water area and the silted land area; **volume weight $\gamma = 1.4 \text{ t} \cdot \text{m}^{-3}$

5. EVALUATION OF THE IMPACTS OF VEGETATION DESTRUCTION AND RECOVERY ON SEDIMENT PRODUCTION SINCE THE END OF THE 1950'S IN THE JIULONGDIAN CATCHMENT FROM VARIATIONS OF CAESIUM-137, EXCESS LEAD-210 IN RESERVOIR DEPOSIT PROFILES

5.1. Study area

The Jiulongdian Reservoir is located in the upper part of the Zidianhe River catchment (75°14'30" of Northern Latitude and 101°40'48" of Eastern Longitude), which is a tributary of the Longchuanjiang River in the Jinshajiang River Basin (Fig. 8). The reservoir, which was built and put in operation in 1958, has an earth dam of 38.5 m high and 265 m long, a storage capacity of 63 million m³, in which dead storage and flood prevention volumes are 3.88 million m³ and 19.32 million m³, respectively. Its maximum water area is 3.3 km². The reservoir has a drainage area of 257.6 km² and a channel length of 42 km. The elevations of the former river channel at the dam site and of riverhead at the Moujiangpu Hill were 1871.5 m and 2812 m above sea level, respectively, with a relative relief of 940.5 m.

The Zidianhe River Basin, located in Chuxiong City and Mouding County of Chuxiong Yi Autonomous Prefecture, Yunnan Province, has typical landforms of the Hilly Central Yunnan Plateau. River valleys are quite wide at the reservoir area with a width of 600~700 m and mostly quite narrow above the reservoir area with a width of 20 m~100 m. Hillslopes on both sides of the valley are not very steep and slopes mostly vary between 15° and 20°. The catchment is underlain by Mesozoic mudstones, siltstones and sandstones. The 'purple soil' of weathering products of the Mesozoic rocks is predominant over the catchment while there are alluvial soils and paddy soils in the valleys and yellow brown soils in the mountain regions where elevation is greater than 2300 m above sea level. The catchment experiences a subtropical monsoon plateau climate monsoon climate, and is characterised by an annual mean temperature of 15.6° C and annual precipitation of 864 mm, 86% of which occurs in the wet season from May to October. Except for a limited area of paddy fields in the valleys and sloping rainfed farmland on the slopes nearby the villages, the catchment had excellent forests

until 1958, most of which were natural subtropical evergreen forests while the rest were secondary forests of Yunnanese Pine. However, during the Great Leap Forward Period of 1958-1960, vegetation in the catchment suffered from disastrous damages and 80% of the forests disappeared as the wood was used to make charcoal for iron and copper smelting. Additionally, in the spring of 1960 after the Great Leap Forward, grain shortage became serious in the region and local farms started to fire some of the remaining forest land for crop production. However, since then, timber harvesting has stopped and natural vegetation has been recovered due to the suitable climate. Most of the present secondary vegetation is Yunnanese Pine forest, and the rest is composed of dense shrubs and grasses. Forest coverage ratio was 58% in 2004 in the catchment. Nevertheless, cultivation of steep farmland has increased because of the fast population growth in the catchment since 1960s. Due to the state policy of 'closing land for rehabilitation', reclaiming land for cultivation has been prohibited and cultivation on some of sloping land has stopped. The current population is about 10,000, of which the Yi minority accounts for 20%. Farming land in the studied catchment occupies 1022 ha with a reclamation ratio of 0.04, of which rainfed farmland accounts for 60% while paddy fields for 40%, in the catchment. Field investigation in 2004 showed that soil erosion was not severe in the catchment and mainly consisted of sheet erosion and the erosion of slopes (cultivated, forested or shrub-grasses), and gully erosion and river bank erosion.

The Fengtun Hydrological station, set up in 1977, is located in the upper reach of Zidianhe River above the Jiulonhdian Reservoir and has a drainage area of 186 km². Based on the monitoring data, the estimated annual runoff depth and runoff yield of the catchment were 28 mm and 71.33 million m³. Major functions of the reservoir are irrigation and water supply to Chuxiong City. However, the reservoir has also played a considerable role in flood prevention and generating electricity. Reliable annual runoff yields from the reservoir for agricultural irrigation and for city water supply are 25 million m³ and 16 million m³, respectively. The reservoir is located in the Central Yunnan Plateau Region where water shortage is quite serious and water resources are very valuable, therefore, water runoff is captured by the reservoir as much as possible under the condition of dam safety during the wet season and in most years no runoff gets through the spill way. Based on interviews with the staff in charge of the reservoir, the water in the reservoir is clean and contains little sediment. The effective storage capacity of the reservoir is 59.12 million m³ and accounts for 83% of the annual delivered water. Nearly all water from floods occurring during the wet seasons were captured by the reservoir. Therefore, also nearly all sediment coming with the floods is deposited in the reservoir. The reservoir was emptied completely in 1985 because of severe drought and in 2004 because of reservoir maintenance. In 2004 the reservoir silted just up to the dead water level of 1881 m with a maximum silting depth of 9.5m. The dead storage volume of 3.88 million m³ was filled up by 2004. Taking a bulk density of $\gamma = 1.4 \text{ t m}^{-3}$ for the deposited sediments, the total deposited sediment weight in the reservoir was estimated to be $543.2 \times 10^4 \text{ t}$ during the period of 1958-2004 and the mean annual deposition rate was $11.81 \times 10^4 \text{ t a}^{-1}$.

5.2. Sampling and measurements

In April 2004 the reservoir was drained completely for maintenance. This occasion was used to carry out a sediment sampling campaign to a depth of 393 cm in the centre of the dry reservoir bottom. The profile was 2.1 km away from the dam and 3.4 km from the entrance of the Zidianhe River (Fig. 8). The upper part of the profile was sampled (0–45 cm) by using a pit and the obtained sample was sectioned into 5~6 cm layers. It was noticed that there was a fine charcoal layer of 2~3mm at a depth of 21cm. After inquiring of the local farmers, the charcoal layer could be linked to a forest and shrub fire in 1998, which burnt an area of

approximately 18 ha* in the nearby Xinzhuang Gully catchment. The gully outlet to the reservoir was 1.9 km upstream of the sampled profile site. The lower part of the profile was collected by drilling a core with a diameter of 98 mm and it was sectioned into sections 6~7 cm thick. A total of 64 sediment samples were collected from the deposit profile. In addition, surface soils of 0~5cm in depth were collected from the forest and shrub slopes and from the cultivated slopes nearby the reservoir with 4 samples for each type of slope.

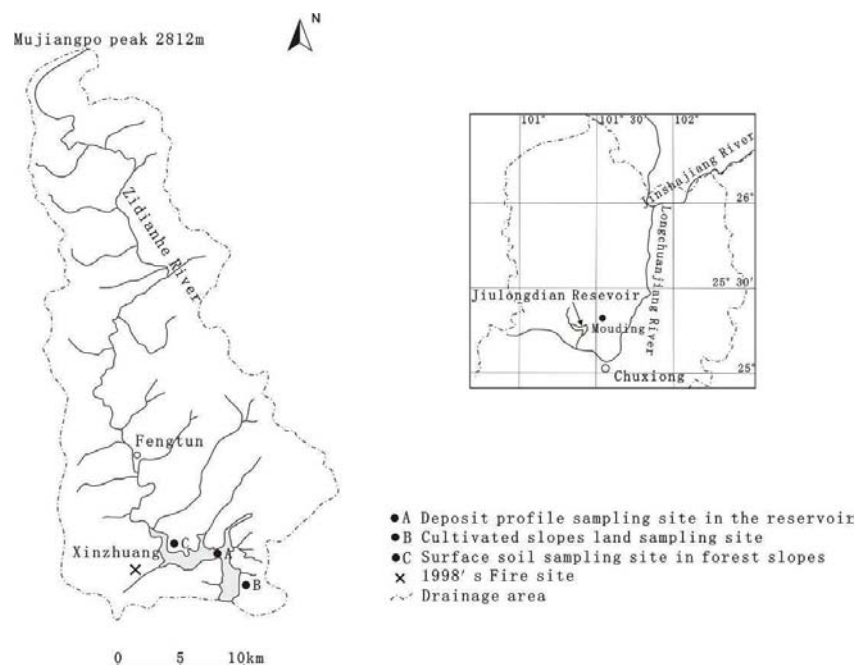


FIG. 8. A sketch map of the Jiulongdian Reservoir Catchment and sampling locations.

5.3. Results and discussion

Depth distributions of ^{137}Cs , $^{210}\text{Pb}_{\text{ex}}$ and fine particle (<0.002 mm) contents are shown in Fig. 9. There are two unusual peaks of extremely high radionuclide contents: (1) the upper peak at a depth of 15~21cm with both high ^{137}Cs content of $10.90 \pm 0.49 \text{ Bq kg}^{-1}$ and $^{210}\text{Pb}_{\text{ex}}$ content of $59.2 \pm 3.4 \text{ Bq kg}^{-1}$ and (2) the lower peak at 331~337cm with only high $^{210}\text{Pb}_{\text{ex}}$ content of $43.4 \pm 6.4 \text{ Bq kg}^{-1}$ and no ^{137}Cs .

If the two unusual peaks are not considered, variations of ^{137}Cs and $^{210}\text{Pb}_{\text{ex}}$ contents with depth are generally normal. The 1963's ^{137}Cs peak occurred at a depth of 231~237cm with a concentration of $4.26 \pm 0.35 \text{ Bq kg}^{-1}$. ^{137}Cs content rapidly decreased as the depth increased from the peak and ^{137}Cs was detected in a few layers below the depth of 250cm, while it gradually generally decreased as the depth decreased above the 1963's peak. The top layer at a depth of 0~5cm had a ^{137}Cs content of $0.92 \pm 0.17 \text{ Bq kg}^{-1}$. The ^{137}Cs contents were fluctuating over the profile and the differences of those between neighbouring layers are often very large. The $^{210}\text{Pb}_{\text{ex}}$ content gradually decreased in general as the depth decreased over the profile and its fluctuations were not as much as ^{137}Cs . The top layer (0~5cm) had a $^{210}\text{Pb}_{\text{ex}}$ content of $17.87 \pm 1.17 \text{ Bq kg}^{-1}$, while it was $2.94 \pm 0.22 \text{ Bq kg}^{-1}$ in the bottom layer at a depth of 387~393 cm.

* The fire area was provided by the local forest department and might be under estimated.

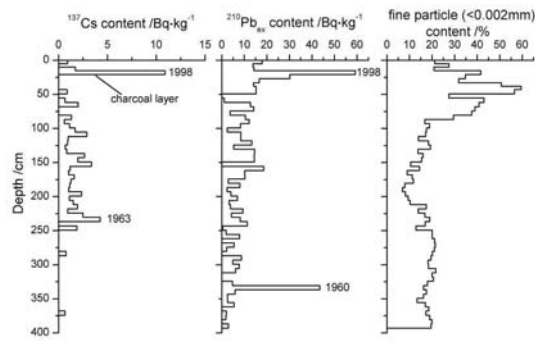


FIG. 9. Depth distributions of ^{137}Cs , $^{210}\text{Pb}_{\text{ex}}$ and fine particle (<0.002mm) contents.

With regards to fine particle content (< 0.002 mm) in the profile, it was not very variable and ranged between 16% and 21% below the depth of 250 cm. The sediment became coarse upward and the fine particle content decreased to 8% in the layer at a depth of 193~199cm. However, it became again fine upward from the coarsest layer and the fine particle content increased up to 59% in the layer of 38~43 cm. Nevertheless, it became coarse again upward from the finest layer and the fine particle content was 21% in the top layer of 0~5cm.

The ^{137}Cs reference inventory in the Qingfeng Gully catchment next to the Zidianhe River was 919.6 Bq m^{-2} in 1997 [3,2] and the decay-corrected value for 2004 is 783 Bq m^{-2} . Four surface soil samples on forest and shrub slopes had a mean ^{137}Cs content of $6.77 \pm 0.43 \text{ Bq kg}^{-1}$ with a range of 4.78 ± 0.33 to $9.35 \pm 0.54 \text{ Bq kg}^{-1}$, and a mean $^{210}\text{Pb}_{\text{ex}}$ content of $52.73 \pm 3.05 \text{ Bq kg}^{-1}$ with a range of 35.33 ± 2.24 to $68.69 \pm 3.94 \text{ Bq kg}^{-1}$. Four surface soil samples on cultivated slopes had a mean ^{137}Cs content of $2.28 \pm 0.25 \text{ Bq kg}^{-1}$ with a range of 1.98 ± 0.20 to $2.64 \pm 0.29 \text{ Bq kg}^{-1}$ and a mean $^{210}\text{Pb}_{\text{ex}}$ of $17.73 \pm 1.04 \text{ Bq kg}^{-1}$ with a range of 11.37 ± 0.62 to $27.24 \pm 1.67 \text{ Bq kg}^{-1}$.

^{137}Cs and $^{210}\text{Pb}_{\text{ex}}$ content of sediment in the top layer of 0~5 cm depth in the profile were 0.92 ± 0.17 and $17.87 \pm 1.17 \text{ Bq kg}^{-1}$, respectively, which accounted for 19% and 34% of the mean values in the surface soils on the forest and shrub slopes. The ^{137}Cs content of the sediments in the top layer accounted for 46% of the mean values in the surface soils on the cultivated slopes, while the $^{210}\text{Pb}_{\text{ex}}$ proportions are similar.

According to the erosion rate of $6271 \text{ t km}^{-2} \cdot \text{a}^{-1}$ for this type of cultivated slopes, estimated by using the ^{137}Cs technique in the study carried out in the nearby Qingfeng Gully catchment in 1997, and as the drainage basin above the reservoir has only 6.13 km^2 of cultivated slopes, the estimated annual soil losses are 38,441 t, which only accounts for 33% of the mean annual silting rate in the reservoir. It is thus obvious that the cultivated slopes were not the major sediment source of the reservoir sediments, however, other sources, such as forest and shrub slopes, stream channels, channel banks and roads, may be the main sources of the reservoir sediments.

The surface soils on slopes covered by forest and shrub were rich in ^{137}Cs and $^{210}\text{Pb}_{\text{ex}}$ while those producing sediments resulting from other sources contained little of those radionuclides. However, ^{137}Cs and $^{210}\text{Pb}_{\text{ex}}$ contents of the sediments in the top layer were much lower than the contents in the surface soils on forest and shrub slopes and only accounted for 19% and 34% of the latter. It also indicated that forest and shrub slopes were not the major source to the reservoir sediments although those slopes accounted for more than 90% of the catchment area and that erosion of soil from stream channels, channel banks and roads containing little ^{137}Cs and $^{210}\text{Pb}_{\text{ex}}$ make a large contribution to the reservoir sediments.

The upper unusual peak with high ^{137}Cs and $^{210}\text{Pb}_{\text{ex}}$ contents and the lower unusual peak with high $^{210}\text{Pb}_{\text{ex}}$ content could be caused by a sudden increase of sediment production from surface soils on forest and shrub slopes. However, fluctuations of ^{137}Cs and $^{210}\text{Pb}_{\text{ex}}$ contents in the deposition profile of the reservoir may be induced by several causes, such as changes of relative contributions between different sources, sediment silting selection, variations of the radionuclide fallout fluxes and precipitation, land use/coverage changes or forest fires.

The coincidence of the thin charcoal layer at the depth of 21 cm with the peak of very high ^{137}Cs and $^{210}\text{Pb}_{\text{ex}}$ contents at depth of 15-21cm in the profile indicated that the high ^{137}Cs and $^{210}\text{Pb}_{\text{ex}}$ contents could result from the forest and shrub fire in the Xinzhuang Gully catchment in the spring of 1998. It is well known that ^{137}Cs and $^{210}\text{Pb}_{\text{ex}}$ are concentrated in surface soil horizons of 0-5 cm depth and decline rapidly with depth, however the soils below the depth of 20 cm contain little of those radionuclides [3]. As soils became bare and prone to soil erosion, sheet erosion in particular should become very severe after forest and shrub fires. Therefore, sediment yields and ^{137}Cs - $^{210}\text{Pb}_{\text{ex}}$ contents in the delivering sediments should suddenly increase after the 1998 fire. As the study profile was just located downstream of the Xinzhuang Gully mouth (Fig. 8), the fire induced the very high ^{137}Cs and $^{210}\text{Pb}_{\text{ex}}$ contents in the upper unusual peak although the fire area was not very large (18ha). In light of the upper unusual peak it was suggested that the very high $^{210}\text{Pb}_{\text{ex}}$ content of the lower unusual peak at a depth of 331~337cm was related to the fire of reclaiming land for cultivation in the spring of 1960 when China was in 'the difficult period'. No ^{137}Cs was detected in the lower peak layer, probably because the eroded soils during the GLF period contained little ^{137}Cs . As mentioned above, variations in ^{137}Cs and $^{210}\text{Pb}_{\text{ex}}$ contents in deposit profiles of lakes and reservoirs may be related to dozens of causes and it is difficult to determine the causes for other small variations of ^{137}Cs and $^{210}\text{Pb}_{\text{ex}}$ contents in the profile.

According to the unusual ^{137}Cs and $^{210}\text{Pb}_{\text{ex}}$ peaks in the profile and the reservoir history, the reservoir deposits in the profile are dated as following: 0~21cm, 1998~2003; 21~237cm, 1963~1997; 237~337cm, 1960~1962; >337cm, 1958~1959. Additionally, based on the reservoir storage volume curve, deposited sediment amounts, annual deposition rates and specific sediment yields for the above periods were estimated in Table 5.

TABLE 5. DEPOSITED SEDIMENT AMOUNTS*, ANNUAL DEPOSITION RATES AND SPECIFIC SEDIMENT YIELDS OF THE JIULONGDIAN RESERVOIR FOR DIFFERENT PERIODS

Period	Depth (cm)	Sediment amounts (10^4t)	Deposition rate ($10^4\text{t}\cdot\text{a}^{-1}$)	Specific sediment yield ($\text{t}\cdot\text{km}^{-2}\cdot\text{a}^{-1}$)
1998~2003	0~21	30.94	5.16	200.2
1963~1997	21~237	262.78	7.51	291.5
1960~1962	237~337	81.76	273.25	1058.0
1958~1959	337~950	167.72	83.86	3255.4
Σ		543.2	$\Sigma = 11.81$	$\Sigma = 458.4$

* Taking bulk density of the deposited sediments of $\gamma=1.4\text{t}\cdot\text{m}^{-3}$

The highest deposition rate of $83.86 \times 10^4 \text{ t a}^{-1}$ and the relevant highest specific sediment yield for the catchment occurred in the period of 1958~1959 when the reservoir started to store water. Annual precipitations in Chuxiong varied between 486 and 1213 mm with a mean value of 864 mm (Fig. 10). It was quite dry in 1958 and 1959 in Chuxiong, when the annual precipitations were 639 mm and 757 mm, respectively. No doubt, the highest deposition rate in 1958~1959 was caused by the severe soil erosion, not due to heavy rainfalls, but due to the timber harvesting at large scale occurring in the catchment during that period. When timber harvesting was reduced and consequently vegetation started to rehabilitate, the sediment yields into the reservoir largely decreased.

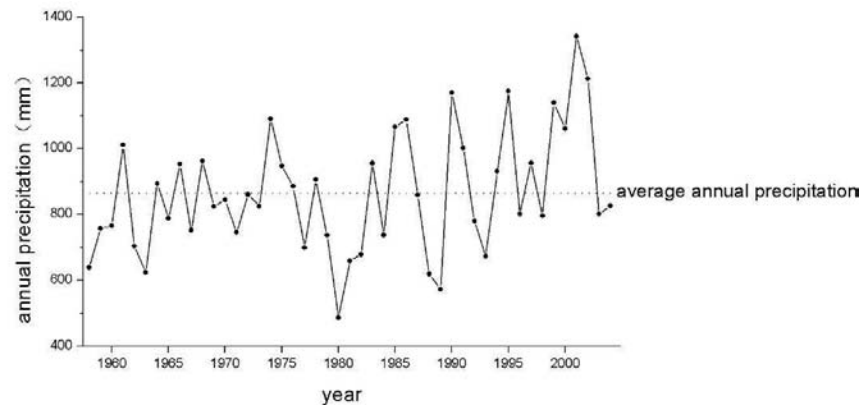


FIG. 10. Variations of annual precipitations from 1958 to 2004 in Chuxiong.

The deposition rates and relevant specific sediment yields have decreased to $40.88 \times 10^4 \text{ t a}^{-1}$ and $1587.0 \text{ t km}^{-2} \text{ a}^{-1}$, respectively, in the period of 1960~1962; to $6.19 \sim 7.73 \times 10^4 \text{ t a}^{-1}$ and $240.2 \sim 291.5 \text{ t km}^{-2} \text{ a}^{-1}$, respectively, since 1963. Sediments are quite coarse and their fine particle contents range between 16~21% in the lower part of the profile below the depth of 250 cm, which was deposited before about 1965. It should be related to the severe soil erosion and sediment production during the period of the 'Great Leap Forward'.

Sediments become coarser upward in the middle part of the profile at a depth of 193~250 cm, which was deposited probably in 1965~1974, and fine particle content of the layer with a depth of 193~199 cm is only 8%. Vegetation rehabilitation since 1960 should result in the reduction of soil erosion severities on slopes and of sediment concentrations in runoff water, and consequently in river channel changes. The channel changes probably increased the relative contribution of the coarse channel sediments to the reservoir. As soil erosion was reduced and river channels stabilized by vegetation rehabilitation, sediments become finer in the upper-middle part of the profile at a depth of 193~38 cm, which was deposited in approximately 1970-1993, and fine particle content of the layer at a depth of 38~43 cm reaches up to 59%. However, sediments in the very upper part of the profile at a depth of 0~38 cm become coarser again and the top layer (0~5 cm) has a fine particle content of 21%. It is suggested this is caused by the fact that particle size compositions of deposited sediments at the profile site in the middle of the reservoir have been gradually affected by expansion of the subaqueous delta of the Zidianhe River since 1993.

6. CONCLUSIONS

(1) Evaluation of soil loss reduction by traditional cultivation measures in the Sichuan Hilly Basin:

The annual soil losses estimated from the $^{210}\text{Pb}_{\text{ex}}$ measurement are comparative to the values from the ^{137}Cs measurements. The results obtained from this study confirm the potential for using $^{210}\text{Pb}_{\text{ex}}$ measurement to estimate soil erosion rates at a medium term of 50-100 a. By combination of the erosion accumulation rates from the ^{137}Cs and $^{210}\text{Pb}_{\text{ex}}$ measurements, the weighted mean net soil erosion rates were estimated to be $4870 \text{ t km}^{-2} \text{ a}^{-1}$ for the upper subfield and $1691 \text{ t km}^{-2} \text{ a}^{-1}$ for the lower subfield. Those rates are considerably lower than the erosion rates from the runoff plot measurements. It is suggested that the traditional drainage system, in combination with the 'Tiaoshamiantu' cultivation measure, has significant effects on the conservation of the valuable farmland in the Sichuan Hilly Basin.

(2) Sediment source identification by using ^{137}Cs and ^{210}Pb radionuclides in a small catchment of the Hilly Sichuan:

By using the double nuclide tracing technique of ^{137}Cs and ^{210}Pb , the relative sediment contributions from steep forestland, gentle cultivated terraces, and bare slopes and banks in the Wujia Gully catchment of the Hilly Sichuan Basin, were estimated to be 18%, 46% and 36%, respectively. Cultivated terraces and bare slopes (including channel banks) were the first and the second most important sediment sources in the catchment. Specific sediment yield in the catchment was $642 \text{ t km}^{-2} \text{ a}^{-1}$ from the deposited sediment volume in the reservoir since 1956. Soil erosion rates for the forested slopes and cultivated terraces, which accounted for 2/3 and 1/3 of the drainage area in the catchment, were estimated to be $173 \text{ t km}^{-2} \text{ a}^{-1}$ and $886 \text{ t km}^{-2} \text{ a}^{-1}$, respectively.

(3) Investigation of erosion severities and sediment production by ^{137}Cs dating of reservoir and pond deposits in small catchments of the Hilly Sichuan Basin and the Three Gorges Region:

The 1963 ^{137}Cs peak was easily identified for dating the reservoir and pond deposits in the Hilly Sichuan Basin and the Three Gorge Region and for estimating deposit volumes and the related specific sediment yields since 1963. The yields of the four study catchments with a drainage area of $<1 \text{ km}^2$ were estimated to range between $566 \text{ t km}^{-2} \text{ a}^{-1}$ and $1869 \text{ t km}^{-2} \text{ a}^{-1}$. Considering the small catchment sizes and the steep topographies, and that the ^{137}Cs depth distribution in the paddy field of the valleys showed little ^{137}Cs accumulation, the sediment delivery ratio should be close to 1. It was suggested that the specific sediment yields can be representative of the soil loss rates in the region and the soil erosion rates are recommended to range between $1000 \text{ t km}^{-2} \text{ a}^{-1}$ and $2000 \text{ t km}^{-2} \text{ a}^{-1}$. Those values were much less than the reported values by the state remote sensing survey.

(4) Evaluation of the impacts of vegetation destruction and recovery on sediment production since the end of 1950s in the Jiulongdian catchment from the variations of ^{137}Cs , $^{210}\text{Pb}_{\text{ex}}$ in reservoir deposit profiles:

Except for the 1963 ^{137}Cs peak of $4.26 \pm 0.35 \text{ Bq kg}^{-1}$ at a depth of 231~237 cm, a deposition profile with a length of 393 cm in the Jiulongdian Reservoir showed two other unusual ^{137}Cs and $^{210}\text{Pb}_{\text{ex}}$ peaks: the upper peak at the depth of 15~21cm, which had a ^{137}Cs concentration of $10.90 \pm 0.49 \text{ Bq kg}^{-1}$ and a $^{210}\text{Pb}_{\text{ex}}$ concentration of $59.20 \pm 3.4 \text{ Bq kg}^{-1}$, respectively; and the lower peak at the depth of 231~237 cm, which had only a high $^{210}\text{Pb}_{\text{ex}}$ concentration of $43.40 \pm 6.4 \text{ Bq kg}^{-1}$. The upper peak was related to the 1998's forest and shrub fire while the lower peak to the deforestation during the Great Leap Forward Period of 1958~1959. No ^{137}Cs was detected in the lower peak layer, probably because the eroded soils during the GLF period contained little ^{137}Cs . Vegetation changes had great impacts on sediment yields in the

catchment. The highest mean specific yield of $3255.4 \text{ t km}^{-2} \text{ a}^{-1}$ occurred in 1958~1959, then it decreased to $1587.0 \text{ t km}^{-2} \text{ a}^{-1}$ in 1960~1962, to $291.5 \text{ t km}^{-2} \text{ a}^{-1}$ in 1963~1997, and to $200.2 \text{ t km}^{-2} \text{ a}^{-1}$ in 1998-2003, because vegetation was recovering after the ceasing of timber harvesting in 1960.

ACKNOWLEDGEMENTS

This research is supported by International Atomic Energy Agency (12322/RO), National Natural Sciences Foundation of China (40271015, 90502002) and Chinese Academy of Sciences (Grant Nos. KZCX3-SW 422 and 330). Geography and Archaeology Department, Exeter University, UK is gratefully acknowledged for sample analyses.

REFERENCES

- [1] QUINE, T.A., et al., "Investigation of Soil erosion terraced fields near Yangting, Sichuan Province, China, using caesium-137. Erosion, Debris Flows and Environment in Mountain Regions", Proc. of the Chengdu Symposium (July 1992), IAHS Publ. **209** (1992) 155-168.
- [2] ZHANG, X., et al., Soil loss evaluation by using ^{137}Cs technique in the Upper Yangtze River Basin, China. *Soil and Tillage Research* **69** (2003) 99-106.
- [3] ZHANG, X., et al., $^{210}\text{Pb}_{\text{ex}}$ depth distribution in soil and calibration models for assessment of soil erosion rates from $^{210}\text{Pb}_{\text{ex}}$ measurements, *Chinese Science Bulletin* **48** (2003) 813-818.
- [4] HUH, C.-A., SU, C.-C., Distribution of fallout radionuclides (^7Be , ^{137}Cs , ^{210}Pb and $^{239,240}\text{Pu}$) in soils of Taiwan, *Journal of Environmental Radioactivity* **77** (2004) 87-100.
- [5] QIAN, J., et al., Atmospheric depositional fluxes of ^{210}Pb near East Sea, *Donghai Marine Science* **4** (1986) 27-33.
- [6] LIU, H., et al., Constraints from Pb-210 and Be-7 on wet deposition and transport in a global three-dimensional chemical tracer model driven by assimilated meteorological fields. *Journal of Geophysical Research D: Atmospheres*, **106** (2001) 12109-12128.
- [7] APPLEBY, P.G., OLDFIELD, F., "Application of Lead-210 to sedimentation studies", *Uranium-series disequilibrium: Application to earth, Marine and environmental sciences*, (IVANOVICH, M., HARMAN, R.S. Eds.), Clarendon Press, Oxford, (1992) 731-738.
- [8] HENDERSON, G.M., MAIER-REIMER, E., Advection and removal of ^{210}Pb and stable Pb isotopes in the oceans: a general circulation model study, *Geochimica et Cosmochimica Acta* **66** (2002) 257-272.
- [9] Zhang, X., Feng, M., ^7Be distribution in soil and its reference inventory in the Central Sichuan Hilly Basin, China. *Journal of Nuclear Techniques*, in press.
- [10] ZHANG, J., LIN, Z., *Climate in China*, Shanghai Publication House, Shanghai, (1985) 603.
- [11] ZHANG, X. et al., Application of the Caesium-137 technique in a study of soil erosion on gully slopes in a yuan area of the Loess Plateau near Xifeng, Gansu Province, China, *Geografiska. Annaler*. **76** (1994) 103-120.
- [12] ZHANG, X., et al., Use of reservoir deposits and Caesium-137 measurements to investigate the erosional response of a small drainage in the Rolling Loess Plateau region of China. *Land Degrad. Develop.* **8** (1997) 1-16.

- [13] ZAPATA, F., Handbook for the Assessment of Soil Erosion and Sedimentation Using Environmental Radionuclides, Kluwer Academic Publishers, Dordrecht/Boston/London, (2002).
- [14] ZHANG, X., et al., A preliminary assessment of the potential use of Caesium-137 to estimate rates of soil erosion in the Loess Plateau of China, Hydrological Sciences Journal **35**(1990) 243-252.
- [15] WALLING, D.E., HE, Q., Using Fallout Lead-210 Measurements to Estimate Soil Erosion on Cultivated Land, Soil Sci. Am. J. **63** (1999) 1404-1412.
- [16] YANG, W., Characteristics and control of soil erosion in a small watershed in the Sichuan Basin, Water and Soil Conservation **1** (1997) 76-84.
- [17] JIA, C., et al., Atmospheric depositional fluxes of ⁷Be and ²¹⁰Pb at Xiamen. Journal of Xiamen University, Natural Science, **42** (2003) 352-358.
- [18] WALLBRINK, P.J., MURRAY, A.S., Determining soil loss using the inventory ratio of excess lead-210 to cesium-137, Soil Sci. Soc. Am. J. **60** (1996) 1201-1208.
- [19] WALLING, D.E., et al., Use of Caesium-137 and Lead-210 as tracers in soil erosion investigations, Tracer Technologies for Hydrological Systems, IAHS Publ. **229** (1995) 163-172.
- [20] WALLING, D.E., WOODWARD, J.C., Tracing sources of suspended sediment in river basins, Marine and Freshwater Research **46** (1995) 327-336.

THE USE OF EXCESS LEAD-210, BERYLLIUM-7 AND CAESIUM-137 IN INVESTIGATIONS OF SEDIMENT DELIVERY DYNAMICS IN THE HOMERKA AND DUNAJEC CATCHMENTS IN THE POLISH FLYSH CARPATHIANS

W. FROEHLICH

Polish Academy of Sciences,
Institute of Geography and Spatial Organization, HOMERKA Laboratory of Fluvial Processes,
Nawojowa, Malopolska, Poland

D.E. WALLING

University of Exeter, Department of Geography
Exeter, Devon, United Kingdom

Abstract

The paper summarizes the findings of the research conducted in the small (19.7 km²) instrumented Homerka catchment and the larger basin of the Dunajec River upstream from the Roznowski reservoir in the Polish Flysch Carpathians, where a combination of conventional and fallout radionuclide methods have been used over the past 35 years to investigate sediment mobilization, transfer and deposition. This paper focuses on the use of ²¹⁰Pb_{ex}, ⁷Be and ¹³⁷Cs to trace the main sources of the suspended sediment exported from the study catchment and to investigate sediment delivery dynamics during high energy flood events. Information on sediment sources has been assembled using the 'fingerprinting' approach. Monitoring of the spatial distribution of ⁷Be activity immediate after each period of heavy rainfall provided a basis for investigating sediment mobilised by dispersed overland flow and linear flow. The results show that ⁷Be transport is connected with land use and soil surface cover. Since changes in land use affected the volume of sediment mobilized from a small catchment, these changes may prove to be significant within larger basins. The depth distribution of ²¹⁰Pb_{ex}, ⁷Be and ¹³⁷Cs in undisturbed soils provided a means for establishing the intensity of surface erosion during different flood events. Changes in the ²¹⁰Pb_{ex}, ⁷Be and ¹³⁷Cs content of suspended sediment transported during flood events reflected changes in the relative contribution of different sediment sources. During extreme storm events, the contributing area was greatly expanded and sediment mobilized from areas which are unconnected to the stream during 'normal' events. The information on soil erosion and sediment delivery dynamics provided by ²¹⁰Pb_{ex}, ⁷Be and ¹³⁷Cs measurements were compared with existing results from conventional investigations. Unmetalled roads were identified as the main source for sediment in suspension, with the channels and active gullies also providing significant contributions.

1. INTRODUCTION

In mountain environments the high energy of flood events and the high spatial variability of extreme rainfall introduce important technical difficulties in the application of traditional techniques for investigating soil erosion, sediment sources and sediment delivery. Data obtained using these methods are primarily limited to small areas, for example experimental plots or slopes, and generally relate to 'normal events' involving only short recording periods. Fallout radionuclides offer considerable potential to overcome the limitations of these traditional monitoring techniques.

To date, most applications of the fallout radionuclides (FRNs) ¹³⁷Cs, ²¹⁰Pb_{ex} and ⁷Be in investigations of soil erosion, sediment sources and sediment delivery dynamics have been limited to hilly or lowland areas. Relatively little work has been undertaken in mountain areas, where altitudinal variations in precipitation and vegetation cover, frozen soils, snow cover, and the high energy environment necessitate modifications to the approach [1,2]. In

such areas, land and water conservation strategies are usually developed at the scale of the small drainage basin (e.g. 1-30 km²). Little is known about the residence times of sediment particles moving through the fluvial system of mountainous drainage basins of different scales.

In the Polish Carpathians, present day land use changes are an important aspect of soil conservation and watershed management. They reflect the political and social changes and the impact of the 'free market' during the past 20 years. In general, arable cultivation is currently rapidly decreasing on steep slopes. The Polish government has promoted campaigns (including giving subsidies) to encourage reduced tillage, especially on steep slopes. Such areas are converted to pasture or afforested. However questions have been raised concerning the effectiveness of such land management practices in controlling soil erosion. To date, little or no attention has been paid to the influence of changing land use patterns and farming activities on changes in soil erosion.

A range of studies have been carried out by the authors, in order to evaluate the potential use of ²¹⁰Pb_{ex}, ⁷Be and ¹³⁷Cs measurements to assess the impact of short term changes in land use practices and to evaluate the effectiveness of soil conservation measures in the Polish Carpathians. Particular attention has been given to refining the ⁷Be technique for documenting short term sediment mobilisation and sediment delivery dynamics during rainfall and snowmelt events of different magnitude. Measurement of the ⁷Be activity of suspended sediment during rainfall and snowmelt floods can provide information on the relative importance of sediment mobilization by diffuse surface flow and linear flow [3,4].

2. MATERIALS AND METHODS

2.1. Study area

The Polish Flysch Carpathians are characterized by highly active erosion, sediment transport and fluvial sedimentation processes, which in turn reflect the climate, the high relief energy, the erodible nature of the soils and rock, and the effects of land management. Steep (15-35°), convex and rectilinear slopes are characteristic of the headwaters, whereas in the foothills more gentle (5-15°) slopes are found. The valley floors of third- and higher-order streams are flat and covered by alluvium and most of the river channels have no direct contact with the adjacent foothill slopes. The headwater zones and steep slopes are characterized by extensively exploited forests, accessed by a network of unmetalled roads (i.e. dirt roads without surface covering and rutted tracks). In the lower parts, much of the land is used for agriculture. The cultivated land is commonly divided into small plots bounded by terraces and is also traversed by an extensive network of unmetalled roads, which frequently extend to the stream and river network. The wetter areas at the base of the slopes and on the valley floors are occupied by meadows and pasture [1,2].

The critical threshold for the widespread occurrence of dispersed overland flow is a storm rainfall of ca. 20 mm and an intensity of 1 mm min⁻¹. During heavy downpours exceeding 20 mm, overland flow occurs on the loamy soils [5]. It may cause mud and earth flows¹ and also give rise to intensive erosion along unmetalled roads. Local rill erosion can occur during heavy rainfall, and earth flows have been observed on some potato fields [6]. These extreme

¹A flow is the down slope movement of water-saturated soil, regolith, weak shale, or weak clay layers. *Earth flows* are fairly slow, occurring over a few hours or so slow that they are almost imperceptible. Earth flows are accompanied with slumping, but unlike slumping, there is no backward rotation. Earth flows differ from mudflows in that they (1) tend to be slower, (2) are not confined to channels, (3) are more common in humid areas than dry, and (4) have a lower water content.

rainfall events may also give rise to intensive erosion along unmetalled roads. The rates of soil erosion for areas under potatoes are as high as $22 \text{ t ha}^{-1} \text{ year}^{-1}$, whilst typical values for winter crops, meadows and forest are $2.4 \text{ t ha}^{-1} \text{ year}^{-1}$, $0.1 \text{ t ha}^{-1} \text{ year}^{-1}$ and $0.03 \text{ t ha}^{-1} \text{ year}^{-1}$ respectively [7]. Sediment yield from the larger river basins are in the range $90\text{-}1000 \text{ t km}^{-2} \text{ a}^{-1}$ [cf. 8].

The clear dominance of suspended sediment mobilised by linear flow over sediment mobilised by overland flow from interchannel areas is an important characteristic of small Carpathian drainage basins [9]. It is unfortunately difficult to make direct comparisons between estimates of the intensity of erosion processes on the slopes and the sediment yields of Carpathian rivers, because of the wide range of techniques of unknown accuracy and precision which have been used and the different periods of record involved [1,9].

2.2. Selected catchments

The work reported was undertaken in the small (19.6 km^2) Homerka instrumented catchment near Nowy Sacz (Fig. 1), and the larger basin of the Dunajec River above Roznowski reservoir, where classical monitoring techniques have also been used over the past 35 years [9]. The basin of the Dunajec River upstream from this reservoir has an extension of about 4700 km^2 and, as the main river of the Polish Carpathians, its catchment is representative of the larger Carpathian drainage basin.

The 19.6 km^2 drainage basin of the Homerka stream lies at an altitude of 375-1060 m a.s.l. and is representative for the Polish Flysch Carpathians with regards to land use, crop rotations and general drainage basin management (Fig. 1). The mean annual precipitation is 937 mm with a dominance of summer rains (30-40%) and snowfall in winter. The Homerka catchment has a mean discharge of $0.362 \text{ m}^3 \text{ s}^{-1}$, and a mean annual flood discharge of $9.15 \text{ m}^3 \text{ s}^{-1}$ (Fig. 2). Fluvial processes are dominant, and the channel network is being actively deepened. The area is also characterized by rapid flood generation (with extreme floods with peak discharges in excess of $3 \text{ m}^3 \text{ s}^{-1} \text{ km}^{-2}$), significant soil erosion and high loads of suspended sediments. The high annual suspended sediment yield of the Homerka catchment is approx. $550 \text{ t km}^{-2} \text{ year}^{-1}$ and suspended sediment concentrations during floods may even exceed $3 \times 10^4 \text{ mg L}^{-1}$ [9]. The critical threshold for the widespread occurrence of dispersed overland flow is a storm rainfall of approx. 20 mm with a minimum intensity of approx. 1 mm min^{-1} [5].

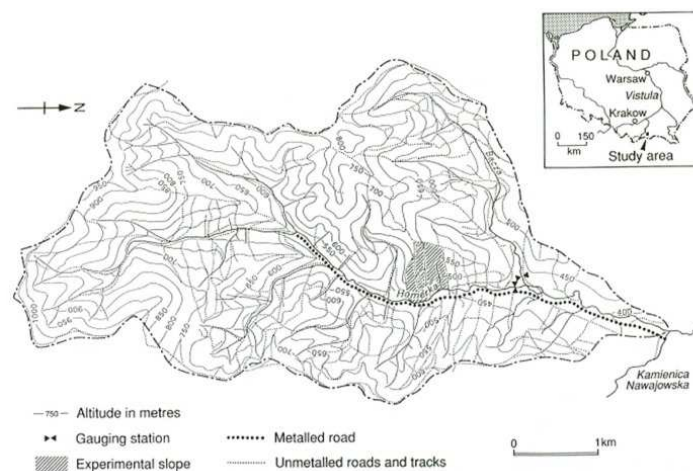


FIG. 1. The Homerka drainage basin and the experimental slope, and its location within Poland (based on Froehlich et. al. 1993).

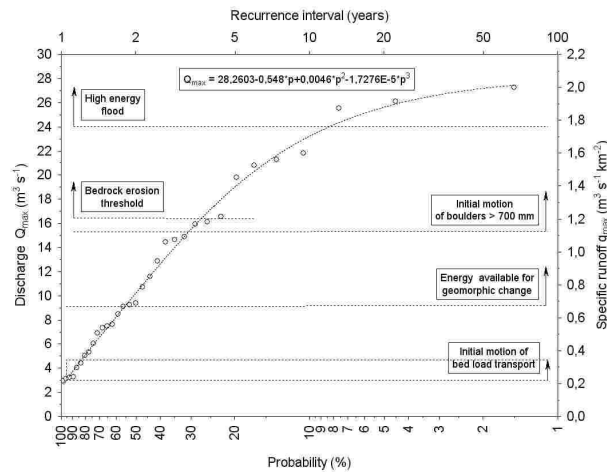


FIG. 2. Probability and recurrence interval of maximum annual discharge at a gauging station on the Homerka stream (14.04 km^2) during the period 1971-2006 and thresholds of sediment transport and effectiveness of fluvial processes.

The Homerka catchment comprises two main zones, representing the montane headwater and the lower foothill zones. The headwater areas, which are predominantly forested, are characterized by steep ($15\text{--}35^\circ$) convex and straight slopes and shallow permeable skeletal soils. These forest areas, which account for 52% of the total basin area, are dissected by a dense network of unmetalled roads and lumber tracks. The foothill zone lies below 650 m a.s.l., this part of the drainage basin is underlain by shale-sandstone flysch series and is characterized by more gentle slopes ($5\text{--}15^\circ$). The silt-clay soils support small traditional farms and the associated mosaic of arable fields is bounded by agricultural terraces and crossed by a dense network of unmetalled roads, which are commonly sunken below the level of the surrounding land. The valley floors of the third order streams are flat, covered by alluvium and occupied by meadows and permanent pasture. In this lower zone of the catchment, most of the stream channels are not in direct contact with the slopes.

Unmetalled⁶ roads are a characteristic feature of both the Carpathian landscape in general and the Homerka catchment in particular. They date back to the original clearing and cultivation of the land. The network of roads serving the fields is related to the field pattern. The primary roads tend to be located along both watercourses and ridges and are linked by a dense network of secondary roads, which run downslope or at an inclination to the slope. In the narrow valley bottoms, unmetalled roads often run along the stream channels, which in forest areas are often used for log transport. The density of unmetalled roads within the catchment as a whole is 5.3 km km^{-2} [9,10].

In order to permit detailed investigation of erosion and sediment delivery from a representative cultivated zone in the lower part of the basin, an area of 26.5 ha located on the boundary between the forest and the agricultural areas has been established as an 'experimental slope' (Fig. 3). The slope is 500–700 m long and its shape is convex-concave. The silty-clay soils increase in depth towards the base of the slope. The slope is subdivided into numerous field plots, which are tilled across the slope and separated by terraces and ditches and by the unmetalled roads, which traverse the area from the watershed to the stream channel. During times of heavy rainfall, these unmetalled roads act as channels for surface runoff and in many places they are deeply incised. The length of unmetalled road traversing the experimental slope is 3.3 km, equivalent to a density of 11.9 km km^{-2} [11].

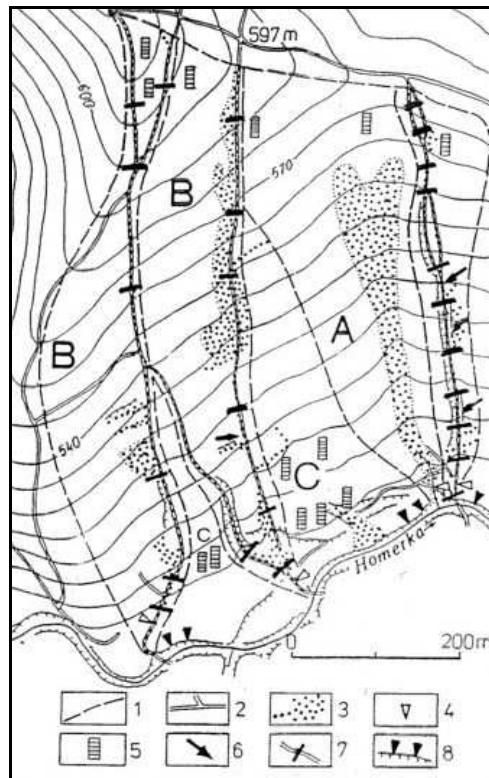


FIG. 3. The experimental slope in the Homerka drainage basin: 1 - drainage divides; A - drainage basin of the Holocene gully; B - drainage basin of the unmetalled roads; C - drainage basin of the interchannel areas; 2 - unmetalled roads; 3 - contributing areas; 4 - points for measuring concentrated flow and collecting water samples; 5 - containers for measuring sheet flow and collecting water samples; 6 - outflow of furrows; 7 - sites for measuring unmetalled road surface changes; 8 - sites for measuring channel erosion rates.

2.3. Application of fallout radionuclides to assess soil erosion, to identify sediment source and understand sediment delivery dynamics

Traditional approaches to determine sediment sources, involving detailed monitoring of rates of sediment production from potential sources, are beset by numerous problems and alternative approaches are needed. One alternative approach, which offers considerable potential, is 'fingerprinting'. In this case the physical or chemical properties of potential sediment sources are matched with those of the sediment transported by the river, in order to determine the dominant sources [12,13]. A variety of sediment properties have been used as 'fingerprints', but $^{210}\text{Pb}_{\text{ex}}$, ^7Be and ^{137}Cs would appear to be particularly valuable. Despite the growing interest in the potential of fingerprinting techniques there have been few attempts to provide an objective assessment of the validity of the results by comparing them with the findings of more traditional monitoring techniques.

In the instrumented drainage basin of the Homerka stream, soil erosion, sediment source and sediment delivery dynamics have been studied using $^{210}\text{Pb}_{\text{ex}}$, ^7Be , and ^{137}Cs . Detailed investigations of soil erosion and sediment delivery dynamics have been carried out on the experimental slope within areas of different land use. The fingerprinting technique has also been used to identify suspended sediment sources within the larger (4692 km²) basin of the Dunajec River flowing to Roznowski reservoir. The information on soil erosion and sediment

delivery dynamics provided by the fallout radionuclides has been compared with existing results from classical investigations.

Measurements of $^{210}\text{Pb}_{\text{ex}}$, ^7Be and ^{137}Cs activity have been carried out on rainwater, on surface soils and on suspended sediment collected during individual floods generated by rainfall and snowmelt. Samples of wet and dry fallout were collected after each rainfall and snowfall event at the meteorological station (412 m a.s.l.) of the Homerka Laboratory of Fluvial Processes. Eight plastic containers of 60 L capacity fitted with glass funnels of 40 cm diameter were installed for sampling dry and wet radionuclide fallout. The samples of rainwater were collected during each precipitation event. In order to obtain reference data, the $^{210}\text{Pb}_{\text{ex}}$, ^7Be , and ^{137}Cs activity of rainfall, samples of rainwater have been analysed by gamma ray spectrometry [cf. 14]. The relationships between rainfall depth and event inter-arrival time (i.e. the time elapsed between rainfall events) and the $^{210}\text{Pb}_{\text{ex}}$, ^7Be , and ^{137}Cs activity of rainwater have been explored (Fig. 4).

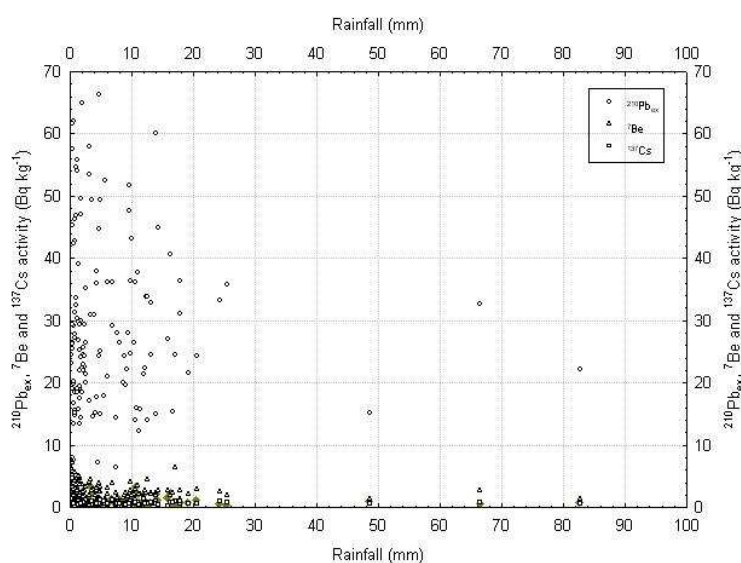


FIG. 4. The relationship between depth of rainfall and the $^{210}\text{Pb}_{\text{ex}}$, ^7Be and ^{137}Cs of rainwater at 420 m a.s.l within the Homerka catchment.

A 75 mm diameter steel corer was used to collect soil cores to depths of 50 cm for the majority of the measurements undertaken on surface soils, and in most cases the cores were sectioned at 2 cm intervals prior to analysis. Where more detailed information of the vertical distribution of ^7Be within a soil profile was required, samples were collected at 5 – 10 mm depth increments using a 40 × 20 cm steel frame and scraper in order to obtain samples of adequate mass for analysis. The vertical activity distribution of ^7Be has been determined for soil cores collected after heavy rainfall and snowmelt events with different inter-arrival times. Bulk samples of surface runoff and stream water were collected from gauging stations on the Homerka stream and its tributaries and within the experimental slope from the outlet of an unmetalled road and a Holocene gully, during periods of flood discharge, when suspended sediment concentrations exceeded ca. 20 mg L⁻¹. The water samples collected from the streams ranged between 200 and 1000 L in volume and were pumped from the stream into 120 L plastic containers using an electromagnetic pump. Occasional bulk samples were also collected during flood event from sites upstream of the main gauging stations on the Homerka and Bacza streams. The suspended sediment was recovered from the bulk water samples by sedimentation and centrifugation, and the <0.063 and >0.063 mm fractions were separated by

wet sieving. Samples of fine sediment recently deposited on the streambed were collected at 16 locations along the mainstream channel of the Homerka stream and its tributaries shortly after flood flow conditions. Measurements of FRN activity were made on the <0.063 mm size fraction. The measurements of $^{210}\text{Pb}_{\text{ex}}$, ^7Be , and ^{137}Cs activity undertaken on suspended sediment samples collected from the catchment outlet integrate the source contributions from the entire upstream catchment.

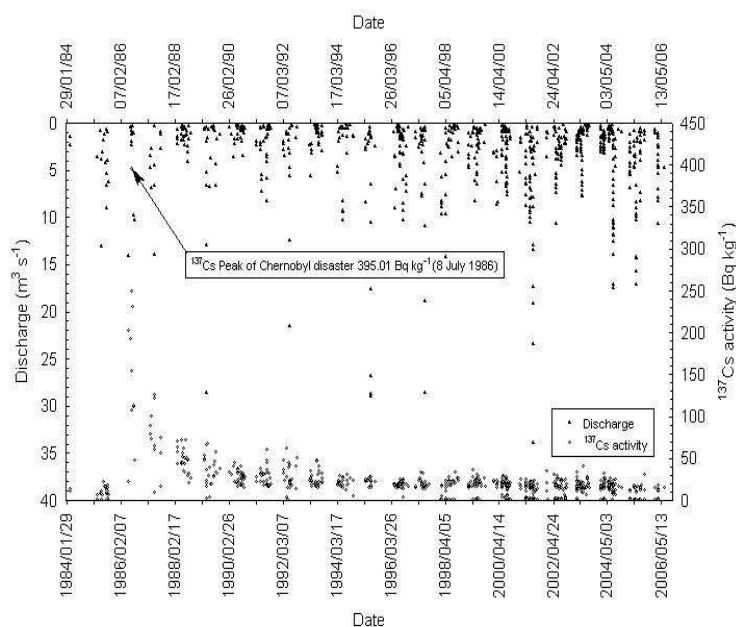


FIG. 5. Variation of the ^{137}Cs content of the <0.063 mm fraction of suspended sediment transported by the Homerka stream during the period 1984–2006.

Information on suspended sediment sources has been assembled using the ‘fingerprinting’ approach (cf. 12,13,15]. Samples of surface material from potential sources (forest, pasture, cultivated areas, unmetalled roads, gully walls and channel banks) were collected from an area of 1 m^2 , using a steel frame. It is not possible to compare directly the $^{210}\text{Pb}_{\text{ex}}$, ^7Be , and ^{137}Cs content of these source materials with that of the suspended sediment transported by the stream, because of contrasts in the grain size composition of source materials and suspended sediment and the known enrichment of the finer fractions in $^{210}\text{Pb}_{\text{ex}}$, ^7Be , and ^{137}Cs . The <0.063 mm fraction of the source materials was therefore separated for gamma spectrometry analysis and the resultant values of radionuclide content were used for comparisons with those associated with the suspended sediment.

The $^{210}\text{Pb}_{\text{ex}}$, ^7Be and ^{137}Cs gamma assay was undertaken in the Laboratory of Fluvial Processes of the Institute of Geography and Spatial Organization of the Polish Academy of Sciences. All soil and sediment samples were dried, disaggregated and passed through a 2 mm or <0.063 mm sieve before being packed into 500 mL Marinelli-beakers for gamma-ray spectrometry using an ORTEC HPGe coaxial detector with a relative efficiency of 45%, calibrated with Standard Reference Materials: IAEA Soil-6; IAEA Soil-375 and IAEA Soil-327 and also artificial standards. Due to its very short half-life, ^7Be activity was measured immediately after sampling. The activities of Pb^{210} , Ra^{226} , Be^7 and ^{137}Cs were determined from the photopeaks produced at 46.52; 185.99; 477.56 and 661.62 keV, respectively. Count times were in the range 42 300 – 84 600 s and provided results with a precision of the order of $\pm 5\%$ at the 95% level of confidence.

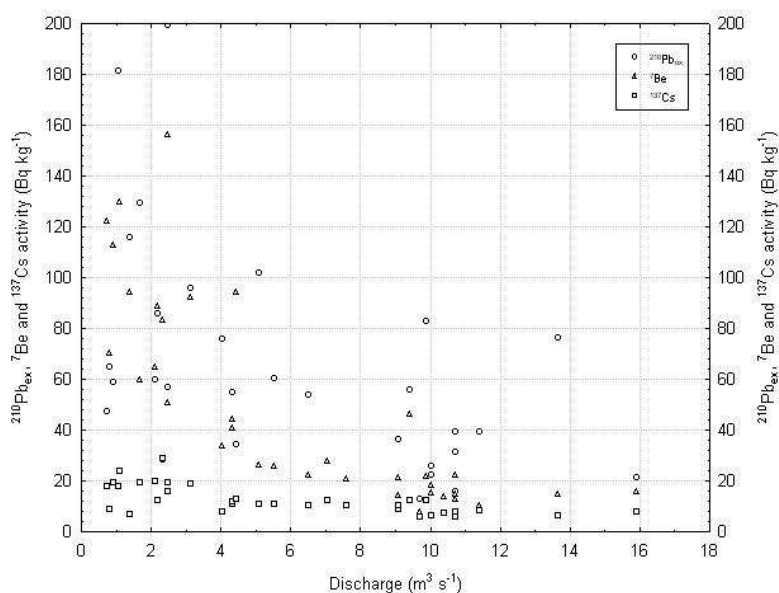


FIG. 6. The relationship between the discharge at the main gauging station on the Homerka stream and the $^{210}\text{Pb}_{\text{ex}}$, ^7Be and ^{137}Cs activity of suspended sediment.

3. RESULTS AND DISCUSSION

3.1. Exploratory studies on the use of ^7Be as a sediment tracer

^7Be does not penetrate far into the soil profile, and the net activity per unit area at any time reflects the recent fallout input, radioactive decay, local soil properties, and the inter-arrival time of recent events. The half penetration depths, at which the concentrations decreased to half the surface value, varied between 5 and 25 mm, depending of the land use and infiltration rate. The smallest penetration depths were observed on road surfaces and these varied between 5 and 10 mm due to surface compaction. The greatest penetration occurred in cultivated plots and soils with grass cover (5 - 25 mm).

The amount of ^7Be deposited at the soil surface depends on the depth of rainfall (Fig. 4). In order to compare the ^7Be deposited within areas under different land uses with a known input, the total input of ^7Be in wet and dry fallout to Homerka drainage basin has been measured since January 2001. Individual rainfall measurements included preceding dry fallout to the collection funnels and thus represented the total fallout input. The average total annual fallout to the site was $3750 \pm 150 \text{ Bq m}^{-2} \text{ a}^{-1}$.

In this area the average depth of ^7Be penetration was between 5 and 25 mm, whereas about 90% of the total ^{137}Cs activity was detected in the top 5 to 20 cm of the soil profile. The radionuclide is therefore capable of providing good discrimination between sediment derived from the immediate soil surface and that derived from depths >20 mm where concentrations will be effectively zero. Monitoring of the spatial distribution of ^7Be activity across plots bounded by terraces, immediately after heavy rains provide a basis for investigating sediment mobilised by sheet and rill erosion and sediment production from unmetalled roads.

Soil particles under forest litter were characterized by lower ^7Be activity than particles from a similar depth in ploughed fields, while in permanent pasture ^7Be concentration was higher at greater depths. This is evidence that canopy interception is an important factor in reducing

fallout to the forest soil surface. On the average, total inventories found on arable soils are lower than those found on grass covered soils, as a result of soil erosion processes linked to short term events. The results show that ^7Be diffusion is connected with land use and soil surface cover. The greatest research need in the Polish Carpathians remains the assessment of soil erosion/deposition rates using ^7Be measurements to evaluate the impact of short term land use changes and the effectiveness of soil conservation practices during extreme events.

3.2. Fingerprinting sediment sources

There is an increasing need for reliable information on the main sources of the suspended sediment transported by a river. Such information may, for example, be needed to provide a basis for establishing sediment control strategies, to afford an improved understanding of sediment-associated transport of contaminants, or to provide a more meaningful assessment of rates of erosion within a drainage basin. Information on sediment mobilisation and transfer through the fluvial system and on sedimentation is important for improving land management, predicting sediment loads and reducing rates of reservoir siltation.

Measurements of the ^{137}Cs content of the $<0.063\text{ mm}$ and $>0.063\text{ mm}$ fractions of suspended sediment collected from the main flow gauging station at the outlet of the Homerka catchment during the pre-Chernobyl period indicated a range of activity between 6.3 and 22.6 Bq kg^{-1} for the $<0.063\text{ mm}$ fraction. Activities for the coarser $>0.063\text{ mm}$ fraction were much lower and consistently approx. $1\text{--}2\text{ Bq kg}^{-1}$. These activities have been plotted against the discharge at the time of sampling in Figs. 5 and 6. The discharges in the main stream associated with the threshold for the initiation of surface runoff as linear flow on unmetalled roads and in gullies, ditches and furrows, and as overland flow from cultivated plots, pasture areas and forest areas, derived from conventional monitoring, have also been defined in Fig. 7. These thresholds show that linear flow from unmetalled roads and in gullies, ditches and furrows occurs above a relatively low threshold discharge in the main channel. However based on the same thresholds it can be concluded that at higher flows overland flow from cultivated, pasture and forest areas progressively occurs, with overland flow from forest areas only occurring when flows in the main channel exceed approximately $4\text{ m}^3\text{ s}^{-1}$. The range of ^{137}Cs activities associated with both suspended sediment and potential source materials have also been plotted in Fig. 7.

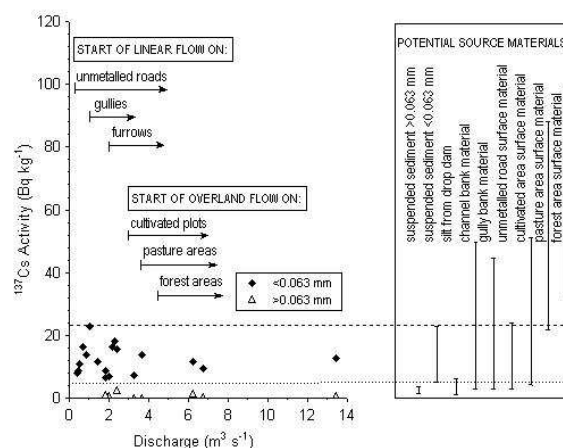


FIG. 7. The relationship between the ^{137}Cs content of suspended sediment and discharge, the discharge thresholds associated with the occurrence of storm runoff from various sources within the Homerka catchment and the range of ^{137}Cs concentrations associated with suspended sediment and potential source materials (based on Froehlich and Walling, 1992).

Two key features of Fig. 7 are worthy of comment in relation to identifying the dominant sources of fine (suspended) sediment in the Homerka catchment. First, comparison of the range of ^{137}Cs activity associated with suspended sediment with the typical ranges associated with potential source materials suggests that this most closely matches that associated with material collected from the surface of unmetalled roads [cf.15,16,17]. Sediment eroded from the surface of forest and pasture areas is unlikely to represent an important sediment source, since its ^{137}Cs activity is substantially higher. If the contribution from this source was appreciable, the overall concentration in the suspended sediment would increase to levels considerably above those recorded. Material eroded from the surface of cultivated land and from gully and channel banks could represent a significant sediment source, but is thought unlikely to represent a major source, since the range of ^{137}Cs activities associated with these materials again extends well above that which is representative of suspended sediment. Secondly, there is no evidence that the dominant sediment sources change significantly during storm runoff events of different magnitude. The ^{137}Cs activity of the suspended sediment remains essentially similar across a wide range of flows, despite crossing a range of thresholds for surface runoff generation within the catchment. This suggests that unmetalled roads represent the main suspended sediment source within the catchment over the entire range of flows.

Fig. 5 provides a longer term perspective on sediment sources in the Homerka catchment, by plotting the values of ^{137}Cs activity recorded in suspended sediment over the entire period of sediment sampling, from its inception in 1984 through to 2006. This plot clearly shows the impact of the Chernobyl accident and the associated fallout of ^{137}Cs in 1986, since ^{137}Cs activities in suspended sediment increased by ~20 times during the immediate aftermath of the Chernobyl accident to reach nearly 400 Bq kg^{-1} . The rapid decline of ^{137}Cs activity in suspended sediment, to reach a new 'equilibrium' after 3–4 years is consistent with unmetalled roads representing the dominant source, since Chernobyl fallout accumulating on these source areas could be expected to be rapidly removed by erosion of the road surface, so that after ca. 10 years, the ^{137}Cs activities are of a similar magnitude to those found before the Chernobyl accident, taking account of radioactive decay. If the catchment surface more generally was the main source, ^{137}Cs activities could be expected to remain higher for an extended period, since ^{137}Cs activities in catchment soils were significantly increased by Chernobyl fallout and still remain substantially higher than those recorded prior to the Chernobyl event.

Fig. 8 introduces a spatial dimension to the identification of the dominant sediment sources in the catchment, by comparing the $^{210}\text{Pb}_{\text{ex}}$, ^7Be and ^{137}Cs activity associated with fine (<0.063 mm) sediment collected from deposits at various locations along the channel of the Homerka stream after a flood in July 2003. The low $^{210}\text{Pb}_{\text{ex}}$, ^7Be and ^{137}Cs activities associated with the sediment are again indicative of the dominance of unmetalled roads as a sediment source. However, although this plot evidences significant scatter, it still shows a tendency for $^{210}\text{Pb}_{\text{ex}}$, ^7Be and ^{137}Cs activities to decrease downstream, in passing from the upper reaches of the catchment to the lower reaches. This is consistent with the progressive increase in the importance of unmetalled roads as a sediment source in the agricultural areas towards the lower part of the catchment, where road densities are frequently highest, and the associated reduction in the relative importance of channel and gully erosion. This trend could also suggest that although unmetalled roads are the dominant source, there is some limited contribution from the catchment surface more generally. Since pasture and forest areas dominate in the upper part of the catchment, any surface contribution from this area is likely to have a higher ^{137}Cs activity than sediment contributed from the catchment surface in its lower areas, where cultivated areas are more important and the forested area is very limited.

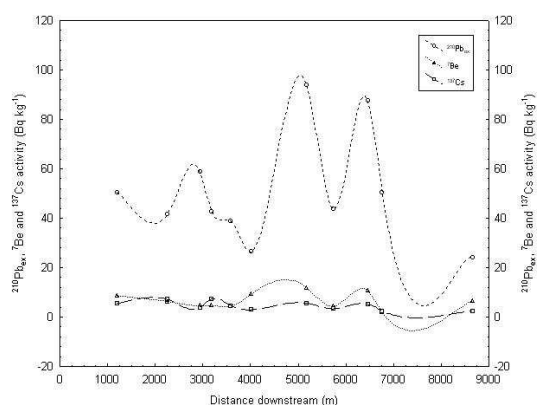


FIG. 8. Downstream changes in the $^{210}\text{Pb}_{\text{ex}}$, ^7Be and ^{137}Cs content of the <0.063 mm fraction of fine sediment deposits in the main channel of the Homerka catchment sampled after the flood of July 2004.

3.3. Suspended sediment delivery dynamics during flood events

During extreme rainfalls, a greatly expanded contributing area could mobilise sediment in areas which are unconnected to the stream under 'normal' events. However, there is a lack of field evidence that documents sediment delivery dynamics during individual extreme rainfall events. It should also be emphasized that only samples from a single flood event should be used to examine the main source of fallout $^{210}\text{Pb}_{\text{ex}}$, ^7Be and ^{137}Cs in sediment samples, because sediment deposited during different storm events may originate from various sources with different radionuclide contents.

Figs. 9, 10 and 11 provide further information on sediment source dynamics within the Homerka catchment, by considering the variation of the $^{210}\text{Pb}_{\text{ex}}$, ^7Be and ^{137}Cs content of suspended sediment during individual events. The three examples illustrated relate to a snowmelt event occurring during March 2003 (Fig. 9), during a flood in July 2003 (Fig. 10) and a 'flash flood' resulting from an intense summer rainstorm occurring in August 2004 (Fig. 11).

The pattern of variation of the $^{210}\text{Pb}_{\text{ex}}$, ^7Be and ^{137}Cs content of suspended sediment during the snowmelt event of March 2003 shows an increase in the $^{210}\text{Pb}_{\text{ex}}$, ^7Be and ^{137}Cs activity during high flows, although there is considerable hysteresis in the relationship, with the increase in $^{210}\text{Pb}_{\text{ex}}$, ^7Be and ^{137}Cs activity lagging the increase in water discharge by 6 h or more. Furthermore, there is a very rapid decline in the $^{210}\text{Pb}_{\text{ex}}$, ^7Be and ^{137}Cs activity associated with the second increase in water discharge that occurred around midday on 11 March. This behaviour is again consistent with unmetalled roads providing the main suspended sediment source in the Homerka catchment. During the early stages of storm events, runoff and sediment generation is likely to be primarily restricted to the network of unmetalled roads, and particularly those parts of the network close to the channel system. As the event proceeds and discharge increases, sediment from parts of the unmetalled road network further from the channel network, which may only contribute during higher magnitude events, will reach the channel system. Equally, during the period of peak runoff, increased sediment inputs are likely to be generated from active gullies and eroding channel banks, and also from cultivated areas connected to the channel system by furrows and ditches, either directly or via the unmetalled roads. These inputs will introduce sediment with a higher $^{210}\text{Pb}_{\text{ex}}$, ^7Be and ^{137}Cs content, causing the $^{210}\text{Pb}_{\text{ex}}$, ^7Be and ^{137}Cs content of the overall sediment load to increase.

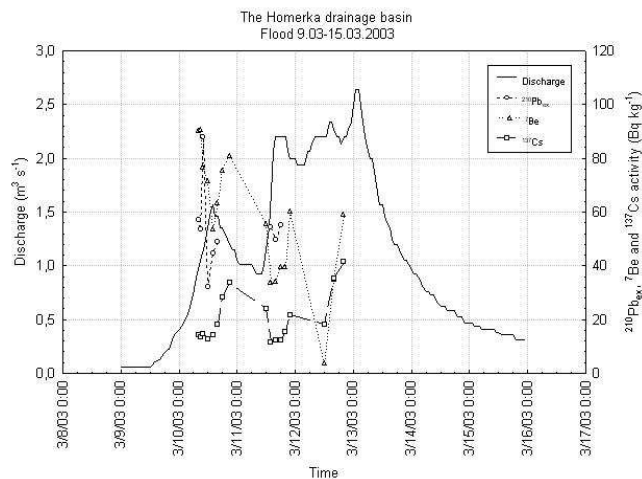


FIG. 9. Variation in the $^{210}\text{Pb}_{ex}$, ^7Be and ^{137}Cs content of the <0.063 mm fraction of suspended sediment transported by the Homerka stream during a snowmelt flood in March 2003.

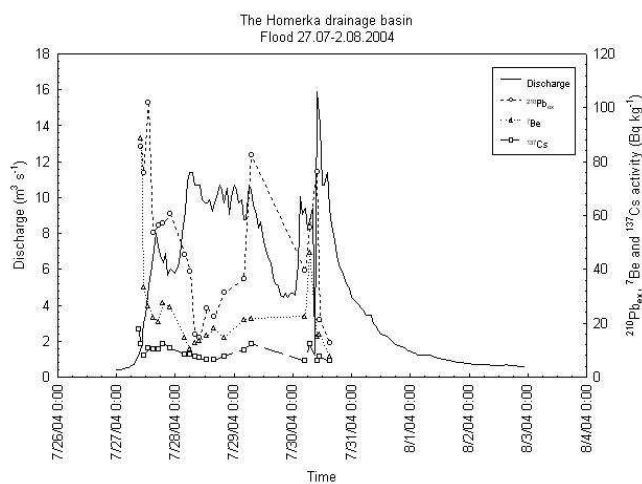


FIG. 10. Variation in the $^{210}\text{Pb}_{ex}$, ^7Be and ^{137}Cs content of the <0.063 -mm fraction of suspended sediment transported by the Homerka stream during a flood in July 2003.

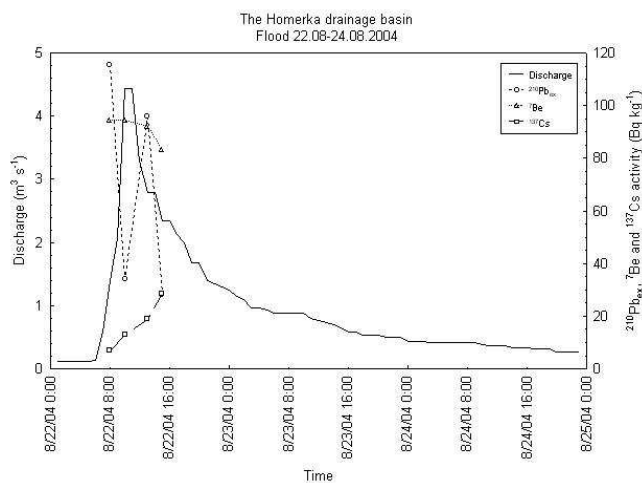


FIG. 11. Variation in the $^{210}\text{Pb}_{ex}$, ^7Be and ^{137}Cs content of the <0.063 -mm fraction of suspended sediment transported by the Homerka stream during a flash flood in August 2004.

3.4. Comparison with conventional measurements

The results from the $^{210}\text{Pb}_{\text{ex}}$, ^7Be and ^{137}Cs measurements presented above, which emphasize the importance of unmetalled roads as the dominant suspended sediment source in the Homerka catchment, are consistent with other information provided by the more traditional monitoring techniques deployed in the study catchment and the adjacent region. Studies of surface runoff generation in forested areas of the Carpathians have emphasized that surface runoff rarely occurs and it can therefore be inferred that direct supply of sediment from the forested areas to the stream channels and the network of unmetalled roads is of very limited importance. Similarly, measurements of suspended sediment concentrations in diffuse surface flow from pasture areas in the Homerka catchment have shown that values are typically in the range 25–65 mg L⁻¹, and were always an order of magnitude or more less than those measured in suspended sediment samples collected from the river at the catchment outlet.

Although surface runoff and sediment mobilization have frequently been documented on the cultivated plots investigated within the experimental slope [see 3], these areas have been shown not to represent a significant source for sediment transfer to the stream channel. In most locations, the slopes are poorly coupled to the stream channels and the existence of terraces and also pasture areas adjacent to most stream channels, which act as buffer strips, serve to reduce slope–channel connectivity. The evidence available from conventional monitoring undertaken within the Homerka catchment therefore provides a strong indication that the high suspended sediment concentrations found in the stream channel, and which sometimes exceed 3×10^4 mg L⁻¹, could not have been produced by sediment mobilized from the catchment slopes, but primarily reflect sediment mobilization from the dense network of unmetalled roads in the catchment. The magnitude of the suspended sediment concentrations measured in samples of surface runoff collected from unmetalled roads has been shown to reflect a number of characteristics of the roads, including their age, their degree of incision, and their frequency of use [11]. Suspended sediment concentrations in excess of 15×10^4 mg L⁻¹ have been recorded for samples collected from sunken roads that are frequently used. Attempts to document the rate of incision of such unmetalled roads have generated estimates of average rates of incision over the past 30 years of approx. 6–7 mm year⁻¹.

The relationships between erosion, sediment redistribution and storage and sediment transfer in headwater areas in the Polish Carpathians include several pathways and linkages within the fluvial system. There is a need to cover spatial scales extending from plots and small hollows on the slopes of first order basin to the outlets of large river system. Rainfall-runoff mechanisms determine the delivery dynamics of suspended sediment to the stream channel. The key requirement is to identify linkages between the sediment sources and the stream channel. The Partial Area and the Variable Source Area models, in which saturated zones expand upslope during the rainfall [18], remain the best guides to the location of suspended sediment source areas. During extreme rainfall, a greatly expanded contributing area could mobilise sediment from areas, which are unconnected to the stream under 'normal' events. Although these models can provide valuable guidance on where soil conservation works need to be located for maximum effect, there remains a need to document sediment delivery dynamics during individual extreme events, in order to develop an improved understanding of sediment mobilisation and routing through the fluvial system.

4. CONCLUSIONS

The study reported confirms the ability of the conjunctive use of $^{210}\text{Pb}_{\text{ex}}$, ^7Be and ^{137}Cs to provide additional information on sediment mobilisation and sediment delivery within a small

drainage basin in Polish Flysch Carpathians. The different depth distributions of $^{210}\text{Pb}_{\text{ex}}$, ^7Be and ^{137}Cs in undisturbed soils can provide a means of identifying the depth of surface erosion during different events. Changes in the $^{210}\text{Pb}_{\text{ex}}$, ^7Be and ^{137}Cs content of suspended sediment transported during flood events reflect changes in the relative contribution of different sediment sources. More detailed analysis of the ^7Be content of suspended sediment during individual flood events may provide valuable information concerning the dynamics of changing sediment sources and contribution areas. Furthermore, there is a need to assess the extent to which conclusions based on the Homerka drainage basin are representative of the Flysch Carpathians more generally, and an attempt has been made to understand the sediment delivery dynamics of fluvial systems in drainage basins of different scale.

Monitoring of the spatial distribution of ^7Be activity immediately after each heavy rainfall event can provide a basis for investigating sediment mobilised by dispersed overland flow and linear flow. Since changes in land use can affect the volume of sediment mobilised from a small catchment, it can be concluded that these changes may prove to be significant at the larger basins. During extreme rainfall events of more than 35 mm with an intensity of ca. 0.5 mm min⁻¹ sediment storage within the edge of agricultural terraces is ca. 5 mm (average) within the agricultural experimental slope in the Homerka drainage basin. This value reflects sediment transport by dispersed wash and is comparable with the intensity of erosion measured by ^7Be on agricultural plots. It is likely that during extreme runoff events some of the eroded sediment cascades over the terrace onto the adjacent downslope plot, but assessment of the $^{210}\text{Pb}_{\text{ex}}$, ^7Be and ^{137}Cs inventories suggests that this is not a major process. It is clear that any attempt to reduce the sediment yield of the study catchment would need to target the network of unmetalled roads in the catchment, with a view to reducing surface runoff and sediment mobilization from these sediment sources and attenuating the transfer of sediment from the roads to the stream system, by, for example, diverting runoff to temporary sinks.

ACKNOWLEDGEMENTS

The work reported in this contribution was undertaken as part of the International Atomic Energy Agency's Co-ordinated Research Project on 'Assessing the effectiveness of soil conservation techniques for sustainable watershed management using fallout radionuclides' (CRP D1.50.08), under Research Contract no. POL-12327. The support of the IAEA, Institute of Geography and Spatial Organization of the Polish Academy of Sciences and the University of Exeter is gratefully acknowledged. Thanks are also extended to Felipe Zapata for his valuable comments on the draft manuscript and to Mr Jim Grapes from the Department of Geography at Exeter University for assistance in undertaking the gamma spectrometry measurements.

REFERENCES

- [1] FROEHLICH, W., WALLING, D.E., "The use of fallout radionuclides in investigations of erosion and sediment delivery in the Polish Flysch Carpathians", *Erosion, Debris Flows and Environment in Mountain Regions* (ed. by D.E. Walling, T.R. Davies and D.E. Walling) (Proc. Chengdu Symp., July 1992), IAHS Publication **209** (1992) 61-76. Enter first reference here.
- [2] FROEHLICH, W., WALLING, D.E., "Using environmental radionuclides to elucidate sediment sources within a small drainage basin in the Polish Flysch Carpathians", *Sediment Budgets 1* (Proc. of symposium S1 held during the Seventh IAHS Scientific Assembly at Foz de Iguacu, Brazil, April 2005), IAHS Publication **291** (2005) 102-112.

- [3] BURCH, G. J. et. al., "Detection and prediction of sediment sources in catchments: use of ^7Be and ^{137}Cs ", Proc. Hydrology and Water Resources Symp. Australian National University, Canberra, Australia (1988) 146–151.
- [4] WALLBRINK, P.J., MURRAY, A.S., Distribution and variability of ^7Be in soils under different surface cover conditions and its potential for describing soil redistribution processes, *Water Resources Research* **32** (1996) 467-476.
- [5] SLUPIK, J., Zróźnicowanie spływu powierzchniowego na fliszowych stokach górskich. Dokumentacja Geograficzna, IG i PZ PAN **2** (1973) 1-118.
- [6] GIL, E., SŁUPIK, J., Hydroclimatic conditions of slope wash during snow melt in the Flysch Carpathians. Symposium International de Geomorphologie, Univ. Liege, **67** (1972) 75-90.
- [7] GIL, E., Ruissellement et erosion sur le versants du flysh d'apres les resultats de parcelles experimentales, *Bull. Assoc. Geogr. Francais* **63** (1986) 357-361.
- [8] BRAŃSKI, J., Zmącenie wody i transport rumowiska unoszonego w rzekach polskich, *Prace PIHM* **95** (1968) 49-67.
- [9] FROEHLICH, W., Mechanizm transportu fluwialnego i dostawy zwietrzelin do koryta w górskiej zlewni fliszowej, *Prace Geogr. IG i PZ PAN* **143** (1982) 1-144.
- [10] FROEHLICH, W., SLUPIK, J., Importance of splash in erosion process within small flysch catchment basin, *Studia Geomorph. Carpatho-Balcanica* **14** (1980) 77-112.
- [11] FROEHLICH, W., et. al., "The use of caesium-137 to investigate soil erosion and sediment delivery from cultivated slopes in the Polish Carpathians", *Farm Land Erosion in temperate Plains Environment and Hills*, (ed. by S. Wicherek), Elsevier Sci. Pub. B.V. (1993) 271-283.
- [12] PEART, M. R., WALLING, D. E., "Fingerprinting sediment source: The example of a drainage basin in Devon, UK", *Drainage Basin Sediment Delivery* (ed. by R. F. Hadley) (Proc. Albuquerque Symp., August 1986), IAHS Publication. **159** (1986) 41–55.
- [13] WALLING, D.E., WOODWARD, J.C., "Use the radiometric fingerprints to derive information on suspended sediment source", *Erosion and Sediment Transport Monitoring Programmes in River Basins* (ed. by J. Bogen, D. E. Walling & T. Day) (Proc. Oslo Symp., August 1992), IAHS Publication **210** (1992) 153–164.
- [14] BASKARAN, M., A search for the seasonal variability on the depositional fluxes of Be-7 and Pb-210, *Journal of Geophysical Research* **100** (1995) 2833-2840.
- [15] FROEHLICH, W., WALLING, D.E., "The role of unmetalled roads as a sediment source in the fluvial systems of the Polish Flysch Carpathians)", *Human Impact on Erosion and Sedimentation* (ed. by D.E. Walling and J.L. Probst) (Proc. Rabat Symp., April 1997), IAHS Publication **245** (1997) 159-168.
- [16] FROEHLICH, W., "Sediment Dynamics in the Polish Flysch Carpathians", *Sediment and Water Quality in River Catchments* (ed. by I. Foster, A. Gurnell & B. Webb), J. Wiley & Sons, Chichester (1995) 453-461.
- [17] FROEHLICH, W., WALLING, D.E., "Impact of Anthropogenic Sediment Sources of Reservoir Sedimentation in the Polish Carpathians", *Proc. of International Workshop on Ecological, Sociological and Economic Implications of Sediment Management in Reservoirs*, Paestum, Italy, 8-10 April, 2002 (ed. Giampaolo Di Silvio, Rollin Hotchkiss) UNESCO-IHP (2003) 108-112.
- [18] WALLING, D.E., The sediment delivery problem, *J. Hydrol.* **65** (1983) 209-237.

APPLICATION OF THE RADIONUCLIDE TECHNIQUE AND OTHER METHODS FOR ASSESSING THE EFFECTIVENESS OF SOIL CONSERVATION MEASURES AT THE NOVOSIL STUDY SITE, OREL REGION, CENTRAL RUSSIA

V.N. GOLOSOV, V.R. BELYAEV, M.V. MARKELOV,
N.N. IVANOVA, Y.S. KUZNETSOVA
Laboratory for Soil Erosion and Fluvial Processes,
Faculty of Geography, Moscow State University,
Moscow, Russian Federation

Abstract

In the present paper, the findings are presented of a detailed study about the long term (70-75 years) effectiveness of soil conservation measures, which was conducted at the Novosil study site located in the Orel region of the Central Russian Plain. At the Novosil Experimental station, three pairs of transects of different morphology were selected on relatively steep arable farmland. One transect in each pair underwent introduction of soil conservation measures in the past, while the other was kept under regular cultivation. On all three transects under soil conservation practices artificial terraces were installed in combination with forest belts located parallel to the topography contour lines and spaced at approximately 100 m from each other. The construction of terraces and tree planting was initiated in 1932. The ^{137}Cs and $^{210}\text{Pb}_{\text{ex}}$ radioisotopes were used as tracers for the quantitative assessment of long term soil conservation effectiveness within each pair of transects. Simultaneously soil profile morphology method and empirically based erosion modelling were used to complement the datasets collected by using fallout radionuclide techniques. The study, based on soil profile morphology and ^{137}Cs based methods, concluded that slopes with soil-protective measures are characterized by a reduction of the average annual soil redistribution rates by 25-80%. Good coincidence of the spatial patterns of soil redistribution rates provided by these two techniques suggests general reliability of the results. Observed discrepancies in values obtained can be attributed to differences in temporal resolution of methods as well as to possible influence of individual extreme events on results yielded by the ^{137}Cs method. However, more significant decrease of average soil degradation rates on slopes under soil conservation practices (up to 70-75% for each pair of slopes) was predicted by empirically based modelling. This substantial differences between predicted and directly measured values is attributed to a high degree of soil degradation prior to the introduction of protective measures (reflected by the soil-morphological method) and lack of funding for maintaining the appropriate conditions of terraces and forest belts after collapse of the former Soviet Union (reflected by the ^{137}Cs technique). Investigation undertaken in the study area confirmed that the radionuclide based technique is an efficient tool for quantitative evaluation of the effectiveness of soil conservation measures within the Central Russian Plain region. However further study is needed for improving the application of the radionuclide technique in the domain of sediment and pollutant transfer into the river system.

1. INTRODUCTION

Since the early intensification of the agricultural sector in the 19th century, deterioration of the soil fertility and its productive capacity, due to soil structure degradation, compaction, and hence erosion, have been an important threat for the agricultural land in Russian Federation. The central part of European Russia is one of the agricultural regions with the longest history of intensive cultivation. The most intensive expansion of arable lands in this region took place during the second part of the 19th century after the land ownership reform was introduced in 1861, resulting in severe sheet, rill and gully erosion. Some of cultivated land was abandoned because of severe soil degradation and slope dissection by very intensive rill and gully erosion. In the beginning of the 20th century the famous Russian scientist Dokuchaev elaborated a national program of conservation measures for protecting soil from water and wind erosion. Several experimental stations were established in different landscape zones of Russia during the first decades of the 20th century to study the effectiveness of different conservation measures.

Both snowmelt and rainfall-induced erosion are observed in Central European Russia. Erosion rates during snowmelt range from 1 to 10 t ha⁻¹ a⁻¹ according to long term observations within erosion plots and experimental slope catchments undertaken in different parts of Central Russia. However intensive rainstorms produce soil losses in a range of 20-220 t ha⁻¹ per event [1]. Despite the fact that they have a 10-20-year return period, such storms are the main cause of soil losses in Central European Russia.

The present study focused on the evaluation of the effectiveness of long term conservation measures initiated 70-80 years ago at the Novosil study site located in the Orel region of the Central Russian Plain. Fallout radionuclide based tracer techniques were used in combination with more traditional methods and approaches for the quantitative assessment of soil redistribution on cultivated slopes.

2. MATERIALS AND METHODS

2.1. Background

The study area is located in the Zusha River basin at the centre of the Orel Region. The Orel Region is the main agricultural region of European Russia within the forest-steppe agroecological zone. Area of agricultural land within the Orel region is 87%. The average annual water erosion rate for the region is estimated at 4.5 t ha⁻¹ a⁻¹ (Fig. 1), which is also the average value considering all regions of Central European Russia (Fig.1). However, the area of arable land affected by noticeable erosion is relatively the highest in the Orel Region (Fig. 1).

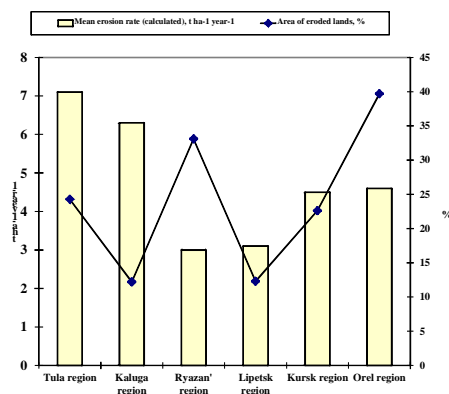


FIG. 1. Mean annual erosion rate (calculated by empirical based model) and eroded arable land as a percentage of the total cultivated area for some main regions of Central European Russia.

The Zusha River basin is a territory with a well-known history of intensive cultivation. Farmland area increased especially significantly in the second half of the 19th century (Fig 2) and reached its maximum after the onset of the collectivization program in 1938 (Fig 2). That was a period of arable field enlargement because of transformation of individual parcels into large collective farm fields. Preliminary assessment of gully erosion rates using historical maps shows that maximum numbers of gullies were formed after the land ownership reform in 1861 (Fig. 3). During this period even very steep slopes became cultivated in many places, which enhanced the development of new gullies. The maximum surface (sheet and rill) erosion was observed in 1930-1940 immediately after the collectivization (Fig. 3).

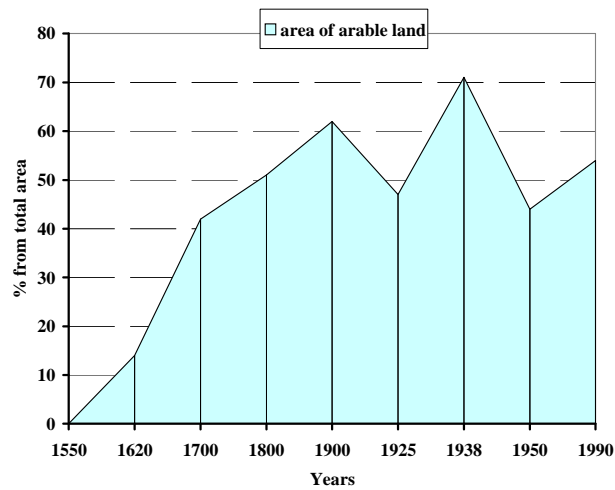


FIG. 2. Temporal variability of arable land as a percentage of the total area of the Zusha River basin for the 1550-1990 time period.

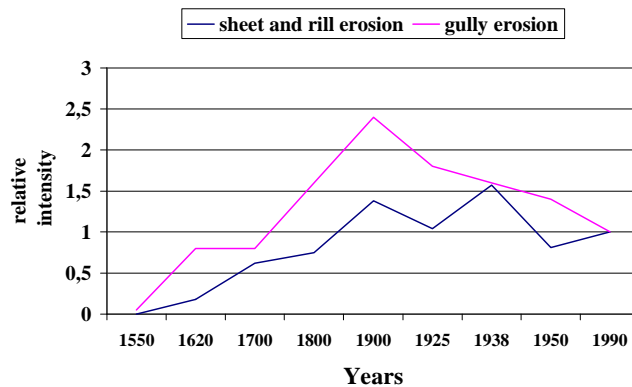


FIG. 3. Relative intensity of surface (sheet and rill) and gully erosion for the 1550-1990 time period within the Zusha River basin (the intensity in 1990 is equal to 1).

2.2. Description of the Novosil study site

The study site is located at the Novosil agro-forestry and land-improvement research station situated in the central part of the Zusha River basin (Fig. 4). The Novosil experimental station was founded in 1923 with the main objective to study processes of soil and gully erosion and to develop effective and economically sound soil conservation measures. The main focus has been put on the improved spatial organization of agricultural land use, crop rotations, use of slope terracing and forest belts for optimal soil protection. For example, at the site analyzed in the present study construction of terraces and tree planting (forest belts) was initiated in 1932. Terraces and forest belts were located parallel to the contour lines and spaced at approximately 100 m from each other. In addition, water retention ditches were dug within the central parts of some of forest belts in the 1960s. Also some other conservation measures were tested on the lands belonging to the Novosil experimental station. The list of conservation measures is presented in Table 1.

There is no detailed information available on the soil cover conditions prior to the foundation of the Novosil experimental station and introduction of soil conservation measures. However, it is generally known that a large part of the present experimental station's landownership was

characterized by moderately to severely degraded subtypes of the *Grey forest soils* (*Phaeozems* according to the World Reference Base (WRB) on Soil resources) [2]. In addition, extreme soil degradation occurred on the steepest parts at the lower slope position above the adjacent valley slope. In many cases these parts of the slopes were completely devoid of productive topsoil as a result of severe sheet and rill erosion. Degradation of these lower located slopes by erosion was often so severe that their surfaces could be characterized as a ‘mini-badland’ [2]. Agricultural productiveness of the degraded soil was completely lost. It must be noted that such most severely degraded zones were first selected for soil conservation and counter-erosion measures application, as this fact has important implications for the analysis of the soil recovery.

TABLE 1. TYPES OF CONSERVATION MEASURES TESTED AT THE NOVOSIL’ EXPERIMENTAL STATION FOR THE PERIOD OF 1923-2000

Conservation measures			
Agronomic/soil management	Vegetative	Structural	Overall management
a/mulching; b/deep tillage; c/minimum tillage; d/deep ripping; e/counter cultivation; f/contour ridging.	a/windbreaks; b/zero grazing; c/relay cropping; d/hedge barrier; e/planting forest; f/reseeding trees along field boundary.	a/retention ditch; b/forward sloping terraces; c/dam; d/level banks; e/waterway (convey water at the gully top and gully bottom); f/level banks with level ditch g/stone concrete over-falls.	a/exclusion of natural waterways; b/change from cropping to grassland; c/better soil cover by vegetation.

The study area is underlain by the Devonian limestones and marls mantled by the Middle-Late Pleistocene sands and loams on which the present soils have been formed. The most typical soils are the *Grey forest soils* (*Phaeozems* according to the WRB) (about 80%) and *Podzolized chernozems* (*Luvic chernozems* according to the WRB) (about 20%) with a heavy loamy texture. The permeability of soils is very low. The typical particle size distribution of these soils is shown in Table 2. A soil surface crust appears very quickly after the first spring rains.

TABLE 2. PARTICLE SIZE DISTRIBUTION OF TYPICAL LOCAL SOIL UNITS AT THE NOVOSIL EXPERIMENTAL STATION [13]

Soil unit	1-0.25 mm (%)	0.25-0.05 mm (%)	0.05-0.01 mm (%)	0.01-0.005 mm (%)	0.005-0.001 mm (%)	<0.001 mm (%)	Sum <0.01 mm (%)
Podzolized chernozem (Luvic chernozem)	1.7	60.9	14.9	5.1	12.8	4.6	22.5
Grey forest soil (Phaeozem)	2.6	55.3	15.9	8.2	10.8	7.2	26.2
Dark-grey forest soil (Haplic Phaeozem)	5.5	79.8	3.0	2.0	4.6	5.1	11.7

The main crops are winter and spring cereals, maize, sugar beans and perennial grasses (forage). According to the local meteorological record the annual average temperature is +5.2°C (the monthly average minimum temperature is reported for February and is -9.7°C; the monthly average maximum temperature is measured in July and is +19.6°C). The annual

average precipitation for the period observed (1959-2003) is 536 mm (range of 350-800 mm), with about 30% of the precipitation falling as snow. Rainfall events with maximum intensity mainly occur during the period of June to August. The mean water equivalent of the snow before the spring snowmelt is 170 mm [3].

From 1959 to 1990 (in 1991 the program was stopped because of insufficient funding), surface runoff and sediment delivery have been measured on large scale runoff plots at the Novosil station (size 200 × 20m) focusing on the spring snowmelt period. The main task of these measurements was to collate information about the effectiveness of different soil conservation measures for reducing soil losses and surface runoff during snowmelt [4]. From 1959 to 1974 observations yielded a relatively higher runoff coefficient (Table 3), which can be explained by deep freezing of the topsoil during the winter time. The second period from 1975 until 1990 was wetter and warmer, resulting in a three-fold decrease of a mean surface runoff coefficient as compared to that observed during the 1959-1974 period (Table 3).

TABLE 3. MEAN VALUES OF WATER STORAGE IN SNOW BEFORE SNOWMELT, SURFACE RUNOFF LAYER AND RUNOFF COEFFICIENT FOR TWO TIME INTERVALS OF DIRECT OBSERVATIONS (THE NOVOSIL EXPERIMENTAL STATION)

Period of observations, year	1959-1974	1975-1990	1959-1990
Water storage in snow before snowmelt (mm)	101.9	105.4	104.0
Surface runoff layer (mm)	49.0	12.3	31.0
Runoff coefficient	0.46	0.14	0.3

Unfortunately the erosion rate data measured on the runoff plots during the spring snowmelts cannot be used for evaluation of soil losses, because the most intensive erosion during snowmelt takes place in hollows which dissect the cultivated slopes. According to observations in the study area, erosion intensity in hollow catchments exceeds erosion from simple straight, convex or concave slopes by a factor of 10 [5]. In addition, the runoff plot observations do not reflect the influence of slope length and slope aspect, because the length of runoff plots is smaller than the typical length of cultivated slopes. According to observations in the Russian forest-steppe zone, snowmelt soil losses vary between 0.64 and 3.2 t ha⁻¹ a⁻¹ [6]. For the forest-steppe zone only a limited number of studies are available on soil losses induced by the typical heavy rainstorms in the summer period. These studies showed that soil losses vary between 20 and 220 t ha⁻¹ for a single rainfall event.

In 1984, average annual soil erosion rates were estimated (including water erosion by snowmelt and rainfall-induced runoff) for the entire area of the Orel Region by using the modified version of the USLE (rainfall period) and the erosion model developed by the Russian State Hydrological Institute (snow-melting). The results of this study [6, 14] showed that about 40% of arable land loses more than 4 t ha⁻¹ of productive topsoil each year (Fig. 1). This topsoil is essential for sustaining the productivity of the grey-forest soils and chernozems.

In the current study three pairs of transects were selected with minimal differences in aspect, length, gradient and morphology between each pair. One transect in each pair was conventionally cultivated, while another had soil conservation measures introduced. All six transects studied generally have convex long profiles typical for this part of Central European

Russia (Fig. 4). Between pairs of slopes there are differences in aspect, length and morphology. In addition to slope aspect, major differences are found in the length of the gentle upper parts and gradients of the steeper bottom parts of slopes. The length of cultivated parts of the studied pairs of transects varies from <500 m for transects 1 and 2 through 700-750 m for transects 5 and 6 up to ca. 800 m for transects 3 and 4 (Table 4). The duration of intensive cultivation could not be established exactly. However, five out of the six transects studied are shown as arable on the State Landownership Survey maps dating back to 1784. Based on this information and the archive data stating that the major expansion of arable land before 1861 in the region occurred between 1620 and 1696 [7], the authors took a figure of 300 years as the cultivation period for transects 1-3, 5 and 6. The only exception is the transect 4, for which a 100-year period of intensive cultivation was established from comparison of topographic maps from 1861 and the early 20th century.

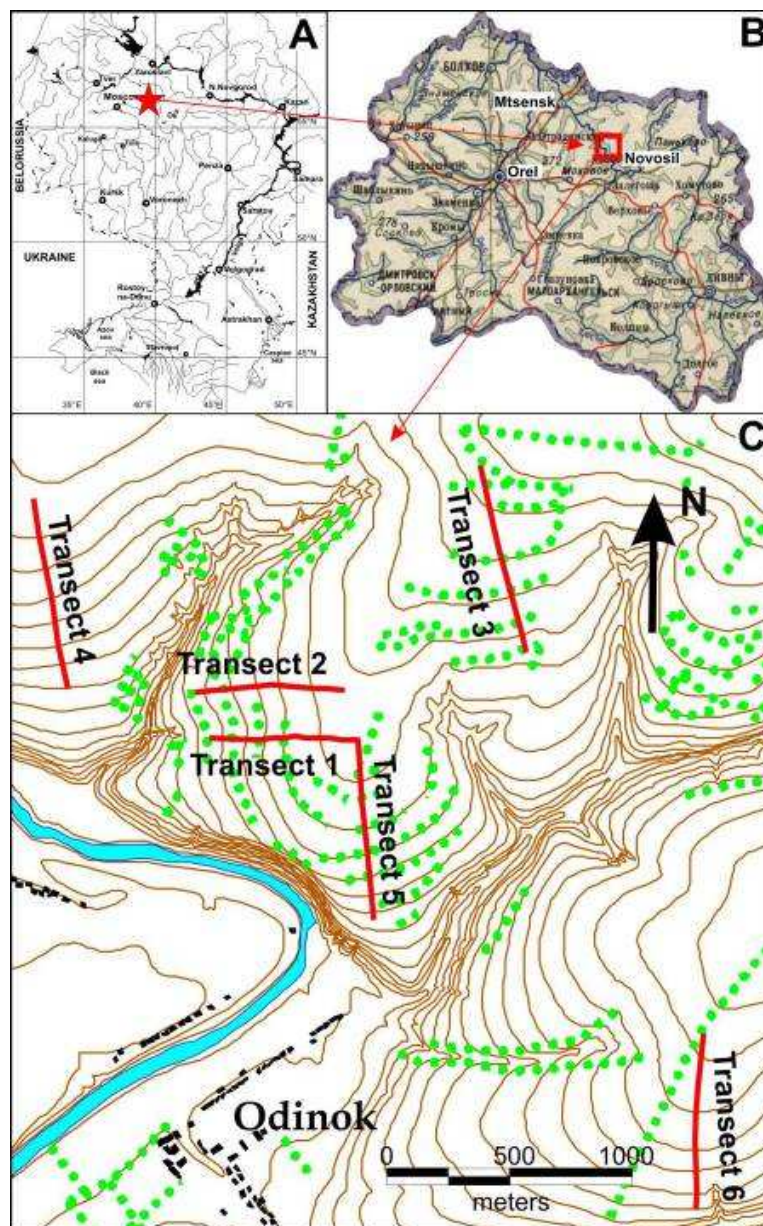


FIG. 4. Location of the case study site within European Russia (A) and the Orel Region (B), and locations of all six transects within the study area at the Novosil experimental station (C). Green dots on C designate locations of forest belts.

TABLE 4. GENERAL CHARACTERISTICS OF THE STUDIED TRANSECTS

Pairs of slopes	Transects	Documented cultivation period, years	Orientation	Relative height, m	Length, m (entire transect /upper gentle part)	Gradient, degrees (upper part/average/lower part)
1	¹⁾ Transect 1	300	west	17	460/110	0.8/2.2/3.2
	²⁾ Transect 2	300	west	18	490/100	0.8/2.2/3.2
2	¹⁾ Transect 3	300	south	25	800/230	1.0/1.7/2.3
	²⁾ Transect 4	100	south	30	770/250	1.3/2.2/3.0
3	¹⁾ Transect 5	300	southeast	31	750/280	1.0/2.3/3.7
	²⁾ Transect 6	300	southeast	28	730/300	1.0/2.2/4.3

1) Transects with contour terraces and forest belts;

2) Conventionally cultivated transects.

2.3. The ¹³⁷Cs and ²¹⁰Pb_{ex} radionuclide tracers

The ¹³⁷Cs method can in most cases be used to derive an average soil redistribution rate for the period since the commencement of the global fallout (1954 for the Northern hemisphere). However, for the Novosil experimental station it was only possible to calculate average soil redistribution rates since the Chernobyl fallout (1986), as it represents more than 90% of the total isotope amount contained in the studied soil profiles. The ¹³⁷Cs method cannot distinguish between the effects of different soil redistribution processes (mainly those including erosion by wind and water as well as tillage translocation), but gives an integrated assessment of their combined action [8]. It has also been argued that the technique is limited to sites where sheet and shallow rill erosion predominates, as development of deep rills and gullies involves redistribution of subsoil material having no ¹³⁷Cs content, in proportions increasing with depth of incision [8]. Nevertheless, it has been demonstrated that not only total soil losses, but also the relative contributions to it from different erosion processes can be obtained when ¹³⁷Cs data and other field based and modeling techniques are combined [9]. The use of ²¹⁰Pb_{ex} measurements for assessing sediment redistribution was also tested. Special attention was given to reliable determination of the initial variability of ²¹⁰Pb_{ex} fallout that allows better estimation of soil loss or deposition based on the evaluation of ²¹⁰Pb_{ex} concentrations in different soil and geomorphic units.

The field sampling for radionuclide analysis involved three phases. Firstly, 5 reference sites were selected across the study area. Depth-incremental sampling was undertaken at some of these reference sites for assessing the vertical distribution of ¹³⁷Cs and ²¹⁰Pb_{ex} (Fig 5). It was established based on the radionuclide vertical distributions that both ¹³⁷Cs and ²¹⁰Pb_{ex} are kept within the upper 30 cm of the soil profile. Secondly, 9 to 12 bulk cores were collected using an 8.0 cm diameter cylindrical metal corer from the 0-30 cm topsoil layer at each reference site. Thirdly, soil sampling was carried out along all six transects by the same corer. Two individual bulk core samples were combined for each single sampling point at the transects. Distance between the sampling points depended on slope morphology and location of forest belts.

All soil samples were subsequently dried, disaggregated and passed through a 2 mm sieve. Measurements of the ¹³⁷Cs activity of the <2 mm fraction were undertaken by gamma-ray spectrometry using an ORTEC HpGe detector. The analytical precision at the 95% level of confidence was typically ±4%. Measurements of the ²¹⁰Pb activities of the <2 mm fraction were undertaken by HPGe X-ray detector with Be window.

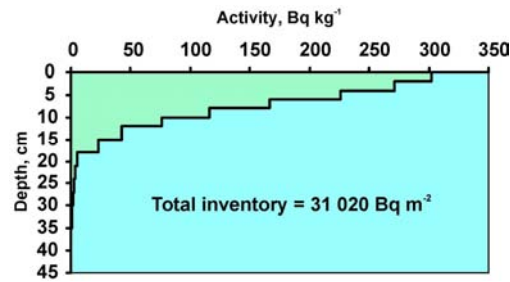


FIG. 5. Depth-incremental ^{137}Cs profile recorded for reference site 1 within the Novosil experimental station.

As the isotope fallout after the Chernobyl reactor explosion in 1986 occurred essentially as a single event, it was possible to employ less sophisticated calibration models for calculating soil redistribution rates. The proportional and simple mass balance models [10] used in this study cannot take into account temporal variability of the ^{137}Cs fallout. On the other hand, both models require only limited and easily measurable input data, such as the reference value, fallout date, plough layer depth and soil bulk density. By using these models it was possible to omit uncertainties associated with obtaining input values for the more sophisticated mass balance models [10]. The equation of the proportional model for an eroding site can be represented as:

$$Y = 10 \frac{B d X}{100 P T} \quad (1)$$

where: Y is the mean annual soil loss ($\text{t ha}^{-1} \text{a}^{-1}$); d is the depth of the plough or cultivation layer (m); B is the bulk density of soil (kg m^{-3}); X is the percentage reduction in total ^{137}Cs inventory (defined as $(A_{ref}-A)/A_{ref} \times 100$); A_{ref} is the local ^{137}Cs reference inventory (Bq m^{-2}); A is the measured total ^{137}Cs inventory at the sampling point (Bq m^{-2}); T is the time elapsed since initiation of ^{137}Cs accumulation, or, in our case, since the date of the Chernobyl fallout event (a); P is the particle size correction factor [10].

The equation of the Proportional Model for a depositional site is essentially the same, except for the introduction of the X' instead of X as the percentage increase in total ^{137}Cs inventory (defined as $(A-A_{ref})/A_{ref} \times 100$) and the use of another particle size correction factor P' [10].

Equation of the simple mass-balance model for an eroding site in the case where only the Chernobyl fallout event is considered can be expressed as follows:

$$Y = \frac{10dB}{P} \left[1 - \left(1 - \frac{X}{100} \right)^{1/(t-1986)} \right] \quad (2)$$

where: t is the year of soil sampling and other notations are the same as for the proportional model.

For a depositional site, assuming a constant deposition rate Y' ($\text{t ha}^{-1} \text{a}^{-1}$) at a point, in case when only the Chernobyl fallout event is considered, the sediment deposition rate can be estimated from the ^{137}Cs concentration of the deposited sediment $C_d(t')$ (Bq kg^{-1}) according to:

$$Y' = \frac{10}{P'} \frac{A(t) - A_{ref}}{\int_{1986}^t C_d(t') e^{-\lambda(t-t')} dt'} = \frac{10}{P'} \frac{\Delta A(t)}{\int_{1986}^t C_d(t') e^{-\lambda(t-t')} dt'} \quad (3)$$

where: $\Delta A(t)$ is the excess ^{137}Cs inventory of the sampling point over reference inventory at year t (defined as measured inventory at a point $A(t)$ less local reference inventory A_{ref}) (Bq m^{-2}), $C_d(t')$ is the ^{137}Cs concentration of deposited sediment in year t' (Bq kg^{-1}); λ is the radioactive decay constant for ^{137}Cs (a^{-1}).

2.4. Soil profile morphology comparison

This approach involves comparing the thickness and horizon composition of the upper productive topsoil in areas affected by various soil redistribution processes to that in locations where the soil profile can be regarded as undisturbed. The decrease or increase of the topsoil thickness within a cultivated field can be used to estimate the total soil loss or gain for the entire period of cultivation, although it is not possible to determine the particular process or processes responsible for that [11]. Some refinement of this approach is possible by choosing different geomorphic locations for the survey pits within a single arable field [12], for example local interfluvies and concentrated flow zones [9].

Limitations of the technique are often associated with variations in natural soil horizon thickness. However, it has been shown that in cases of severe soil losses this variation is less than that due to erosion [9]. In addition, if multiple observations from undisturbed locations are made, then natural soil variability can be described and accounted for. In our case it was not possible to find undisturbed locations for statistically sufficient number of reference soil pits. Therefore the authors used a single reference pit for each of transects comparing its detailed description with the already available information on variation of the A+AE+EB soil horizon thickness in natural settings of the general study region published by Surmach [13]. That refined information on soil profile morphology was used to compare with our observations in pits dug on arable slopes.

2.5. Empirical model

The application of the empirical model in this particular study aimed to show the comparability and possible discrepancies between regional erosion estimations commonly based on such models and detailed small scale case studies employing the field based techniques. To achieve this, model estimations of erosion were carried out along the same transects as those to which the field based techniques had been applied. The empirical model employed in this study utilizes a combination of the USLE based approach for estimating rainfall-induced erosion and the model developed in the Russian State Hydrological Institute for estimating erosion from snowmelt runoff. The model was developed by Larionov [14] especially for the application in Russia and is supported with a large spatially distributed dataset of input coefficients. Modifications from the initial USLE model include an improved set of equations for determining topographic factors [15], a novel approach calculating and mapping a rainfall erosivity index for European Russia [16], as well as adaptation of land use factors and soil protection techniques specific to the Russian agricultural system. The model yields estimates of sheet erosion rates from both rainfall- and snowmelt-generated overland flow. Data required for the model inputs include detailed topography of transects oriented along the surface runoff flow lines, local soil properties, precipitation records and land use information. The output is generated as a series of points with values of soil loss, which can

then be exported to various GIS tools for visual presentation and manipulation with other spatial data. Available information about crop rotations and their changes during the period of cultivation was collected. The most accurate data about crop rotations and cultivation practices at different arable fields of the study area were available for the last 20 years. Information about local soil properties (local distribution of soil subtypes, typical soil profile structures, texture (table 2) and humus content) was available [13]. Information obtained from detailed description of soil pits along the case study transects as well as from grain size and humus content analysis of samples was also taken into account. In addition meteorological information was collected from the nearest meteorological stations.

3. RESULTS

3.1. The ^{137}Cs reference inventories

Evaluation of the initial ^{137}Cs fallout is a key issue for using the ^{137}Cs technique. Five locations within or nearby the Novosil experimental station (Fig. 6, Table 5) were selected to establish a baseline fallout value and evaluate its possible spatial variation associated with the irregularity and single event-controlled nature of the Chernobyl fallout. The main statistical characteristics of the reference sampling sites are presented in Table 5. Firstly, levels of the ^{137}Cs contamination far exceed possible values associated with pre-Chernobyl global fallout. It was calculated that more than 90% of the total ^{137}Cs content in soil is attributed to the Chernobyl input. This value is supported by published data from other sources [17]. Secondly, the comparison of average baseline fallout inventories calculated for each of the reference sites and analysis of their relative position led us to conclusion that the initial ^{137}Cs fallout after the Chernobyl accident was characterized by an increasing trend in north-western direction. From the available data it can be approximately estimated as $7.0 \text{ Bq m}^{-2} \text{ m}^{-1}$ (Fig. 6a).

Further support of our findings regarding spatial irregularity of the Chernobyl ^{137}Cs fallout and existence of the north-west oriented increase came from the published results of the large scale program of radio-ecological monitoring from airborne detectors [17]. On the inset map (Fig. 6B) it is shown that the ^{137}Cs contamination values, its trend direction and magnitude closely correspond with the field observations of the present study. Based on this information, it was possible to calculate the so-called ‘local reference values’ for the studied transects 1-5 using average values from the examined reference sites and observed trend of increase in the northwest direction (Fig. 6A). However, the transect 6 is located outside the area where interpolation based on the reference locations is possible and, as shown by the inset map, outside the area where the north-western directed trend of ^{137}Cs Chernobyl fallout is significant (Fig. 6B; [17]). Therefore the authors took a constant reference value for that transect, with a value approximately 31700 Bq m^{-2} , based mainly on the more general spatial pattern of the isotope fallout distribution (Fig. 6B).

Based on the information presented above, it has been possible to establish statistically significant baseline fallout values with a coefficient of variation (CV) at all the reference sites of less than 20% (Table 5). The baseline fallout values are considered variable along the slopes of transects 1-5 and constant for transect 6. Those values were then used for the quantification of soil redistribution rates from the ^{137}Cs data. Local reference values with $\pm 90\%$ confidence intervals for each of the studied transects are graphically represented in Figs. 4-6. Observed variability of the isotope atmospheric input is mainly associated with the local specifics of the Chernobyl ^{137}Cs fallout, most of which occurred with a few rainfall events during the period of late April – early May, 1986 [17]. According to the available

precipitation records from the three closest meteorological stations, these rains were characterized by relatively low magnitude and intensity ($<10 \text{ mm day}^{-1}$). However, at the same time, notable differences in rainfall magnitude existed between individual observation stations. This distinctive spatial pattern of local rainfall, mainly controlled by interaction of rainfall cloud movement with local topography features [18], determined spatial distribution of the Chernobyl ^{137}Cs fallout. As shown by the established trend in Fig. 6, one of the rainfall cloud systems with relatively higher intensive rainfall (and hence ^{137}Cs deposition) passed at a few kilometers distance from the case study area. Trajectory of its central part with maximum precipitation is represented by the elongated zone of local maximum of the ^{137}Cs contamination observed on the map (Fig. 6B) between the cities of Orel and Mtsensk. Such rainfall pattern was responsible for the formation of the observed northwestern trend of the isotope fallout at the study site. At the same time, areas further to the southeast, unaffected by the main rainfall cluster, received relatively lower amounts of the isotope, with local differences mainly depending on topography features [18].

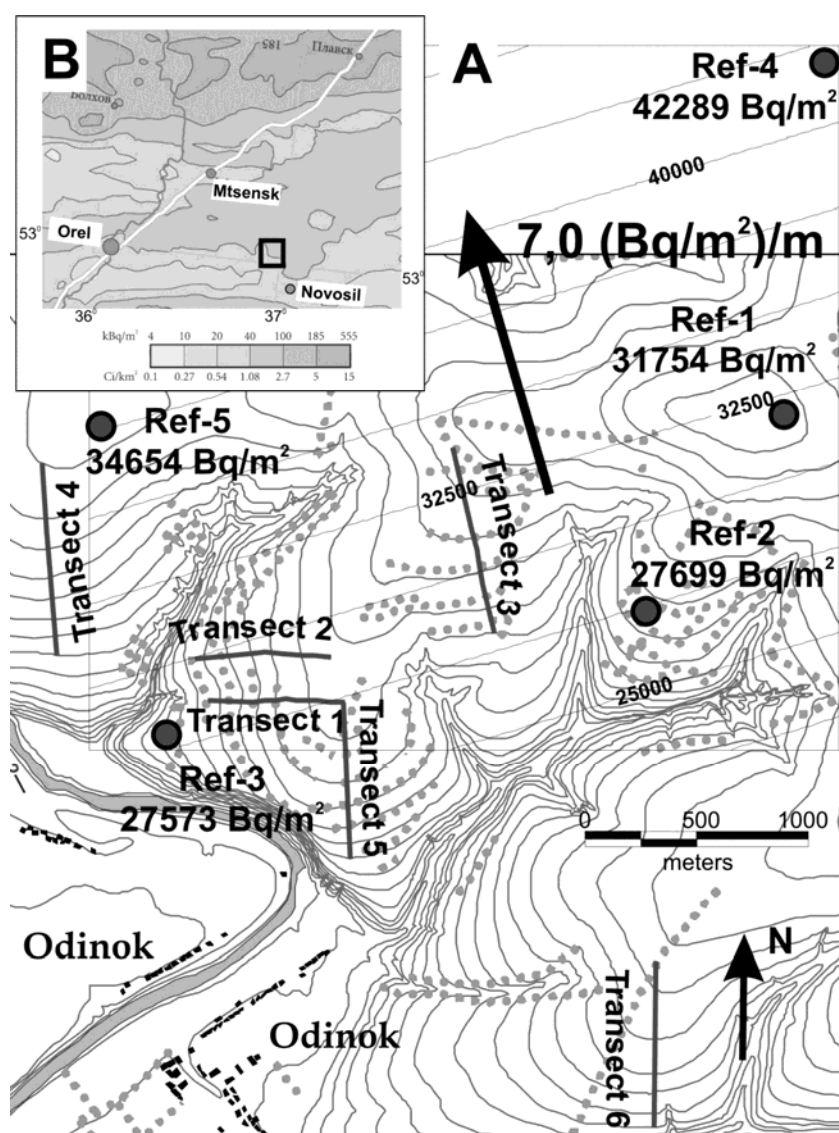


FIG. 6. The ^{137}Cs inventory spatial trend established from field data (A) and published information [17] (B).

TABLE 5. GENERAL CHARACTERISTICS AND CAESIUM-137 INVENTORY STATISTICS FOR THE REFERENCE SITES

Reference site	Land use	¹ N	The ¹³⁷ Cs inventory (Bq m ⁻²)		CV,%	² N ₀
			Range of values	Average ± 90% confidence interval		
Ref-1	Open meadow	12	30470-33038	31754±1284	9	2
Ref-2	Abandoned (>10 years) arable with tree shootings	11	18164-37128	27699±2573	19	12
Ref-3	Permanent pasture with adjacent trees	9	23209-32051	27573±1688	11	4
Ref-4	Meadow with adjacent trees	12	31696-52512	42289±3431	16	8
Ref-5	Arable	4	30175-37944	34654±1942	10	6

¹ actual number of samples taken;

² minimal numbers of samples, necessary to be taken to obtain the average value with a 90% level of confidence for a known coefficient of variation, can be calculated using the following formulae:

$$N_0 = \left[\frac{t_{(\alpha, N-1)} \times CV}{AE} \right]^2 \quad (4)$$

where: $t_{(\alpha, n-1)}$ is the inverse Student's distribution t -value with $N-1$ degrees of freedom (N – actual number of samples taken) and confidence probability α (in our case, $\alpha=1-0.9=0.1$); CV is the coefficient of variation of a sampled dataset; AE is the allowable error (in our case, $AE=0.1$).

The lowest CV was reported for the reference site 1 (Table 5). This site is the most appropriate area for determining a reference value, because it is located in a meadow on the very flat upper part of an interfluvial area. Accuracy of the calculation of soil redistribution using calibration models strongly depends on the quality of the reference value determination.

3.2. The ¹³⁷Cs inventories in soils along transects

The distributions of the ¹³⁷Cs inventories for all sampling points along the six studied transects are shown in Figs. 7-9. From comparison of the isotope topsoil content variation along the transects with the local reference values, it can be observed that generally substantial ¹³⁷Cs redistribution has taken place, even though less than 20 years have passed since the Chernobyl fallout occurred.

Considering the spatial patterns of the isotope redistribution, substantial differences are evident between the transects with and without forest belts. The latter (transects 2 and 4) are characterized by significant depletion of the ¹³⁷Cs inventories along most of the transect (Fig. 7B, 8B). Only short sections at the lower slope position of the above transects exhibit ¹³⁷Cs topsoil inventories higher than the local reference values. Thus, both distributions provide clear evidence of substantial soil losses from most of the arable slopes with limited deposition along the lower field boundaries.

The isotope inventory is slightly different along the transect 6 (Fig. 9B). At the upper slope position it is similar to the other transects without forest belts. However, the lower half of the transect is characterized by an alternation of points with ¹³⁷Cs inventories above and below the local reference value. Such spatial pattern can most likely be explained by complex micro-topography, i.e. local depressions, adjacent to the lower part of the transect. These local depressions, too small to be seen at the map scale used in Fig. 6B or transect Fig. 9B, could probably divert a substantial proportion of the overland flow off the transect line, creating 'local interfluvial' zones where only localized soil redistribution takes place. Some localized

sediment deposition may also occur at the bottom of such depressions. Another possible cause for the observed alternation in ^{137}Cs inventories is the change in land use. During most of the post-Chernobyl period two separate parcels (upper – arable, lower – meadow or pasture) were situated where now the present single arable field is located. Nevertheless, in general ^{137}Cs depletion is also significant within this transect.

By contrast, the transects with contour terraces and forest belts exhibit a much more variable spatial distribution of ^{137}Cs . The downslope change in the isotope inventories exhibit fluctuations, which seem to be largely determined by the presence of slope terraces and forest belts, though certain scatter at some points must be explained by other factors. At transect 1 (Fig. 7A) locally increased ^{137}Cs inventories are observed upslope of all forest belts (soil redeposition), though the magnitude of this increase varies substantially from place to place. Only at one sampling point a substantial gain of the ^{137}Cs inventory relatively to the local reference value is observed. More complex is the isotope distribution along transects 3 (Fig. 8A) and 5 (Fig. 9A). The transect 3 is characterized by relatively limited ^{137}Cs redistribution. The isotope inventories substantially differ from the local reference value at three out of six slope sections only (Fig. 8A). Substantial excess of the isotope inventory is observed at two sampling points located in the central or upper parts of the slope sections between forest belts. It may be explained by natural slope profile concavities prominent at these points, promoting local soil redeposition (Fig. 8A). Spatial variation of the ^{137}Cs distribution along transect 5 is also largely limited, though local increase of the isotope inventories towards the forest belts is observed at most of the slope sections (Fig. 9A). Significant increase in comparison with the local reference value is found at five points, three of which are located closely upslope of the forest belts. An opposite situation (low ^{137}Cs inventories at points immediately upslope of the forest belts), found above the 2nd and 3rd forest belts, can be explained by their improper maintenance, evidence of which (traces of runoff concentration, erosion and sediment transport along or across forest belt margins) was observed in the field.

In general, it can be concluded that forest belts and terraces have exerted significant influence on the post-fallout spatial redistribution of ^{137}Cs . Transects with these features exhibit evidences of localized isotope redistribution limited to separated slope sections, whereas conventionally cultivated transects show evidences of severe isotope losses at most sampling points. More significant ^{137}Cs redistribution at transect 1 compared to transects 3 and 5 (Figs. 7-9) can be explained by different crop rotations after 1986. The field where transects 1 and 2 are located (Fig. 1c) was mainly sown with winter and summer cereals and row crops (sugar beetroot, maize and buckwheat), whereas fields with transects 3 and 5 (Fig. 8c) were primarily used for growing permanent or annual grasses. During the last few years prior to the present study the entire field at transect 5 and lower half of transect 3 were left under permanent pasture. Therefore transect 1 has been much more vulnerable to erosion, which is well reflected by more substantial redistribution of the ^{137}Cs topsoil inventories (Figs. 7-9).

3.3. The $^{210}\text{Pb}_{\text{ex}}$ reference inventories

A detailed study of the initial fallout of $^{210}\text{Pb}_{\text{ex}}$ was conducted for different areas of the Russian Plain. The aim of the study was to evaluate the possibilities of the use of $^{210}\text{Pb}_{\text{ex}}$ for soil redistribution assessment within the Russian Plain region.

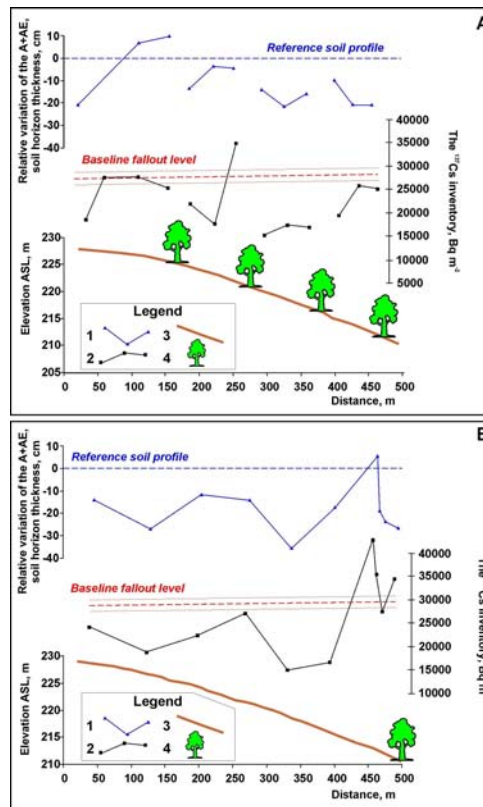


FIG. 7. Distribution of relative soil horizon (A+AE) thickness (1) and ¹³⁷Cs inventories (2) along slope transects (3) 1 (A) and 2 (B). Tree signs (4) designate forest belts.

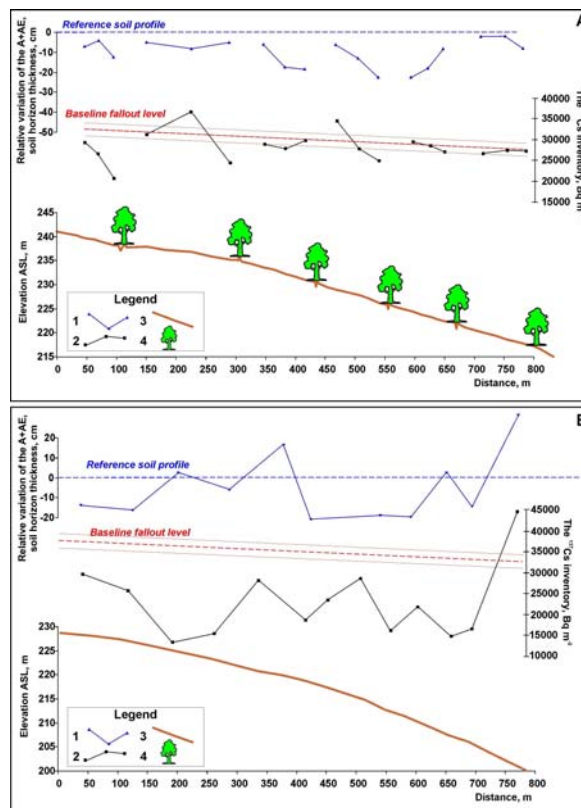


FIG. 8. Distribution of relative soil horizon (A+AE) thickness (1) and ¹³⁷Cs inventories (2) along slope transects (3) 3 (A) and 4 (B). Tree signs (4) designate forest belts.

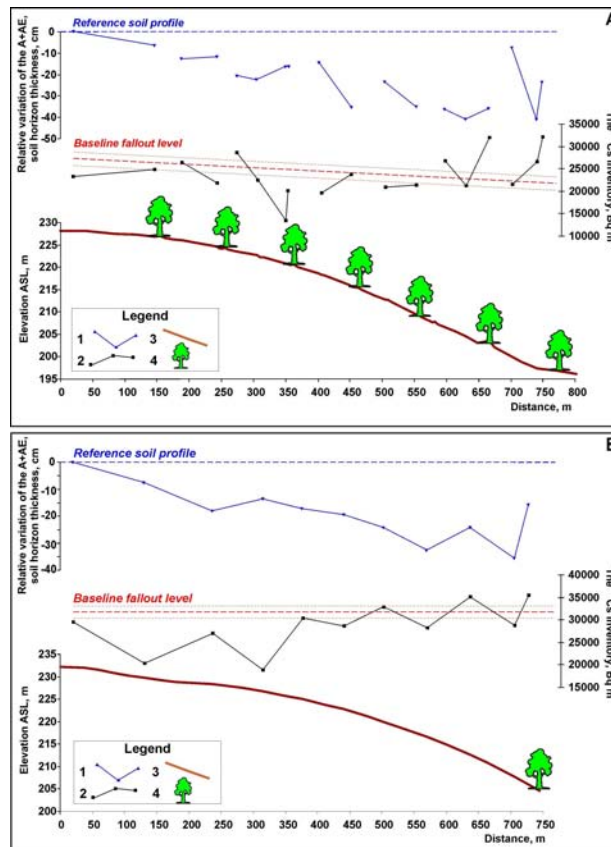


FIG. 9. Distribution of relative soil horizon (A+AE) thickness (1) and ¹³⁷Cs inventories (2) along slope transects (3) 5 (A) and 6 (B). Tree signs (4) designate forest belts.

Four locations in different landscape zones were selected to establish baseline ²¹⁰Pb_{ex} fallout values. Statistical characteristics of the reference sampling sites are presented in Table 6. The average value ranges between 3200 and 5200 Bq m⁻², which is in agreement with available data from literature [19; 20]. Similarly high variation in the reference values was reported for the adjacent locations in the Zusha River basin (Table 6). Unlike the bomb-derived ¹³⁷Cs fallout which occurred mostly during the warm period of the year, ²¹⁰Pb_{ex} fallout occurs near Moscow relatively uniformly during the year with a maximum during the winter months according to results of the ‘Radon’ monitoring company (Unpublished data). Hence, the essential part of the ²¹⁰Pb_{ex} fallout is observed during the cold period of the year and is therefore kept in the snow until the spring snowmelt. Therefore it is very likely that part of the ²¹⁰Pb_{ex} fallout is washed out with snowmelt surface runoff before it is absorbed by the soil particles. This happens in the open areas rather than under forests, because of differences in soil freeze depth and surface runoff intensity.

The variation of initial ²¹⁰Pb_{ex} fallout is relatively high as compared to ¹³⁷Cs fallout (Table 5 and 6). Only one reference site, located within an abandoned cultivated field surrounded by forest belts, is characterized by relatively uniform ²¹⁰Pb_{ex} fallout. Other researches also found relatively high variability of ²¹⁰Pb_{ex} fallout changing within the range 26-45% [19,20]. Therefore it is only possible to assess soil loss based on ²¹⁰Pb_{ex} inventories for each morphological unit separately. In addition, each morphological unit should have a separate reference value and be characterized by several samples to address the inherent variability.

TABLE 6. GENERAL CHARACTERISTICS AND EXCESS LEAD-210 INVENTORY STATISTICS FOR THE REFERENCE SITES LOCATED IN DIFFERENT LANDSCAPE ZONES OF THE RUSSIAN PLAIN REGION

Area	Landscape zone	Unsupported ²¹⁰ Pb inventory		CV,%
		Mean, Bq m ⁻²	Range, Bq m ⁻²	
Timiryazevskiy park, Northern part of Moscow, open area within park	Forest	3515	1724-5116	32
Podgozhee, Tula region, cultivated field	Forest	5179	1712-7320	30
The Zusha River basin, Orel region, meadow	Forest-steppe	3873	2344-6518	39
The Zusha River basin, Orel region, abandoned field with shrubs	Forest-steppe	4978	3972-7280	17
The Vorozba River basin, Kursk region, cultivated field	Forest-steppe	3202	1460-5871	38
The Kalaus River basin, Stavropol region, pasture	Steppe	3340	1980-4700	41

3.4. Soil redistribution within transects

3.4.1. Average annual soil redistribution rates calculated from the ¹³⁷Cs data

From the analysis of the ¹³⁷Cs inventory values and depth distributions in undisturbed locations and their comparison with published data [17] it was established that the Chernobyl fallout represents more than 90% of the total ¹³⁷Cs loading in soil. Therefore the authors decided to regard the global isotope fallout as negligible and concentrate on assessing average soil redistribution rates since 1986, when the Chernobyl accident happened. This allowed us to assume that the isotope fallout took place as a single event. This assumption is valid for the majority of territories that experienced serious Chernobyl ¹³⁷Cs contamination. As stated above, the available precipitation data from the three neighboring meteorological stations suggest that in 1986 there were only two to four low-intensity rains from late April until early May during a few successive days. Therefore, for this case study the assumption of the Chernobyl ¹³⁷Cs fallout as a single event is reliable. In addition, it can be assumed that no overland flow and subsequent ¹³⁷Cs redistribution prior to its absorption by the clay minerals of the soil particles could have been associated with such low-intensity rainfall event.

Average annual soil redistribution rates at the sampled locations calculated by the proportional and simple mass balance models are shown for all six analyzed transects in figures 10-12. The calculated gross and net soil redistribution rates for the entire transects are summarized in Table 7 together with the extent of the erosion and deposition zones. As stated above, these values are applicable for the period since the Chernobyl fallout (April 1986) only.

The values obtained for most of the sampled locations indicate very intensive soil redistribution over the last 20 years (Table 7). When converting the above values to gross erosion rates (erosion is recalculated for the entire transect without accounting for within slope redeposition) and net erosion rates (gross within-slope redeposition is subtracted from

gross erosion) differences between transects with and without soil-protective measures become more obvious (Table 7).

The spatial pattern of erosion and deposition calculated from ^{137}Cs data (Fig. 10-12) obviously resembles that of the isotope inventory (Figs. 6-8). Nevertheless, it must be noted that, even for transects with forest belts, the extent of deposition is very limited (Fig. 10-12). It can be suggested that significant sediment redeposition should have occurred within the forest belts and especially in runoff-intercepting retention ditches. However, soil sampling in these locations was not carried out because of time and labor limitations. Therefore, the authors have assumed in calculating net erosion rates that neither erosion nor deposition took place within forest belts and regarded them as stable slope sections. This assumption is obviously not realistic because a substantial proportion of sediment eroded upslope should have been trapped within these forest belts. Hence, our calculations of net erosion rates (Table 7) for entire transects with forest belts give us overestimated values. Implications of this fact for the final conclusions will be discussed below.

TABLE 7. GROSS AND NET SOIL REDISTRIBUTION RATES CALCULATED FOR THE STUDIED TRANSECTS BASED ON CAESIUM-137 DATA (UPPER FIGURES – PROPORTIONAL MODEL, LOWER FIGURES – MASS BALANCE MODEL)

Pairs of slopes	Transects	Length of erosion zones (m/%)	Average annual erosion within zones ($\text{t ha}^{-1} \text{a}^{-1}$)	Gross erosion ($\text{t ha}^{-1} \text{a}^{-1}$)	Length of deposition zones (m/%)	Average annual deposition within zones ($\text{t ha}^{-1} \text{a}^{-1}$)	Gross deposition ($\text{t ha}^{-1} \text{a}^{-1}$)	Net erosion ($\text{t ha}^{-1} \text{a}^{-1}$)
1	1) Transect 1	320	62.5	43.5	80	20.6	3.6	39.9
		/69.6	75.9	52.8	/17.4	23.5	4.1	48.7
	2) Transect 2	460	58.5	54.9	30	61.0	3.7	51.2
		/93.9	72.0	67.6	/6.1	72.8	4.5	63.1
2	1) Transect 3	590	19.3	14.2	60	24.9	1.9	12.3
		/73.8	21.4	15.8	/7.5	26.7	2.0	13.8
	2) Transect 4	740	61.7	59.3	30	62.3	2.4	56.9
		/96.1	82.1	78.9	/3.9	79.8	3.1	75.8
3	1) Transect 5	590	30.1	23.7	80	47.3	5.0	18.7
		/78.7	34.3	27.0	/10.7	49.4	5.3	21.7
	2) Transect 6	630	30.9	26.7	100	15.9	2.2	24.5
		/86.3	36.0	31.1	/13.7	16.9	2.3	28.8

1) Transects with contour terraces and forest belts.

2) Conventionally cultivated transects.

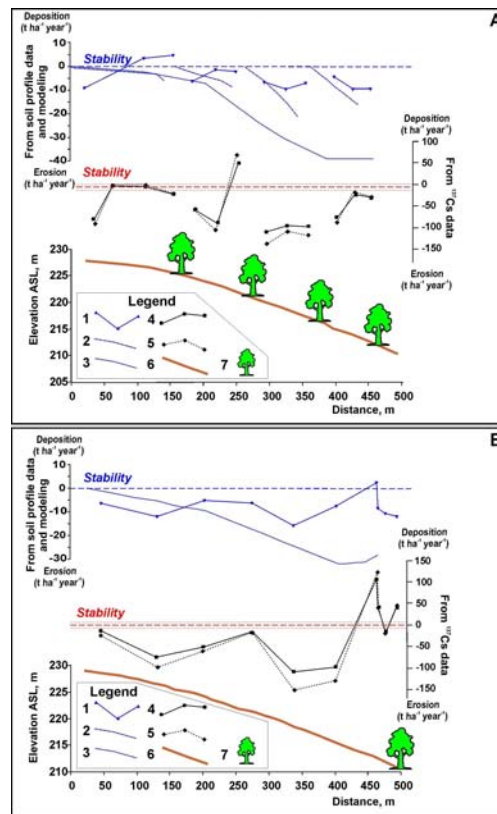


FIG. 10. Results of soil redistribution rate calculations by soil profile comparison (1), empirical model with (2) and without (3) forest belts, ^{137}Cs proportional (4) and simple mass-balance (5) models for slope transects (6) 1 (A) and 2 (B). Tree signs (7) designate forest belts.

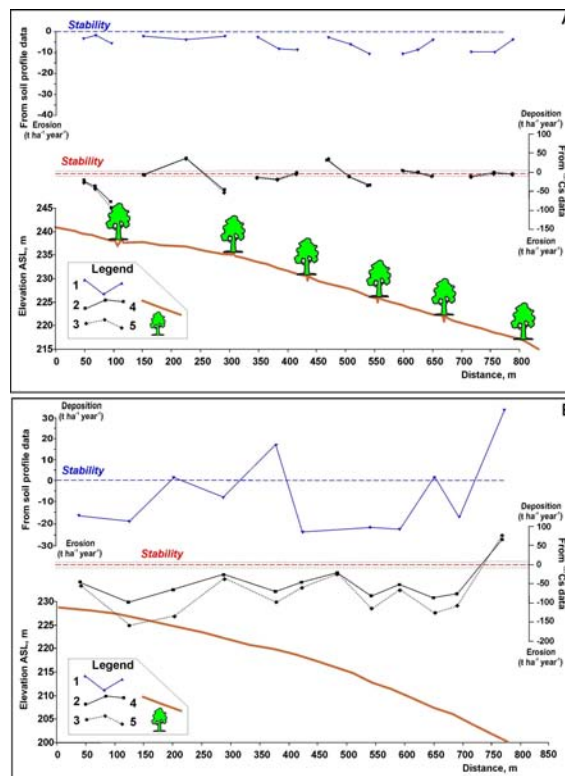


FIG. 11. Results of soil redistribution rate calculations by soil profile comparison (1), ^{137}Cs proportional (2) and simple mass-balance (3) models for slope transects (4) 3 (A) and 4 (B). Tree signs (5) designate forest belts.

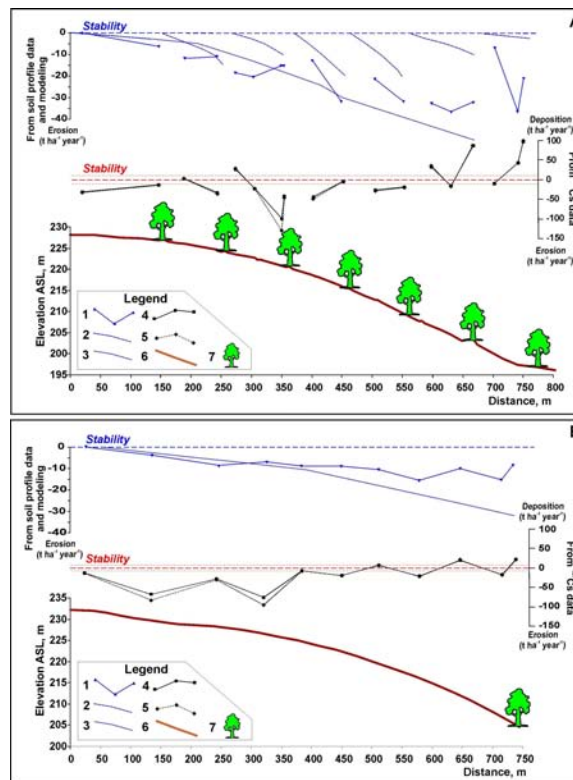


FIG. 12. Results of soil redistribution rate calculations by soil profile comparison (1), empirical model with (2) and without (3) forest belts, ^{137}Cs proportional (4) and simple mass-balance (5) models for slope transects (6) 5 (A) and 6 (B). Tree signs (7) designate forest belts.

3.4.2. Selection of the reference soil profiles

As mentioned above, it was not possible to find undisturbed locations for a statistically sufficient number of reference soil pits within the study area. Therefore, the authors used a single reference pit for each of the studied transects and compared it with the available information on the variation of the A+AE soil horizon thickness in natural settings of the general study region published by Surmach [13].

The typical profile of the uneroded arable *Grey forest soil (Phaeozem)* at interfluvial landscape positions consists of the following characteristic soil horizons: Ap (plough horizon with an average thickness of 27-30 cm, brownish-grey); AE (transitional horizon with an average thickness of about 15 cm, characterized by generally darker colour, very distinctive structure with sharp edges and abundant pale silica skeletons); EB (upper transitional part of illuvial horizon with an average thickness of about 30 cm, characteristic mottling due to presence of abundant humus cutanes, and non-uniform presence of pale silica skeletons); B (non-carbonate illuvial horizon to a depth of 180-190 cm); at 190 cm depth (on average) soil profile is underlain by pale yellow loessy loam with high carbonate content (C horizon). This information was evaluated by analyzing a large number of soil profiles at undisturbed locations from within the area of grey forest soils [13]. Important morphological characteristic of soil horizons AE and EB, which are diagnostic for the grey forest soil type, can be visually determined in a soil section even when partly eroded or incorporated into a plough layer.

The authors used this information to identify soil profiles at the upper slope positions of the studied transects, which were meant to be used as reference baseline for comparison with soil

profiles at disturbed locations. It was found that all four soil profiles used as reference (soil profile at the top of the transect 5 was used as reference for transects 1, 2 and 5 because those are located close to each other) have the characteristic horizon thickness very close to the average figures provided by Surmach [13]. It has been concluded that the available reference soil profiles provide reliable baseline data for estimations of soil redistribution rates according to the soil profile comparison method.

3.4.3. Soil profile characteristics of the studied transects

The results of the soil profile description along the six studied transects are graphically represented in Figs. 7-9. These graphs demonstrate a relative decrease or increase of the A+AE soil horizon thickness as compared with the reference soil profile characteristics selected for each particular transect. Soil survey pits were in most cases located at the same points where ^{137}Cs samples were taken, thus allowing direct comparison of the resulting spatial patterns.

Just as with the ^{137}Cs inventories, substantial differences in soil profile structure were observed comparing transects with and without forest belts. The former were characterized by relatively more frequent fluctuations of soil horizon thickness, resulting from direct influence of soil conservation measures. The latter were characterized by more gradual variation of soil horizon thickness, mainly controlled by slope morphology and the associated pattern of soil redistribution. Sampling locations where soil profile accretion was reported, are rare, suggesting that soil degradation remains the long term tendency of soil development for all studied transects, and that the cumulative effect of soil conservation measures on soil thickness still remains lower than the effect of severe soil degradation prior to tree planting.

3.4.5. Average annual soil redistribution rates calculated from the soil profile comparison

In the present calculation of soil redistribution rates, based on soil profile data, the authors compared the total thickness of the A+AE soil horizons of the reference soil profiles with the thickness of the observation points along the studied transects. The duration of intensive cultivation was assumed to be 300 years for all transects except transect 4, for which a duration of 100 years was estimated (Table 4). This assumption was based on analyses of available maps and historical sources for different periods of time (earliest information dated back to 1695). Soil bulk density values needed for the transition from layer of soil loss/gain to mass per unit area figures were taken from analysis of the ^{137}Cs soil samples, which were taken with corers up to a depth of 30 cm. The results of the quantitative assessment of soil redistribution rates obtained by the soil profile comparison method are graphically represented in Figures 8-10. The estimated gross and net soil redistribution rates for each of the studied transects are summarized in Table 8.

In contrast to the ^{137}Cs method, the soil-morphological method yielded relatively moderate values of soil redistribution rates ($4.7\text{-}9.7 \text{ t ha}^{-1} \text{ a}^{-1}$), which were almost identical to general regional averages ($4.5 \text{ t ha}^{-1} \text{ a}^{-1}$; [6]). The only exception is the transect 4, which experienced significant soil loss ($14.7 \text{ t ha}^{-1} \text{ a}^{-1}$) over relatively short period of time. The main explanation for such moderate values is the longer timeframe of the technique, as it integrates the changes in soil thickness by soil redistribution over a period of 300 years. In reality, during this long period of 300 years there were probably relatively short time spans with severe soil redistribution (caused by different factors such as initial clearance of natural vegetation, 1861 landownership reform, collectivization in 1930s, individual extreme events) alternated with longer periods of less intensive soil redistribution.

TABLE 8. GROSS AND NET SOIL REDISTRIBUTION RATES CALCULATED FOR THE STUDIED TRANSECTS FROM SOIL PROFILE MORPHOLOGY COMPARISON DATA

Pairs of slopes	Transects	Length of erosion zones (m/%)	Average annual erosion within zones ($t\ ha^{-1}\ a^{-1}$)	Gross erosion ($t\ ha^{-1}\ a^{-1}$)	Length of deposition zones (m/%)	Average annual deposition within zones ($t\ ha^{-1}\ a^{-1}$)	Gross deposition ($t\ ha^{-1}\ a^{-1}$)	Net erosion ($t\ ha^{-1}\ a^{-1}$)
1	¹⁾ Transect 1	350 /76.1	6.7	5.1	50 /10.9	3.8	0.4	4.7
	²⁾ Transect 2	470 /95.9	9.4	9.0	20 /4.1	2.5	0.1	8.9
2	¹⁾ Transect 3	650 /81.3	5.7	4.7	0 /0	0	0	4.7
	²⁾ Transect 4	680 /88.3	18.5	16.3	90 /11.7	13.3	1.6	14.7
3	¹⁾ Transect 5	670 /89.3	10.6	9.4	0 /0	0	0	9.4
	²⁾ Transect 6	730 /100.0	8.5	8.5	0 /0	0	0	8.5

- 1) Transects with contour terraces and forest belts;
2) Conventionally cultivated transects.

For the transects with forest belts the situation is even more complex. As it was mentioned above, those steep slopes selected for constructing contour terraces and planting forest belts were initially characterized by the highest degree of soil degradation. Nevertheless, after less than 80 years under soil conservation, two to three times lower average soil redistribution rates are reported from direct evaluation of the soil profiles on transects 1 and 3 as compared with transects 2 and 4 (table 8). The exception of the third pair of slopes can be explained by the above-mentioned severe erosion at the transect 5 prior to tree planting, where the entire productive topsoil layer was lost at the lower slope position [2]. More time will be required for the soil conservation measures to have a quantitatively distinctive effect on transect 5 soil cover or thickness. Nevertheless, soil profile descriptions on that transect have already shown that productive topsoil layer is now (after 80 years of forest belts) at least partly recovered at all parts of the slope, indicating the effect of soil conservation measures.

3.4.6. Application of $^{210}Pb_{ex}$ fallout for the evaluation of soil redistribution

The authors decided not to use calibration models for the transformation of the $^{210}Pb_{ex}$ fallout concentration into soil loss/gain values because of the high initial variation of $^{210}Pb_{ex}$ fallout (Table 4). However the authors compared relative values of ^{137}Cs and $^{210}Pb_{ex}$ loss or gain for two slope pairs. It was expected that relative values should demonstrate a similar pattern along the slope for both radionuclides because of the similar nature of their redistribution processes. In general it is possible to conclude that trends of inventory changes along each transect are similar for both radionuclides (Figs. 13-16). This is in particular true for transect 6 (Fig. 16). On the other hand, essential differences between both types of radionuclides were found in the lower part of transect 2 (Fig. 14). However, it is difficult to explain the reason of this discrepancy. At the same time, $^{210}Pb_{ex}$ values usually show the deposition prior to

planting of forest belts more clearly as compared with ^{137}Cs (Fig.13, 15), because $^{210}\text{Pb}_{\text{ex}}$ allows estimating mean erosion and deposition rates for a longer period of time (ca. 100-150 years) [19,20] than ^{137}Cs (ca. 50 years for the global fallout and ca. 20 years for the Chernobyl fallout) [8,10]. Hence it is possible to conclude that $^{210}\text{Pb}_{\text{ex}}$ can be used as tracer for evaluation of soil loss/gain from arable lands, but it is better to have several samples within one morphological unit for receiving more precise absolute values.

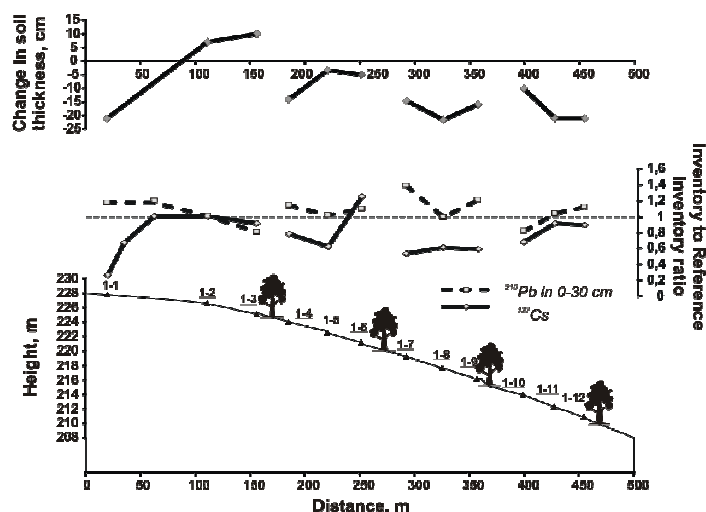


FIG. 13. Relationship between relative radionuclide inventories (^{137}Cs and ^{210}Pb) in sampling locations and reference sites for Transect 1. Tree symbols designate locations of forest belts.

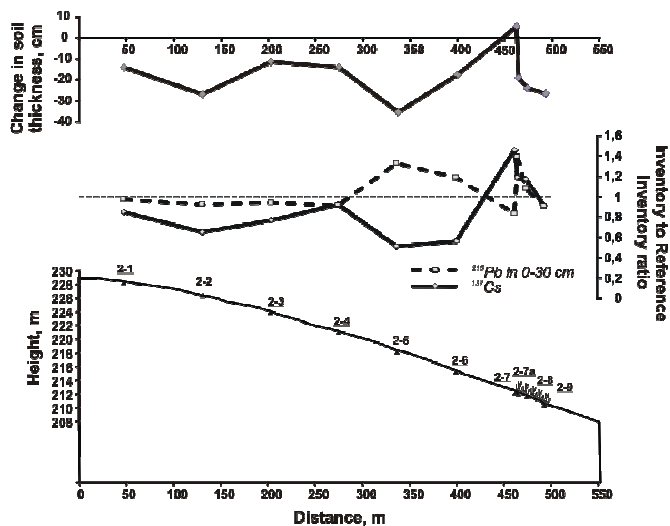


FIG. 14. Relationship between relative radionuclide inventories (^{137}Cs and ^{210}Pb) in sampling locations and reference sites for the Transect 2.

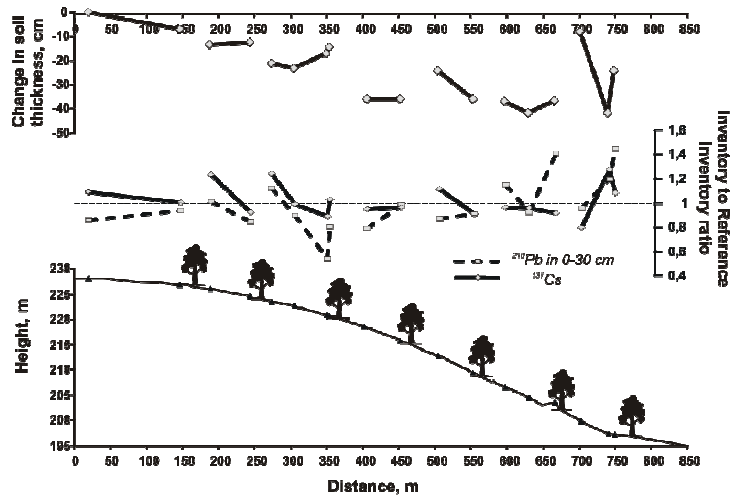


FIG. 15. Relationship between relative radionuclide inventories (^{137}Cs and ^{210}Pb) in sampling locations and reference sites for the Transect 5. Tree symbols designate locations of forest belts.

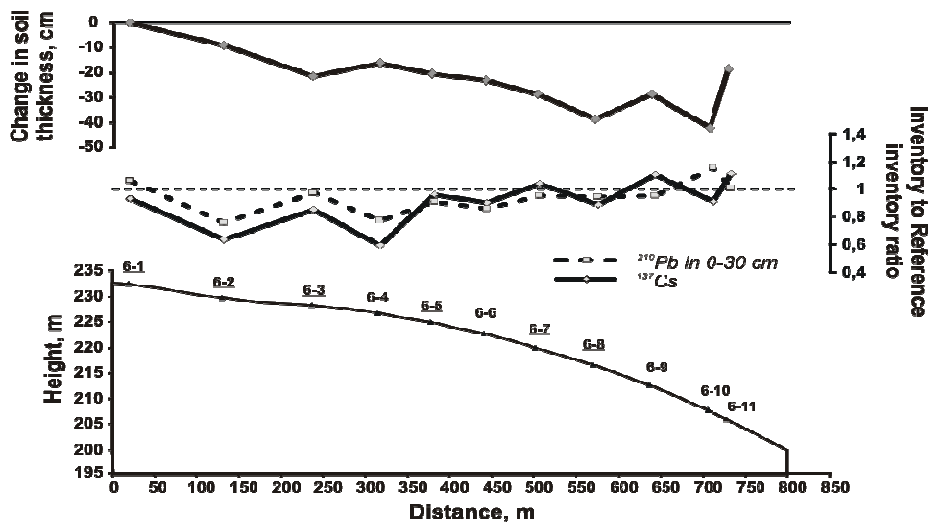


FIG. 16. Relationship between relative radionuclide inventories (^{137}Cs and ^{210}Pb) in sampling locations and reference sites for the Transect 6. Tree symbols designate locations of forest belts.

4. DISCUSSION

The results of the present study have shown that slopes with soil-protective measures are characterized by a substantial reduction of average soil redistribution rates, as shown by soil-morphological and ^{137}Cs methods (Table 9). The maximum relative decrease of average net erosion rate was reported for the transects 3 and 4 (more than 80% by the ^{137}Cs method and up to 70% by the soil-morphological method). Intermediate values were observed for the transects 1 and 2 (about 50% by the soil-morphological method and about 25% by the ^{137}Cs method). For the transects 5 and 6 the ^{137}Cs method also showed approximately a reduction by 25% of the net soil loss rate, but the soil-morphological method gave a figure of about 10% more soil degradation for the transect 5 with forest belts (Table 9). This can be explained by the above-mentioned fact that the transect 5 is located on the slope that was most severely

eroded prior to introduction of soil-protective measures. It is known that all productive topsoil layers were lost from the lower third of that slope [2], its surface was a 'badland' with large rills and ephemeral gullies. Therefore, the present state of the soil profile thickness, along the transect 5, although substantially improved and partly recovered, still reflects effects of that severe degradation. A substantially longer period (assuming the appropriate maintenance of the soil conservation measures) will be required for the complete recovery of the soil profile.

The reasonably good coincidence of the spatial soil redistribution pattern provided by the soil-morphological and ^{137}Cs methods (Fig. 10-12) suggests generally good reliability of the obtained results. However, at the same time, large discrepancies in soil redistribution rates obtained by the two field based methods require more detailed consideration. Soil redistribution rates estimated by the ^{137}Cs method are extremely high if compared with the typical average values for the general study region ($4.5 \text{ t ha}^{-1} \text{ a}^{-1}$; [6]), while soil-morphological method and empirical model provide more comparable results. The most extreme soil redistribution rates are yielded by the ^{137}Cs method for the studied transects 1, 2 and 4 (Table 9). However, even relatively low values for transects 3 and 5 (Table 9) seem to be overestimated if one takes into account the fact that both fields after the year 1986 have been mainly used for growing annual or perennial grasses. As very low soil redistribution rates are normally expected for fields under such crop rotations, values of net erosion rates obtained by ^{137}Cs method for these two transects may roughly represent a range of overestimation by this method in our case.

With regards to the reasons for such a substantial degree of overestimation, two main explanations can be proposed. First of all, extremely high soil redistribution rates yielded by the ^{137}Cs method for many sampling points can be attributed to possible influence of individual extreme runoff events on ^{137}Cs redistribution prior to soil mixing by tillage operation. It is known from the available precipitation data that 5-10 rainfall events, potentially able to generate overland flow ($>10 \text{ mm}$), took place during the summer period of the year 1986. Especially heavy rainstorm was reported on August 26 (25-35 mm at different meteorological stations). At that time, the fields of transects 1 and 2 were sown partly with maize and partly with barley, while the fields of transect 4 was used partly for oats, and partly left under bare fallow. Very severe erosion could have occurred on these slopes, along transect 4 because of the presence of fields under bare fallow, and transects 1 and 2, as maize and barley at site of those transects were likely already harvested to the date when the rainstorm occurred. If this was the case, substantial proportion of the Chernobyl ^{137}Cs fallout could have been eroded from the topsoil before its incorporation into the plough layer, as the isotope initially has an exponential depth distribution with peak located at the soil surface [8]. The authors believe that this erosion event (or a few events) in 1986 unaccounted for by calibration models is the most reasonable explanation for overestimating soil redistribution rates obtained from the ^{137}Cs data.

On the other hand, certain increase of soil redistribution rates during the last 20 years might indeed have taken place as a result of general economic disorder after the collapse of the socialistic economy system. Until now, the Novosil experimental station does not receive funding for the maintenance of the different soil conservation measures, such as the contour terraces, forest belts or soil-protective crop rotations (the station director A.I. Petelko, personal communication). As a result, the runoff-intercepting potential of the forest belts decreased at some places. In the field the authors observed flow retention ditches which cannot trap any more runoff at transect 1, as they are completely filled with sediments, forest belts partly devoid of trees, ephemeral gullies cutting across contour terraces, and traces of runoff and erosion along forest belts at transect 5. The authors also found similar increase of

erosion rates over the post-Soviet period resulting from general lack of funding for soil conservation measures at other case study sites in different regions within European Russia [1]. However, the magnitude of that increase in these case studies was certainly much lower (in a range of 10-20%) as compared with the magnitude of excess of ^{137}Cs -estimated net erosion rates over those obtained by soil-morphological method at the present case study (Table 9).

TABLE 9. COMPARISON OF SOIL REDISTRIBUTION RATES CALCULATED FOR THE STUDIED TRANSECTS BY DIFFERENT TECHNIQUES

Pairs of slopes	Transects	Soil redistribution rates ($\text{t ha}^{-1} \text{a}^{-1}$) (gross erosion/gross deposition/net erosion)		³⁾ Potential soil loss estimated by empirical model ($\text{t ha}^{-1} \text{a}^{-1}$)
		^{137}Cs (proportional model)	Soil profile morphology	Without forest belts With forest belts
1	1) Transect 1	^{137}Cs (simple mass balance model)		
		43.5/3.6/39.9	5.1/0.4/4.7	23.9
	2) Transect 2	52.8/4.1/48.7		6.0
		54.9/3.7/51.2	9.0/0.1/8.9	19.9
		67.6/4.5/63.1		-
2	1) Transect 3	14.2/1.9/12.3	4.7/0.0/4.7	24.0
		15.8/2.0/13.8		9.2
	2) Transect 4	59.3/2.4/56.9	16.3/1.6/14.7	21.6
		78.9/3.1/75.8		-
3	1) Transect 5	23.7/5.0/18.7	9.4/0.0/9.4	25.9
		27.0/5.3/21.7		6.8
	2) Transect 6	26.7/2.2/24.5	8.5/0.0/8.5	20.5
		31.1/2.3/28.8		-

¹⁾ Transects with contour terraces and forest belts;

²⁾ Conventionally cultivated transects.

A more significant decrease of average soil degradation rates on slopes with soil conservation measures (60-75%) was predicted by the empirical model (Table 9, 10) based on calculations along the same transects as discussed above (section 2.5). It is important to notice for comparison with the other techniques that the erosion model calculates only potential rates of gross erosion, without accounting for any within-slope redeposition (Table 10). It is obvious from comparison of the model estimates with the field based method results (Table 9, 10) that the real observed effectiveness of soil conservation measures is lower than the potential one. As discussed above, this can be explained firstly by insufficient time for a complete soil recovery passed since the terrace construction and forest belts planting, and secondly by improper maintenance of the terraces and forest belts because of a lack of funding since 1991.

5. CONCLUSIONS

At the Novosil research station in the Orel Region of Central European Russia experimental soil conservation measures have been applied now for about 70-80 years. The use of radionuclide techniques for assessing redistribution rates confirmed that the applied conservation measures (contour terraces with forest belts and retention ditches for runoff interception) were effective in decreasing erosion (20-80%). This result was also supported by conventional research methods, such as the empirical based erosion model calculation and the soil morphological method.

TABLE 10. PERCENTAGE DIFFERENCE OF SOIL REDISTRIBUTION RATES BETWEEN TRANSECTS WITHOUT AND WITH FOREST BELTS WITHIN EACH PAIR OF TRANSECTS CALCULATED BY DIFFERENT TECHNIQUES

Transects	¹³⁷ Cs technique		Soil profile morphology		Empirical model
	Gross erosion	Net Erosion	Gross erosion	Net Erosion	Gross erosion
2-1	21-22%	22-23%	43%	47%	75%
4-3	76-80%	78-82%	71%	68%	62%
6-5	11-13%	24-25%	-11%	-11%	74%

However the radionuclide techniques seem to overestimate actual erosion rates on all of the six studied transects. It is very likely that this overestimation is the result of the influence of extreme erosion prior to tillage mixing of a fresh fallout isotope in 1986. Therefore there is a need for more research on the possible influence of high-magnitude erosion events prior to homogenization of the vertical ¹³⁷Cs distribution in the plough layer by tillage mixing.

Based on the detailed study of ¹³⁷Cs initial fallout inventory spatial distribution, it was found that local scale variability of Chernobyl-derived ¹³⁷Cs fallout (within individual reference sites) is relatively low, but its larger scale change (between neighboring reference sites) is significant. This spatial trend was determined by the selection of several reference locations around the study area and taken into account when estimating relative ¹³⁷Cs gain/loss at individual points and transforming it into soil redistribution rates using calibration models.

However, ²¹⁰Pb_{ex} fallout within the case study area is characterized by substantially higher local variability (17-39%) than that of the ¹³⁷Cs (9-16%). That poses an essential limitation for ²¹⁰Pb_{ex} application for soil redistribution calculations. Nevertheless, it was found out that variations of ¹³⁷Cs and ²¹⁰Pb_{ex} relative inventories along the study transects followed the similar pattern in most parts of the studied transects. Results generally support the conclusion that ²¹⁰Pb_{ex} can potentially be employed for quantification of soil redistribution rates on cultivated slopes. However, more research is needed to evaluate quantitatively contributions of various factors influencing its initial fallout variability, determine sufficient number of reference sites and sampling points, establish the most suitable and effective approaches for selecting locations and density of sampling points within different agricultural landscape units.

ACKNOWLEDGEMENTS

This research work has been made possible by the financial support of the Russian Foundation for Basic Research (RFBR grant no. 04-05-64215) and the International Atomic Energy Agency grant (RUS /12329). Authors gratefully acknowledge the cooperation of the Novosil experimental station director A.I Petelko in providing access to the study sites, research information and consultations. Assistance of a number of the Moscow State University researchers and students involved in fieldwork activities is gratefully acknowledged.

REFERENCES

- [1] SIDORCHUK, A.Yu. et al., "European Russia and Belarus", Soil erosion in Europe, (J. BOARDMAN, POESEN, J., Eds), J. Wiley & Sons, Chichester (2006) 95-106.
- [2] KOZMENKO, A.S., Basics of soil conservation melioration, Kolos Publ., Moscow (1954) 232 p. (in Russian).
- [3] PRONIN, V.V., Development of erosion processes in Orel region, Nauchnye Trudy VNIIZ **59** (1973) 78-85 (in Russian).
- [4] BARABANOV, A.T., Agro- and forest melioration for soil conservation agriculture, VNIALMI, Volgograd (1993) 156 p. (in Russian).
- [5] LITVIN, L.F. et al., Monitoring of soil erosion during snow-melting in the Central Non-chernozem zone, Eroziya pochv i ruslovye processy **11** (1998) 57-76(in Russian).
- [6] LITVIN, L.F., Geography of soil erosion on Russian agricultural lands, Akademkniga Publ., Moscow (2002) 256 p. (in Russian).
- [7] TSVETKOV, M.A., Changes of forested area in European Russia from the end of 18 century since 1914, Publishing House AN SSSR, Moscow **213** (1957) 213 p. (in Russian).
- [8] WALLING, D.E., QUINE, T.A., Calibration of caesium-137 measurements to provide quantitative erosion rate data, Land Degrad. Rehabil. **2** (1990) 161-175.
- [9] BELYAEV, V.R., et al., A comparison of methods for evaluating soil redistribution in the severely eroded Stavropol region, southern European Russia, Geomorphology **65** (2005) 173-193.
- [10] WALLING, D.E., HE, Q., Improved models for estimating soil erosion rates from cesium-137 measurements, J. Environ. Qual. **28** (1999) 611-622.
- [11] LARIONOV, G.A., et. al., Determination of slope wash rates by the method of paired soil pits descriptions, Soil Erosion and Channel Processes, **3** (1973) 162-167 (in Russian).
- [12] KIRYUKHINA, Z.P., SERKOVA, YU.V., Podsolich soils morphometric characteristics variability and the diagnostics of soil erosion, Soil Erosion and Channel Processes, **12**, (2000) 63-70 (in Russian).
- [13] SURMACH, G.P., Soil and erosion investigations on Srednerusskaya vozvyshehnost', Sel'skokhozyastvennaya eroziya i bor'ba s nei, Publishing House AN SSSR, Moscow (1956) 71-80 (in Russian).
- [14] LARIONOV, G.A., Soil erosion and deflation, Moscow University Publ., Moscow (1993) 200 p. (in Russian).
- [15] LARIONOV, G.A., et. al., Theoretical-empirical equation of topography factor for a statistical model of soil erosion by water, Soil Erosion and Channel Processes, **11** (1998) 25-44 (in Russian).
- [16] KRASNOV, S.F. et. al., Spatial and temporal aspects of the rainfall erosivity evaluation, Soil Erosion and Channel Processes, **13** (2001) 8-17(in Russian).
- [17] Atlas of caesium deposition for the European part of Russia, Belorussia and the Ukraine (IZRAEL, YU. A., ed), Rosgidromet, Roskartografiya **142** (1998) 142 p. (in Russian).
- [18] ISAEV, A.A., Atmospheric precipitation, Part 2, Mezostructure of rainfall spatial pattern, MSU Publ., Moscow (2002) (in Russian) 100 p.
- [19] WALLING, D.E., et. al., Use of caesium-137 and lead-210 as tracers in soil erosion investigations, International Association of Hydrological Sciences Publication N°. **229** (1995) 163-172.
- [20] WALLING, D.E., et. al., Using unsupported lead-210 measurements to investigate soil erosion and sediment delivery in a small Zambian catchment, Geomorphology **52** (2003) 193-213.

ESTIMATES OF LONG AND SHORT TERM SOIL EROSION RATES ON FARMLAND IN SEMI-ARID WEST MOROCCO USING CAESIUM-137, EXCESS LEAD-210 AND BERYLLIUM-7 MEASUREMENTS

M. BENMANSOUR, A. NOUIRA, A. BENKIDAD, M. IBN MAJAH
Centre National de l'Energie, des Sciences et des Techniques Nucléaires,
Rabat, Morocco

H. BOUKSIRAT, M. EL OUMRI, R. MOSSADEK
Institut National de Recherche Agronomique,
Rabat, Morocco

M. DUCHEMIN
Institut de Recherche et de Développement en Agroenvironnement,
Quebec, Canada

Abstract

The aim of the present work was to investigate both long and short term soil erosion and deposition rates on agricultural land in Morocco and to assess the effectiveness of soil conservation techniques by the combined use of environmental radionuclides (^{137}Cs , excess ^{210}Pb and ^7Be) as tracers. The study area is an experimental station located in Marchouch 68 km from Rabat (western part of Morocco). Experimental plots have been installed in the study field to test the no-till practice under cereals as a soil conservation technique, and comparing it to the conventional tillage system. Fallout ^{137}Cs and $^{210}\text{Pb}_{\text{ex}}$ allowed a retrospective assessment of long term (50 and 100 yrs respectively) soil redistribution rates while fallout ^7Be with a short half-life (53 days) was used to document short term soil erosion associated with short rainfall events for different tillage systems and land uses. From ^{137}Cs and $^{210}\text{Pb}_{\text{ex}}$ measurements the rates of soil redistribution induced by water erosion were quantified by using the Mass Balance 2 model. The net soil erosion rates obtained were $14.3 \text{ t ha}^{-1} \text{ a}^{-1}$ and $12.1 \text{ t ha}^{-1} \text{ a}^{-1}$ for ^{137}Cs and $^{210}\text{Pb}_{\text{ex}}$ respectively resulting in a high sediment delivery ratio of about 92%. Data on soil redistribution generated by the use of both radionuclides are similar, indicating that the soil erosion rate did not change significantly during the last 100 years. In addition, the soil redistribution rates due to tillage were estimated using the Mass Balance 3 model. The global results obtained from ^7Be measurements during the period 2004-2007 suggest that the soil loss is reduced by up to 30% when no-till management is practised when compared to the conventional tillage or uncultivated soil.

1. INTRODUCTION

Agriculture plays a major economic and social role in Morocco. The sector employs about half of the active population and contributes to 17% of the GDP. However, land degradation due to accelerated soil erosion undermines the sustainability of the agricultural sector. In addition to the specific natural conditions of Morocco, inadequate agricultural intensification accentuates this phenomenon. More than 15 million hectares of agricultural land are under serious threat. It has been estimated that 100 million tons of soil are annually lost [1]. On the other hand, the decrease of the capacity of reservoirs caused by sedimentation is estimated at about 50 million m^3 each year.

Despite the severity of land degradation in Morocco, there are still only limited datasets available about the actual state of water and wind erosion and other related problems such as stoniness, desertification, salinity and soil compaction. Reliable information about soil erosion over several spatial and time scales is essential in order to evaluate the severity of the

phenomenon and to develop soil conservation strategies and sustainable crop production. In addition, the majority of the previous studies focused on the use of experimental plots or the empirical RUSLE equation to estimate water soil erosion. However, environmental radionuclides such as caesium-137 (^{137}Cs), excess lead-210 ($^{210}\text{Pb}_{\text{ex}}$) and Beryllium-7 (^7Be) constitute an excellent tool for soil erosion studies and possess many advantages compared to the traditional methods like experimental runoff plots or empirical erosion modelling.

The ^{137}Cs technique was extensively and successfully applied in several regions of the world [2-7]. In Morocco, the potential of the use of ^{137}Cs technique was demonstrated [8-12]. The main studies were carried out in watersheds located at the north, in the Atlas mountain range, and the west of Morocco. Measured soil erosion rates ranged between 6 and 70 t ha⁻¹ a⁻¹ with generally high soil erosion rates in the north. Nevertheless some constraints in the use of the ^{137}Cs technique were identified depending on the local conditions and concerned particularly the difficulty to identify appropriate reference sites, the stoniness and heterogeneity of the study soils and the complex geomorphology in some cases.

In contrast to the ^{137}Cs technique, studies reporting the use of excess or unsupported ^{210}Pb ($^{210}\text{Pb}_{\text{ex}}$) and particularly ^7Be as natural tracers for soil erosion assessment are still scarce [13-16], therefore these techniques require further development. Fallout ^{210}Pb has been particularly applied to establish the chronology of deposited sedimentation [17-19], whereas the use of ^7Be has shown to be suitable to understand short term erosion processes, linked with rainfall events, and to assess the efficiency of soil conservation measures [15,16].

The objectives of this work carried out in the capacity of FAO/IAEA CRP D1.50.08 project on 'Assess the Effectiveness of Soil Conservation Techniques for Sustainable Watershed Management Using Fallout Radionuclides' were:

- To examine the potential of the combined use of environmental radionuclides (^{137}Cs , ^{210}Pb , ^7Be) to investigate both long and short term rates of soil erosion in agricultural fields in Morocco,
- To better evaluate the efficiency of no-till management used as a soil conservation method.

One experimental pilot site located 68 km from Rabat in the western part of Morocco, with a semi-arid climate was selected to undertake the study.

2. MATERIALS AND METHODS

2.1. ^{137}Cs , $^{210}\text{Pb}_{\text{ex}}$ and ^7Be as tracers

Over the past 30 years the potential for using natural and anthropogenic radionuclides to study erosion and sedimentation has drawn much attention. ^{137}Cs , the most common radionuclide in such studies, is an artificial radionuclide with a half-life of 30.1 years produced by the atmospheric testing of thermonuclear weapons during the 1950s and 1960s, while ^{210}Pb and ^7Be are naturally occurring radionuclides, with a half-life of 22.3 years and 53.1 days respectively. ^{210}Pb is derived from the decay of gaseous ^{222}Rn , a daughter of ^{226}Ra . Decay of ^{222}Rn produces ^{210}Pb in the atmosphere, so that the subsequent fallout of ^{210}Pb to the

landscape surface provides an input of this radionuclide (termed excess $^{210}\text{Pb} - ^{210}\text{Pb}_{\text{ex}}$) which is not in equilibrium with its parents ^{226}Ra , and can serve as tracer of soil. ^7Be is a 'cosmogenic' radionuclide produced by the bombardment of the atmosphere by cosmic rays. All these radionuclides are rapidly and strongly adsorbed at the soil surface upon their deposition with precipitation. Under these conditions subsequent redistribution of ^{137}Cs , ^{210}Pb and ^7Be reflects the movement of the soil. Estimates of erosion or deposition rates can be provided by the measurement of loss or gain in the radionuclide inventory relative to the local reference level that represents the radionuclide amount at a stable site. Appropriate models allow converting radionuclide activities to erosion or deposition rates. ^{137}Cs and ^{210}Pb measurements provide estimates of long term (~ 45 years and 100 years respectively) soil redistribution rates. The technique based on the measurement of excess ^{210}Pb with half-life of 22 years may be used in regions where the ^{137}Cs level is low, such as in the Southern Hemisphere, and those regions affected by the Chernobyl accident. ^7Be with its short half-life of 53 days appears to be an interesting tracer to document short term soil erosion on agricultural land associated with individual rainfall events.

2.2. Study area

The study area is an agricultural field of about one hectare located in Marchouch (6°42' W, 33° 47' N) 68 km south east from Rabat. This site belongs to one of the experimental stations of the 'Institut National de Recherche Agronomique' (INRA). The mean annual precipitation at the site is 405 mm, of which about 50% falls from December to March. The mean monthly temperature ranges from 10 to 23°C. The altitude is about 350 to 400 m a.s.l. Agriculture is one of the main land uses and covers 84% of the total area of Marchouch. The soil texture is predominantly clay, 46%, with 28% sand and 26% silt. The organic matter is about 2.5% in the first ten centimetres of soil. The mean slope gradient and the length of the experimental plot are 17% and 100 m respectively. A general view of the experimental site is given in Fig. 1.



FIG. 1. Experimental site (Marchouch station).

In 2004 experimental plots have been installed at the Marchouch study site along a transect from the upper to lower slope position. On the plots cultivated with wheat in rotation with lentils the no-till practice has been used as a soil conservation measure and compared to cultivated plots under conventional tillage. Each treatment has been replicated three times in the field. In addition, uncultivated plots under bare fallow were also monitored. The

comparison between these three treatments was carried out in 2004 and 2005. In 2006, the fields of the study site were not cultivated, while in 2007, conventional tillage was practiced again.

In the study area highly erosive rainfall and high soil temperature accelerate the loss of soil organic matter and hence reduce the soil fertility and thus crop productivity. Furthermore, the erosion phenomenon is accentuated in the study area by unsustainable agricultural practices, increasing the pace of the gradual impoverishment of the arable layer. Improvement of the agricultural productivity under such conditions requires the use of appropriate soil conservation methods, which also enhances the water availability for the crops.

The essential objective of this study was the determination of a production system which ensures agronomic and economic viability. The no-till practice appears to be a good method for soil and water conservation. The non-disturbance of the soil-atmosphere interface allows control of the infiltration and evaporation of water. No-till also minimizes erosion because crop seeds are planted directly through the crop residue layer and the soil surface is permanently covered by mulch left from the previous crop. In addition the soil organic matter increases, improving soil structure.

2.3. Field sampling

Two sampling campaigns were carried out in 2003 and 2004 in order to estimate long term soil erosion and deposition rates in the study site using ^{137}Cs and excess ^{210}Pb . A transect approach was adopted, which consists of a sequence of samples along the line with the steepest slope from the top to the bottom of the studied field. In total 50 samples were collected along 5 parallel transects using a motorized cylindrical tube (diameter of ca. 9 cm) or the so-called Column Cylinder Auger (Fig.2.a), which was inserted to a depth of 30-40 cm to ensure that all ^{137}Cs or ^{210}Pb was measured. Bulk soil cores were collected for measuring the ^{137}Cs and ^{210}Pb inventories, but also incremental samples were collected at 1 to 2 cm depth intervals to obtain the vertical distributions of ^{137}Cs and ^{210}Pb . One reference site (undisturbed field) had been identified located at 3 km from the study area, and both bulk and sectioned soil cores were collected at this site.

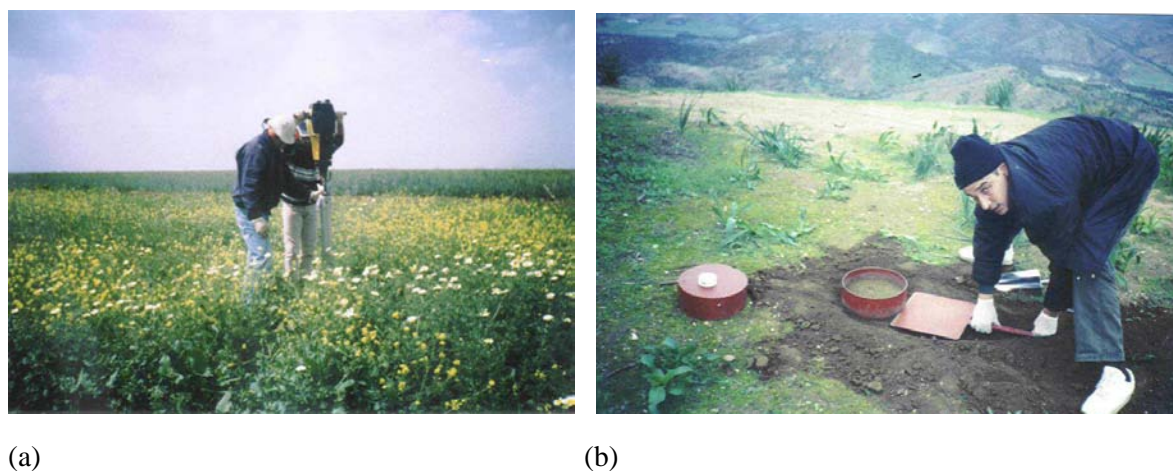


FIG. 2. Sample collection by (a) a motorized tube or so-called Column Cylinder Auger for fallout ^{137}Cs and ^{210}Pb and (b) a surface collector for fallout ^7Be .

For the use of ^7Be as a tracer to document rates of soil erosion associated with short rainfall events, four sampling campaigns were conducted from 2004 to 2007: i.e. one campaign per year at the end March or early April, at the end of the Mediterranean winter season with heavy rainfall.

As ^7Be is only found in the immediate surface layer due to its short half-life, soil cores of 3 cm depth were collected along the experimental plots to measure ^7Be inventories (Fig. 2.b) using a cylindrical tube (diameter of 15 cm). Incremental soil samples were also taken. Collection of very thin sections of soil is required (0-3 mm) for fallout ^7Be . Around 50 samples were collected each year. Two reference sites were used for ^7Be . The first one is the same as the site used for ^{137}Cs and $^{210}\text{Pb}_{\text{ex}}$. The second site without any slope gradient was selected near to the cultivated study field. As ^7Be has a short half-life, the past land use is of no importance, as long it was not disturbed during the experiments, In addition, precipitation samples were collected in the period of December until March in order to measure ^7Be inventories in the rainwater.

2.4. Laboratory analysis

All soil samples were dried, lightly ground, sieved (< 2 mm) and homogenised prior to the measurement of ^{137}Cs , ^{210}Pb , ^{226}Ra (from ^{214}Bi) and ^7Be by gamma spectrometry using HPGe detectors. Two high resolution coaxial detectors (Canberra p-type 30% and Oxford n-type 50%) were used for the measurements. The calibration of the detection systems was done by preparing standards from a certified multi-gamma source (Amersham) and IAEA reference materials (IAEA 327, IAEA 375). Generally, samples were placed in Marinelli bakers (0.5 L) or cylindrical containers (200 mL). ^{137}Cs , ^7Be , ^{210}Pb and ^{214}Bi activities were determined from the net peak areas of gamma rays at 662, 478 and 46.5 keV respectively. The counting rates varied from 12 to 24 hours providing a precision of about 5 to 20% at 95% level of confidence. The detection limits reached in these experimental conditions were 0.5, 5 and 0.7 Bq kg⁻¹ for ^{137}Cs , ^7Be , ^{210}Pb respectively. The short half-life of ^7Be combined with low ^7Be inventories required measurement of the activity as soon as possible. On the other hand, indirect determination of excess ^{210}Pb activity from total ^{210}Pb and ^{226}Ra gave a low precision with regards to the activity value (30 to 50%). To improve precision of ^{210}Pb activity, measurements by alpha spectrometry through ^{210}Po , daughter of ^{210}Pb , was performed for some soil samples. The method requires a total digestion of soil samples containing ^{210}Pb , ^{210}Po and tracer ^{209}Po , using acids (HNO_3 , HCl , and HF) and spontaneous deposition of polonium isotopes in silver discs. The counting is carried out by using silicon detectors (EG&G Ortec). The alpha spectrometry provides a good precision for measuring ^{210}Pb but needs more time as compared to gamma spectrometry. Quality control procedures were applied using control charts (efficiency, resolution and background), certified reference materials and regular participation in inter-comparison exercises and proficiency tests organised by IAEA.

2.5. Fallout Radionuclides conversion models and RUSLE 2 model

The refined mass balance 2 model (MB2) [20] has been used for estimating long term rates of water-induced soil erosion (50 and 100 years for ^{137}Cs and $^{210}\text{Pb}_{\text{ex}}$ respectively). This model can be expressed as follows:

$$d(A)/dt = (1-\Gamma) I(t) - (\lambda + (P R/d)) A(t) \quad (1)$$

where: $A(t)$ is the ^{137}Cs ($^{210}\text{Pb}_{\text{ex}}$) inventories (Bq m^{-2}); t is the time since the onset of ^{137}Cs ($^{210}\text{Pb}_{\text{ex}}$) fallout (a); R is the soil erosion rate ($\text{kg m}^{-2} \text{a}^{-1}$); d is the cumulative mass depth representing the average plough depth (kg m^{-2}); λ is the decay constant for ^{137}Cs ($^{210}\text{Pb}_{\text{ex}}$) (a^{-1}); $I(t)$ is the annual deposition flux at time t ($\text{Bq m}^{-2} \text{a}^{-1}$); Γ is the proportion of the freshly deposited ^{137}Cs ($^{210}\text{Pb}_{\text{ex}}$) removed by erosion before being mixed into the plough layer; P is the particle size factor.

For ^{137}Cs , the annual flux $I(t)$ is expressed as [5,20]:

$$I(t) = I_n A_{\text{ref}}/A_n$$

where :

I_n is a hypothetical record of annual ^{137}Cs deposition flux for a site in the northern hemisphere based on the record of ^{137}Cs deposition to the northern hemisphere ($\text{Bq m}^{-2} \text{a}^{-1}$);

A_n (Bq m^{-2}) is the current inventory for the hypothetical ^{137}Cs fallout record;

A_{ref} (Bq m^{-2}) is the ^{137}Cs reference inventory for the study site;

For $^{210}\text{Pb}_{\text{ex}}$, the annual flux is expressed as $I(t) = \lambda A_{\text{ref}}$ [13];

Γ is expressed as $\Gamma = p \gamma (1 - e^{-R/H})$ where γ is the proportion of the annual ^{137}Cs input susceptible to removal by erosion and H (kg m^{-2}) is the relaxation mass depth of the initial distribution of fallout ^{137}Cs in the soil profile.

The application of the mass balance 3 model (MB3) [21,22] permitted an estimate of the tillage effect. This model is based on ^{137}Cs measurements carried out along slope transects parallel to the down-slope direction of the water flow. It is based on the following equation:

$$d(A)/dt = (1-\Gamma) I(t) + R_{t,\text{in}} C_{t,\text{in}}(t) - R_{t,\text{out}} C_{t,\text{out}}(t) - R_{w,\text{out}} C_{w,\text{out}}(t) - \lambda A(t) \quad (2)$$

where:

$R_{t,\text{in}}$ and $R_{t,\text{out}}$ ($\text{kg m}^{-2} \text{a}^{-1}$) are the soil redistribution rates associated with the tillage input and tillage output at the study point. Thus they represent the rates of soil loss and soil gain at this point due to tillage and are expressed as follows:

$$R_{t,\text{in}} = \phi \sin \beta_i / L_i \text{ and } R_{t,\text{out}} = \phi \sin \beta_{i-1} / L_i$$

where ϕ is a constant related to the tillage practice used; β_i and β_{i-1} are slope angles of the i^{th} and $(i-1)^{\text{th}}$ segments and L_i (m) is the slope length of the i^{th} segment.

In equation (2) $R_{w,\text{out}}$ represents the rate of soil loss produced by water erosion, and $C_{t,\text{in}}$, $C_{t,\text{out}}$, and $C_{w,\text{out}}$ (Bq kg^{-1}) are the ^{137}Cs concentrations of the sediment associated with tillage input, tillage output and water output.

The net erosion rate R is:

$$R = R_{t,\text{out}} - R_{t,\text{in}} + R_{w,\text{out}} \quad (3)$$

More details on equations (1) and (2), as well as those corresponding to the points at which deposition has occurred and the determination of the parameters corresponding to MB2 and MB3 models are reported in references [5,20,21,22].

The conversion model used to quantify soil erosion rates from ^7Be measurements is based on the exploitation of the ^7Be concentration profile [23]. The decline of ^7Be concentration with depth can be described by an exponential function:

$$C(x) = C(0) e^{-x/h_0} \quad (4)$$

where: x (kg m^{-2}) is the mass depth from soil surface, $C(0)$ (Bq kg^{-1}) is the initial concentration of ^7Be and h_0 (kg m^{-2}) is the relaxation mass depth profile.

The use of radionuclide based methodologies allowed the assessment of results obtained by empirical prediction models. The RUSLE [24] model using the RUSLE 2 [25] software was applied to estimate rates of water-induced soil erosion in the study field. This empirical model is based on the following equation:

$$A = R K L S C P \quad (5)$$

where: A represents the potential, long term average annual soil loss in tonnes per hectare per year; R is the rainfall factor; K is the soil erodibility factor; L and S are the slope length and steepness factors, respectively; C is the cropping-management factor; P is the support practice factor.

3. RESULTS AND DISCUSSIONS

3.1. Long term soil erosion rates using ^{137}Cs and $^{210}\text{Pb}_{\text{ex}}$

3.1.1. Vertical distribution and inventories

Figure 3 shows the depth distribution of ^{137}Cs and $^{210}\text{Pb}_{\text{ex}}$ concentrations associated with the reference site. Most of ^{137}Cs and $^{210}\text{Pb}_{\text{ex}}$ were being contained in the top 10 cm and concentrations decreased, as expected, exponentially with depth. The ^{137}Cs concentration in the reference site was the highest at the surface (0-3 cm) with a value about 13 Bq kg^{-1} while the $^{210}\text{Pb}_{\text{ex}}$ concentration at the soil surface in the reference site was about 25 Bq kg^{-1} . The patterns of the vertical distributions associated with both radionuclides are similar. However, one minor difference was observed: a bioturbation processes which produce near-constant ^{137}Cs concentration in the upper 4 cm. This result can be explained by the origin of the ^{137}Cs fallout which ceased in the 1970s. In contrast, the continuous inputs of $^{210}\text{Pb}_{\text{ex}}$ have maintained a layer of maximum activity at the surface. For the cultivated site, concentrations are almost uniform throughout the plough layer ($\sim 16 \text{ cm}$) as a result of mixing caused by cultivation (Fig. 4). The concentrations derived from all explored points of the cultivated field ranged between 1.9 and 5.9 Bq kg^{-1} and between 2.2 and 16.7 Bq kg^{-1} for ^{137}Cs and $^{210}\text{Pb}_{\text{ex}}$ respectively. Similar forms of ^{137}Cs profiles were generally observed in other regions of the world in a variety of environments as reported by Walling and Quine [4]. Concerning the $^{210}\text{Pb}_{\text{ex}}$, the observed profiles were comparable to those obtained in other studies [26,27].

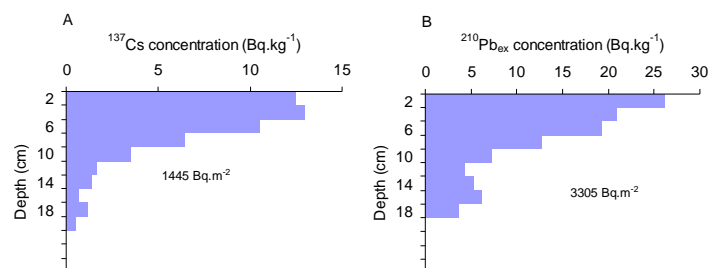


FIG. 3. Vertical distribution of ^{137}Cs (A) and $^{210}\text{Pb}_{\text{ex}}$ (B) associated with the reference site.

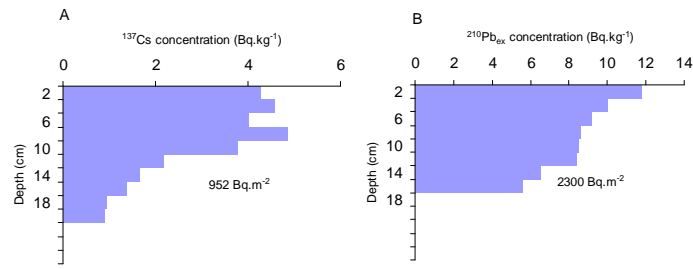


FIG. 4. Vertical distribution of ^{137}Cs (A) and $^{210}\text{Pb}_{\text{ex}}$ (B) associated with the cultivated site.

The ^{137}Cs inventories were measured on the study field along five parallel transects. The values were found to range between 600 and 1900 Bq m^{-2} . For the undisturbed site near to the study field representing the reference inventory the mean ^{137}Cs obtained from 12 soil cores was estimated to be 1445 Bq m^{-2} with a standard deviation of 18%. As observed elsewhere [28], the variability in ^{137}Cs inventories at the reference site has several sources; random spatial variability, systematic spatial variability, sampling variability and measurement precision. The reference inventory of the present study appears to be within the expected range based on previous studies on soil erosion in Morocco using the ^{137}Cs technique and the correlation between mean annual precipitation and ^{137}Cs reference values [9-12,29]. The ^{137}Cs activities of the soil cores collected in the cultivated field were generally lower than the reference inventory, particularly those of the upslope area, indicating the loss of soil. In contrast, high ^{137}Cs inventories were observed generally around the down slope boundaries, indicating soil deposition. Illustration of the observed patterns along the five studied transects is given in figure 5.A.

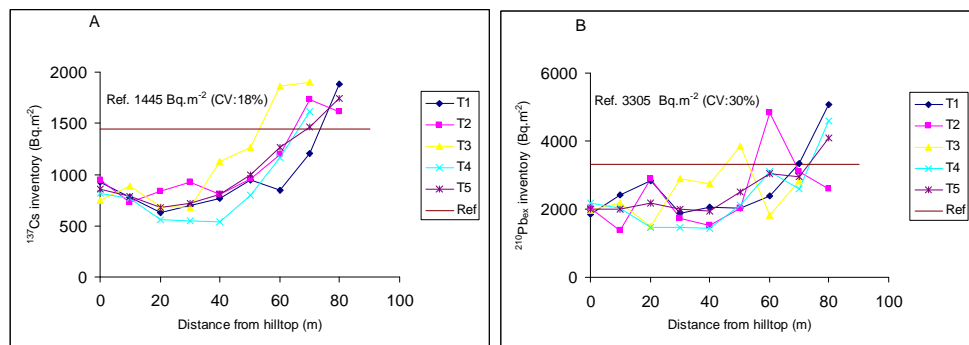


FIG. 5. Distribution of ^{137}Cs (A) and $^{210}\text{Pb}_{\text{ex}}$ (B) inventories along the studied transects.

For fallout $^{210}\text{Pb}_{\text{ex}}$, the reference inventory was found to be 3305 Bq m^{-2} with 30% of standard deviation. $^{210}\text{Pb}_{\text{ex}}$ inventories obtained along the transects in the study field ranged between 1700 and 5000 Bq m^{-2} . This variation is shown in Fig. 5.B representing the redistribution of $^{210}\text{Pb}_{\text{ex}}$ inventories.

As in the case of ^{137}Cs , erosion could be observed at the upslope boundary while deposition was found at the down slope boundary. However the lateral variation of $^{210}\text{Pb}_{\text{ex}}$ inventories appeared to be more important than that of ^{137}Cs . These fluctuations observed for $^{210}\text{Pb}_{\text{ex}}$ are due to the poor precision accompanied with $^{210}\text{Pb}_{\text{ex}}$ measurements.

3.1.2. Assessment of soil redistribution rates

From the ^{137}Cs measurements the rates of water-induced soil erosion were estimated by using the mass balance 2 model. The values of the mass balance 2 model parameters based on local

conditions were selected as follows: ^{137}Cs : $\gamma = 0.6$, $H = 4.0 \text{ kg m}^{-2}$, $d = 217 \text{ kg m}^{-2}$, $A_{\text{ref}} = 1445 \text{ Bq m}^{-2}$, $p = p' = 1$ ^{210}Pb : $\gamma = 0.6$, $H = 4.0 \text{ kg m}^{-2}$, $d = 217 \text{ kg m}^{-2}$, $A_{\text{ref}} = 3305 \text{ Bq m}^{-2}$, $p = p' = 1$.

The global results (for all transects) indicated that the erosion rates in the study field ranged between 4 and 30 $\text{t ha}^{-1} \text{ a}^{-1}$. The eroding zones in the upslope part of the field represented 70% of the total area, soil deposition occurred at the lower slope position on the remaining 30% of the area. The mean and gross erosion rates were estimated to be 17.9 and 15.4 $\text{t ha}^{-1} \text{ a}^{-1}$ respectively, and the mean and gross deposition rates were 6.3 and 1.2 $\text{t ha}^{-1} \text{ a}^{-1}$ respectively. The net soil loss was about 14.3 $\text{t ha}^{-1} \text{ a}^{-1}$ resulting in a sediment delivery ratio of 92%. Data on soil erosion and deposition rates derived from the $^{210}\text{Pb}_{\text{ex}}$ approach were found comparable to those obtained by ^{137}Cs . Gross erosion and deposition rates were about 12.9 $\text{t ha}^{-1} \text{ a}^{-1}$ and 0.8 $\text{t ha}^{-1} \text{ a}^{-1}$ respectively. The net erosion rate was estimated to be 12.1 $\text{t ha}^{-1} \text{ a}^{-1}$ and the sediment delivery ratio was 93%.

The ^{137}Cs technique provided more reliable results due to its good precision with regards to the activity measurement compared to $^{210}\text{Pb}_{\text{ex}}$. Taking into account the errors provided by the two techniques (^{137}Cs and $^{210}\text{Pb}_{\text{ex}}$), the overall data related to soil redistribution rates over 45 years (for ^{137}Cs) and 100 years (for $^{210}\text{Pb}_{\text{ex}}$) seem to be similar and indicate that the soil erosion rate did not change drastically during the last decades.

Such relatively high soil erosion rates obtained for the study field are most likely the result of the steep topography, the clay-rich soil and the heavy rainfall during the winter season without major vegetative cover, but also the unsustainable agricultural practices used in the past. Comparable erosion rates, ranging between 5 and 16 $\text{t ha}^{-1} \text{ a}^{-1}$, were obtained in areas in Northern Morocco with similar characteristics as the study field using the same methodology (^{137}Cs technique) [9].

To include the impact of tillage erosion, erosion rates were also estimated using the mass balance 3 (MB3) model with the same parameters as for the run of MB2 model. The table 1 shows that the total gross erosion and deposition rates were about 22.0 $\text{t ha}^{-1} \text{ a}^{-1}$ and 7.6 $\text{t ha}^{-1} \text{ a}^{-1}$ respectively and indicate that the contribution of the tillage on the site during the last 45 years was significant. However, the net erosion rate was about 15.4 $\text{t ha}^{-1} \text{ a}^{-1}$ practically the same value as that determined by the mass balance model 2. This result confirms that the water erosion is the main origin of the soil exported from the field, and that tillage erosion is more a translocation process within the field.

TABLE 1. LONG term SOIL REDISTRIBUTION RATES BASED ON THE FRN MEASUREMENTS (CAESIUM-137 AND EXCESS LEAD-210) AND THE EMPIRICAL RUSLE MODEL

Erosion Rates ($\text{t ha}^{-1} \text{ a}^{-1}$)	From $^{210}\text{Pb}_{\text{ex}}$ Period: ~ 100 years	From ^{137}Cs Period : ~ 50 years		From RUSLE2 Period: 10 years
		<i>Mass balance 2</i>	<i>Mass balance 3</i>	
Erosion range	8-27	4-30	8-70	4-56
Mean erosion	15.0	17.9	26.0	19.5
Mean deposition	4.1	6.3	12.8	14.3
Gross erosion	12.9	15.4	22.0	17.4
Gross deposition	0.8	1.2	6.5	5.3
Net erosion	12.1	14.3	15.5	12.1
Sediment delivery ratio	93%	92%	70%	69%

In addition, to test the validity of the empirical RUSLE model for the study site, the RUSLE2 software was run taking into account the available parameters such as daily precipitation, soil texture, soil management and topographic factors. The parameters were computed for a period of 10 years. The data obtained showed that the soil erosion rates along all transects of the field ranged between 3.5 and 56 t ha⁻¹ a⁻¹. The gross erosion and deposition rates were found to be 17.4 t ha⁻¹ a⁻¹ and 5.3 t ha⁻¹ a⁻¹. The net erosion was estimated to be 12.0 t ha⁻¹ a⁻¹. The results derived from the prediction model- RUSLE2 - were firstly compared to the ¹³⁷Cs and ²¹⁰Pb_{ex} techniques using the mass balance 2 model as the two approaches estimate soil erosion induced by water. In general, the data on erosion rates obtained by RUSLE 2 and radionuclides using MB2 were similar. However, the sedimentation (or deposition within the field) was found to be higher with the RUSLE2 model than the sedimentation estimated by the radionuclides, leading to a sediment delivery ratio obtained from the RUSLE2 model slightly lower than that obtained by the MB2 model. The comparison with the MB3 model output showed that the RUSLE2 model provided values of soil erosion rates slightly lower than those obtained by the MB3 model as this model also takes into account the tillage effect (Table 1). Indeed, the mean erosion rates derived from MB3 and RUSLE 2 models were 19.5 and 26.0 t ha⁻¹ a⁻¹ respectively and the gross erosion rates were estimated to be 17.4 and 22.0 t ha⁻¹ a⁻¹ for MB3 and RUSLE2 respectively. The same results were obtained when MB2 and MB3 models were compared as mentioned above. However, due to the high deposition rate estimated by RUSLE2 model (5.3 t ha⁻¹ a⁻¹) relative to the value provided by MB2 (1.2 t ha⁻¹ a⁻¹), the sediment delivery ratio obtained by RUSLE2 model was not found to be higher than that provided by the MB3 model (69% and 70% respectively), as expected, in contrast to comparison between MB2 and MB3 models (92% and 70% respectively). The uncertainties related to the two approaches (RUSLE2 and Radionuclides) combined with the different periods of estimation of soil redistribution (10 years, 50 years for RUSLE2 and ¹³⁷Cs respectively) could explain the difference between the two approaches. The outputs of the different techniques are presented in Table 1.

3.2. Short term soil erosion rates using ⁷Be

3.2.1. Vertical distribution and inventories

Fig. 6 shows the vertical distribution of ⁷Be in two sectioned shallow cores from both the undisturbed and cultivated sites. As expected the majority of ⁷Be was found within the upper layers of the surface (< 1 cm) due to its short half-life. The ⁷Be concentration declined with depth following an exponential form and varied with precipitation intensity. Its value at the surface, for example at the end of March of the year 2005 was about 14 Bq kg⁻¹ (Fig. 6). Similar behaviour of ⁷Be in soil was obtained in previous studies [15,16,23]. The value of h₀ associated with the study field measured from the vertical distribution of ⁷Be was 4.7 kg m⁻².

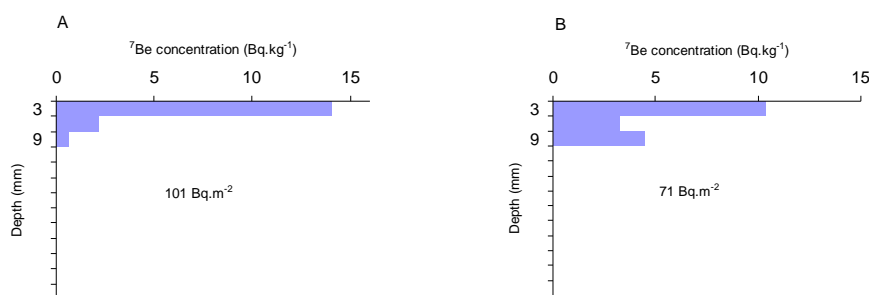


FIG. 6. Vertical distribution of ⁷Be associated with cores collected in the undisturbed (A) and cultivated (B) sites.

However, as successive erosion events occurred during the winter rainfall period without sufficient separation, it was not straight forward to determine the exact period corresponding to the soil erosion rates derived from ^7Be inventories measured at the end of March. However, by taking into account the ^7Be inventories of the rainwater during the period of December until March, in 2004 and 2005, and assuming the low contribution to the total ^7Be inventories from the October and November rains of each year, because of their sufficient separation from March, it was considered acceptable that the soil erosion rates determined at the end of March based on the ^7Be inventories corresponded with the rainfall period from December to March. ^7Be inventories were measured from 2004 to 2007 at the end of March and beginning of April after the winter rainfall period (December- March). The no-till practice was compared to the conventional tillage during the years 2004 and 2005. In 2006, the field was not cultivated, while in 2007, the conventional tillage with cereals was practiced. The local ^7Be reference inventories associated with all four studied years (2004, 2005, 2006 and 2007) were estimated to be 120, 101, 132 and 74 Bq m^{-2} respectively with standard deviations ranging between 15 to 20%. The precipitations corresponding to the period from December until March were 192, 141, 288 and 98 mm respectively. The measured inventories in the rainwater were generally close to the values obtained from the fallout-derived ^7Be inventories resulting from precipitation since December to March. During these four years, ^7Be inventories were found to range between 50 and 180 Bq m^{-2} , and erosion and deposition zones could be identified. Results obtained in 2004 and 2005 permitted comparison between both soil tillage practices. In 2004 for example, the mean value of ^7Be inventory obtained from the plots under no-till management was about $99 \pm 5 \text{ Bq m}^{-2}$ while for the plots under conventional tillage, the mean value of ^7Be inventory was estimated to be $88 \pm 4 \text{ Bq m}^{-2}$. This result indicates that the soil loss has been reduced under no-till as compared to conventional tillage. In the same year, the mean ^7Be inventory corresponding to the plots without crop was found to be about $78 \pm 5 \text{ Bq m}^{-2}$. In 2005, the same result was obtained but less difference was observed between both tillage systems as compared to 2004. In 2006, when no crops were cultivated on the fields, ^7Be inventories were found significantly lower than the reference inventory. Finally, in 2007, the conventional tillage practiced in the site conducted to an equivalent reduction of ^7Be inventory relative to the reference inventory (12%) as obtained in 2004 (10%). Table 2 summarizes ^7Be inventories associated with different experimental plots. The coefficients of variation (CV) associated with the ^7Be inventories of plot inventories were about 5% to 6% and those corresponding to the reference inventories were about 15 to 20%.

TABLE 2. BERYLLIUM-7 INVENTORIES DURING 4 YEARS (PERIOD FROM DECEMBER UNTIL MARCH) ASSOCIATED WITH THE REFERENCE SITE AND PLOTS UNDER DIFFERENT LAND USES - NO TILL (NT)- CONVENTIONAL TILLAGE (CT), UNCULTIVATED SOIL (NC)

Year	Precipitation (mm)	^7Be inventories (Bq m^{-2}) Reference site	^7Be inventories (Bq m^{-2}) Experimental Plots		
			NT	CT	NC
2003-2004	192	120 ± 18	99 ± 5	88 ± 4	78 ± 5
2004-2005	141	101 ± 10	94 ± 5	89 ± 4	86 ± 5
2005-2006	288	132 ± 19	-	-	80 ± 4
2006-2007	99	74 ± 7	-	67 ± 3	-

3.2.2. Assessment of soil redistribution rates and effectiveness of soil conservation methods

Soil erosion and deposition rates were calculated from the ^7Be measurements and the ^7Be depth profile. The value of relaxation mass depth (h_0) associated with the study field measured from the vertical distribution of ^7Be was 4.7 kg m^{-2} . The average of mean erosion rates, corresponding to the period of 2004 in the plots under no-till management (NT) and conventional tillage (CT) were estimated to be 10.3 and 14.6 t ha^{-1} respectively. In the same period of 2005, the mean soil erosion rates were lower than those of 2004 certainly due to the difference in precipitations. Their values were about 6.6 and 8.3 t ha^{-1} for NT and CT plots respectively [30]. Therefore, soil erosion for the plots under no-till management was reduced by 30% and 20% in 2004 and 2005 respectively. This difference can be clearly observed in Fig. 7 and indicates that the no-till technique reduces soil loss compared to the conventional tillage system. Gross erosion and net erosion rates were also observed to be lower in the plots under no-till as compared to those rates under conventional tillage. On the other hand, the deposition was found higher in the NT plots than the CT plots leading to a sediment delivery ratio significantly lower in the NT plots (mean value: $\sim 72\%$) as compared to the CT plots (mean value: $\sim 85\%$). It seems that the no-till practice retains the eroded soil within the field and reduces the rate of sediment exported from the field. The mean soil erosion rates measured in the uncultivated plots (NC) during the two years 2004 and 2005 were about 20.0 and 10.2 t ha^{-1} respectively. The results show that erosion was significantly higher on the plots without protection by the crop (NC), as compared to the cultivated plots under both tillage systems. The mean value of the sediment delivery ratio was found to be 87%, practically similar to the value obtained for the plots under conventional tillage but significantly higher than that determined for the plots under no-till. In 2006, the uncultivated plot led equally to high soil erosion (25.3 t ha^{-1}). In 2007, when the conventional tillage was practiced again, the mean soil erosion rate in the study field was about 7.2 t ha^{-1} . All data are summarized in Table 3. The efficiency of the no-till practice to counteract soil erosion was already reported in other regions of the world, in the scope of soil erosion studies using FRNs or other conventional methods in for instance the USA [31], Chile [31], Canada [32] and Mali [33]. Also in Morocco, the benefits of the no-till technique compared to the conventional tillage have been demonstrated. Experiments conducted during 11 years in the experimental station of INRA located near Settat city and other sites, showed that the no-till management increased the organic matter amount, preserved nitrogen, ensured good soil aggregate stability and to improved the productivity yield [34,37]. Indeed, after 11 years of experimentation, the no-till practice had modified the soil proprieties. The results obtained through the measurement of physical and chemical parameters (structural stability, organic matter, total nitrogen, particular organic matter and pH) indicate that the soil quality had been improved under minimum tillage (no-till) and such practice constitutes a very good soil conservation measure.

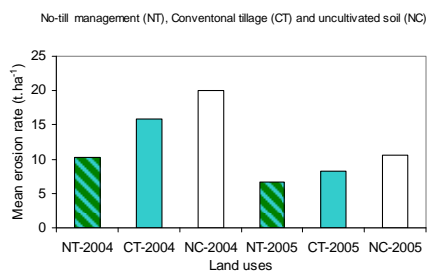


FIG. 7. Mean erosion rates under different land uses using fallout ^7Be .

TABLE 3. SHORT term SOIL REDISTRIBUTION RATES USING BERYLLIUM-7 DURING 4 YEARS (PERIOD FROM DECEMBER UNTIL MARCH) UNDER DIFFERENT LAND USES - NO TILL (NT)- CONVENTIONAL TILLAGE (CT), UNCULTIVATED SOIL (NC)

Years (Dec – March)	Precipitation (Dec – March) mm	Land use	Erosion rates (t ha ⁻¹)		Deposition rates (t ha ⁻¹)		Net erosion rates (t ha ⁻¹)	Sediment ratio delivery
			Mean	Gross	Mean	Gross		
2003 - 2004	192	NT	10.3	6.2	9.0	2.0	4.2	68%
		CT	14.6	13.4	4.4	1.5	11.9	89%
		NC	20.0	15.4	6.7	2.2	13.2	89%
2004 - 2005	141	NT	6.6	4.8	3.5	1.1	3.7	77%
		CT	8.3	5.9	3.2	1.1	4.8	82%
		NC	10.5	8.3	5.1	1.0	7.3	88%
2005 - 2006	288	NC	25.3	18.2	11.0	3.2	15.0	82%
2006 - 2007	99	CT	7.2	5.7	3.9	0.8	5.0	88%

4. CONCLUSIONS

Experiments conducted in this work demonstrated the potential of the use of fallout ¹³⁷Cs and ²¹⁰Pb_{ex} and ⁷Be to estimate both long and short term soil erosion rates in agricultural fields in Morocco and to assess the effectiveness of soil conservation techniques. Fallout ¹³⁷Cs and ²¹⁰Pb_{ex} allowed the estimation of soil erosion and deposition rates associated with long time periods of 50 and 100 years respectively. The behaviour of both radionuclides in soil was generally observed being similar.

Reference inventories were about 1445 and 3305 Bq m⁻² for ¹³⁷Cs and ²¹⁰Pb_{ex} respectively. Taking into account the previous studies on soil erosion in Morocco using the ¹³⁷Cs technique, the reference inventory appears to be well correlated with the mean annual precipitation. From ¹³⁷Cs and ²¹⁰Pb_{ex} inventories and using the Mass Balance 2 model (MB2) the rates of water-induced soil erosion have been quantified. The mean and gross soil erosion rates were estimated to be 17.9 and 15.4 t ha⁻¹ a⁻¹. The net soil erosion rate was about 14.3 t ha⁻¹ a⁻¹ indicating a high sediment delivery ratio of about 92%. Data on soil redistribution generated by the use of both radionuclides are similar. This result indicates that soil erosion in the study field did not change significantly during the last decades. However, the ¹³⁷Cs technique provided more reliable results due to the good precision on ¹³⁷Cs activity measurement as compared to ²¹⁰Pb_{ex}. Nevertheless, ²¹⁰Pb_{ex} can provide an alternative for the areas with low ¹³⁷Cs activities.

Soil erosion rates due to tillage were also estimated using the Mass Balance 3 model (MB3). The total gross erosion and deposition rates including both water and tillage erosion were about 22.0 t ha⁻¹ a⁻¹ and 7.6 t ha⁻¹ a⁻¹ respectively indicating that the contribution of tillage to erosion in the last 50 or 100 years was not negligible. But, the net soil erosion rate value was found practically the same as that determined by the Mass Balance 2 model confirming that the water erosion is the main origin of the soil exported from the field while the tillage erosion is more a translocation process within the field. A validation of the empirical RUSLE2 model for estimating soil redistribution rates induced by water was carried out and the prediction model provided comparable results to those obtained by ¹³⁷Cs and ²¹⁰Pb_{ex}, in particular for the data on soil erosion rates. Deposition rates provided by RUSLE2 model were found higher than those obtained by MB2 model conducting to a sediment delivery ratio slightly lower than that derived from MB2 model.

Fallout ^7Be was exploited to document short term rates of soil erosion associated with short events and to assess the effectiveness of no-till practiced in the study field. ^7Be reference inventories measured at the end of March or early April from 2004 to 2007 were about 120, 110, 132 and 74 Bq m⁻². As successive erosion events occurred during the high rainfall period without sufficient separation, it was more realistic to consider that soil erosion rates determined at the end of March were mostly associated to the rainfall period from December to March. The mean erosion rates ranged between 6.6 and 10.5 t ha⁻¹ for the no-till management (NT), 7.2 and 14.6 t ha⁻¹ for the conventional tillage (CT) and 10.5 and 25.3 t ha⁻¹ for uncultivated soil. The results obtained from ^7Be measurements during 2004-2007 agree with studies elsewhere and suggest that soil loss is reduced when no-till management is practiced compared to conventional tillage or soil without any crop cultivation. A reduction of up to 30% is achieved. Therefore the no-till management constitutes an effective approach for conserving soil and ensuring a sustainable crop production in the agricultural sector of Morocco.

ACKNOWLEDGEMENTS

The authors are thankful to the IAEA for the financial and technical support provided under Research Contract MOR-12325. They also acknowledge the support of Mr. Souihka from INRA, Head of the 'Marchouch' experimental site and the contribution of Mr. Bizi and Mr. Sebbar from CNESTEN.

REFERENCES

- [1] SECRETARIAT D'ETAT CHARGE DE L'EAU ET DE L'ENVIRONNEMENT DEPARTEMENT DE L'ENVIRONNEMENT Rapport National sur l'Etat de l'Environnement du Maroc (2002) 292 pp.
- [2] WALLING, D.E., QUINE, T.A., The use of ^{137}Cs measurements to investigate soil erosion in arable fields in the U.K: potential applications and limitations, *J. Soil Sci.* **2** (1991) 147-165.
- [3] LOUGHRAN, R.J., et al., Estimation of soil erosion from ^{137}Cs measurements in a small cultivated catchment in Australia, *J. Appl. Radiat. Isot.* **39** (1988) 1153-1157.
- [4] WALLING, D.E., QUINE, T.A., Use of ^{137}Cs as a tracer of erosion and sedimentation: Handbook for the application of the ^{137}Cs technique, University of Exeter (1993) 196 pp.
- [5] ZAPATA, F., (ed), Handbook for the assessment of soil erosion and sedimentation using environmental radionuclides, Kluwer Academic Publishers, Dordrecht (2002) 219 pp.
- [6] QUERALT I., et al., (Eds) Assessment of soil erosion and sedimentation through the use of the ^{137}Cs and the related techniques, *Acta Geologica Hispanica* **35** (2000) 195-367.
- [7] RITCHIE, J.C., MCHENRY, J.R., Application of Radionuclide fallout ^{137}Cs for measuring soil erosion and sediment accumulation rates and patterns. A review, *J. Environ. Qual.* **19** (1990) 215-233.
- [8] BOUHLASSA, S., et al., ^{137}Cs fallout as tracer of erosion and sedimentation in big catchment, *App. Radiat. Isot.* **46** (1994) 659.
- [9] BENMANSOUR, M., Use of the ^{137}Cs technique in soil erosion in Morocco - Case study of the Zitouna basin in the north. Proc. of International Symposium on Nuclear Techniques in Integrated Plant Nutrients, Water and Soil management held in Vienna 16-20 october 2000, IAEA -CSP-11/C (2002) 308-315.

- [10] BOUHLASSA, S., et al., Estimates of soil erosion and deposition of cultivated soil of Nakhla watershed, Morocco, using ^{137}Cs technique and calibration models, *Acta Geologica Hispanica* **35** (2000) 239-249.
- [11] NOUIRA, A., et al., Use of ^{137}Cs technique for soil erosion study in the agricultural region of Casablanca in Morocco, *Journal of Environment Radioactivity* **68** (2003) 11-26
- [12] DAMNATI, B., et al., Utilisation du ^{137}Cs pour l'estimation des taux d'érosion dans un bassin versant du nord du Maroc, *Sécheresse*, **15** (2004) 195-199.
- [13] WALLING, D.E., HE, Q., Using fallout ^{210}Pb to estimate soil erosion on cultivated land, *Soil Sci. Soc. Am. J.*, **63** (1999)1404-1412.
- [14] WISE, S.M., ^{137}Cs and ^{210}Pb : "A review of techniques and some applications in geomorphology", *Timescales in geomorphology* (CULLINGFORD, R.A, et al., Eds),. Wiley, New York (1980) 109-127.
- [15] WALLBRINK, P.J., MURRAY, A.S., Distribution of and variability of ^7Be in soils under different surface cover conditions and its potential for describing soil redistribution processes, *Water Res. Res.* **32** (1996) 467-47.
- [16] WALLING, D.E., et al., Use of ^7Be and ^{137}Cs measurements to document short- and medium-term rates of water - induced soil erosion on agricultural land, *Water Res. Res.* **35** (1999) 3864-3874.
- [17] JENSEN, A., Historical deposition rates of Cd, Cu, Pb and Zn in Norway and Sweden estimated by ^{210}Pb dating and measurement of trace elements in cores of peat bogs, *Water air Soil Pollut.***95** (1997) 205-220.
- [18] BENNINGER, L.K.,KRISHNASWAMI S., Sedimentary process in the inner New York Bight : Evidence from excess ^{210}Pb and $^{239+240}\text{Pu}$, *Earth Planet. Sci. Lett* **53** (1981) 158-174.
- [19] BENMANSOUR,M., et al., Distribution of anthropogenic radionuclides in Moroccan coastal waters and sediments, *Radioactivity in the Environment - Book series - 8* (2006) 145-150.
- [20] WALLING D.E., QUINE T.A., Calibration of ^{137}Cs measurements to provide quantitative erosion rate data, *Land degradation and Rehabilitation* **2** (1990) 161-175.
- [21] WALLING, D.E., HE, Q., Improved models for deriving estimates of soil redistribution rates from ^{137}Cs measurements, *J. Environ. Quality* **28** (1999) 611-622.
- [22] GOVERS, G., et al., The role of tillage in soil redistribution on hill slopes, *European Journal of Soil Science* **45** (1994) 469-478
- [23] BLAKE, W.H, et al., Fallout beryllium as a tracer in soil erosion investigations, *Applied Radiation and Isotopes* **51** (1999) 599-605.
- [24] RENARD, K.G., et al., Predicting Soil Erosion by Water: A Guide to Conservation Planning with the Revised Universal Soil Loss Equation (RUSLE), *Agricultural Handbook* **703**, U.S. Department of Agricultural Research Service, Washington D.C. (1997) 404 pp.
- [25] USDA., Revised Universal Soil Loss Equation, Version 2 (RUSLE2), USDA-ARS National Soil Erosion Research Laboratory, Purdue University, West Lafayette, IN.(2005),
Site internet
(http://fargo.nserl.purdue.edu/rusle2_dataweb/RUSLE2_Index.htm).
- [26] WALLING, D.E., et al., Use of ^{137}Cs and ^{210}Pb as traces in soil erosion investigations, *IAHS Publ.* **229** (1995)163-172.
- [27] HE, Q., WALLING, D.E., The distribution of fallout ^{137}C and ^{210}Pb in undisturbed and cultivated soils, *Applied Radiation and Isotopes* **48** (1997) 677-690.
- [28] OWENS, P.N.,WALLING., D.E., Spatial variability of ^{137}Cs inventories at reference sites and example from two contrasting sites in England and Zimbabwe, *Applied Radiation and isotopes* **47** (1996) 699-707.

- [29] NOUIRA, A., Application de la technique de ^{137}Cs pour l'étude de l'érosion et déposition du sol à l'échelle d'une parcelle culturale Ain Harouda et l'échelle du bassin versant de Trigrigra, Thèse de Doctorat, Faculté de Casablanca (2003) 112-194.
- [30] BENMANSOUR M., et al., "Use of fallout radionuclides to estimate short and long-term rates of soil erosion on agricultural lands in Morocco", Proc. of 14th International Soil Conservation Organisation Conference, Marrakech, Session Isotopes 11 (2006) 4 pp.
- [31] INTERNATIONAL ATOMIC ENERGY AGENCY, Report of the Third Research Coordination Meeting of the FAO/IAEA Coordinated Research Project, Assess the Effectiveness of Soil Conservation Techniques for sustainable Watershed Management Using Fallout Radionuclides, Vienna (2006) 11-13.
- [32] DUCHEMIN, M., et al., "Mesure et modélisation de l'érosion hydrique des sols agricoles au Maroc et au Québec", Proc. of 14th International Soil Conservation Organisation Conference, Marrakech, Session Isotopes 11 (2006) 4pp.
- [33] DRISSA, D., Influence des pratiques culturales et du type de sols sur les stocks et pertes de carbone par érosion en zones soudanienne du Mali. Gestion de la biomasse, érosion et séquestration du carbone, IRD, Montpellier, 09/2002, Bulletin du Réseau Erosion **22** (2004) 193-206.
- [34] SABER, N., MRABET, R., Influence du travail du sol et des rotations de cultures sur la qualité d'un sol argileux gonflant en milieu semi-aride marocain, Étude et Gestion des Sols **9** (2002) 43-53.
- [35] BESSAM, F., MRABET, R., "Time influence of no tillage on organic matter and its quality of a vertic Calcixeroll in a semiarid area of Morocco", proc of International Congress on Conservation Agriculture, Madrid, Vol **2** (2001) 281-286.
- [36] MRABET R., et al., Total Particulate Organic Matter and Structural Stability of a Calcixeroll soil under different wheat rotations and tillage systems in a semiarid area of Morocco, Soil and Tillage Research **57** (2001) 225-235.
- [37] MRABET R., et al., Soil chemical quality changes and implications for fertilizer management after 11 years of no-tillage wheat production systems in semiarid Morocco, Land Degradation and Development **12** (2001) 505-517.

THE USE OF CAESIUM-137 MEASUREMENTS FOR ASSESSING SOIL EROSION AND SEDIMENTATION IN THE RIVA BASIN (ISTANBUL, NW TURKEY)

S. HACIYAKUPOGLU, M.S. KIZILTAS, H. SAYGIN
Istanbul Technical University, Energy Institute,
Istanbul, Turkey

F. GOKBULAK, A. HIZAL
Istanbul University, Forestry Faculty,
Istanbul, Turkey

D.E. WALLING
University of Exeter, School of Geography,
Exeter, Devon, United Kingdom

T.A. ERTEK
Istanbul University, Department of Geography,
Istanbul, Turkey

A.E. ERGINAL
Canakkale Onsekiz Mart University, Department of Geography,
Canakkale, Turkey

Abstract

The paper summarizes the findings of an assessment of soil redistribution in the Riva basin, upstream of the Omerli reservoir, based on use of the fallout radionuclide Caesium-137. This reservoir is located at the eastern side of Istanbul, Turkey, and is the main provider for water to Istanbul. In the Riva basin, soil erosion and associated sediment deposition and potential mass movements are natural landscape forming processes. However, these processes are being accelerated by human intervention, creating a serious threat for sustainable intensification of the agricultural production, watershed management and the conservation of the local natural resources. To determine soil redistribution rates and patterns using the fallout radionuclide approach, samples were collected from an uncultivated flat reference sites and the cultivated sloping farmland (two transects). According to the results of gamma spectroscopy measurements of Caesium-137 and the outputs from the proportional model and simplified mass balance model for both transects, erosion rates varied between $-2.4 \text{ t ha}^{-1} \text{ a}^{-1}$ and $-36.0 \text{ t ha}^{-1} \text{ a}^{-1}$ and deposition rates between $+1.7 \text{ t ha}^{-1} \text{ a}^{-1}$ and $+10.5 \text{ t ha}^{-1} \text{ a}^{-1}$.

1. INTRODUCTION

Istanbul is one of the largest and oldest cities in Turkey. Its population growth rate is almost twice the overall rate for Turkey. Migration from other parts of Turkey to Istanbul, rapid industrial development and uncontrolled urbanization create extra pressure on the limited land and water resources [1].

The domestic water supply in the over-populated and rapidly growing city of Istanbul has always been a serious problem. Due to the decline of rainfall in recent years, the Omerli reservoir, the main source of domestic water supply to Istanbul, is currently filled with water to only 28% of its capacity [2]. Hence, there is a water shortage in the city. It is thus very important to establish a management plan and define principles for soil and water

conservation because water production and water quality as influenced by forest ecosystems and other land use practices are equally critical in the watershed of the Omerli reservoir.

With the degradation of the natural resources raising serious concerns worldwide, governments and non-governmental organisations such as WOCAT (The World Overview of Conservation Approaches and Technologies) have started to take actions for improving natural resource management. WOCAT showed that the necessary definitive soil and water conservation technology and approach should be selected and planned together with the land users [3].

With the rapidly growing population around Istanbul, the need for sustainable management of its land and water resources and improved information concerning rates of soil loss from agricultural land gained increasing importance. However, to date no systematic monitoring of soil erosion has been undertaken for agricultural land and rangelands. The Forest Service has planted forests in some areas to protect watersheds from erosion, but the effectiveness of these measures has not been assessed.

In the water-producing watersheds of Istanbul, including the catchment of the Omerli reservoir, the total forest area decreased by 4% from 1970 to 1992 [4], mainly due to urbanization projects such as the construction of the Formula 1 Istanbul circuit and other large scale recreational facilities [5]. As a result, destruction of the forest vegetation increased the frequency of flooding events in some parts of the city. To support and promote sustainable watershed management analyses of soil redistribution rates and patterns are needed. Recent advances in the application of fallout radionuclides (FRN's) for documenting soil redistribution rates offer the possibility to collect such information [6,7].

The use of environmental fallout radionuclides such as Caesium-137 (^{137}Cs) has received increasing attention due to the growing importance of determining soil erosion rates throughout the world. The advantages of this methodology include the potential for deriving retrospective estimates of erosion and deposition rates based on a single site visit, and for assembling distributed information for individual points in the landscape which can be used to study spatial patterns of soil redistribution. ^{137}Cs is the Caesium radionuclide with mass number 137 and it is an artificial radionuclide with a half-life of 30.17 year produced by nuclear fission [8]. Widespread global distribution of ^{137}Cs in the environment began with high-yield atmospheric tests of atomic weapons in the 1950's and early 1960's. Because more atmospheric nuclear tests took place in the northern hemisphere, ^{137}Cs fallout inputs were much greater in the northern hemisphere than in the southern hemisphere. Local events, such as the Chernobyl accident have had important impacts on the fallout patterns at the regional level but are of limited significance for global fallout patterns and rates. Theoretical models have been developed to estimate soil erosion rates and soil redistribution patterns by using natural and artificial fallout radionuclides. In most environments, soils and sediments rapidly and strongly adsorb these fallout radionuclides and an understanding of their distribution between different size fractions is important for their use as a tracer [9, 10].

When considering the rates and patterns of total soil loss and accumulation within individual fields, it is important to identify all contributing processes and there is a growing evidence that the effects of soil tillage should also be taken into account. In the light of this evidence, several studies have attempted to assess the relative importance of water erosion and tillage processes in determining the rates and patterns of total soil redistribution. This study attempts to address the need for information on soil redistribution rates by applying the fallout

radionuclide methodology within an area of cultivated farmland in the catchment of the Omerli reservoir located within the Riva Basin.

2. MATERIALS AND METHODS

2.1. Study site characteristics

The Omerli reservoir was built in 1972 and supplies most of the water consumed in Istanbul. The Istanbul Water and Sewerage Administration (ISKI) report states that 70% of the water, which Istanbul needs in the future, will be supplied by this reservoir [2]. Therefore, the Omerli reservoir and its watershed are of strategic importance for Istanbul (Fig.1).

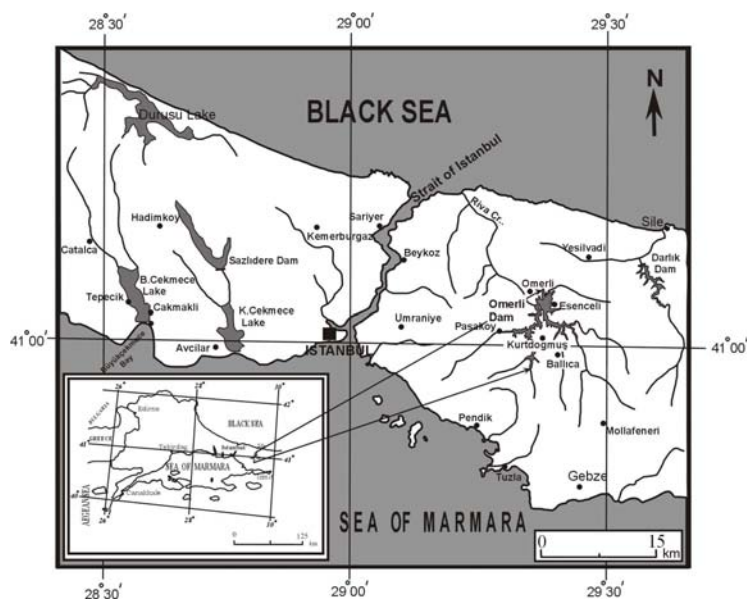


FIG.1. The location of the study area.

The Omerli watershed, is located in the Riva basin between $40^{\circ} 51' N$ - $41^{\circ}07' N$ and $29^{\circ}11' E$ – $29^{\circ}40' E$ and covers an area of 57,820 ha. The mean annual temperature is $12.8^{\circ} C$ and average annual precipitation, based on 40 years of data, is around 705 mm. Topography is fairly steep. In total 55% of the total area of the watershed has a slope gradient of more than 15%. The parent material includes Devonian schist, Eocene limestone, Triassic conglomerates, sandstones, grit, limestone, and Silurian arkoses. The soil texture generally varies from sandy to loam and soil depths range between deep to moderate deep. Non-calcic brown forest soils are dominant in the watershed.

The vegetation cover of the Omerli watershed is mainly composed of oak coppice, beech, pine tree species and some machia vegetation, however, much of the watershed (34,653 ha) is covered by forest vegetation. Open areas (herbaceous covered areas, forest clearings, agricultural fields, settlements and industry) and water surfaces cover 23,167 ha of the watershed.

The cultivated area (under oats) where soil redistribution rates were estimated is located 0.5 km north from Ballica village (Fig. 2). The study area has an altitude that varies between 109 and 120 m a.s.l. with a slope gradient toward the north of less than 15%. The soil type of the

site is mainly a brown coloured forest soil, developed on arkoses⁷ of the Paleozoic era, with an average depth of 30 to 40 cm [11]. This type of geological formation is prone to both erosion and mass movements. Based on visual observations, the soils in the cultivated study area are characterised by high erosion rates. The selected reference area, where according to local farmers, no cultivation has been performed since the 1960s, is located in the catchment near to the cultivated area associated with Ballica village. The in-situ-measured soil thickness was similar to the cultivated study area. The slope gradient varied between 0 and 1° reducing the erosion risk to almost zero.



FIG. 2. The cultivated area at north of the Ballica village.

2.2. Collection of soil samples

According to the standard procedures for applying the fallout radionuclide methodology, bulk and depth incremental soil samples were collected from an uneroded reference area and along transects across the sloping eroded farmland within the Omerli catchment in the Riva Basin. Surface soil samples were also collected from the cultivated field from points adjacent to the cores for particle size analysis. A motorized percussion corer with a diameter of 6.9 cm was used for soil sample collection. Within the reference sampling site, soil sampling was carried out to a depth of 36 cm at six positions, uniformly distributed across the site. Additionally, one sectioned core (sectioned at 2 cm depth increments) was also collected from the reference site to determine the ¹³⁷Cs depth distribution. Within the sloping cultivated area, 22 bulk soil cores were collected to a depth of 50 cm at 10 m intervals along the two transects (Fig. 3). Finally, one sectioned core was collected from a representative eroding zone and one from a representative depositional zone within the study area.

2.3. Particle size analysis

Because ¹³⁷Cs is strongly and rapidly adsorbed by the fine soil particles and subsequent redistribution of the fallout ¹³⁷Cs reflects the movement of soil particles, the absolute grain size composition of the soil must be taken into account when estimating soil redistribution rates. The absolute grain size composition of the <2 mm fraction of each of the surface soil samples collected from the cultivated field was therefore determined using a Saturn Digisizer laser particle size analyzer, following pre-treatment with hydrogen peroxide to remove the organic component and chemical dispersion with sodium hexametaphosphate. This analysis was undertaken in the laboratory of the Department of Geography at the University of Exeter, UK.

⁷A sedimentary rock composed of sand size fragments that contain a high proportion of feldspar in addition to quartz and other detrital minerals.

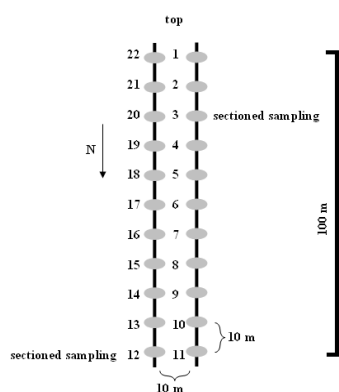


FIG.3. A sketch of the soil sample collection transects in the Omerli-Ballica cultivated area.

The values of median particle size or volume median diameter (d_{50}) given in Table 1 represent the values of particle size which divides a population exactly into two equal halves i.e. there is 50% of the distribution above this value and 50% below. The proportions of the sample classes are for clay ($<2 \mu\text{m}$), silt ($2-63 \mu\text{m}$) and sand ($>63 \mu\text{m}$ - 2 mm).

TABLE 1. CHARACTERISTICS OF THE SURFACE SOIL SAMPLES OF THE CULTIVATED FIELD IN BALLICA VILLAGE (BASED ON ANALYSES UNDERTAKEN AT EXETER UNIVERSITY)

Core N ^o	d_{50} (μm)	Clay ($<2 \mu\text{m}$) (%)	Silt (2-63 μm) (%)	Sand ($>63 \mu\text{m}$) (%)
1	9.97	10.7	74.9	14.4
2	14.03	9.1	72.1	18.8
3	13.87	8.6	72.7	18.7
4	9.426	12.7	74.4	12.9
5	11.75	11.5	73.6	14.9
6	9.425	13.2	75.4	11.4
7	9.158	13.5	77.0	9.5
8	10.58	12.2	76.0	11.8
9	9.758	12.2	77.6	10.2
10	10.09	12.5	74.6	12.9
11	9.189	12.4	76.2	11.4
12	9.835	11.7	77.5	10.8
13	9.298	12.7	76.0	11.3
14	10.96	11.4	75.1	13.5
15	10.12	11.8	73.5	14.7
16	12.05	10.1	73.3	16.6
17	12.76	8.3	75.1	16.6
18	10.51	11.6	74.1	14.3
19	13.25	9.9	72.0	18.1
20	11.56	10.6	71.8	17.6
21	26.44	5.6	65.6	28.8
22	12.77	8.4	74.7	16.9

2.4. Estimation of the soil redistribution rates

Several different approaches have been used within the FRN methodology to convert ^{137}Cs measurements into quantitative estimates of erosion and deposition rates for cultivated soils. In an attempt to standardize the methods and procedures employed, Walling and He (2001) developed PC-compatible software that implements a number of the available conversion models or procedures [9,10]. The reliability of the conversion models depends heavily on the specification of the relevant parameters. Some of these are more difficult to determine than others. The reference inventory is a critical parameter for any study using fallout radionuclides such as ^{137}Cs , ^{210}Pb and ^7Be . By comparing measured inventories with the reference inventory, it is possible to establish whether a sampling point has undergone erosion or deposition. The ^{137}Cs profile of a soil core from an undisturbed reference site is commonly characterized by a concentration peak at or near the soil surface and an exponential decline in concentration with depth below the peak. For a cultivated soil, the ^{137}Cs can be expected to be relatively uniformly distributed through the plough layer.

All conversion models are different in their underlying assumptions, process descriptions and representation of temporal variation in fallout inputs and soil redistribution rates. Their advantages and limitations should be considered when selecting an appropriate model and this decision should take account of the intended use of the estimated erosion and deposition rates, the land use history of the study site, and the availability of the information needed to establish the relevant parameters or the feasibility of estimating them if they are not directly available. In this study, the proportional model and simplified mass balance model applicable to cultivated sites have been selected from the available theoretical conversion models and these two models have been used to estimate the soil redistribution rates in the Omerli-Ballica cultivated site.

The proportional model has been widely used for estimating soil erosion rate from the ^{137}Cs measurements on cultivated soils. It is based on the premise that ^{137}Cs fallout inputs are completely mixed within the plough or cultivation layer and that the soil loss is directly proportional to the amount of ^{137}Cs removed from the soil profile since the beginning of ^{137}Cs accumulation or the onset of cultivation, whichever is later. Thus, if half of the ^{137}Cs input has been removed, the total soil loss over the period is assumed to be 50% of the plough depth. The model can be represented as follows:

$$Y = 10 \frac{B d X}{100 T P} \quad (1)$$

where: Y is the mean annual soil loss ($\text{t ha}^{-1} \text{ a}^{-1}$), d is the plough depth or cultivation layer (m), B is the soil bulk density (kg m^{-3}), X is the reduction (%) in total ^{137}Cs inventory (defined as $((A - A_{\text{ref}})/A_{\text{ref}}) \times 100$), T is the time elapsed since the initiation of ^{137}Cs accumulation or the commencement of cultivation whichever is later (a), A_{ref} is the local ^{137}Cs reference inventory (Bq m^{-2}), A is the measured total ^{137}Cs inventory at the sampling point (Bq m^{-2}) and P is the particle size correction factor for erosion. For this study, the plough depth d was estimated to be 20 cm, based on the specification of the ploughs used by the local farmers and evidence obtained from sampling the soil profile in cultivated areas. In the absence of direct evidence of size selective sediment mobilisation and transport, no particle size correction was applied and the parameter P was therefore set to 1.0.

This model oversimplifies reality, by making the assumption that the depth of the plough layer is progressively reduced by erosion and that the ^{137}Cs concentration of the eroded sediment therefore remains constant through time. The ^{137}Cs concentration of sediment deposited at a depositional point is also assumed to be constant.

The mass balance model takes into account the effects of ongoing cultivation in maintaining the depth of the plough layer and the progressive reduction in the ^{137}Cs concentration of the soil within the plough layer, due to the incorporation of soil containing negligible ^{137}Cs from below the original plough depth. It thus represents an improvement over the proportional model. This model is also easy to use and only requires information on plough depth and bulk density. This model also assumes that the total ^{137}Cs fallout occurred in 1963, instead of over the longer period extending from the mid 1950s to the mid 1970s. This assumption is an oversimplification. With this model the erosion rate can be estimated as follows:

$$Y = \frac{10 d B}{P} \left[1 - \left(1 - \frac{X}{100} \right)^{1/(t-1963)} \right] \quad (2)$$

where: Y is the mean annual soil loss ($\text{t ha}^{-1} \text{ a}^{-1}$), A_{ref} is the local reference inventory (Bq m^{-2}), X is the reduction (%) in total ^{137}Cs inventory (defined as $((A - A_{ref})/A_{ref}) \times 100$). A value of 1.0 was again assumed for the particle size correction factor P .

3. RESULTS

In this study ^{137}Cs inventories and related soil redistribution rates were evaluated for the study area within the Omerli watershed in the Riva basin on the eastern side of Istanbul. The local reference inventory for the Ballica undisturbed reference site was estimated to be $2257.1 \pm 458.3 \text{ Bq m}^{-2}$. Fig. 4 shows the ^{137}Cs depth profiles for both from the Ballica reference site and for eroding and depositional points within the cultivated study area.

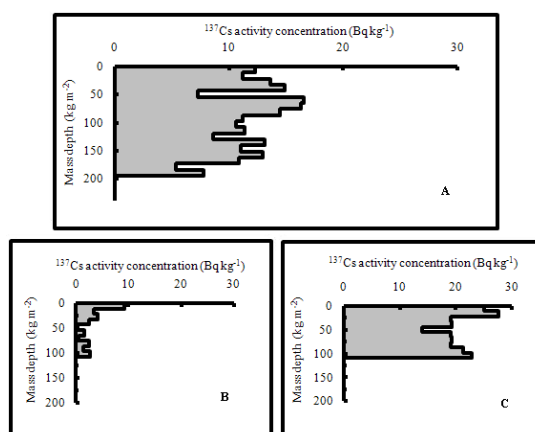


FIG. 4. ^{137}Cs depth profiles from the Ballica reference site (A) and for eroding (B) and depositional (C) points within the cultivated area.

The characteristics of the surface soil samples collected from the cultivated field at Ballica are given in Table 1. Particle size will affect erodibility and erodibility will influence the erosion rate. However the process of erosion may be size selective and the particle size of the surface layer may reflect the local erosion (or deposition) rate due to selective erosion (or deposition) rather than the inherent erodibility of the soil. If erosion preferentially mobilises the fine material, the remaining soil will become coarser.

The proportional and simplified mass balance models were used to derive estimates of mean annual soil redistribution rates for the 22 bulk cores collected from the cultivated study area at Ballica. The results are presented in Table 2 [12]. As the proportional model oversimplifies the mobilization of ^{137}Cs erosion process in comparison with mass balance model 1, the second column shows the more realistic soil erosion rates for the cultivated land in Ballica. Nevertheless values derived from both approaches are quite close to each other.

As documented in Table 2, negative values represent erosion, positive values deposition. Table 3 shows estimates of soil loss/deposition for the two transects in this cultivated study area based on the simplified mass balance model using the reference site inventory for Ballica. The mean erosion rate is equal to the total erosion per unit width divided by the eroding length. The gross erosion rate is equal to the total erosion per unit width divided by total length. The mean aggradation rate is equal to the total aggradation per unit width divided by the aggrading length. The gross aggradation rate is equal to the total aggradation per unit width divided by total length. The net erosion rate is the rate of soil movement (loss) from the sampled area and is equal to the difference between gross erosion and the gross aggradation rates.

4. CONCLUSIONS

Using the proportional and simplified mass balance models, the results showed that soil erosion rates varied between -2.4 and $-36.0 \text{ t ha}^{-1} \text{ a}^{-1}$ while soil aggradation rates between $+1.7$ and $+10.5 \text{ t ha}^{-1} \text{ a}^{-1}$ for the Ballica study area (Table 2). Estimates of soil loss/deposition for the two transects in this cultivated study area based on the simplified mass balance model also indicated (Table 3) that gross soil loss is considerable higher than soil deposition, suggesting that sediment delivery to the streams is high. According to Table 3, net soil redistribution rates estimates are -12.1 and $-16.2 \text{ t ha}^{-1} \text{ a}^{-1}$ for the two transects. Since the soil loss tolerance value is considered to be $10 \text{ t ha}^{-1} \text{ a}^{-1}$ for deep brown forest soils in Turkey [13], the erosion rates which are in excess of $10 \text{ t ha}^{-1} \text{ a}^{-1}$ indicate that soil erosion is a serious problem at the site and that appropriate control measures should be implemented to prevent soil loss due to erosion. In order to achieve sustainable water production in the watershed, a sediment control strategy should be developed. Forest areas must be protected and soil protection measures implemented. This study was aimed at estimating soil redistribution rates using the fallout radionuclide methodology, in order to assess present soil erosion and thereby improve future management of the catchment and thus protect the important Omerli reservoir from siltation. According to the results of this study, soil erosion rates are not within the soil loss tolerance limits for the studied area and soil conservation measures are urgently required.

TABLE 2. CAESIUM-137 INVENTORIES AND SOIL REDISTRIBUTION RATES OBTAINED FOR THE 22 BULK CORES COLLECTED FROM THE CULTIVATED FIELD AT BALLICA

Core N ^o	¹³⁷ Cs activity (Bq kg ⁻¹)	¹³⁷ Cs activity inventory (Bq m ⁻²)	Soil redistribution rate using proportional model for Ballica cultivated area (t ha ⁻¹ a ⁻¹)	Soil redistribution rate using simplified mass balance model for Ballica cultivated area (t ha ⁻¹ a ⁻¹)
1	6.14	1660.5	-11.0	-12.0
2	3.68	994.8	-23.3	-22.8
3	5.52	1491.6	-14.1	-15.0
4	3.17	856.3	-25.8	-24.8
5	4.09	1104.9	-21.3	-21.1
6	2.66	718.2	-28.4	-26.7
7	2.25	607.7	-30.4	-28.2
8	6.23	1684.9	-10.6	-11.6
9	8.69	2347.8	1.7	2.1
10	9.10	2458.3	3.7	4.8
11	5.72	1546.8	-13.1	-14.0
12	7.87	2126.8	-2.4	-2.9
13	7.77	2099.2	-2.9	-3.5
14	9.91	2679.3	7.8	10.5
15	8.99	2430.7	3.2	4.1
16	5.93	1602.0	-12.1	-13.0
17	5.62	1519.2	-13.6	-14.5
18	5.42	1463.9	-14.6	-15.4
19	4.09	1104.9	-21.3	-21.1
20	1.12	303.8	-36.0	-32.1
21	2.76	745.8	-27.9	-26.3
22	5.52	1491.6	-14.1	-15.0

TABLE 3. ESTIMATES OF SOIL LOSS/DEPOSITION FOR THE STUDY AREA IN BALLICA BASED ON THE SIMPLIFIED MASS BALANCE MODEL

	Measure	Estimated using simplified mass balance model results (t ha ⁻¹ a ⁻¹)
Ballica cultivated area	First transect	
	Mean erosion rate for eroding area	-21.7
	Gross erosion rate	-13.6
	Mean aggradation rate for aggrading area	+5.0
	Gross aggradation rate	+1.5
	Net soil redistribution rate	-12.1
	Second transect	
	Mean erosion rate for eroding area	-32.2
	Gross erosion rate	-16.6
	Mean aggradation rate for aggrading area	+2.2
Gross aggradation rate	+0.4	
Net soil redistribution rate	-16.2	

ACKNOWLEDGEMENTS

The financial and technical support provided by IAEA Coordinated Research Programme D1-50-08, through contracts TUR-12330 is gratefully acknowledged by the authors. Thanks are also extended to the staff of the Cekmece Nuclear Research Centre of Turkish Atomic Energy Agency (CNAEM) and the General Directorate Istanbul Water and Sewerage Administration (ISKI) for their help during the study.

REFERENCES

- [1] HIZAL, A., OZER, C., The vegetation changes of Omerli watershed and their effects on the water yield, International Symposium on Water Supply and Treatment, Istanbul Water and Sewerage Administration, Istanbul Technical University, Water Trusty, 25-26 May 1998, Istanbul, Turkey (1998).
- [2] ISTANBUL WATER AND SEWERAGE ADMINISTRATION (ISKI), Turkey, <http://www.iski.gov.tr/surezervleri/dol5b.phtm> (2007).
- [3] WOCATEER (WOCAT Newsletter), N°. 11 - Autumn/Winter 2005, <http://www.wocat.org/MATERIALS/WOCATEER11.PDF> (2005).
- [4] WOCATEER (WOCAT Newsletter), N°. 11 - Autumn/Winter 2005, <http://www.wocat.org/MATERIALS/WOCATEER11.PDF> (2005).
- [5] SERENGIL, Y., et al., Su üretim havzalarının havza amenajmanında yeni yaklaşımlar açısından değerlendirilmesi (Ömerli barajı havzası örneği). Istanbul ve Su Sempozyumu TMMOB Mimarlar Odası Istanbul Büyükkent Şubesi, 251-259; 8-9 January 2004, Istanbul, Turkey (2004).
- [6] FORMULA 1 ISTANBUL PARK RACING, Turkey, <http://www.formula1-istanbul.com/f1/en/?Map> (2007).
- [7] WALLING, D.E., QUINE, T.A. Use of ^{137}Cs as a tracer of erosion and sedimentation, Handbook for the application of the ^{137}Cs technique, University of Exeter, Exeter, United Kingdom (1993).
- [8] ZAPATA, F., Handbook for the Assessment of Soil Erosion and Sedimentation Using Environmental Radionuclides, Kluwer Academic Publishers, Boston (2002).
- [9] LEDERER, C. M., SHIRLEY, V.S., Table of Isotopes /ed. New York: John Wiley and Sons, USA (1978).
- [10] WALLING, D.E., et al., Models for Converting Radionuclide (^{137}Cs , $^{210}\text{Pb}_{\text{ex}}$, and ^7Be) Measurements to Estimates of Soil Erosion and Deposition Rates (Including Software for Model Implementation), Department of Geography, University of Exeter, Exeter, U.K. (2006).
- [11] WALLING, D.E., et al., Using ^{137}Cs measurements to validate the application of the AGNPS and ANSWERS erosion and sediment yield models in two small Devon catchments, Soil & Tillage Research **69** (2003) 27–43.
- [12] ERTEK, T.A., et al., Use of ^{137}Cs radionuclide in erosion investigations: Case studies of Turkey. Geography Journal of Department of Geography of Istanbul University, Nr.12, P.47-62, Istanbul 2004 (in Turkish + English abstract at http://www.istanbul.edu.tr/edebiyat/edebiyat/dekanlik/dergi/cd/Archives/number_12/12-04.pdf (2004).
- [13] KAYA, M., Using fallout radionuclides in erosion and sedimentation research, Master Science Thesis, Istanbul Technical University, Institute of Energy, May 2005 (in Turkish), full CD is available from The Turkish Higher Education System (2005).
- [14] DOGAN, O., GUCER, C., Su erozyonunun nedenleri-oluşumu ve universal denklem ile toprak kayıplarının saptanması (in Turkish). Topraksu Genel Müdürlüğü Merkez Topraksu Araştırma Enstitüsü, Genel Yayın Nr: 41, Teknik Yayın Nr: 21, Ankara, Turkey (1976).

EROSION/DISPOSITION DATA DERIVED FROM FALLOUT RADIONUCLIDES (FRNS) USING GEOSTATISTICS

L. MABIT

International Atomic Energy Agency,
Soil and Water Management and Crop Nutrition Laboratory,
FAO/IAEA Agriculture & Biotechnology Laboratory,
IAEA Laboratories Seibersdorf,
Seibersdorf, Austria

Abstract

FRN (Fallout Radionuclides) methodologies to assess erosion and sedimentation processes have been used worldwide for more than 40 years. However, some aspects of the methodology in particular data spatialisation and interpretation need further improvement. The aim of this work is to characterize the spatial distribution of FRN and to establish an isotope and sediment budget using FRN data and geostatistics. The spatial correlation of ^{137}Cs , soil organic matter content (SOM) and soil erosion-sedimentation patterns was estimated in a 2.16 ha field (located in the southern part of the Boyer River watershed, in Eastern Canada) using geostatistics coupled with a Geographic Information System (GIS). The spatial variability of the parameters was characterized through a geostatistical approach which considers the randomized and structured nature of spatial variables and the spatial distribution of the samples. Semivariograms were produced to take into account the spatial structure present in the data. A strong spatial dependence was found for each tested parameter ($0.87 \leq R^2 \leq 0.95$ and $0.7 \leq \text{Scale/Sill} \leq 0.96$). SOM spatial redistribution was correlated to soil erosion and sedimentation as shown by the significant relationship ($r^2 = 0.63$; $p < 0.001$; $n = 42$) between ^{137}Cs and SOM. The spatial distribution of FRN was estimated by Ordinary Kriging (OK) to design contour maps. Using different interpolation methods and 'area weighted mean' of the ^{137}Cs redistribution map, a radioisotope budget was established. Since 1954, around 2×10^7 Bq of ^{137}Cs were exported from the studied field. The net sediment production was estimated at $16.6 \text{ t ha}^{-1} \text{ a}^{-1}$ with a sediment delivery ratio (SDR) of 99%. The paper demonstrates the efficient contribution of geostatistics in studies using environmental radionuclides to estimate soil redistribution rates and isotope and sediment budgets. This approach could be used for ^{210}Pb or ^7Be as well as ^{137}Cs .

1. INTRODUCTION

There is a clear need for quantitative data on soil erosion to improve soil and water conservation action. Implementation of conservation measures needs also better understanding of spatial erosion and sedimentation patterns. Soil erosion data are often provided from experimental plots, elementary geomorphological units, river sediment discharge or empirical models. The implementation of nuclear techniques and particularly the use of fallout radionuclides (FRN) – ^{137}Cs , ^{210}Pb and ^7Be – as soil movement tracers provide an alternative and cost-effective way to collect valuable punctual data on soil erosion rates under different climatic and geographical conditions [1].

However, some limitations of the FRN methodology have been identified, especially with regards to sampling and the spatialisation of the data [2,3]. A bibliography record [4] – a contribution of the USDA-ARS Hydrology and Remote Sensing Laboratory to the IAEA Coordinated Research Project (CRP) D1.50.08 on 'Assessing the effectiveness of soil conservation techniques for sustainable watershed management and crop production using fallout radionuclides' – demonstrated clearly the paucity of studies using this concept. According to this record (more than 4000 publications) only a limited number of publications refer to the use of geostatistics to spatialize data sets. During the recommendation session of the third Research Co-ordination Meeting of the CRP D1.50.08 this problem was also identified [5], and the corresponding IAEA report emphasized the necessity to consider this new approach to process FRN data. Therefore, IAEA through the SSU/SWMCN section

tested geostatistical tools to treat spatial variability and mapping of FRN in order to respond to the lack of information in this necessary step [6,7,8].

In order to effectively assess soil redistribution patterns it is necessary to ensure sufficient sample numbers for a reliable data interpolation. The optimum number of samples depends mainly on the spatial variability in the FRN, the topographical and pedological complexity of the site. Several sampling strategies exist, i.e. random, stratified random, systematic, quadrat and transect sampling. Because traditional descriptive statistics showed limitations for dealing with this aspect, geostatistics have been utilized since the 1960's as a tool to spatialise information from punctual data and to inter- and extrapolate results. Variography can be used to quantify and to model the spatial correlation between locations and to characterize the spatial data behaviour [9]. There are two main types of interpolators: firstly those ignoring spatial autocorrelation of the data such as Inverse Distance Weighting (IDW); and secondly those accounting for spatial autocorrelation of the data such as Ordinary Kriging (OK) [6].

To improve the information on erosion and sedimentation processes provided by the redistribution of FRN in the landscape, this paper reports on the use of geostatistics to assess soil redistribution, as indicated by ^{137}Cs measurements, and its spatial relationship with soil organic matter (SOM) content. As the development of an appropriate variogram model for a data set requires the understanding and application of advanced statistical concepts and tools, this paper provides necessary practical recommendations on the choice and the application of geostatistics, in particular interpolation methods [10].

Through the presentation of a case study, the objectives of this paper are (i) assess the relationship between SOM and ^{137}Cs , (ii) determine at the field scale the structure of spatial dependence of SOM, ^{137}Cs and soil redistribution, (iii) assess the ^{137}Cs budget, and (iv) establish sediment budget using the information provided by geostatistical approaches.

2. MATERIALS AND METHODS

2.1. Study area

High levels of suspended solids and adsorbed phosphorus and high sedimentation rates through erosion processes have been identified as the cause of the decline of the Rainbow Smelt fish in the Boyer River watershed located in Québec, eastern Canada. Soil erosion magnitude was investigated using a GIS-oriented sampling strategy for ^{137}Cs measurements in selected fields representing the main soil-slope-land use combinations encountered in this 217 km² watershed [11,12].

A typical 2.16 ha field (46° 40.800' N, 70° 51.000' W), located in the upstream part of the Boyer watershed was investigated (Fig.1). The soil is a sandy loam with an average composition of 54% sand, 33% silt, 13% clay and an average of SOM content of 4.3%. The slope is < 2% with a maximum elevation relief difference of only four meters. No evidence of erosion was noticed in the selected study site.

2.2. Sampling strategy

An appropriate sampling design adapted to the field condition of the study site was selected. This experimental site was sampled using a transect approach along the length of the field to capture the observed variations of the local microtopography at the sampling time (Fig. 2).

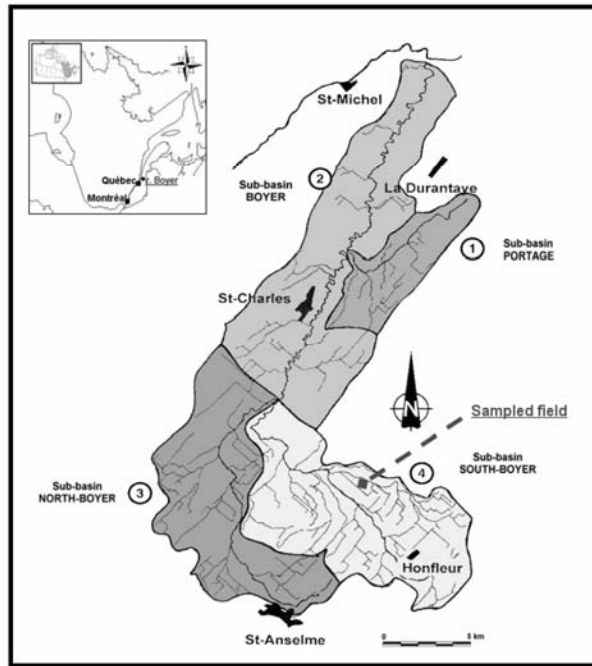


FIG. 1. Study area in the Boyer River watershed.

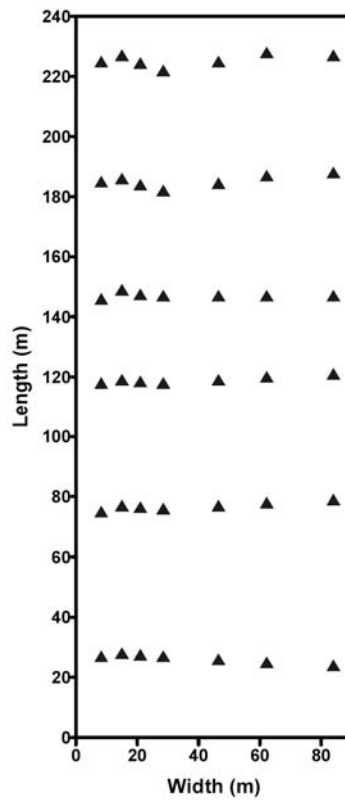


FIG. 2. Field sampling design (NB: triangles representing the position of the soil samples collected).

In total 42 points were sampled along seven parallel transects at different soil depth, i.e. 0-20, 20-30 and 30-40 cm. The points were not all at equal distance; in order to obtain a pattern with a variety of distances between sampled points, which is required for the establishment of a robust variogram. A recent study on soil parameters adopted a similar sampling strategy with a sampling density of 40 points for a 6.9 ha field [13].

It is well known that permanent pasture as well as forestland can be used to assess reference fallout values [14]. In the present study an undisturbed forest was selected to assess the reference inventory of fallout ^{137}Cs because no grassland left idle since the early 60's could be found and used for that purpose. The reference inventory of ^{137}Cs fallout was then estimated from 9 samples collected in three different undisturbed forested sites located next to the field under investigation.

2.3. Sample preparation, radionuclides activities measurements and assessment of soil redistribution

Soil samples were dried and sieved through a 2 mm mesh. Soil organic matter content (SOM (%)) was analysed and the ^{137}Cs measurements were carried out on the fine fractions (<2 mm) by gamma spectroscopy. Counting times ranged between 10,000 and 50,000 seconds, depending on the ^{137}Cs activity of the soil. This was sufficient to obtain a counting error less than 10% at the 95% confidence level. For each sample, the ^{137}Cs activities (Bq kg^{-1}) were converted to areal activities (Bq m^{-2}) using bulk density. The conversion of the areal activities of ^{137}Cs into soil movement ($\text{t ha}^{-1} \text{ a}^{-1}$) was done using the Mass Balance Model 2 (MBM 2) [15]. For the particle size factor and the relaxation depth, default values of MBM 2 were used. The proportional factor – proportion of the annual radionuclide fallout that is susceptible to mobilisation by heavy rainfall, prior to its incorporation into the soil – that depends on the temporal distribution of the local rainfall in relation to the timing of cultivation, was preset at 0.8 due to the snowing period (5 to 6 months/year) and field conditions.

2.4. Spatial analysis of ^{137}Cs , SOM content and soil redistribution

The spatial distribution of ^{137}Cs , SOM content and soil movement was analyzed and described using geostatistics and variography concepts. Two different spatial interpolation methods were used.

2.4.1. Inverse Distance Weighting (IDW)

IDW is a deterministic estimation method where unknown values are determined by a linear weighted moving averaging of values at known sampled points. The formula used for IDW is:

$$Z^*(x_a) = \sum_{b=1}^n \lambda_b \cdot Z(x_b) \quad (1)$$

where: $Z^*(x_a)$ is the estimated value Z for location x_a , λ_b is the weighting factor assigned to the known variable Z for location x_b and n is the number of observations. The weighting factor λ_b is based on the inverse of the distance between locations of observed and estimated values [8]:

$$\lambda_b = \frac{1/d_b^\alpha}{\sum_{b=1}^n 1/d_b^\alpha} \quad (2)$$

where d_b is the distance between the measurement points of b and the points being estimated and α is the power. In IDW, the samples closer to the unsampled location are more representative of the value to be estimated than samples further away. In this study the value of the weighting power was set to 2.

2.4.2. Ordinary Kriging (OK)

OK is the most popular type of Kriging. The difference between IDW and OK lies in the way the weighting factor is calculated. In Kriging weights are based on the spatial structure of the data, and not only on the distance between the measured points. Structural analysis involves describing and modeling the estimated variogram. The variogram is a mathematical description of the relationship between the variance of pairs of observations, and the distance separating these observations (h). It describes the between-population variance within a distance class according to the geographical distance between pairs of populations.

The fitted curve minimizes the variance of the errors. The variogram model is used to define the weights of the Kriging function and the semivariance is an autocorrelation statistic defined as:

$$\gamma(h) = \frac{1}{2N(h)} \sum_{i=1}^{N(h)} \{Z(x_i) - Z(x_i + h)\}^2 \quad (3)$$

where: $\gamma(h)$ is the semivariance for interval distance class or lag interval h . For more information on the concepts of geostatistics see paper [10], which complements Chapter 2 in Zapata (2002) [2] on site selection and sampling design.

The different spatial interpolation methods IDW power 1, IDW power 2 and OK were first compared to assess the ^{137}Cs budget in this field. Furthermore, after demonstration of spatial autocorrelation dependence, the OK method was used to map SOM content and soil movement. Spatial continuity of the parameters was investigated by calculating semivariograms. Four semivariogram models (spherical, Gaussian, exponential and linear) were considered. Geostatistical and spatial correlation analysis was performed with GS⁺ version 7 software [16]. Afterwards the different variographic parameters and fitted models were introduced into the GIS software Surfer 8.00 [17]. A spatial soil movement distribution was produced through mapping, using OK interpolation. On the basis of the resulting map, a sediment budget was also produced, using the Surfer 8 package.

3. RESULTS AND DISCUSSION

3.1. Descriptive statistics of the dataset and relationship between SOM and ^{137}Cs

The SOM content ranged from 2.3 to 7.3% with an average of $4.3 \pm 0.4\%$ (average \pm 95% confidence interval). The mean value of the ^{137}Cs reference sites was estimated at 2970 ± 110 Bq m⁻² with a coefficient of variation of 4% ($n = 9$). The ^{137}Cs activity in the agricultural field varied from 531 to 4180 Bq m⁻² with a mean value of 2034 ± 745 Bq m⁻² (mean \pm SD). A significant relationship between SOM and ^{137}Cs surface inventory was found [18]:

$$Y = 0.0867 X^{0.5487} \quad (4)$$

$(n = 42; r^2 = 0.63; p < 0.001)$

where: Y is the SOM (%) and X the ^{137}Cs areal activity (Bq m⁻²).

Soil erosion is a selective process and the spatial redistribution of soil should be translated into soil depletion in eroding areas, and into enrichment in sedimentation areas. Therefore, soil degradation through erosion is associated with soil quality depletion that will decrease crop productivity. Similar results underlining a significant relationship between SOM and ^{137}Cs were found by other authors under different climatic conditions [19,20,21].

3.2. Spatial autocorrelation of SOM, ^{137}Cs and soil movement

Experimental variograms for ^{137}Cs and SOM were fitted to theoretical models using their average semivariance of four distance values (11, 25, 41, 55 m) estimated with 36, 41, 131 and 100 pairs, respectively. The experimental variograms for soil movement, after conversion of the ^{137}Cs activity using the MBM 2, were fitted using the average semivariance of five distance values (11, 32, 48, 71, 89 m) estimated with 42, 87, 158, 156, and 100 pairs, respectively. The number of pairs represents the average variogram value for the group of pairs separated by a specified distance (h). The value of the variable varies similarly in all directions and the semivariance depends only on the distance between sample points. The geo-statistical and key parameters of the best-fit model determined by the variogram analysis for SOM, ^{137}Cs and soil movement are indicated in (Table 1).

TABLE 1. VARIOGRAM PARAMETERS AND PARAMETERS VALIDITY

	^{137}Cs inventory	SOM content	Soil movement
Best –fit model	Isotropic spherical	Isotropic spherical	Isotropic spherical
Range (m)	30	38	65
Sill	408 kBq m ⁻²	1.99%	197 t ha ⁻¹ a ⁻¹
Nugget	17 kBq m ⁻²	0.362%	39 t ha ⁻¹ a ⁻¹
R ²	0.91	0.95	0.87
Nugget to sill ratio (%) ^a	4	18	20
Spatial dependence ^b	Strong	Strong	Strong

^a Nugget to sill ratio (%)=(Nugget semivariance/total semivariance) x 100; ^b Spatial dependence was defined as strong, moderate, or weak for nugget to sill ratios < 25, 25 to 75, or > 75, respectively, and weak if the best-fit semivariogram model R² was lower than 0.50 [13].

The nugget variance information from the variogram integrates the various sources of unexplained error and uncertainty: measurement error, sampling error, inter-sample error and unexplained and inherent variability and give also an indication of short distance variation. The sill corresponds to the model asymptote (scale and the nugget variance) and should be equal to the variance of the data set.

All semivariograms are well-structured with a small nugget effect. Effectively, each variogram showed a strong spatial dependence for soil movement, ^{137}Cs activity, as well as for SOM.

In general, the number of points needed for reliably estimating variogram depends on the accuracy required versus resources available for the survey. Table 1 results (e.g. small nugget value, strong spatial dependence) confirm that the number of samples and the sampling density is sufficient to capture the spatial variability of ^{137}Cs redistribution in that field. It proves clearly that the sampling strategy along seven transects was adapted to the field condition.

3.3. Isotope budget assessment using OK, IDW 1 and IDW 2

The spatial redistribution of ^{137}Cs was estimated by the spatial interpolation methods OK, IDW 1 and IDW 2 to produce contour maps. A radioisotope budget was established for the 2.16 ha agricultural field under investigation. It was estimated that around 2×10^7 Bq of ^{137}Cs was missing, around 30% of the total fallout since the first major introduction of ^{137}Cs in the global environment (1954), and has been exported by physical processes (runoff and erosion processes) from the field [10]. This represents a loss of around 0.62% per year of the initial ^{137}Cs inputs during the 1954-2003 period. Overall similar results were obtained with the different interpolation methods. However, the relative importance of the ^{137}Cs intervals is different from one interpolation to the other. This has an impact in terms of the magnitude and spatial distribution of erosion rates that could be calculated from the ^{137}Cs redistribution data. The cross-validation analysis showed that in the case of spatially structured data, OK is a better interpolation method than IDW 1 or IDW 2 for the mapping FRN landscape redistribution [10]. Effectively, IDW 1 and IDW 2 models are currently used to spatialize data by scientists especially when they are not familiar with geostatistics concept. But as demonstrated in many environmental studies using geostatistics – if there is a spatial structure – Kriging has to be used in order to integrate the spatial dependence of the data [10].

3.4. Sediment budget assessment using OK

After conversion of the ^{137}Cs data into soil movement and interpolation with OK in order to take into account the structure of the data, a complete soil movement budget (Table 2) was calculated based on the resulting soil redistribution map (see Fig. 3).

The data showed that around 85% of the field was affected by a high erosion rate exceeding $6 \text{ t ha}^{-1} \text{ a}^{-1}$, the suggested soil loss tolerance level for most Canadian soils [22]. The sediment delivery ratio (SDR), which corresponds to the ratio between the net erosion rate and the gross erosion, represents 99% (Table 2). This means that over the 49 year period 1954-2003 99% of the sediment mobilized in the study area effectively leaves it. This high value could be explained by the combined effects of snow melt erosion, water erosion and tillage erosion, and also by the fact that erosion areas represent 98% of the field surface and sedimentation only 2%.

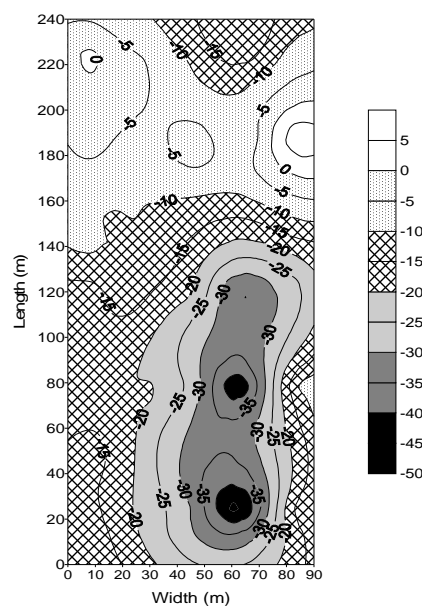


FIG. 3. Map of soil movement ($\text{t ha}^{-1} \text{ a}^{-1}$) in the studied field using OK interpolation.

TABLE 2. SEDIMENT BUDGET INFORMATION

Summary of soil movement statistics	
Maximum erosion rate (t ha ⁻¹ a ⁻¹)	62
Maximum sedimentation rate (t ha ⁻¹ a ⁻¹)	17
Erosion area (%)	98%
Sedimentation area (%)	2%
Sediment budget	
Gross erosion (t ha ⁻¹ a ⁻¹)	16.7
Net erosion rate (t ha ⁻¹ a ⁻¹)	16.6
Sediment Delivery Ratio (SDR)	99%

Soil texture analysis revealed no significant variation between sampling points affected by erosion and sedimentation processes. So a clear protocol is needed to estimate soil selectivity processes for using any conversion model.

4. CONCLUSIONS

This study confirms that the ¹³⁷Cs technique coupled with geostatistics and variography can be a reliable complement to more conventional methods for assessing erosion and sedimentation and its impact on soil quality:

- A significant correlation was found between ¹³⁷Cs and SOM ($r^2 = 0.63$; $p < 0.001$);
- SOM, ¹³⁷Cs/soil redistribution semivariograms are well-structured with a small nugget effect demonstrating a strong spatial dependence;
- Based on this spatial structure a ¹³⁷Cs budget and sediment budgets were established using Ordinary Kriging. The Sediment Delivery Ratio for the 49 year period 1954-2003 was estimated at 99%.

Geostatistics can be applied to soil parameters, such as ¹³⁷Cs (or all other FRN like ⁷Be and ²¹⁰Pb), SOM content as well as soil movement processes, and then used to optimise the spatial interpolation and mapping of data. The use of spatial analysis techniques and tools helps to improve the interpretation and representation of spatially distributed data for better understanding the impact of land and water management practices on soil redistribution, so that the best and most cost-effective conservation practices can be identified for maximum efficiency in terms of soil and water conservation.

Spatialisation of soil movement variability through geostatistics is a first step towards an efficient resource management policy and towards implementing conservation actions successfully. However, these spatial based approaches need to be further developed and refined using adapted protocols and tools like GIS and geostatistics under a wide range of environmental conditions.

ACKNOWLEDGEMENTS

This study was conducted as laboratory support to the IAEA Co-ordinated Research Project D1.50.08 'Assess the effectiveness of soil conservation measures for sustainable watershed management using fallout radionuclides'. The authors acknowledge Mr. Felipe Zapata & Mr. Gerd Dercon (SWMCN) and Mr. Gudni Hardarson, Head of the Soil Science Unit for editorial comments and suggestions.

REFERENCES

- [1] MABIT, L., BERNARD, C, Study of water erosion processes using radioisotopes, IAEA-Soils Newsletter, Laboratory Activities – Research **28** (2005) 20-21.
- [2] ZAPATA, F. (Ed), Handbook for the assessment of soil erosion and sedimentation using environmental radionuclides. Kluwer Ac. Publ., Dordrecht (2002).
- [3] INTERNATIONAL ATOMIC ENERGY AGENCY, Report of the third Research Co-ordination Meeting of the Coordinated Research Project “Assess the effectiveness of soil conservation techniques for sustainable watershed management using fallout radionuclides”, Vienna (2006).
- [4] RITCHIE, J.C., RITCHIE, C.A. Bibliography of publications of ^{137}Cs studies related to erosion and sediment deposition, <http://www.ars.usda.gov/Main/docs.htm?docid=15237> (2007).
- [5] MABIT, L., MELERO URZAINQUI M., “Study of ^{137}Cs redistribution at the field scale using geostatistics”, CD-ROM of Third Research Co-ordination Meeting of the Co-ordinated Research Project D1.50.08 “Assess the effectiveness of soil conservation techniques for sustainable watershed management using fallout radionuclides”, IAEA, Vienna, presentations n° 23 (2006).
- [6] MABIT, L., The use of geostatistics in environmental sciences to spatialise fallout radionuclides to assess soil erosion/sedimentation (Part 1-Geostatistics concepts), IAEA-Soils Newsletter, Laboratory Activities – Research **29** (2006) 22-23.
- [7] MABIT, L. (2007), The use of geostatistics in environmental sciences to spatialise fallout radionuclides to assess soil erosion/sedimentation (Part 2- a case study), IAEA-Soils Newsletter, Laboratory Activities – Research **30** (2007) 26-27.
- [8] MABIT, L., “Use of Geostatistics to establish soil movement map and sediment budget using Fallout RadioNuclides (FRN)”, Proc. of the 10th International Symposium On River Sedimentation: Effects of river sediments and channel processes on social, economic and environmental safety, 1-4 August 2007, Moscow, **1** (2007) 247-254.
- [9] GOOVAERTS, P., Geostatistical modelling of uncertainty in soil science, *Geoderma* **103** (2001) 3-26.
- [10] MABIT, L., BERNARD, C., Assessment of spatial distribution of Fallout RadioNuclides through geostatistics concept, *Journal of Environmental Radioactivity*, **97** (2007) 206-219.
- [11] MABIT, L., et al., Sediment production using ^{137}Cs and GIS in an agricultural watershed. IAEA-Soils Newsletter, Laboratory Activities – Research **29** (2006) 16-18.
- [12] MABIT, L., et al., Assessment of erosion in the Boyer River watershed (Canada) using a GIS oriented sampling strategy and ^{137}Cs measurements, *Catena*, **71** (2007) 2 242-249.
- [13] DUFFERA, M., et al., Spatial variability of Southeastern U.S. Coastal Plain soil physical properties: Implications for site-specific management, *Geoderma* **137** (2007) 327-339.
- [14] SUTHERLAND, R. A., Caesium-137 soil sampling and inventory variability in reference locations: a literature review, *Hydrological Proceedings* **10** (1996) 43-53.

- [15] WALLING, D.E., et al., "Conversion models for use in soil-erosion, soil-redistribution and sedimentation investigations", Handbook for the Assessment of Soil Erosion and Sedimentation using Environmental Radionuclides. Zapata, F. (Ed)., Kluwer Ac. Publ., Dordrecht (2002) 111-164.
- [16] GAMMA DESIGN SOFTWARE,. GS⁺ Version 7, GeoStatistics for the Environmental Sciences, User's guide, Gamma Design Software, LLC (2004).
- [17] GOLDEN SOFTWARE, Surfer 8, Contouring and 3D Surface Mapping for Scientists and Engineers, User's guide, Golden Software, Inc. (2002).
- [18] MABIT, L., et al., "Application of geostatistics concept in agri-environmental sciences: A case study addressing soil and organic matter redistribution by erosion processes to assess soil fertility and establish sediment budget", Proc. of the International Symposium SOPHYWA, Soil Physics and Rural Water Management-Progress, Needs and Challenges, Vienna (2006) 183-186.
- [19] MABIT, L., BERNARD, C., Relationship between soil inventories and chemical properties in a small intensively cropped watershed, CRA Sciences, Earth and Planetary Sciences **327** (1998) 527-532.
- [20] LI, Y., et al., Changes in soil organic carbon induced by tillage and water erosion on a steep cultivated hillslope in the Chinese Loess Plateau from 1898–1954 and 1954–1998, Journal of Geophysical Research **112** (2007) Article Number: G01021.
- [21] ZHANG, J.H, et al., Distribution of soil organic carbon and phosphorus on an eroded hillslope of the rangeland in the northern Tibet Plateau, China, European Journal of Soil Science **57** (2006) 365-371.
- [22] MABIT, L., et al., Quantification of soil redistribution and sediment budget in a Canadian watershed from fallout caesium-137 (¹³⁷Cs) data, Can. J. Soil Sci. **82** (2002) 423-431.

APPLICATION OF CAESIUM-137 AND BERYLLIUM-7 TO ASSESS THE EFFECTIVENESS OF SOIL CONSERVATION TECHNOLOGIES IN THE CENTRAL HIGHLANDS OF VIETNAM

P.S. HAI, T.D. KHOA, N. DAO, N.T. MUI, T.V. HOA
Center for Environment Research & Monitoring, Dalat Nuclear Research Institute
Dalat

P.D. HIEN
Vietnam Atomic Energy Commission
Hanoi

T.C. TU
National Institute for Soil and Fertilizer
Hanoi

Vietnam

Abstract

Over the last decade large areas in Vietnam have become more vulnerable to erosion due to fast economic changes leading to increasing and often unsustainable land use intensification. In the present study soil erosion rates at medium (40-50 years) and short (event based) term have been assessed for steep farmland protected by or without soil conservation measures in the Central Highlands of Vietnam using fallout radionuclide (^{137}Cs and ^7Be) based techniques. A 2.5 ha mulberry field with a slope gradient of about 15% was selected as study site in the Lamdong province, which is located in the south-east part of the Central Highlands. Widely spaced shrubby contour hedgerows composed of *Leucaena glauca* and *Lantana camara* have been utilized at this site as a soil conservation measure for 22 years. In order to assess the effectiveness of additional novel soil conservation measures, such as the use of Vetiver grass barriers (*Vetiveria zizanioides* L.), additional research plots were installed in the year 2000 on a field with a slope gradient of about 15%, adjacent to the previous study site. On the mulberry field, where widely spaced hedges have been utilized as a soil conservation measure for 22 years, about 55% of the area suffered from erosion with rates varying between 0.6 and 70 t ha⁻¹ a⁻¹ (an average of 31 t ha⁻¹ a⁻¹). Deposition occurred on 45% of the area with deposition rates ranging between 0.2 and 74 t ha⁻¹ a⁻¹, (an average of 36 t ha⁻¹ a⁻¹), resulting in a sediment delivery ratio of only 9%. The medium term erosion rate assessed by the use of the ^{137}Cs radionuclide was 1.2 ± 0.6 t ha⁻¹ a⁻¹. The short term soil erosion rate at this field estimated by ^7Be in 2006 was 1.5 ± 0.24 t ha⁻¹ a⁻¹, coming close to the medium term soil erosion rate. For the mulberry plot without hedgerows, net erosion rates assessed by the runoff plot method in the period of 2000 – 2003 ranged between 21 t ha⁻¹ a⁻¹ and 41 t ha⁻¹ a⁻¹, i.e. 18 to 35 times the net erosion rate at the mulberry field with shrubby hedgerows. The ^{137}Cs and ^7Be techniques were also used for assessing novel soil conservation measures. For the plot without soil conservation, soil erosion could be observed at all sampled points, with medium term erosion rates ranging between 1 t ha⁻¹ a⁻¹ and 35 t ha⁻¹ a⁻¹ (the average erosion rate was 23 ± 1 t ha⁻¹ a⁻¹). The short term soil erosion rate estimated by the ^7Be technique in the year 2005 was 33 ± 6 t ha⁻¹ a⁻¹ for this plot. However, the short term soil erosion rate at the plot with Vetiver grass barriers was for the same year 2 t ha⁻¹ a⁻¹ (estimated by the ^7Be technique), and showed that by using this kind of grass barriers as a soil conservation measure soil erosion was almost completely controlled.

1. INTRODUCTION

The Central Highlands of Vietnam (11° - 16°N, 107° - 108°E) are located at elevations between 150 m - 1500 m a.s.l., covering an area of 57,370 km² or about 18% of the total area of Vietnam. This region is the main producer of agricultural export products such as natural rubber, timber and coffee beans. The Central Highlands are also home to ethnic groups that mainly practice subsistence farming systems. Over the last three decades, governmental programmes helped to establish 'new economic zones' in this region stimulating immigration

from other areas of the country. However, reforestation is not keeping pace with deforestation and large areas have become more vulnerable to erosion under the heavy monsoon rainfalls. Some studies, which were carried out in the period of 1992 - 1997 [1] using conventional runoff plots, reported soil erosion rates ranging between 5 t ha⁻¹ a⁻¹ and 90 t ha⁻¹ a⁻¹ depending on the type of vegetation cover and soil conservation practices. The average soil erosion rates estimated using amounts of sediment in reservoirs varied in some catchments from 3 t ha⁻¹ a⁻¹ to 8 t ha⁻¹ a⁻¹ [2].

In order to control soil erosion, farmers usually use contour hedgerows composed of shrubs, which can be used as well as green manure for the crops in the alleys. For an effective reduction of runoff and improved soil retention, hedgerows are typically 1.0 to 1.5 m wide. However, the land area utilised by these hedgerows is relatively high. Consequently, by the year 2000 in some areas hedgerows have started to be replaced by more narrow green barriers composed of Vetiver grass, a grass species widely used in the tropics for soil conservation purposes. The width of Vetiver barriers is usually about 0.3 – 0.5 m. The land occupied by Vetiver is thus much less than that by the traditional hedgerows.

However, there is a need to assess the effectiveness of this novel soil conservation measure and the more traditional shrubby hedgerows in reducing soil erosion losses. Fallout radionuclides in particular ¹³⁷Cs have been successfully used in soil erosion and redistribution studies [3,4]. A variety of conversion models for soil erosion investigations has been developed [5]. Besides ¹³⁷Cs, which is suitable for soil erosion assessment at medium term (40-50 years), in recent years the radionuclide ⁷Be has also been used for studying short term or event based soil erosion [6,7]. In this study, ¹³⁷Cs and ⁷Be were applied for assessing soil redistribution patterns and rates of soil loss on sloping land cultivated with coffee and mulberry plantations in the Central Highlands of Vietnam.

2. MATERIALS AND METHODS

2.1. Study area

The studies were carried out in coffee and mulberry plantations in the Lamdong province (11⁰20 – 12⁰20 N, 107⁰20 - 108⁰40 E), which is located in the south-east part of the Central Highlands of Vietnam (Fig. 1). The elevation of the study sites varies from 900 m to 1000 m a.s.l. There are two distinct seasons in the study area. The dry season lasts about 5 months, from November to March and the rainy season from April to October. The annual rainfall ranged over the last 25 years between 2145 mm and 5190 mm, and the contribution of rainfall in the dry season to the total rainfall was only between 8 and 25%.

2.2.2. Study sites

The first study site (Fig. 1, Site A) was a field of 60 m wide and 80 m long with a slope gradient of 25%, which is located in a coffee plantation (11° 35' N, 108° 03' E) at an elevation of 980 m above sea level with an average annual rainfall of 2590 mm. The soil type at this site is classified as a Xanthic Ferralsol according to the FAO-UNESCO soil classification system. In this study site the efficiency of Vetiver grass (*Vetiveria zizanioides* L.) as soil conservation measure was assessed and compared with a control without any protection.

The second study site (site B) was a mulberry field of 2.5 ha (11⁰35' N, 107⁰48' E) situated at 900 m above sea level with an average annual rainfall of 2950 mm. The mean slope gradient of the field is about 15%. As soil conservation measures, five 1.5 m wide shrubby hedgerows composed of *Leucaena glauca* and *Lantana camara* were planted along the contour lines in

1982, at a distance of 35-40 m. The hedgerows divided the field into 5 subplots from the upper to the lower slope position. This area was under forest until 1975.

In order to further assess the effectiveness of soil conservation by different types of hedgerows or barriers, an additional experiment was implemented in the year 2000 on a mulberry field adjacent to the site B. Each plot had an area of 405 m² (13.5m × 30m) and a slope gradient of about 12 – 15%. In each plot four 30 cm wide hedgerows or barriers were planted 7 metres apart for soil conservation. Vetiver grass (*Vetiveria zizanioides* L.), mimosa (*Mimosa pudica* L.) and cherry tree (*Prunus fruticosa*) were the species used for establishing the hedgerows or barriers. A fourth plot was used as a control (no hedgerows). A ditch was dug at the bottom end of each plot for retaining eroded materials, which were collected twice per year for assessing the soil erosion rate.

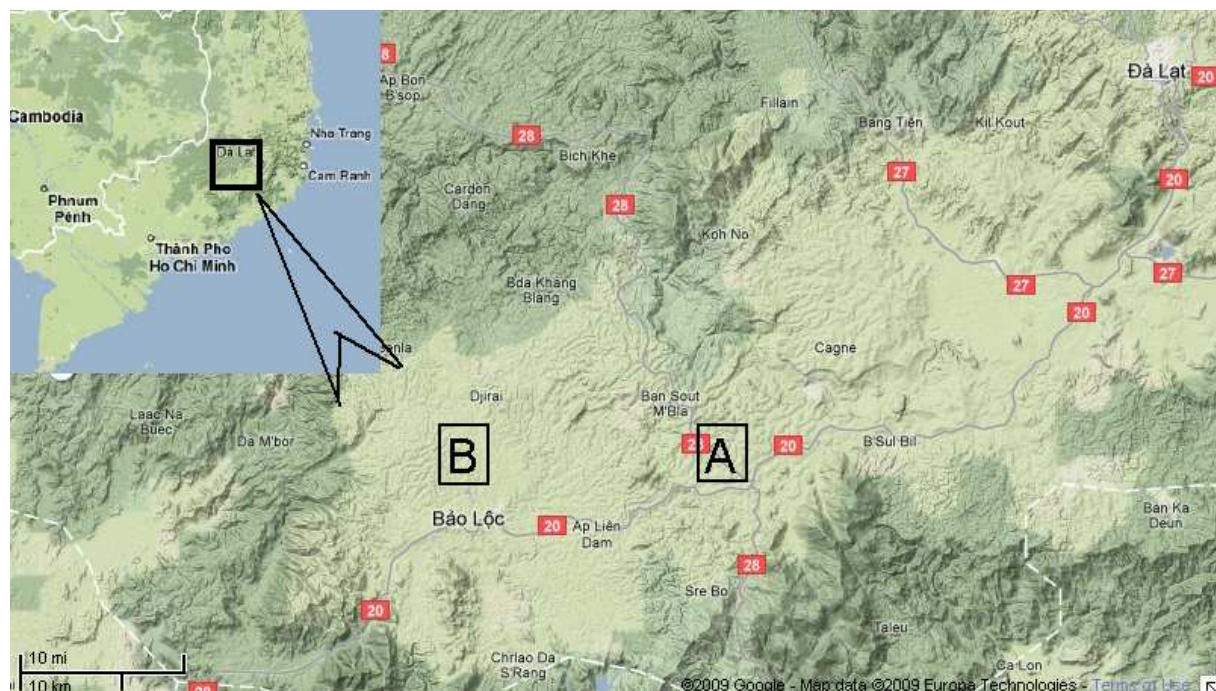


FIG. 1. The location of the study areas in the Central Highlands of Vietnam.

2.3. Experimental methods

2.3.1. Soil sampling method for the ¹³⁷Cs and ⁷Be analysis

For the assessment of the redistribution pattern of ¹³⁷Cs and ⁷Be in site A in the coffee plantation, bulk soil samples were taken in November 2005 at 28 points along two transects in the plot with Vetiver grass barriers and at 8 points along a transect in the control plot without hedgerows. For the ¹³⁷Cs measurements, soil cores with a diameter of 10 cm were collected to a depth of 30 cm. For the ⁷Be measurements, soil samples were collected using a frame made of steel (thickness 5 mm, width 20 cm, height 40 cm), which allows taking samples in an area of 800 cm² and up to a depth of 5 cm.

With regards to site B in the mulberry field with the 22 year old hedges, the soil redistribution was investigated in March 2004 using ¹³⁷Cs as tracer. At this site, 57 bulk soil cores were collected along 3 transects. Among them 21 cores were in the larger subplot, 1 and 9 cores were in each of the remaining subplots. On each transect, sampling points were separated from each other in the range of 10 – 15 m. Short term soil redistributions within this field

were studied using ^7Be in November 2006. The sampling diagram for ^7Be measurements was the same as that for ^{137}Cs measurements. Bulk soil samples for ^7Be and ^{137}Cs measurements were taken by the same devices as those used at site A.

Both reference sites, needed to convert ^{137}Cs and ^7Be inventories into soil redistribution patterns and soil erosion rates, were located at uneroded spots on neighbouring hills, about 1.5–3 km from the study sites. In total 10 bulk soil samples were collected at each site for determining the mean reference values [8].

At each study site, depth incremental samples at 1 – 2 cm intervals were also collected down to 35cm for assessing the vertical distribution of ^7Be and ^{137}Cs .

2.3.2. ^{137}Cs and ^7Be analysis

Radionuclides ^{137}Cs and ^7Be were determined by gamma spectrometry using high purity germanium detectors with a 30% relative efficiency. Gamma counting usually lasts for 24 hours. For this analysis, all samples were prepared as a fine homogeneous powder and were cast using polyester resin in the desired geometry. Radionuclide ^{137}Cs was measured by its gamma emission at 662 keV and ^7Be was measured at 478 keV.

2.3.3. Conversion models for the assessment of soil erosion rates

For the ^{137}Cs technique the two following conversion models were utilized to estimate soil erosion and deposition rates from the ^{137}Cs measured inventories:

(1) An Empirical Model was developed by the Dalat team using experimental data at 15 runoff plots in the Central Highlands in the period of 1999 – 2005 [9]:

$$Y = 19.275X^{0.998} \quad (1)$$

where Y is soil loss (t ha^{-1}) and X is percentage decrease in the total ^{137}Cs inventory per hectare (%).

(2) The Proportional Model (He and Walling, 1996)[11]:

$$Y = 10 \frac{BdX}{100TP} \quad (2)$$

where: Y is soil loss ($\text{t ha}^{-1} \text{ a}^{-1}$); X is percentage decrease in the total ^{137}Cs inventory in comparison with the reference inventory; d is the ploughing depth or cultivation layer (m); B is the soil bulk density (kg m^{-3}); T is the time elapsed since initiation of ^{137}Cs accumulation (a); P is the ratio of the ^{137}Cs concentration of mobilized sediment to that of the original soil.

(3) A Profile-Distribution Model for converting ^7Be measurements into soil erosion rates:

Based on ^7Be inventories, soil erosion rates were assessed using the assumption that the initial depth distribution of ^7Be fallout inputs within the surface soil is exponential [10]:

$$C_{Be}(x) = C_{Be}(0)e^{-x/h_0} \quad (3)$$

where: x is the mass depth from the soil surface (kg m^{-2}); $C_{Be}(x)$ is the initial concentration of ^7Be at depth x (Bq kg^{-1}); $C_{Be}(0)$ is the initial concentration of ^7Be in the surface soil (Bq kg^{-1}); h_0 is the relaxation mass depth describing the shape of the initial ^7Be depth distribution (kg m^{-2}).

The soil erosion amount R_{Be} was calculated using the following equation, which was inferred from the Profile-Distribution Model (3) taking into account the grain size selectivity associated with the erosion process [10]:

$$R_{Be} = h_0 \ln \frac{PA_{Be,ref}}{PA_{Be,ref} - A_{Be,ref} + A_{Be}} \quad (4)$$

where: $A_{Be,ref}$ is the 7Be reference inventory; A_{Be} is the 7Be inventory; P is the ratio of the 7Be concentration of mobilized sediment to that of the original soil and it is estimated by the method proposed by He and Walling [11]. According to this method, P can be estimated by using the specific surface area of the original soil, S_{sl} ($m^2 g^{-1}$), and that of mobilized sediment, S_{ms} ($m^2 g^{-1}$). An estimate of the specific surface area of a sediment or soil sample can be derived from its particle-size distribution, by assuming spherical particles. In order to determine P factor, five surface soil samples (20 cm wide, 40 cm long, 5 cm depth) were taken at erosion areas, and five surface soil samples (20 cm wide, 40 cm long, 2 cm depth) were taken at deposition areas within each study site. Then all soil samples at erosion areas were mixed together to make one sample for analysis of particle size. The same procedure was applied for soil samples at deposition areas. From the measured particle size distributions S_{sl} and S_{ms} were estimated and the P factor calculated from:

$$P = \left(\frac{S_{ms}}{S_{sl}} \right)^{0.65} \quad (5)$$

The deposition amount R'_{Be} is calculated as:

$$R'_{Be} = \frac{A_{Be} - A_{Be,ref}}{C_{Be,d}} \quad (6)$$

where: $C_{Be,d}$ is the 7Be concentration of the deposited sediment and is estimated by following equation:

$$C_{Be,d} = \frac{A_{Be,ref} (1 - e^{-R_{Be}/h_0})}{R_{Be}} \quad (7)$$

3. RESULTS AND DISCUSSION

3.1. ^{137}Cs and 7Be inventories and depth distribution at reference sites

The depth distribution of ^{137}Cs at the reference sites is shown in Fig. 2. The maximum depth of ^{137}Cs penetration was in the range of 20 – 25 cm for all sites. The majority (> 80%) of ^{137}Cs was contained in the top 10 cm of the soil profiles with a peak in activity concentration at about 2-5 cm depth. This result is consistent with that obtained by Walling et al. [7]. The mean reference inventories of ^{137}Cs at site A and site B obtained from bulk soil cores were $430 \pm 26 Bq.m^{-2}$ and $585 \pm 30 Bq.m^{-2}$ respectively.

Hien et al. [12] described the relationship between the ^{137}Cs inventory at uneroded site i ($Bq m^{-2}$) and latitude L (degree) and annual rainfall AR (m) by following regression model:

$$\ln(i) - \varepsilon = (3.53 \pm 0.09) + (0.092 + 0.004)L + (0.62 + 0.03)AR \quad (6)$$

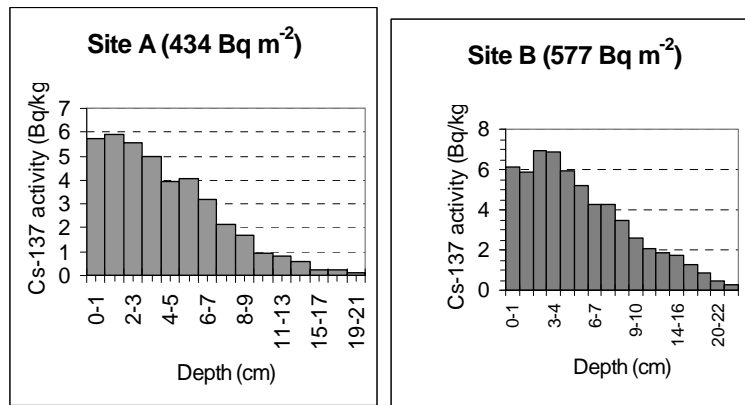


FIG. 2. The depth distribution of ^{137}Cs in undisturbed soils at two uneroded reference sites.

where: ε is the residual and it follows a normal distribution with zero mean ($\bar{\varepsilon} = 0$) and a standard deviation of 0.30. The expression (6) with latitude and rainfall parameters corresponding to study sites gave ^{137}Cs inventories at site A ranging between 365 and 666 Bq m^{-2} (the mean value: 493 Bq m^{-2}) and ^{137}Cs inventories at site B ranging between 457 and 832 Bq m^{-2} (the mean value: 617 Bq m^{-2}). These predicted values were consistent with the measured experimental values.

The depth distributions of ^7Be at these reference sites were shown in Fig. 3. The maximum penetration depth of ^7Be was in the range of 3 – 4 cm for all sites and the majority of ^7Be (> 80%) was concentrated in the top 2 cm of the soil profiles. These results agree with those reported by Walling et al. [7] and He et al. [10]. The ^7Be activity exhibits an exponential decline with depth for both reference sites with high correlation coefficients. This evidence suggests that the Profile-Distribution Model (3) is appropriate for the assessment of soil erosion rates at the study sites. The relaxation mass depth h_0 estimated from these distributions was 8.5 kg.m^{-2} for site A and 7.8 kg.m^{-2} for site B. The mean reference inventory of ^7Be obtained from bulk soil samples at the reference sites was 450 Bq.m^{-2} at the time of sampling and this was used for both sites.

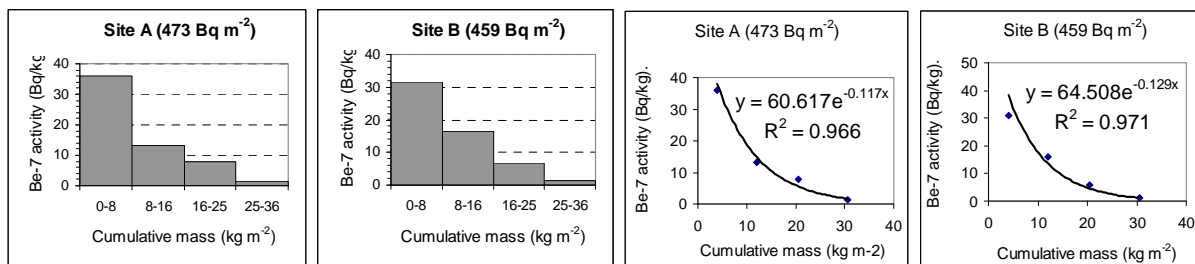


FIG. 3. The depth distribution of ^7Be in undisturbed soil at two reference sites.

3.2. Soil erosion rates at site A

3.2.1. Medium term soil erosion rates assessed by ^{137}Cs

Soil erosion rates within the coffee field assessed by ^{137}Cs inventories using the Empirical Model (1) and the Proportional Model (2) with $P = 1.24$ are given in Table 1. The estimated soil erosion rates varied from 19.5 to 21.6 $\text{t ha}^{-1} \text{a}^{-1}$ for the plot having Vetiver grass barriers and from 20.7 to 25.8 $\text{t ha}^{-1} \text{a}^{-1}$ for the plot without Vetiver grass barriers. The data with regards to soil erosion and deposition rates estimated by the conversion models differed from

each other by 10% to 20%. The mean soil erosion rate for the plot with soil conservation and without soil conservation was $20.4 \pm 0.6 \text{ t ha}^{-1} \text{ a}^{-1}$ and $22.7 \pm 1.2 \text{ t ha}^{-1} \text{ a}^{-1}$, respectively.

After taking uncertainties into account the difference between soil erosion rate for the plot with Vetiver grass barriers and for the other without Vetiver grass barriers was estimated to be $0.5 \text{ t ha}^{-1} \text{ a}^{-1}$. As the ^{137}Cs technique describes the erosion for the last 40-50 years, and as the grass barriers were installed only 5 years ago, it is clear that the ^{137}Cs technique did not reflect accurately the ability of Vetiver grass barriers in retaining eroded soil, and revealed limitations in assessing soil redistribution rates for short term erosion as mentioned by Zapata [4].

TABLE 1. THE NET EROSION RATES ESTIMATED BY CAESIUM-137 AND BERYLLIUM-7 AT SITE A

Study site	Medium term (40-50 year) net erosion rates ($\text{t ha}^{-1} \text{ a}^{-1}$)			Short term erosion rates ($\text{t ha}^{-1} \text{ a}^{-1}$)
	Empirical Model	Proportional Model	Average	
Plot without Vetiver grass barriers	-20.7 ± 1.5	-25.8 ± 1.9	-22.7 ± 1.2	-32.7 ± 6.1
Plot with Vetiver grass barriers	-19.5 ± 0.8	-21.6 ± 0.9	-20.4 ± 0.6	-2.3 ± 0.9

(-) denotes soil erosion and (+) denotes sediment deposition.

The soil redistribution pattern within both plots is shown on Fig. 4. Although the net erosion rates for both plots with and without Vetiver grass barriers are not too different from each other as mentioned above, the difference in soil redistribution patterns within two areas is obvious. Therefore, although the use of ^{137}Cs for a quantitative assessment of the effectiveness of Vetiver grass barriers in retaining eroded soil is not feasible, the qualitative assessment is quite possible in this case. The pattern of medium term soil redistribution reflects areas where local erosion and concentrated flow occurred.

For the plot without Vetiver grass barriers, soil erosion occurred at all sampling points with medium term erosion rates ranging between $1.2 \text{ t ha}^{-1} \text{ a}^{-1}$ and $35 \text{ t ha}^{-1} \text{ a}^{-1}$ (the mean value was $23 \text{ t ha}^{-1} \text{ a}^{-1}$). For the plot with Vetiver grass barriers, about 93% of the area suffered from erosion with the erosion rates varying from $3 \text{ t ha}^{-1} \text{ a}^{-1}$ to $33 \text{ t ha}^{-1} \text{ a}^{-1}$ (the mean value was $22.2 \text{ t ha}^{-1} \text{ a}^{-1}$). Deposition occurred for only 7% of the area with the deposition rates ranging between 1.3 and $1.4 \text{ t ha}^{-1} \text{ a}^{-1}$, resulting in a sediment delivery ratio of 99.4%.

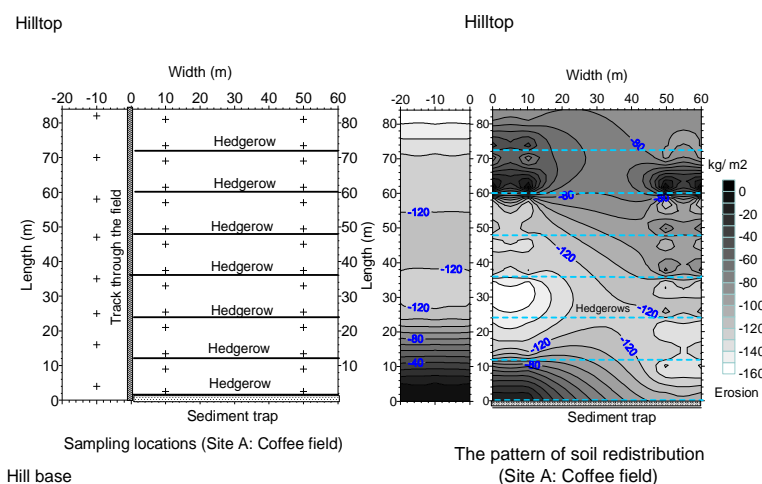


FIG. 4. The pattern of soil redistribution (units of kg m^{-2}) obtained from ^{137}Cs data in the study site A.

3.2.2. Short term soil erosion rates assessed by ^7Be

The fallout radionuclide ^7Be was used for estimating the soil loss at the coffee field over a seven month rainy season in the year 2005. Short term erosion rates estimated by the Conversion Models ($h_0 = 8.5$, $P = 1.65$, $C_{Be,d} = 28 \text{ Bq kg}^{-1}$) for the plot without Vetiver grass barriers and the other with Vetiver grass barriers were $32.7 \pm 6.1 \text{ t ha}^{-1} \text{ a}^{-1}$ and $2.3 \pm 0.9 \text{ t ha}^{-1} \text{ a}^{-1}$ respectively (Table 1). According to data provided by the Centre for Experimental Research on Agriculture & Silviculture of Lamdong, the net soil erosion rate obtained by the conventional run-off plot method for the plot with Vetiver grass barriers was $2.9 \text{ t ha}^{-1} \text{ a}^{-1}$ for 2005, a rate consistent with the value obtained by the ^7Be technique. With the presence of Vetiver grass barriers soil erosion was nearly controlled and the net erosion rate was reduced from $32.7 \text{ t ha}^{-1} \text{ a}^{-1}$ to $2.3 \text{ t ha}^{-1} \text{ a}^{-1}$.

The patterns of short term soil redistribution within both plots are shown in Fig. 5. For the plot without soil conservation, soil erosion occurred for all sampling points with erosion rates ranging between $18 \text{ t ha}^{-1} \text{ a}^{-1}$ and $56 \text{ t ha}^{-1} \text{ a}^{-1}$ (the mean value was $33 \text{ t ha}^{-1} \text{ a}^{-1}$). For the plot with soil conservation practices, sediment deposition occurred for most of the sampling points up-slope of Vetiver grass barriers with deposition rates varying from $1.2 \text{ t ha}^{-1} \text{ a}^{-1}$ to $100 \text{ t ha}^{-1} \text{ a}^{-1}$ (the mean value was $22.4 \text{ t ha}^{-1} \text{ a}^{-1}$), whereas soil erosion occurred for most of sampling points down slope of Vetiver grass barriers with the erosion rates varying from $0.4 \text{ t ha}^{-1} \text{ a}^{-1}$ to $33 \text{ t ha}^{-1} \text{ a}^{-1}$ (the mean value is $8.0 \text{ t ha}^{-1} \text{ a}^{-1}$). The sediment delivery ratio was 34.3% for the plot with Vetiver grass barriers.

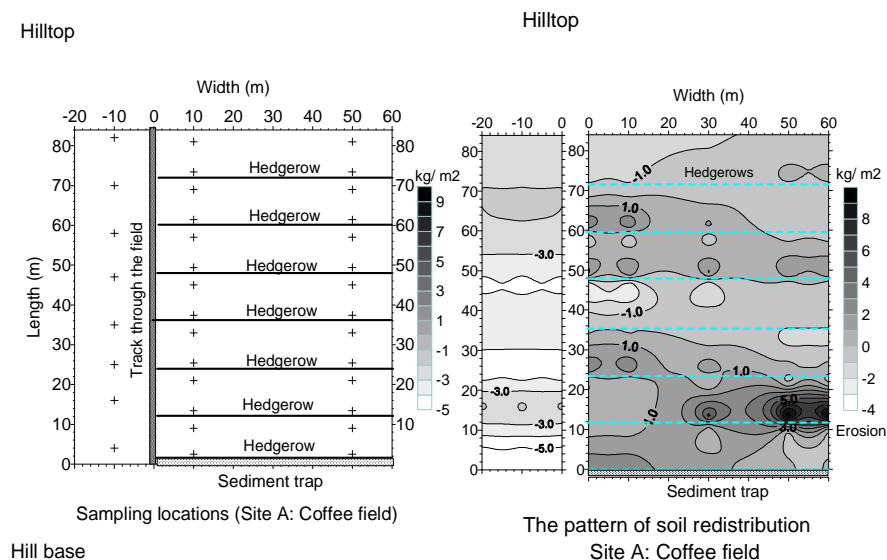


FIG. 5. The pattern of soil redistribution (kg m^{-2}) obtained from ^7Be data in the study site A.

In comparison with the medium term soil redistribution pattern obtained by ^{137}Cs data, the short term soil redistribution pattern obtained by ^7Be for the plot with soil conservation practices suggested that for the last five years soil erosion has been declining due to the presence of Vetiver grass barriers.

3.3.1. Medium term soil erosion rates assessed by ^{137}Cs

Soil erosion and deposition rates assessed by using the Empirical Model and the Proportional Model with $P = 1.27$ for each part of the mulberry field are given in Table 2. Both models produced data on soil erosion and deposition rates with a difference of 5% - 17%. The upper

and largest subplot 1 was eroded the most seriously of all with a soil erosion rate of $11.5 \text{ t ha}^{-1} \text{ a}^{-1}$, whereas deposition was recorded for subplots 2 and 3 with deposition rates of 21.7 and $1.0 \text{ t ha}^{-1} \text{ a}^{-1}$ respectively. The data suggest that most eroded soil from subplot 1 was retained in subplots 2 and 3. Soil loss also occurred on subplot 4 with an erosion rate of $2.5 \text{ t ha}^{-1} \text{ a}^{-1}$, resulting in deposition at subplot 5 with a deposition rate of $0.29 \text{ t ha}^{-1} \text{ a}^{-1}$. The net erosion rate for the 2.5 ha mulberry field was $1.20 \pm 0.55 \text{ t ha}^{-1} \text{ a}^{-1}$ for the time scale of 40-50 years.

TABLE 2. SOIL EROSION AND DEPOSITION RATES ESTIMATED BY CAESIUM-137 AND BERYLLIUM-7 AT SITE B

	Medium term (40-50 year) net erosion rates ($\text{t ha}^{-1} \text{ a}^{-1}$)			Short term erosion rates ($\text{t ha}^{-1} \text{ a}^{-1}$)
	Empirical Model	Proportional Model	Average	
Subplot 1	-10.6 ± 1.6	-12.8 ± 1.9	-11.5 ± 1.2	-3.8 ± 0.6
Subplot 2	19.6 ± 2.4	25.2 ± 3.1	21.7 ± 1.9	4.3 ± 0.5
Subplot 3	1.4 ± 0.2	0.9 ± 0.1	1.0 ± 0.1	-2.6 ± 0.4
Subplot 4	-2.0 ± 0.4	-4.0 ± 0.7	-2.5 ± 0.3	-2.2 ± 0.4
Subplot 5	0.25 ± 0.06	0.34 ± 0.07	0.29 ± 0.05	0.5 ± 0.1
Whole field	-1.07 ± 0.71	-1.40 ± 0.88	-1.20 ± 0.55	-1.5 ± 0.2

(-) denotes soil erosion and (+) denotes sediment deposition.

The pattern of medium term soil redistribution for the mulberry field is shown in Fig. 6. The soil redistribution pattern allowed assessment of erosion and deposition areas and rates for the subplots (Table 3). For the whole field, about 55% of the area suffered from erosion with rates varying from 0.6 to $70 \text{ t ha}^{-1} \text{ a}^{-1}$ (the average was $31 \text{ t ha}^{-1} \text{ a}^{-1}$). Deposition occurred on 45% of the area with rates ranging between 0.2 and $74 \text{ t ha}^{-1} \text{ a}^{-1}$ (the average was $36 \text{ t ha}^{-1} \text{ a}^{-1}$), resulting in a sediment delivery ratio of 9%. The net erosion rate was $1.2 \text{ t ha}^{-1} \text{ a}^{-1}$.

TABLE 3. SOIL EROSION AND DEPOSITION AREAS AND RATES FOR SUBPLOTS ASSESSED BY CAESIUM-137 AT SITE B.

Subplot	Eroded area (%)	Max. erosion rates ($\text{t ha}^{-1} \text{ a}^{-1}$)	Min. erosion rates ($\text{t ha}^{-1} \text{ a}^{-1}$)	Average erosion rates ($\text{t ha}^{-1} \text{ a}^{-1}$)	Deposition area (%)	Max. deposition rates ($\text{t ha}^{-1} \text{ a}^{-1}$)	Min. deposition rates ($\text{t ha}^{-1} \text{ a}^{-1}$)	Average deposition rates ($\text{t ha}^{-1} \text{ a}^{-1}$) ¹
1	62.0	50	0,6	35	38.0	74	3	33
2	-	-	-	-	100	51	0,2	22
3	71.0	32	18	24	29.0	65	61	63
4	58.6	70	15	35	41.4	70	9	41
5	66.5	39	8	27	34.5	65	44	53

3.3.2. Short term soil erosion rates assessed by ⁷Be

The fallout radionuclide ⁷Be was used for estimating the soil loss at the mulberry field over a seven month rainy season in the year 2006. The short term soil erosion and deposition rates for the entire mulberry field and each subplot are given in Table 2 ($h_0 = 7.8$, $P = 1.65$, $C_{Be,d} = 35 \text{ Bq kg}^{-1}$). Soil erosion was reported on subplots 1, 3 and 4 with net erosion rates ranging between $2.2 \text{ t ha}^{-1} \text{ a}^{-1}$ and $3.8 \text{ t ha}^{-1} \text{ a}^{-1}$. As mentioned above, soil deposition occurred for

subplot 3 at medium term ($1.0 \text{ t ha}^{-1} \text{ a}^{-1}$), whereas at short term soil loss occurred for this subplot. Soil deposition also was observed on the remaining subplots. The deposition rates at subplots 2 and 5 was $4.3 \text{ t ha}^{-1} \text{ a}^{-1}$ and $0.5 \text{ t ha}^{-1} \text{ a}^{-1}$, respectively. The net erosion rate for the whole mulberry field was $1.5 \pm 0.2 \text{ t ha}^{-1} \text{ a}^{-1}$ for 2006, close to the medium term erosion rate estimated by ^{137}Cs .

The pattern of short term soil redistribution in the mulberry field is shown on Fig. 6. Soil erosion and deposition areas, and erosion and deposition rates for all subplots assessed by ^7Be inventories are given in Table 4. For the whole field, about 62% of the area suffered from erosion with erosion rates varying from 1.1 to $21 \text{ t ha}^{-1} \text{ a}^{-1}$ (the average was $7.4 \text{ t ha}^{-1} \text{ a}^{-1}$), and deposition occurred for 38% of the area with deposition rates ranging between 1.4 and $16 \text{ t ha}^{-1} \text{ a}^{-1}$ (the average was $8.7 \text{ t ha}^{-1} \text{ a}^{-1}$), resulting in a net erosion rate of $1.5 \text{ t ha}^{-1} \text{ a}^{-1}$ and a sediment delivery ratio of 33%.

Both medium and short term soil redistribution patterns showed that (i) erosion occurred downslope of the hedgerows, (ii) the translocated soil by erosion was trapped in 10 to 15 m wide strips slope upwards from the hedges for all parts of the field. The large and wide subplot 1 was eroded the most seriously of all for both medium and short periods due to the long distance between the hedgerow and hilltop (93 m); (iv) The movement of eroding soil from subplot 1 to subplot 2 was concentrated in a cross section of about 35 – 40 m at the hedgerow.

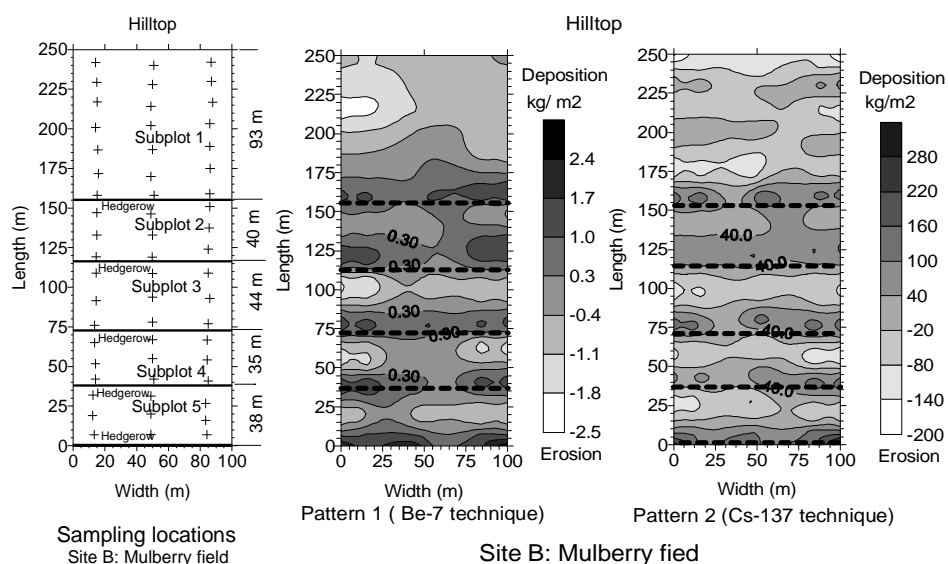


FIG. 6. The patterns of medium- and short term soil erosion rates (kg m^{-2}) in the study site B.

TABLE 4. SOIL EROSION AND DEPOSITION AREAS AND RATES FOR SUBPLOTS ASSESSED BY BERYLLIUM-7 AT SITE B.

Subplot	Eroded area (%)	Max. erosion rates ($\text{t ha}^{-1} \text{ a}^{-1}$)	Min. erosion rates ($\text{t ha}^{-1} \text{ a}^{-1}$)	Average erosion rates ($\text{t ha}^{-1} \text{ a}^{-1}$)	Deposition area (%)	Max. deposition rates ($\text{t ha}^{-1} \text{ a}^{-1}$)	Min. deposition rates ($\text{t ha}^{-1} \text{ a}^{-1}$)	Average deposition rates ($\text{t ha}^{-1} \text{ a}^{-1}$) ¹
1	66.0	20.6	4.3	11.9	34.0	12.9	1.4	6.6
2	21.4	1.5	1.1	1.3	78.6	14.6	1.4	6.7
3	70.4	15.0	2.7	6.6	29.6	13.4	10.3	11.6
4	69.3	11.3	2.7	7.3	30.7	15.7	12.9	14.5
5	43.4	8.2	6.6	7.5	56.6	14.9	1.4	9.4

3.3.3. Runoff plots method

In order to assess the effectiveness of different types of hedgerows as soil conservation measure, four runoff plots were built in a mulberry field adjacent to the study site B in 2000. Soil erosion rates and the effectiveness of the studied soil conservation measures are given in Table 5. Soil erosion rates for the plot without hedgerows ranged between 21 and 41 t ha⁻¹ a⁻¹. The efficiency of hedgerows in retaining soil ranged between 31% and 76%, and increased with the years because of the hedgerow becoming denser and thus acting as better sediment traps. The efficiency of Vetiver hedgerows in retaining soil was the highest. By comparing soil erosion rates at the control plot CT1 with the medium term erosion rate at the study site B, we can conclude that soil erosion at site B was controlled by the shrubby hedgerows and the net erosion rate was reduced considerably.

TABLE 5. SOIL EROSION RATES FOR DIFFERENT SOIL CONSERVATION MEASURES OBTAINED BY RUNOFF PLOTS WITHIN MULBERRY FIELD NEAR SITE B

Plot code	Soil erosion rate (t ha ⁻¹ y ⁻¹) and effectiveness of soil conservation measures (%)							
	2000	%	2001	%	2002	%	2003	%
CT1	41.4	0	25.2	0	21.4	0	25.6	0
CT2	26.3	36.5	11.3	55.2	8.4	60.7	6.2	75.8
CT3	28.4	31.4	13.2	47.6	10.9	49.1	7.8	69.5
CT4	28.2	31.9	13.8	45.2	11.3	47.2	8.3	67.6

CT1: control (no hedges); CT2: Vetiver hedgerows; CT3: mimosa hedgerows; CT4: cherry tree hedgerows

4. CONCLUSIONS

For the coffee plot without soil conservation, soil erosion occurred for all sampling points with medium term erosion rates estimated by ¹³⁷Cs ranging between 1.2 t ha⁻¹ a⁻¹ and 35 t ha⁻¹ a⁻¹, resulting in a net erosion rate of 23 ± 1 t ha⁻¹ a⁻¹. For the coffee plot with Vetiver grass barriers, about 93% of the area suffered from erosion with medium term erosion rates varying from 3 t ha⁻¹ a⁻¹ to 33 t ha⁻¹ a⁻¹ (the average was 22 t ha⁻¹ a⁻¹), and deposition occurred for only 7% of the area with deposition rates ranging between 1.3 and 1.4 t ha⁻¹ a⁻¹, resulting in the net erosion rate of 20.4 ± 0.6 t ha⁻¹ a⁻¹ and a sediment delivery ratio of 99%. The short term soil erosion rate at the plot without Vetiver grass barriers estimated by ⁷Be technique in the year 2005 was 33 ± 6 t ha⁻¹ a⁻¹. By using Vetiver grass barriers as a soil conservation measure, soil erosion was almost completely controlled and the net erosion rate was reduced from 33 t ha⁻¹ a⁻¹ to 2 t ha⁻¹ a⁻¹.

For the mulberry field, where 1.5 m wide contour hedgerows have been utilized as a soil conservation measure for 22 years, about 55% of the area suffered from erosion with erosion rates varying from 0.6 to 70 t ha⁻¹ a⁻¹ (the average was 31 t ha⁻¹ a⁻¹), and deposition occurred for 45% of the area with the deposition rates ranging between 0.2 and 74 t ha⁻¹ a⁻¹ (the average was 36 t ha⁻¹ a⁻¹), resulting in a sediment delivery ratio of 9%. The medium term erosion rate assessed by ¹³⁷Cs radionuclide was 1.2 ± 0.6 t ha⁻¹ a⁻¹. Short term soil erosion rate at this field estimated by ⁷Be in 2006 was 1.5 ± 0.24 t ha⁻¹ a⁻¹, close to the medium term soil erosion rate. For the mulberry plot without hedgerows, net erosion rates assessed by runoff plot method in the period of 2000 – 2003 ranged between 21 t ha⁻¹ a⁻¹ and 41 t ha⁻¹ a⁻¹, from 18 times to 35 times as much as the net erosion rate at the mulberry field with shrubby hedgerows.

ACKNOWLEDGEMENTS

The authors gratefully acknowledge Ms. N. B. Thu, Centre for Soil and Fertilizer Research (Ho Chi Minh City), Mr. N. V. Trung, Centre for Experimental Research on Agriculture & Silviculture of Lamdong (CERASL) for assistance in the field and information on the experimental runoff plots. This research was funded by the Ministry of Science, Technology and Environment (MOSTE) and the International Atomic Energy Agency through the FAO/IAEA Co-ordinated Research Project on 'Assessing the effectiveness of soil conservation techniques for sustainable watershed management and crop production using fallout radionuclides' (IAEA research contract No. VIE – 12331).

REFERENCES

- [1] LUONG, D.L., et al., "Cultivation measures for conserving and improving soil fertility on coffee and some annual crops in the Western Plateau", Sustainable farming on sloping lands in Vietnam (Research Results 1990 – 1997) (THAI, P., NGUYEN, T.S., Eds), Agriculture Publisher, Hanoi (1998) 60-79.
- [2] PHAN, S.H., et al., "Assessment of erosion and accretion in catchment areas based on Pb-210 and Cs-137 concentrations in soil and sediment", Proc. 3ICI, Isotope Production and Applications in the 21st Century (STEVENSON N.R., Ed), World Scientific Publishing Co. Pte., Vancouver (2000) 415–418.
- [3] WALLING, D.E., "Use of ^{137}Cs and other fallout radionuclides in soil erosion investigations: Progress, problems and prospects", Use of ^{137}Cs in the study of soil erosion and sedimentation, IAEA-TECDOC-1028, Vienna (1998) 39–62.
- [4] ZAPATA, F., "The use of environmental radionuclides as tracers in soil erosion and sedimentation investigations: recent advances and future developments", Soil and Tillage Research **69** (2003) 3–13.
- [5] WALLING, D.E., et al., "Conversion models for use in soil-erosion, soil-redistribution and sedimentation investigations", Handbook for the assessment of soil erosion and sedimentation using environmental radionuclides (ZAPATA, F., Ed), Kluwer Academic Publishers, Dordrecht (2002) 111 – 158.
- [6] WALLBRINK, P.J., MURRAY, A.S., "Distribution and variability of Be-7 in soil under different surface cover conditions and its potential from describing soil redistribution processes", Water Resources Research, **32** (1996) 467–476.
- [7] WALLING, D.E., et al., Use of ^7Be and ^{137}Cs measurements to document short- and medium-term rates of water-induced soil erosion on agricultural land, Water Resources Research **35** (1999) 3865–3874.
- [8] PHAN, S.H., et al., "Spatial variability of ^{137}Cs inventory at reference sites and influence of sampling strategy on the uncertainty in estimation of soil erosion rates", Proc. of the fifth National Conference on Nuclear Physics and Techniques, Ho Chi Minh City (2003) 234–237.
- [9] PHAN, S.H., et al., Establishment of relationship between ^{137}Cs loss and soil erosion rates for the region of Central Highlands, J. Vietnam Soil Science **26** (2006) 92–94.
- [10] HE, Q., et al., "Alternative methods and radionuclides for use in soil erosion and sedimentation investigations". Handbook for the assessment of soil erosion and sedimentation using environmental radionuclides (ZAPATA, F., Ed), Kluwer Academic Publishers, Dordrecht (2002) 185 – 215.
- [11] HE, Q., WALLING, D.E., Interpreting the particle size effect in the adsorption of ^{137}Cs and unsupported ^{210}Pb by mineral soils and sediments, Journal of Environmental Radioactivity **30** (1996) 117–137.
- [12] HIEN, P.D., et al., Derivation of ^{137}Cs deposition density from measurements of ^{137}Cs inventories in undisturbed soils, Journal of Environmental Radioactivity **62** (2002) 295–303.

ASSESSMENT OF EFFECTIVENESS OF SOIL CONSERVATION MEASURES IN REDUCING SOIL EROSION AND IMPROVING SOIL QUALITY IN CHINA USING FALLOUT RADIONUCLIDE TECHNIQUES

Y. LI, H.Q. YU, X.C. GENG,
Chinese Academy of Agricultural Sciences, Institute of Environment
and Sustainable Development in Agriculture,
Beijing, China

M.L. NGUYEN
Joint FAO/IAEA Division of Nuclear Techniques in Food and Agriculture,
Soil and Water Management & Crop Nutrition Section
Vienna, Austria

R. FUNK
Leibniz-Centre for Agricultural Landscape Research, Institute
of Soil Landscape Research,
Müncheberg, Germany

Abstract

China is one of the countries perhaps suffering from the most serious soil erosion in the world. Soil erosion and associated sediment production has become a major environmental problem. A wide variety of soil conservation measures, such as re-vegetation, terracing, and conservation agriculture practices, exist in China but they require an effective evaluation to establish specific regional recommendations of integrated soil and water management practices. Using fallout radionuclide techniques, IAEA-funded studies for the assessment of soil erosion and soil conservation have been undertaken in three sites from SW China through to NE China (Baiquan County of North East China, Fengning County of Northern China and Xichang city of South Western China). In the Baiquan County of North East China, the study showed that soil erosion, measured by the fallout ^{137}Cs tracer, decreased by 16% due to terracing and 54% due to contour cultivation as compared to downslope cultivation practice. In the Fengning County of Northern China, the authors assessed the short term impact of conservation agriculture practices on soil erosion and soil quality parameters. The data from ^7Be measurements indicated that all sites with conservation practices contained higher ^7Be inventories than the conventional tillage treatment site. Four years of no tillage with high amount of crop residues reduced soil erosion by 44% and no tillage with low residue amounts reduced soil erosion rates by 33% as compared with conventional tillage practices in the Fengning site. In Xichang city of South Western China, the results showed that shrubs and grasses increased soil organic carbon (SOC) stocks more than trees as compared with bare land. Re-vegetation, especially by using shrubs and grasses increased SOC, available nitrogen (AN) and available phosphorus (AP) indicating a significant positive role of vegetation restoration in improving soil quality. Re-vegetation increased SOC stocks under trees, shrubs and grasses by 61%, 1.53 and 1.86 fold, respectively. The AN under shrubs and grasses increased by 9.5% and 10.5%, respectively, but the mean value of AN was less than the bare land on the entire eroded hillslope. Trees increased AP by 2.9 times and AP in the shrub-land and grassland increased 4.5 and 5.7 fold in SW China.

1. INTRODUCTION

Accelerated soil erosion is considered as a major land degradation process which poses a significant threat to soil quality, food production, and water quality throughout China. This accelerated soil erosion is primarily the result of intensive tillage, over-grazing and deforestation that reduce vegetation cover and result in a loss of surface soil and deterioration of soil quality. Over the last decade a large soil conservation program for erosion control through terracing, contour farming, planting trees, shrubs and grasses on previous sloping cultivated sloping land has been conducted through the northern and western regions of China

[1,2]. According to information from the Water Resources Minister, China has spent billions of Yuan planting trees, converting marginal farmland to forest and grasslands and fighting soil erosion since 2001. Over more than half a million km² of land hillsides have been set aside for afforestation or pastures closed to farmers. A total of 350,000 km² of plants and grassland have been restored and conserved. Eleven major state-level water and soil conservation projects are currently in operation, covering more than 500-plus counties and cities [3]. Research is urgently needed to assess the effectiveness of these soil conservation measures at local and regional scale.

Environmental radionuclides, in particular Caesium-137 (¹³⁷Cs), are an effective way for studying soil redistribution within the agricultural landscape [4,5,6]. Caesium-137 is an artificial radionuclide (half-life 30.2 years) produced as a consequence of atmospheric testing of nuclear weapons, which commenced in the mid 1950s. Since the ¹³⁷Cs technique can be used to provide estimates of soil loss and deposition rates quickly and efficiently, the approach has been used in numerous studies undertaken throughout the world [7]. The ¹³⁷Cs technique was originally used to study soil erosion by water in the United States [8,9,10], and later in Europe; for example by Vanden Berghe and Gulinck [11] in Belgium and Walling and Quine [12] in the United Kingdom. The technique and its important advantages are well described by Vanden Berghe and Gulinck [11], Walling and Quine [12,13], Quine and Walling [14], Zapata and Garcia Agudo [15,16].

The effectiveness of soil conservation measures is commonly described based on soil properties for sustained plant growth [17,18]. The sustainability of soil management is related to a positive soil nutrient balance and the capability to maintain adequate soil conditions for root development. Soil physical parameters such as soil bulk density (BD) and soil nutrients such as soil organic carbon (SOC), available nitrogen (AN) and available phosphorus (AP), are commonly used to characterize constraints for root growth of different vegetation. Nitrate is a key plant elemental nutrient. Available nitrogen is the readily and easily available form of N in soil for root uptake [19]. Nitrogen is a key element for microbial activity, the latter being considered as a major source of soil organic carbon (SOC). Therefore, it is often hypothesized that release of SOC is influenced by changes in N availability.

A study from Pennock [20] indicated that soil redistribution is a major determinant of changes in nutrient status. Mabit and Bernard [21] found a significant correlation between the ¹³⁷Cs and soil organic matter contents. Ritchie and McCarty [22] proposed that both ¹³⁷Cs and SOC are moving along similar physical pathways, but there is a lack of direct field evidence to support this proposal. Another fallout radionuclide for estimation of sedimentation rate is ²¹⁰Pb [23]. The ²¹⁰Pb produced in the soil is termed 'supported' while the additional ²¹⁰Pb from radionuclide fallout is termed unsupported or excess ²¹⁰Pb (²¹⁰Pb_{ex}). Lead-210 with a half-life of 22.3 years is formed in the atmosphere by the normal decay of ²²²Rn, which diffuses as a gas from the soil. The approach employed using unsupported ²¹⁰Pb, which has been relatively constant over time, but does vary spatially [24], is similar to that used for ¹³⁷Cs. In previous studies [25,26], the authors estimated SOC redistribution affected by intensive tillage and linked SOC to profile variations of ¹³⁷Cs and ²¹⁰Pb_{ex} inventories. The authors therefore tried to establish values for these soil quality parameters under different land uses with soil conservation measures by using fallout radionuclides and related techniques.

The objective of this paper is to assess the effectiveness of soil conservation measures in reducing soil erosion and improving soil quality using fallout radionuclides and related techniques in studies conducted in three sites from SW China throughout NE China (Baiquan County of North East China, Fengning County of Northern China and Xichang city of South Western China).

2. MATERIALS AND METHODS

2.1. Study sites

The studies were conducted in three locations: Baiquan County in NE China (47°30'N, 125°51'E), Fengning County in northern China (41°12' N, 116°38' E) and Xichang city in south-western China (27°43'N, 102°13'E) (Fig. 1).

In Baiquan County, NE China, the mean annual precipitation is over 500 mm. The precipitation and runoff are seasonally variable, more than 70% of it occurs in the rainy season from July to September, normally with a high rainfall intensity during a short period, and thus easily producing concentrated runoff and creating severe soil erosion. Water erosion is a recurrent problem on eroded hillslopes of the study area, and resulting in reduction of soil depth from 1 m to about 30 cm, and soil organic matter decrease from 8% to 3.7%.

In Fengning County in northern China, average annual precipitation is 460 mm. In this study site, the soil is classified as dark chestnut soil, and it is affected by severe wind erosion and dust storms caused by heavy wind from north-western direction during the winter and spring seasons when crop cover is not protecting the soil. However, water erosion is also a problem caused by heavy rainfall events, which are common during thunderstorms in the cropping season.

In the Majiasongpo catchment nearby Xichang city in south-western China, climatic conditions are typical of a subtropical monsoon region. The altitudes range from 1500 to 1600 m a.s.l. above the sea level. Mean annual temperature is 17.1°C and mean annual precipitation is 1013 mm. The precipitation and runoff are seasonally variable, with more than 70% of them occurring in the rainy season from June to October. The soil in the study area has a silt-loamy texture with 26% clay, 45% silt and 29% sand. The slope gradient of the eroded sloping land varies from 8% to 70%. Water erosion and overgrazing are recurrent problems on the eroded hillslopes of the study area.

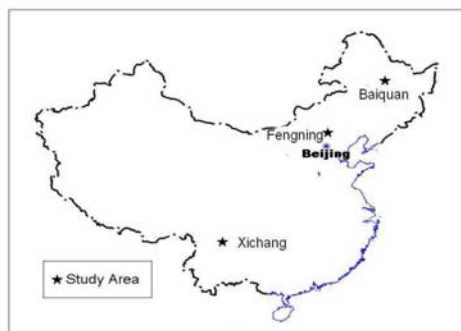


FIG. 1. Study sites to assess the effectiveness of soil conservation measures in reducing soil erosion from Baiquan of NE China, Fengning of northern China, to Xichang of SE China.

2.2. Field survey and soil sampling

In the Baiquan County of NE China, two study catchments were selected. Soil samples were collected on (1) downslope (control) and (2) terraced farmland in Dingjiagou catchment, and (3) contour cropping farmland in Xingsheng catchment to assess the effectiveness of terracing and contour tillage (Figs. 2 and 3). Corn and soybean are major crops grown in the study site. Soil samples were also collected in a sediment deposition site of a gully in the Xingsheng catchment, to assess the effects of soil conservation measures on gully evolution (Fig. 4).

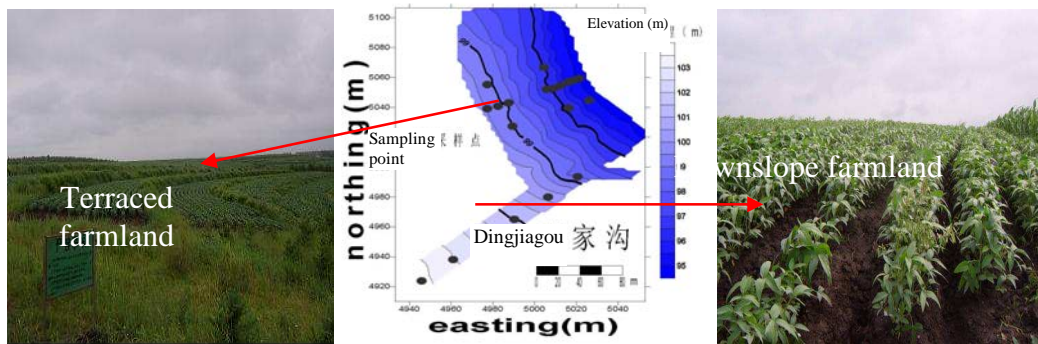


FIG. 2. Soil sampling in terraced fields and downslope farmland in Dingjiagou catchment, Baiquan County, NE China.

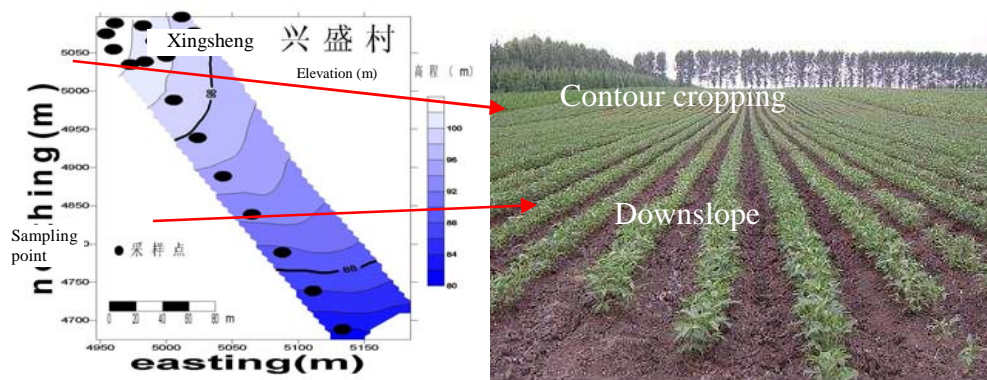


FIG. 3. Soil sampling strategy in downslope and contour cropping farmlands in the Xingsheng catchment, Baiquan County, NE China.

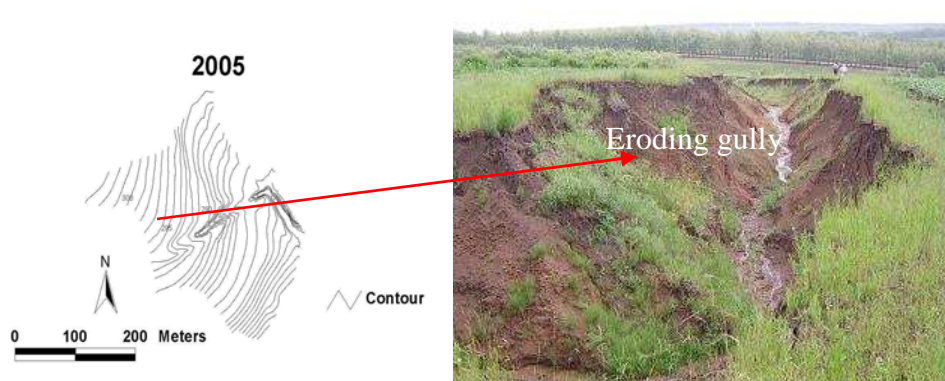


FIG.4. Gully survey in the Xingsheng catchment, Baiquan County, NE China.

In the Fengning County of northern China, the major objective was to evaluate the use of the fallout radionuclide ^{7}Be to assess short term changes in soil redistribution rates and soil quality parameters due to conservation tillage practices in northern China. Five treatments were selected: (1) Ref–undisturbed never-cultivated grassland; (2) CT–conventional tillage, spring wheat-fallow rotation; (3) NT+HR–no-till for 3 years, spring wheat–surface residue cover with 50-56 cm high wheat straw fallow rotation; (4) NT+LR–no-till for 3 years, spring wheat–surface residue cover with 25 cm wheat straw fallow rotation, and (5) T-G–conversion of cultivated land into grassland for 5 years.

In the Majiasongpo catchment of Xichang, SW China, trees (*Eucalyptus*) and shrubs (*Camelliaoleifera Abel*) were planted in 1970s, and grasses (*Eulaliopsis binata*) were left to re-establish as natural regrowth of local species on the eroded hillslopes of the study site. Some areas without vegetation growth (i.e. bare land) can be found on the eroded hillslopes due to overgrazing and erosion. Overgrazing is considered the major driving force for soil loss and soil degradation of the hillslopes. Therefore, four treatments in the Majiasongpo catchment of Xichang were identified: (1) tree-growth area, trees, (2) shrub-growth area, shrubs, (3) grasses, natural regrowth area, and (4) vegetation loss area, bare land. For the determination of soil quality parameters soil samples were taken to a depth of 10 cm in all three replicates of all treatments at the top, upper, mid, lower positions of the eroded hillslope in April of 2004, using a 6.74 cm diameter hand operated core sampler (Fig. 5).



FIG. 5. GPS survey and soil sampling with core and scraper plate in Majiasongpo catchment of Xichang, SW China.

2.3. Laboratory analyses

Soil samples were air-dried, weighed, and divided into two parts, one passing through a 0.15 mm sieve for the measurement of soil physical properties and the other passing through a 2 mm sieve for the measurements of ^{137}Cs , $^{210}\text{Pb}_{\text{ex}}$ and ^7Be activities. Soil samples for measuring ^{210}Pb were sealed in containers and stored for 28 days to ensure equilibrium between ^{226}Ra and its daughter ^{222}Rn (half-life 3.8 days). The amounts of $^{210}\text{Pb}_{\text{ex}}$ of the samples were calculated by subtracting ^{226}Ra -supported ^{210}Pb concentration from the total ^{210}Pb concentrations. Measurements of ^{137}Cs , $^{210}\text{Pb}_{\text{ex}}$ and ^7Be activities were conducted using a Hyper pure coaxial Ge detector coupled to a multi-channel analyzer (Genie-2000 spectroscopy system) and other standard nuclear electronics [25]. Caesium-137 activity was detected at 662 keV peak while total ^{210}Pb activity was determined at 46.5 keV and the one from ^{226}Ra was obtained at 609.3 keV using counting time over 80,000 s, which provided an analytical precision of $\pm 5\%$ for ^{137}Cs and $\pm 8\%$ for ^{210}Pb [26].

Soil organic carbon concentration (*SOC%*) was measured by the combustion method as *SOC* percentage [27]. The soil bulk densities (g cm^{-3}) were calculated with the volume of bulked soil cores and oven-dried soil mass. Available phosphorus (mg kg^{-1}) was determined by sodium bicarbonate (NaHCO_3) extraction and subsequent colorimetric analysis [28]. Available soil nitrogen (mg kg^{-1}) was determined by using the micro-diffusion technique after alkaline hydrolysis [29].

2.4. Data analysis

One-way analysis of variance (ANOVA) was performed to assess the effectiveness of different soil conservation treatments in improving soil quality and reducing soil erosion. All statistical analyses were performed using Statistical Analysis System (SAS) General Linear Model procedures [30].

Using fallout radionuclides to estimate sediment production involves the comparison of the measured inventories (total activity in the soil profile per unit area) at the study sites with an estimate of the total atmospheric input obtained from a 'reference site'. By this comparison one can determine whether erosion (a reduction in fallout radionuclides compared to the reference site) or deposition (an increase in fallout radionuclides compared to the reference site) has occurred. In our studies, the following ^{137}Cs mass balance model was used for estimating soil redistribution rates at individual sampling points on the terraced and cultivated slopes [31]:

$$\frac{dA(t)}{dt} = (1 - \Gamma)I(t) - \left(\lambda + P \frac{R}{d}\right)A(t)$$

where:

$A(t)$ = cumulative ^{137}Cs activity per unit area (Bq m^{-2});

R = erosion rate ($\text{kg m}^{-2} \text{a}^{-1}$);

d = cumulative mass depth representing the average plough depth (kg m^{-2});

λ = decay constant for ^{137}Cs (a^{-1});

$I(t)$ = annual ^{137}Cs deposition flux ($\text{Bq m}^{-2} \text{a}^{-1}$);

Γ = percentage of the freshly deposited ^{137}Cs fallout removed by erosion before being mixed into the plough layer;

P = particle size correction factor.

3. RESULTS AND DISCUSSION

3.1. Evaluating the effectiveness of soil conservation measures in reducing soil erosion in Baiquan County, NE China

3.1.1. Reference inventories of fallout ^{137}Cs and $^{210}\text{Pb}_{\text{ex}}$

In order to make an accurate assessment of reference inventories of ^{137}Cs and $^{210}\text{Pb}_{\text{ex}}$ five sites were sampled on undisturbed and uncultivated land covered by open forest, in Baiquan County, NE China. The average values of ^{137}Cs and $^{210}\text{Pb}_{\text{ex}}$ from the five reference sites were $2532 \pm 670 \text{ Bq m}^{-2}$ and $9550 \pm 2341 \text{ Bq m}^{-2}$, respectively (Fig. 6). The depth profiles of both fallout ^{137}Cs and $^{210}\text{Pb}_{\text{ex}}$ at the reference sites showed a typical exponential decrease with soil depth, and the majority of the ^{137}Cs and $^{210}\text{Pb}_{\text{ex}}$ was concentrated within the soil surface (0-10 cm) in the study area.

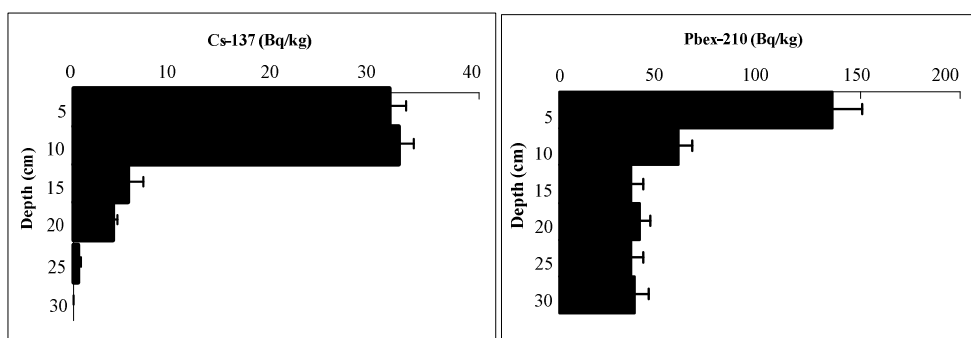


FIG. 6. Depth distribution of ^{137}Cs and excess ^{210}Pb at the reference site in Baiquan County, NE China.

3.1.2. Effectiveness of terracing and contour cropping in reducing soil loss from farmland of Baiquan County, NE China

At this study site of the Baiquan County the authors examined, during July 2005 to August 2006, the effectiveness of two typical soil conservation measures, terracing and contouring cropping, in reducing soil erosion rates by using fallout ^{137}Cs measurements. This study was conducted on gently sloping farmland with terracing and contour ridge farming. Since 1980s, terraced fields have been constructed and cultivated, and most downslope oriented farming has been changed into farming with the crops planted along the contour lines.

Because of the shallow depth of ^{137}Cs in the cultivated soil, soil samples for the determination of the fallout radionuclide inventories were taken to a depth of 15 cm at different slope positions on the farmland without any conservation measures. Additionally, in total five samples were collected at the top, middle and lower position of the terraced hillslopes.

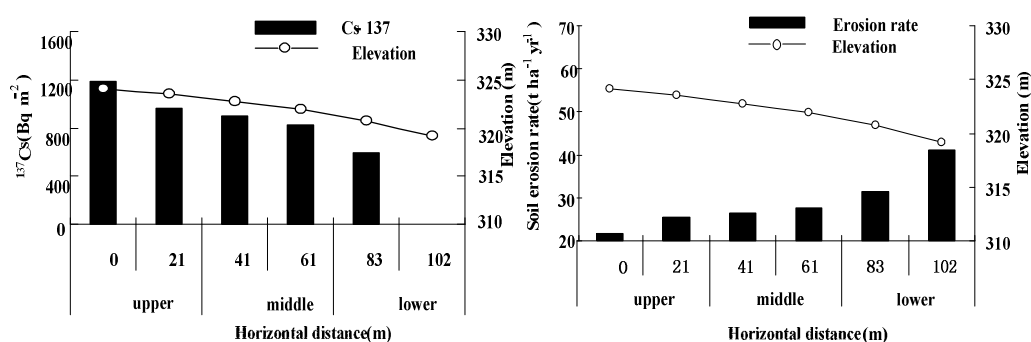


FIG. 7. Inventory of ^{137}Cs and erosion rates at the different slope positions on farmland without any soil conservation measures in the Dingjiagou catchment, Baiquan County, NE China.

For the sloping farmland without any soil conservation measures, the soil at the upper position contained the highest amount of ^{137}Cs whereas the lower position had the lowest ^{137}Cs (Fig. 7). ^{137}Cs inventories of 1079 ± 84 , 862 ± 66 , 296 ± 27 Bq m^{-2} were recorded, corresponding to soil erosion rates of 24, 27 and 36 $\text{t ha}^{-1} \text{a}^{-1}$ at the upper, middle and lower slope positions, respectively. The sediment budget calculated using ^{137}Cs inventories showed high soil losses from the studied eroded sloping farmland without any soil conservation.

Figure 8 shows the distribution of ^{137}Cs inventory and soil erosion rates at the different slope positions on terraced farmland in Dingjiagou catchment, Baiquan County, NE China. The

recorded amounts of ^{137}Cs also decreased from the upper to the lower slope position. ^{137}Cs inventories of 1184 ± 95 , 948 ± 78 , 832 ± 65 Bq m^{-2} were recorded, corresponding to soil erosion rates of 22, 26, 28 $\text{t ha}^{-1} \text{a}^{-1}$ at the upper, middle and lower slope positions, respectively. As compared with farming land without any soil conservation measures, the terracing of fields reduced soil erosion rates by 7.7, 5.4 and 31.5% on the upper, middle and lower slope positions, respectively. Terracing the fields reduced soil erosion rates by 16% for the entire slope (Table 1).

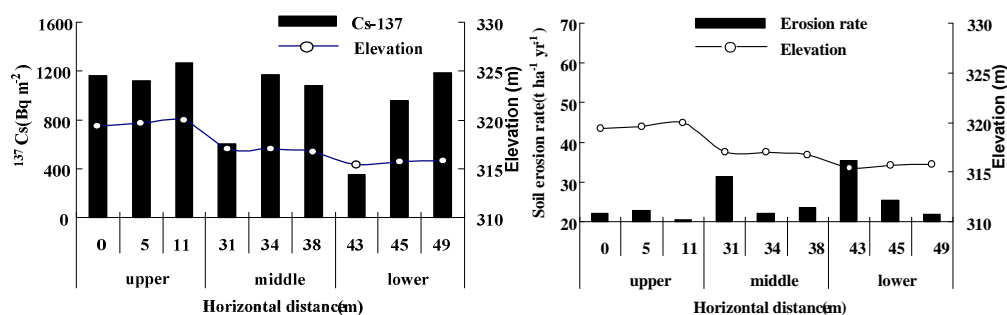


FIG. 8. ^{137}Cs inventory and erosion rates at different slope positions on terraced farmland in the Dingjiagou catchment, Baiquan County, NE China.

TABLE 1. EFFECTIVENESS OF TERRACING FARMLAND ON SOIL EROSION REDUCTION AS COMPARED WITH FARMLAND WITHOUT SOIL CONSERVATION MEASURES

Slope position	^{137}Cs inventory (Bq m^{-2})				Soil erosion rate ($\text{t ha}^{-1} \text{a}^{-1}$)		Soil erosion reduction percent by terraced farmland (%)
	Terraced farmland	Uncertainty	No soil conservation	Uncertainty	Terraced farmland	No soil conservation	
Upper	1184	95	10793	84	22	24	7.7
Middle	948	78	862	66	26	27	5.4
Lower	832	65	296	27	28	36	31.5
Total	988	79	746	59	25	29	15.7

From the distribution of the ^{137}Cs concentration on the farmland without soil conservation practice in the Xingsheng catchment (Fig. 9), it was observed that the upper and lower slope positions contained the higher amount of ^{137}Cs whereas the middle position had the lowest ^{137}Cs content. The inventory of ^{137}Cs was 809 ± 71 , 612 ± 53 , 929 ± 72 Bq m^{-2} on the upper, middle and lower slope positions, respectively. These inventories corresponded to soil erosion rates of 33, 40 and 32 $\text{t ha}^{-1} \text{a}^{-1}$ on the upper, middle and lower slope positions respectively (Fig. 9).

For the farmland with crops grown following the contour lines in the Xingsheng catchment the amount of ^{137}Cs and the corresponding soil erosion rates were not significantly different along the slope (Fig. 10). The inventories of ^{137}Cs were 1053 ± 97 Bq m^{-2} , 1191 ± 116 Bq m^{-2} , 1197 ± 96 Bq m^{-2} corresponding to soil erosion rates on the contour cropping farmland of 23, 22, 23 $\text{t ha}^{-1} \text{a}^{-1}$ on the upper, middle and lower slope positions, respectively. Compared with downslope farmland without soil conservation, contour cultivation reduced soil erosion rates by 41% on the upper, 84% on the middle, and 38% on the lower slope positions, and by 54% for the entire slope (Table 2).

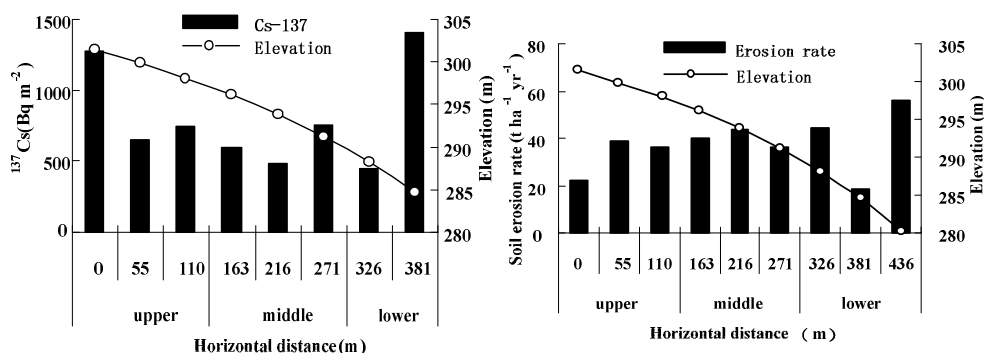


FIG. 9. ¹³⁷Cs inventory and erosion rates at the different slope positions on farmland without soil conservation practice in the Xingsheng catchment, Baiquan County, NE China.

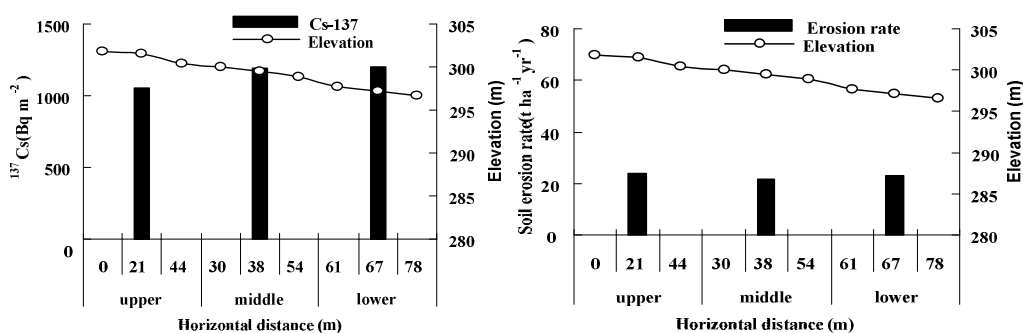


FIG. 10. ¹³⁷Cs inventory and erosion rates at the different slope positions on farmland with contour cultivation in Xingsheng catchment, Baiquan County, NE China.

TABLE 2. EFFECTIVENESS OF CONTOUR CULTIVATION ON SOIL EROSION REDUCTION AS COMPARED WITH FARMLAND WITHOUT SOIL CONSERVATION MEASURES

Slope position	¹³⁷ Cs inventory (Bq m ⁻²)				Soil erosion rate (t ha ⁻¹ a ⁻¹)		Soil erosion reduction percent by contour cultivation (%)
	Contour	Uncertainty	Downslope	Uncertainty	Contour	No soil conservation	
Upper	1151	97	809	71	23	33	40.9
Middle	1191	116	612	53	22	40	83.5
Lower	1197	96	929	72	23	32	37.6
Total	1179	103	784	65	23	35	53.5

3.1.3. Historical reconstruction of gully development in Baiquan County, NE China, using ¹³⁷Cs as tracer and GPS survey

Gullies are extensively distributed in the gently sloping regions of north-eastern China. Gullies have been recognized as contributing significantly to total sediment budgets. In addition, in a range of agroecosystems gullies are effective links between upland areas and channels, transferring both overland flow and sediment rapidly to lower parts of the agricultural landscape. The specific objectives of the present study were: a) to quantify gully erosion rates as affected by land use change over the last 50 years, and b) to assess relative contribution of gully and rill or sheet erosion on sediment production in selected gully

catchments. The study was carried out in the Xinsheng catchment in Baiquan County, NE China, for the period from July 2005 until August 2006. The authors measured the gully system using RTK-GPS (Real time kinetic-global position system) and established a precise Digital Elevation Model (DEM) of the gully catchment (Fig. 11). Sediment production by the gully was estimated from DEMs based on RTK-GPS survey data and the ^{137}Cs dating method. By establishing a sediment chronology within the gully systems using ^{137}Cs dating the authors intended to develop a relationship between gully development and the history of land use in the corresponding catchment. Sediment production by rill or sheet erosion on the slopes of the catchment was estimated by ^{137}Cs measurements.

Based on a comparison of the map from the RTK-GPS survey in 2005 with the contour map from 1983, a clear gully with a total length of 182.5m seems to have been developed during the period of 1983 to 2005 (Figs. 12, 13). According to several individual interviews with local farmers, no gullies were found in 1950s at that site. This information was further supported by a clear ^{137}Cs peak recorded in the profile distribution of ^{137}Cs at the outlet of the Xingsheng gully (Fig. 14). Therefore, the initiation of this gully is estimated to have occurred 42 years ago.

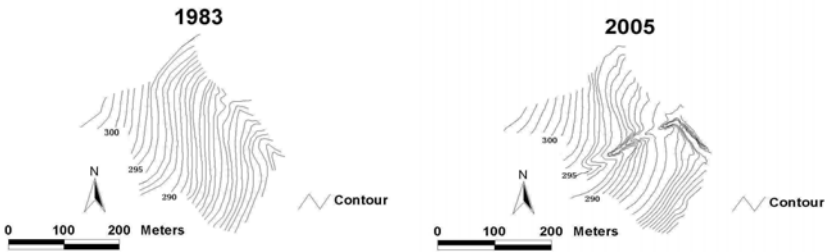


FIG. 11. Contour map from 1983, created by digitizing the topographical map at that time, and map from 2005 derived from GPS survey data in the Xingsheng gully catchment.

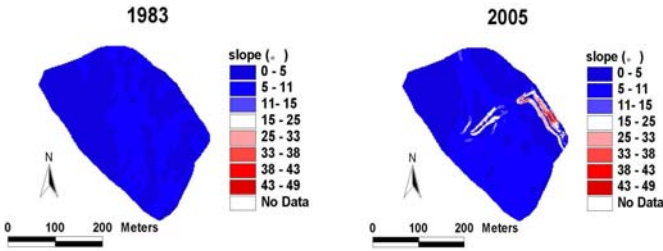


FIG.12. Slope gradient map for 1983 and 2005.

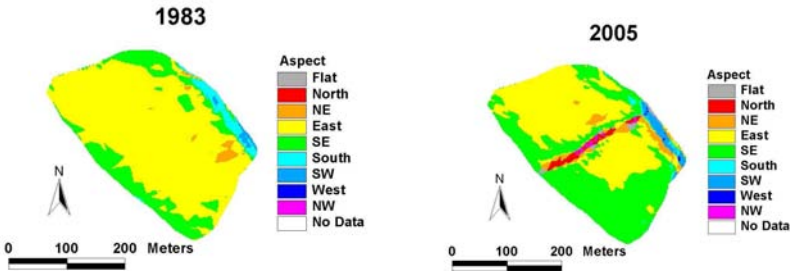


FIG. 13. Slope aspects for 1983 and 2005.

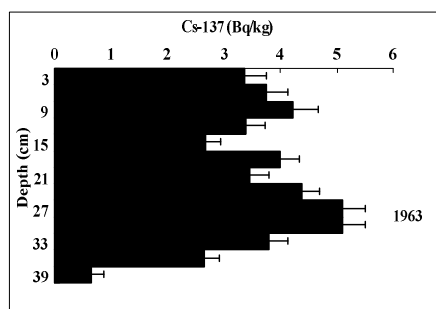


FIG. 14. Profile Distribution of ^{137}Cs at the outlet of the Xingsheng gully in Baiquan County.

Parameters of the Xingsheng gully estimated from the ^{137}Cs dating and RTK-GPS survey are shown in Table 3. Over the last 42 years, the Xingsheng gully developed at a rate of 4.35 m a^{-1} . The total erosion amount of the gully is 4093 t with an annual erosion rate of $77 \text{ t ha}^{-1} \text{ a}^{-1}$. Taking average sediment yields by sheet erosion as $35 \text{ t ha}^{-1} \text{ a}^{-1}$, derived by the ^{137}Cs tracing method, gully erosion contributed 69% of the total sediment yield in the study catchment (Table 3). An average bulk density of 1.3 g cm^{-3} from measurements was used for calculating the sediment yields and gully erosion rate.

TABLE 3. GULLY PARAMETERS OF THE XINGSHENG GULLY ESTIMATED FROM CAESIUM-137 DATING AND GPS SURVEY

*Gully depth (m)		Gully width (m)		Gully length (m)	Drainage area (m^2)	Gully erosion amount (t)	Gully erosion rate ($\text{t ha}^{-1} \text{ a}^{-1}$)
Mean	Maximum	Mean	Maximum				
1.2	6.42	13.2	20.7	182.5	11916	4093	76.47

3.2. Assessing short term impacts of conservation agriculture practices on soil erosion and soil quality parameters in Fengning, Northern China.

The aim of the study in Fengning was to assess the effectiveness of conservation agriculture practices in reducing soil erosion by measurement of ^7Be . The depth distribution of ^7Be concentration under different conservation agriculture practices is shown in Fig. 15. Unlike ^{137}Cs and ^{210}Pb , the ^7Be concentration sharply decreased with soil depth within 0-20 mm top-surface layer, and no ^7Be was detected below 20 mm depth at all treatment sites.

The highest fallout ^7Be inventories were observed in autumn and the lowest in spring (Fig. 16). The coefficients of variation (CV) of ^7Be inventories ranged from 89 to 134% whereas CV values of ^{137}Cs inventories were below 41% for all treatments during the same periods.

A higher inventory of ^7Be under no tillage than under conventional tillage suggested a soil erosion reduction under conservation agriculture practices (Figs. 15 and 16). All sites with conservation agriculture practices contained higher ^7Be inventories as compared with the conventional tillage (CT) treatment site. The mean fallout ^7Be inventory increased by 57% for T-G, 44% for NT+HR, and 33% for NT+LR. As compared with the reference site, conventional tillage operation resulted in more than 50% loss of total ^7Be amounts, which was much higher than the conservation tillage practices (Table 4).

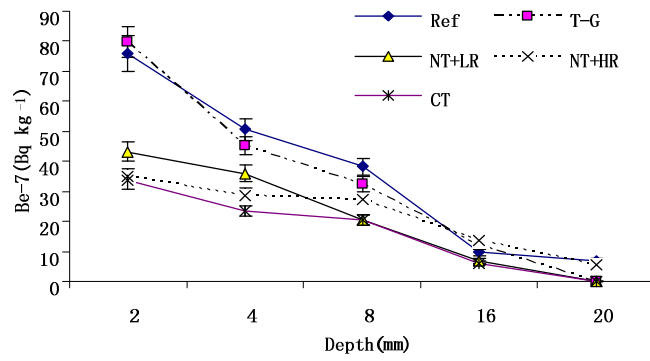


FIG. 15. Depth distribution of ^7Be in soils under different soil management practices: Ref–undisturbed never-cultivated grassland; CT–conventional tillage, spring wheat- fallow rotation; NT+HR–no-till for 3 years, spring wheat–surface residue cover with 50-56 cm high wheat straw fallow rotation; NT+LR–no-till for 3 years, spring wheat–surface residue cover with 25 cm wheat straw fallow rotation, and T-G-conversion of cultivated land to grassland for 5 years.

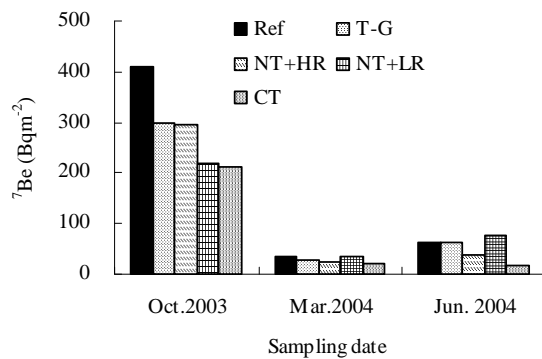


FIG. 16. Seasonal changes of fallout ^7Be under different soil management practices: Ref–undisturbed never-cultivated grassland; CT–conventional tillage, spring wheat- fallow rotation; NT+HR–no-till for 3 years, spring wheat–surface residue cover with 50-56 cm high wheat straw fallow rotation; NT+LR–no-till for 3 years, spring wheat–surface residue cover with 25 cm wheat straw fallow rotation, and T-G-conversion of cultivated land to grassland for 5 years.

TABLE 4. SUMMARY STATISTICS FOR SEASONAL CHANGES IN BERYLLIUM-7 INVENTORIES UNDER DIFFERENT SOIL CONSERVATION PRACTICES

Treatments*	Mean (Bq m ⁻²)	SD (Bq m ⁻²)	CV (%)	Change with CT (%)	Change with reference (%)
Ref	169.3	209.6	123.8	104.5	0.0
T-G	129.8	146.9	113.2	56.8	-23.3
NT+HR	119.6	152.2	127.2	44.4	-29.4
NT+LR	109.7	97.1	88.5	32.5	-35.2
CT	82.8	111.3	134.4	0.0	-51.1

*Ref–undisturbed never-cultivated grassland; CT–conventional tillage, spring wheat- fallow rotation; NT+HR–no-till for 3 years, spring wheat–surface residue cover with 50-56 cm high wheat straw fallow rotation; NT+LR–no-till for 3 years, spring wheat–surface residue cover with 25 cm wheat straw fallow rotation, and T-G-conversion of cultivated land to grassland for 5 years.

3.3. Evaluation of the effectiveness of re-vegetation on eroded hillslopes of SW China

In the Majiasongpo catchment of Xichang in SW China, the authors assessed the long term (15-30 year) effects of vegetation restoration on soil erosion, using fallout ^{137}Cs and excess ^{210}Pb inventories, and soil organic carbon (SOC) content. The study was carried out in the time period of September 2004 - August 2005. The terraced hill slope contained 9 terraced fields, which were constructed in the 1940s. The terraced fields had been cultivated since their construction until the 1950s. The present vegetation, composed of a mixture of trees, shrubs and grasses, was established in the 1970s on the terraced hillslope. Despite the revegetation, at the time of the assessment some areas were still without vegetative protection (i.e. bare land) due to overgrazing and erosion. Overgrazing is considered one of the major driving forces for soil loss and soil degradation in general. Therefore, four typical land uses were included in this study: (1) forest, (2) shrub vegetation, (3) natural grassland (regrowth of local grass species), and (4) bare land. For the determination of soil quality parameters soil samples were taken to a depth of 10 cm at all three replicates of the four treatments at the top, upper, mid, lower position of the terraced hillslope. To ensure that complete profiles of ^{137}Cs and excess ^{210}Pb inventories were included, soil samples were taken to a depth of 40 cm in each terraced field of all three replicates.

Fig. 17 indicates the spatial variability in ^{137}Cs and excess ^{210}Pb , on the terraced hillslope covered sparsely by trees, shrubs or grasses. The top slope position contained the highest amount of ^{137}Cs and excess ^{210}Pb whereas the upper position the lowest for the terraced hillslope. Compared to the values of ^{137}Cs ($802\pm 49 \text{ Bq m}^{-2}$) and excess ^{210}Pb ($7283\pm 1382 \text{ Bq m}^{-2}$) at the reference sites, the upper slope position lost 26% of ^{137}Cs and 58% of excess ^{210}Pb whereas the mid and lower positions of the terraced hillslope did not have a significant loss of ^{137}Cs and ^{210}Pb . However, a significant gain was found at the top slope position, i.e. 36% for ^{137}Cs and 75% for excess ^{210}Pb inventories, which suggested that some additional soil material was delivered from the upland areas of the hillslope.

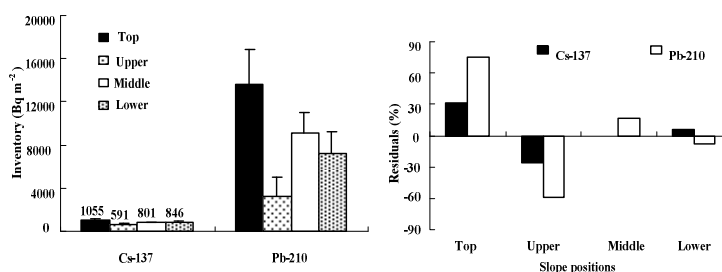


FIG. 17. Spatial pattern in ^{137}Cs and excess ^{210}Pb inventories on the terraced hillslope and their residuals as compared to the values from the reference sites at the Majiasongpo catchment.

Figs. 18-21 summarize the distribution of soil organic carbon (SOC), available nitrogen, available phosphorus, and bulk density grouped by slope position and respective land use on the studied eroded hillslope at the Majiasongpo catchment. The differences between slope positions and land use are clear. Fig.18 shows that re-vegetation increased carbon storage significantly, but shrub and grasses increased SOC more than trees compared with bare land where slope position did not significantly affect SOC. The mean SOC concentration of 22.1 g kg^{-1} and 19.5 g kg^{-1} in the 0-10 cm layer under grass and shrubs, respectively, was significantly higher than the SOC of 12.4 g kg^{-1} under trees. As compared with the SOC under bare land of 7.7 g kg^{-1} , trees increased SOC stocks by 61%, shrubs and grasses increased SOC stocks by a factor of 1.53 and 1.86 times. However, slope position did not significantly affect SOC ($p < 0.05$), except for a difference between the top and lower position.

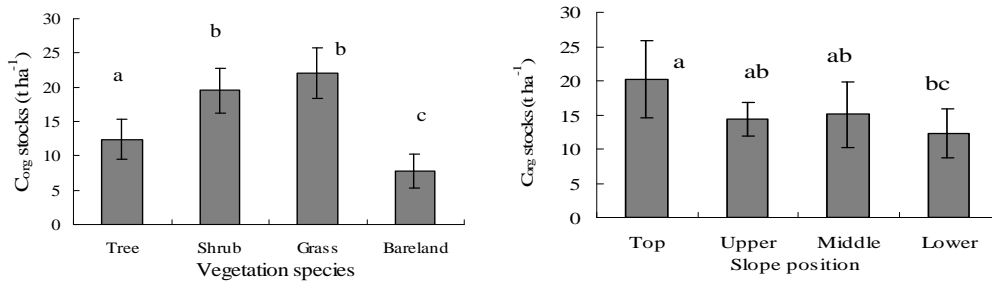


FIG. 18. Distribution of soil organic carbon (SOC) stocks (0-10 cm) grouped by slope position and respective land use on the studied eroded hillslope at the Majiasongpo catchment (The same letters indicate the absence of significant difference).

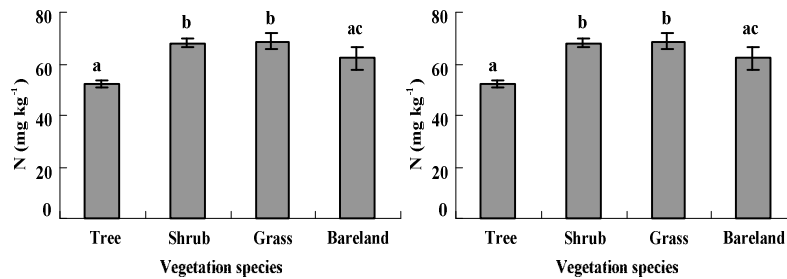


FIG. 19. Distribution of available nitrogen (0-10 cm) grouped by slope position and respective land use on the studied eroded hillslope at the Majiasongpo catchment (Same letters indicate the absence of significant difference).

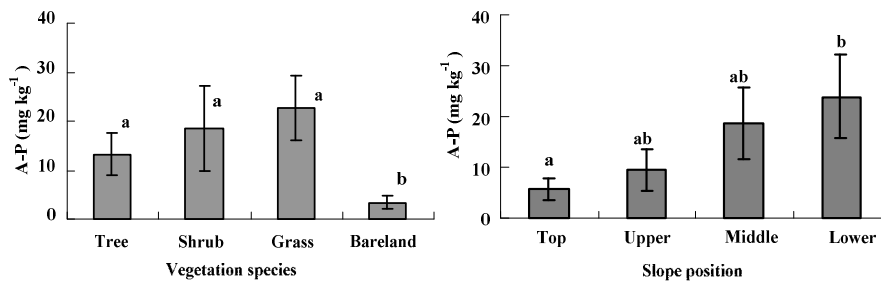


FIG. 20. Distribution of available phosphorus (A-P) (0-10 cm) grouped by slope position and respective land use on the studied eroded hillslope at the Majiasongpo catchment (Same letters indicate the absence of significant difference).

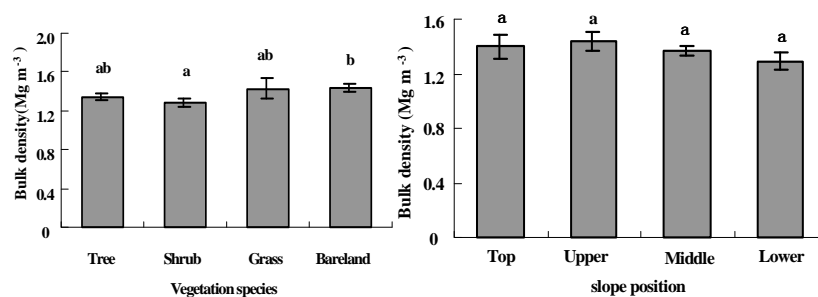


FIG. 21. Distribution of soil bulk density (0-10 cm) grouped by slope position and respective land use on the studied eroded hillslope at the Majiasongpo catchment (same letters indicate the absence of significant difference).

Shrubs and grasses increased available nitrogen (AN) significantly, as compared to bare land, while slope positions did not have any significant effect on AN ($p < 0.05$) (Fig. 20). The mean value of AN with 68.8 mg kg^{-1} and 68.1 mg kg^{-1} in the 0-10cm layer under grasses and shrubs, respectively, was significantly higher than AN under bare land (62.2 mg kg^{-1}). As compared with bare land, shrubs and grasses increased AN by 9.5% and 10.5% respectively.

The available phosphorus (AP) in the bare land was very low with a mean value of 3.38 mg kg^{-1} for the entire eroded hillslope (Fig. 21). Revegetation, especially shrub and grasses, increased AP significantly. The positive effect of vegetation on AP increased in the following order: tree<shrub<grasses, while AP also increased along the downslope direction. The surface soil layer (0-10 cm) under grasses (22.6 mg kg^{-1}) and shrubs (18.5 mg kg^{-1}) was significantly higher in AP than under trees (13.3 mg kg^{-1}). As compared with bare land, soil AP was higher by 2.9 times, by 4.5 and 5.7 times under trees, shrubs and grasses respectively.

As indicated in Fig. 21, the soils (0-10 cm) under shrubs had a lower bulk density (1.28 Mg m^{-3}) than under the adjacent trees (1.35 Mg m^{-3}), grasses (1.43 Mg m^{-3}) or bare land (1.43 Mg m^{-3}). The bulk density of the upper 0-10 cm surface soil under planted trees and natural re-growth grasses did not differ between them. The planted shrubs were the only species that significantly reduced bulk density of the surface soil as compared with the bare land area. Slope positions had no significant relation with the bulk density of surface soil.

4. CONCLUSIONS

Accelerated soil erosion is considered as a major land degradation process resulting in reduced soil quality, increased sediment production and sediment-associated nutrient inputs to the rivers throughout China.

The combined use of fallout ^{137}Cs and $^{210}\text{Pb}_{\text{ex}}$ measurements suggested that shrubs and grasses are more effective in reducing soil erosion and eroded hillslopes than grasses on grazed hillslopes while planting trees alone cannot effectively control soil erosion and improve soil quality in the Xichang study site, SW China.

The net soil erosion rate, measured by the fallout ^{137}Cs tracer, decreased by 16% on terraced farmland as compared to a 53% soil loss reduction using contour tillage in the Baiquan study site, NE China. These results indicate that soil losses can be controlled by changing tillage practices from downslope cultivation to contour cultivation.

The data from ^7Be measurements indicated that four years of no tillage with high crop straw cover reduced soil erosion by 44% and no tillage with low crop straw cover reduced soil erosion rates by 33% as compared with conventional tillage practices in the Fengning site of northern China.

In Xichang city of South Western China, shrubs and grasses increased soil organic carbon (SOC) stocks more than trees, which in turn were higher compared with bare land. Revegetation, especially shrubs and grasses increased SOC, available phosphorus and nitrogen, indicating a significant positive role of the restoration of vegetation in improving soil quality.

ACKNOWLEDGEMENTS

We thank Dr. G. Dercon for commenting on this manuscript. This study was supported by the International Atomic Energy Agency (IAEA) under Research Contract No. 12323 and National Natural Science Foundation of China (No. 40671097 and No. 40701099) and National Key Basic Research Special Foundation Project of China (2007CB407204). Field sampling and soil analysis were carried out with the assistance of X.C. Zhang, F.H. He, D.H. Liu, L. Li, Q.W. Zhang, L. Sun, R. Li, L.Y. Bai and J. Li.

REFERENCES

- [1] UNITED NATIONS CONVENTION TO COMBAT DESERTIFICATION, China national report to implement the United Nation's Convention to Combat Desertification, UNCCD (2002) p. 66.
- [2] FENG, Z. M., et al., Grain-for-green policy and its impacts on grain supply in West China, *Land Use Policy* **22** (2005) 301–312
- [3] MINISTRY OF COMMERCE OF THE PEOPLE'S REPUBLIC OF CHINA, China reverses soil erosion on 960,000 km² of land. <http://english.mofcom.gov.cn/aarticle/newsrelease/commonnews/200706/20070604837264.html>. Last accessed November 2007 (2007).
- [4] WALLBRINK, P.J., A.S. MURRAY, Use of fallout radionuclides as indicators of erosion processes, *Hydrol. Process.* **7** (1993) 297-304.
- [5] ZAPATA, F., The use of environmental radionuclide as tracers in soil erosion and sedimentation investigation: recent advances and future developments, *Soil Till. Res.* **69** (2003) 3-13.
- [6] LI, Y., J. et al. (2003), Evaluating gully erosion using ¹³⁷Cs and ²¹⁰Pb/¹³⁷Cs ratio in a reservoir catchment, *Soil Till. Res.* **69** (2003) 107-115.
- [7] RITCHIE, J.C., RICHIE, C.A., Bibliography of publication of ¹³⁷Cs study related to erosion and sediment deposition, Document Contribution to the IAEA CRP on the Assessment of Soil Erosion Through the Use of ¹³⁷Cs and Related Techniques as a Basis for Soil Conservation, Sustainable Agricultural Production, and Environmental Quality (D1.50.05) and the IAEA CRP on Soil Erosion and Sediment Assessment Studies by Environmental Radionuclides and Their Application to Soil Conservation Measures (F3.10.01) (2000).
- [8] ROGOWSKI, A.S., TAMURA, T., Movement of Cs-137 by run off, erosion and infiltration on the alluvial Captina silt loam. *Health Phys.* **11** (1965) 1333–1340.
- [9] MCHENRY, J.R., Use of tracer techniques in soil erosion research, *Trans. Am. Soc. Agric. Eng.* **11** (1968) 619–625.
- [10] RITCHIE, J.C., et al., „The use of fallout caesium-137 as a tracer of sediment movement and deposition“, *Proc. of the Mississippi Water Resource Conference*, (1970) 149–163.
- [11] VANDEN BERGHE, I., GULINCK, H., Fallout 137-Cs as a tracer for soil mobility in the landscape framework of the Belgian loamy region, *Pedologie* **37** (1987) 5–20.
- [12] WALLING, D.E., QUINE, T.A., Use of 137-Cs measurements to investigate soil erosion on arable fields in the UK: potential applications and limitations, *J. Soil Sci.* **42** (1991) 147–165.
- [13] WALLING, D.E., QUINE, T.A., 1995. „Use of fallout radionuclide measurements in soil erosion investigations“, *Nuclear Techniques in Soil–Plant Studies for Sustainable Agriculture and Environmental Preservation*, IAEA, Vienna, pp. 597–619.

- [14] QUINE, T.A., WALLING, D.E., Rates of soil erosion on arable fields in Britain: quantitative data from caesium-137 measurements, *Soil Use Management* **7** (1991) 169–176.
- [15] ZAPATA, F., GARCIA AGUDO, E., Assessment of soil erosion through the use of ^{137}Cs and related techniques as a basis for soil conservation, sustainable agricultural production and environmental production, IAEA Report on the Third Research Co-ordination Meeting on the Co-ordinated Research Projects (D1-RC-629.3 and F3-RC-644.3), Barcelona, (1999).
- [16] ZAPATA, F., et al., Future prospects for the Cs-137 technique for estimating soil erosion and sedimentation rates, *Acta Geol. Hispanica* **35** (2000) 197–205.
- [17] INTERGOVERNMENTAL PANEL ON CLIMATE CHANGE, *Climate Change 2001: The Scientific Basis*, Cambridge University Press, Cambridge (2001) 12–14.
- [18] JENS, L., et al., Carbon stocks in Swiss agricultural soils predicted by land-use, soil characteristics and altitude, *Agr. Eco. Environ.* **105** (2005) 255-266.
- [19] RASIAH, V., et al., The impact of deforestation and pasture abandonment on soil properties in the wet tropics of Australia, *Geoderma* **120** (2004) 35–45.
- [20] PENNOCK, D.J. FRICK, A.H., The role of field studies in landscape-scale applications of processes models: an example of soil redistribution and soil organic carbon modeling using CENTURY, *Soil Tillage Res.* **58** (2001) 183-191.
- [21] MABIT, L., BERNARD. C., Relationship between soil ^{137}Cs inventories and chemical properties in a small intensively cropped watershed, *Earth Planet. Sci. Lett.* **327** (1998) 527-532.
- [22] RITCHIE, J.C., et al., $^{137}\text{Caesium}$ and soil carbon in a small agricultural watershed, *Soil Till. Res.* **69** (2003) 45-51.
- [23] WALLING, D. E., et al., Using unsupported lead-210 measurements to investigate soil erosion and sediment delivery in a small Zambian catchment, *Geomorphology* **52** (2003) 193-213.
- [24] CANNIZZARO, F., et al., Determination of ^{210}Pb concentration in the air at ground-level by gamma-ray spectrometry, *Appl. Radiat. Isot.* **51** (1999) 239-45.
- [25] LI, Y., et al., Evaluating gully erosion using ^{137}Cs and $^{210}\text{Pb}/^{137}\text{Cs}$ ratio in a reservoir catchment, *Soil Till. Res.* **69** (2003) 107-115.
- [26] LI, Y., Q.W. et al., Using ^{137}Cs and $^{210}\text{Pb}_{\text{ex}}$ for quantifying soil organic carbon redistribution affected by intensive tillage on steep slopes, *Soil Till. Res.* **86** (2006) 176-184.
- [27] NELSON, D.W., SOMMERS, L.E., “Total carbon, organic carbon and organic matter”, *Methods of Soil Analysis. Part 2. Chemical and Microbiological Properties* (PAGE, A.L., Ed.), American Society of Agronomy, Madison (1982) 539–579.
- [28] OLSEN, S.R., et al., Estimation of available phosphorus in soil by extracting with sodium bicarbonate, USDA circular 939, Washington (1954).
- [29] BAO, S.D., *Soil and agricultural chemistry analysis*, Beijing: China Agricultural Press, (2000) 39-58 (in Chinese).
- [30] SAS INSTITUTE, *SAS user’s guide, Statistics, Statistical Analysis System Institute Inc., Cary, NC* (1990).
- [31] WALLING, D.E., HE, Q., Improved models for estimating soil erosion rates from caesium-137 measurements, *J. Environ. Qual.* **28** (1999) 611–622.
- [32] HUNTINGTON, T.G., Carbon sequestration in an aggrading forest ecosystem in the South-eastern USA, *Soil Sci. Soc. Am. J.* **59** (1995) 1459–1467.
- [33] ELLERT, B., GREGORICH, E.G., Storage of C, N, and P in cultivated and adjacent forest soils of Ontario, *Soil Sci.* **1619** (1996) 587–603.

- [34] BASHKIN, M.A., BINKLEY, D., Changes in soil carbon following afforestation in Hawaii. *Ecology* **79** (1998) 828–833.
- [35] POST, W.M., KWON, K.C., Soil carbon sequestration and land use change: Processes and potential, *Global Change Biol.* **6** (2000) 317–327.
- [36] LUGO, A.E., SANCHEZ, M.J., Land use and organic carbon content of some tropical soils, *Plant Soil* **96** (1986) 185–196.
- [37] BOUWMAN, A.F. LEEMANS, R., “The role of forest soils in the global carbon cycle”, *Carbon forms and functions in forest soils*, (MCFEE, W.F., KELLY F.M., Ed), SSSA, Madison (1995) 503-525.
- [38] SIX, J., et al., Measuring and understanding carbon storage in afforested soils by physical fractionation, *Soil Sci. Soc. Am. J.* **66** (2002) 1981-1987.
- [39] LI, Y., LINDSTROM, M. J., Evaluating soil quality-soil redistribution relationship on terraces and steep hillslope, *Soil Sci. Soc. Am. J.* **65** (2001) 1500-1508.
- [40] WU, H. B., et al., Land use induced changes of organic carbon storage in soils of China, *Global Change Biol.* **9** (2003) 305-315.
- [41] LI, Y., et al., Preliminary study on mechanism of plant roots to increase soil anti-scourability on the Loess Plateau, *Sci. China (Ser. B)* **35** (1992) 1085-1092.
- [42] LI, Y, et al., Effectiveness of plant roots on increasing the soil permeability on the Loess Plateau, *Chinese Sci. Bull.* **37** (1992) 1735-1738.

ASSESSING THE IMPACTS OF RIPARIAN ZONES ON SEDIMENT RETENTION IN BRAZILIAN SUGARCANE FIELDS BY THE CAESIUM-137 TECHNIQUE AND WEPP MODELING

O.O.S. BACCHI

Center for Nuclear Energy in Agriculture,
Piracicaba

G. SPAROVEK, M. COOPER, S.B.L. RANIERI

Department of Soils and Plant Nutrition,
"Luiz de Queiroz" College of Agriculture,
Piracicaba

V. CORRECHEL

Federal University of Goias,
Goiania

Brazil

Abstract

Erosion and sediment deposition studies are essential for understanding the functional aspects and impacts of riparian zones on sediment retention. This understanding is useful to improve the related environmental legislation and to increase the probability of success of public intervention in restoring the riparian systems in private lands. However, one of the main difficulties to carry out this approach is the choice of the method to predict soil loss and sediment deposition in complex landscapes. In more recent years, process based models like WEPP are being used for this purpose which has the advantage to be applicable in conditions where no long term statistical relations are available and for environmental studies that also consider soil deposition and sediment enrichment processes (and not only soil loss as estimated by first empirical models). On the other hand, the number of input parameters needed to run process based models increases significantly if compared to statistical models, contributing to rising costs and some times making its practical application unfeasible. Sensitivity analysis can be performed in order to reduce this problem, identifying the more relevant parameters to be calibrated. However, it is necessary to compare the model results with other direct measures of soil erosion and deposition (validation). In this project techniques based on the measurement of fallout radionuclide ^{137}Cs , the soil organic carbon isotopic ratios and soil morphology were used and integrated as tools for this purpose. Comparable results were obtained by ^{137}Cs and WEPP for different slope transects showing abrupt changes from soil loss (sugarcane field) to sediment deposition (riparian forest). Complementary soil carbon isotopic ratio analysis and soil morphology allowed a better interpretation of sediment redistribution along the transects.

1. INTRODUCTION

Riparian zones are typically located between the aquatic and terrestrial ecosystems. They are key areas in ensuring the stability of global biodiversity, serving as protection niches for wildlife, and acting as ecological corridor between forest fragments [1,2,3,4]. Besides its ecological function, these areas, also called 'buffer zones', are considered important for protecting waterways and consequently improving surface water quality. The main mechanism involved in this function is the filtering and trapping of sediments which are produced by erosion in upland agricultural fields. These mechanisms are related to the increase in roughness and water infiltration rate, the presence of root biomass and the good structure of the soil matrix caused by the intense microbiologic activity in the soil [5,6,7].

The Brazilian Environmental Law (Law 4.771/65) protects natural ecosystems by fixing widths of riparian zones which have to be preserved around surface waterbodies, called 'Legally Protected Areas' (LPA). However, the application of Law 4.771/65 has produced many conflicts between land owners and monitoring organisms due to the governmental strategy to preserve natural ecosystems in private lands, based on strict control mechanisms, as well as the lack of the scientific background that ensures the real benefits of fixed widths of riparian zones on water quality improvement, or on maintenance of the landscape biological value [8,3,9].

Some authors [8] believe that these fixed strips are not well linked with the hydrological aspects of the watersheds. For these authors, the riparian zone should vary as a function of the local climate, geology and soils, land use and management and these aspects are not considered in the minimum width established by law. The importance of the width of riparian zones for water resources protection also has been a focus of interest by various researchers [10,11,12]. However, studies conducted in Brazil [13] indicate that the fixed widths of LPA are not always large enough to ensure the filter function for nutrients (mainly Phosphorus and Nitrogen) and sediments carried from agricultural lands.

Erosion and sediment deposition studies are essential for understanding the functional aspects and impacts of riparian zones on sediment retention. This understanding is useful to improve the related environmental legislation and to increase the probability of success of public intervention in restoring the riparian systems in private lands. However, one of the main difficulties to carry out this approach is the choice of the method to predict soil loss and sediment deposition in complex landscapes. Traditional approaches involve direct measurements of soil loss at plot scale, using natural or simulated rainfall. The first empirical erosion models to assess soil loss worked at this relatively small scale and under uniform conditions and were based on statistical relationships between rainfall and runoff parameters (driving force) and soil, crop management and erosion control practices (resistance). This approach is appropriate to predict the on-site impacts of erosion, e.g. the loss of fertile soil layer and the consequent loss in agricultural production. However, this scale does not properly reflect the off-site effects of erosion, which include sedimentation, water eutrophication and contamination by fertilizers and pesticides.

The need to predict the environmental consequences of soil loss, deposition and sediment yield from complex hillslopes, led to the development of a new generation of prediction models [14]. In more recent years, process based models are being used for this purpose [15]. These models have the advantage to be applicable under conditions where no long term statistical relations are available and for environmental studies that also consider soil deposition and sediment enrichment processes (and not only soil loss as estimated by the first empirical models). On the other hand, the number of input parameters in process based models increases significantly if compared to statistical models, contributing to rising costs and sometimes becoming unfeasible its practical application. Sensitivity analysis can help to reduce this problem, by identifying the more relevant parameters to be calibrated. In addition, it is necessary to compare the model results with other direct measurements of soil erosion (validation).

The Water Erosion Prediction Project (WEPP) [16] is a continuous simulation computer program which predicts soil loss and sediment deposition from overland flow on hillslopes. WEPP has been used as a tool for scenario simulation with different buffer zone widths in small watersheds in Brazil, but there was a lack of methods to validate it in the short term. In

the present study the ^{137}Cs technique complemented by soil carbon isotopic ratio analysis and soil morphology studies were used as tools to calibrate and validate the model.

The main objectives of this study were:

(1) To check the efficiency of riparian ecosystems in sediment retention using the WEPP model in a subtropical agricultural area of Brazil, and

(2) To validate the data generated by the WEPP model through the use of the ^{137}Cs technique in combination with soil carbon isotopic ratio analysis and soil morphology studies providing scientific support to Brazilian legislation and contributing to sustainable and agricultural production programs and environmental protection.

2. MATERIALS AND METHODS

2.1. Study areas

The selection of areas was based on the need to find case studies which presented abrupt and clearly marked borders between soil loss and sediment deposition zones, in order to analyze the sensitivity of both the ^{137}Cs technique and the WEPP model to assess the impacts of riparian zones on sediment retention. Contrasting land uses, such as agriculture and forest, were considered ideal.

Six transects were used for this study. Four of them are situated in Iracemópolis (State of São Paulo, Brazil) 22°35' S and 47°33' W. According to Köppen's classification, the climate is of the type 'Cwa', with an annual mean temperature of 21°C and a mean precipitation of 1360 mm per year. The mean altitude is 610 m a.s.l. and the predominant soil is classified as a Rhodic Hapludox according to Soil Taxonomy (Soil Survey Staff, 1993). The main crop of region is sugarcane, which has been continuously grown over more than 50 years. The first transect, called 'Forest Transect 1' (FT-1) consists of an upper slope segment (800 m) cultivated with sugarcane and a lower slope segment (120 m) covered by secondary forest, from the lower edge of the sugarcane field until reaching the water body (reservoir). The second transect, called 'Sugarcane Transect 1' (ST-1) is approximately 1,000 meters long and at the time of the assessment completely cultivated with sugarcane. The transects are 300 m apart and run parallel to each other, having similar slope gradients of about 10%. The third transect (Restoration Transect 1) RT-1 and the fourth transect (Restoration Transect 2) RT-2 are also located in Iracemópolis, 22°35' S 47°31' W, and the soil, climate and topography are similar to the other transects. It is composed of an upper slope segment (460m) cultivated with sugarcane and a lower slope segment (50 m) with a recovered riparian forest. The lower slope segment of RT-1 is covered by an 18 years old forest of native species, and in RT-2 it is covered by a 7 years old forest of similar native species, which edges the margin of a water reservoir. Additional two transects FT-2 (Forest Transect 2) and ST-2 (sugarcane transect 2) with the same dimensions of FT-1 and ST-1 were established in another sugarcane field in Orindiuva-SP (20°14' N; 49°21' W), where the soil is also classified as a Rhodic Hapludox but with a more sandy texture as compared to the other transects. Figure 1 shows the positions of the six studied transects in the field.

Erosion and sediment deposition were studied in the transects FT-1, ST-1, RT-1 and RT-2 by using ^{137}Cs , WEPP, and soil morphology methodologies. Soil carbon isotopic ratio analysis was applied in the transects FT-1 and ST-1. Transects FT-2 and ST-2 were studied using only the ^{137}Cs technique.

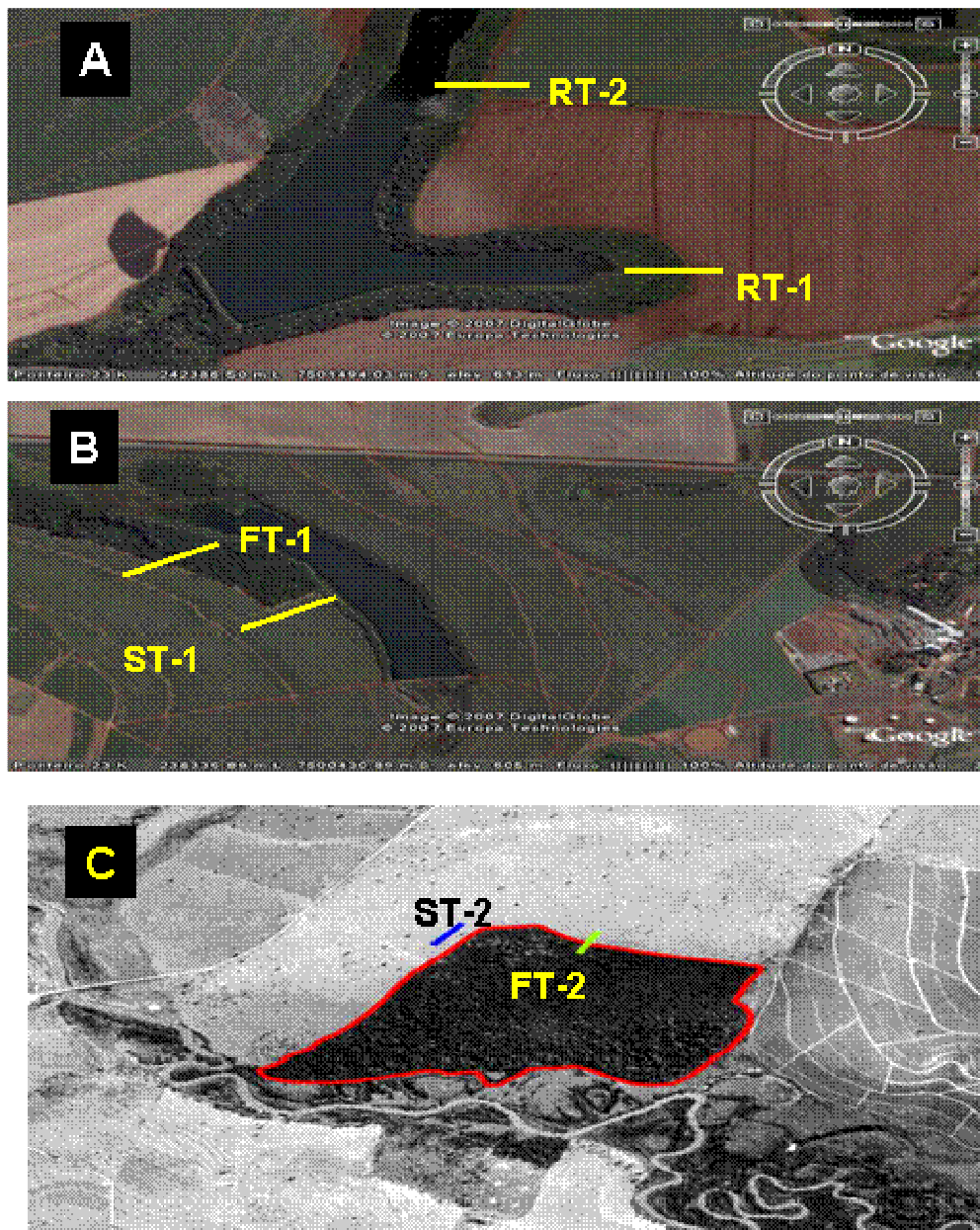


FIG.1. Study areas and respective transects: A and B (Iracemapolis-SP - 22°35' S; 47°33' W), C (Orindiuva-SP - 20°14' N; 49°21' W), FT-forest transect, ST-sugarcane transect, RT-reforestation transect.

2.2. WEPP model

Soil erosion estimates were calculated using an interface of the WEPP (Water Erosion Prediction Project) model and a Geographic Information System (GIS) [17]. The climate and soil parameters, topography and land use-management input data for the WEPP model were adapted following the methods indicated in [18]. The climatic information was based on measured data from the ESALQ meteorological station located at Piracicaba (State of São Paulo, Brazil), 22°42' S, 47°38' W and at an altitude of 560 m a.s.l. The climate file was generated using CLIGEN [19]. Soil input parameters as total sand, very fine sand, organic matter and Cationic Exchange Capacity were obtained for different soil depths, i.e. 0-0.2, 0.2-0.4 and 0.4-0.6 m, from three sampling locations along the transects (one from sugarcane and two from forest soil). Saturated Hydraulic Conductivity was adjusted to the measured values in the field, using Guelph Permeameter. The values found for conductivity were comparable

to results obtained by other authors [20], working on similar soils. Topographic data were obtained from topographic maps at scale 1:10.000 and were improved locally using Global Position System (GPS) and a 'Sokia' station, with a 9' precision, through Trigonometric Leveling [21,22]. Land use and management input parameters were compiled from the literature and information obtained from local specialists.

2.3. ^{137}Cs technique

The assessment of the ^{137}Cs redistribution is based on a comparison of measured inventories (total activity per unit area) at individual sampling points with a measure of the inventory of a representative site of the cumulative fallout input which was not subject to soil erosion or deposition. The sampling points with lower inventories than the reference site are expected to be locations of soil loss. Similarly, sampling points with inventories in excess of the reference level are considered as sediment deposits. Quantitative estimates of erosion and deposition rates from ^{137}Cs measurements are made through calibration procedures or conversion models that relate the erosion or deposition rate to the magnitude of the reduction or increase in the ^{137}Cs inventory [23]. For the transects FT (FT-1 and FT-2), the sampling points were located at the following positions: a) five points on the sugarcane field segment of the transect spaced 10 m from each other (points -50m, -40m, -30m, -20m, -10m); b) twelve points in the riparian forest segment of the transect spaced 5 m from each other (points 5m and 10m) and 10 m from each other (points from 10m to 110m). The transition zone between the sugarcane and riparian forest segments of FT is represented by a 5 m wide dusty road. Samples from each profile were taken with a 10 cm diameter Riverside auger down to 60 cm depth in three layers of 20 cm. For each transect point a composite sample was obtained from five samples collected (5 m distant from each other) on contour lines, perpendicularly to the transect.

Depth incremental samples were also taken down to 0.6 m depth in layers of 0.05 m, from pits located at 5 and 10 m from the forest border. The same number of sampling points were taken for the parallel sugarcane transects ST (ST-1 and ST-2). At RT, the sampling was done at 10 and 5 m in the sugarcane field segment of the transect (points -5m and -10m) and at 5, 10, 20, 30 and 40 m inside the restoration area.

The samples were dried and passed through a 2 mm sieve. A 1-liter Marinelli Beaker was filled with approximately 1 kg of the sieved soil and sealed for gamma ray analyses. Gamma-ray analyses were carried out using an EG&ORTEC Spectroscopy System using a high purity coaxial germanium detector GEM 20-180p presenting a detection efficiency of 0.7% in this geometry. The counting time for each sample varied from 24 to 72 hours according to sample activities. The results (Bq m^{-2}) were converted in sediment loss or deposition by the Proportional Model [24,25], using a particle size correction factor P equal to 1. The reference value was taken as $314 \pm 34 \text{ Bq m}^{-2}$ obtained at a flat grass land area [26,27], located at the Campus of São Paulo State University (ESALQ), Piracicaba, SP, 25 km far from the experimental site, but considered close enough to be taken as a reference for fallout deposition of the studied area. The minimum detectable activity of the system is of the order of 0.2 Bq kg^{-1} .

The results of ^{137}Cs loss or gain were obtained by comparison of each inventory point with the reference site inventory according to:

$$Cs_{red} = \left(\frac{Cs_{ref} - Cs_p}{Cs_{ref}} \right) \quad (1)$$

where: $C_{s_{red}}$ is the fraction of redistributed ^{137}Cs , loss (positive values) or gain (negative values), C_{s_p} and $C_{s_{ref}}$ ($\text{Bq}\cdot\text{m}^{-2}$) are the ^{137}Cs inventories at each sampled point and at the reference site, respectively.

The Proportional Model [28] was used to convert the values of $C_{s_{ref}}$ (%) into soil erosion or deposition rates E ($\text{t ha}^{-1} \text{a}^{-1}$):

$$E = \left(\frac{C_{s_{red}} \rho_b D}{T P 100} \right) \cdot 10 \quad (2)$$

where: ρ_b is the soil bulk density (kg m^{-3}); D the ploughing depth (m); T is the time lapse since fallout (years); P is a particle size correction factor (taken as unity in the present study); and the constant 10 adjusts the units.

2.4. Soil morphology

Detailed soil morphological descriptions were made for the riparian zones segments of FT-1, RT-1 and RT-2. Disturbed samples (samples taken with an auger) were taken from points located at each 10 meters from the upper border of the forest downslope to the reservoir margin, and at 0-0.05, 0-0.10, 0.10-0.20, 0.20-0.40, 0.40-0.60, 0.60-0.80 e 0.80-1 m depth from three pits located at 5, 10 and 20 m from the forest border. The geometrical distribution of the soil horizons and sediments was described [29]. For micromorphological observations and image analysis, thin sections of 5 by 7 cm were prepared from blocks impregnated with a non-saturated polyester resin diluted with styrene monomer. A fluorescent dye allowed distinguishing the pores when illuminated with UV light. Digital images were acquired from the thin sections and impregnated blocks using a color CCD camera with a resolution of 1024×768 pixels (area of $156 \mu\text{m}^2$ pixel $^{-1}$). Images were processed using the Noesis Visilog® image analysis software. Total porosity was calculated as the sum of the areas of all pores divided by the total area of the field in percentage. Particle size distribution was determined by sieving and the Bouyoucus method, using a hydrometer, after dispersion with a sodium hydroxide and sodium hexametaphosphate solution [30].

2.5. Soil stable carbon isotopic ratio analysis

Stable isotopes of carbon (C) are characterized by having 6 protons plus 6 (^{12}C) or 7 (^{13}C) neutrons in their nuclei. The carbon isotopic composition of a given sample $\delta^{13}\text{C}$ can be expressed in relative terms [31,32] by the ratio between the abundance of ^{13}C and ^{12}C ($^{13}\text{C}/^{12}\text{C}$) as indicated in the following equation:

$$\delta^{13}\text{C} \text{ ‰} (sample) = \left(\frac{^{13}\text{C}/^{12}\text{C} (sample)}{^{13}\text{C}/^{12}\text{C} (std)} - 1 \right) \cdot 1000 \quad (3)$$

where: the marine carbon with an abundance of about 1.1% of ^{13}C is taken as a standard (*std*).

To determine the relative contribution of C of sugarcane plants to the forest total soil C, the following equation was used:

$$f_C = \frac{\delta^{13}\text{C}_{OM-SAMPLE} - \delta^{13}\text{C}_{OM-C3}}{\delta^{13}\text{C}_{OM-C4} - \delta^{13}\text{C}_{OM-C3}} \quad (4)$$

where: f_c represents the sugarcane C fraction; $\delta^{13}C_{OM-SAMPLE}$ is the mean value of $\delta^{13}C$ for the OM (organic matter) of samples; and $\delta^{13}C_{OM-C4}$ and $\delta^{13}C_{OM-C3}$ are the mean values of $\delta^{13}C$ for sugarcane (C_4) and the specific forest plants (C_3), respectively. The reference $\delta^{13}C$ value for sugarcane OM was determined according to Eq. 3 as -13 ‰ and for the specific studied forest OM as -26.5 ‰.

Isotopic determinations of soil samples were made using a Thermo Quest-Finnigan Delta Plus Isotope Ratio Mass Spectrometer (Finnigan-MAT - USA) in interface with an Elemental Analyzer (Carla Erba model 1110 - Italy).

Values of f_c according to Eq. 4 were determined for 24 superficial soil samples (0-5 cm) taken at each 5 m along the forest segment of FT-1 and 4 samples taken along the upper slope sugarcane segment of FT-1. Depth incremental soil samples taken down to 2.10 m at two locations inside the forest located at 5 and 20 m from the forest border and in one point in the sugarcane field were also analyzed to verify the depth of contribution of C derived from sugarcane plants to the total soil C.

The results of soil loss and deposition estimated by WEPP model and ^{137}Cs technique were compared by regression analysis. Results from the soil morphological and the soil carbon isotopic ratio analyses were used in order to help the interpretation of results generated by both the ^{137}C and WEPP methods.

3. RESULTS AND DISCUSSION

3.1 Transect FT-1

Figure 2 presents the estimated erosion (+) and sediment deposition rates (-) determined by ^{137}Cs technique and WEPP model for FT-1.

The WEPP model and ^{137}Cs technique were both sensitive to the presence of the riparian forest. Both approaches indicated the predominant occurrence of erosion in the sugarcane segment and sediment deposition in the forest segment. However, the abrupt deposition in the border of riparian zone was not clearly detected by ^{137}Cs technique.

The average estimated soil erosion rates were 82.3 and 84.2 $t\ ha^{-1}\ a^{-1}$ and sediment deposition rates were 158.4 and 96.5 $t\ ha^{-1}\ a^{-1}$ by the ^{137}Cs technique and the WEPP model, respectively. The estimated sediment redistribution in the riparian forest zone estimated by the ^{137}Cs technique presented oscillations along the transect with slight erosion between 20 and 40 m. This behavior probably resulted from the presence of fallen tree trunks and branches, and of changes in the micro-relief which defined the preferential pathways for water and sediments coming from the upland areas.

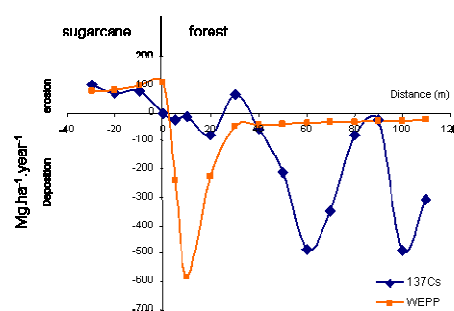


FIG. 2. Estimated erosion (+) and sediment deposition (-) rates ($t\ ha^{-1}\ a^{-1}$) determined by the ^{137}Cs technique and the WEPP model for FT-1.

Figure 3 shows the soil horizon distribution within the forest transect segment determined with the aid of morphological and micro-morphological analysis.

The FT-1 transect was characterized by a layer of sediments covering the original soil that thinned gradually down slope. However the thinning of the sediment layer was not homogeneous, but depended on the slope shape. Depressions at the soil surface or changes in the micro-relief could be associated with thicker layers of sediment deposition [29]. The analysis of pore morphology showed a great contrast between the sediment layers and the original soil. Probably during the deposition process, the soil particles carried by the water were deposited and densely packed favoring the formation of micropores to the detriment of macropores. The sediment layers in this case could be easily distinguished by field morphological description and their main difference in relation to the original soil was the aggregation and porosity [29,33].

Although the estimated sediment redistribution in the riparian forest zone given by ^{137}Cs presented oscillations along the transect, the depth distributions of ^{137}Cs evaluated at two positions in the transect (5m and 10m) were in agreement with the soil horizon distribution determined by soil morphology. The other deposition sites in the transect detected by ^{137}Cs were not observed through the soil morphology approach.

The contribution of sugarcane carbon to the total soil carbon of the surface riparian forest soil (upper 5 cm layer) is shown in Fig. 4.

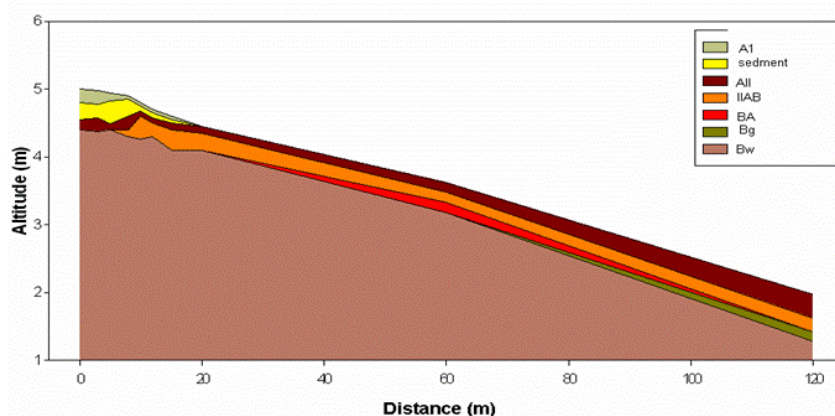


FIG. 3. Bi-dimensional soil horizon distribution within the forest segment of FT-1 determined with the aid of morphological and micro-morphological analysis (The legend refers to soil horizons).

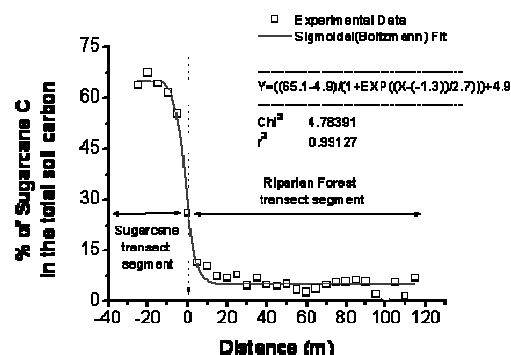


FIG. 4. Contribution of the sugarcane carbon in the total soil carbon of the sugarcane transect segment and in the riparian forest transect segment.

The percentage of sugarcane carbon contribution (%SC) to the total soil carbon in the upper 5 cm layer was high in the sugarcane segment, as expected, and there was a tendency of a decrease in this %SC along the forest segment as expected. The main sources of carbon in the sugarcane crop field soil resulted from the practice of burning the sugarcane leaves and trash before harvest, the decomposition of remaining leaves and other residues after harvest. After about 15 m distance inside the forest segment the amount of sugarcane carbon found in the total soil carbon practically oscillates around an average value of 4.7%. One of the sources of the sugarcane carbon present in the soil of the forest segment comes from sugarcane field runoff, which transported both soil suspended sediments and carbon from the upland sugarcane field. This decrease in the sugarcane carbon concentration in the riparian forest is in agreement with the soil morphology analysis, which could not be clearly understood in light of the ^{137}Cs redistribution analysis.

The sugarcane segment presented the heaviest $\delta^{13}\text{C}$ values, varying from -18.2 to -17.4‰, with an average of $-17.8 \pm 0.3\text{‰}$ (n=4). Such isotopic low values fall in the range typically found for C_4 plants. The highest $\delta^{13}\text{C}$ values, varying from -26.5 to -23.0‰, with an average of $-25.7 \pm 0.7\text{‰}$ (n=24) were found for the forest segment. Typically $\delta^{13}\text{C}$ values for C_3 plants range between -25 and -34‰, and the most common values vary from -26 and -29‰ [34,35].

The input of the sugarcane carbon to the soil of the riparian forest did not only originate from suspended sediment transported by runoff. The traditional practice of burning the sugarcane fields before harvest to facilitate the manual cut of stalks produces very high amount of carbon as CO_2 and as ash particles that are suspended and spread in the atmosphere and then are deposited over neighbouring areas enriching the soil with carbon coming from C_4 plants. Analysis of the percentage of the sugarcane carbon in the total soil carbon in depth inside the FT segment was also made in order to evaluate the contribution of this process. The results obtained in two soil profiles at positions of the forest segment situated at 5 and 10 m from the upper forest border, respectively, show a tendency of increase in the %SC contribution with depth for both soil profiles down to 2 m depth. Leaching of the sugarcane carbon is an explanation for this result.

3.2. Transect ST-1

Figure 5 shows the results obtained by the ^{137}Cs technique and the WEPP model for ST-1. For ST-1, the average soil loss estimated by the WEPP model for the entire hillslope was around $35.0 \text{ t ha}^{-1} \text{ a}^{-1}$. As for FT-1, changes in soil loss values were related with slope changes along the transect. There was no deposition suggested or estimated by the WEPP model for this transect. The ^{137}Cs and WEPP methods showed mainly soil losses, except for the first point where the ^{137}Cs technique suggested soil deposition. This soil deposition point can be coincident with the position of an old terrace, commonly used in sugarcane fields. The average soil loss rates were very similar ($33.9 \text{ t ha}^{-1} \text{ a}^{-1}$ for the ^{137}Cs technique and $35.0 \text{ t ha}^{-1} \text{ a}^{-1}$ for the WEPP approach) and these values were smaller than the values observed by both methods for the sugarcane segment of FT-1 (82.2 and $84.2 \text{ t ha}^{-1} \text{ a}^{-1}$ for the WEPP and ^{137}Cs approaches, respectively). This difference likely occurred due to the higher slope steepness of FT-1 (reaching values of 13.3%) as compared to ST-1 (around 6.7%) at the same position. The same behavior of oscillation in ^{137}Cs values found for FT-1 was observed for ST-1, probably caused by micro-relief changes which determined the selection of particles in the sedimentation process. The WEPP model was not sensitive to these changes in micro-relief.

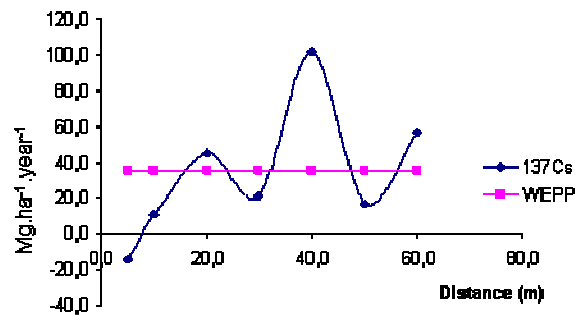


FIG. 5. Estimated erosion (+) and sediment deposition (-) rates ($t\ ha^{-1}\ a^{-1}$) determined by the ^{137}Cs technique and the WEPP model for ST-1.

3.3 Transect RT-1

Figure 6 shows the results obtained by the ^{137}Cs technique and the WEPP model for RT-1. As for FT-1, both the WEPP and ^{137}Cs approaches were sensitive to land use changes at RT-1, with predominantly soil losses for the sugarcane fields and sediment deposition at the riparian zone. When the entire transect was considered, WEPP estimated an average soil loss of $16.3\ t\ ha^{-1}\ a^{-1}$ and changes in soil loss values along the hillslope reflecting the changes in slope steepness. WEPP and ^{137}Cs showed similar average erosion values, and also a similar behavior with regards to sediment distribution along the transect. Abrupt sediment deposition was estimated by WEPP for RT-1, although the pattern of deposition has been different from FT-1. At RT-1, the sedimentation did not decrease over distance, but continued increasing until next to the border of the reservoir. The erosion prediction by WEPP for RT-1 was made considering that for a part of the simulation time (1962-1987) the hillslope was occupied only by sugarcane. After 1987 the restoration of 50 meters of native forest at the riparian zone was started in the study area [35]. This forest is younger than the native forest of FT-1 and consequently the infiltration rates and soil coverage by a leaf and litter layer are smaller than in FT-1, and these parameters were considered in WEPP input data. In this case, the effects of high infiltration and roughness are still not dominant in RT-1. Probably the oscillation in deposition estimated by WEPP is reflecting changes in slope steepness in the riparian zone.

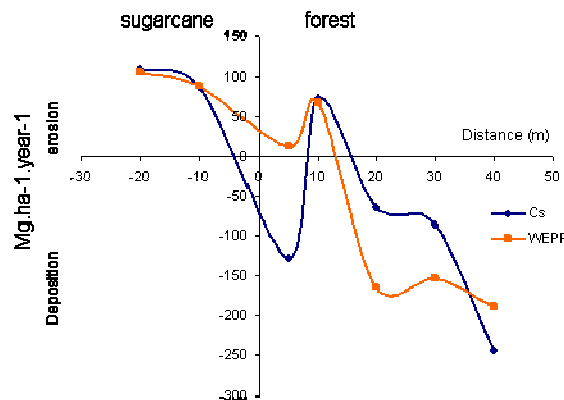


FIG. 6. Estimated erosion (+) and sediment deposition (-) rates ($t\ ha^{-1}\ .a^{-1}$) determined by the ^{137}Cs technique and the WEPP model for RT-1.

Figure 7 shows the soil horizon distribution within the forest transect segment of RT-1 determined with the aid of morphological and micro-morphological analysis. The morphological analysis showed a thick layer of sediments (0.6m) which became thin or null over distance (around 10 m), before increasing at 20 m distance. The thickness of this second package of sediments increased and reached the maximum value (0.4 m) at 27 m distance, decreasing to 0.28 m at 33 m distance. Differences in colour and structure were observed

between the layers of this second package of sediments, showing that there are two kinds of sediments deposited at this position. The hypothesis to explain this sediment deposition pattern is that probably there were three moments of deposition at RT-1. In the first moment, when the whole transect was covered by sugarcane, deposition could have happened on the alluvial plain, next to the reservoir. As there was no forest, the sediments did not experience much resistance to reach the reservoir. The second moment could have been between the beginning of forest restoration and the current soil coverage by forest, when the soil was still exposed to erosion. After forest restoration, the sediment started to deposit closer to the forest border. The morphological analysis of the RT-1 agrees with both the WEPP and ^{137}Cs predictions.

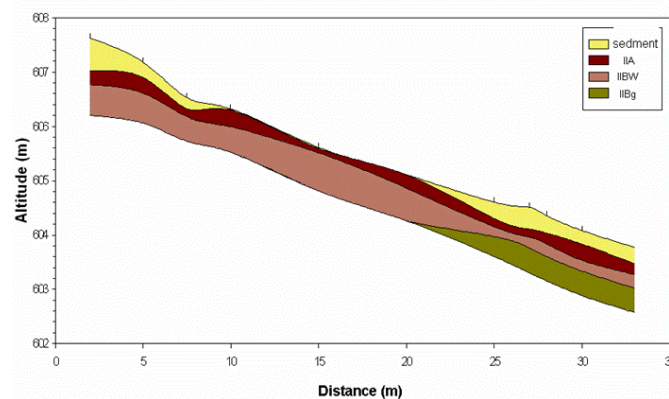


FIG. 7. Bi-dimensional soil horizon distribution within the forest segment of RT-1 determined with the aid of morphological and micro-morphological analysis (The legend refers to soil horizons).

3.4. Transect RT-2

Figure 8 shows the results obtained by the ^{137}Cs technique and the WEPP model for RT-2.

As it can be observed in the RT-2 both the ^{137}Cs technique and the WEPP model estimate erosion rates for the sugarcane segment and deposition rates for the forest segment. Although the sediment redistribution trends are the same for both models the absolute magnitude of erosion and deposition are not the same, as was observed for RT-1. Erosion rates estimated by ^{137}Cs were much lower and sediment deposition much higher than the WEPP based values. Since the age of the riparian forest in RT-2 is different from RT-1, it is possible that a better adjustment of WEPP input parameters related to infiltration and roughness should be made. It is important to emphasize the same trend of continuous increase in sediment deposition along the forest segment right up to the reservoir edge.

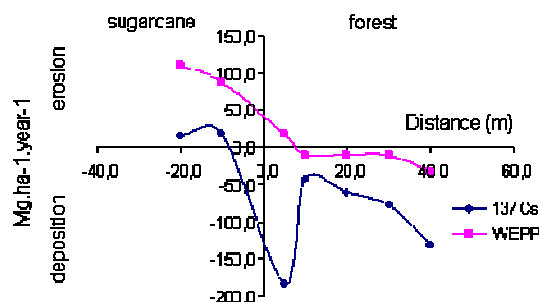


FIG. 8. Estimated erosion (+) and sediment deposition (-) rates ($\text{t ha}^{-1} \cdot \text{a}^{-1}$) determined by the ^{137}Cs technique and the WEPP model for RT-2.

Figure 9 shows the soil horizon distribution within the forest transect segment of RT-2 determined with the aid of morphological and micro-morphological analysis. Only one deposition site was observed in RT-2 forest segment transect situated at the upper part of the riparian forest and presented a length of 8m and a maximum depth of 0.22m. As in the case of FT-1, the other deposition sites detected by ^{137}Cs in RT-2 were not observed by soil morphology.

3.5. Transect FT-2

Figure 10 shows the results obtained by the ^{137}Cs technique for FT-2. The results obtained by the WEPP model for this transect were not considered reliable due to the lack of adequate input parameters.

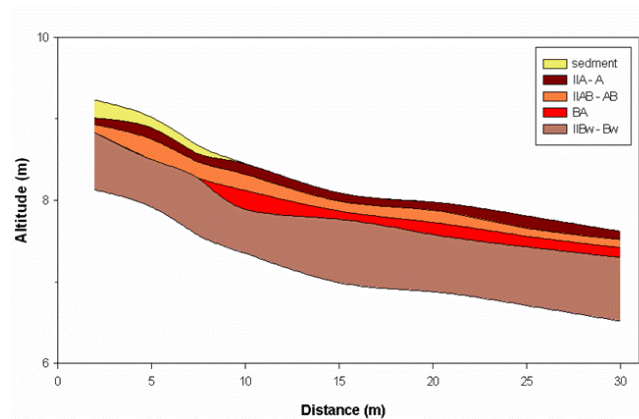


FIG. 9. Bi-dimensional soil horizon distribution within the forest segment of RT-2 determined with the aid of morphological and micro-morphological analysis (The legend refers to soil horizons).

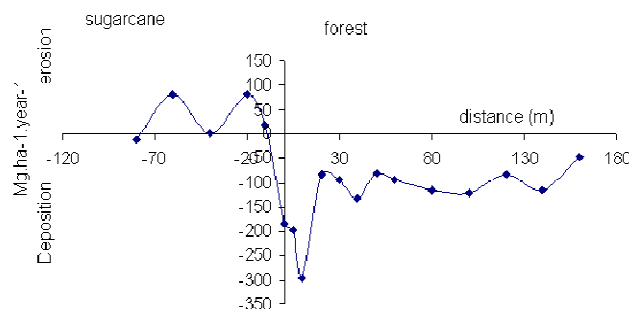


FIG. 10. Estimated erosion (+) and sediment deposition (-) rates ($\text{t ha}^{-1} \text{a}^{-1}$) determined by the ^{137}Cs technique for FT-2.

As in the case of the other forest transects (FT-1, RT-1 and RT-2) the ^{137}Cs based estimates indicated a predominance of erosion in the sugarcane segment with an average rate of $34.4 \text{ t ha}^{-1} \text{a}^{-1}$ and deposition in the forest segment with an average rate of $125 \text{ t ha}^{-1} \text{a}^{-1}$. However in FT-2 the Cs redistribution inside the forest showed an abrupt rise of the sediment deposition rate in the first 10 meters ($225 \text{ t ha}^{-1} \text{a}^{-1}$). Nevertheless, the oscillation was not so high as in the other transects and the average of deposition rates after the first 10 m was much lower ($96 \text{ t ha}^{-1} \text{a}^{-1}$) than the initial values of the forest segment.

3.6. Transect ST-2

Figure 11 shows the results obtained by ^{137}Cs for ST-2. As in the case of FT-2, the results obtained by WEPP for this transect were also not of good quality due to the lack of adequate input parameters for the local soil and climatic conditions.

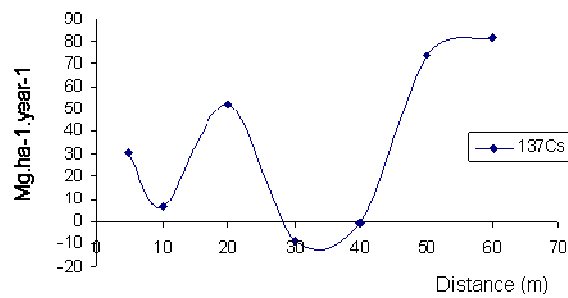


FIG. 11. Estimated erosion (+) and sediment deposition (-) rates ($t\ ha^{-1}\ yr^{-1}$) determined by the ^{137}Cs technique for ST-2.

The ^{137}Cs estimates indicated a predominance of erosion in the sugarcane segment transects with an average rate of $33.6\ t\ ha^{-1}\ a^{-1}$. This value is comparable to the estimates for the parallel sugarcane segment of FT-2.

According to the results obtained on the six transects, it can be observed that the WEPP and ^{137}Cs methods were generally not fully comparable mainly in terms of spatial sediment distribution patterns. Due to its adsorption at clay particles, the fallout radionuclide ^{137}Cs is sensitive to micro-relief oscillations and preferential pathways of sediments caused by tree branches and soil movement due to agricultural mechanization. The WEPP model is not sensitive to these specific variations, mainly for long hillslopes. However, the average soil loss and deposition rates estimated by both methods are similar. The averages of erosion rates estimated by both the ^{137}Cs technique and the WEPP model for all sugarcane transect segment points were 63.3 and $79.1\ t\ ha^{-1}\ a^{-1}$, respectively, while the averages of deposition rates for the forest transect segment points were -120.8 and $-69.1\ t\ ha^{-1}\ a^{-1}$, respectively. The erosion estimates are comparable to values obtained in sugarcane fields by other authors under similar conditions [37,38]. On the other hand, there are no reported data of sediment deposition rates in Brazilian riparian forests.

The disagreement of the ^{137}Cs with the WEPP based estimates of sediment redistribution along the forest segments of FT-1, RT-1 and RT-2 was initially assumed to be a consequence of possible selective transport of fine sediments inside the forest and therefore the need for corrections using the P factor of Eq. 2. However soil textural analysis along the forest segment of the transect FT-1 did not show the expected textural gradient. Also the complementary study using soil carbon isotopic ratio analysis along FT-1 did not confirm the suspected selective transport. The sediment redistribution pattern along the forest segment of FT-2 (sandy soil) estimated by the ^{137}Cs technique also did not indicate a selective sediment transport process.

As it was expected, the WEPP model is not able to detect details of the sediment deposition variation along the riparian zones caused by small changes in soil roughness and water infiltration rates. It was also clear that specific WEPP input parameters are required for each kind of riparian zone with specific characteristics of vegetation and consequent differences in runoff dynamics and sediment trapping abilities.

Despite the spatial disagreements found mainly at sediment deposition sites, this prospective analysis showed the potential use of the ^{137}Cs technique for WEPP validation, and proves the efficiency of riparian forests in trapping sediments coming from agricultural lands. One of the main reasons for the observed disagreements between the different methods can be the spatial variability of erosion and sediment deposition processes and the different sensitivity of the methods to detect it. It is strongly advisable to adopt an appropriate grid sampling procedure for ^{137}Cs analysis as well as for morphological profile description and to run the WEPP model for many parallel transects covering the grid sampling area. The sediment deposition rate

variations observed in reforested riparian zones when running WEPP model simulations with different input parameters according to the forest age enhanced also the need of a precise knowledge of the soil use history.

The results obtained using the ^{137}Cs technique aiming at the validation of the WEPP model and adjustment of its input parameters are of high practical importance for land use planning and environmental legislation. After validation the WEPP model would allow expeditious large scale surveys and could be an easy and useful tool for simulations and estimations of optimal width of riparian forests for sediment trapping at the watershed scale [39].

In addition to the mentioned validation aspects the results obtained allowed to achieve important data regarding the trapping efficiency of riparian vegetation. For example, the sediment delivery from FT-1 to the reservoir was estimated as $2.8 \text{ t ha}^{-1} \text{ a}^{-1}$. It means that 97% of sediments produced at this hillslope are being trapped in the 120m wide riparian zone. For ST-1, with similar conditions of slope length and steepness, soil and climate, 100% of sediments produced in the sugarcane field would be delivered to the reservoir ($21.6 \text{ t ha}^{-1} \text{ a}^{-1}$). For the 18 years old 50m wide reforested riparian zone in RT-1, about $12.5 \text{ t ha}^{-1} \text{ y}^{-1}$ of sediments reached the reservoir (or 77% of sediment produced).

4. CONCLUSIONS

- The WEPP model and the ^{137}Cs technique were not fully comparable mainly in terms of spatial sediment distribution patterns at deposition sites.
- The disagreement of the ^{137}Cs with the WEPP based estimates of sediment redistribution along the transects can be attributed to differences in intrinsic sensitivity of both methods to micro-relief oscillations and preferential pathways of sediments caused by tree branches and soil movement due to agricultural mechanization.
- After adjustments of key WEPP input parameters, guided by ^{137}Cs method estimations, both methods presented average erosion and deposition rates of the same order of magnitude. This prospective analysis shows the potential use of ^{137}Cs for WEPP validation and improvement on input parameters.
- The results showed the high efficiency of riparian vegetation in trapping sediments coming from agricultural lands and its importance as a conservation measure at the watershed scale.
- The results were able to show that the minimum established width of 30m for ‘Legally Protected Areas’ (LPA) of riparian forests, according to the Brazilian Environmental Law (Law 4.771/65), is not always enough to assure the sediment trapping function of the riparian vegetation.

ACKNOWLEDGEMENT

The authors are grateful to CNPq and IAEA for its financial support under research contract BRA-12320.

REFERENCES

- [1] RITCHIE, J.C., MCCARTY, G.W., ^{137}Cs Cesium and soil carbon in a small agricultural watershed. *Soil and Tillage Research* **69** (2003) 45-51.
- [2] RODRIGUES, R.R., GANDOLPHI, S., “Restauração de Florestas tropicais: Subsídios para uma Definição Metodológica e Indicadores de Avaliação e Monitoramento”, *Recuperação de Áreas Degradadas* (DIAS, L.E., MELLO, J.W.V., Eds) 203-206, SBCS, São Paulo, SP (1998).

- [3] RODRIGUES, R.R., GANDOLPHI, S., “Conceitos, tendências e ações para a Recuperação de Florestas Ciliares”, *Matas Ciliares: Conservação e Recuperação* (RODRIGUES, R. R., LEITÃO FILHO, H. F., Eds), EDUSP/FAPESP, São Paulo, SP, (2001)
- [4] LLANO, F.L.C. DE, *Restauración Hidrológica Forestal de Cuencas y Control de la Erosión*, 2nd Edn, Madrid (1998) 21 – 40.
- [5] AMPONTUAH, E. O., et al., Assessment of soil particle redistribution on two contrasting cultivated hillslopes, *Geoderma*, **132** (2006) 324-343.
- [6] IZIDORIO, R., et al., Perdas de Nutrientes por erosão e sua distribuição espacial em área sob cana-de-açúcar, *Eng.Agríc., Jaboticabal*, **25** (2005) 660-670.
- [7] KLAPPROTH, J.C., JOHNSON, J.E., *Understanding the Science Behind Riparian Forest Buffers: Effects on Water Quality*, Virginia Cooperative Extension, Publication N° **420-151**, Virginia Polytechnic Institute and State University (2000), www.ext.vt.edu/pubs/forestry/420-151/420-151.html.
- [8] LIMA, W. P.; ZAKIA, M. J. B., *Hidrologia de Florestas ribeirinhas, Matas Ciliares: Conservação e Recuperação* (RODRIGUES, R. R.; LEITÃO FILHO, H. F., Eds), EDUSP/FAPESP, São Paulo, SP (2001).
- [9] LOWRANCE, R., et al., Water quality functions of riparian buffers in Chesapeake Bay watersheds, *Environmental Management* **21** (1997) 687-712.
- [10] MALANSON, G.P., *Riparian Landscapes*, Cambridge University Press, Cambridge (1995).
- [11] MANDER, U., et al., Efficiency and dimensioning of riparian buffer zones in agricultural catchments, *Ecological Engineering* **8** (1997) 299-324.
- [12] NILSON, C., et al., Long-term responses of river-margin vegetation to water-level regulation. *Science*, **276** (1997) 798-800.
- [13] SIMÕES, L. B., *Integração entre um modelo de simulação hidrológica e sistema de informação geográfica na delimitação de zonas tampão ripárias*, PhD thesis, 125f, Faculdade de Ciências Agrônômicas, Universidade Estadual Paulista, Botucatu, 2001.
- [14] RENARD, K.G., MAUSBACH, M.J., “Tools for conservation”, *Proc. of Soil Erosion and Productivity Workshop*, University of Minnesota, Minneapolis (1990) 55-64.
- [15] NEARING, M.A., et al., “Soil erosion and sedimentation”, *Agricultural non-point source pollution*. (RITTER, W. F., SHIRMOHAMMADI, A. Eds), CRC Press LLC, Lafayette (2001) 29-54.
- [16] FLANAGAN, D.C., NEARING, M.A., *Water Erosion Prediction Project: Hillslope Profile and Watershed Model Documentation*, West Lafayette: NSERL Report n. 10, West Lafayette (1995).
- [17] RANIERI, S.B.L., et al., Erosion database interface (EDI): a computer program for georeferenced application of erosion prediction models, *Computers Geosciences* **28** (2002) 661-668.
- [18] SPAROVEK, G., SCHNUG, E., Temporal erosion-induced soil degradation and yield loss. *Soil Science Society of America Journal* **65** (2001) 1479-1485.
- [19] NICKS, A.D., et al., “Weather Generator”, *USDA-Water Erosion Prediction Project: Hillslope profile and watershed model documentation* (FLANAGAN, D.C., NEARING, M.A., Eds), USDA-ARS-MWA-SWCS, West Lafayette (1995) 2.1-2.22.
- [20] POTT, C.A., DE MARIA, I.C., Comparação de métodos de campo para determinação da velocidade de infiltração básica, *Revista Brasileira de Ciência do Solo*, Campinas **27** (2003) 19-27.
- [21] SPARTEL, L. LUDERITZ, J., *Caderneta de campo*, 3th edn, Globo, São Paulo (1968).
- [22] GODOY, R., *Topografia Básica*, FEALQ, Piracicaba (1988) pp. 349.

- [23] ZAPATA, F.G., The use of environmental radionuclides as tracers in soil erosion and sedimentation investigations: recent advances and future developments, *Soil and Tillage Research* **69** (2003) 3-13.
- [24] MITCHELL, J.K., et al., "Soil loss estimation from fallout cesium-137 measurements", *Assessment of erosion* (DE BOODT, M., GABRIELS, D., Eds), Wiley, London (1980) 393-401.
- [25] DE JONG, E., et al., Preliminary investigations on the use of ^{137}Cs to estimate erosion in Saskatchewan, *Canadian Journal of Soil Science* **62** (1982) 673-683.
- [26] CORRECHEL, V., et al., "Primeira aproximação de um estudo sobre as atividades de ^{137}Cs em áreas de referência" (Compact disc), Congresso Brasileiro de Ciência do Solo 29, Ribeirão Preto (2003)
- [27] CORRECHEL, V., et al., Random and systematic spatial variability of ^{137}Cs inventories at reference sites in south-central Brazil, *Scientia Agricola* **62** (2005) 173-178.
- [28] WALLING, D.E., HE, Q., Models for converting ^{137}Cs measurements to estimates of soil redistribution rates on cultivated and uncultivated soils, A contribution to the IAEA Coordinated Research Projects D1.50.05 and F3.10.01, University of Exeter, Exeter (1997) pp. 29.
- [29] BOULET, R., et al., Analyse structurale et cartographie en pédologie, I Prise en compte de l'organisation bidimensionnelle de la couverture pédologique: les études de toposéquences et leurs principaux apports à la connaissance des sols, *Cah. ORSTOM, Pedol.* **19** (1982) 309-320.
- [30] CAMARGO, A.O. DE, et al., Métodos de análise química, mineralógica e física de solos do IAC, Instituto Agronômico de Campinas, *Boletim Técnico*, **106** (1986) pp. 94.
- [31] BOUTTON, T.W., Stable carbon isotopes ratios of soil organic matter and their use as indicators of vegetation and climate change. *Mass Spectrometry of Soils* (BOUTTON, T.W., YAMASAKI, S., Eds.), Marcel Decker, New York (1996) 47-82.
- [32] CERRI, C.C.; et al., Aplicação do traçage isotópico natural em ^{13}C , à l'étude de la dynamique de la matière organique dans les sols, *Comptes Rendus de l'Académie des Sciences de Paris, Série II*, **9** (1985) 423-428.
- [33] COOPER, M., et al., Origin of microaggregates in soils with ferrallic horizons, *Scientia Agricola*, **62** (2005) 256-263.
- [34] O'LEARY, M.H., Carbon isotopes in photosynthesis, *BioScience* **38** (1988) 328-336.
- [35] BOUTTON, T.W., "Stable isotope ratio of natural material: II. Atmospheric, terrestrial, marine, and freshwater environments", *Carbon Isotopic Techniques* (COLEMAN, D.C., FRAY, D., Eds.), San Diego Academic Press, San Diego (1991) 173-185.
- [36] ESTEVÃO, C., et al., Plano diretor de uso e manejo da microbacia hidrográfica do ribeirão Cachoeirinha - Iracemápolis - SP: Avaliação de 18 anos de implantação, Monografia (Especialização em Gerenciamento Ambiental) - Escola Superior de Agricultura "Luiz de Queiroz", Universidade de São Paulo, Piracicaba (2006).
- [37] FERNANDES, E.N.; et al., EROSYS: Support system for evaluation of environmental impacts of farming activities, *Revista Brasileira de Agroinformática*, **4** (2002) 1-12.
- [38] BACCHI, O.O.S., et al., Sediment spatial distribution evaluated by three methods and its relation to some soil properties, *Soil and Tillage Research*, **69** (2003) 117-125.
- [39] SPAROVEK, G., et al., A conceptual framework for the definition of the optimal width of riparian forest, *Agriculture Ecosystems and Environment* **90** (2001) 171-177.

USE OF FALLOUT CAESIUM-137 AND BERYLLIUM-7 TO ASSESS THE EFFECTIVENESS OF CHANGES IN TILLAGE SYSTEMS IN PROMOTING SOIL CONSERVATION AND ENVIRONMENTAL PROTECTION ON AGRICULTURAL LAND IN CHILE

P. SCHULLER, A. CASTILLO
Universidad Austral de Chile,
Facultad de Ciencias, Instituto de Física,
Valdivia, Chile

D.E. WALLING
University of Exeter,
Department of Geography
Exeter,
Devon, United Kingdom

A. IROUMÉ
Universidad Austral de Chile,
Facultad de Ciencias Forestales,
Instituto de Manejo Forestal,
Valdivia, Chile

Abstract

The current study developed a simplified method for using ^{137}Cs depth distribution datasets to estimate soil loss or accumulation at a sampling point under conventional tillage and after the shift to a no-till system. Previous applications of ^{137}Cs measurements had been limited to the estimation of erosion rates during the period extending from the beginning of fallout receipt to the time of sampling. The new procedure allows the change in erosion rates associated with a shift in land tillage practices to be estimated. In an additional study to assess no-till systems with and without burning of crop residues after harvesting, ^7Be was used to quantify the erosion that occurred within the same field area, as a result of burning and a period of extreme rainfall (400 mm in 27 days, May 2005). The studied site is located in the Coastal Mountains of the Araucanía Region, Chile. The soil is Ultisol (Typic Hapludult), and the area has a temperate climate and a mean annual precipitation of 1100 mm year⁻¹. The obtained fallout radionuclide (FRN) data showed that 16 years after implementing the no-till system there was a reduction in the erosion rate of about 87% (from 11 t ha⁻¹ year⁻¹ to 1.4 t ha⁻¹ year⁻¹). In addition, the proportion of the study area, subject to erosion, decreased from 100% to 57%. The net erosion associated with crop residue burning and an extreme rainfall event (400 mm in 27 days occurring in May 2005) as estimated from the FRN was approximately 12 t ha⁻¹. This indicated that large proportions of soil and ashes were mobilized by erosion and transported beyond the study area during the period of heavy rainfall. Comparing these results with those estimated for the medium long term net erosion rate (1.4 t ha⁻¹ year⁻¹) during a prolonged period of no-till without the burning of crop residues, it would appear that burning in autumn is a highly undesirable practice, since it could promote soil loss in the following rainy season, especially under high magnitude erosive events. In combination, the use of ^{137}Cs and ^7Be provided a valuable means of investigating soil erosion and assessing erosion risk associated with the changes in tillage system.

1. INTRODUCTION

Intensification of agricultural production in south-central Chile since the 1970s has increased soil erosion and associated soil degradation [1,2]. In this region conventional tillage (CT) on crop land involves the burning of stubble after harvesting, ploughing and subsequent disk harrowing operations for seedbed preparation. These practices leave the soil bare for

considerable periods before a new crop cover develops and the bare soils can be subject to intense rainfall, which frequently causes soil erosion. Due to CT operations, over 80% of the Ultisols of the Coastal Mountains of south-central Chile show evidence of compaction below the plough depth and the erosion rates of these soils are described as being amongst the highest for any agricultural land in Chile [1,2,3]. CT affects the long-term sustainability of both the soil resource and crop production, and contributes to diffuse source pollution of water courses and river systems. The introduction of a no-till/minimum-tillage system (NT) is seen as a key strategy for reducing soil erosion and soil and fertiliser loss from agricultural land. The NT system involves the management of crop residues, to ensure that the soil is partially covered with stubble and straw during the fallow period, and direct seeding, using seed drills which cut throughout crop residues and open slots in the soil, into which seeds and fertilisers are placed. The implementation of NT has been shown to cause significant improvements in soil quality for the Ultisols, as reflected by an increase in aggregate stability (typically from ca. 17 to ca. 78%), and an increase in macroporosity (from ca. 12 to 17.5%) [2]. NT is currently being widely applied, in order to maintain and improve soil quality and to reduce soil and nutrient losses to water courses. However, there is a need to assemble more information on the precise magnitude of the decrease in soil loss associated with the shift from CT to NT systems, in order to provide a more rigorous confirmation of the likely impact, and therefore effectiveness, of such changes in land management.

A mixed tillage system is also employed in south-central Chile. This tillage practice involves no-till with burning of crop residues remaining after harvesting in late summer (NTWB), leaving the soil bare during the subsequent period of rainfall, which commonly commence around May (autumn). Due to the implementation of the NTWB system, the exposure of the bare soil to the autumn rains increases its susceptibility to raindrop impact and surface sealing. In addition, it is likely that the burning will increase the bulk density of the surface soil, through removal of organic matter, destroy the soil aggregates, thereby increasing the potential for soil crusting, and reduce the hydraulic conductivity of the surface horizons. There is also evidence that burning may result in hydrophobic conditions at the soil surface [4]. All of these changes are likely to lead to increased surface runoff and thus increased erosion risk.

Faced with the need to assess the impact of the shift in tillage systems from CT to NT on rates of soil loss, the use of ^{137}Cs measurements has been explored. This paper describes the development of a novel procedure for using the ^{137}Cs depth distribution to estimate rates of soil loss at a sampling point under the original CT and after the shift to NT. It also reports the application of this procedure in a field cultivated annually for crop production, which was under CT until 1986, when there was a change to a NT system.

Additionally, this paper reports the use of ^7Be measurements to document soil redistribution in the same field, associated with the implementation of NTWB in 2005, which was followed immediately by a period of very heavy autumn rainfall. The field investigated had been cultivated using a NT system for about 18 years, but because of the slow decomposition of the residual stubble, after the harvest in early March 2005, the crop residue was burnt leaving the field bare at the onset of the autumn rains in May 2005. Therefore, the event related results obtained using the ^7Be method provide information on the role of high magnitude, low frequency, rainfall events in contributing to the longer term erosion from the site and permit some preliminary conclusions regarding the influence of burning within the no-till systems (i.e. a shift from NT to NTWB) in increasing soil loss.

2. METHODS

2.1. Use of ^{137}Cs measurements to document changes in soil erosion rates associated with changes in the soil tillage system

The standard and simplified approaches for documenting medium term soil erosion rates and their spatial distribution during a period of CT and the subsequent period of NT described below were developed by Schuller et al. [5].

2.1.1. The standard method

The standard method is based on the observation of the ^{137}Cs (Half life is 30.2 years) distribution in soil profiles. The medium term erosion rate ($R_{NT} < 0$) or sedimentation rate ($R_{NT} > 0$) at selected sampling points, associated with the NT period ($\text{kg m}^{-2} \text{ year}^{-1}$), can be estimated by comparing the mass depth of the zone of homogeneous mixing of ^{137}Cs in the soil ($h(t)$, kg m^{-2}) at the time of sampling (t , year), with the estimated plough depth (H , kg m^{-2}) at the time of cessation of CT (t' , year). Assuming that the whole study area was affected by erosion during the CT period and that no ^{137}Cs fallout occurred during the NT period, the depth of the zone of homogeneous mixing of ^{137}Cs in the soil at the time when CT ceased, t' , would be equal to the plough depth H . The reduction or increase in $h(t)$ relative to H (i.e. $h(t) - H$, kg m^{-2}) represents the total amount of soil erosion or deposition occurring during the period extending from the time of introduction of the NT system to the time of sampling. The annual erosion or deposition rate R_{NT} can therefore be estimated as:

$$R_{NT} = \frac{h(t) - H}{t - t'} \quad (1)$$

The ^{137}Cs depth distribution in the soil at the end of the period of CT can be reconstructed by assuming that the zone of homogeneous mixing would have extended to depth H and that the mean ^{137}Cs mass activity density ($\bar{C}(t)$, Bq kg^{-1}) in the upper part of the residual portion of the zone of homogeneous mixing (i.e. down to $h' \leq h$) at the time of sampling is a direct reflection of that existing in the plough layer at the end of the period of conventional tillage. The loss (negative value) or gain (positive value) in the areal activity density ($\Delta A(t)$, Bq m^{-2}) during the subsequent NT period can thus be estimated as:

$$\Delta A(t) = [h(t) - H] \bar{C}(t) \quad (2)$$

The total areal activity density ($A(t')$, Bq m^{-2}) at the measuring points at the end of the period of CT (or the beginning of the period of NT) can therefore be estimated in the following way:

$$A(t') = [A(t) - \{h(t) - H\} \bar{C}(t)] \exp[\text{Ln}(2)(t - t') / T_m] \quad (3)$$

where: $A(t)$ (Bq m^{-2}) represents the areal activity density at each sampling point measured at the time of sampling and T_m (year) is the half-life of ^{137}Cs .

Comparison of the estimates of the total ^{137}Cs areal activity density at the end of the period of CT for the sampling points with the local reference value enables the erosion rate during the period of CT (R_{CT}) to be estimated for these points using one of the conversion models for cultivated soils documented by Walling and He [6]. In this situation, it is simply assumed that

the samples were collected at the same time as the shift from CT to NT and that the estimated erosion rate applies to the period extending from the onset of ^{137}Cs fallout to that date.

2.1.2. The simplified method for extending the application of the standard method

The standard method, described above, requires appreciable effort, both in terms of the need to collect depth incremental samples and the resulting large number of samples requiring analysis for ^{137}Cs activity. The latter limitation is particularly significant for sites where ^{137}Cs activities are low and extended gamma count times are required. A simpler approach, that uses bulk cores and can be applied to additional sampling points in the study field to estimate the erosion rates associated with the periods under CT and a NT system, was proposed and validated by Schuller et al. [5].

The depth distributions of ^{137}Cs obtained for individual sampling points along a slope transect at a site under a NT system at the time of sampling, where the standard method was applied, indicated that only a small proportion of the total areal activity density was found below mass depth h . In addition, a significant linear relationship was found between A_h , the areal activity density down to h , and the total areal activity density, A [5]:

$$A_h(t) = 1.006 A(t) - K, \quad (r = 0.999, p < 0.01) \quad (4)$$

where the value of the constant K (Bq m^{-2}) represents the ^{137}Cs areal activity density, which migrated below the mass depth of homogeneous mixing, h .

The well-defined relationship between these two variables makes it possible to estimate A_h for additional points at the study site, where only the total areal activity density, A , has been measured using bulk (unsectioned) cores. Assuming that the ^{137}Cs mass activity density is approximately constant down to depth h and that the bulk density of the soil will also be almost constant down to this depth, $h(t)$ can be estimated using the following relationship:

$$h(t) = \frac{A_h(t)}{\bar{C}(t)} \quad (5)$$

where: $\bar{C}(t)$ (Bq kg^{-1}) is the mean ^{137}Cs mass activity density measured in the upper part of the soil profile (down to $h' \leq h$) at the sampling points.

Using the relationship between $A(t)$ and $A_h(t)$, and Eq. (5), measurements of $A(t)$ and $\bar{C}(t)$ at additional sampling points enables the key parameters for the ^{137}Cs depth distributions associated with the two tillage periods to be estimated for those points. These in turn allow the mean annual soil redistribution rates for the periods under CT and NT systems to be estimated. This simplified approach was validated by Schuller et al. [5], by demonstrating a very close correspondence between the results obtained using this method and those provided by the standard method for the same sampling points.

One limitation of the approach for comparing rates of soil loss under CT and under a subsequent NT system, described above, is that it is not applicable to sampling points where deposition occurred during the period of CT, since this would result in the depth of homogeneous mixing exceeding the plough depth H at the beginning of the NT period. This would make it impossible to estimate the rate of soil loss associated with the NT period, since the method employed assumes that the depth to which appreciable ^{137}Cs activity is found at the onset of the NT system corresponds to the plough depth H . For this reason the approach can only be used to assess the change in soil redistribution rate at sampling points that were

eroding under CT. The approach is able to determine whether the introduction of a NT system at these sampling points resulted in either an increase or decrease in the erosion rate or a shift to deposition.

To apply the simplified method, the relationship between $A_h(t)$ and $A(t)$ described in Eq. (4) must be established by depth incremental sampling for the date of sampling, and for the specific soil and climatic conditions of the study site, which affect the migration of the ^{137}Cs in the soil profile, and consequently the value of K .

2.2. Use of ^7Be measurements to document short term soil redistribution associated with a period of highly erosive rainfall following burning of the crop residue

2.2.1. Use of cosmogenic ^7Be for tracing soil redistribution

The successful use of the natural radionuclide ^7Be (*Half life* is 53.3 days), generated in the stratosphere and upper troposphere, to document both the magnitude and spatial pattern of short term (event based) soil redistribution on agricultural land has been reported by Blake et al. [7] and Walling et al. [8]. Existing field and laboratory evidence suggests that the initial vertical distribution of the ^7Be areal activity density (Bq m^{-2}) within the soil is characterised by a rapid exponential decrease with depth, with most of the radionuclide being found within the upper few millimetres of the surface soil [9,7,10]. The approach used to estimate soil redistribution rates is based on comparison of the ^7Be areal activity density (Bq m^{-2}) measured at a sampling point with a reference areal activity density determined for a nearby undisturbed and stable reference site, where neither erosion nor deposition have occurred. Depletion of the ^7Be areal activity density, relative to the reference value, provides evidence of erosion, whereas areas of sediment deposition are associated with increased areal activity densities. By coupling information on the extent of the decrease or increase in the areal activity density with information on the characteristic depth distribution of ^7Be within the surface soil of the reference site, the depth or amount of soil eroded or deposited can be estimated.

Based on the known rapid and strong fixation of ^7Be fallout by the surface soil and assuming an exponential decrease of the initial ^7Be areal activity density with depth, Blake et al. [7] and Walling et al. [8] proposed a conversion model for estimating soil redistribution from measurements of the extent of the increase or decrease in the areal activity density, relative to the reference value. The components of this model as presented by Schuller et al. [10] are described below, using terms defined according to the International Commission on Radiation Units and Measurement (ICRU) [11].

2.2.2. The ^7Be method

The exponential decrease of the ^7Be areal activity density in a soil with depth can be represented as:

$$A(x) = A_{ref} \exp(-x/h_o) \quad (6)$$

where: x (kg m^{-2}) represents the mass depth of the soil measured from the surface (positive downward), $A(x)$ (Bq m^{-2}) is the areal activity density below mass depth x , and A_{ref} (Bq m^{-2}) the reference areal activity density, i.e., the areal activity density at an uneroded stable site or reference site in the study area. The relaxation mass depth h_o (kg m^{-2}) describes the shape of the depth distribution of the areal activity density of ^7Be in the soil. According to Eq. (6), the

areal activity density below h_o is 36.8% of the total areal activity density, A_{ref} , i.e. $A(h_o) = 0.368 A_{ref}$

Assuming that erosion has removed a thin layer of mass depth R (kg m^{-2}) at a sampling point within the study site, the ^7Be areal activity density remaining at this eroded point, A (Bq m^{-2}) will be lower than A_{ref} . The soil mass eroded per unit area, R , is equal to the mass depth removed. By setting $x = R$ in Eq. (6), the remaining areal activity density at the sampling point can be calculated as:

$$A = A(R) = A_{ref} \exp(-R/h_o) \quad (7)$$

The mass of soil per unit area lost from the sampling point, R , can therefore be calculated as:

$$R = h_o \text{Ln} \left[\frac{A_{ref}}{A} \right] \quad (8)$$

An estimate of the sediment mass deposited per unit area, R' , kg m^{-2} , can be obtained by dividing the areal activity density in excess of A_{ref} ($A' - A_{ref}$, Bq m^{-2}) by the mean ^7Be mass activity density of the deposited sediment, C_d (Bq kg^{-1}) i.e.:

$$R' = \frac{A' - A_{ref}}{C_d} \quad (9)$$

The ^7Be mass activity density of the sediment eroded from a point, C_e (Bq kg^{-1}) can be estimated from the areal activity density lost at that point divided by the mass of sediment eroded per unit area, i.e.:

$$C_e = \left[\frac{A_{ref} - A}{R} \right] = A_{ref} [1 - \exp(-R/h_o)] / R \quad (10)$$

Consequently, the mean ^7Be mass activity density of the deposited sediment C_d can be estimated as the weighted mean mass activity density, C_e , of sediment mobilised from the upslope contributing area S :

$$C_d = \frac{\int_S C_e R dS}{\int_S R dS} \quad (11)$$

Using the parameters A_{ref} and h_o established for the initial ^7Be vertical distribution in the soil (i.e. for the reference site), and Eqs. (8) and (9), the amounts of soil eroded or deposited at individual sampling points within a study site, and thus the spatial pattern of soil redistribution, can be established.

The use of the ^7Be method outlined above to estimate soil redistribution, involves three key assumptions [see 8,10]:

- (1) Prior to the erosion event to be investigated, any pre-existing ^7Be within the soil should be uniformly distributed across the study area.
- (2) The deposition of ^7Be fallout associated with the erosion event should also be spatially uniform across the study area.

- (3) The ^7Be deposited during an erosion event will be rapidly fixed by the surface soil particles and can only be redistributed by mobilisation and redistribution of those particles.

Considering the first assumption, any pre-existing spatial variability of the ^7Be areal activity density introduced by soil redistribution caused by previous erosion events will rapidly disappear through radioactive decay, providing the erosion episodes are separated by a period of sufficient length (e.g. longer than ca. two half-lives). Contributions to the ^7Be areal activity density in the soil, associated with low intensity rainfall, which does not result in significant soil redistribution, can be assumed to be spatially uniform. The second assumption can be expected to be fulfilled at the scale of a small field, where the spatial distribution of both rainfall input and ^7Be fallout can be considered to be spatially uniform. The third assumption has been widely confirmed by experimental investigations of the fixation of ^7Be fallout inputs by soil particles, such as those reported by Wallbrink and Murray [12] and Blake et al. [7].

3. RESULTS AND DISCUSSION

3.1. A case study involving the use of the ^{137}Cs method to document the changes in soil erosion rates associated with the shift from conventional tillage to no-till

3.1.1. Site selection, sample collection and laboratory procedures

The ^{137}Cs method described above was applied in a field located on a farm in the Coastal Mountains of the Araucanía Region of Chile ($38^{\circ}37'S$ $73^{\circ}04'W$), characterized by Araucano series Ultisols (Typic Hapludult), a temperate climate and a mean annual precipitation of 1100 mm year^{-1} . The field had been cultivated annually for crop production and was under CT until May 1986, when there was a change to a NT system [5,13]. A second site was located close to the site described above and with a similar soil type, but where CT had continued through to the sampling year. This last site was selected to estimate the historical plough depth.

In the region of the study site, significant atmospheric deposition of ^{137}Cs was last recorded in 1983 [14] and it can therefore be safely assumed that the existing ^{137}Cs inventory was mixed homogeneously within the plough layer by CT prior to the implementation of the NT system. This is an important assumption of the approach proposed by Schuller et al. [5].

Samples were collected from within an area of ca. 5000 m^2 , which was selected to be representative of a site likely to be susceptible to erosion during the period of CT. Initially, in 2001 and 2002, depth incremental samples were collected from points situated along a single slope transect, in order to implement the standard method and to establish the relationship between A_h and A , required to use the simplified method. To apply this simplified method, bulk soil samples for determining the total ^{137}Cs areal activity density A and the ^{137}Cs mass activity density \bar{C} down to $h' \leq h$, were collected during 2003, from between seven and eight points, located at 15 m intervals along four additional parallel slope transects extending down the upper and middle portions of the slope. At each point, three 25 cm long and two 8 cm long cores were collected by using an 11 cm diameter corer, in order to determine A and \bar{C} , respectively.

At the additional site, located close to the study field where CT was continued until 2003, depth incremental samples were collected to determine the historical plough depth H , from the ^{137}Cs depth distribution. A depth increment of 1 cm was used around the expected plough depth, in order to define this as precisely as possible.

The ^{137}Cs content of the soil samples was measured by gamma spectrometry, using a Canberra high-purity Ge detector (Canberra Industries, Inc., Meriden, USA), with a relative efficiency of 28%. The gamma spectra were analysed using Genie 2000 software (Canberra Industries, Inc., Meriden, USA). Due to the low ^{137}Cs concentrations in the samples analysed, the count time was set to 20 h per sample, which provided a measurement precision of better than $\pm 10\%$ at the 95% level of confidence. The ^{137}Cs detection limit for this measuring time was estimated to be approximately 0.3 Bq kg^{-1} for the Marinelli geometry (bulk cores) and 10 Bq kg^{-1} for the Petri dish geometry (sectioned cores) employed.

3.1.2. Estimation of soil redistribution rates

To extend the area documented using the standard method through use of the simplified method, A_h was estimated for the sampling points using the linear regression between $A_h(t)$ and $A(t)$ described in Eq. (4). As documented by Schuller et al. [5], for the given site and sampling date, this relation is:

$$A_h(t) = 1.006 A(t) - 31.5 \quad (12)$$

Soil redistribution rates during the NT period were estimated using Eqs. (5) and (1). The erosion rates associated with the period of CT were estimated using Eq. (3) coupled with the mass balance conversion model incorporating soil redistribution caused by tillage developed by Walling and He [6]. As tillage will result in the redistribution of soil within a field, the ^{137}Cs contained in the soil will also be redistributed, and this redistribution needs to be taken in account when using ^{137}Cs measurements to derive estimates of water-induced soil erosion per se [6]. The reference inventory used for the calculations was based on that determined previously for a neighbouring site [15], taking account the influence of local variation in annual precipitation. This value, $525 \pm 12 \text{ Bq m}^{-2}$ for 1998, whilst relatively low from a global perspective, was consistent with existing understanding of the dependence of ^{137}Cs areal activity density on the local mean annual precipitation for the 9th and 10th Regions of Chile [16]. The other parameters used to apply the mass balance model incorporating soil movement by tillage were: Proportion factor (γ) = 0.8; relaxation mass depth = 6.2 k m^{-2} ; tillage flux (ϕ) = $210 \text{ kg m}^{-2} \text{ year}^{-1}$; particle size correction = 1.0 [13].

3.1.3. Results

Fig. 1 shows the ^{137}Cs depth distribution observed at a point susceptible to erosion located within the site where CT has continued to be practiced until the present day [17]. Using this information and the ^{137}Cs depth distributions documented at other eroding locations within the site, the historical plough depth for the study site was estimated to be 170 kg m^{-2} , based on the mean mass depth of the zone of ^{137}Cs homogeneous mixing in the annually ploughed soil.

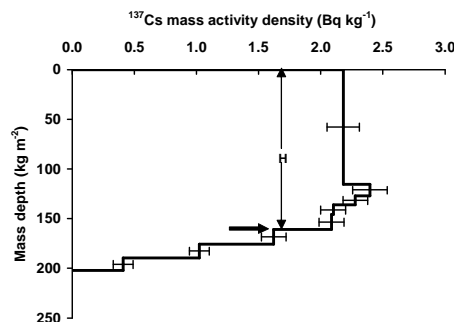


FIG. 1. Determination of the historical plough mass depth H (kg m^{-2}) under CT practice, for conditions similar to those of the study area (source: [5,13]).

The results obtained for the 29 sampling points in the study field using the simplified method, have been combined with those obtained from the previous application of the standard method for a single slope transect (5 points) within the same area, to provide information from five slope transects [5, 13]. Fig. 2 presents the spatial distributions of the soil redistribution rates obtained for the CT period (I) and NT period (II). These were mapped using a Kriging procedure.

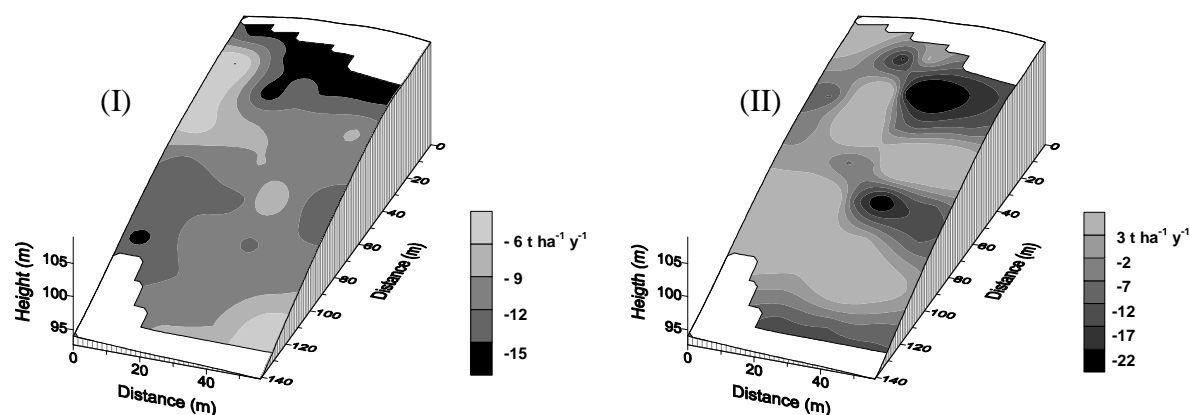


FIG. 2. The spatial patterns of mean annual erosion (negative values) and deposition (positive values) rates, established for the study area using ^{137}Cs measurements, for the period of CT (I) and during the subsequent period of NT system (II) (source: [13]).

Summary statistics for the study area relating to the periods of CT and NT have been derived using an areal weighting procedure applied to the soil redistribution rates estimated for the 34 sampling points within the study area and these are presented in the first two columns of Table 1.

For the CT period, extending from the beginning of ^{137}Cs fallout in 1954 to the shift to NT practice in 1986, an area-weighted mean annual erosion rate for the study area of $11 \text{ t ha}^{-1} \text{ year}^{-1}$ was estimated. This value is seen to be representative of the upper and middle portions of the study field, where erosion was expected to be the predominant soil redistribution process during the CT period. The results obtained corroborate this assumption, because all points investigated in the area evidenced erosion and the study area was therefore characterized by a sediment delivery ratio of 100%.

During the NT period extending from 1986 to 2003, only 57% of the study area was affected by erosion and this was characterized by an area-weighted mean erosion rate of $13 \text{ t ha}^{-1} \text{ year}^{-1}$. The remainder of the area was affected by deposition, with an area-weighted mean annual deposition rate of $14 \text{ t ha}^{-1} \text{ year}^{-1}$. These results demonstrate that in the study area the shift from CT to a NT system has caused soil erosion to decrease significantly to produce a net erosion rate of about $1.4 \text{ t ha}^{-1} \text{ year}^{-1}$, a gross erosion rate of $7.3 \text{ t ha}^{-1} \text{ year}^{-1}$, and a sediment delivery ratio of ca. 19%. Interestingly, the results obtained from the ^{137}Cs measurements show that within the study area, the shift to a NT system caused erosion rates in parts of the area to increase. The increase might reflect compaction in some areas as a result of the cessation of cultivation. This would be most likely to occur in those areas where previous erosion had caused the highest rates of soil loss and thus soil degradation (e.g. reduced organic matter content and increased bulk density), and could result in local increases in surface runoff. However, this increase was coupled with a shift from erosion to deposition over more than 40% of the study area, with the result that the sediment delivery ratio

decreased and both the gross and net soil loss from the study area decreased. In terms of soil degradation, the increased rates of soil loss over parts of the area must clearly be seen as undesirable, but more than 40% of the study area now experiences no soil loss and, equally importantly, the export of soil towards the stream network has been reduced to ca. 19% of that occurring during the period of CT. Overall, therefore, the introduction of NT management can be seen to have coincided with a significant reduction in both gross and net soil loss within the study area and to have greatly reduced the potential for diffuse source pollution of the local watercourses by eroded sediment.

TABLE 1. A COMPARISON OF THE SOIL REDISTRIBUTION DOCUMENTED FOR THE SAME AREA OF THE STUDY FIELD DURING THE PERIODS UNDER CONVENTIONAL TILLAGE (1954-1986), NO-TILL WITHOUT BURNING (1986-2003) AND NO-TILL WITH BURNING IN COMBINATION WITH HEAVY RAINFALL (MAY 2005)

	Conventional tillage	No-till, no burning	No-till with burning
	Mean annual values for a 32 year period estimated using ¹³⁷ Cs. Source: [13]	Mean annual values for a 16 year period estimated using ¹³⁷ Cs. Source: [13]	Values documented for a 27 day period of heavy rainfall, estimated using ⁷ Be. Source: [17]
<i>Year</i>	1954-1986	1986-2003	May 2005
<i>Period</i>	32 years	16 years	27 days
<i>Precipitation</i>	~1100 mm year ⁻¹	~1100 mm year ⁻¹	400 mm
<i>Length of the slope (m)</i>	130	130	130
<i>Sampling points</i>	34	34	27
<i>Eroding Zone</i>			
Mean erosion	11 ±2 t ha ⁻¹ year ⁻¹	13 ±2 t ha ⁻¹ year ⁻¹	18 ±2 t ha ⁻¹
Fraction of total area (%)	100	57	78
<i>Aggrading zone</i>			
Mean sedimentation	0 t ha ⁻¹ year ⁻¹	14 ±2 t ha ⁻¹ year ⁻¹	9 ±2 t ha ⁻¹
Fraction of total area (%)	0	43	22
<i>Total area</i>			
Net erosion	11 ±2 t ha ⁻¹ year ⁻¹	1.4 ±2 t ha ⁻¹ year ⁻¹	12 ±2 t ha ⁻¹
Sediment delivery ratio (%)	100	19	86

The mean annual soil redistribution rates for the periods under conventional tillage and no-till without burning were derived using ¹³⁷Cs measurements and the soil redistribution associated with a period of heavy rainfall occurring under no-till with burning was documented using ⁷Be measurements (source: [13,17]).

Although the results presented above clearly demonstrate that the shift to a NT system coincided with a reduction of both gross and net erosion rates and the area subject to erosion, it is important to consider whether the change in soil erosion associated with the NT period could reflect the influence of other factors, and, more particularly, reduced annual rainfall. The mean annual rainfall for Temuco Airport (38°45'S 72°38'W, some 45 km from the study site) over the period 1960 to the present is ca. 1230 mm, and therefore a little higher than the 1100 mm estimated for the study site, using the available record. However, it is thought that both stations would have experienced similar trends in annual rainfall over the past 40 years.

The years since 1986 at Temuco have generally been marked by reduced annual rainfall, with the mean for the period 1986 to 2003 being 1151 mm and ca. 11% lower than that for the preceding period extending from 1960 to 1985 (i.e. 1290 mm). It is clear that the reduced annual rainfall associated with the period since the introduction of NT is likely to have contributed to the reduced soil loss during this period, but in view of the substantial length of the period and the occurrence of many years with annual rainfall totals similar to those associated with the preceding period under CT, it is suggested that the shift to a NT system represents the primary cause of the reduced rates soil loss and sediment delivery documented for the period under a NT system [13].

The use of the ^{137}Cs approach to document the influence of a change from CT to NT possesses four key advantages over conventional plot based approaches for assembling such data. These are as follows:

- (1) The ability to generate information for individual fields or landscape units that is likely to prove more representative than the information provided by small plots, particularly when assessing net soil loss and sediment delivery to water courses.
- (2) The ability to produce medium term estimates of erosion rates associated with both CT and NT systems that will take account of the temporal variability of erosion rates.
- (3) The ability to undertake ‘before’ (i.e. with CT) and ‘after’ (i.e. with NT) investigations of the same field or study area.
- (4) The retrospective nature of the approach, which can provide information relating to medium term erosion rates operating in the landscape over the past ca. 45 years on the basis of a single site visit for the collection of soil samples.

3.2. A case study to document soil redistribution associated with a period of heavy rainfall occurring after the implementation of a no-till with burning of crop residues system by using ^7Be measurements

3.2.1. Site selection, sample collection and laboratory procedures

The investigation was undertaken at Buenos Aires farm in the previously described field, when the tillage system shifted from NT to a no-till with burning of the crop residue (NTWB) system, two years after the study described above [13]. The field had previously been under NT system for 18 years. After harvesting in early 2005 (summer) and before the wet season began, the crop residue remaining on the field was burnt in March 2005, leaving the soil bare until the onset of a period of very heavy rainfall in early May 2005 (autumn). The rainfall record for the period between January 1st and June 1st, 2005 is shown in Fig. 3.

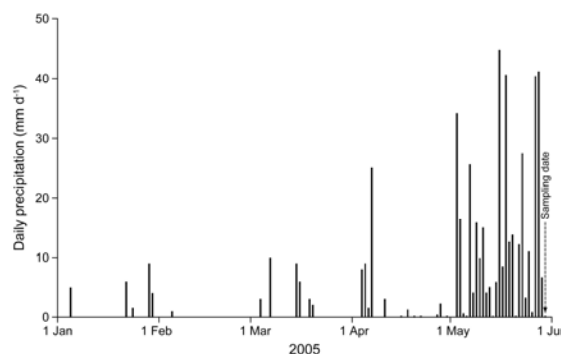


FIG. 3. The daily precipitation record for the study site for the period from January 1st to June 1st, 2005. The arrow shows the date of collection of the soil samples used for ^7Be measurements (source: [17]).

After a prolonged dry period with little precipitation, extending from January 1st to May 2nd, a period with an unusually high amount of precipitation occurred, extending from May 3rd to 29th, 2005. This period was characterized by a total rainfall of 400.5 mm in 27 days, including a 1 hour period on May 18th with 11.4 mm of rain. In the absence of a long rainfall record for the study site, it is not possible to provide a value for the recurrence interval of this period of heavy rainfall. However, based on the 52 year (624 month) record of monthly rainfall for the measuring station at Temuco Airport, some 45 km from the study site, it is estimated that a monthly rainfall total in excess of 400 mm was only recorded on three occasions, and therefore it can be considered as 'extreme rainfall'.

On May 30, one day after cessation of the extreme rainfall period, the field was sampled for ^7Be measurements, using the method described by Walling et al. [8] and Schuller et al. [10]. To document the variation in areal activity density produced by erosion and deposition associated with the period of NTWB and heavy rainfall, across the same study area where the ^{137}Cs approach was applied, soil cores were collected from 9 sampling points located at 15 m intervals along each of three slope transects spaced 15 m apart, superimposed onto the grid used to apply the ^{137}Cs models. At each sampling point, two soil cores (11 cm in diameter and 4 cm long) were collected.

To determine A_{ref} and h_o , two groups of nine cores, collected from a reference site, were sectioned into 2-mm slices, and the slices from each group representing specific depth increments were bulked for measurement as a single composite sample. A special device was used to facilitate slicing the cores. This device was designed and successfully used by Schuller et al. [10] and comprised a piston (with the same diameter as the internal diameter of the core tube), the movement of which is controlled by a screw thread. The piston is inserted into the base of the core tube and can be used to extrude 1 mm of core per full turn of the screw. The 2 mm slices of soil extruded by rotating the screw two turns were separated from the remaining core using a sharp pallet knife. The samples were analysed for their ^7Be content using gamma spectrometry using similar procedures to those described in section 3.1.1.

3.2.2. Results

The mean reference inventory measured for the two groups of cores collected from the reference site was $473 \pm 50 \text{ Bq m}^{-2}$. The linear regression between the natural logarithm of the mean areal activity density, $\text{Ln}[A(x)]$, and the mean mass depth, x , based on the two groups of sectioned cores collected from the reference site showed a high correlation coefficient ($r = 0.997$), which is significant at the 99% level of confidence, and confirms the expected exponential decrease of the areal activity density with depth. The values for the relaxation mass depth, h_o , and the reference areal activity density, A_{ref} , obtained from this relationship were $3.4 \pm 0.1 \text{ kg m}^{-2}$ and $499 \pm 10 \text{ Bq m}^{-2}$, respectively.

The calculated relaxation mass depth indicates that, at the reference site, 63% of the total areal activity density was found in the soil above a mass depth of 3.4 kg m^{-2} , i.e. the upper 2.5 mm. Removal of the upper 1 mm (about 1.4 kg m^{-2}) of the soil by erosion would result in a 34% reduction in the ^7Be areal activity density at an eroding point. Due to the low value of the relaxation mass depth and the exponential depth distribution of the areal activity density, small amounts of erosion and deposition associated with individual events or short periods of rainfall will be reflected by significant decreases or increases in the areal activity density, relative to the reference value, A_{ref} . The ^7Be method is therefore highly sensitive to relatively small amounts of erosion and deposition.

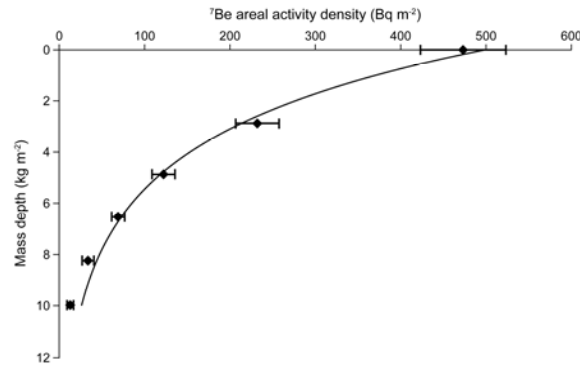


FIG. 4. The exponential decrease of the ${}^7\text{Be}$ areal activity density with mass depth documented for the reference site (source: [17]).

Fig. 4 indicates the depth distribution of the mean ${}^7\text{Be}$ areal activity density at the reference site. The exponential form of the distribution is characterized by the relaxation mass depth. By setting $h_o = 3.4 \text{ kg m}^{-2}$, $A_{ref} = 499 \text{ Bq m}^{-2}$ in Eq. (6), the resulting expression for the areal activity density is:

$$A(x) = 499 \exp(-x/3.4) \quad (13)$$

which is shown as a continuous line on Fig. 4. Because the ${}^7\text{Be}$ activity falls below the detection limit at mass depth 11.8 kg m^{-2} ($\sim 12 \text{ mm}$), the ${}^7\text{Be}$ areal activity density contained below this depth was subtracted from the total areal activity density estimated using the linear regression, i.e.:

$$499 - \int_{11.8}^{\infty} 147 \exp(-x/3.4) dx = 483 \text{ Bq m}^{-2} \quad (14)$$

The resulting value, 483 Bq m^{-2} , is in very close agreement with the mean areal activity density of $473 \pm 50 \text{ Bq m}^{-2}$ measured at the reference site and the former value was used as the reference areal activity density, when estimating the magnitude of soil redistribution associated with the period of extreme rainfall.

Summary statistics for the magnitude of the soil redistribution associated with the period of heavy rainfall occurring in May 2005, estimated from the ${}^7\text{Be}$ measurements for 27 sampling points (54 samples) located on three slope transects using Eqs. (8) and (9), and covering the same area studied previously using the ${}^{137}\text{Cs}$ approach, are provided in Table 1. The results indicate that about 78% of the sampled area experienced erosion, whereas deposition occurred over 22% of the area. The mean erosion estimated for the eroding area was 18 t ha^{-1} and the mean sedimentation for the areas experiencing deposition was 9 t ha^{-1} . Combining these data, the net erosion from the sampled area was estimated to be 12 t ha^{-1} . This indicates that a large proportion of the soil mobilised by erosion from the sampled area during the period of heavy rainfall was transported beyond that area [17].

The results presented above confirm the potential for using ${}^7\text{Be}$ measurements to document soil redistribution associated with individual periods of heavy rainfall. The ${}^7\text{Be}$ technique should therefore be seen as representing a valuable complement to ${}^{137}\text{Cs}$ measurements for soil erosion investigations in south-central Chile.

3.2.3. A comparison of the soil redistribution associated with the period of heavy rainfall occurring under a NTWB system, estimated using the ^7Be method, with that documented for the CT and NT periods

The magnitude of the values of short term soil redistribution presented above can usefully be compared with the longer term values of mean annual net erosion of $1.4 \text{ t ha}^{-1} \text{ year}^{-1}$ and $11 \text{ t ha}^{-1} \text{ year}^{-1}$ reported for the study field under the NT system and the original CT system, respectively, by Schuller et al. [13]. These data indicate that, while the value of net erosion recorded for the 27 day period of extreme rainfall in May 2005 was an order of magnitude greater than the mean annual rate of net erosion reported for the field for the period of 16 years when it was managed with a NT system, it is little different from the mean annual rate of net erosion reported for the previous 32 years when the field was managed under a CT.

The relatively high amount of net erosion associated with the period of NTWB and the heavy rainfall could be seen as reflecting both the extreme nature of the rainfall and the impact of the burning in modifying the erosion response associated with the standard NT system. It is not possible to ascribe a relative importance to these two controls, due to their close interaction and the availability of only a single measurement of event based soil redistribution for a period of heavy rainfall. A more comprehensive measurement programme, based on an experimental (factorial) design and involving several periods of rainfall of different magnitude with the presence and absence of burning, would be necessary to isolate the effects of the two controls. Nevertheless, some tentative conclusions can be drawn from the available information.

Table 1 compares the soil redistribution documented at the study site for the period of NTWB and heavy rainfall that occurred in May 2005 with the medium term mean annual rates of soil redistribution for the study site under both CT (1954-1986) and NT (1986-2003) documented using ^{137}Cs measurements. Based on this comparison, several observations, related to the impact of both the burning of the crop residue and the heavy rainfall associated with the May 2005 event on soil redistribution rates within the study area, can be made:

- (1) The net erosion associated with the period of NTWB and heavy rainfall is of similar magnitude to the mean annual rate of net erosion from the study field during the period under CT. Because it reflects an extreme event, the net erosion associated with the period of heavy rainfall is likely to considerably exceed the longer term mean annual rate of net erosion associated with the NTWB system under normal climatic conditions. It is therefore suggested that annual rates of soil erosion associated with the NTWB system under normal rainfall conditions are substantially less than under CT. If under the described scenario, it is assumed that the longer term mean annual net rate of soil erosion under NTWB management could be approximately 33% of that under conventional tillage, the rate under NTWB can be estimated to be ca. $4 \text{ t ha}^{-1} \text{ year}^{-1}$ [17].
- (2) The net erosion associated with the period of NTWB and heavy rainfall, is almost an order of magnitude greater than the mean annual rate of erosion from the study field during the period under NT system. Part of this increase reflects the extreme nature of the rainfall event and part the impact of burning the crop residues. However, if, following observation (1) above, it can be suggested that the net erosion associated with the extreme event is approximately 3 times greater than the mean annual rate of net soil erosion under the NTWB system under normal precipitation conditions, whilst the latter is approximately three times greater than the mean annual net soil loss under NT. In this situation, the extreme nature of the rainfall, rather than the burning of the crop residue, is the more important control on the high amount of erosion documented for the NTWB

period. Under the above scenario, the mean annual net soil loss increases from 1.4 t ha⁻¹ year⁻¹ under NT to 4 t ha⁻¹ year⁻¹ under NTWB, but the period of extreme rainfall increases the annual soil erosion for the year including the study period to >12 t ha⁻¹ year⁻¹.

- (3) There are important differences between the magnitude and nature of the soil redistribution reported for the three periods in Table 1. Under conventional tillage, there was no net deposition of sediment within the sampled area. However, significant deposition occurred during both the period of NT and the period of heavy rainfall following the burning. In the case of the period under NT, the erosion rates documented for the eroding area were essentially the same as those estimated for the period of CT. However the occurrence of significant rates of deposition over nearly half (43%) of the sampled area resulted in a net erosion rate that is almost an order of magnitude less than that associated with the period under conventional tillage. The key impact of the introduction of the NT system was therefore to increase redeposition of the sediment mobilised from the eroding areas, rather than to reduce rates of erosion from those areas. In the case of the period of heavy rainfall in May 2005, which followed the burning of the harvest residue, the soil mobilisation within the eroding zone was greater than the mean annual rates reported for the periods under NT and CT. However in contrast to the situation under CT, some deposition occurred over 22% of the sampled area, and as a result the net erosion was similar to the mean annual rate of net erosion reported for the period under conventional tillage.

4. CONCLUSIONS

The ¹³⁷Cs method provides a valuable alternative to conventional techniques for assessing the impact of changes in tillage system on soil erosion rates. This method was successfully employed in a study of a field located on a farm in south-central Chile. The results demonstrated a significant decrease in the rate of net soil loss and the portion of the study area subject to erosion, as well as in the sediment delivery ratio for the study area. The shift from CT to a NT system was found to be associated with a decrease in the net soil erosion rate of about one order of magnitude (from 11 t ha⁻¹ year⁻¹ to 1.4 t ha⁻¹ year⁻¹) and a reduction of the proportion of the eroded soil exported from the study area (the sediment delivery ratio) by 81% (from 100% to 19%). Additionally, the proportion of the study area subject to erosion decreased from 100% to 57%. The reduced soil loss has important benefits for the sustainable use of the soil resource, and the reduced sediment delivery ratio will result in a reduction in sediment transfer to the local watercourses, which will in turn reduce the offsite effects of soil erosion and, more particularly, diffuse source pollution associated with sediment inputs to the stream network. These changes clearly demonstrate the potential environmental benefits of a shift from CT to a NT system. Since the simplified ¹³⁷Cs method requires far fewer measurements, it also allows data to be assembled for a larger number of sampling points and thus from a larger area, thereby providing a more rigorous assessment of the changes in soil erosion rates associated with the change in tillage system.

⁷Be measurements were successfully used within the same field, to investigate the influence on soil erosion of the shift from NT to a NTWB system, two years after the original study. The field had previously been under NT system for 18 years. After harvesting in early 2005 (summer) and before the wet season began, the crop residue remaining on the field was burnt, leaving the soil bare until the onset of a period of very heavy rainfall (400 mm in 27 days). The results obtained for the NTWB with extreme rainfall period indicate that about 78% of the sampled area experienced erosion, whereas deposition occurred over 22% of the area. The

net erosion from the area was estimated to be 12 t ha⁻¹ and the sediment delivery ratio 86%, demonstrating that a large proportion of the soil mobilised from the sampled area by erosion during the period of heavy rainfall was transported beyond that area. The relatively high amount of net erosion associated with the period of NTWB and heavy rainfall could be seen as reflecting both the extreme nature of the rainfall and the impact of the burning in modifying the results obtained for the NT system. It is not possible to ascribe a relative importance to these two controls, due to their close interaction and the availability of only a single measurement of event based soil redistribution for a period of heavy rainfall. Nevertheless, some tentative conclusions have been drawn by comparing these results with the available information obtained for the CT and NT periods using ¹³⁷Cs measurements.

The application of ⁷Be measurements to document gross and net erosion on agricultural land in south-central Chile, associated with a period of heavy rainfall following the burning of crop residues, clearly confirms the potential for using this technique. The information on event-related erosion generated by the ⁷Be measurements provides a useful complement to that provided by the use of ¹³⁷Cs measurements to document the mean annual erosion rates associated with both CT and NT systems. In combination, the two radionuclides provide a valuable means of investigating soil erosion and assessing erosion risk in the study area. Although the use of ⁷Be measurements involves a number of important requirements and assumptions, related to both the preceding conditions and the occurrence of a discrete period of heavy rainfall that can be expected to cause significant erosion, the approach is likely to be applicable in many parts of the world, in addition to south-central Chile.

ACKNOWLEDGEMENTS

The financial support provided by IAEA Coordinated Research Programme D1-50-08, through contracts CHI-12321 and UK-12094; by FONDECYT Research Grants 1060119, 7060075 and 7070073; and by the Dirección de Investigación y Desarrollo, Universidad Austral de Chile, through contract S-2006-12, is gratefully acknowledged by the authors. Thanks are also extended to Mr. Werner Schürch, the landowner of Buenos Aires farm, for generously permitting access to the study site and the collection of soil cores, and to Helen Jones, Department of Geography, University of Exeter, for producing the figures.

REFERENCES

- [1] COMISIÓN NACIONAL DEL MEDIOAMBIENTE, Resúmenes de talleres: Diagnóstico y propuesta para la conservación de suelos (2000), <http://www.conama.cl/portal/1255/fo-article-26251.pdf>.
- [2] ELLIES, A., Soil erosion and its control in Chile - An overview, *Acta Geologica Hispanica* **35** (2000) 279-284.
- [3] INSTITUTO NACIONAL DE INVESTIGACIONES AGROPECUARIAS, Diagnóstico sobre el estado de degradación del recurso suelo en el país. Ed. INIA Centro Regional de Investigación Quilamapu, Chillán. *Boletín INIA* 15 (2001) 196 pp.
- [4] LIMON-ORTEGA, A., et al., Soil aggregate and microbial biomass in a permanent bed wheat-maize planting system after 12 years, *Field Crops Res.* **97** (2006) 302-309.

- [5] SCHULLER, P., et al., Use of ^{137}Cs measurements to estimate changes in soil erosion rates associated with changes in soil management practices on cultivated land, *Appl. Radiat. Isotopes* **60** (2004) 759-766.
- [6] WALLING, D.E., HE, Q., Improved models for estimating soil erosion rates from ^{137}Cs measurements, *J. Environ. Qual.* **28** (1999) 611-622.
- [7] BLAKE, W., et al., Fallout beryllium-7 as a tracer in soil erosion investigations, *Appl. Radiat. Isotopes* **51** 5 (1999) 599-605.
- [8] WALLING, D.E., et al., Use of ^7Be and ^{137}Cs measurements to document short- and medium-term rates of water-induced soil erosion on agricultural land, *Water Resource Res.* **35** (1999) 3865-3874.
- [9] WALLING, D.E., WOODWARD, J., Use of radiometric fingerprints to derive information on suspended sediment sources. In: *Erosion and Sediment Transport Monitoring Programmes in River Basins*. IAHS Publ. No. 210, IAHS Press, Wallingford, UK, (1992) 153-164.
- [10] SCHULLER, P., et al., Use of Beryllium-7 to document soil redistribution following forest harvest operations, *J. Environ. Qual.* **35** (2006) 1756-1763.
- [11] INTERNATIONAL COMMISSION ON RADIATION UNITS AND MEASUREMENTS, Quantities, unit and terms in Radioecology, Nucl. Tech. Publishing, Pep. 65. IRCU, Ashford, Kent, UK, (2001).
- [12] WALLBRINK, P., MURRAY, A., Distribution of ^7Be in soils under different surface cover conditions and its potential for describing soil redistribution processes, *Water Resources Res.* **32** (1996) 467-476.
- [13] SCHULLER, P., et al., Changes in soil erosion associated with the shift from conventional tillage to a no-tillage system, documented using ^{137}Cs measurements, *Soil Tillage Res.* **94** (2007) 183-192.
- [14] JUZDAN, Z.R., Worldwide deposition of ^{90}Sr through 1985. Environmental Measurements Laboratory, Report EML-515, U.S. Department of Energy, New York, NY 10014-3621 (1988).
- [15] SCHULLER, P., et al., Use of ^{137}Cs to estimate tillage- and water-induced soil redistribution rates on agricultural land under different use and management in central-south Chile, *Soil Tillage Res.* **69** (2003) 69-83.
- [16] SCHULLER, P., et al., Global weapons fallout ^{137}Cs in soils and transfer to vegetation in south-central Chile, *J. Environ. Radioact.* **62** (2002) 181-193.
- [17] SEPÚLVEDA, A., et al., Use of ^7Be to document erosion associated with a short period of extreme rainfall, *J. Environ. Radioact.* **99** (2007) 35-49.

USING CAESIUM-137 TECHNIQUES TO ESTIMATE SOIL EROSION AND DEPOSITION RATES ON AGRICULTURAL FIELDS WITH SPECIFIC CONSERVATION MEASURES IN THE TUTOVA ROLLING HILLS, ROMANIA

N. POPA, E. FILICHE, G. PETROVICI

Research and Development Center for Soil Erosion Control (RDCSEC)

Perieni

R.M. MARGINEANU

National Institute of Physics and Nuclear Engineering (NIPNE)

Magurele, Bucharest

Romania

Abstract

In the period from 2003 until 2007 a study was conducted at four representative micro-catchments in the Tutova Rolling Hills of Romania to estimate soil erosion and deposition rates on agricultural fields and to assess the efficiency of soil conservation measures. In the study several categories of soil conservation measures were evaluated, such as strip farming, bench terraces and forest belts. As a first step in the analysis, two reference sites were selected on an uneroded meadow and in an old rural cemetery. The ^{137}Cs inventory calculated for the first site was 6.90 kBq m^{-2} and for the second site 4.98 kBq m^{-2} . The ^{137}Cs results revealed that the highest erosion rates could be found in the centre of the strip crops where ^{137}Cs inventory varied between 2.12 and 4.77 kBq m^{-2} , while deposition of sediments was the largest on the bench terraces with a maximum inventory of ^{137}Cs of 14 kBq m^{-2} (exceptionally 44 kBq m^{-2}). The forest belts were characterized by high spatial variability in the deposition pattern; ^{137}Cs inventory ranged between 7.98 and 11.22 kBq m^{-2} . The comparative analysis between in situ and laboratory measurements of the ^{137}Cs inventories revealed that the portable detector has to be used with care, especially on steep slopes with strong roughness. Nevertheless, generally in situ measurements gave good estimates of soil erosion and sedimentation rates. Conventional measurements made on the runoff plots at the Perieni Center in the period of 1985-2006 indicated that annual erosion rates ranged between 2.1 and $8.9 \text{ t ha}^{-1} \text{ a}^{-1}$, depending on the crop rotation. A maximum value of $52.3 \text{ t ha}^{-1} \text{ a}^{-1}$ was registered for the plot of 150 m^2 under bare fallow. The smallest differences between the conventionally measured and the empirically and ^{137}Cs based estimated values have been observed in the case of those plots well covered by vegetation throughout the years, especially by brome grass. On the plots with annual crops like maize, bean, soybean and especially under bare fallow the values measured were often higher than those estimated by the empirical ROMSEM model, but came closer to the values calculated with the conversion models. This study showed that the use of the ^{137}Cs technique on agricultural lands from the Tutova Rolling Hills region, Romania, represents an alternative tool that can provide a valuable means for investigating soil erosion and assessing the efficiency of soil conservation measures. Nevertheless because of the complex landscapes further fine-tuning of the tool using fallout radionuclides is recommended.

1. INTRODUCTION

In Romania, about 43% (6.4 million hectares) of the total agricultural land is located on moderate to steep slopes and is subject to soil erosion. In addition, since 1991, the extension of the area under soil conservation practices has declined by more than 60%, which is attributed to a particular government policy developed in 1991. The related law n° 18/1991 stipulated that the land has to be reassigned to the original landowners resulting in the division of the agricultural land in long and narrow plots, which are often downslope oriented. The major impact of the law was the revival of the old traditional agricultural system leading to increased soil erosion.

Therefore, the use of fallout radionuclide (^{137}Cs) based techniques became an integrated part of the search for efficient measures to protect the soils and improve water quality in Romania. The first studies using fallout radionuclides started in 1996 in Eastern Romania in the scope of the FAO/IAEA Coordinated Research Project on ‘Assessment of Soil Erosion through the Use of ^{137}Cs and Related Techniques as a Basis for Soil Conservation, Sustainable Production and Environmental Protection’. Field measurements of the spatial distribution of ^{137}Cs in a small area of Upper Gaiceana in the Moldavian Plateau region were conducted until 2001 by Ionita et al. [5,6]. The ^{137}Cs technique was also successfully used to evaluate the development of gullies near Perieni and to assess reservoir sedimentation rates in the same Moldavian Plateau region.

The specific research objectives of the present study were:

- To measure soil erosion over several spatial and time scales in the Tutova Rolling Hills region of Romania using the ^{137}Cs technique,
- To assess the impact of changes in land use practices and the effectiveness of specific soil conservation measures commonly used in Romania.

2. MATERIALS AND METHODS

2.1. Study sites

The present study has been conducted at four representative micro-catchments located in the Tutova Rolling Hills region of Romania ($46^{\circ} 15' - 46^{\circ} 16' \text{N}$, $27^{\circ} 35' - 27^{\circ} 39' \text{E}$): (1) Tarnii (300 ha), with uniform gentle¹ to rolling slopes, (2) Crang (30 ha), with gentle to hilly slopes, (3) Gheltag (100 ha), also with gentle to hilly slopes and finally (4) a research site of 20 ha in the Seaca catchment with slope gradients of about 8-9% (Fig. 1). All study areas comprise a range of categories of soil conservation measures according to WOCAT [12]: strip farming, buffer strips, bench terraces, forest belts and an adequate agricultural exploitation road network.

All four study sites are characterized by a temperate-continental climate, with an annual average rainfall of 490 mm, and an annual average temperature of 9.8°C . The dominant soil in the area is Cambic Chernozem, which is moderately to severely eroded. The most common crops are: winter wheat, maize, peas, soybean, bean, sunflower and alfalfa. Typical crop rotations are composed of winter wheat, peas and maize.

In the Tarnii micro-catchment eight conventional runoff plots, fully instrumented for measuring runoff and soil loss under different conditions concerning vegetative cover have been used since 1985. The soil type at these plots, with a slope gradient of 12%, is a moderately deep Cambic Chernozem, medium clay loam textured, characterized by moderate erosion.

In order to assess the effectiveness of conservation practices compared with the ‘traditional’ downslope-oriented long and narrow strips, an experimental site of 20 ha arable land, located on the western hillside of Seaca Micro-catchment, was selected (Fig. 2). Soil type and gradient slope are similar to those in the runoff plot site at the Tarnii micro-catchment. At this site two different land management practices were identified:

¹The authors used the WOCAT classification for slope gradients with following ranges: flat 0-2%; gentle 2-5%; moderate 5-8%; rolling 8-16%; hilly 16-30%; steep 30-60%.

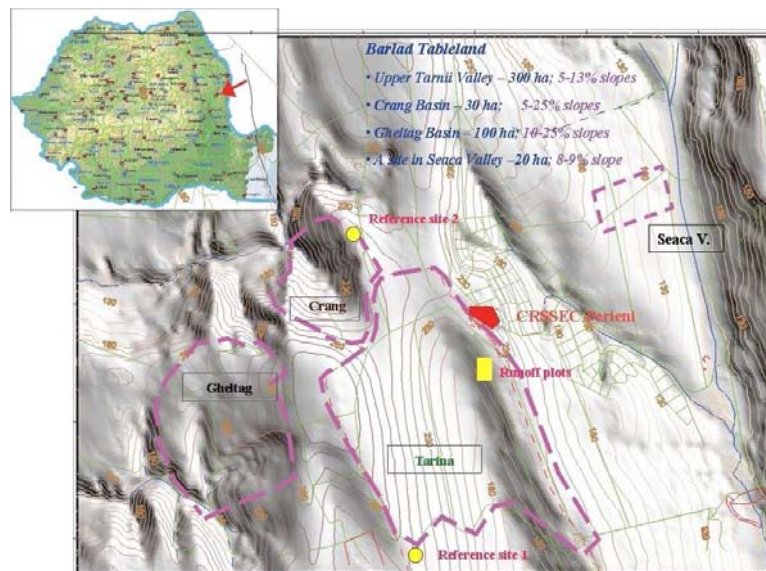


FIG. 1. Selected study sites from the Tutova Rolling Hills, Romania.



FIG. 2. Comparative study on soil erosion by the ^{137}Cs technique under two different agricultural systems in the Seaca Micro-catchment, Eastern Romania.

- (1) On the first site, soil conservation was initiated during the 1960s – 1970s, mainly by using contour strip-cropping, adequate crop rotation and soil fertility management. Since then, this site has been managed continuously by RDCSEC – Perieni.
- (2) On the second site, the land was protected with the same soil conservation measures, but was reassigned to the original landowners in 1991, according to the Law 18/1991 and divided into small long and narrow downslope oriented parcels. Since 1992 until present, a traditional subsistence agricultural system has been used.

2.2. Experimental methods

2.2.1. Reference sites

The approach used to estimate erosion and deposition rates was based on the comparison of the measured ^{137}Cs inventories (kBq m^{-2}) along representative transects through each study-

site with a reference value that represents the inventory at a site where neither erosion nor deposition was observed. The reference value provides an assessment of the total ^{137}Cs fallout input to the site, corrected for the radioactive decay at the time of sampling. The estimates of the erosion or deposition rate ($\text{t ha}^{-1} \text{ a}^{-1}$) represents an average rate for the period extending back from the time of sampling to the beginning of ^{137}Cs fallout.

The flat and uneroded reference sites have been continuously covered by vegetation over the last 60 years. The first one is an old rural cemetery and the second is a meadow.

2.2.2. ^{137}Cs sampling and measurements

The ^{137}Cs distribution at the upper Tarnii micro-catchment has been assessed by a single transect which went through three bench terraces and two forest belts. The slope gradient of the selected transect varies between 12 and 14%, and the width of strip cropping fields is about 100m. The measurements were made in the upper part, middle part and platform of the terraces to determine relationships between ^{137}Cs activity and the redistribution of eroded soil along the slope.

In the Crang micro-catchment, a transect was selected crossing two terraces which comprised ten sampling locations, while in the Gheltag micro-catchments seven sampling points were located along a single transect to characterize the effectiveness of narrow terraces in reducing soil erosion on hilly slopes. On the research site at the Seaca catchment the measurements were carried out along two transects on each of the previously described locations. On each transect five sampling points were established (Fig. 2).

Data referring to the aggradation of the platform of terraces owing to tillage translocation, were obtained by topographical measurements made on five parallel transects at 1 m distance [9].

For soil sampling, a scraper device [2,7,11] and conventional soil augers have been used. Where the depth of sediment in depositional areas was thin or in reference sites where neither soil loss nor sediment deposition occurred, the samples were collected at 1 or 2 cm intervals [13]. In deep sediments, depth increments were usually 10 or 20 cm, depending on the auger bucket. The mass of soil collected varied between 0.5-1.5 kg and depended on the dimensions of the scraper (20×50cm), the bulk density and the depth increment involved.

The following procedure for sample processing has been used:

- spreading on a tray and dried at room temperature for 3 – 10 days;
- removing of the gravel and vegetal debris;
- sieving through 2 mm steel sieve
- dried at 105° C for constant weight
- 100 g of sample was put into a cylindrical box
- evaluation of ^{137}Cs activity
- calculation of uncertainties

Counting time for gamma spectrometry ranged between 15000 and 67000s using a Canberra S100 system equipped with a Ge(HP) detector (18% rel. efficiency, HV=+3500V, FWHM=1.95 keV). Spectra were analyzed with SAMPO 90 dedicated computer code.

2.2.3. Runoff plots

In the year 1985 eight runoff plots, with a slope gradient of 12%, were located at the north-east hillside of the Tarnii micro-catchment (Latitude 46° 15' 50' N, Longitude 27° 37' 30' E) at an elevation of 218 m a.s.l. Five out of eight of them have a surface area of 100m² (25×4m with 1 m border areas between them) and the other two are 150m² (37.5×4m). Runoff water and eroded soil are collected in three tanks placed in cascade. Six plots are cultivated with the following crops: maize, beans, soybeans, winter wheat and brome grass. Two control plots of 100 and 150 m² are kept under bare fallow, continuously free of weeds. Besides total runoff and eroded soil, information is collected concerning lost organic matter, nitrogen (total N, NO₃⁻, NH₄⁺), phosphorus and potassium.

In the present study analysis of the soil erosion data has been carried out based on the records since 1985. In addition, from each plot, samples to determine ¹³⁷Cs activity were collected. Sample points were set along six transects for short plots and nine for long plots placed at 5 m intervals. On each transect three samples were taken for obtaining a single composite sample.

2.2.4. Conversion model comparisons

In the present study conversion models were used to convert the fallout radionuclide data into soil erosion and deposition rates. A comparison between measured and simulated data for all assessed conversion models (Proportional Model, Mass Balance (MB) Model 1, MB 2, MB 3 [10] and ROManian Soil Erosion Model (ROMSEM) has been made.

The proportional model is based on the premise that ¹³⁷Cs fallout inputs are completely mixed within the plough or cultivation layer and that the soil loss is directly proportional to the amount of ¹³⁷Cs removed from the soil profile since the beginning of the ¹³⁷Cs accumulation. Thus, if half of the ¹³⁷Cs input has been removed, the total soil loss over the period is assumed to be 50% of the plough depth.

Mass Balance Model 1 takes account of both inputs and losses of ¹³⁷Cs from the profile over the period since the onset of ¹³⁷Cs fallout and assumes that the total ¹³⁷Cs fallout occurred in 1963 instead of over a longer period extending from the mid 1950s to the mid 1970s.

Mass Balance Model 2 requires consideration of the time-variant fallout ¹³⁷Cs input and the fate of the freshly deposited fallout before its incorporation into the plough layer by cultivation.

Mass Balance Model 3, in addition to MB2, incorporates soil redistribution introduced by tillage.

In Romania, as an alternative to the USLE, the ROMSEM has been developed to estimate soil erosion on hillslopes [8]:

$$Es = K \cdot S \cdot L^m \cdot I^n \cdot C \cdot C_s \quad (1)$$

where: Es (t·ha⁻¹·a⁻¹) is the computed soil loss per unit area and year; K is the erosivity factor obtained by multiplying the amount of precipitation by the maximum 15-min. intensity (i_{15} - in mm per min), for a given rainstorm; S is the soil erodibility ($S = 1$ for cambic chernozem severely eroded); L^m (m) is the field slope length, $m=0.3$; I^n (%) is the mean slope, $n=1.4$; C is the cover management factor that shows the influence of crops and tillage ($C = 1$ for corn

cultivated year by year); C_s is the support practice factor (C_s is 1 for land where there are no measures to control soil erosion).

The main differences as compared with USLE are:

- the dimensional factor is no longer erodibility but erosivity;
- the topographic factor ($L \cdot i$) is no longer the ratio of soil loss per unit area as measured on a standard plot but directly L (m) i (%).

Developed on the basis of long term studies conducted on runoff plots, ROMSEM has been widely used in Romania in scientific planning for soil and water conservation. For more than 40 years the model helped for selecting the control practices best suited to the particular need of agricultural land.

2.2.5. *In situ* measurements of ^{137}Cs activity

Besides fallout radionuclide measurements in the lab, additional *in situ* measurements of ^{137}Cs activity were carried out in all study sites over the period of 2003-2006 by using a Canberra Ge HP portable detector, 18% efficiency. In 2007, a new Ortec Ge HP portable detector, High Voltage 4500 V, 33% efficiency has been used.

The portable gamma spectroscopy system provides a practical way to characterize dispersed fallout radionuclides in or on the soil. *In situ* gamma spectroscopy detects all the radioactivity. The main advantage of this system is that there is no need to collect soil samples and the period of investigation is reduced significantly. With laboratory analyses, there is much labour involved, and a long processing time to get the analysis results.

Usually *in situ* measurements were performed in the same locations as those where soil samples were collected. All *in situ* measurements were compared with the measurements carried out in the laboratory. *In-situ* gamma spectrometry efficiency calibration of the detector was performed according to Beck's methodology (HASL 258, 1972) [1].

3. RESULTS

3.1. ^{137}Cs technique

3.1.1. ^{137}Cs activity in reference sites

For the reference site N° 1 (Fig. 3) the calculated ^{137}Cs inventory was 6.90 kBq m^{-2} while for the reference site N° 2 (Fig. 4) ^{137}Cs inventory was 4.98 kBq m^{-2} . These sites have been continuously covered by vegetation over the last 60 years, and the high inventories indicate significant deposition of fallout from both thermonuclear weapons test and Chernobyl. The lower level of ^{137}Cs activity in reference site N° 2 was likely explained by the fact that the surface of terrain is flat but distinctly convex. The wind-driven effect on ^{137}Cs deposition is much more severe close to the top of the hill [3] and it is assumed that this has reduced initial deposition of ^{137}Cs .

3.1.2. ^{137}Cs results from the Tarnii micro-catchment

At the Tarnii micro-catchment the studied transect crossed three terraces and two forest belts (Fig. 5). As the transect was located at equal distance from both reference sites, an average of 5.94 kBq m^{-2} for the ^{137}Cs inventory reference was used.

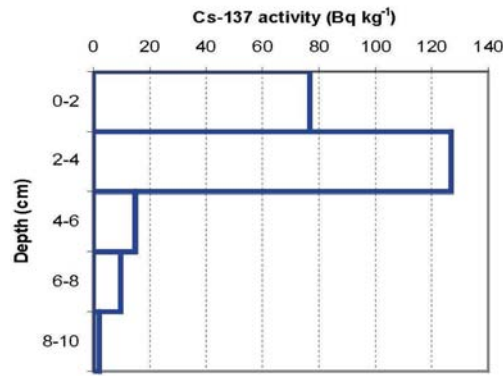


FIG. 3. ^{137}Cs activity at reference site N° 1.

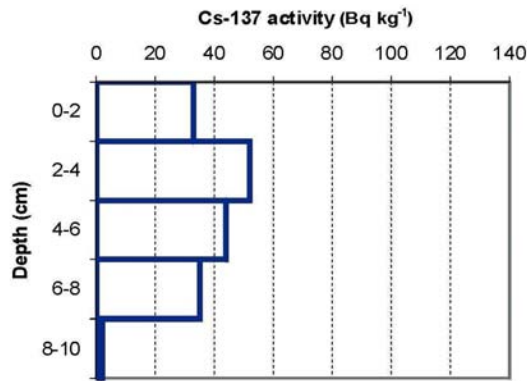


FIG. 4. ^{137}Cs activity at reference site N° 2.

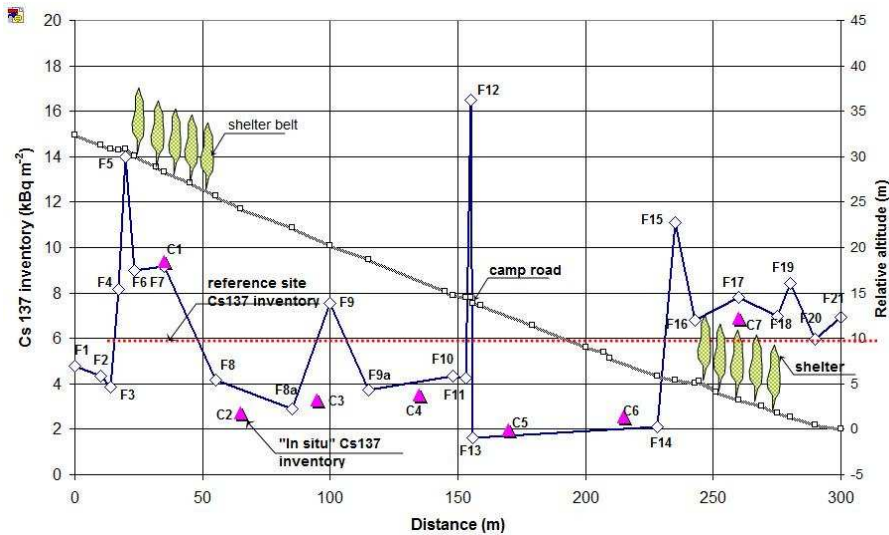


FIG. 5. ^{137}Cs inventory of 21 soil profiles from the Tarnii micro-catchment.

The ^{137}Cs inventory for sampling points F1, F2, F3, F8, F10, F11, and F14 presented values below the reference line indicating soil erosion and varied between 2.12 and 4.77 kBq m⁻².

The high ^{137}Cs inventory at F9 could initially not be explained, as there was clearly erosion taking place at the site. Moreover, the additional sampling points at F8a and F9a located around F9, undergoing similar erosion as in F9, indicated low ^{137}Cs inventories. More detailed

investigation about F9 and its history, showed that exactly at the sampling point a pit for a soil profile was made some years ago, which affected the measurements.

In F8, the low ^{137}Cs inventories or soil loss was explained by the influence of tillage erosion.

The lowest ^{137}Cs activity was observed in F13 (1.95 kBq m⁻²) where a significant part of the topsoil was removed in 1993 when a road was constructed.

For the sampling points F4, F5, F12, F15 and F16, which were located on the terraces with a slope gradient of less than 5%, high values of the ^{137}Cs inventory with a maximum of 13.97 kBq m⁻² reflected the dominant sedimentation process.

The points F6, F7, F17 and F18, inside the forest belts, were characterised by a high spatial variability in the ^{137}Cs inventory (7.98 – 11.22 kBq m⁻²), which can be linked with the process of tree toppling and root throw resulting in sediment disturbance. The soil associated with the root wad was upheaved in the form of a root plate, which eventually disintegrates [4]. The disintegrating sediment may either have been returned to the pit or landed on the ground forming a mound, which was then susceptible to transport by other processes. In addition, the heterogeneity in soil cover by the tree canopy can be as well part of the reason for the observed spatial variability in the ^{137}Cs inventory. However, the average inventories (11.04 kBq m⁻² for SB1 and 8.66 kBq m⁻² for SB2) are above the reference inventory, indicating overall soil deposition in the forest belts. Nevertheless, field observations show that this sedimentation process inside the shelter belts is rather limited.

In addition, the *in situ* measurements of the ^{137}Cs inventories, from C1 to C7 in Fig. 5, indicated values that were generally close to the laboratory measurements.

Fig. 6 shows that for soil profile F-5 the high ^{137}Cs activity of 11.8 Bq kg⁻¹ at a depth of 0-20 cm still remained at 11.4 Bq kg⁻¹ at a depth of 60-80 cm. This illustrates the large deposition of translocated sediments on the nearly levelled platform of the terraces. Soil translocation was linked with water erosion but also with tillage erosion. Taking into account that this maximum value of ^{137}Cs activity at a depth of 80 cm corresponds to the year 1986 when the Chernobyl nuclear plant accident happened, the calculated annual rate of sediment deposition for this terrace platform is about 4.2 cm a⁻¹ in comparison with 4.5 cm a⁻¹, measured by a conventional topographical method.

Fig. 7 shows that most of the ^{137}Cs activity for soil profile F-7 is present only at the soil surface. This confirms that the forest belts retained just a small part of sediment in comparison with the terraces. Net erosion of the this transect, calculated by the conversion model Mass Balance 3 [10], was 8.5 t ha⁻¹yr⁻¹. In running the model the following parameters have been used: reference inventory = 5.94 Bq m⁻², alpha factor = 1.146, year of sample collection = 2005, bulk density = 1200 g cm⁻³, proportion factor gamma = 0.5, relaxation depth = 4 cm, plough depth = 0.15m and tillage flux phi = 11.6.

3.1.3. ^{137}Cs results from the Crang micro-catchment

In Table 1 data for the transect through two terraces at the Crang micro-catchment are presented, where additional measurements concerning tillage erosion were initiated in 1998. The topographical measurements made after ploughing and seeding in 1998 and 2003, showed significant modifications of the terrace height because of soil deposition mainly due to soil translocation by tillage. The average rise of the terraces was 3.8 cm a⁻¹.

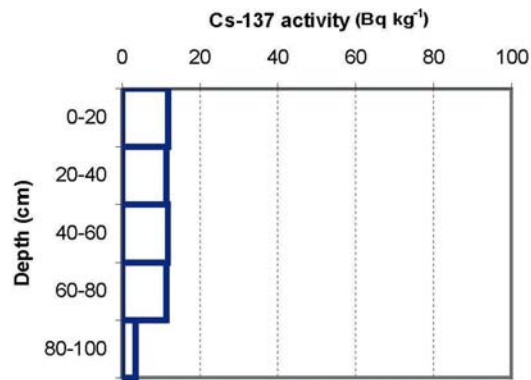


FIG. 6. ¹³⁷Cs activity of the soil profile F-5 at the Tarnii micro-catchment.

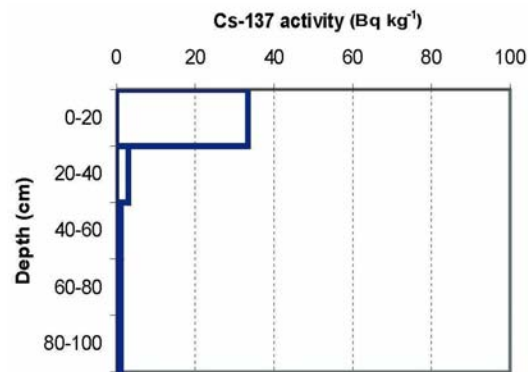


FIG. 7. ¹³⁷Cs activity of the soil profile F-7 at the Tarnii micro-catchment.

TABLE 1. CAESIUM-137 INVENTORY OF 10 SOIL PROFILES AT THE CRANG MICRO-CATCHMENT

Point	Distance from the edge of transect (m)	Relative altitude (m)			Slope (%)	Land use	¹³⁷ Cs kBq m ⁻²
		year 1998	year 2003	difference			
	0						
C-F1	1.5	0.556	0.760	0.204	93.8	C	44.40*
C-F2	3	0.629	0.819	0.190	-4.6	C	8.31
C-F3	15	2.311	2.315	0.005	13.9	C	4.17
C-F4	34	4.827	4.804	-0.023	13.8	C	6.96
C-F5	36	5.182	5.142	-0.040	13.8	C	8.07
C-F6	40	6.125	6.399	0.274	-2.5	C	12.45
C-F7	41.5	6.182	6.395	0.213	-0.4	C	10.74
C-F8	60	8.521	8.510	-0.011	12.9	C	9.93
C-F9	74	10.642	10.604	-0.038	13.0	C	5.28
C-F10	76	11.158	11.113	-0.045	15.2	C	6.84

C- Cultivated land; *: a deposit of sediments of about 1.4m thickness, next to a road.

The highest values of ^{137}Cs inventory were determined at positions C-F1 and C-F6, situated on the platform of the terraces where the sedimentation process was much more evident. The low values of ^{137}Cs activity at C-F4, C-F5, C-F9 and C-F10 confirmed that tillage erosion is more intensive in the upper part of the cropping strips. The C-F3 sampling position that was placed in the lower part of the strip showed the lowest value of ^{137}Cs activity, probably due to water erosion.

The conversion of the inventories into soil erosion rates by the Mass Balance 3 Model showed that net erosion for this transect was about $2.5 \text{ t ha}^{-1} \text{ a}^{-1}$.

3.1.4. ^{137}Cs results from the Gheltag micro-catchment

The results from the Gheltag micro-catchment, concerning the ^{137}Cs inventories, are presented in Table 2. A transect through two terraces from the lower part of the hillslope was made. The reference inventory was calculated as an average of the values determined at reference site N° 1 and reference site N° 2.

On the narrow terraces, soil redistribution could be mainly assigned to tillage erosion. Thus, measurements at positions G-F1, G-F3 and G-F4 whose ^{137}Cs inventories were below the reference value, indicated that significant erosion had occurred since 1986. Year by year, soil was translocated to the lower edge of terraces, a process that was reflected by the high values of ^{137}Cs activity at the G-F2 and G-F5 sampling points.

Values of soil losses calculated by Mass Balance 3 Model ranged between 8.3 and $18.6 \text{ t ha}^{-1} \text{ a}^{-1}$ while values of deposition were situated between 22.1 and $57.8 \text{ t ha}^{-1} \text{ a}^{-1}$. Net erosion for the entire transect was $1.8 \text{ t ha}^{-1} \text{ a}^{-1}$.

TABLE 2. CAESIUM-137 INVENTORY FOR 7 SOIL PROFILES FROM THE GHELTAG MICRO-CATCHMENT

Point	Distance from the edge of transect (m)	Relative altitude (m)			Slope (%)	Land use	^{137}Cs (kBq m ⁻²)
		year 2003	year 2005	difference			
G-F1	12.0	1656	1626	-0.03	10.5	C	1.6
G-F2	15.6	3229	3429	0.20	43.7	C	9.2
G-F3	23.0	3459	3559	0.10	6.9	C	4.5
G-F4	28.0	4143	4143	0.00	15.2	C	4.8
G-F5	31.0	6091	6241	0.15	64.9	C	15.5
G-F6	35.7	6384	6384	0.00	9.7	C	6.2
G-F7	40.5	6769	6569	-0.20	8.5	C	4.8

C – Cultivated land

3.2. Comparison of *in situ* and laboratory measurements of ^{137}Cs activities

In the period from 2005 until 2007 some *in situ* measurements were made, firstly by means of a Canberra Ge HP portable detector and finally by a new Ortec Ge HP detector. Count times ranged between 3,000 and 10,000 seconds and it was assumed that the distribution of ^{137}Cs in the soil is uniform, considering that the land is arable.

Figure 8 shows a relatively good relationship between values of ^{137}Cs inventory measured *in situ* and those determined in the laboratory.

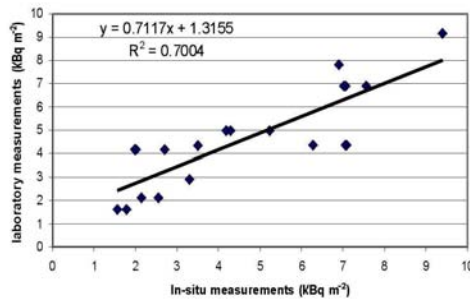


FIG. 8. The relationship between laboratory and in situ measurements of ^{137}Cs activity.

However a few differences have been noticed that can be explained by the fact that the portable detector mounted on a tripod 1 m above the ground surface is a circle of about 20 m^2 . Also, the detector was set perpendicular to the ground surface to ensure that gamma ray is collected symmetrical from the whole area. The result of *in situ* measurement can therefore average the ^{137}Cs inventory over all points located inside the circle. Therefore the correlation between the *in situ* and laboratory measurements is often lower near the boundary of different land uses or on steeper slopes. 3.3. Runoff, soil and nutrient losses on runoff plots at Perieni Center, Romania

Through time, each runoff plot was affected by erosion. In Table 3 soil erosion data since 1985 are presented.

Major differences among the measured data can be explained by the crops grown on the plots (Figure 9). Among the cultivated plots, plot N° 2 was the most eroded with $8.6\text{ t ha}^{-1}\text{ a}^{-1}$ of soil removed by water. On this plot, maize and beans were cultivated with a frequency of 27-26% during the period of time between 1985 and 2006.

Theoretically, concerning vegetative cover the best crop rotation offering appropriate protection of the soil against erosion can be observed on plot N° 4 where crops such as bromus grass, winter wheat and flax were cultivated in 15 out of 22 years. However, the plot with the lowest erosion rates was plot N° 5 from which only $2.0\text{ t ha}^{-1}\text{ a}^{-1}$ of soil was lost. During 22 years, crops like bromus (29%), flax (14%) and winter wheat (19%) covered and protected the soil against erosion for about 62% of the whole period while the crops, which made the soil vulnerable to erosion were grown for the remaining time (corn 14%, bean 19% and soybean 5%). The difference in soil erosion was due to two main rain events from 1993 when plot N° 4 was not so well covered (protected) by beans. The recorded erosion was 31.6 t ha^{-1} while on plot N° 5, covered by bromus grass, soil loss was clearly lower with 0.289 t ha^{-1} .

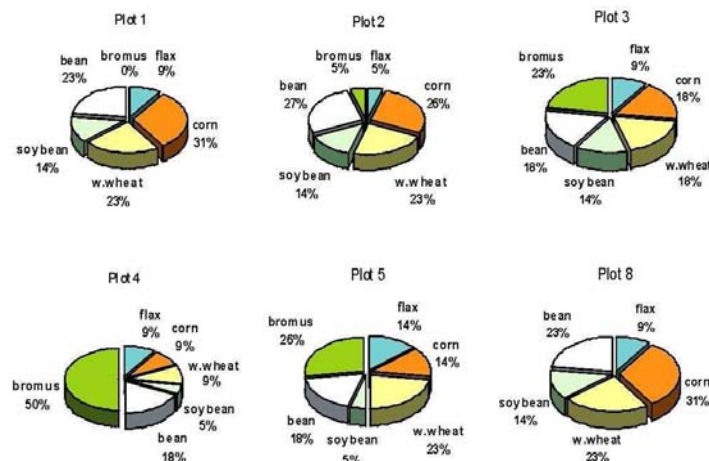


FIG. 9. Crop frequency on runoff plots at Perieni, Romania, between 1985 and 2006.

TABLE 3. EROSION ON RUNOFF PLOTS AT THE PERIENI CENTER DURING THE PERIOD OF 1985-2006 ($t\ ha^{-1}$)

Year	Plot 1		Plot 2		Plot 3		Plot 4		Plot 5		Plot 6		Plot 7		Plot 8	
	crop	erosion	crop	erosion	crop	erosion	crop	erosion	crop	erosion	crop	erosion	crop	erosion	crop	erosion
1985	flax	1.000	bean	2.000	corn	6.565	bromus	0.000	w.wheat	0.163	B. fallow	12.502	B. fallow	14.404	flax	2.001
1986	bean	0.865	w.wheat	0.105	bromus 1	3.381	flax	0.447	corn	1.153	B. fallow	6.925	B. fallow	8.781	bean	1.425
1987	w.wheat	3.447	corn	48.105	flax	24.879	bean	12.810	bromus 1	2.259	B. fallow	71.647	B. fallow	84.793	w.wheat	3.422
1988	corn	14.902	bromus 1	2.897	bean	17.436	w.wheat	0.014	flax	0.043	B. fallow	18.917	B. fallow	24.263	corn	8.042
1989	corn	7.252	flax	3.614	w.wheat	1.524	bromus	0.463	bean	0.193	B. fallow	58.016	B. fallow	78.343	corn	15.834
1990	flax	0.452	bean	0.164	corn	0.662	bromus	0.000	w.wheat	0.000	B. fallow	1.193	B. fallow	1.216	flax	0.000
1991	Bean	2.908	w.wheat	8.893	bromus 1	2.661	flax	0.000	corn	2.858	B. fallow	70.174	B. fallow	84.028	bean	11.590
1992	w.wheat	0.000	corn	2.778	bromus 2	0.000	bean	1.606	flax	0.000	B. fallow	4.477	B. fallow	5.113	w.wheat	0.000
1993	corn	27.691	bean	31.580	bromus 3	0.289	bean	31.580	bromus 1	0.289	B. fallow	48.890	B. fallow	78.332	corn	31.456
1994	bean	0.000	w.wheat	0.000	bromus 4	0.000	corn	1.026	flax	0.000	B. fallow	8.249	B. fallow	15.707	bean	0.000
1995	w.wheat	0.209	corn	2.962	flax	6.697	bromus 1	0.000	bean	3.497	B. fallow	21.939	B. fallow	31.719	w.wheat	2.763
1996	corn	2.426	bean	8.305	soy bean	7.083	bromus 2	0.011	w.wheat	0.000	B. fallow	29.684	B. fallow	56.391	corn	3.125
1997	soybean	19.846	w.wheat	0.449	corn	9.494	bromus 3	0.000	bean	7.631	B. fallow	123.450	B. fallow	145.388	soy bean	97.082
1998	corn	0.000	soy bean	0.000	bean	0.000	bromus 4	0.000	w.wheat	0.000	B. fallow	7.149	B. fallow	7.960	corn	0.000
1999	bean	23.686	corn	39.887	w.wheat	0.153	soy bean	18.120	bromus 1	0.230	B. fallow	219.018	B. fallow	239.682	bean	12.393
2000	w.wheat	0.000	soy bean	0.739	bean	0.737	corn	0.000	bromus 2	0.000	B. fallow	7.316	B. fallow	10.244	w.wheat	0.000
2001	soybean	0.163	corn	2.990	w.wheat	0.000	bean	0.000	bromus 3	0.000	B. fallow	18.230	B. fallow	24.200	soy bean	1.474
2002	corn	10.512	bean	2.573	soy bean	4.059	w.wheat	2.506	bromus 4	0.000	B. fallow	59.345	B. fallow	89.444	corn	18.128
2003	bean	0.000	w.wheat	0.000	corn	0.000	bromus 1	0.000	soy bean	0.000	B. fallow	6.886	B. fallow	8.529	bean	0.000
2004	w.wheat	0.033	soy bean	0.037	bean	0.720	bromus 2	0.090	corn	1.275	B. fallow	53.833	B. fallow	63.689	w.wheat	0.026
2005	soybean	30.170	corn	30.486	w.wheat	0.010	bromus 3	0.000	bean	25.000	B. fallow	39.003	B. fallow	42.460	soy bean	32.303
2006	corn	0.052	bean	0.340	soy bean	0.040	bromus 4	0.000	w.wheat	0.000	B. fallow	31.691	B. fallow	36.951	corn	0.528
TOTAL ($t\ ha^{-1}$)		145.6		188.9		86.4		68.7		44.6		918.5		1151.6		241.6
Annual erosion rate ($t\ ha^{-1}\ a^{-1}$)		6.6		8.6		3.9		3.1		2.0		41.8		52.4		11.0

Runoff, soil and nutrient losses in water and sediments have been monitored after every rainfall event that produced runoff and sediments. Generally the values of nutrient losses from each plot (Table 4) were strongly correlated with the values of runoff and erosion. Correlation coefficient calculated for each plot ranged between 0.53 and 0.87. Some exceptions were noticed in the period of spring, after applying of fertilizers when low values of runoff and soil losses were associated with high values of nutrient losses.

TABLE 4. ANNUAL RUNOFF, SOIL AND NUTRIENT LOSSES ON RUNOFF PLOTS CALCULATED FOR THE PERIOD OF 1985-2006

Plot No.	Runoff m ³ ha ⁻¹	Nutrient losses in runoff				
		NO ₃ kg ha ⁻¹	NH ₄ kg ha ⁻¹	N kg ha ⁻¹	P ₂ O ₅ kg ha ⁻¹	K ₂ O kg ha ⁻¹
Plot 1	136.2	0.202	0.137	0.339	0.086	0.556
Plot 2	149.9	0.222	0.151	0.373	0.095	0.612
Plot 3	131.9	0.205	0.134	0.338	0.083	0.551
Plot 4	117.3	0.195	0.119	0.315	0.072	0.508
Plot 5	73.7	0.116	0.076	0.191	0.046	0.313
Plot 8	163.8	0.239	0.162	0.410	0.102	0.675
		Soil and nutrient losses				
		Erosion t ha ⁻¹	Org. Matter. kg ha ⁻¹	N kg ha ⁻¹	P ₂ O ₅ kg ha ⁻¹	K ₂ O kg ha ⁻¹
Plot 1		6.9	149	7.6	0.456	1.069
Plot 2		9.0	164	8.4	0.502	1.176
Plot 3		4.1	135	6.9	0.410	0.963
Plot 4		3.3	108	5.5	0.323	0.764
Plot 5		2.1	71	3.6	0.214	0.504
Plot 8		11.5	240	12.6	0.716	1.289

In Table 5 the ¹³⁷Cs inventories for the transects on all eight plots are presented. As the runoff plots are located approximately at equal distance from the reference site N°1 and N° 2, the average of 5.94 kBq m⁻² as ¹³⁷Cs inventory reference appears to be the most probable value. However, taking into account the slope orientation to the west (direction of predominant wind) the maximum value of 6.9 kBq m⁻² has been chosen. On the cultivated plots, the minimum ¹³⁷Cs inventories were generally measured approximately in the centre of the plots (in F3 for the plot 5, in F4 for the plots 2 and 4 and, in F5 for the plots 1 and 3). They varied between 4.70 and 6.08 kBq m⁻². The lowest values of ¹³⁷Cs inventory were found for plots 7 and 8 under bare fallow

TABLE 5. CAESIUM-137 INVENTORY ON RUNOFF PLOTS FROM PERIENI, ROMANIA (kBq m⁻²)

Point sample	Plot 1	Plot 2	Plot 3	Plot 4	Plot 5	Plot 6	Plot 7	Plot 8
F2	6.518	6.693	6.652	6.789	6.697	6.018	6.138	6.644
F3	6.305	5.922	6.360	5.745	6.079	3.805	5.086	6.471
F4	5.251	4.697	5.922	5.554	6.393	2.751	3.150	6.111
F5	5.066	5.075	5.322	6.412	6.455	1.856	2.255	5.514
F6	5.446	5.975	6.795	6.211	6.417	2.460	1.710	5.623
F7	6.872	6.678	6.852	6.884	7.147	6.772	2.172	5.388
F8							1.983	5.590
F9							5.569	5.456
F10							6.813	6.883

At the upper and the lower edges of the plots, values of ^{137}Cs inventory were relatively high. A single value of 7.15 kBq m^{-2} , corresponding to F7 from Plot 5, was higher than the reference value, indicating a small amount of sedimentation.

3.4. Estimating soil redistribution rates from the ^{137}Cs measurements

Table 6 presents the soil erosion rates based on the conversion of the ^{137}Cs measurements by the Proportional Model, Mass Balance Model (MB) 1, MB2 and MB3 [10] for all eight runoff plots under cultivation.

The following input parameters have been used: reference inventory = 6.9 kBq m^{-2} , year of sample collection = 2005, bulk density = 1200 g dm^{-3} , plough depth = 0.2 m, alpha factor = 0.968, proportion factor $\gamma = 0.5$, relaxation depth = 4 cm and tillage flux $\phi = 11.6$.

The maximum erosion rates (78.4 t ha^{-1}) were estimated by MB1 in the middle of the plot 7 which has an area of 150 m^2 and was maintained all the time under bare fallow. On plot 6, similar to plot 7 except for the area being 100 m^2 , the erosion rate was at its maximum, i.e. 73.9 t ha^{-1} in F5, at 15m from the upper edge of the parcel. As a general rule, whether the parcels were planted or kept under bare fallow, soil losses were minimal at the upstream and downstream ends and maximum values have been recorded around the middle position.

Figure 10 illustrates the variation of soil losses along of each plot using data calculated by the Mass Balance Model 3.

In the upper part of the plots, erosion is low because of the limited slope length. At the lower part of the plots erosion is also limited, even sedimentation can be observed. This sedimentation can be explained by the fact that the discharge device functions like a weir and favours deposition of sediments.

Figure 11 presents a comparative graph with regards to the measured and estimated soil erosion rates by the Proportional Model, Mass Balance Model 1, MB2, MB3 and the empirical ROMSEM model.

The smallest differences between measured and estimated values can be observed on those parcels, which were very well covered by crops (plots 3, 4 and 5). The longer the time the land was protected by vegetation, the better seems to be the performance of the models for estimating soil losses by erosion. On plots with annual crops like maize, bean, soybean or under bare fallow the agreement between the empirical ROMSEM model and other estimates is slightly lower, as the chance is very high that a torrential rainfall occurs exactly at that moment when the land was still unprotected by the vegetation cover. In addition, during the last years the occurrence of several exceptional rainfalls significantly changed the statistical series which had been used to validate ROMSEM. This can also explain why the values measured on plots 1, 2, 6, 7 and 8 are higher than those estimated by the empirical ROMSEM model.

TABLE 6. EROSION ON RUNOFF PLOTS FROM PERIENI (UNDER CULTIVATION), CALCULATED BY THE PROPORTIONAL MODEL AND MASS BALANCE MODELS 1, 2, AND 3 ($t\ ha^{-1}\ a^{-1}$)

Point sample	Proportional Model							
	Plot 1	Plot 2	Plot 3	Plot 4	Plot 5	Plot 6	Plot 7	Plot 8
F2	1.95	1.57	1.27	0.57	1.04	6.02	5.20	1.75
F3	3.04	5.00	2.76	5.91	4.20	21.11	12.37	2.93
F4	8.44	11.27	5.00	6.89	2.59	28.30	25.58	5.38
F5	9.43	9.34	8.07	2.50	2.28	34.40	31.68	9.45
F6	7.44	4.73	0.64	3.52	2.47	30.28	35.40	8.71
F7	0.14	0.68	0.25	0.08	-1.40	0.87	32.25	10.31
F8							33.54	8.93
F9							9.08	9.85
F10							0.59	0.12
Net erosion	4.92	5.57	3.25	3.35	2.06	19.54	23.36	6.72
Point sample	Mass Balance Model 1							
	Plot 1	Plot 2	Plot 3	Plot 4	Plot 5	Plot 6	Plot 7	Plot 8
F2	2.44	1.95	1.57	0.70	1.28	7.80	6.68	2.16
F3	3.86	6.54	3.49	7.83	5.42	33.77	17.37	3.67
F4	11.67	16.41	6.54	9.28	3.27	51.98	44.39	6.93
F5	13.28	13.12	11.10	3.14	2.86	73.87	63.06	12.78
F6	10.11	6.16	0.66	4.50	3.11	58.22	78.41	11.67
F7	0.17	0.83	0.30	0.10	-5.22	1.07	65.15	14.09
F8							70.21	12.00
F9							12.22	13.38
F10							0.73	0.14
Net erosion	6.75	7.77	4.30	4.42	2.58	36.88	45.74	8.99
Point sample	Mass Balance Model 2							
	Plot 1	Plot 2	Plot 3	Plot 4	Plot 5	Plot 6	Plot 7	Plot 8
F2	2.29	1.83	1.47	0.65	1.20	5.55	4.74	1.52
F3	3.64	6.22	3.28	7.49	5.13	26.09	12.71	2.58
F4	11.32	16.24	6.22	8.92	3.07	42.95	35.64	4.92
F5	12.97	12.81	10.74	2.95	2.68	66.84	54.50	9.22
F6	9.75	5.85	7.12	4.25	2.92	49.32	72.35	8.39
F7	0.17	0.77	0.28	0.10	-9.50	0.75	56.80	10.21
F8							62.53	8.64
F9							8.80	9.68
F10							0.51	0.10
Net erosion	6.53	7.58	4.70	4.22	2.39	31.25	39.62	6.47
Point sample	Mass Balance Model 3							
	Plot 1	Plot 2	Plot 3	Plot 4	Plot 5	Plot 6	Plot 7	Plot 8
F2	4.52	3.61	2.90	1.29	2.37	10.93	9.34	3.00
F3	3.86	6.62	3.52	8.03	5.50	27.78	13.40	2.77
F4	11.85	16.91	6.47	9.09	3.07	43.97	37.17	5.14
F5	13.16	12.74	11.08	2.77	2.76	68.21	55.60	9.55
F6	9.71	5.64	7.05	4.42	3.03	48.86	73.33	8.45
F7	0.66	0.62	0.38	0.44	-2.15	-1.80	56.41	10.41
F8							62.93	8.67
F9							7.51	9.83
F10							-0.32	0.72
Net erosion	6.94	7.94	5.00	4.40	2.67	32.51	40.41	6.72

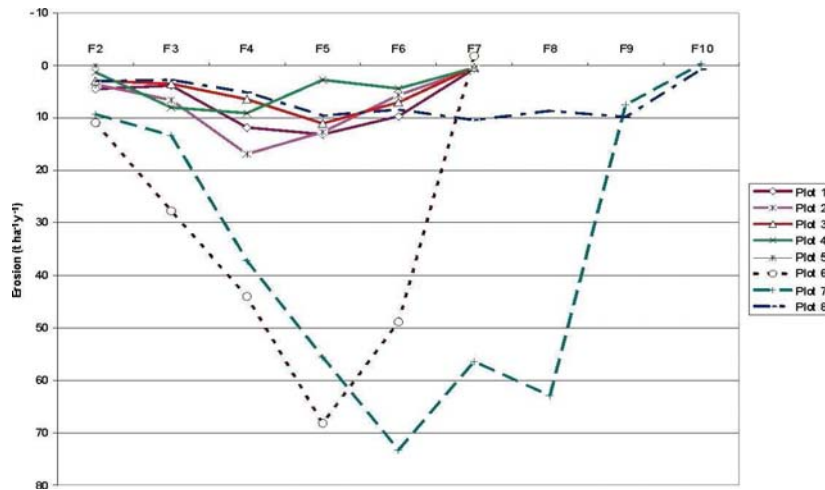


FIG. 10. Erosion rates on the runoff plots from Perieni calculated by Mass Balance Model 3.

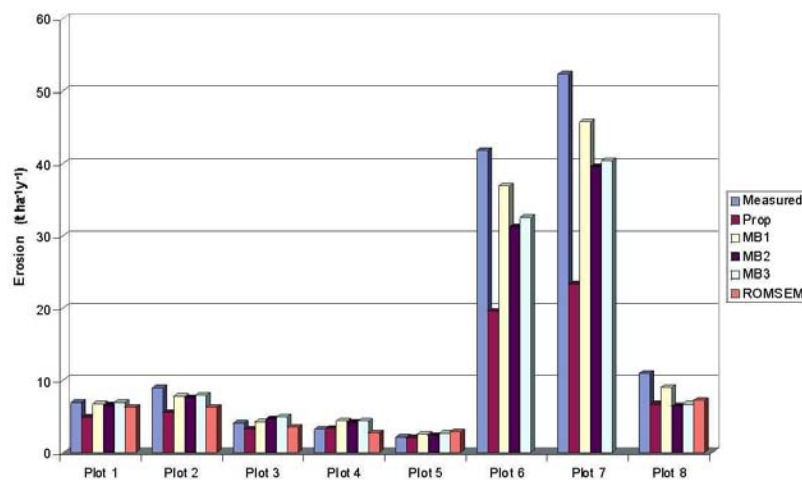


FIG. 11. Comparison of soil erosion rates from runoff plots at Perieni (Romania) vs. data estimated by the empirical ROMSEM model and four conversion models.

The differences that arose among the values estimated by the conversion models are due to the fact that the models have been progressively improved and differ in complexity and type of input parameters. The simplest and most easily to apply is the Proportional Model, and as it can be observed, soil losses were underestimated by this model for almost all plots. For this reason the use of the proportional model is recommended in our case only for approximate estimates. The estimated soil losses by the MB1, MB2 and MB3 models come closer to the conventionally measured soil loss, in particular those values estimated by MB1.

The annual soil losses from both sites located in the Seaca micro-catchment are illustrated in Fig. 12 and 13 and Table 7. On the first transect located on farmland under soil conservation practices, estimates regarding annual soil losses by conversional models (PM and MB1) indicated an increase from $1.13 \text{ t ha}^{-1} \text{ a}^{-1}$ and $1.39 \text{ t ha}^{-1} \text{ a}^{-1}$, respectively, corresponding to point S₁ (upper slope position), to $4.53 \text{ t ha}^{-1} \text{ a}^{-1}$ and $5.86 \text{ t ha}^{-1} \text{ a}^{-1}$, respectively, which correspond to point S₉ (lower slope position). All values were lower than the acceptable soil tolerance limit of $4\text{-}6 \text{ t ha}^{-1} \text{ a}^{-1}$, corresponding to soils in this area.

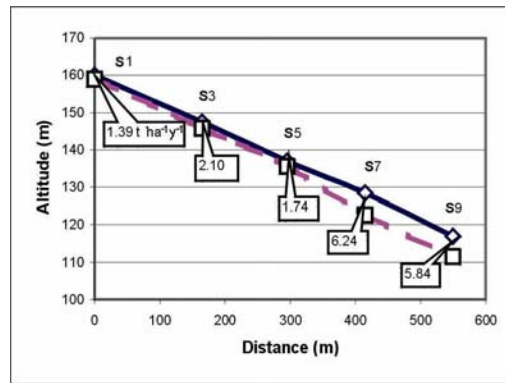


FIG. 12. Annual soil losses on farmland with soil conservation measures at the Seaca micro-catchment.

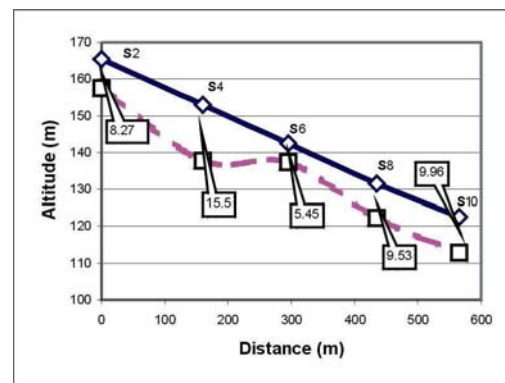


FIG. 13. Annual soil losses on land in private property, without conservation practices at the Seaca micro-catchment.

TABLE 7. SOIL LOSSES ($t\ ha^{-1}\ a^{-1}$) ESTIMATED BY CAESIUM-137 TECHNIQUE USING THE PROPORTIONAL, MB1 AND ROMSEM MODELS

Transect 1	S ₁	S ₃	S ₅	S ₇	S ₉	Average
PM	1.13	1.70	1.42	4.81	4.53	2.72
MB1	1.39	2.10	1.74	6.24	5.84	3.46
ROMSEM	1.52	2.42	2.63	2.88	2.57	2.40
Transect 2	S ₂	S ₄	S ₆	S ₈	S ₁₀	Average
PM	6.23	10.75	4.24	7.08	7.36	7.13
MB1	8.27	15.51	5.45	9.53	9.96	9.74
ROMSEM	5.38	7.13	8.50	7.48	10.26	7.75

PM – proportional model; MB1 – Mass balance 1 model; ROMSEM – Romanian model.

On the second transect on farmland with downslope oriented long and narrow strips, the annual soil losses were significantly (up to 3 times) larger than on the first transect. Fluctuations of the erosion rates along both transects can be explained by the fact that the terrain has undergone land reclamation works during the 1970s, such as levelling which induced certain disturbances in soil structure. Therefore, at point S₃ on the second transect a maximum soil loss of $15.5\ t\ ha^{-1}\ a^{-1}$ was measured, and at point S₅ located immediately downslope S₃, a much lower rate of $5.45\ t\ ha^{-1}\ a^{-1}$ was estimated, which was followed by another increase in the rate of up to $9.53\ t\ ha^{-1}\ a^{-1}$ at point S₇.

If taken into account the fact that the reference (starting) year was 1992 for both cases, it is estimated that over the last 15 years until now the erosion rates were:

- 36 t ha⁻¹ (calculated by ROMSEM), or 51.9 t ha⁻¹ (MB1) for land with conservation practices, and
- 116.3 t ha⁻¹ (ROMSEM), or 146.1 t ha⁻¹ (MB1) for land without conservation practices.

4. CONCLUSIONS

The present study of long term soil erosion and deposition rates on agricultural fields with specific conservation measures in the Tutova Rolling Hill region of Romania proved the usefulness of the ¹³⁷Cs technique. The results of the measurements also showed that the long term application of soil conservation practices, as compared with traditional agricultural practices (soil tillage system performed up and down the hill) led to a significant reduction of soil losses by about three times. The net soil erosion rate of a transect which crossed three terraces and two forest belts, on a terrain with a slope gradient ranging between 10 and 12%, calculated by the conversion model Mass Balance 3, was about 8.5 t·ha⁻¹·a⁻¹, which is under the soil loss tolerance limit.

The estimated soil erosion rates by the Proportional Model, Mass Balance Model 1, 2 and 3, and the empirical ROMSEM model revealed that where the parcels were planted or kept under bare fallow, soil losses were minimal at the upstream and downstream ends and reached maximum values around the middle position. The smallest differences between the measured (runoff plots) and estimated values with any of models, have been observed on those parcels, which were very well protected by vegetation (plots 3, 4 and 5), while the values measured on plots 1, 2, 6, 7 and 8 were higher than those estimated by the empirical ROMSEM model and the conversion models. However, for the conversion models this difference was smaller. Therefore, it is recommended to further calibrate and validate the empirical ROMSEM model. The reason for the smaller differences with the values estimated by the conversion models might be found in the complex slope micro-topography, however, this needs some more attention in future research.

ACKNOWLEDGEMENTS

The authors would like to thank for the financial support provided by the IAEA Coordinated Research Project D1.50.08, through the Contract RO-12328, and by the National Authority for Scientific Research, Romania, through the Contract 51-053/2.

REFERENCES

- [1] BECK, HL, DECOMPO J., GOGOLAK C., In situ Ge (Li) and NaI (Tl) Gamma-ray spectrometry. USAEC Report HASL-258, 1972
- [2] CAMPBELL B.L., LOUGHRAN R.J., ELIOT G.L., 'A method for determining sediment budgets, using Caesium-137', Sediment budgets (BORDAS, M.P. WALLING, D.E. (Eds)), International Association of Hydrological Sciences Publication (1988) 174, 171-179.
- [3] E. C. C. CHOI, Modelling of wind-driven rain and its soil detachment effect on hill slopes Journal of Wind Engineering and Industrial Aerodynamics, Volume 90, Issue 9, September. (2002) pp 1081-1097.

- [4] GALLAWAY, J.M., et al., "Tree root throw and sediment transport: Field and modelling studies in a Canadian Rocky Mountain Forest", Proc. 93rd ESA Annual Meeting, Milwaukee (2008)
<http://eco.confex.com/eco/2008/techprogram/P11238.HTM>
- [5] IONITA I., M. MARGINEANU, R.M., Application of ¹³⁷Cs for measuring soil erosion/deposition rates in Romania, *Acta Geologica Hispanica* **35** (2000) 311-319.
- [6] IONITA I., et al., Assessment of the reservoir sedimentation rates from ¹³⁷Cs measurements in the Moldavian Plateau, *Acta Geologica Hispanica* **35** (2000) 357-367.
- [7] LOUGHRAN R.J., CAMPBELL B.L. SHELLY D.J., ELIOT G.L., Developing a sediment budget for a small drainage basin in Australia. *Hydrological processes*. (1992) 6. 145-158.
- [8] MOTOC M., SEVASTEL, M., Evaluation of the factors, which determine surface water erosion risk, Editura BREN, Romania (2002) pp. 140.
- [9] POPA N., E. et al., "Tillage Translocation in some representative Basins from Tutova Rolling Hills-Romania", Proc. of International Symposium of the State Agricultural of Moldova Chişinău, Vol.3 (2003) pp.105.
- [10] WALLING D.E., et al., Models for converting radionuclide (¹³⁷Cs, Excess ²¹⁰Pb, and ⁷Be) measurements to estimates of soil erosion and deposition rates (Including Software for Model Implementation), <http://www-naweb.iaea.org/nafa/swmn/swmcn-databases.html>
- [11] WALLING D.E., QUINE T.A. Use of Caesium-137 as a tracer of erosion and sedimentation: handbook for the application of the Caesium-137 technique. Exeter. University of Exeter. (1993) pp.15-97.
- [12] WORLD OVERVIEW OF CONSERVATION APPROACHES AND TECHNOLOGIES, <http://www.wocat.net>
- [13] ZAPATA F., Handbook for the assessment of soil erosion and sedimentation using environmental radionuclides, Kluwer Academic Publishers, Dordrecht, (2002) pp. 215.

COMBINED USE OF CAESIUM-137 METHODOLOGY AND CONVENTIONAL EROSION MEASUREMENTS IN THE MISTELBACH WATERSHED (AUSTRIA)

L. MABIT, A. TOLOZA

International Atomic Energy Agency,
Soil and Water Management and Crop Nutrition Laboratory,
FAO/IAEA Agriculture & Biotechnology Laboratory,
Seibersdorf, Austria

A. KLIK

Institute of Hydraulics and Rural Water Management, University of Natural Resources and Applied Life Sciences,
Vienna, Austria

A. GEISLER, U.C. GERSTMANN

Helmholtz Zentrum München, German Research Center for Environmental Health,
Institute of Radiation Protection,
Neuherberg, Germany

Abstract

Over the past thirty years, many studies identified water erosion worldwide as one of the major causes of soil degradation on arable land. However, in order to develop appropriate soil conservation strategies more quantitative long term assessments of the soil erosion process are still needed. Therefore, in the present study, the magnitude of erosion and sedimentation was quantified using Fallout RadioNuclides (FRN) in combination with conventional runoff plots measurements in a small agricultural watershed under conventional and conservation cropping practices at Mistelbach located in Austria. A preliminary test of the use of the FRN Caesium-137 (^{137}Cs) was successfully implemented in the Mistelbach watershed. A valid reference site – a small forest within the watershed – was identified and characterized (texture and physicochemical parameters). In this undisturbed area, a classical exponential depth distribution of ^{137}Cs activity was found with 90% of the ^{137}Cs in the first 15 cm; no ^{137}Cs was detected below 20 cm. Seventy six (76) samples were collected on integrated grids basis. The reference value was $1954 \pm 91 \text{ Bq m}^{-2}$ (mean \pm 95% confidence interval) with a coefficient of variation of 20.4%. Two one meter soil profiles were also collected in the sedimentation area and analysed using the ^{137}Cs method combined with the conversion model Mass Balance Model 2 (MBM 2). Using the ^{137}Cs data, the sedimentation rates down slope of the field containing the runoff plots were estimated to be $26 \text{ t}^{-1} \text{ ha}^{-1} \text{ a}^{-1}$ using the ^{137}Cs depth distribution profile and at $20 \text{ t}^{-1} \text{ ha}^{-1} \text{ a}^{-1}$ using the MBM 2. In the lowest part of the watershed sedimentation rates of up to $51 \text{ t}^{-1} \text{ ha}^{-1} \text{ a}^{-1}$ were estimated through the ^{137}Cs depth distribution profile. These results were linked to long term erosion measurements (1994-2006) from runoff plots just up-slope from the sedimentation area. The average soil erosion reached $29 \text{ t ha}^{-1} \text{ a}^{-1}$ from the conventional tilled plot, $4 \text{ t ha}^{-1} \text{ a}^{-1}$ from the conservation tillage plot and $3 \text{ t ha}^{-1} \text{ a}^{-1}$ from the direct seeding treatment. This study demonstrates the complementarity of both approaches in order to assess erosion and sedimentation processes under different conservation cropping practices.

1. INTRODUCTION

Erosion is a major form of soil degradation, leading to decreased soil productivity (on-farm impacts) and environmental pollution by sediments, nutrients and pesticides (off-farm impacts) [1]. The magnitude and relative importance of direct (rainfall energy absorption) or indirect (soil quality improvement) impacts of conservation practices need to be evaluated under various agroecological conditions. It is therefore important that relationships linking agronomic parameters and erosion are developed and validated. In this way, the benefits from the implementation of conservation practices can be assessed more accurately.

As traditional monitoring techniques for soil erosion require many years of measurements to integrate climatic interannual variability [2,3], there is need for more efficient and cost-effective methods. Soil erosion can also be measured by techniques based on the use of fallout radionuclides ‘FRNs’ such as ^{137}Cs , ^7Be , $^{210}\text{Pb}_{\text{ex}}$ [4,5]. FRNs, in particular ^{137}Cs [6], have proven to be very powerful tracers of soil movements within the landscape, and this methodology can complement conventional approaches.

FRNs can be used to assess the result of many years of erosive processes, while direct measurements are related to single rainfall events or rather short periods of time [7]. Since radionuclide based measurements also produce information on the spatial distribution of erosion/deposition rates, they can be used to confirm the results of distributed soil erosion models. The efficiency of conservation practices can also be assessed from radionuclide measurements. As conventional sediment loading measurements were carried out for 13 years by BOKU University on erosion plots in the Mistelbach watershed (18 ha) located 60 km north of Vienna in Austria, the objectives of this contribution are:

- To measure soil erosion magnitude under eastern Austrian conditions under conventional and conservation cropping practices using conventional runoff plots,
- To test and confirm the potential use of FRNs (especially ^{137}Cs) as soil tracers under Austrian field conditions,
- To evaluate the initial fallout and establish the physico-chemical characterisation of the reference site selected,
- To assess the sedimentation rates using ^{137}Cs .

2. MATERIALS AND METHODS

2.1. Study area and set up of runoff and erosion measurements using conventional erosion plots

In 1994 a field experiment was started in Lower Austria to investigate the impact of three tillage systems on surface runoff, soil erosion, nutrient and pesticide losses. Such measurements have to be carried out over long periods of time to integrate the inter-annual variability of climate and cropping practices.

The experiments were carried out on plots of agricultural schools in Mistelbach (Fig. 1 and 2) [8]. Mistelbach is situated 60 km north of Vienna in the so-called Wine Quarter. This region is one of the warmest and also driest parts of Austria. Long term annual average precipitation reaches 643 mm (Table 1) and air temperature 9.6 °C. The landscape is characterized by gentle to fairly steep slopes. Soil texture ranges from silt loam to loam. Crop rotation consists mainly of cereals.



FIG. 1. Location of the Mistelbach site.



FIG. 2. Investigated erosion plots.

TABLE 1. MONTHLY AND ANNUAL PRECIPITATIONS IN MM (1994-2006)

Year	January	February	March	April	May	June	July	August	September	October	November	December	Mean
1994	14	6	31	50	115	164	80	50	14	44	38	36	642
1995	23	19	49	49	54	140	15	8	145	16	39	45	601
1996	43	30	17	85	118	87	67	145	94	56	24	28	794
1997	15	14	45	33	78	64	220	29	15	21	77	27	637
1998	30	2	27	14	55	128	69	31	150	108	32	21	668
1999	16	54	26	43	73	103	142	31	57	12	52	41	649
2000	30	31	71	7	30	18	79	93	65	78	151	53	706
2001	23	5	41	39	38	51	143	44	160	12	52	38	648
2002	9	23	48	36	48	77	105	146	38	82	55	53	718
2003	51	2	1	26	36	32	30	25	45	47	34	62	390
2004	51	51	93	16	36	91	45	41	31	24	36	14	529
2005	28	38	7	40	84	49	158	170	46	14	20	54	707
2006	32	30	69	72	93	86	42	193	10	21	17	12	676
Av.	28	23	40	40	66	84	92	77	67	41	48	37.2	643

The study design consisted of 3 m wide and 15 m long runoff plots, for each tillage management system. Runoff and soil loss were measured continuously during the growing season using an automated erosion wheel (AEW) [9]. The AEW (Fig. 3) consists of four equal sections. The soil particles in suspension are collected from the experimental plot in a trough and then diverted by a 100 mm PVC pipe to the AEW. This equipment can be used for different plot sizes with the same resolution of runoff measurement. The maximum tipping bucket volume is approximately five liters. The number of tippings and the corresponding time are recorded by a data logging system. The soil suspension from the tipping bucket passes a 3 mm sieve to hold back any plant residues and therefore to avoid the clogging of the subsequent multi-tube divisor (Fig. 4). The runoff water is then divided by an adapted multi-tube divisor which is located in the 100 mm wide tube. It consists of 19 aluminum tubes with an outside diameter of 20 mm and an inside diameter of 16 mm. The length of these tubes is 150 mm. The central tube with a length of 410 mm collects then a representative runoff sample. Area of this sampling tube is 3.52% of the possible cross sectional area. This runoff sample is then diverted through a 16 mm PVC pipe to a 60 liter plastic container. The rest of the runoff which is not sampled is conducted away by the 100 mm PVC pipe.

Representative samples of the soil suspension were also collected for further physical and chemical analyses. Precipitation and air temperature were measured at 5 minutes intervals with an automated data logging system.

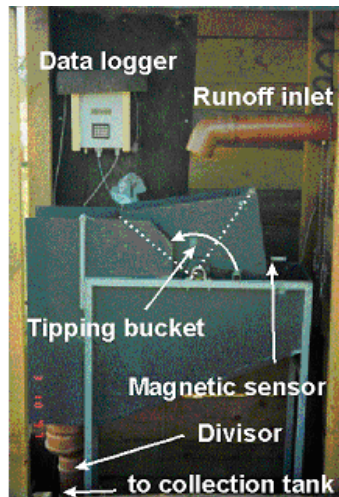


FIG. 3. Automated Erosion Wheel.



FIG. 4. Multi-tube divisor with sampling tube.

Following tillage treatments were compared: (1) conventional tillage system with mechanical plough and a tillage depth of 30 cm (CT), (2) conservation tillage (CS) with reduced tilling and cover crops during winter and (3) direct seeding (DS) with cover crops during winter. The soil of the experimental plot is of the Loess type and can be classified as typical Argiudoll (Soil Taxonomy). The soil texture is silt loam with a sand content of 9%, silt content of 71% and clay content of 20%. The soil has an organic carbon content of about 1%, a pH (CaCl₂) of 8.1 and a CaCO₃ content of 4%. Total nitrogen and total phosphorus values reach 1.6 and 0.8 g kg⁻¹, respectively.

2.2. Preliminary test and sampling strategy to assess soil redistribution using FRN

Our first activity was to test the potential application of ¹³⁷Cs methodology, to assess at different specific landscape locations the total activity ¹³⁷Cs and simultaneously to evaluate the potential impact of the Chernobyl accident in 1986. In the Mistelbach watershed different landscape positions were sampled (upper/top, middle part lower/bottom part of agricultural slope, a sedimentation/deposition area and two potential reference sites one in a forest and one in vineyard) to implement a first preliminary study test for a potential use of FRN to assess erosion and sedimentation processes.

As 80% of the total deposition linked to Chernobyl has affected Europe [10], it is common in Europe to carry out a pre-test evaluation of the FRN amount before to implement a full survey using this approach. Chernobyl fallouts were rather localized and were not as global as those from the 1950s to 1960s. But the impact of the Chernobyl accident, which introduced significant new radio-caesium amounts in most European countries, has particularly affected Austria.

Surface contamination of the Austrian territory by ^{137}Cs based on 2115 measurements showed a very high variability of the fallout linked to the Chernobyl event [11,12]. In Austria the total ^{137}Cs fallout linked directly to the Chernobyl accident represents 1.6 PBq. That represents around 2% of the total ^{137}Cs sprayed by the accident that took place in April 1986. The average ^{137}Cs soil contamination was evaluated at 21.0 kBq m^{-2} of which 18.7 kBq m^{-2} is due to the Chernobyl accident [12].

While Austria has particularly been affected by the Chernobyl deposition, the north-east region of Austria, where our experimental watershed is located, has not been significantly affected. It was verified with the assessment of the reference site values (Section 3.2 of the present manuscript).

2.3. Selection and sampling design of the reference site

After the successful implementation of the preliminary study, it was decided to estimate the initial fallout of ^{137}Cs on so-called reference sites. One of the most important steps in using the ^{137}Cs method – as well as for ^{210}Pb and ^7Be – is to select and determine a suitable reference inventory, against which other values spatially distributed in the watershed will be compared [4]. To assess this base inventory, three different criteria to select the reference site were considered:

- The reference site should not be cultivated or disturbed since the beginning of the 1950's.
- The reference site should be selected within the study area or near to it (e.g. around 1 km) in order to be as representative as possible of the initial input of radioisotopes,
- The reference site should not be influenced by erosive processes that imply quasi flat topography.

Because of the restricted number of permanent pastures and after compilation of background information and consultation of available documents (maps, aerial photography) coupled with field reconnaissance, an undisturbed forest within the watershed was selected as the reference site. This small area was about 2500 m^2 ($50 \times 50\text{m}$) with a small slope gradient and limited canopy density (Fig. 5).

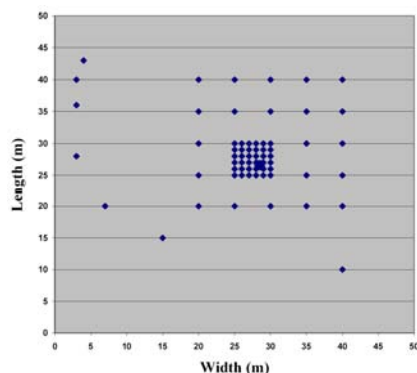


FIG. 5. Sampling design for the reference site.

The sampling was adapted to the forest conditions. Avoiding forest borders to minimize the possible interrelation and disturbance linked to agricultural fields, a relatively flat area with reduced trees and canopies was selected. A homogenous 400 m² surface (20 × 20 m) inside the forest was selected. A systematic multi-grid design was used for sample collection including three different scales (20 × 20 m, 5 × 5 m and 1 × 1 m) to estimate the spatial variability of the initial fallout using geo-statistical methods and tools. Soil sampling points were shifted slightly in consideration of trees/trunk ‘runoff’ interaction or the presence of tree roots at the surface.

Collection of samples was carried out according to a consistent spacing pattern of 5 m between each sampling point (n=25). Inside this first grid, another internal 5 × 5 m grid was investigated with a spacing of 1 m, involving 32 additional samples and 4 common samples with the 20 × 20 m grid (Fig. 6).



FIG. 6. Aerial photograph of the investigated watershed, indicating the location of the reference site (forest), erosion plots and sedimentation area.

In the cultivated fields, the tillage of the soil uniformly mixed the ¹³⁷Cs in the plough layer. In the undisturbed area ¹³⁷Cs was concentrated within the first few centimetres of the soil, and vertical migration of this element was negligible. As a total inventory at each sampling point should be taken into account the sampling depth strategy in the forest was adapted to the results obtained through the first evaluation of the depth distribution of ¹³⁷Cs.

Soil pits of 50 cm deep were dug. Care was taken to obtain a free-standing and stable pit wall. Sampling was done on the best free-standing and stable pit wall with a bulk density cylinder of 558 cm³. In order to measure the complete stock of ¹³⁷Cs present in the soil, samples were collected in the first 20 cm. Each reference sample corresponded to a composite of two mixed increments (0-10 cm and 10-20 cm) in order to, later on, simplify and reduce the number of gamma analysis.

Using the same sampling procedure, 10 additional samples were taken to characterise the physical and chemical soil properties of the reference site.

In the 1 × 1 m grid 12 complementary samples were taken from a soil pit (50 cm deep) including 11 classic samples based on two increments in combination (0-10 and 10-20 cm) as

well as 4 special samples to estimate the ^{137}Cs activity distribution in the soil profile. These samples were collected with smaller bulk density cylinders every 5 cm up to 30 cm. The different layers were grouped to create a composite sample per layer including 4 sub-samples (0-5, 5-10, 10-15, 15-20, 20-25 and 25-30 cm). This sample confirmed the depth distribution of ^{137}Cs and the maximum depth presence of the isotope, i.e. 20 cm. The maximum of 20 cm depth with regards to the ^{137}Cs penetration in this soil was confirmed by the soil texture differentiation. Effectively, below 20 cm depth the soil is composed of more than 80% stones and gravel.

To complete our investigation, 7 random additional samples were collected in the forest around the 20×20 sampling grid (Fig. 5). Based on the sampling protocol applied by Mabit et al. [13], 174 samples increments were taken in the reference site for 76 future gamma analyses. The overall spatial distribution of the samples is presented in Fig. 5.

2.4. Sampling strategy in the sedimentation area

In the sedimentation area of the watershed, 3 different cores were collected in a radius of 2 m with a mechanised soil corer to 1 m depth and divided into 5 cm increments. The inner diameter of the tube inserted in the soil was 9 cm. The same increments from each core were combined to obtain a composite profile (profile 1).

Another single sample (profile 2) was collected in the 'talweg' runoff convergence and divided into 10 cm increments. It was expected that the sedimentation rates for profile 2 were higher than for profile 1 based on the basin geomorphology (Fig. 6).

2.5. Laboratory analysis

2.5.1. Samples pre-treatment, gamma measurements and conversion of the ^{137}Cs activity into soil redistribution

All soil samples were oven dried for 48 hours at 70°C , sieved at 2 mm and homogenized prior to measurement of ^{137}Cs content by gamma spectrometry using high resolution HPGe detector. The material <2 mm was used since it is assumed that material >2 mm has negligible ^{137}Cs activity.

The samples of the preliminary test were analyzed in Seibersdorf by the Soil Science Unit in collaboration with the Chemistry Unit. The ^{137}Cs was measured at 662 keV using a GEM30 γ -ray spectrometric system consisting of a high-purity germanium (HPGe) detector of 27% relative efficiency and a resolution of FWHM of 1.8 keV at 1.3 MeV mount in a 5 cm thick lead shield. Counting times ranged between 6 and 90 hours in order to obtain a measurement precision of $\pm 10\%$ at the 95% confidence level.

The ^{137}Cs activity measurements of the samples collected in the reference site and in the agricultural fields were carried out with the gamma detector of the Soil Science Unit at the IAEA Seibersdorf Laboratory. The system set includes a sampler changer system with a capacity of 12 samples [14] and the detector itself is an HPGe coaxial detector (p-type). The performance specifications of the detector measured are as following: resolution (FWHM) at 1.33 MeV, $^{60}\text{Co} = 1.89$ keV, Peak-to-Compton Ratio, $^{60}\text{Co} = 95.1$; relative efficiency at 1.33 MeV, $^{60}\text{Co} = 115.6\%$; peak shape (FWTM/FWHM), $^{60}\text{Co} = 1.93$; resolution (FWHM) at 122 keV, $^{57}\text{Co} = 0.82$ keV. The spectra were evaluated with the software Gamma Vision-32 [15]. The detector was calibrated using the sealed radioactive source FG 607 from Amersham (ISO

classification C.11111, active volume 1300 mL, density approx. 1.0 g/cm³). Counting times ranged between 10000 - 50000 seconds, depending on the ¹³⁷Cs activity. This was sufficient to obtain an average counting error of 6.2% ± 1.8% at 2 sigma precision.

Additional verification/control test on the ¹³⁷Cs measurements were done using subsamples of 200 g in the Institute of Radiation Protection of the GSF-National Research Center for Environment and Health demonstrating an overall difference of 5% on the samples tested. The samples were analysed with coaxial HPGe detectors with relative efficiencies (1.33 MeV) ranging from 15 to 80%.

Counting times ranged from 60000 to 1100000 s, depending on the ¹³⁷Cs activity of the samples. In general, the counting rate uncertainties were <5% (1 sigma) for the samples with ¹³⁷Cs activity concentrations >2 Bq kg⁻¹. Minimum detectable activities were in the range of 0.1 to 0.2 Bq kg⁻¹.

The detectors were calibrated with standard sources purchased by the Physikalisch-Technische Bundesanstalt (PTB), Brunswick, Germany. The spectra were evaluated with Canberra Genie VMS software and quality assurance was performed regularly measuring certified reference materials and by participating in national interlaboratory tests.

After gamma measurement of the samples collected in the sedimentation area, the areal activities of ¹³⁷Cs were converted into sedimentation rates (t ha⁻¹ a⁻¹) using the information provided by the ¹³⁷Cs depth profile. It is possible to estimate the sedimentation rate assuming that the sedimentation area has been cultivated since the time of the interception of the ¹³⁷Cs fallout [16,17]. If no sedimentation has occurred, ¹³⁷Cs will only be found until a layer equivalent of the initial plough depth. However, if some sedimentation has occurred, ¹³⁷Cs will be present below the plough depth. The comparison of the plough depth D_{pl} (kg.m⁻²) with the information provided by the ¹³⁷Cs depth profile distribution D_b (kg.m⁻²) allows estimating the sedimentation rate R' that can be calculated using the following equation:

$$R' = \frac{D_b - D_{pl}}{T_s} \quad (1)$$

where: T_s (a) is the time since the beginning of significant fallout and the collection of the sediment core.

Additional estimates were made for profile 1, which is representative of the sedimentation originating from the field containing the three experimentation runoff plots. These assessments were made using the Mass Balance Model 2 (MBM 2) [18]. The results obtained were then related to the net average erosion rates provided by the erosion plot measurements.

2.5.2. Physicochemical analysis of the reference site soil

The soil of the forest was characterized through physicochemical analysis. The measured parameters were: bulk density, particle size distribution (% sand,% silt and% clay) measured with wet sieving and pipette method, water content (w/w dry basis), organic carbon/organic matter measured by the modified Walkley-Black method [19], C/N ratio, pH in CaCl₂, cation exchange capacity (CEC) determined by the barium chloride dehydrate method, calcium carbonate content determined by HCl treatment, total nitrogen analyzed by the Kjeldahl method, and total phosphorus determined using ammonium molybdate and extraction with K₂S₂O₃ solution.

3. RESULTS AND DISCUSSION

3.1. Result from the experimental plots

Over the total period of 13 years of investigation the average annual surface runoff from the different treatments was 13.5 mm for CT, 8.4 mm for CS and 10.5 mm for DS (Table 2). A large variability due to precipitation during the growing season and type of crop cover was observed. In 1994 surface runoff was around 72-80 mm from the different treatments. In six of the 13 years no runoff could be determined throughout the growing season. On average, no statistically significant difference ($p < 0.05$) between the tillage treatments could be found. However, in the last five years since 2002 a numerical decrease can be observed in the measured data.

Since the beginning of the experiment in 1994 32 runoff events were registered in Mistelbach from CT, but only 27 from DS and 23 from CS. Between 62% (CT) and 70% (DS) of these events produced less than 1 mm runoff and between 80% (CT) and 94% (DS) of these events produced less than 5 mm runoff (Fig. 7). During the investigation period, only one event was recorded with more than 50 mm runoff, and it occurred on both the CT and DS plots [8].

For soil erosion similar results were obtained. From CS and DS 80% of the erosive events yielded a soil loss less than 1 t ha⁻¹ (Fig. 8). From CT plots only 72% of the events led to this low erosion amount, whereas about 4% of all events exceeded a soil loss of 50 t ha⁻¹. Under DS no soil loss >50 t ha⁻¹ was measured during the whole investigation period; under CS only 1.5% exceeded this threshold.

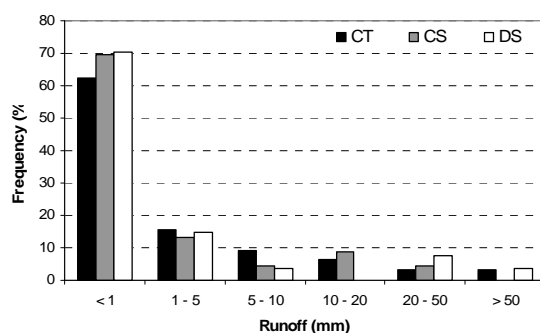


FIG. 7. Frequency of runoff amounts for investigated tillage (conventional tillage system (CT), conservation tillage (CS) with cover crops during winter and direct seeding (DS) with cover crops during winter) in Mistelbach (1994-2006).

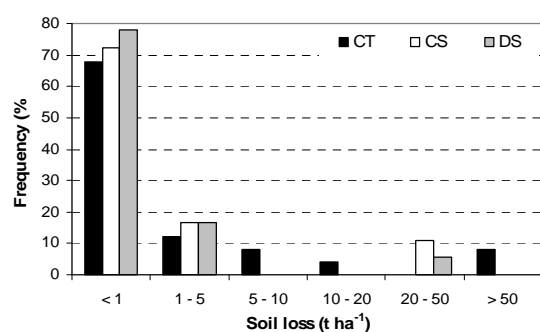


FIG. 8. Frequency of soil losses for investigated tillage practices (conventional tillage system (CT), conservation tillage (CS) with cover crops during winter and direct seeding (DS) with cover crops during winter) in Mistelbach (1994-2006).

Long term average soil erosion could be reduced significantly from 28.4 t ha⁻¹ a⁻¹ under CT to 4.2 and 2.7 t ha⁻¹ a⁻¹ for CS and DS, respectively (Table 2). The 13 years average value is dominated by three rainfall events (total of 257 mm) in 1994 which led up to a soil loss of 319 t.ha⁻¹ under CT. At least one of these events (P = 115 mm) had a reoccurrence of 50 years. This shows that soil erosion is an extreme event process.

Soil erosion is a function of soil erodibility and rainfall erosivity. The rainfall erosivity is expressed by the kinetic energy of the rainfall (E) and the maximum 30-min intensity (I₃₀) throughout the event. E describes the erosive force of the rainfall impact on the soil surface (splash erosion) while I₃₀ represents the kinetic energy of the shallow Hortonian surface runoff [20]. (Fig. 9) shows the relationship between the rainfall erosivity (EI₃₀) and the soil loss for all erosive events. It can be clearly distinguished that CS and DS due to the higher soil cover lead to much lower soil loss (differences up to 2 orders of magnitude) than CT.

TABLE 2. CROP ROTATION AND YEARLY AMOUNTS OF RUNOFF AND SOIL LOSS IN MISTELBACH

Year	crop	Soil loss (t ha ⁻¹)			Runoff (mm)		
		CT	CS	DS	CT	CS	DS
1994	corn	317.20	43.8	26.00	80.6	72.2	79.9
1995	w-wheat	0.12	0.06	0.04	0.2	0	0
1996	sugar beet	3.25	0.60	0.41	10.1	1.5	5.6
1997	s-barley	0.00	0.00	0.00	2.7	0.4	1.8
1998	sunflower	19.75	5.92	5.43	41.1	20.8	31.8
1999	w-wheat	0.00	0.00	0.00	0	0	0
2000	corn	0.00	0.00	0.00	0	0	0
2001	w-wheat	0.00	0.00	0.00	0	0	0
2002	corn	11.98	0.16	0.38	22.0	2.0	3.2
2003	w-wheat	0.03	0.04	0.02	1.3	1.3	1.3
2004	sunflower	0.05	0.03	0.04	2.2	1.6	1.9
2005	w-wheat	n.m.	n.m.	n.m.	n.m.	n.m.	n.m.
2006	corn	0.34	0.08	0.07	1.7	1.4	0
Average		29.38	4.22	2.70	13.5	8.4	10.5

Conventional tillage system (CT), conservation tillage (CS) with cover crops during winter and direct seeding (DS) with cover crops during winter); n.m = not measured.

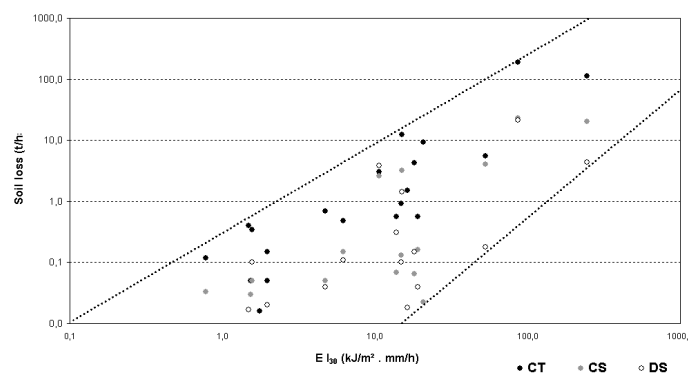


FIG. 9. Relationship between rainfall erosivity (EI₃₀) and soil loss for all erosive events in Mistelbach (1994-2006) (conventional tillage system (CT), conservation tillage (CS) with cover crops during winter and direct seeding (DS) with cover crops during winter).

3.2. Preliminary test of the caesium-137 as soil tracer in Mistelbach area

The ^{137}Cs activity magnitude revealed by the pre-test was between 2 to 4 kBq m⁻² that underlines the fact that this area has not been affected by major fallout from Chernobyl accident. The results are in agreement with what we could expect with variable activity in the agricultural field and very high activity of ^{137}Cs in deposition area.

The ^{137}Cs activity of the different sites ranged from 2112 Bq m⁻² in the eroded area to 4151 Bq m⁻² in the sedimentation area in agreement with the topography and landscape location of the soil sampled. The total ^{137}Cs inventories showed an evident variability related to the topography. The values decreased from the top of the slope to the middle (3045 to 2112 Bq m⁻²) and increased again to 2325 Bq m⁻² in the bottom part. The activity of the full profile reached its maximum in the sedimentation area with the presence of ^{137}Cs below 60 cm soil depth.

Potential reference sites were searched out as uneroded areas. Regarding the reference site, a forest area was chosen based on the the exponential decrease of the ^{137}Cs activity profile, typical for uneroded areas. Detailed enquiries and aerial photography consultation confirmed that this small forest was already present more than 20 years ago. The vineyard area could not be used as reference site due to some minor tillage activity.

The ^{137}Cs measurement underlined quite well the sedimentation process in the deposition area with a global activity twice as high than the reference site located in the forest. Regarding the preliminary result it was decided to further investigate the use of FRNs to assess erosion and sedimentation process with an initial emphasis on an accurate evaluation of the reference value activity.

This pre-study confirmed the potential use of ^{137}Cs in Mistelbach because of the redistribution of the radioisotope in the landscape being linked to the slope/topography and the erosion processes. Secondly based on the ^{137}Cs activity level measured it appeared that the Chernobyl impact on the ^{137}Cs fallout was not significant. According to the yearly precipitation, latitude and longitude of the study site we could expect around 2 kBq m⁻² of ^{137}Cs for the reference site.

3.3. Physicochemical characterisation of the reference site and evaluation of the ^{137}Cs base level

The reference site in the forest area was characterised through its texture (sand %, silt % and clay%) and different chemical parameters. Using the United States Department of Agriculture soil classification system based on grain size the soil was described as a soil with a silt-loam texture (Table 3). The other chemical properties are summarised in Table 4. This alkaline soil with a C/N ratio of about 10-11 indicates a high degree of humification. Regarding the standard deviation to the mean, the different chemical parameters do not indicate large variability between the different soil increments (0-10 and 10-20 cm). The organic carbon content was classified as medium and the electric conductivity as low.

The composite sample was used to determine the profile distribution of ^{137}Cs and its maximum depth presence. A mass activity of 12.1 Bq kg⁻¹ was found in the first 5 cm with an exponential decrease till 3.4 Bq kg⁻¹ in the 15-20 cm increment and no more caesium was detected under the 20 cm layer. Fig. 10 shows the vertical distribution of the ^{137}Cs areal activity in the reference site using the composite sample. In total 90% of the caesium is accumulated in the 15 first cm and the results show an exponential decrease of the ^{137}Cs activity with depth for a total activity profile of 2138 Bq m⁻².

The results of the main descriptive statistics of Mistelbach reference site (n=76) after conversion of the activity in Bq kg⁻¹ into areal activity in Bq m⁻² are presented in (Table 5). The ¹³⁷Cs areal activity of the seventy six (76) samples collected in the forested reference site (Fig. 5) ranged from 1123 to 3354 Bq m⁻²

At the beginning of 2007 the average value of the base level corresponding to the residual amount left from the historic ¹³⁷Cs fallout in the absence of erosion or deposition was 1954±91 Bq m⁻² (mean ± 95% confidence interval; n=76). The coefficient of variation (CV) that measures dispersion of a probability distribution and is defined as the ratio of the standard deviation to the mean (CV (%) = (σ/μ) × 100) is equal to 20.4% [8].

TABLE 5. DESCRIPTIVE STATISTICS OF MISTELBACH REFERENCE SITE VALUES

	Base level of ¹³⁷ Cs (Bq m ⁻²)
Mean	1954
Standard Error of Mean (SEM)	45
Median	1940
Standard Deviation	400
Kurtosis	1.5
Skewness	0.75
Minimum	1123
Maximum	3354
Confidence Level (95.0%)	91

This value is in full agreement with the literature review on reference sites [21, 22, 23] which indicated the median CV for the papers reviewed was 19%, with a range from 1.5 to 86%. The CVs were high in the forested sites (19 to 47%) and lower at the pasture/grassland sites (5 to 41%). This greater variability resulted from the unequal distribution of leaf fall and other organic detritus on the forest floor which may have higher contents of radiocaesium. Also, the pattern is complicated by the spatial variability of canopy throughfall and stemflow which varies with season and vegetation type [21].

From the average reference inventory and the standard error of mean (SEM), it can be statistically estimated that ¹³⁷Cs activities between 1864 and 2044 Bq m⁻² (Mean ± 2SEM) indicate that no net soil movement occurred since the first introduction of major peak fallout in 1954. Values below 1864 Bq m⁻² may be considered as an indicator of a net loss, and those above 2044 Bq m⁻² of net deposition.

The results also proved that the Chernobyl fallouts added only a small amount of ¹³⁷Cs to the soils of the Mistelbach area. It could therefore be concluded that the Chernobyl fallouts on the study watershed were small enough not to significantly influence the relationship between soil and ¹³⁷Cs losses. The value of 1954 ±91 Bq m⁻² can therefore be considered a good estimate of the actual ¹³⁷Cs base level for the experimental watershed, and does not need to be corrected for Chernobyl fallout.

3.4. Evaluation of soil deposition magnitude

The total areal activity of the soil profile 1 was 2836 Bq m⁻² with a maximum activity of 7.5 Bq kg⁻¹ in the 20 and 25 cm increment. Taking into account the bulk density of each increment, the maximum areal activity was found at the depths of 5-10 and 15-20 cm with respective values of 563 and 547 Bq m⁻². ¹³⁷Cs was present up to 40 cm depth. The ¹³⁷Cs areal

activity of the profile 1 is presented in Fig. 11. The ^{137}Cs areal activity of profile 2 is presented in Fig. 12. The total areal activity of the profile 2 was 4776 Bq m^{-2} with a maximum activity at 10-20 cm depth of 11.2 Bq kg^{-1} equivalent of 1344 Bq m^{-2} taking into account the bulk density of this soil layer.

The ^{137}Cs measurements illustrate quite well the sedimentation process in the deposition area with an areal activity significantly higher than the reference site. For both soil profiles, sedimentation magnitude was assessed using the ^{137}Cs depth of penetration. For the profile 1, the depth to the base of the ^{137}Cs profile (D_b) was 40 cm and the plough depth (D_{pl}) was 30 cm. Using the equation 1 and a T_s value of 54 years (1954-2007), the sedimentation rate of the profile 1 was estimated at $26.1 \text{ t ha}^{-1}\text{yr}^{-1}$. However ^{137}Cs was found to a depth of 50 cm in profile 2 corresponding to a sedimentation rate of $50.5 \text{ t ha}^{-1}\text{yr}^{-1}$ which represents 1.9 times the rate of profile 1.

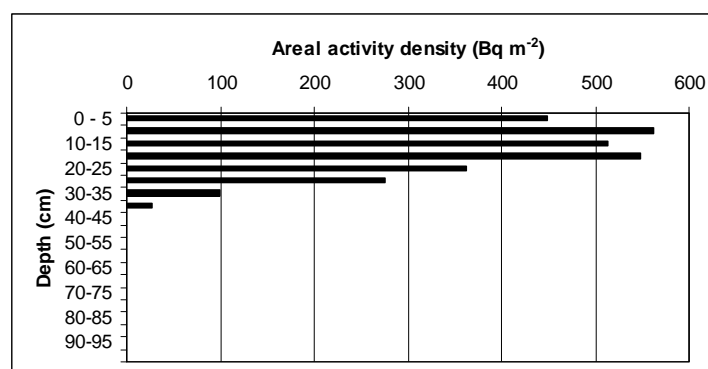


FIG. 11. ^{137}Cs distribution in the sedimentation area – Profile 1.

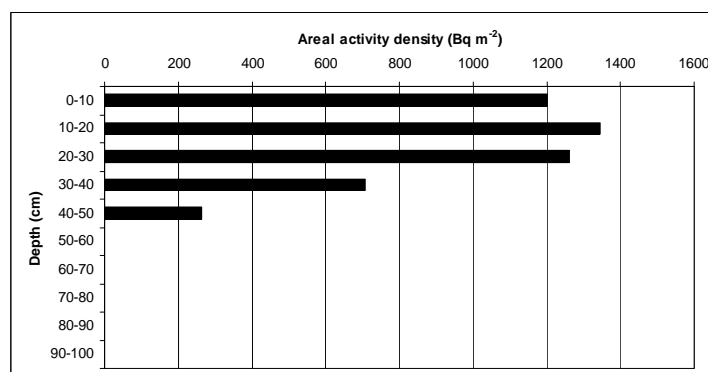


FIG. 12. ^{137}Cs distribution in the sedimentation area – Profile 2.

Taking into account the average bulk density of the different soil layers in the sedimentation area, the sedimentation rates associated with profiles 1 and 2 were 1.8 mm a^{-1} and 3.7 mm a^{-1} equivalent to total deposition during the 54-year period (1954-2007) of 9.7 cm and 20 cm respectively. The sedimentation rates provided by profile 2 were far greater than the average erosion rates measured by the erosion plots (maximum of $29.4 \text{ t ha}^{-1} \text{ a}^{-1}$). This can be explained by the fact that the profile 2 is more representative of sedimentation processes occurring in the study area due to its topographical position and the basin geomorphology, while for profile 1 the main source of deposited material is probably the soil losses originating from the contiguous field containing the experimental runoff plots located upstream.

An additional assessment of sedimentation in the area was done using the conversion model MBM 2 and the data of profile 1 and the erosion plots. In utilising the model MBM 2 conversion parameters have been determined and default values were set for the particle size factor, the relaxation depth and the proportional factor as listed below:

- Bulk density: 1380 kg m^{-3} (mean bulk density of the 30 samples increments collected)
- Particle size factor: 1
- Sampling year: 2007
- Reference inventory: 1954 Bq m^{-2}
- Proportional factor: 1
- Relaxation depth: 4 kg m^{-2}
- Tillage depth: 414 kg m^{-2} ($0.3 \text{ m} \times 1380 \text{ kg m}^{-3}$)
- Year of initial tillage: 1954

As MBM 2 need data on a transect basis and not point single data, the model was run utilising the net erosion rates produced by the CT, CS and DS erosion plots. The ^{137}Cs activity data derived from the plots (685 Bq m^{-2} for CT; 1680 Bq m^{-2} for CS and 1775 Bq m^{-2} for DS) and ^{137}Cs inventory of profile 1 were integrated into MBM 2 and used as point values to assess the sedimentation rates ($\text{t ha}^{-1} \text{ a}^{-1}$) for the different treatments [24].

Using this approach sedimentation rates of $20.3 \text{ t}^{-1} \text{ ha}^{-1} \text{ a}^{-1}$, $13.5 \text{ t}^{-1} \text{ ha}^{-1} \text{ a}^{-1}$ and $13.2 \text{ t}^{-1} \text{ ha}^{-1} \text{ a}^{-1}$ were obtained for the CT, CS and DS systems respectively. These results indicate that the conservation tillage systems CS and DS were effective in reducing sedimentation rates on the average by 65% under the experimental conditions.

Deposition rates provided by the profile 1 using the ^{137}Cs depth distribution information ($26.1 \text{ t ha}^{-1} \text{ yr}^{-1}$) and MBM 2 ($20.3 \text{ t}^{-1} \text{ ha}^{-1} \text{ a}^{-1}$) are closely related to the erosion rates measured by the runoff plot under CT ($29.4 \text{ t ha}^{-1} \text{ a}^{-1}$) in the upper part of the same experimental field. If we take into account that the major erosive events that took place in 1994 (recurrence of 50 years) might introduce an overestimate of the average erosion rate obtained with the erosion plots on a long term basis, the measurements obtained with the erosion plots could be much closer to the MBM 2 - ^{137}Cs results [24].

4. CONCLUSIONS

Soil erosion and sedimentation magnitude in a small agricultural watershed located in Austria (Mistelbach) were evaluated using a combined approach based on conventional runoff plots measurement (13 years) and FRN method (^{137}Cs).

- A forested reference site was identified (classical exponential depth distribution of ^{137}Cs activity) and characterized (texture and physicochemical parameters).
- The initial ^{137}Cs fallout were evaluated at $1954 \pm 91 \text{ Bq m}^{-2}$ ($n=76$) with a CV of 20.4%; Chernobyl fallout contribution was assumed as negligible in the site under investigation.
- Long term erosion measurements (1994-2006) from runoff plots located in the upper part of an agricultural field just up-slope from a deposition area reached $29.4 \text{ t ha}^{-1} \text{ a}^{-1}$ from the conventional tilled plot, $4.2 \text{ t ha}^{-1} \text{ a}^{-1}$ from the conservation tillage plot and $2.7 \text{ t ha}^{-1} \text{ a}^{-1}$ from the direct seeding treatment. Soil losses were reduced significantly by a factor of 10 using no tillage, direct seeding treatment.

- Using the ^{137}Cs data that integrate the 1954-2007 period, the sedimentation rates down slope of the field containing the runoff plots were estimated at $26.1 \text{ t}^{-1} \text{ ha}^{-1} \text{ a}^{-1}$ using the ^{137}Cs depth distribution profile and $20.3 \text{ t}^{-1} \text{ ha}^{-1} \text{ a}^{-1}$ using MBM 2
- The erosion rates under conventional tillage are in agreement with the sedimentation rates estimated down slope of the field by the ^{137}Cs depth distribution profile and MBM 2.
- In the lowest part of the watershed sedimentation rates of $50.5 \text{ t}^{-1} \text{ ha}^{-1} \text{ a}^{-1}$ were highlighted by the ^{137}Cs depth distribution profile. These rates were greater than the average erosion rates measured by the erosion plots because this area is more representative of sedimentation processes occurring in the whole study area due to its topographical position and the basin geomorphology.

In order to better understand and quantify sediment mobilization, transfer and storage fluxes in this watershed, our future investigations will focus on the comparison of the magnitude and spatial distribution of soil erosion/deposition using radionuclide measurements (laboratory and in-situ) and conventional measurement. Also geostatistical tools will be used to evaluate the spatial structure of the initial ^{137}Cs fallout in the forested site.

ACKNOWLEDGEMENTS

This study was conducted as part of the Co-ordinated Research Project D1.50.08 ‘Assess the effectiveness of soil conservation measures for sustainable watershed management using fallout radionuclides’. The authors are grateful to the people who were involved during the sampling collection: Mr. Norbert Jagoditsch (SSU staff member), Mr. Stefan Borovits (previous SSU staff member), Ms. Maitane Melero-Urzainqui (previous SSU staff member), Ms. Sonia Rubio-Martinez (BOKU University), Ms. Johanna Hofmann (BOKU University), Ms. Bai (CU/SSU fellow), Ms. Li (SSU fellow), Mr. Josef Seufzenecker (previous SSU staff member), Ms. Maryalee Walker (SSU fellow), Mr. Daniel Asave (SSU fellow), Ms. Jawahir AL-Meslemani (CU fellow), and all other staff members of the SSU, CU, SWMCN and BOKU University. The authors are also grateful to Prof. Walling from Exeter University (UK) for advising us for data treatment from the sedimentation area and how to link them with the experimental erosion plots. Thanks are expressed to Mr. Felipe Zapata & Mr. Gerd Dercon (Soil Water Management and Crop Nutrition Section) and Mr. Gudni Hardarson (Soil Science Unit) for suggestions to improve this manuscript.

REFERENCES

- [1] MABIT, L., et al., L'étude de l'érosion hydrique au Québec, *Vecteur environnement* **33** (2000) 34-43.
- [2] MABIT, L., et al., Quantification of soil redistribution and sediment budget in a Canadian watershed from fallout caesium-137 (^{137}Cs) data, *Can. J. Soil Sci.* **82** (2002) 423-431.
- [3] MABIT, L., et al., Water erosion: Methods and case studies in Northern France, *Cahiers Agricultures* **11** (2002) 195-206.
- [4] MABIT, L., et al., Comparative advantages and limitations of Fallout radionuclides (^{137}Cs , ^{210}Pb and ^7Be) to assess soil erosion and sedimentation, *J. Environ. Radioact.* **99** (2008) 1799-1807.

- [5] ZAPATA, F. (ed.), Handbook for the assessment of soil erosion and sedimentation using environmental radionuclides, Kluwer Ac. Publ., Dordrecht (2002) 219 pp.
- [6] MABIT, L., FULAJTAR, E., “The use of ^{137}Cs to assess soil erosion and sedimentation processes: advantages and limitations”, Book of the extended Synopses of the International Conference on Environmental Radioactivity: From Measurements and Assessments to Regulation, IAEA Publication, IAEA-cn-145 (2007) 338-339.
- [7] MABIT, L., et al., Assessment of erosion in the Boyer River watershed (Canada) using a GIS oriented sampling strategy and ^{137}Cs measurements, *Catena* **71** (2007) 242-249.
- [8] MABIT, L., KLIK, A., “Test of ^{137}Cs and $^{210}\text{Pb}_{\text{ex}}$ to assess erosion and sedimentation process: A case study in Austria”, Moving ahead from assessments to action: Could we win the struggle with land degradation? (ZDRULI, P, COSTANTINI, E., Eds.), Proc. 5th International conference on land degradation, Valenzano Bari, Italy 18-22 September 2008, Book of abstracts ISBN 2-85352-399-2 Vol I (2008) 61-65.
- [9] KLIK, A., et al., Automated erosion wheel: a new measuring device for field erosion plots, *Journal of Soil and Water Conservation* **59** (2004) 116-121.
- [10] ANSPAUGH, L.R., et al., The global impact of the Chernobyl reactor accident, *Science* **242** (1988) 1513-1519.
- [11] Bossew P., Ditto, M., Falkner, T., Henrich, E., Kienzl, K., Rappelsberger, U., Caesiumbelastung der Boden Oesterreichs, Federal Environmental Agency, Volume 60 (2nd ed.) Vienna (1996).
- [12] BOSSEW, P., et al., Contamination of Austrian soil with caesium-137, *J. Environ. Radioact.* **55** (2001) 187-194.
- [13] MABIT, L, et al., Spatial variability of erosion and soil organic matter content estimated from ^{137}Cs measurements and geostatistics, *Geoderma* **145** (2008) 245-251.
- [14] GV AUTOMATIONPACK., GammaVision Productivity Add-on Version 1.3, Advanced Measurement Technology, Inc. Ortec/Ametek (2003-2004) 19 pp.
- [15] GAMMA VISION-32., Gamma-Ray Spectrum Analysis and MCA Emulator for Microsoft Windows 98, 2000, NT and XP - Software Version 6, Software User's Manual, Advanced Measurement Technology, Inc. Ortec/Ametek (2003) 414 pp.
- [16] ALLISON, M.A., et al., Importance of flood-plain sedimentation for river sediment budgets and terrigenous input to the oceans: insights from the Brahmaputra-Jamuna River, *Geology* **26** (1998) 175-178.
- [17] WALLING, D.E., HE, Q., Improved models for estimating soil erosion rates from cesium-137 measurements, *J. Environ.Qual.* **28** (1999) 611-622.
- [18] WALLING, D.E., et al., “Conversion models for use in soil-erosion, soil-redistribution and sedimentation investigations”, Handbook for the assessment of soil erosion and sedimentation using environmental radionuclides (ZAPATA, F., Ed.), Kluwer Ac. Publ., Dordrecht, (2002) 111-164.
- [19] KLUTE, A., (Ed.), Methods of soil analyses, Part I. Physical and mineralogical methods, 2nd edn, Agron. 9 ASA, SSSA, Madison WI (1986).
- [20] WISCHMEIER, W.H., SMITH, D.D., Predicting rainfall erosion losses – a guide to conservation planning, U.S. Government Printing Office, Agriculture Handbook **537** (1978) 58 p.
- [21] SUTHERLAND, R.A., Examination of caesium-137 areal activities in control (uneroded) locations, *Soil Technology* **4** (1991) 33-50.
- [22] SUTHERLAND, R.A., Caesium-137 soil sampling and inventory variability in reference locations: a literature review, *Hydrological Proceedings* **10** (1996) 43-53.

- [23] OWENS, P.N., WALLING, D.E., Spatial variability of caesium-137 inventories at reference sites: an example from two contrasting sites in England and Zimbabwe, *Appl. Radiat. Isot.* **47** (1996) 699-707.
- [24] MABIT, L, et al., Assessment of erosion and deposition rates within an Austrian agricultural watershed by combining ^{137}Cs , $^{210}\text{Pb}_{\text{ex}}$ and conventional measurements, *Geoderma* **150** (2009) 231-239.

USING THE CONCEPT OF A SOIL QUALITY INDEX (SQI) TO EVALUATE AGRICULTURAL SOILS WITH AND WITHOUT SOIL PROTECTION MEASURES IN LOWER AUSTRIA

A. KLIK

Institute of Hydraulics and Rural Water Management,
University of Natural Resources and Applied Life Sciences Vienna,
Vienna

J. HOFMANN

OMV Austria,
Gänserndorf

Austria

Abstract

Higher environmental standards in developed countries, in particular Europe, demand changes in agricultural land use and management practices. Modern agriculture needs to achieve high crop yields with decreasing equipment and labour inputs while reducing negative environmental impacts. Soil erosion causes many on-site and off-site damages; it has negative effects on the soil functions and soil quality. Improved soil management practices, including reduced tillage are often reported as a potential solution. The investigation and evaluation of different tillage practices and the assessment of soil quality as an indicator for sustainability are nowadays an issue of wide public concern and international debate. The objective of this study was to 1) to investigate the impact of different tillage systems and therefore the effect of soil conservation measures on physical, chemical and biological soil properties, and 2) to develop and adopt a model to assess changes in soil quality due to agricultural practices. Since 1994 the impact of conventional, conservation tillage and direct seeding has been investigated at three sites in Lower Austria. The field studies included continuous measurement of surface runoff, erosion and determination of crop yield. This study was conducted by computing a Soil Quality Index (SQI) for agricultural soils in Lower Austria. The model calculated improved soil quality for reduced tillage practices. For one site this improvement was statistically significant. The results are confirmed by long term erosion measurements from runoff plots and by determination of crop yields. Lower soil erosion led to higher SQI and higher yield. Computing the SQI helps combine different soil properties and processes within a simple tool that explains changes due to different soil tillage/management practices. These results support previous studies suggesting that calculation of soil quality indices can be useful for selecting management practices to maintain or improve soil quality. It was demonstrated that adjusting the system for local conditions can make the function ratings more or less sensitive to the management practices being evaluated.

1. INTRODUCTION

Soil erosion by wind and water is the major threat to the soil resources worldwide. Although erosion is a natural geological process, some human activities like inadequate agricultural and forestry practices, including tourism can dramatically exacerbate erosion rates. An estimated 115 million hectares or 12% of Europe's total land area are subject to water erosion, and 42 million hectares are affected by wind erosion [1].

Soil erosion is an irreversible process and has several impacts on the soil itself. The loss of fertile topsoil has serious effects on crop yields, the disruption of soil functions and overall on soil quality, as it reduces plant rooting depths, removes nutrients and reduces water holding capacity potential. Depletion of soil's filter and buffer capacity and potential accumulation of pollutants in local deposition areas are also impacts caused by soil erosion. The decrease in biodiversity affects soil turnover, degrades soil structure, increases crusting, reduces infiltration rates and exacerbates surface runoff and erosion [2].

The concept of soil functions and soil quality provides a sound basis for assessing, predicting or measuring the impact of soil erosion on sustainable development and sustainable use of soil. Soil quality has been defined as ‘the capacity of a specific kind of soil to function, within natural or managed ecosystem boundaries, to sustain plant and animal productivity, maintain or enhance water and air quality, and support human health and habitation’ [3]. Soil quality cannot be measured directly, so the use of indicators is needed. Indicators are measurable soil attributes that provide clues about how well the soil can function. Various concepts have been developed to assess soil quality, including those that focus on indices assessing soil productivity [4,5] and tilth [6].

Acton and Gregorich [7] stressed the importance of selecting appropriate indicators which could be measured and which influenced the capacity of a soil to perform various crop production or environmental functions. For Doran et al. [8] soil quality indicators should be sensitive enough to detect effects; however they quantified only the physical state of soil and did not consider environmental aspects. Larson and Pierce [9] discussed the need to assess how soils were functioning with regard to environmental issues. They proposed three different functions associated with good soil quality: (1) function as a medium for plant growth, (2) regulating and partitioning water flow through the environment and (3) serving as an environmental filter and buffer for agrochemicals.

In the 1990s field experiments were initiated in three sites in the eastern part of Lower Austria to investigate the effect of different tillage practices on soil erosion, surface runoff and erosion associated nutrient and pesticide losses [10]. Following soil tillage/management systems were compared: 1) conventional tillage (CT), conservation tillage with cover crops during the winter season (CS), and 3) direct seeding with cover crop during the winter season (DS). Eight years later in 2002 the impact of these tillage treatments on physical, chemical and biological soil parameters was determined. A model was developed and applied to evaluate the effects of these agronomic soil conservation measures on soil quality [11].

2. MATERIALS AND METHODS

2.1. Study sites and experimental treatments

In 1994 field experiments were initiated in two study sites, i.e. Mistelbach and Pyhra, and in 1997 one additional study site in Pixendorf. All three sites are located in Lower Austria about 30 to 80 km north and west of Vienna (Fig. 1). The soils in Mistelbach and Pyhra are classified as Typic Argiudolls while the soil in Pixendorf is an Entic Hapludoll. Soil textures ranged from silt loam to loam. Average annual rainfall at the sites amounted between 645 and 947 mm, average annual temperature between 9.4 and 10.4 °C. Table 1 gives an overview of the key data of the experimental fields. As soil conservation measures the following treatments were investigated: (1) conventional tillage system (CT), (2) conservational tillage (CS) with cover crops during winter and (3) direct seeding (DS) with cover crops during winter. Crop rotation consists mainly of cereals.

2.2. Experimental design for runoff plots

Throughout the investigation period from 1994 to 2006 soil erosion, surface runoff and nutrient and pesticide losses due to erosion processes were determined for all sites and the three tillage systems. The study design consisted of 4 m wide and 15 m long runoff plots for each management variation without replication [10,12]. Runoff and sediments were collected for each erosive storm event with an automated measuring device [13].

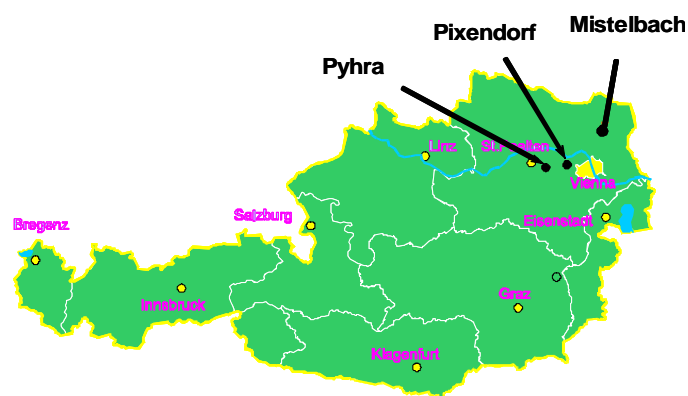


FIG.1. Location of the investigated sites.

TABLE 1. SELECTED CHARACTERISTICS OF THE EXPERIMENTAL SITES MISTELBACH, PIXENDORF AND PYHRA

Parameter	Mistelbach	Pixendorf	Pyhra
latitude	16° 34'E	15° 58'E	15° 41'E
longitude	48° 34'N	48° 17'N	48° 09'N
soil texture	silt loam	silt loam	loam
sand content (%)	9	11	9
silt content (%)	71	64	53
clay content (%)	20	25	38
slope (%)	12	5	15
average annual precipitation (mm)	645	687	947
average annual air temperature (°C)	9.6	10.4	9.4
organic carbon content (%)	0.8 – 1.3	0.8 – 2.5	0.7 – 0.9
CaCO ₃ content (%)	3.5 – 5.4	1.2 – 4.6	0.6 – 0.9
pH	8.1	7.3	6.5

Immediately after each erosive event representative runoff and sediment samples were taken to the laboratory for physical and chemical analyses. Nitrate concentrations were measured by UV absorption method described by Navonne [14]. Ammonium concentrations were analyzed using Na-nitroprussid, Na-salicylic and dichlorisocyanuric acid solution [15]. Phosphate contents were determined by the ammonium molybdate method [16]. These plots have been used to estimate soil erosion/deposition rates using fallout radionuclides [17].

2.3. Laboratory and field methods

Six years (Pixendorf) and eight years (Mistelbach and Pyhra) after initiation of this field study disturbed and undisturbed soil samples were taken in fall after harvest from all treatments. Investigated soil depths were 0-5 cm, 10-15 cm, 25-30 cm, 50-55 cm and 70-75 cm. To avoid potential slope induced differences in soil texture the samples were all taken at the same slope position at the upper third of the slope avoiding the wheel tracks. The rooting depth was also determined at that occasion. Crop yield of 10 m² plots was determined.

Main physical, chemical and biological parameters were determined: aggregate stability (aggregate stability), porosity (POR), total organic carbon (C_{org}), bulk density (BD), rooting depth (root), total nitrogen (N_{tot}), pH, total phosphorus (P_{tot}) and plant available water capacity (PAWC) were determined using standard methods.

Soil porosity (POR) and bulk density (BD) were analyzed from undisturbed soil samples of 200 cm³ volume. Soil pore size distribution was determined from soil water retention curves. The plant available water content (PAWC) was defined as the difference between soil water content at field capacity (300 hPa) and permanent wilting point (15 00 hPa). Soil aggregate stability (AggStab) was determined in fall for the top soil (0 – 2.5 cm) by the wet sieving method [18].

Samples for chemical analyses were air-dried, crushed, mixed and passed through a 2 mm sieve. Total nitrogen (N_{tot}) and total carbon were determined by a C/N-element analyser, type varioMAX CN by Elementar. The organic carbon content (C_{org}) was calculated as the difference of the total carbon content and the inorganic carbon content [19]. Total phosphorus (P_{tot}) was determined following Oenorm L 1085 [20] using a UV/VIS spectral photometer (DU-640, Beckmann). The results of the chemical analyses were converted into tons per hectare by multiplying with the bulk density. Soil pH was determined in a 1:2.5 soil to water solution, following Oenorm L 1083 [21], using a glass electrode by Mentrohm.

2.4. Soil quality assessment

A soil quality framework was adopted to assess changes in soil quality due to soil tillage/management practices. A common approach to assess soil quality is through single indicator-single response studies. These studies are useful for understanding the impact of singular components but they do not provide a comprehensive appraisal of agro-ecosystem performance. One approach that perhaps comes closer to assessing the impact of management on multiple soil functions involves the use of performance based indices [22] based on the general method of multi-attribute ranking. Numerical values for each soil quality indicator are converted into dimensionless scores ranging from 0 to 1. The score of each indicator is calculated from established lower, baseline and upper threshold limits. Indicators are categorized into elements within specific soil functions and then they are weighted based on their relative importance within the soil system. This approach has been demonstrated to be particularly useful in comparing management systems [23,24]. To assess soil quality Larson and Pierce [9] suggested measuring various soil attributes or indicators that controlled or are influenced by the various soil functions.

Arshad and Coen [25] used soil depth to a root restricting layer, available water holding capacity, bulk density or penetration resistance, hydraulic conductivity, aggregate stability, soil organic matter content, nutrient availability, pH and electrical conductivity, as soil quality indicators because those measurements are generally responsive to management practices. Similarly, Larson and Pierce [9] suggested a minimum data set for assessing soil quality; however, they substituted particle size distribution for aggregate stability.

Doran and Parkin [26] mentioned that soil quality could be quantified by using regression equations that describe relationships between the various soil quality indicators and the soil quality functions identified by Larson and Pierce [9]. To quantify these relationships Karlen et al. [27,28] selected three Standard Scoring Functions (SSF) to normalize the indicators (Fig. 2). The scoring functions were (a) more is better, (b) optimum and (c) more is worse. Numerical values for each soil quality indicator were converted into dimensionless scores ranging from 0 to 1. The score for each indicator was calculated after establishing lower threshold limits, baseline values and upper threshold limits with published values [22] or expert opinion.

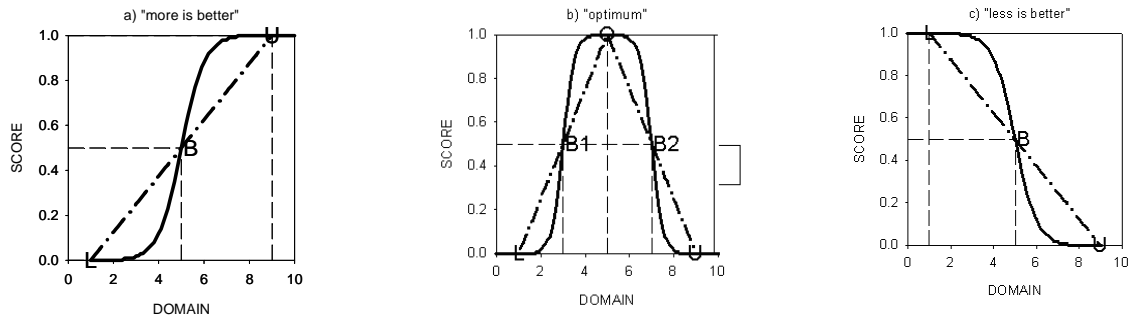


FIG. 2. Standard scoring function (SSF) used for normalization of soil quality indicators.

For this study soil quality assessment models by Harris et al. [22], Hussain et al. [23] and Mausbach and Seybold [28] were combined and adapted focusing on three main soil functions:

- (1) Sustenance of the biological activity (BIO),
- (2) Water regulation and partitioning (WATER),
- (3) Filtering and buffering (FILTER)

For each indicator scoring functions and threshold values needed to normalize the indicator data and to assign values between 0 and 1 were taken from the different sources. Jones [30] developed an empirical regression relationship to distinguish a 'lower' and an 'upper' critical bulk density (BD) for various soil textures. The lower boundary was defined by the value below which an effectively root growth is impeded. It was found to range from about 1.2 to 1.6 g cm⁻³ for soil with silt and clay contents ranging from 90% to 10%. The upper critical bulk density is also defined by root growth as the limiting factor and defined by 20% of the root growth at the lower critical bulk density. Values for the upper critical bulk density were found at 1.4 to 1.8 g cm⁻³. Comparable upper critical limits were proposed by Veihmeyer and Hendrickson [31] who found that root extension in clayey soils could stop completely at bulk densities of 1.5-1.6 g cm⁻³ and in loamy and sandy soils at densities of 1.6 - 1.8 g cm⁻³.

Good crop and root growth, health and function require additionally an adequate and well balanced soil air and soil water storage capacity. Substantial work over the last 30 years suggests that near-surface air-filled soil pore space (i.e. air capacity) should be at least 10 - 15% [32, 33]. It has also been proposed that plant-available water capacity should be larger than 20% [33] or within the range of 15-20% [34].

The carbon content of agricultural soil ranged at the study sites between 0% and 2.5% [35]. Aggregate stability is a very dynamic parameter, therefore it is important to know the time of sampling for data interpretation. More stable aggregates reduce the potential for erosion, soil crusting and surface runoff; therefore a higher amount of stable aggregates is desirable.

The soil functions were described by indices as follows:

$$\text{BIO} = f(a_1 \text{ root} + a_2 \text{ BD} + a_3 \text{ POR} + a_4 \text{ PWC} + a_5 \text{ pH} + a_6 \text{ P}_{\text{tot}} + a_7 \text{ C}_{\text{org}} + a_8 \text{ N}_{\text{tot}}) \quad (1)$$

$$\text{WATER} = (b_1 \text{ AggStab.} + b_2 \text{ POR} + b_3 \text{ BD}) \quad (2)$$

$$\text{FILTER} = f(c_1 \text{ AggStab} + c_2 \text{ POR} + c_3 \text{ C}_{\text{org}} + c_4 \text{ N}_{\text{tot}}) \quad (3)$$

where: a_n , b_n , c_n are weighting factors for the indices (Table 2).

TABLE 2. WEIGHTING FACTORS FOR SOIL QUALITY FUNCTIONS AND INDICATORS

Soil function	Function weight			Indicator weight			Total weight		
	bio	water	filter	bio	water	filter	bio	water	filter
<i>Sustenance of biological activity</i>	0.6	0.2	0.2						
Rooting medium				0.33	0.30	0.25			
Rooting depth							0.6	0.20	0.18
Bulk density							0.4	0.13	0.12
Water relation				0.33	0.40	0.25			
Porosity							0.6	0.20	0.24
PAWC							0.4	0.13	0.16
Nutrient relations				0.33	0.30	0.50			
pH							0.30	0.10	0.09
Total P							0.15	0.05	0.045
Organic C							0.40	0.13	0.12
Total N							0.15	0.05	0.045
<i>Water regulation and partitioning</i>	0.2	0.5	0.2						
Aggregate stability				0.60	0.40	0.30		0.60	0.40
Porosity				0.20	0.30	0.40		0.20	0.30
Bulk density				0.20	0.30	0.30		0.20	0.30
<i>Filtering and buffering</i>	0.2	0.3	0.4						
Aggregate stability				0.60	0.40	0.20		0.60	0.40
Porosity				0.10	0.30	0.40		0.10	0.30
Microbial processes				0.30	0.30	0.40			
Organic carbon							0.50	0.15	0.15
total N							0.50	0.15	0.15

The overall soil quality index was computed using the equation:

$$\text{Soil Quality Index (SQI)} = f(x_1 \text{ BIO} + x_2 \text{ WATER} + x_3 \text{ FILTER}) \quad (4)$$

where: x_n is the weighting factor for each function.

For this study six soil quality indices were computed using a combination of two different types of scoring functions (linear and nonlinear) and three different weighting systems with focus on the three main soil functions: sustenance of the biological activity (BIO), the regulation and partitioning of water (WATER), and the filtering and buffering function (FILTER). To complete the evaluation the six overall soil quality indices and the individual function, ratings were compared.

3. RESULTS

3.1. Impact of tillage practices on soil and nutrient losses, and crop yield

The results show that a reduction in tillage intensity had a positive impact on the long term average soil erosion rates. Average soil loss from conventionally tilled fields (CT) ranged from 3.37 to 9.57 t ha⁻¹ a⁻¹ (Table 3). By using conservation tillage (CS) in combination with a cover crop soil loss was between 1.50 and 1.98 t ha⁻¹ a⁻¹ whereas direct seeding (DS) led to an average soil loss between 0.41 and 1.38 t ha⁻¹ a⁻¹. As compared to conventional tillage, conservation tillage was able to reduce the soil loss by 41% (Pyhra), 52% (Pixendorf) and 84% (Mistelbach), respectively. The corresponding reductions with direct seeding were 59% (Pyhra), 89% (Pixendorf) and 90% (Pyhra).

For surface runoff numerical differences could be found between the investigated tillage treatments but these differences were statistically not significant. Only in Pixendorf, DS

reduced surface runoff significantly (Table 3). Losses of nutrients (nitrogen and phosphorus) depended mainly on the amount of eroded soil. N-losses from CT ranged from 4.0 to 14.9 kg ha⁻¹ a⁻¹ and P-losses from 2.3 to 8.0 kg ha⁻¹ a⁻¹. By using CS these losses were reduced and ranged between 2.2 and 6.2 kg N ha⁻¹ a⁻¹ and between 1.2 and 1.4 kg P ha⁻¹ a⁻¹. Corresponding values for DS ranged from 0.8 to 2.5 kg N ha⁻¹ a⁻¹ and from 0.2 to 1.9 kg P ha⁻¹ a⁻¹ (Table 3). Overall, no significant decrease in crop yield was found by applying soil management systems with reduced tillage intensity under the experimental conditions (Table 3).

TABLE 3. LONG TERM AVERAGE RUNOFF, SOIL LOSS AND SEDIMENT YIELD (1994-2006) FROM THE INVESTIGATED TREATMENTS

Parameter	Mistelbach			Pixendorf			Pyhra		
	CT	CS	DS	CT	CS	DS	CT	CS	DS
Soil loss (t ha ⁻¹ a ⁻¹)	9.57 ^a	1.50 ^b	1.10 ^b	3.99 ^a	1.90 ^b	0.41 ^b	3.37 ^a	1.98 ^b	1.38 ^a
Runoff (mm yr ⁻¹)	13.5 ^a	8.4 ^a	10.5 ^a	23.8 ^a	25.4 ^a	15.0 ^b	26.8 ^a	29.9 ^a	32.1 ^a
N-losses (kg ha ⁻¹ a ⁻¹)	14.9 ^a	2.8 ^b	2.5 ^b	4.0 ^a	2.2 ^b	0.8 ^c	7.2 ^a	6.2 ^a	4.2 ^b
P-losses (kg ha ⁻¹ a ⁻¹)	8.0 ^a	1.2 ^b	0.9 ^a	2.3 ^a	1.2 ^b	0.2 ^c	2.5 ^a	1.4 ^b	1.9 ^b
Relative crop yield (%)	100	94	92	100	103	103	100	104	103

Means within the same site followed by same letter are not significantly different at p=0.05 probability level.

Conventional tillage system (CT), conservational tillage (CS) with cover crops during winter and direct seeding (DS) with cover crops during winter.

3.2. Impact of tillage practices on soil characteristics

The impact assessment showed that soils were generally characterised by a higher bulk density in the top 10 cm layer and therefore lower porosity under reduced tillage systems (Table 4). The change of porosity was always positively correlated to saturated hydraulic conductivity values. In Mistelbach and Pyhra CS and DS improved the plant available water capacity whereas in Pixendorf the tillage system showed no impact on PAWC. At all investigated sites aggregate stability increased significantly under CS and DS (Table 4). Differences in the amount of total nitrogen and phosphorus in the 0 - 20 cm depth were not uniform for all three sites. The amount of organic carbon stored in the top 20 cm increased significantly at all three sites under reduced tillage (Table 4). In Mistelbach (silt loam) the reduced tillage practices resulted in higher amount of stored nitrogen and had no effect on total phosphorus. In Pixendorf (silt loam) no effects due to tillage could be found for nitrogen but amount of phosphorus varied among the treatments (CS > CT > DS). In Pyhra (loam) the total amount of phosphorus and nitrogen increased under reduced tillage. Soil pH did not differ among tillage systems, except in Pyhra where it was lower under direct seeding as compared to CS and CT.

Tillage effects could not be classified as entirely negative or positive with regards to the sustenance of biological activity (bio), water balance (water) or filtering and buffering capacity (filter), because every indicator was analysed separately. Therefore the soil quality framework was applied. Table 4 gives an overview of the obtained results from the laboratory measurements for the chosen parameters that were used to calculate the soil water index and the calculated dimensionless scores.

3.3. Soil function indices

Tables 5 to 7 show the calculated function indices with respect to sustenance of the biological activity (Table 5), water regulation and partitioning (Table 6) and the filtering and buffering function (Table 7), using linear (L) and nonlinear (NL) scoring functions and three types of weights. From these six results mean values were computed and compared.

TABLE 4. EFFECT OF TILLAGE TREATMENTS ON MAIN PHYSICAL AND CHEMICAL CHARACTERISTICS

Parameter	Mistelbach			Pixendorf			Pyhra		
	CT	CS	DS	CT	CS	DS	CT	CS	DS
Bulk density (g cm ⁻³)									
0-5 cm	1.13 ^a	1.35 ^b	1.40 ^b	1.34 ^a	1.24 ^a	1.22 ^b	1.45 ^a	1.43 ^a	1.42 ^a
25-30 cm	1.40 ^a	1.46 ^a	1.46 ^a	1.46 ^a	1.58 ^b	1.51 ^b	1.66 ^{ab}	1.65 ^a	1.69 ^b
50-55 cm	1.45 ^a	1.46 ^{ab}	1.50 ^b	1.36 ^a	1.31 ^b	1.35 ^a	1.62 ^a	1.61 ^a	1.62 ^a
Porosity (%)									
0-5 cm	57.6 ^a	49.6 ^a	47.4 ^b	50.3 ^a	54.6 ^b	55.0 ^b	44.8 ^a	45.6 ^a	45.7 ^a
25-30 cm	48.0 ^a	48.5 ^a	45.3 ^b	46.7 ^a	42.1 ^a	44.7 ^b	38.0 ^{ab}	38.6 ^a	37.0 ^b
50-55 cm	45.8 ^a	45.9 ^a	44.3 ^b	50.3 ^a	52.3 ^b	50.4 ^a	39.9 ^a	40.2 ^a	39.9 ^a
K _{sat} (m·d ⁻¹)									
0-5 cm	49.9 ^a	21.7 ^{ab}	5.03 ^b	3.93 ^a	24.2 ^a	21.3 ^a	0.34 ^a	0.17 ^a	0.45 ^a
25-30 cm	0.92 ^a	1.02 ^a	0.25 ^a	0.80 ^a	0.76 ^b	0.51 ^b	0.02 ^a	0.04 ^a	0.21 ^a
50-55 cm	0.32 ^a	0.24 ^a	0.20 ^a	0.93 ^a	1.79 ^{ab}	1.81 ^b	0.03 ^a	0.04 ^a	0.06 ^a
Rooting depth (cm)	75.0 ^a	80.0 ^b	77.5 ^a	67.5 ^a	75.0 ^b	75.0 ^b	70.0 ^a	47.5 ^c	80.0 ^b
Aggregate stability (%)	8.0 ^a	10.4 ^b	11.6 ^b	7.0 ^a	9.1 ^b	10.7 ^b	11.2 ^a	14.2 ^b	15.3 ^b
C _{org} 0-20 cm (t·ha ⁻¹)	13.8 ^a	17.6 ^b	19.0 ^b	13.2 ^a	29.9 ^b	39.4 ^b	13.1 ^a	14.4 ^b	14.8 ^b
N _{tot} 0-20 cm (t·ha ⁻¹)	2.3 ^a	2.3 ^a	2.6 ^b	2.8 ^a	2.7 ^a	2.7 ^a	2.8 ^a	3.2 ^b	3.1 ^b
P _{tot} 0-20 cm (t·ha ⁻¹)	1.8 ^a	1.8 ^a	1.8 ^a	1.9 ^a	2.0 ^b	1.6 ^c	1.7 ^a	1.9 ^b	1.9 ^b
PAWC 0- 70 cm (mm)	118 ^a	110 ^b	123 ^a	95 ^a	94 ^a	96 ^a	73 ^a	84 ^b	67 ^c
pH	8.3 ^a	8.2 ^a	8.2 ^a	7.4 ^a	7.3 ^a	7.3 ^a	6.8 ^a	6.6 ^a	6.4 ^b

Means within the same site followed by same letter are not significantly different at p=0.05 probability level; Conventional tillage system (CT), conservational tillage (CS) with cover crops during winter and direct seeding (DS) with cover crops during winter. PAWC: Plant Available Water Capacity

TABLE 5. FUNCTION INDEX FOR THE SUSTENANCE OF THE BIOLOGICAL ACTIVITY CONSIDERING NON LINEAR (NL) AND LINEAR (L) SCORING FUNCTIONS AND DIFFERENT INDICATOR WEIGHTS (BIO, WATER, FILTER)

Weights	Mistelbach						Pixendorf						Pyhra					
	CT		CS		DS		CT		CS		DS		CT		CS		DS	
	NL	L	NL	L	NL	L	NL	L	NL	L	NL	L	NL	L	NL	L	NL	L
Bio	0.66	0.51	0.61	0.49	0.59	0.48	0.64	0.51	0.66	0.56	0.69	0.57	0.42	0.41	0.40	0.40	0.42	0.43
Water	0.68	0.54	0.63	0.52	0.63	0.51	0.64	0.54	0.66	0.58	0.69	0.59	0.41	0.42	0.39	0.42	0.40	0.43
Filter	0.52	0.42	0.50	0.41	0.50	0.41	0.59	0.45	0.62	0.51	0.66	0.53	0.44	0.39	0.43	0.39	0.44	0.41
Mean	0.56	a ¹	0.53	a	0.52	a	0.56	a	0.60	a	0.62	a	0.42	a	0.41	a	0.42	a

¹: for each row, means within the same site followed by same letter are not significantly different at p=0.05. Conventional tillage system (CT), conservational tillage (CS) with cover crops during winter and direct seeding (DS) with cover crops during winter.

TABLE 6. FUNCTION INDEX FOR WATER REGULATION AND PARTITIONING CONSIDERING NON LINEAR (NL) AND LINEAR (L) SCORING FUNCTIONS AND DIFFERENT INDICATOR WEIGHTS (BIO, WATER, FILTER)

Weights	Mistelbach						Pixendorf						Pyhra					
	CT		CS		DS		CT		CS		DS		CT		CS		DS	
	NL	L	NL	L	NL	L	NL	L	NL	L	NL	L	NL	L	NL	L	NL	L
Bio	0.40	0.49	0.39	0.51	0.35	0.51	0.37	0.46	0.39	0.51	0.43	0.55	0.16	0.42	0.32	0.48	0.40	0.50
Water	0.59	0.60	0.55	0.59	0.46	0.57	0.54	0.58	0.56	0.61	0.60	0.64	0.19	0.44	0.29	0.49	0.33	0.49
Filter	0.68	0.67	0.64	0.65	0.54	0.61	0.64	0.65	0.66	0.68	0.69	0.70	0.23	0.47	0.29	0.50	0.32	0.51
Mean	0.57	a ¹	0.55	a	0.50	a	0.54	a	0.57	a	0.60	a	0.32	a	0.40	a	0.42	a

¹: for each row, means within the same site followed by same letter are not significantly different at p=0.05. Conventional tillage system (CT), conservational tillage (CS) with cover crops during winter and direct seeding (DS) with cover crops during winter.

TABLE 7. FUNCTION INDEX FOR FILTERING AND BUFFERING CAPACITY CONSIDERING NON LINEAR (NL) AND LINEAR (L) SCORING FUNCTIONS AND DIFFERENT INDICATOR WEIGHTS (BIO, WATER, FILTER)

Weights	Mistelbach						Pixendorf						Pyhra					
	CT		CS		DS		CT		CS		DS		CT		CS		DS	
	NL	L	NL	L	NL	L	NL	L	NL	L	NL	L	NL	L	NL	L	NL	L
Bio	0.18	0.27	0.22	0.32	0.26	0.34	0.19	0.26	0.22	0.33	0.28	0.38	0.20	0.31	0.38	0.46	0.46	0.40
Water	0.38	0.41	0.40	0.43	0.43	0.43	0.39	0.40	0.41	0.47	0.46	0.51	0.28	0.37	0.38	0.42	0.43	0.43
Filter	0.50	0.45	0.51	0.45	0.53	0.44	0.52	0.46	0.53	0.52	0.58	0.56	0.33	0.37	0.38	0.40	0.39	0.40
Mean	0.37	a ¹	0.39	a	0.41	a	0.37	a	0.41	a	0.46	a	0.31	a	0.39	b	0.42	c

¹ : for each row, means within the same site followed by same letter are not significantly different at p=0.05. Conventional tillage system (CT), conservational tillage (CS) with cover crops during winter and direct seeding (DS) with cover crops during winter.

For the indicators of the sustenance of the biological activity (Table 5) none of the sites showed significant differences although at two sites (Pixendorf and Pyhra) the direct seeding (DS) treatment had higher numerical values for the index. This indicates an improvement. The use of non-linear scoring functions resulted in slightly higher values than the linear functions but total indices ranged for Mistelbach from 0.41 to 0.68, for Pixendorf from 0.45 to 0.69 and for Pyhra from 0.39 to 0.44. Overall the spectrum of the results was narrow, because eight different parameters influenced the function of sustaining the biological activity and therefore a single indicator had not such a big impact on the final result.

The results focusing on the water regulation and partitioning are given in Table 6. They show the same pattern as those for the sustenance of the biological activity. Based on the index, for two sites an improvement in water regulation and partitioning was observed under reduced tillage (Pixendorf and Pyhra). Nevertheless these differences were not significant. Overall the spectrum of the results was wider than for the biological indicator. Values at Mistelbach ranged from 0.35 to 0.67, at Pixendorf from 0.37 to 0.70 and at Pyhra from 0.16 to 0.50. As this index is calculated only based on three parameters, the influence of each parameter is higher and therefore the spectrum of the results is also broader.

At all three sites an improvement of the filtering and buffering function under reduced tillage practices could be observed (Table 7). Direct seeding showed always the highest SQI whereas conventional tillage always the minimum. This difference was significant for the loamy soil in Pyhra. Results for Mistelbach ranged from 0.18 to 0.53, for Pixendorf from 0.19 to 0.58 and for Pyhra from 0.20 to 0.43.

The absolute values of the indices varied depending on the used combination of scoring function and weighting but the relative ranking of the treatments always stayed the same. Differences between the index calculations were higher when less parameters were used for the calculation.

3.4. Soil quality index

The Soil Quality Index, calculated using different weighting factors (Table 2) and focusing on sustaining the biological activity, water regulation and partitioning, and filtering and buffering functions respectively are presented in Table 8. The highest overall ratings for SQI in this study were associated with the direct seeding treatment. Similar differences among tillage systems were obtained by Karlen et al. [27]. With the exception of Mistelbach (silt loam) soils under reduced tillage had higher soil quality indices than under conventional tillage. This can be interpreted as an improvement of soil quality.

TABLE 8. SOIL QUALITY INDICES (SQI) CONSIDERING NON LINEAR (NL) AND LINEAR (L) SCORING FUNCTIONS AND DIFFERENT INDICATOR WEIGHTS (BIO, WATER, FILTER)

Weights	Mistelbach						Pixendorf						Pyhra					
	CT		CS		DS		CT		CS		DS		CT		CS		DS	
	NL	L	NL	L	NL	L	NL	L	NL	L	NL	L	NL	L	NL	L	NL	L
Bio	0.51	0.46	0.46	0.46	0.48	0.46	0.49	0.45	0.52	0.50	0.56	0.53	0.33	0.39	0.38	0.41	0.42	0.44
Water	0.54	0.53	0.52	0.53	0.48	0.51	0.52	0.52	0.54	0.56	0.58	0.59	0.26	0.42	0.34	0.45	0.37	0.46
Filter	0.55	0.48	0.53	0.47	0.52	0.46	0.57	0.50	0.59	0.55	0.63	0.58	0.35	0.40	0.38	0.42	0.40	0.43
Mean	0.51	a ¹	0.50	a	0.49	a	0.51	a	0.54	a	0.58	b	0.36	a	0.40	a	0.42	a

¹:for each row, means within the same site followed by same letter are not significantly different at p=0.05

Conventional tillage system (CT), conservational tillage (CS) with cover crops during winter and direct seeding (DS) with cover crops during winter.

The differences in the soil quality index were significant in Pixendorf (silt loam) with DS (0.58) > CS (0.54) > CT (0.51). The differences for Pyhra (loam) were not significant but numerically still high with DS (0.42) > CS (0.40) > CT (0.36). The Mistelbach fields (silt loam) showed the opposite ranking of SQI but these differences were negligible with: CT (0.51) > CS (0.50) > DS (0.49). Overall it could be observed, that the silt loam sites (Mistelbach and Pixendorf) had higher soil quality indices than the loam site (Pyhra).

The calculated SQI and function indices showed a big variation depending on the chosen scoring function or weighing system but the ranking of the sites was not influenced by that. This indicates that a change in the function weight would only change the absolute value but not the relative ranking. Therefore the model can be seen as stable regarding the output and depends only on the soil indicators and not on their scoring functions or weights of the indicators. In terms of overall soil quality assessment, field observations and the SQI indicated that practices with reduced tillage intensity resulted in the best overall soil quality. This reflects a soil with a high sustenance of the biological activity, good water regulation and the improvement of the filtering and buffering function.

4. CONCLUSIONS

In a long term field experiment the effects of different tillage practices on runoff, soil erosion and soil quality were investigated. The results showed that compared to conventional tillage, conservation tillage as well as direct seeding in combination with cover crops during the growing season are very effective measures to significantly reduce soil loss and erosion induced nutrient losses. Long term annual average soil loss from conventionally tilled fields at the investigated sites ranged from 3.4 to 9.6 t ha⁻¹. By using conservation tillage in combination with cover crops during the winter season soil erosion could be reduced by 41 to 84%. Corresponding reductions with direct seeding were between 59 and 90%. No significant impact of tillage type was observed for surface runoff. Reduction in nitrogen loss ranged from 42 to 84% and with regards to phosphorus losses values varied between 24 and 92%. Under the experimental conditions no crop yield decline was reported under CS or DS.

Soil quality and its change due to tillage practice or to soil erosion can not be expressed by a single parameter but it depends on the complex system of various physical, chemical and biological processes. When applying a soil quality model these interactions have to be considered. For this study a Soil Quality Indicator (SQI) was developed.

The SQI calculated based on measurements of physical, chemical and biological soil properties indicated an improvement of soil quality with regards to sustenance of the biological activity, water regulation and partitioning, and filtering and buffering functions. Under reduced tillage practices (CS and DS) soil quality was improved for two of the investigated sites, whereas no improvement was observed for Mistelbach. For Pixendorf and Pyhra the SQI were ranked in the following way: CT < CS < DS. In Pixendorf the SQI value increased from 0.51 under CT to 0.54 and 0.58 for CS and DS, respectively. For the Pyhra fields an increase from 0.36 (CT) to 0.40 (CS) and 0.42 (DS) was reported. Field measurements (soil loss, runoff and crop yield) confirmed these calculations; therefore the chosen soil parameters and the approach to calculate a Soil Quality Index are useful for determining changes in soil quality.

In conclusion, this study demonstrated that computing functional components of an overall soil quality index can provide a comprehensive assessment of soil quality and can be used to identify soil management/soil conservation problems that need to be considered to sustain or improve our soil resources.

ACKNOWLEDGEMENTS

This study was partly funded by the FAO/IAEA Co-ordinated Research Project (CRP) D1.50.08 ('Assessing the effectiveness of soil conservation techniques for sustainable watershed management and crop production using fallout radionuclides'), Research Agreement AUS-12319.

REFERENCES

- [1] COMMISSION OF THE EUROPEAN COMMUNITIES, 2006. Thematic Strategy for Soil Protection, Communication from the Commission to the Council, the European Parliament, the European Economic and Social Committee, and the Committees of the Region – COM (2006) 231 final, Brussels (2006) pp 12.
- [2] VAN CAMP, L., et al., Reports of the Technical Working Groups Established under the Thematic Strategy for Soil Protection, EUR 21319, EN/1, Office for Official Publications of the European Communities, Luxembourg (2004) pp 872.
- [3] KARLEN, D.L., et al., Soil quality: a concept, definition, and framework for evaluation (a guest editorial), *Soil Sci. Soc. Am. J.* 61 (1997) 4-10.
- [4] NEIL, L.L., An Evaluation of Soil Productivity Based on Root Growth and Water Depletion, M.Sc. Thesis, University of Missouri, Columbia (1979).
- [5] PIERCE, F.J., et al., Productivity of soils: assessing long-term changes due to erosion, *J. Soil Water Conserv.* 38 (1983) 39-44.
- [6] SINGH, K.K., et al., Tilth index: an approach to quantifying soil tilth, *Trans. American Society of Agricultural Engineers* 35 (1992) 1777-1785.
- [7] ACTON, D.F., GREGORICH, L.J., "Understanding soil health", *The Health of Our Soils - Toward Sustainable Agriculture in Canada* (ACTON, D.F., GREGORICH, L.J., Eds), Centre for Land and Biological Resources Research, Research Branch, Agriculture and Agr-Food Canada, Ottawa, Ont. (1995) 5-10.
- [8] DORAN, J.W., et al., "Soil health and sustainability", *Advances in Agronomy*, vol. 56 (SPARKS, D.L., Ed), Academic Press, San Diego (1996) 1-54.

- [9] LARSON, W.E., PIERCE, F.J., "The dynamics of soil quality as a measure of Sustainable management", Defining Soil Quality for a Sustainable Environment, Chapter 3, 1st ed (DORAN, J.W., et al., Eds), Soil Sci. Soc. Am. Pub. N° 35, Soil Sci. Soc. Am., Madison (1994) 37-52.
- [10] KLIK, A., 2003, Einfluss unterschiedlicher Bodenbearbeitung auf Oberflächenabfluss, Bodenabtrag sowie Nährstoff- und Pestizidausträge, Österreichische Wasser- und Abfallwirtschaft 55 (2003) 89-96.
- [11] HOFMANN, J., Auswirkungen unterschiedlicher Bodenbearbeitungssysteme auf die Bodengesundheit, Dissertation, Institute of Hydraulics and Rural Water Management, University of Natural Resources and Applied Life Sciences, Vienna (2005).
- [12] KLIK, A., et al., "Tillage Effects on Soil Erosion, Nutrient, and Pesticide Transport", Proc. of the International Symposium „Soil Erosion Research for the 21st Century“, Honolulu, Hawaii, January 2-5, 2001, American Society of Agricultural Engineers, St. Joseph (2001) 71-74.
- [13] KLIK, A., et al., Automated erosion wheel: A new measuring device for field erosion plots, Journal of Soil and Water Conservation 59 (2004) 116-121.
- [14] NAVONNE, R., Proposed method for nitrate in potable waters, Journal AWWA 56 (1964) 781-783.
- [15] OENORM ISO 7150, 1985, Spectrometric analysis of ammonium, Ministry of Agriculture and Forestry, Vienna (1985).
- [16] DEUTSCHE INDUSTRIE NORM (DIN) 38.405, Deutsche Einheitsverfahren zur Wasser- und Schlammuntersuchung. Anionen (Gruppe D), Bestimmung von Phosphorverbindungen (D 11) – Teil 11 (1983).
- [17] MABIT, L. et al., Combined use of caesium-137 methodology and conventional erosion measurements in the Mistelbach watershed (Austria), TECDOC CRP D1.50.08, pp. 293-309.
- [18] KEMPER, W.D., KOCH, E.J., Aggregate stability of soils from the western portions of the United States and Canada, U.S. Dep. Agric. Tech. Bull. 1355 (1966).
- [19] OENORM L 1084, Chemische Bodenuntersuchungen - Bestimmung von Carbonat, Österreichisches Normungsinstitut, Wien (1988).
- [20] OENORM L 1085, Chemische Bodenuntersuchungen - Säureextrakt zur Bestimmung von Nähr- und Schadelementen, Österreichisches Normungsinstitut, Wien (1989).
- [21] OENORM L 1083, Chemische Bodenuntersuchungen - Bestimmung der Acidität, Österreichisches Normungsinstitut, Wien (1988).
- [22] KARLEN, D.L., STOTT, D.E., „A framework for evaluating physical and chemical indicators of soil quality“, Defining soil quality for a sustainable environment, Chapter 4. 1st ed (DORAN, J.W., et al., Eds), Soil Sci. Soc. Am. Pub. N° 35, Soil Sci. Soc. Am., Madison (1994) 53-72.
- [23] HARRIS, R.F, et al., "A conceptual framework for assessment and management of soil quality and health", Methods for Assessing Soil Quality, Chapter 4, 1st ed. (DORAN, J.W., JONES, A.J., Eds), Soil Sci. Soc. Am. Pub. N° 49, Soil Sci. Soc. Am., Madison, (1996) 61-82.
- [24] HUSSAIN I., et al., Adaptation of soil quality indices and application to three tillage systems in southern Illinois, Soil & Tillage research 50 (1999) 237-249.
- [25] ARSHAD, M.A., COEN, G.M., Characterization of soil quality: physical and chemical criteria, Am. J. Alternative Agric. 7 (1992) 12-16.
- [26] DORAN, J.W., PARKIN., T.B., "Defining and Assessing Soil Quality", Defining Soil Quality for a Sustainable Environment, SSSA Special Publication N° 35, Soil Science Society of America, American Society of Agronomy, Madison (1994).

- [27] KARLEN, D.L., et al., Crop residue effect on soil quality following 10-years of no-till corn, *Soil Tillage Res.* 31 (1994) 149-167.
- [28] KARLEN, D.L., et al., Long-term tillage effects on soil quality, *Soil Tillage Res.* 32 (1994) 313-327.
- [29] MAUSBACH, M.J., SEYBOLD, C.A., "Assessment of Soil Quality", *Soil Quality and Agricultural Sustainability* (LAL, R., Ed), Sleeping Bear Press, Chelsea (1998).
- [30] JONES, C.A., Effect of soil texture on critical bulk densities for root growth, *Soil Sci. Soc. Am. J.* 47 (1983) 1208-1211.
- [31] VEIHMEYER, F.J., HENDRICKSON, A.H., Soil density and root penetration, *Soil Sci.* 65 (1948) 487 - 493.
- [32] GRABLE, A.R., SIMMER, E.G., Effects of bulk density, aggregate size, and soil water suction on oxygen diffusion, redox potentials and elongation of corn roots, *Soil Sci. Soc. Am. Proc.* 32 (1968) 180-186.
- [33] COCKROFT, B., OLSSON, K.A., "Case study of soil quality in south-eastern Australia: management of structure for roots in duplex soils", *Soil Quality for Crop Production and Ecosystem Health, Development in Soil Science*, vol. 25 (GREGORICH, E.G.; CARTER, M.R., Eds), Elsevier, New York (1997) pp.339-350.
- [34] CRAUL, P., *Urban Soils: Applications and Practices*. Wiley, Toronto (1999).
- [35] SCHEFFER, F., SCHACHTSCHABEL, P., *Lehrbuch der Bodenkunde*, 14. Auflage, Ferdinand Enke Verlag Stuttgart (1998).

ANALYTICAL PERFORMANCE OF 14 LABORATORIES TAKING PART IN PROFICIENCY TEST FOR THE DETERMINATION OF CAESIUM-137 AND TOTAL LEAD-210 IN SPIKED SOIL SAMPLES

A. SHAKHASHIRO

International Atomic Energy Agency, Chemistry Unit,
IAEA Laboratories Seibersdorf

L. MABIT

International Atomic Energy Agency,
Soil and Water Management and Crop Nutrition Section ,
FAO/IAEA Agriculture & Biotechnology Laboratory,
IAEA Laboratories Seibersdorf
Seibersdorf, Austria

Abstract

One of the most widespread threats to agricultural development is soil erosion. Soil erosion further impoverishes low-income farm households by reducing soil quality and consequently agricultural yields. It also affects productivity in irrigated farming systems by contributing suspended sediment to waterways and reducing storage capacity of reservoirs. The costs of these effects are substantial in many developing and developed countries. To combat soil erosion there is an urgent need for reliable quantitative data on the extent and rates of soil erosion and sedimentation. Fallout radionuclides (FRN) ^{210}Pb and ^{137}Cs are widely used for soil erosion and sedimentation studies. FRN measurements for soil redistribution involve gamma analysis on soil samples. It is therefore important that the analytical data are correct to ensure that the conclusions of such studies are based on reliable and validated analytical results and to ensure the comparability of the results of different countries. Through a collaboration between the Chemistry Unit and the Soil Science Unit of the IAEA's laboratories IAEA organized an intercomparison exercise in order to assess the validity and reliability of the analytical measurements of ^{137}Cs and total ^{210}Pb carried out by the different laboratories participating in the IAEA Co-ordinated Research Project D1.50.08 'Assessing the effectiveness of soil conservation measures for sustainable watershed management using fallout radionuclides' lead by the Soil Water Management and Crop Nutrition Section of the Joint FAO/IAEA Division of Nuclear Techniques in Food and Agriculture. In this proficiency test 90 samples (Proficiency Test¹ (PT) materials) were distributed to the participating laboratories. The laboratories were requested to analyse the samples employing the same methods used in their daily routine gamma measurements. In total 14 out of 18 initially registered laboratories reported their results. The analytical results of the laboratories were compared with the reference values assigned to the PT materials, and a rating system was applied. In the case of ^{137}Cs , the analytical results were satisfactory with 66% of the participants producing acceptable results (only the sample with low ^{137}Cs activity $2.6 \pm 0.2 \text{ Bq kg}^{-1}$ gave less accurate results) while the ^{210}Pb analysis indicated a clear need for corrective actions in the analytical process. 63% of the laboratories involved in the proficiency test did not fulfil the proficiency test criteria for total ^{210}Pb , while this was only 21% for ^{137}Cs . It is recommended that further inter-comparison exercises be organized by IAEA or regional laboratories to ensure the quality of the analytical data produced in Member States through Co-ordinated Research Projects and Technical Co-operation Projects.

1. INTRODUCTION

Studies conducted since the late 1960s showed that fallout radio-nuclides (FRN) can be used to assess temporal and spatial patterns and rates of soil redistribution in the landscape. The most commonly used FRN as a soil tracer is ^{137}Cs (half-life = 30.2 years), resulting from the fallout from high-yield thermonuclear weapons tests. The ^{137}Cs was injected into the stratosphere and circulated globally before being deposited to the land surface through precipitation. While ^{137}Cs is used to assess erosion rates for the last 50 years, ^{210}Pb is another radionuclide that can

¹ Proficiency Testing (PT) is defined as a means of evaluating a laboratory's performance under controlled conditions relative to a given set of criteria through analysis of unknown samples provided by an external source.

be employed to quantify the soil movement that took place over a period of about 100 years (half-life= 22.8 years). ^{210}Pb is a natural radionuclide, that originates by decay of ^{222}Rn which occurs in both soil and atmosphere. The ^{210}Pb originating in the atmosphere is deposited by fallout on the land surface. Soil samples for measuring ^{210}Pb should be stored for 1 month to obtain equilibrium between ^{226}Ra and its daughter ^{222}Rn (half-life = 3.8 days). The amount of $^{210}\text{Pb}_{\text{ex}}$ in the samples is calculated by subtracting ^{226}Ra -supported ^{210}Pb concentration from the total ^{210}Pb concentration. A great advantage of the ^{210}Pb -method is that it can be used also on the southern hemisphere where in some cases fallout ^{137}Cs concentrations can be below the detection limits of the available measuring equipment.

The International Atomic Energy Agency (IAEA), through the Soil and Water Management and Crop Nutrition Programme of the Joint FAO/IAEA Division of Nuclear Techniques in Food and Agriculture, has been actively involved in the development and transfer of erosion/sedimentation assessment approaches based on FRN (fallout radionuclides) since the mid-1990's. These activities are conducted through supporting financially and technically Co-ordinated Research Projects (CRP) and Technical Co-operation Projects (TCP), as well as in house research and training programmes.

Two CRPs on the assessment of erosion and sedimentation with the aid of FRNs were implemented by IAEA during 1995-2000. The major outcome of these projects was the production of a handbook on the use of FRNs for erosion/sedimentation assessment [1], contributing to the overall coordination and standardization of the procedures employed by researchers using the FRN techniques in soil erosion and sedimentation studies worldwide. A follow up CRP on 'Assessing the effectiveness of soil conservation measures for sustainable watershed management using fallout radionuclides' was initiated in 2003.

For more than forty years the IAEA has been implementing the Analytical Quality Control Services (AQCS) programme to assist laboratories in Member States (MS) in testing, improving and maintaining the reliability and the quality of analyses of radioactive materials from different origins [2]. This is accomplished through the provision of matrix reference materials and validated procedures, training in the implementation of quality control, and the evaluation of measurement performance by the organization of proficiency tests and intercomparison exercises (<http://www.iaea.org/programmes/aqcs>). Through the conduct of proficiency tests, the IAEA pursues its tradition to initiate and support improvements in the accuracy of analytical radiometric measurements. It is widely recognised that for a laboratory to produce consistently reliable data it must implement an appropriate programme of quality assurance measures. Amongst such measures, the laboratory should demonstrate that its analytical systems are under statistical control, that it uses methods of analysis which are properly validated, that its results are 'fit-for-purpose', and that it participates in proficiency testing exercises [3]. The competence of laboratories is demonstrated in accreditation processes following the ISO/IEC 17025:2005 [4]. In the frame of accreditation systems, the use of reference materials, both for quality control and proficiency testing, has therefore increased in recent years.

As incorrect decisions can be extremely costly and detrimental to research programmes, it is therefore, essential that such analytical measurements are accurate, reliable, cost-effective and defensible. In addition, measurements performed by laboratories located worldwide should yield traceable and comparable results. Proficiency testing is a method for regularly assessing the accuracy of the analytical data produced by the laboratories of particular measurements. In analytical chemistry proficiency testing usually comprises the distribution of effectively homogenous portions of the test material to each participant for analysis as an unknown. The

laboratories conduct the test under routine conditions, and report the result to the organiser by a deadline. The results generated in proficiency testing should be used for the purpose of a continuing assessment of the technical competence of the participating laboratories [3]. Participation in proficiency testing exercises provides also laboratories with an objective means of assessing and documenting the reliability of the data they are producing.

Following a recommendation given at the first Research Co-ordination Meeting of the CRP on 'Assessing the effectiveness of soil conservation measures for sustainable watershed management using fallout radionuclides', held in Vienna (19-23 May 2003) a proficiency test for ^{137}Cs and total ^{210}Pb measurement was organized in 2006 by the Chemistry Unit in collaboration with the Soil Science Unit of the IAEA's Laboratories. The main purpose of this paper is to report on this proficiency test conducted to assess the analytical performance of 14 participating laboratories in the CRP for the determination of ^{137}Cs and total ^{210}Pb in spiked soil samples. Only the summary of main results is presented in this contribution.

2. MATERIALS AND METHODS

Full details on the organization and implementation of the Proficiency Test (PT) on the determination of ^{137}Cs and total ^{210}Pb in spiked soil have been described elsewhere. The most important steps are described here.

2.1. Preparation and validity test of the PT materials

The proficiency test aimed at checking the validity and reliability of the analytical results produced by the participating laboratories for the determination of ^{137}Cs and total ^{210}Pb in spiked soil and to enable the participating laboratories to compare their performances with those of other laboratories.

A loess soil from China was used to prepare a spiked soil matrix with ^{137}Cs and ^{210}Pb . Before spiking, the soil was milled and sieved to collect the appropriate fraction at mesh size less than 0.1mm, and then homogenised. A number of samples from the Chinese soil matrix were pre-screened for radionuclides prior to spiking. The results showed that the material is free from man made radionuclides, except for ^{137}Cs , which was present at $2.6 \pm 0.2 \text{ Bq kg}^{-1}$ based on dry weight (d.w.). (Ref. date: 2006-01-01) and ^{210}Pb at $48 \pm 1.5 \text{ Bq kg}^{-1}$ d.w. The moisture content determined at 105°C was found to be $2.3 \pm 0.2\%$.

The following set of 5 soil samples was distributed in this proficiency test:

- One soil sample (sample code 03) at low activity: This soil was used to prepare the spiked test materials (blank soil),
- Two soil samples spiked with ^{137}Cs and ^{210}Pb (sample codes 01, 05): The activity level of ^{137}Cs was about 10 times the level of the blank; and for ^{210}Pb it was about 5 times.
- Another two soil samples spiked with ^{137}Cs and ^{210}Pb (sample codes 02, 04): The activity level of ^{137}Cs and ^{210}Pb were about twice the level of the samples 01 and 05.

The participating laboratories received the set of test samples, together with handling instructions and the reporting forms. The participants were given two months to report the results.

2.1.1. Spiking Procedure for ^{137}Cs and ^{210}Pb in the Chinese soil

An aliquot (0.5136 g) of the spiking solution was introduced into polypropylene containers and diluted with 80 mL of methanol. A portion of the Chinese soil was weighed to the second decimal place and transferred to the jar containing the spiking solution. The liquid-to-solid ratio was determined experimentally such that the whole amount of liquid was absorbed by the soil and the whole amount of soil became uniformly moistened.

The samples were kept in an oven at 40°C for 12 hours to become completely dry. They were then allowed to reach equilibrium with ambient humidity before sealing. After such treatment the residual moisture content was found to be $2.4 \pm 0.2\%$, i.e. not very different from the initial humidity of the untreated sample ($2.3 \pm 0.2\%$).

To control the quality of the spiked samples, all of the produced samples were measured by gamma spectrometry and checked for consistency.

2.1.2. Assignment of target values to the PT materials

The target values established for the activity levels, which are close to those measured in developed and also developing countries belonging to south hemisphere, were calculated from the certified activity values assigned to each radionuclide, taking into account the successive dilution steps, the mass of spiking solutions and the amount of matrix being spiked. The target values for ^{137}Cs and ^{210}Pb in the four prepared samples, together with the respective uncertainties, are presented in Tables 1 and 2. The combined standard uncertainty includes three major components: (1) uncertainty of spiking solution, (2) uncertainty originating from heterogeneity and (3) arising from variability of moisture content in samples. The two latter sources are the largest contributors to the overall uncertainties, which are, nevertheless, gratifyingly small for all radionuclides used in the proficiency test. A summary of the target values and associated total uncertainties of the set of test samples is presented in Table 3.

2.1.3. Homogeneity test of the PT materials

The method of spiking soil samples was developed at the Agency's Laboratories in Seibersdorf. It was demonstrated to yield reliable and reproducible results within 1-2% for all radionuclides tested.

In one series of experiments, a homogeneity test was performed on three bottles of spiked samples, by measuring ^{137}Cs and ^{210}Pb in 3 sub-samples with a sample mass of 60g taken from each of the three bottles. The measurements were performed by gamma-spectrometry in the IAEA Laboratories Seibersdorf [5]. The results were evaluated by single factor ANOVA [6]. It could be concluded that the homogeneity of the material is fitting for the purpose of this proficiency test. The homogeneity test results are shown in Table 4.

The results on the homogeneity provided experimental evidence that satisfactory homogeneity (within-bottle) could be attained for both radionuclides for sub-samples weighing 60 g or more.

To check if there was any trend in the activity values for ^{210}Pb and ^{137}Cs during the spiking procedure, a graphical evaluation was made (Figs. 1 and 2). The estimated slope of the linear fitting was found to be negligible, thus illustrating that there was no significant trend with regards to the activity values of the studied radionuclides during spiking.

TABLE 1. TARGET ACTIVITIES AND ASSOCIATED UNCERTAINTIES OF SAMPLES 01 AND 05

(Reference date: 1 January 2006)

Radio-nuclide	Activity (A) Bq/sample	U (A) %	U (homogeneity) Bq/sample	Dry weight %	U (DW) %	Sample mass g	u Sample Mass g	Activity in soil Bq kg ⁻¹ d.w.	Combined uncertainty Bq kg ⁻¹ d.w.			
¹³⁷ Cs	3.968	0.056	1.42	0.078	2.00	97.7	0.25	200.00	0.101	20.3	0.50	2.47
²¹⁰ Pb	56.526	0.750	1.33	1.131	2.00	97.7	0.25	200.00	0.101	289.2	6.98	2.41

d.w. is dry weight.

TABLE 2. TARGET ACTIVITIES AND ASSOCIATED UNCERTAINTIES OF SAMPLES 02 AND 04

(Reference date: 1 January 2006)

Radio-nuclide	Activity (A) Bq/sample	u(A) %	u(homogeneity) Bq/sample	Dry weight %	u(DW) %	Sample mass g	u Sample Mass g	Activity in soil Bq kg ⁻¹ d.w.	Combined uncertainty Bq kg ⁻¹ d.w.			
¹³⁷ Cs	7.509	0.114	1.53	0.113	1.50	97.7	0.25	200.00	0.101	38.4	0.83	2.15
²¹⁰ Pb	103.668	1.544	1.49	1.555	1.50	97.7	0.25	200.00	0.101	530.5	11.3	2.13

d.w. is dry weight.

TABLE 3. SUMMARY OF THE TARGET VALUES AND ASSOCIATED TOTAL UNCERTAINTIES OF THE PROFICIENCY TEST MATERIALS

Sample code	Target value (Bq kg ⁻¹) dw	
	¹³⁷ Cs	²¹⁰ Pb
01 , 05	20.3±0.5	289±7
02 , 04	38.4±0.8	530±11
03	2.6±0.2	48.0±1.5

The uncertainty is expressed as 1 σ (k=1), dw = based on dry weight (dw).

TABLE 4. HOMOGENEITY TEST MEASUREMENTS

Sample ID	²¹⁰ Pb		¹³⁷ Cs	
	R (cps)	u(R)/R (%)	R (cps)	u(R)/R (%)
133-1	6.09E-02	3.5	6.96E-02	2.0
133-2	6.28E-02	3.4	6.79E-02	2.1
133-3	6.27E-02	3.1	6.84E-02	2.1
244-1	6.16E-02	3.5	7.14E-02	2.1
244-2	5.93E-02	3.5	7.03E-02	2.0
244-5	6.41E-02	2.1	6.93E-02	2.1
325-1	5.92E-02	3.5	7.33E-02	2.0
325-2	6.22E-02	1.1	7.05E-02	1.0
325-3	6.25E-02	3.4	6.98E-02	2.1
Average	6.17E-02		7.01E-02	
STDV	0.0016		0.0016	
Rel. STDV	2.7%		2.3%	

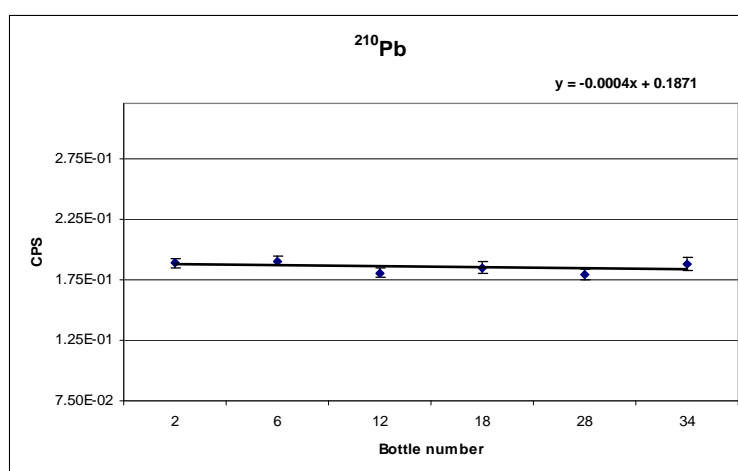


FIG. 1. Trend evaluation of the spiking procedure of ²¹⁰Pb.

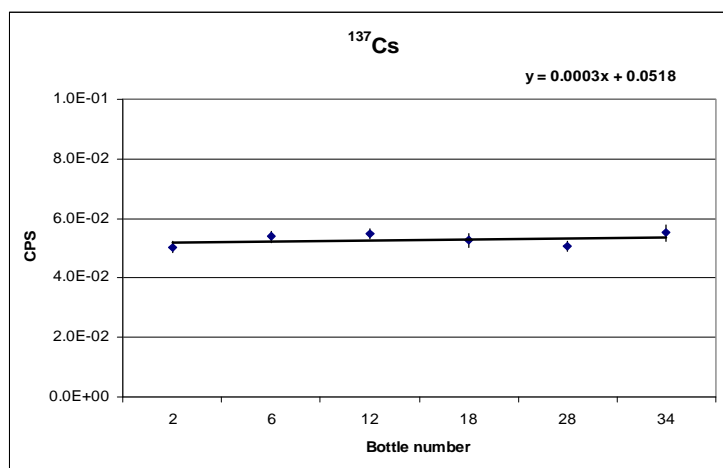


FIG. 2. Trend evaluation of the spiking procedure of ^{137}Cs .

A second experiment was designed to check if there were any losses of the radionuclides due to adsorption on the walls of the bottles in which the samples were spiked. Two empty bottles which had been already used in spiking soil were measured in a gamma-spectrometer. No activity was detected upon 24 hour counting. It was, therefore, concluded that the whole amount of radionuclides was associated with the matrix.

There was no need to check the between-bottle homogeneity, since each bottle was spiked individually with the same amount of radionuclides and each bottle was also individually homogenised. Therefore, the value of between-bottle heterogeneity was limited to the weighing uncertainty. It was estimated that combined uncertainties arising from heterogeneity was less than 2% and they were included in the total uncertainty budget.

2.2. Performance evaluation and scoring

Most of the participating laboratories produced test results accompanied, at best, with an indication of their repeatability. Information on their analytical uncertainty was not provided. However, new requirements coming into force (ISO/IEC 17025:2005) [4] demand that laboratories also have to express their measurement uncertainty.

Several rating systems have been developed for determining a laboratory's performance and the meaning of the results of the different scoring systems are not always comparable. Among various statistical methods, Z-scores and U-scores are the most often used. The drawback of Z-scores is that uncertainty of the participant's measurement result is not taken into account for the evaluation of the performance. In the case of U-scores, the evaluation includes uncertainties of the participant measurements and the uncertainty of the assigned value. Laboratories performing well in classical proficiency testing (Z-Scores) will not necessarily exhibit the same level of performance when their analytical uncertainties are considered in the evaluation.

Three additional statistical parameters namely: Relative bias, Z-score, and U score are calculated as complementary information for the participating laboratories.

2.2.1. Relative bias

The first step in producing a score for a result $Value_{Analyst}$ (a single measurement of analyte concentration in a test material) is obtaining the estimate of the bias. To evaluate the bias of the reported results, the relative bias between the analyst's value and the IAEA value ($Value_{IAEA}$) is calculated and expressed as a percentage:

$$Relative\ bias = \frac{Value_{Analyst} - Value_{IAEA}}{Value_{IAEA}} \times 100\% \quad (1)$$

2.2.2. The Z-score value

The Z-score is calculated from the laboratory results, the assigned value and a standard deviation (σ) in accordance to the following equation:

$$Z_{Score} = \frac{Value_{Analyst} - Value_{IAEA}}{\sigma} \quad (2)$$

On the basis of 'fitness for purpose' principle, the target value for the standard deviation is:

$$0.10 \times Value_{IAEA}$$

The laboratory performance is evaluated as satisfactory if $|z_{Score}| < 2$; questionable for $2 < |z_{Score}| < 3$, and unsatisfactory for $|z_{Score}| \geq 3$.

2.2.3. The U-score value

The value of the u_{test} score is calculated according to the following equation [7]:

$$u_{test} = \frac{|Value_{IAEA} - Value_{Analyst}|}{\sqrt{Unc_{IAEA}^2 + Unc_{Analyst}^2}} \quad (3)$$

The calculated U_{test} value is compared with the critical values listed in the t-statistic tables to determine if the reported result differs significantly from the expected value at a given level of probability. The advantage of U_{test} is that it takes into consideration the propagation of measurement uncertainties when defining the normalised error. This is especially useful when evaluating results, which may overlap with the reference interval.

It should be noted that the choice of the significance level is subjective. For this proficiency test the limiting value for the u-test parameter was set to 2.58 for a level of probability at 99% to determine if a result passes the test ($u_{test} < 2.58$).

2.3. Evaluation criteria of the proficiency test

The proficiency testing scoring system used in this assessment took into consideration the trueness and the precision of the reported data and it includes in the evaluation both the total combined uncertainty associated with the target value of proficiency testing samples and the total uncertainty reported by the participating laboratories. According to the newly adopted approach, the reported results are evaluated against the acceptance criteria for accuracy and precision and assigned the status 'acceptable' or 'not acceptable' accordingly. A result must

pass both criteria to be assigned the final status of ‘acceptable’. The advantage of this approach is that it checks the credibility of uncertainty statement given by the participating laboratories, and results are no longer compared against fixed criteria but participants establish their individual acceptance range on the basis of the uncertainties assigned to the values. Such an approach highlights not only methodological problems affecting accuracy of the reported data but also identifies shortcomings in uncertainty estimation.

The proficiency test results were evaluated against the acceptance criteria for trueness and precision and assigned the status ‘acceptable’ (A), ‘warning’ (W) or ‘not acceptable’ (N) accordingly.

2.3.1. Trueness

The participant result is assigned ‘acceptable’ status if $A1 \leq A2$:

where:

$$A1 = |Value_{IAEA} - Value_{Analyst}| \quad (4)$$

$$A2 = 2.58 \times \sqrt{Unc_{IAEA}^2 + Unc_{Analyst}^2} \quad (5)$$

2.3.2. Precision

The participant result is assigned ‘acceptable’ status if:

$$P = \sqrt{\left(\frac{Unc_{IAEA}}{Value_{IAEA}}\right)^2 + \left(\frac{Unc_{Analyst}}{Value_{Analyst}}\right)^2} \times 100\% \quad (6)$$

The acceptance criterion for precision depends on the concentration or activity concentrations of the considered analytes.

The ^{137}Cs , ^{210}Pb activities are measured using gamma spectrometry: ^{137}Cs activity is detected at 662 keV and ^{210}Pb at 46.5 keV. As it is commonly admitted that the activity of soil sample containing ^{137}Cs and ^{210}Pb should be provided with an analytical precision less than $\pm 10\%$ [1], applying the above reported equation the participant result is assigned ‘acceptable’ status if P is:

- $\leq 10\%$ for ^{137}Cs
- $\leq 10\%$ for total ^{210}Pb

A result must obtain ‘acceptable’ status in both criteria to be assigned final status of ‘acceptable’. If a result obtained a ‘not acceptable’ status for trueness or precision, then the relative bias is compared to a predetermined limit (20% for ^{137}Cs and 25% for ^{210}Pb), and if a result bias is below this limit then the status ‘warning’ is assigned as a final score, otherwise the status ‘not acceptable’ is assigned as a final score. Obviously, if a result obtained ‘not acceptable’ status for both trueness and precision the final score will be assigned as ‘not acceptable’.

3. RESULTS AND DISCUSSIONS

3.1. Analytical performance

In total, 14 out of 18 initially registered laboratories reported their results to the IAEA. Altogether 130 results were submitted. The participant's data along with the performance evaluation criteria and evaluation scores were compiled and presented in the summary report [8].

Fig. 3 shows the percentage of acceptable scores for each sample. Performances for samples 1, 2, 4 and 5 are comparable with a non acceptable level inferior to or equal to 20%. However, it can be noticed that the sample number 3 with low activity of ^{137}Cs ($2.6\pm 0.2 \text{ Bq kg}^{-1}$) had the lowest number of acceptable scores. This could be due to several reasons related to the available analytical facilities and procedures for sample measurement in the participating laboratories. However, this low activity level is greater than or close to the activity that can be found under the plough depth in agricultural fields. For example, in Canada (Quebec) in 24 sampled fields from the Boyer River watershed Mabit et al [9] found 3.2 Bq kg^{-1} of ^{137}Cs in the soil depth interval of 20-30 cm and 0.47 Bq kg^{-1} in the depth interval of 30-40 cm ($n = 412$). This outcome demonstrates the potential impact that incorrect measurements of low ^{137}Cs activities can have on estimating erosion and sedimentation rates. Therefore, particular care and appropriate measures should be taken to produce acceptable levels in samples with low level ^{137}Cs activity.

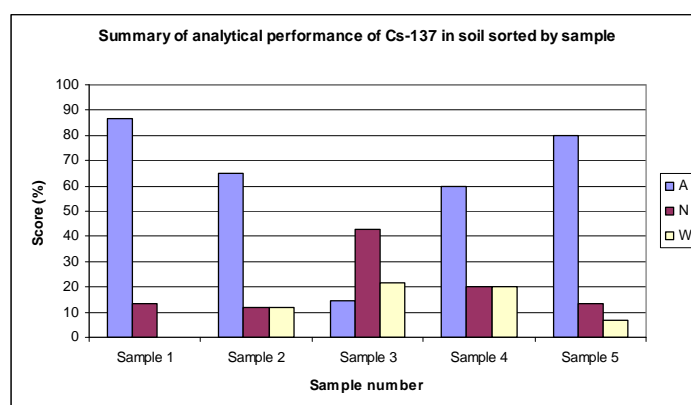


FIG. 3. Summary of analytical performance of ^{137}Cs in soil sorted by sample ('acceptable' (A), 'warning' (W) or 'not acceptable' (N)).

The performance evaluation of ^{210}Pb results is shown in Fig. 4. It is well known that the determination of ^{210}Pb by gamma spectrometry in a soil matrix is more complicated than ^{137}Cs determination. This is mainly related to the relatively low emission probability and low energy (46.5 keV) of the gamma ray used in the ^{210}Pb measurement. Hence, particular care is needed when performing efficiency calibrations and sample self-attenuation corrections.

Although such a bias in ^{210}Pb measurements could arise in a number of ways, there are three most likely sources of error which may be investigated:

- Firstly, the laboratory has used a biased calibration source. There may be a problem with the calibration of the detector's efficiency. For example, the use of an extrapolated ^{210}Pb efficiency calibration can lead to large discrepancies.

- Secondly, many laboratories do not report the use of proper matrix reference materials to check the validity of the detector's efficiency calibration.
- Thirdly, the underestimation of the correction coefficient for self-attenuation of the gamma ray in the sample could be a source of negative bias.

The second and third sources of bias are the most probable causes of problems for ^{210}Pb measurements because the emitted gamma ray is in the low energy part of the spectrum.

The results from the overall performance evaluation showed that the ^{137}Cs measurements had a higher number of acceptable scores than those of ^{210}Pb determination. Figs. 5 and 6 illustrate the summary results of this proficiency test. 66% and 31% of the data reported by the participating laboratories were scored as 'acceptable' for ^{137}Cs and ^{210}Pb measurements respectively [10]. In the case of ^{210}Pb analysis corrective actions in the analysis procedures are needed to improve the quality of the results.

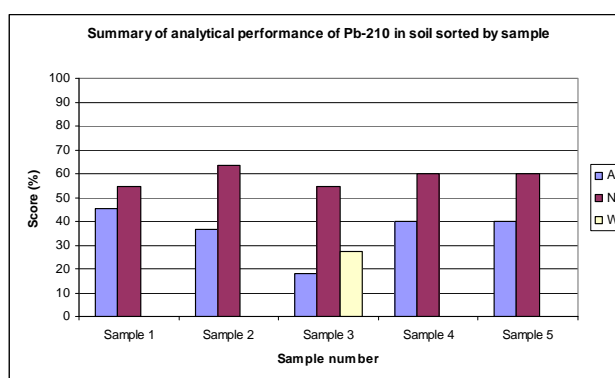


FIG. 4. Summary of analytical performance of ^{210}Pb in soil sorted by sample ('acceptable' (A), 'warning' (W) or 'not acceptable' (N)).

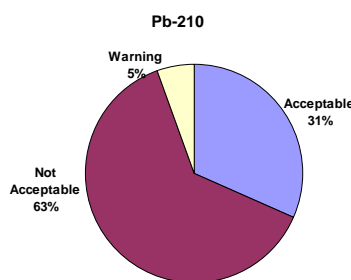


FIG. 5. Summary evaluation of the analytical data (Total ^{210}Pb measurements) of the proficiency test completed by the 14 laboratories.

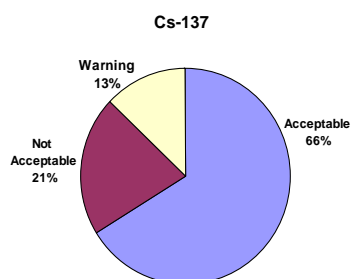


FIG. 6. Summary evaluation of the analytical data (^{137}Cs measurements) of the proficiency test completed by the 14 laboratories.

3.2. Further issues for FRN measurements by gamma spectrometry

The analysis of FRN by gamma spectrometry using High Purity Germanium (HPGe) detectors in soil/sediment samples is a complex task that demands specific and expensive equipment and staff with high skills and experience to achieve accurate results with good precision.

Different factors can influence and affect the precision of gamma measurement of soil/sediment samples: (1) detector and associated equipment (performance of the detector – relative efficiency–, detector type, size, configuration, calibration, internal background interference, geometry and lead-shield thickness), (2) collection, preparation, pre-treatment and configuration of the sample (sample mass and sample activity), (3) laboratory radiation exposition (external background interference, constancy of the background) and (4) software for data acquisition and evaluation.

As a result of this proficiency test some recommendations are provided to optimize FRN measurements with appropriate analytical facilities [10]:

- The sample size (quantity) should be the maximum possible. This means that the sampling strategy should be adapted in order to collect sufficient amount of soil for accurate analysis and adapted to the geometry calibration employed in the laboratory.
- Different sample geometries for measurement should be prepared in the laboratory.
- The gamma detector should be installed in a low and constant background environment (to reduce environmental radiation) and the lead shield should have a minimum thickness of 100 mm to protect the measurement from external background.
- For calibration old standard or certified solutions with expired validity should not be used.
- Standards with an appropriate matrix should be used for calibration and an appropriate correction factor should be applied depending on the density of the material.
- Gamma spectra information should be collected and evaluated using appropriate modern software.
- The calibration of the detector should be controlled regularly with reference material and blank samples. In order to assess the precision of gamma analysis, a quality control and quality assurance protocol should be instituted and respected by all laboratories to obtain accurate and valid measurement at mid term and long term.
- The IAEA recommends to the national laboratories to organize and run their own inter-comparison exercises at the regional level; thus the data obtained by national laboratories can be compared on a regular basis.
- The IAEA also recommends that the participating laboratories of the inter-comparison exercise develop and improve their analytical quality assurance system including diagnosis and standard operating procedures (quality control based on standards of radioactive materials with known activity level) to assess the accuracy and precision of their analytical data.

4. CONCLUSIONS

The measurement of the radionuclides by HPGe gamma spectrometry is an essential component of the application of FRN techniques in soil erosion and sedimentation studies.

From the performance evaluation of this proficiency test it was found that 66% of the laboratories reported 'acceptable' results for the ^{137}Cs measurements and only 31% of the participants were able to provide acceptable results for total ^{210}Pb analyses. Also, difficulties

were found in measuring low levels of activity of ^{137}Cs ($2.6\pm 0.2 \text{ Bq kg}^{-1}$) with more than 40% of results scored as unacceptable. In general, the analytical uncertainties associated with the results were appropriate for the analytes and matrices considered in the current proficiency test.

The results from this proficiency test underline the necessity for the IAEA to organize regularly inter-comparison exercises of FRN analyses for laboratories participating in CRPs and TCPs and working in soil erosion/sedimentation studies. It is worthy to note that proficiency testing should be conducted within the context of a complete quality assurance system.

ACKNOWLEDGEMENTS

This study was conducted as part of the Co-ordinated Research Project D1.50.08 ‘Assessing the effectiveness of soil conservation measures for sustainable watershed management using fallout radionuclides’. The authors are grateful to the laboratories participating in this proficiency test.

We would like to thank the IAEA collaborating centre: Hungarian Agricultural Authority (HAA), Budapest, Hungary, for milling and testing the homogeneity of the soil used in this proficiency test at no cost to the IAEA. Thanks are expressed to Mr. Felipe Zapata & Mr. Gerd Dercon (Soil Water Management and Crop Nutrition Section) and Mr. Gudni Hardarson (Soil Science Unit) for suggestions to improve this manuscript.

We acknowledge also the contribution and support provided by Mr. Claude Bernard (previous staff member of the SWMCN section), Ms. Adelaide Maria Condin Da Foseca Azeredo (SSU), Mr. Umberto Sansone (Head of the CU), Mr. Chang-Kyu Kim (CU), Mr. Gyula Kis-Benedek (CU), Mr. Marek Makarewicz (CU), Mr. Alexander Trinkl (CU), Mr. Thomas Benesch (CU), Ms. Renate Schorn (CU) and Ms. Karin Will (CU).

REFERENCES

- [1] ZAPATA, F. (Ed.), Handbook for the Assessment of Soil Erosion and Sedimentation Using Environmental Radionuclides, Kluwer Academic Publishers, Dordrecht-Boston-London (2002).
- [2] INTERNATIONAL ATOMIC ENERGY AGENCY, Analytical Quality Control Services (AQCS) 1994-1995, IAEA publication, IAEA, Vienna (1995).
- [3] ISO GUIDE 34:2000 (E), General requirements for the competence of reference material producers, ISO, Geneva (2000).
- [4] ISO/IEC 17025:2005, General Requirements for the Competence of Testing and Calibration Laboratories, ISO, Geneva (2005).
- [5] MAKAREWICZ, M., Gamma Analysis report CU-06-019, Chemistry Unit, IAEA Laboratories, IAEA, Seibersdorf (2006).
- [6] ISO/IEC GUIDE 35:2000, Certification of reference materials-General and statistical principles, ISO, Geneva (2000).
- [7] BROOKES, C.J., et al., Fundamentals of Mathematics and Statistics, Wiley (1979).
- [8] INTERNATIONAL ATOMIC ENERGY AGENCY, Report on the IAEA-CU-2006-02, Proficiency test on the determination of ^{137}Cs and ^{210}Pb in spiked soil, Seibersdorf, IAEA/AL/166, IAEA, Vienna (2006).

- [9] MABIT, L., et al., Assessment of erosion in the Boyer River watershed (Canada) using ^{137}Cs measurements and a GIS oriented sampling strategy, *Catena* **71** (2007) 242-249.
- [10] SHAKHASHIRO, A., MABIT, L., Results of an IAEA inter-comparison exercise to assess ^{137}Cs and total ^{210}Pb analytical performance in soil, *Appl. Radiat. Isot.* **67-1** (2009) 139-146.

**RECENT IAEA PUBLICATIONS
ON SOIL AND WATER MANAGEMENT AND CROP NUTRITION**

- 2001 Use of Isotope and Radiation Methods in Soil and Water Management and Crop Nutrition –Manual (IAEA Training Course Series No. 14).
- 2002 Water Balance and Fertigation for Crop Improvement in West Asia (IAEA-TECDOC-1266).
- 2002 Assessment of Soil Phosphorus Status and Management of Phosphatic Fertilisers to Optimise Crop Production (IAEA-TECDOC-1272).
- 2002 Nuclear Techniques in Integrated Plant Nutrient, Water and Soil Management (Proc. Symp. Vienna, 2000) (IAEA C+S Paper Series 11/P).
- 2002 Irradiated Sewage Sludge for Application to Cropland (IAEA-TECDOC-1317).
- 2003 Neutron and Gamma Probes: Their Use in Agronomy (Second Edition) (IAEA Training Course Series No. 16).
- 2003 Les Sondes à Neutrons et à Rayons Gamma: Leur Applications en Agronomie (Deuxième Édition) (Collection Cours de Formation No.16).
- 2003 Las Sondas de Neutrones y Gamma: Sus Aplicaciones en Agronomía (Segunda Edición) (Colección Cursos de Capacitación No. 16).
- 2003 Management of Crop Residues for Sustainable Crop Production (IAEA-TECDOC-1354).
- 2003 Guidelines for the Use of Isotopes of Sulfur in Soil-Plant Studies (IAEA Training Course Series No. 20).
- 2003 Maximising the use of biological nitrogen fixation in agriculture (Developments in Plant and Soil Sciences No. 99. FAO, Rome, and Kluwer Academic Publishers, Dordrecht).
- 2004 Use of phosphate rocks for sustainable agriculture. (FAO Fertilizer and Plant Nutrition Bulletin 13. Joint FAO/IAEA Division of Nuclear Techniques in Food and Agriculture and the Land and Water Development Division-AGL, FAO, Rome).
- 2004 Use of Isotope and Radiation Methods in Soil and Water Management and Crop Nutrition (An interactive CD).
- 2005 Nutrient and water management practices for increasing crop production in rainfed arid/semi-arid areas (IAEA-TECDOC-1468).
- 2007 Management Practices for Improving Sustainable Crop Production in Tropical Acid Soils Results of a Coordinated Research Project organized by the Joint FAO/IAEA Programme of Nuclear Techniques in Food and Agriculture, Proceedings Series, STI/PUB/1285.
- 2008 Guidelines on Nitrogen Management in Agricultural Systems, Training Course Series No. 29: IAEA-TCS-29/CD - ISSN 1998-0973.
- 2008 Field Estimation of Soil Water Content, A Practical Guide to Methods, Instrumentation and Sensor Technology, Training Course Series No. 30. IAEA-TCS-30/CD - ISSN 1998-0973.
- 2008 Management of Agroforestry Systems for Enhancing Resource use Efficiency and Crop Productivity Details, IAEA TECDOC Series No. 1606, ISBN 978-92-0-110908-8.

LIST OF PARTICIPANTS

- Bacchi, O. Laboratório de Física do Solo
Centro de Energia Nuclear na Agricultura
Universidade de Sao Paulo
Avenida Centenario 303
Caixa Postal 96
13400-970 Piracicaba, SP
Brazil
Email: osny@cena.usp.br
- Benmansour, M. Centre National de l'Energie, des Sciences et des Techniques Nucléaires
B.P. 1382
10001 Rabat, Agdal
Morocco
Email: benmansour64@yahoo.fr; benmansour@cnesten.org.ma
- Froehlich, W. Institute of Geography and Spatial Organization
Polish Academy of Sciences
Frycowa 113
33-335 Nawojowa
Poland
Email: wfroehlich@pro.onet.pl
- GolosoV, V. Laboratory for Soil Erosion and Fluvial Processes
Faculty of Geography
M.V. Lomonosov Moscow State University
Leninskiye Gory
P.O. Box GSP-1
119991 Moscow
Russian Federation
Email: golossov@rambler.ru; golosov@river.geogr.msu.su
- Haciyakupoglu, S. Institute of Nuclear Energy
Istanbul Technical University
Maslak
80626 Istanbul
Turkey
Email: haciyakup1@itu.edu.tr
- Klik, A. Institut für Hydraulik und landeskulturelle Wasserwirtschaft (IHLW)
Universität für Bodenkultur (BOKU)
Muthgasse 18
1190 Wien
Austria
Email: andreas.klik@boku.ac.at

- Li, Y. Institute of Environment and Sustainable Development in Agriculture
Chinese Academy of Agricultural Sciences
12 Zhongguancun South Street
Beijing 100081
China
Email: yongli32@yahoo.com.cn
- Lobb, D. University of Manitoba
362 Ellis Building
Winnipeg, Manitoba R3T 2N2
Canada
Email: lobbda@cc.umanitoba.ca; lobbda@ms.umanitoba.ca
- Onda, Y. School of Life and Environment Science
University of Tsukuba
1-1-1 Ten-nodai
Tsukuba, Ibaragi-ken 305-8572
Japan
Email: onda@geoenv.tsukuba.ac.jp
- Phan, S.Hai. Center for Environment Research and Monitoring
Nuclear Research Institute
Vietnam Atomic Energy Institute
01 Nguyen Tu Luc Street
P.O. Box 61100
Dalat
Vietnam
Email: phansh_nri@vnn.vn; nrigovn@hcm.vnn.vn
- Popa, N. Development Center for Soil Erosion Control Perieni
Bacau Road, km7
P.O. Box 1
731240 Barlad, Vaslui
Romania
Email: nelu_c_popa@yahoo.com
- Ritchie, J.C.[†] USDA Agriculture Research Service
Hydrology and Remote Sensing Laboratory
BARD-West Bldg-007, Beltsville, MD 20705
United States of America
- Schuller, P.S. Instituto de Física, Facultad de Ciencias
Universidad Austral de Chile
Independencia 641
Casilla 567
Valdivia
Chile
Email: pschulle@uach.cl

[†] Deceased.

- Sheikh, M. Radiation and Isotope Applications Division
Pakistan Institute of Nuclear Science & Technology Pakistan Atomic
Energy Commission
P.O. Box 1482, Nilore
Islamabad
Pakistan
Email: manzoor@pinstech.org.pk; rafiq@pinstech.org.pk
- Wallbrink, P. Commonwealth Scientific and Industrial Research Organisation
Land and Water
Black Mountain laboratory
GPO Box 1666
Canberra ACT 2600
Australia
Email: Peter.Wallbrink@csiro.au; Peter.Wallbrink@cbr.clw.csiro.au
- Walling, D. School of Geography
Sediment Research Centre
University of Exeter
Rennes Drive
Exeter, Devon EX4 4RJ
United Kingdom
Email: d.e.walling@exeter.ac.uk
- Zhang, X. Institute of Mountain Hazards and Environments
Chinese Academy of Sciences
P.O. Box 417
Chengdu, Sichuan 610041
China
Email: zxbao@imde.ac.cn

Consultants Meeting

Vienna, Austria: 28-30 May 2001

Research Coordination Meetings

Vienna, Austria: 19-23 May 2003
Istanbul, Turkey: 4-8 October 2004
Vienna, Austria: 27-30 March 2006
Vienna, Austria: 15-19 October 2007



IAEA

International Atomic Energy Agency

No. 22

Where to order IAEA publications

In the following countries IAEA publications may be purchased from the sources listed below, or from major local booksellers. Payment may be made in local currency or with UNESCO coupons.

AUSTRALIA

DA Information Services, 648 Whitehorse Road, MITCHAM 3132
Telephone: +61 3 9210 7777 • Fax: +61 3 9210 7788
Email: service@dadirect.com.au • Web site: <http://www.dadirect.com.au>

BELGIUM

Jean de Lannoy, avenue du Roi 202, B-1190 Brussels
Telephone: +32 2 538 43 08 • Fax: +32 2 538 08 41
Email: jean.de.lannoy@infoboard.be • Web site: <http://www.jean-de-lannoy.be>

CANADA

Bernan Associates, 4501 Forbes Blvd, Suite 200, Lanham, MD 20706-4346, USA
Telephone: 1-800-865-3457 • Fax: 1-800-865-3450
Email: customercare@bernan.com • Web site: <http://www.bernan.com>

Renouf Publishing Company Ltd., 1-5369 Canotek Rd., Ottawa, Ontario, K1J 9J3
Telephone: +613 745 2665 • Fax: +613 745 7660
Email: order.dept@renoufbooks.com • Web site: <http://www.renoufbooks.com>

CHINA

IAEA Publications in Chinese: China Nuclear Energy Industry Corporation, Translation Section, P.O. Box 2103, Beijing

CZECH REPUBLIC

Suweco CZ, S.R.O., Klecakova 347, 180 21 Praha 9
Telephone: +420 26603 5364 • Fax: +420 28482 1646
Email: nakup@suweco.cz • Web site: <http://www.suweco.cz>

FINLAND

Akateeminen Kirjakauppa, PO BOX 128 (Keskuskatu 1), FIN-00101 Helsinki
Telephone: +358 9 121 41 • Fax: +358 9 121 4450
Email: akatilais@akateeminen.com • Web site: <http://www.akateeminen.com>

FRANCE

Form-Edit, 5, rue Janssen, P.O. Box 25, F-75921 Paris Cedex 19
Telephone: +33 1 42 01 49 49 • Fax: +33 1 42 01 90 90
Email: formedit@formedit.fr • Web site: <http://www.formedit.fr>

Lavoisier SAS, 145 rue de Provigny, 94236 Cachan Cedex
Telephone: + 33 1 47 40 67 02 • Fax +33 1 47 40 67 02
Email: romuald.verrier@lavoisier.fr • Web site: <http://www.lavoisier.fr>

GERMANY

UNO-Verlag, Vertriebs- und Verlags GmbH, Am Hofgarten 10, D-53113 Bonn
Telephone: + 49 228 94 90 20 • Fax: +49 228 94 90 20 or +49 228 94 90 222
Email: bestellung@uno-verlag.de • Web site: <http://www.uno-verlag.de>

HUNGARY

Librotrade Ltd., Book Import, P.O. Box 126, H-1656 Budapest
Telephone: +36 1 257 7777 • Fax: +36 1 257 7472 • Email: books@librotrade.hu

INDIA

Allied Publishers Group, 1st Floor, Dubash House, 15, J. N. Heredia Marg, Ballard Estate, Mumbai 400 001,
Telephone: +91 22 22617926/27 • Fax: +91 22 22617928
Email: alliedpl@vsnl.com • Web site: <http://www.alliedpublishers.com>

Bookwell, 2/72, Nirankari Colony, Delhi 110009
Telephone: +91 11 23268786, +91 11 23257264 • Fax: +91 11 23281315
Email: bookwell@vsnl.net

ITALY

Libreria Scientifica Dott. Lucio di Biasio "AEIOU", Via Coronelli 6, I-20146 Milan
Telephone: +39 02 48 95 45 52 or 48 95 45 62 • Fax: +39 02 48 95 45 48
Email: info@libreriaaeiou.eu • Website: www.libreriaaeiou.eu

JAPAN

Maruzen Company, Ltd., 13-6 Nihonbashi, 3 chome, Chuo-ku, Tokyo 103-0027
Telephone: +81 3 3275 8582 • Fax: +81 3 3275 9072
Email: journal@maruzen.co.jp • Web site: <http://www.maruzen.co.jp>

REPUBLIC OF KOREA

KINS Inc., Information Business Dept. Samho Bldg. 2nd Floor, 275-1 Yang Jae-dong SeoCho-G, Seoul 137-130
Telephone: +02 589 1740 • Fax: +02 589 1746 • Web site: <http://www.kins.re.kr>

NETHERLANDS

De Lindeboom Internationale Publicaties B.V., M.A. de Ruyterstraat 20A, NL-7482 BZ Haaksbergen
Telephone: +31 (0) 53 5740004 • Fax: +31 (0) 53 5729296
Email: books@delindeboom.com • Web site: <http://www.delindeboom.com>

Martinus Nijhoff International, Koraalrood 50, P.O. Box 1853, 2700 CZ Zoetermeer
Telephone: +31 793 684 400 • Fax: +31 793 615 698
Email: info@nijhoff.nl • Web site: <http://www.nijhoff.nl>

Swets and Zeitlinger b.v., P.O. Box 830, 2160 SZ Lisse
Telephone: +31 252 435 111 • Fax: +31 252 415 888
Email: info@swets.nl • Web site: <http://www.swets.nl>

NEW ZEALAND

DA Information Services, 648 Whitehorse Road, MITCHAM 3132, Australia
Telephone: +61 3 9210 7777 • Fax: +61 3 9210 7788
Email: service@dadirect.com.au • Web site: <http://www.dadirect.com.au>

SLOVENIA

Cankarjeva Založba d.d., Kopitarjeva 2, SI-1512 Ljubljana
Telephone: +386 1 432 31 44 • Fax: +386 1 230 14 35
Email: import.books@cankarjeva-z.si • Web site: <http://www.cankarjeva-z.si/uvoz>

SPAIN

Díaz de Santos, S.A., c/ Juan Bravo, 3A, E-28006 Madrid
Telephone: +34 91 781 94 80 • Fax: +34 91 575 55 63
Email: compras@diazdesantos.es, carmela@diazdesantos.es, barcelona@diazdesantos.es, julio@diazdesantos.es
Web site: <http://www.diazdesantos.es>

UNITED KINGDOM

The Stationery Office Ltd, International Sales Agency, PO Box 29, Norwich, NR3 1 GN
Telephone (orders): +44 870 600 5552 • (enquiries): +44 207 873 8372 • Fax: +44 207 873 8203
Email (orders): book.orders@tso.co.uk • (enquiries): book.enquiries@tso.co.uk • Web site: <http://www.tso.co.uk>

On-line orders

DELTA Int. Book Wholesalers Ltd., 39 Alexandra Road, Addlestone, Surrey, KT15 2PQ
Email: info@profbooks.com • Web site: <http://www.profbooks.com>

Books on the Environment

Earthprint Ltd., P.O. Box 119, Stevenage SG1 4TP
Telephone: +44 1438748111 • Fax: +44 1438748844
Email: orders@earthprint.com • Web site: <http://www.earthprint.com>

UNITED NATIONS

Dept. I004, Room DC2-0853, First Avenue at 46th Street, New York, N.Y. 10017, USA
(UN) Telephone: +800 253-9646 or +212 963-8302 • Fax: +212 963-3489
Email: publications@un.org • Web site: <http://www.un.org>

UNITED STATES OF AMERICA

Bernan Associates, 4501 Forbes Blvd., Suite 200, Lanham, MD 20706-4346
Telephone: 1-800-865-3457 • Fax: 1-800-865-3450
Email: customercare@bernan.com • Web site: <http://www.bernan.com>

Renouf Publishing Company Ltd., 812 Proctor Ave., Ogdensburg, NY, 13669
Telephone: +888 551 7470 (toll-free) • Fax: +888 568 8546 (toll-free)
Email: order.dept@renoufbooks.com • Web site: <http://www.renoufbooks.com>

Orders and requests for information may also be addressed directly to:

Marketing and Sales Unit, International Atomic Energy Agency

Vienna International Centre, PO Box 100, 1400 Vienna, Austria
Telephone: +43 1 2600 22529 (or 22530) • Fax: +43 1 2600 29302
Email: sales.publications@iaea.org • Web site: <http://www.iaea.org/books>